University of Naples FEDERICO II

Department of Structural Engineering

PH.D. PROGRAMME IN MATERIALS AND STRUCTURES

COORDINATORS PROFF. D. ACIERNO AND G. MENSITIERI

XXIV CYCLE

REMO CHIODI

PH.D. THESIS

WIND RISK ASSESSMENT IN A MULTI HAZARD PERSPECTIVE: THE CASE OF STEEL AIRCRAFT HANGARS

TUTOR PROF. GAETANO MANFREDI

CO-TUTOR PROF. ANDREA PROTA

CO-TUTOR PROF. FRANCESCO RICCIARDELLI

ACKNOWLEDGEMENTS

The PhD Thesis is the culmination of a process of scientific growth started when I was a young teenager. I have met people who have brought out my passion for structural engineering and it has been a changeling experience. Unfortunately, I have no time to say what I would say. I need to express a particular acknowledgment to Italian Air Force for the support in this activity; many thanks for Professor Ricciardelli and Professor Andrea Prota who have spent a lot of time to revise this document and make it look even better. Many thanks for Professor Edoardo Cosenza and Gaetano Manfredi for the support in this activity. I thank my laptops that have been a very good fellow adventures. And, of course, my girlfriend and my family for their patience.

Remo Chiodi

Naples, November 30th, 2011.

CONTENTS

1 INTRODUCTION

Fatalities and economic losses due to natural catastrophic events have increased in the last decades. This is not only due to the growth of population density in hazard risk zones, but also to the consequent and concomitant increase of possible "cascade effects" (Marzocchi, et al., 2009). For instance, topped only by 2007, 2010 was the year with the second-highest number of natural catastrophes since 1980 (Munich RE, 2010).

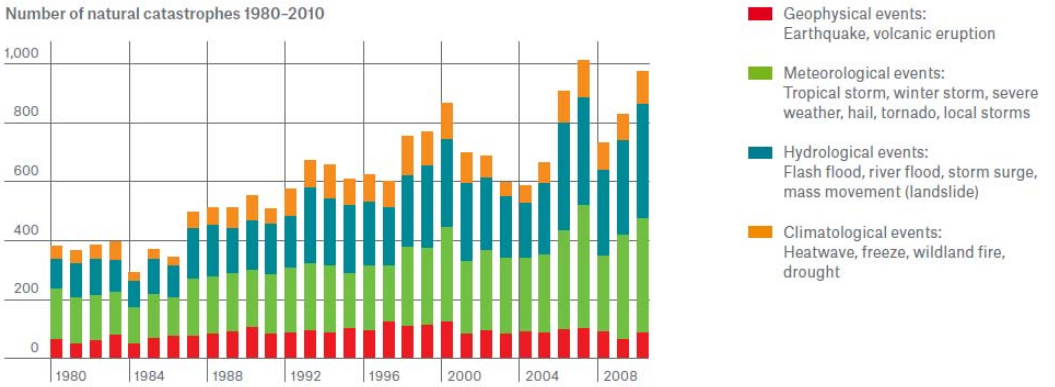

Figure 1.1 Number of natural catastrophes 1980-2010 (Munich RE, 2010)

The Figure 1.1 clearly shows an increasing tendency of the number of natural disasters, especially weather-related disasters such as floods and windstorms, and the majority of disasters are caused by wind storm and flood. With 960 loss events due to natural hazards, the number of catastrophes documented in 2010 far exceeded the average for the last ten years (785 events). Overall losses amounted to approximately US$ 150bn, with the year's four major earthquakes (Haiti, Chile,

China and New Zealand) accounting for no less than one-third of this sum (Munich RE, 2010), as shown in the Figure 1.2.

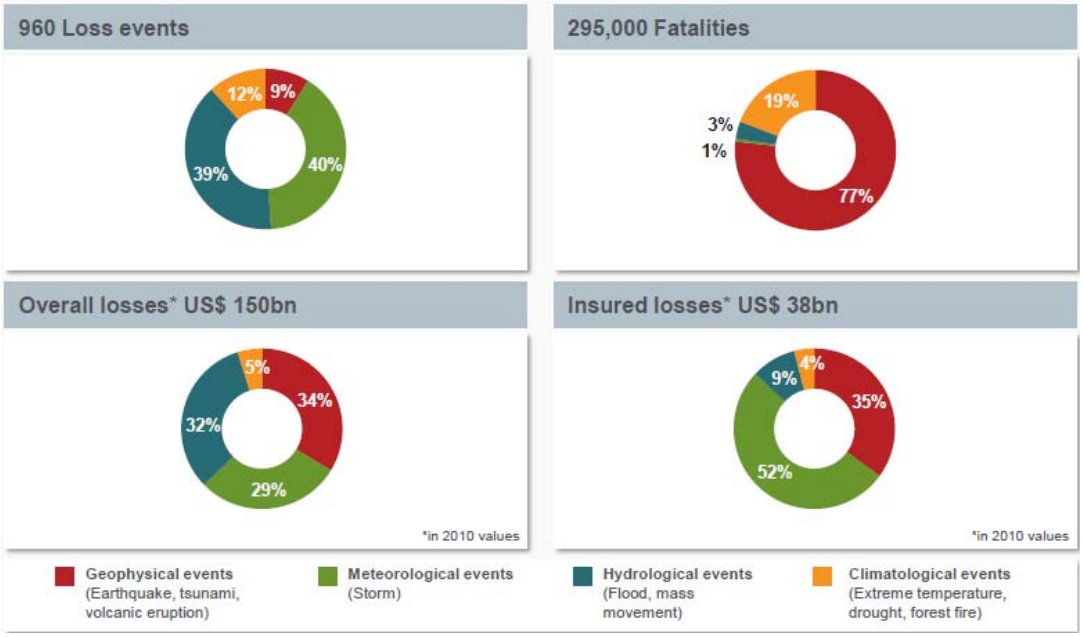

Figure 1.2 Natural Catastrophes worldwide 2010 – Percentage distribution (Munich RE, 2010)

Furthermore, as shown in the Figure 1.3, the trend is the same if it refers only to great or devastating natural disasters, defined as the events with losses exceeding US$ 650 m and/or more than 500 fatalities.

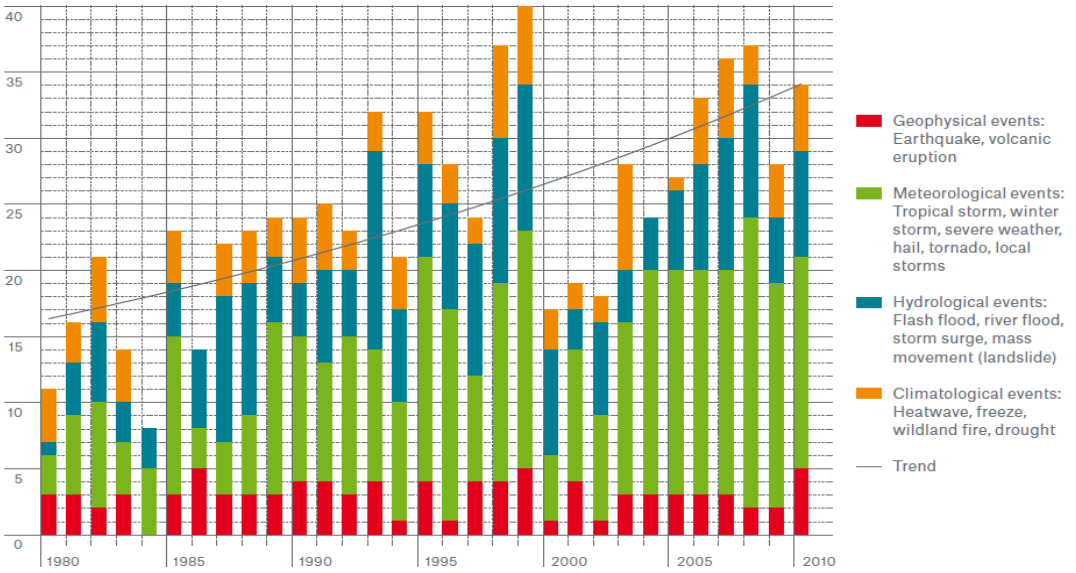

Figure 1.3 Number of great and devastating natural catastrophes 1980-2010 (Munich RE, 2010)

Figure 1.4 also shows a clear increasing tendency of related economic losses.

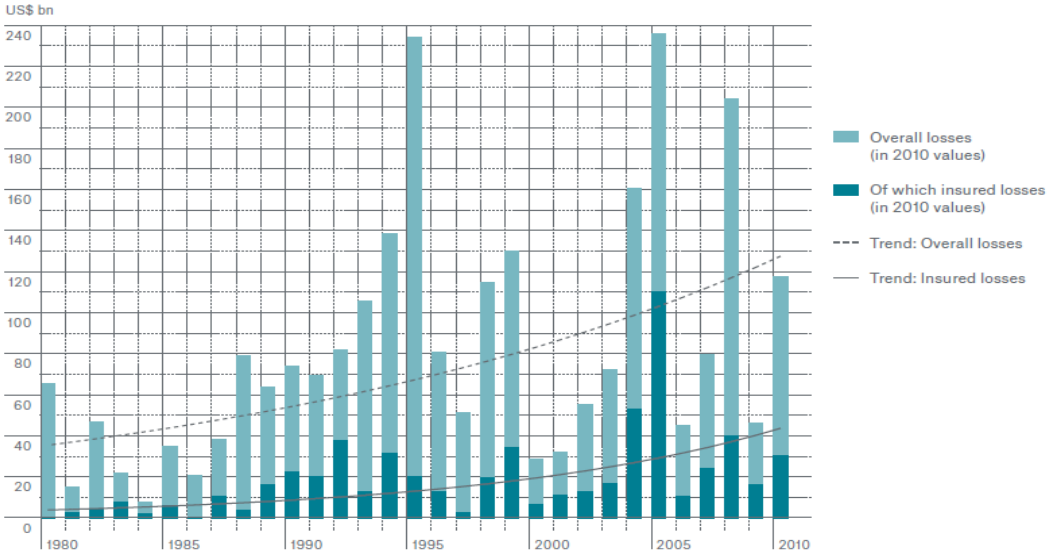

Figure 1.4 Overall losses and insured losses for great and devastating naturalcatastrophes 1980-2010 (Munich RE, 2010)

It is also said that about 80% of natural disaster economic losses in the world are caused by extreme wind and its relevant events, i.e. combined effects of wind and water. In the context of climate change, hydro-meteorological natural hazards continue to strike and are expected to increase in magnitude, complexity and frequency all over the world. However, the discussions of climate change and the effects of global warming on weather-related disasters should be made very carefully. Rapid urbanization in Asian countries, increasing population in urban areas, development of living regions to inappropriate areas vulnerable to wind and water hazards, and so on can also be reasons for the recent increasing tendency of wind-related disasters. Thus, even if the meteorological conditions were the same, if society was becoming more and more vulnerable to weather-related natural disasters, devastating disasters would increase (Tamura, et al., 2011).

1.1 Background concepts

Assessment and mitigation of the impact of catastrophic events in a given area require innovative approaches allowing a comparison of different risks and accounting for all the possible cascade events. The multi-risk approach is not an alternative to single risk analysis; in fact, the probabilistic single risk analysis is a necessary pre-requisite for a multi-risk analysis. The evaluation of risks related to different sources is generally done through independent analyses, adopting disparate procedures and time-space resolutions. In most of cases, only qualitative estimates of the risk level are available. Such a strategy of risks evaluation has some evident major drawbacks: 1) it is difficult, if not impossible, to compare risks of different origins; 2) the implicit assumption of independence of the risk sources leads to neglect possible interactions among threats and/or cascade effects. In practice, this means that a potential multi-risk index could be higher than the simple aggregation of single risk indexes calculated considering each source as independent from the others (Marzocchi, et al., 2009). A joint analysis and quantification of all the anthropogenic and natural risks which can affect a territory (multi-risk approach) is a basic factor for the development of a sustainable environment and land use planning as well as for a competent emergency management before and during catastrophic events (Durham, 2003).

However, the quantification of risks and thus the implementation in a multi-risk framework can be a very difficult issue. For environmental and natural issues, risk factors can be conveniently defined as a function of the probability that a certain event will occur and of the extent of the damage caused to man, environment and objects. In particular, the following expression is generally used to quantify risks due to natural events:

$$Risk = (hazard\ index) \times (vulnerability) \times (value\ at\ risk) \quad \textbf{(1.1)}$$

This definition indicates that the risk is related to a specific source (or hazard) as a function of the magnitude of the potential damage that may result from the considered hazard and from the probability that it will occur (also a function of the frequency and duration of the exposure, of the probability it will occur and of the possibility to avoid or limit the damage).

A mathematical form to shown the concept of the multi hazard assessment is represented by a matrix in which each row and column represent a hazard. It is very difficult to define correlation between different hazards and therefore to define non-diagonal terms different from zero. Nevertheless, for instance, it is clear that the devastating tropical cyclones are generally accompanied by high waves, storm surge, heavy rains, floods, landslides, lightning and so on.

Furthermore, with respect to wind risk, the constructions are becoming more and more vulnerable to wind action as their weight decreases (Augusti, et al., 2001) and many dramatic failures have happened during the last century. It's worth point out the collapse of the 3-km long railway bridge over the Tay in Scotland in 1879, the failure of ultra-light suspension bridge over the Tacoma Narrows due to non-expected and unpredicted wind effects, the collapse of four cooling towers in Ferrybridge in England in 1965 and also the collapses and the damages occurred to steel aircraft hangars belonging to Italian Air Force during the last ten years whose details are presented in the Chapter 5.

Less spectacular, but much more frequent, damages depend on the turbulent nature of the wind. Although the wind-induced stresses remain below the yielding and fatigue stress, the large amplitude oscillations may make the structure unable to function as planned or, even, unsafe.

1.2 Aim and organization of thesis

In the field of structural engineering, current design procedures use the envelope of individual hazard demands on a structure to ensure safety against multiple hazards. With regard to wind and seismic hazard, these actions can reasonably considered uncorrelated and, therefore, the design can be carried out separately; however, a difficulty in multi-hazard design for wind and earthquake is that the load and resistance factor method makes use of different design philosophies developed by different subdisciplines. Seismic design explicitly allows for inelastic behavior. In contrast, wind design assumes that the structures behaves in elastic range both for damage limit state (DLS) and ultimate limit state (ULS), although ULS typically refers to return periods shorter than those used for seismic design. In this context, a probabilistic multi-hazard approach can be employed to investigate the performance of a structure under critical events and to ensure its acceptable performance during its entire lifetime. Following the approach proposed by the Pacific Earthquake Engineering Research Center (PEER) for Performance-Based Earthquake Engineering, the purpose of the thesis is to define a reliable methodology for probabilistic estimation of the annual wind risk associated to the achievement of specific limit states. Such approach must be implemented in probabilistic terms due to the stochastic nature of both resistance and loading parameters. These uncertainties affect the wind field, the structural response and also the aerodynamic interaction between the environment and the structure. Therefore, a reliable evaluation of structural performances needs the statistical treatment of recorded data, that is the first step towards the investigation of the performance of wind-exposed structures, the characterization of the interaction by wind tunnel testing or computational fluid dynamics (CFD) techniques and also the knowledge of the structural behavior, i.e. the analysis of all possible failure mechanism induced by wind loads. Starting from this point, the main statistical

methods for treatment of extreme wind speeds are presented in the Chapter 2, including the methods for correction of non-standard conditions in terms of roughness and orography. The theoretical background is then applied by performing the statistical analyses of observed data collected starting from 1951 by the Air Force meteorological service. Some of the results are presented in the Chapter 3 whereas the detailed results in terms of fitted parameters, 50-year return period wind speeds, directional and seasonal coefficients estimated by different methods are presented in the Appendixes. The effect of the dowsampling is also investigated and the underestimation of 50-year return period wind speeds is quantified for all the stations available. A further step of the research activity has consisted in the characterization of the structural vulnerability. In fact, the Chapter 4 provides a brief review of properties of materials, structural details and structural types adopted in the past for steel hangars, that are considered as representative wind-exposed structures. These structural types are characterized by large spans and, in some cases, have borrowed design solutions from other industrial buildings. The attention is focused on historical evolution of structural types and adopted design standards; some failure cases which occurred during the last years due to extreme wind events are illustrated. Hence the main elements of vulnerability are discussed. Furthermore, the aerodynamic interaction is investigated; the role of the location and size of the openings is outlined and, in particular, the main theories about the propagation of the internal pressure due to a dominant opening are examined. In fact, due to their particular use, the steel aircraft hangars have a dominant opening that allows increased internal pressures to occur. By assembling of all the previously mentioned tools, a methodology for assessing wind risk is proposed aiming at the evaluation of the annual probability of achievement a fixed limit state due to wind actions. In a multihazard framework, the resulting value can be compared with the same probability referred to seismic actions obtained by

applying the IDA approach. Finally, in order to implement and explain the multihazard risk assessment, two case studies are presented and briefly discussed.

2 STATISTICAL MODELS FOR EXTREME WIND SPEEDS

The calculation of appropriate design wind speeds is a critical first step towards the calculation of design wind loads for structures. It is also usually one of the most uncertain part of the design process for wind loads and requires analysis of historical recorded wind speeds.

The statistical analysis of extreme winds has traditionally been performed considering values of annual maximum wind speed by the extreme value theory. The classical extreme value theory is based on three asymptotic extreme value distributions: Gumbel, Frechet and reversed Weibull distribution also known as Type I, Type II and Type III distribution, respectively. Nevertheless, the Type II distribution is very unlike to be appropriate for extreme wind speeds (Simiu, et al., 1978), both for mathematical and physical reasons. The Generalized Extreme Value (GEV) distribution combines them into a single mathematical form whose shape factor affects the distribution's tail and shows which extreme value distribution fits well the measured data.

However, since 2009, the current ISO-document 4354 "Wind action on structures" states that "*in the general case, yearly extremes do not form an appropriate basis for the extreme value analysis of wind speeds. This is especially true if the respective storm phenomenon tends to occur in families or cluster. … the ensemble therefore should consist of independent extremes above an appropriate threshold for each storm type*".

In fact, the major criticism of traditional extreme value theory is that it only considers a single maximum each epoch. An analysis of only yearly extremes may lead to a loss of important information if the second and third strongest storm in

one year is stronger than the yearly extreme of another year (Kasperski, 2011) showed that yearly extremes and yearly directional extremes can contain a lot of irrelevant data. Furthermore, yearly and yearly directional extremes can neglect relevant data, e.g. the second-, third to seventh-strongest storm during a season, and yearly directional extremes can contain dependent events, e.g. the second-, third- and fourth-strongest storm hour if these hours show a change of the wind direction relative to wind direction in the strongest hour of the storm.

To overcome these restrictions, the model parameters can be estimated to first n annual maxima (Lagomarsino , et al., 1992) or to monthly maxima (Simiu, et al., 1982) (Grigoriu, 1984) using a Type I distribution. These estimates are based on an empirical model which assumes that first n annual maxima and monthly maxima wind speeds are independent, stationary and Type I distributed. The assumption of independence seems to be satisfactory. In particular, Grigoriu (Grigoriu, 1984) showed that estimates of extreme wind speeds derived from monthly observations are superior to those based on yearly data for short wind records and provided the upper confidence limits for the development of probability-based specifications for wind design.

Furthermore, the ensemble of yearly extremes contains events that can hardly be described as ‘extreme storms’. The fact that this approach doesn’t consider other extreme events that may have occurred in each epoch suggests that alternative approaches based on shorter reference period than a year or on all maximum values can become the most chosen model to estimate the extreme values. In the first one, The second method, known as Peak-Over-Threshold (POT) approach, is based on the Generalized Pareto Distribution (GPD); it considers all values greater than a given value and is based on the fact that exceedances of a sufficiently high threshold are rare events and so the Poisson distribution can’t be applied. Nevertheless, the POT method can take into account more or less non-independent events, i.e. those associated to a specific storm.

With the aim at overcome this incongruence, Cook (Cook, 1982) proposed the Method of Independent Storms (MIS) that analyzes a time series of storm maxima modeled by the Gumbel distribution. The method was refined by Harris (Harris, 1999), and it is performed by obtaining a subset of independent maxima by identifying storms and then by fitting the storm maxima by the Gumbel distribution. Moreover, POT method's estimates exhibit significant dependence on threshold (An, et al., 2005); in particular, for low threshold, the estimates of the extreme wind speeds increase almost monotonically as the threshold increases. Furthermore a very high threshold increases the sampling uncertainty (variance) associated with a quantile estimate whereas, on the contrary, the lower the threshold the bigger the POT sample and, therefore, the quantile bias tends to increase (Pandey, 2002).

Another alternative approach to the prediction of extreme speeds, known as process analysis, is based on the knowledge of the Parent distribution (Gomes , et al., 1977). The main advantage of this method is that a comparatively short length of record is sufficient to estimate the parent distribution.

2.1 Parent distribution

The term "parent" is conventionally used to denote the original set of observations which, in the case of wind speed, is usually collected as an ordered time series. In the majority of synoptic wind climates the parent wind distribution, irrespective of wind direction, is reasonably well represented by a Weibull distribution whose probability density function is defined by the equation:

$$f(v) = \frac{k}{c}\left(\frac{v}{c}\right)^{k-1} exp\left[-\left(\frac{v}{c}\right)^{k}\right] \qquad (2.1)$$

Where k and c are the shape and the scale parameters of the distribution, respectively.

The cumulative distribution function assumes the form:

$$F(v) = 1 - exp\left[-\left(\frac{v}{c}\right)^{k}\right] \tag{2.2}$$

Maxima from a Weibull parent are in the domain of attraction of the Type I asymptote and, therefore, extreme wind speeds have been usually fitted to the Gumbel distribution (Galambos, 1978). The Weibull distribution coincides with the exponential distribution for k=1 and with the Rayleigh's distribution for k=2 and imposes conditions:

$$f(v) = F(v) = 0 \tag{2.3}$$

However, since much of the anemometric recordings include a lot of wind calms and very low wind speeds, the CDF and the PDF of the current values are usually described by the hybrid model (Takle, et al., 1978):

$$F(v) = C + (1 - C)\left\{1 - exp\left[-\left(\frac{v}{c}\right)^{k}\right]\right\} \tag{2.4}$$

In Eq. (4.4) C is the fraction of measurements corresponding to (either true or false) wind calms, and c and k are the distribution parameters regressed to the data without calms.

2.2 Extreme value theory

The extreme value theory was firstly applied to flood analysis and then to extreme wind speeds. As stated in the introduction, the classical extreme value theory is based on three asymptotic extreme value distributions (Gumbel, Frechet and Weibull distribution). The Generalized Extreme Value (GEV) distribution

(Jenkinson, 1955) combines them into a single mathematical form with the following expression:

$$F(v) = exp\left\{-\left[1 + k\left(\frac{v-u}{a}\right)^{-1/k}\right]\right\} \quad (2.5)$$

Where $F(v)$ is the cumulative probability distribution function of random variable v and the parameters a, u and k are the scale factor, the location factor and the shape factor, respectively. The shape parameter k governs the tail behavior of the distribution and, in particular, when k tends to 0 the equation above become the Type I extreme value distribution or so called Gumbel distribution, when k < 0 the GEV distribution is called the Type II (or Frechet) distribution whereas when k >0 the GEV distribution is called the Type III (or Weibull) distribution. The Type II is characterized by a long right tail instead of the Type III that has the shorter right tail. Therefore Type III distribution is appropriate for variables that are bounded on the high side whereas both Type I and Type II predict unlimited values and they are suitable distributions for variables that are unbounded. However, because of the atmosphere, wind speeds have an upper limit and the Type III distribution may also be appropriate for treatment of recorded data.

Although unrealistic because of the lack of an upper bound, the Type I is the most used for describing extreme winds, whose cumulative distribution function can be written in the following form:

$$F(v) = exp\left[-exp\left(-\frac{v-u}{a}\right)\right] \quad (2.6)$$

The associate probability density function is:

$$f(v) = \frac{1}{a} exp\left(-\frac{v-u}{a}\right) exp\left[-exp\left(-\frac{v-u}{a}\right)\right] \quad (2.7)$$

Where u and a are the mode and the scale factor of the distribution, respectively

With respect to the estimation of extreme wind speeds by the Type I distribution, two main methods are used; the first one is referred to Gumbel (Gumbel, 1958) and the second one to Gringorten (Gringorten , 1963).

The Gumbel's method provides the following procedure:

- The largest recorded wind speed in each calendar year is selected;
- The series is ranked in order of smallest to largest: 1, 2, …m, … to N;
- Each value is assigned a probability of non-exceedence, p, according to:

$$p \approx \frac{m}{N+1} \tag{2.8}$$

- A reduced variate, y, is formed from:

$$y = -\ln(-\ln p) \tag{2.9}$$

- The wind speed, v, is plotted against y, and a line of "best fit" is drawn, usually by means of linear regression.
- The distribution's parameters are estimated by the following expression:

$$a = \frac{1}{b} \tag{2.10}$$

$$u = -\frac{c}{b} \tag{2.11}$$

Where b and c are the slope and the intercept of the fitted line.

The Gumbel procedure, however, is biased and, in particular, it gives distorted values for probability of non-exceedence referred to high values of p (as defined in the Eq. (2.8)) near 1. A simple and good modification to the Gumbel procedure, which gives nearly unbiased estimates for the probability distribution, is due to Gringorten (Gringorten , 1963). In Gringorten's method, the Type I distribution is also assumed as the best fitting distribution but the Eq. (2.8) is replaced by the following formula:

$$p \approx \frac{m - 0.44}{N + 1 - 0.88} = \frac{m - 0.44}{N + 0.12} \tag{2.12}$$

Except for the estimation of each probability of non-exceedence, the produce is identical to Gumbel method and, therefore, it is easy to evaluate the distribution's parameters.

2.3 Peak over threshold approach

As stated in the introduction, the approach of consider a single maximum value of wind speed from each year of historical data obviously has limitations in that there may be many storms during any year and only one value from all these storm is being used. Furthermore, often the data are not enough to allow a good estimation of model's parameters. Therefore, with the aim of overcoming these difficulties the so called Peak-Over-Threshold (POT) approach has been proposed (Simiu, et al., 1996). The POT method considers, instead of just annual maxima, all wind speeds above a particular threshold wind speed. Given a threshold u, the distribution of excess values of x over u is defined by:

$$F_u(y) = Pr\{X - u \leq x | X > u\} = \frac{F(x) - F(u)}{1 - F(u)} \tag{2.13}$$

Which represents the probability that the value of x exceeds u by at most an amount y, where $y = x - u$. For a reasonable high threshold u, the distribution function of the excess $F_u(y)$ converges to the Generalized Pareto Distribution (GPD) which has a cdf characterized by the following expression:

$$G(x) = 1 - \left(1 + \frac{cx}{a}\right)^{-1/c} \qquad \text{for } c \neq 0 \tag{2.14}$$

$$G(x) = 1 - exp\left(-\frac{x}{a}\right) \qquad \text{for } c = 0 \tag{2.15}$$

where x are excesses, a is a scale parameter and c is a shape parameter.

The distribution is characterized by the fact that has unbounded upper tail if $c \geq 0$ and is bounded between 0 and a/c if $c < 0$.

The POT is a useful alternative to the popular Gumbel method in the field of extreme value estimation. However, the threshold sensitivity of quantile estimates is a very important topic. The experience suggests that a very high threshold resulting in a small POT sample would increase the sampling uncertainty associated with a quantile estimate. On the other hand, as threshold is lowered to include more data, quantile bias tends to increase. In this sense, it is expected that an optimal threshold might exist that would minimize both bias and variance.

2.4 Probability of exceedence and return period

For design purposes, estimates of wind speeds corresponding to various mean recurrence intervals are of interest. Typically the return period is defined as the reciprocal of the rate of occurrence; this does not imply that a generic intensity event will be exceeded exactly once every interval time equal to return period, but rather that the average time between exceedences is equal to return period. In hypothesis of homogeneous Poisson's distribution of events, the rate of occurrence is constant and it is quite easy to be estimated. The Poisson model assumes that occurrences of extreme wind speeds are independent in time and that the probability of more than one occurrence in a very short interval is negligible; in other words the probability of an extreme event in a window of time is related only to the size of window and it is independent of anything such as the time since the most recent occurrence (otherwise homogeneous Poisson is not suitable to predict extreme events). Under the assumption of Poisson occurrences, the probability of observing at least one event in a period of time t is equal to:

$$P(at\ least\ one\ event\ in\ time\ t) = 1 - e^{-\lambda t} \qquad (2.16)$$

Where λ is the rate of occurrence of events.

If λt is small (less than approximately 0.1), then the probability can also be approximately by:

$$P(at\ least\ one\ event\ in\ time\ t) = 1 - e^{-\lambda t} \cong \lambda t \tag{2.17}$$

Under these assumptions, the annual (t=1) rate of occurrence is equal to the probability of exceedence and the return period T_r can be calculated by the following expression:

$$T_r = \frac{1}{\lambda} = \frac{1}{P_{exc}(v)} = \frac{1}{1 - F(v)} \tag{2.18}$$

Where $P_{exc}(v)$ is the annual probability of exceedence and $F(v)$ is the cumulative distribution function of the data.

In the framework of POT method, the definition of crossing rate, λ*, as the expected number of peaks above threshold per year, is required in order to estimate wind speeds corresponding to various return periods. (Davison, et al., 1990) estimated a required quantile value as:

$$v(T_r) = G^{-1}\left(1 - \frac{1}{\lambda^* T_r}\right) + u \tag{2.19}$$

Where u is the threshold and $G^{-1}(\dots)$ is the Generalized Pareto inverse cdf.

2.5 Hypothesis test

In order to verify the goodness of fit of the distribution models to wind speed data, the hypothesis tests should be implemented. Kolmogorov-Smirnov test is an easy and effective tool to compare the distributions of the values; according to the test method, the following function shall be calculated:

$$Dn = max(|F(v) - E(v)|) \tag{2.20}$$

Where F(v) and E(v) represent the fitted and empirical cumulative distribution functions associated to the data. Therefore, the test returns a measure of "distance" between recorded and fitted distributions and, in particular, the result is 1 if the test rejects the hypothesis that the distributions are from the same continuous distribution at a specific significance level.

2.6 Correction for non-standard conditions

In Europe, typically, the fundamental value of the basic wind velocity is the characteristic 10 minutes mean wind velocity, irrespective of wind direction and time of year, at 10 m above ground level in open country terrain with low vegetation such as grass and isolated obstacles with separations of at least 20 obstacle heights (CEN, 2005). This terrain corresponds to terrain category II, as defined in the following table, where z_0 is the roughness length.

Table 2.1 Terrain categories and corresponding roughness lengths

	Terrain category	z_0 m
0	Sea or coastal area exposed to the open sea	0.003
I	Lakes or flat and horizontal area with negligible vegetation and without obstacles	0.01
II	Area with low vegetation such as grass and isolated obstacles (trees, buildings) with separations of at least 20 obstacle heights	0.05
III	Area with regular cover of vegetation or buildings or with isolated obstacles with separations of maximum 20 obstacle heights (such as villages, suburban terrain, permanent forest)	0.3
IV	Area in which at least 15 % of the surface is covered with buildings and their average height exceeds 15 m	1.0

The basic values are characteristic values having annual probabilities of exceedence of 0.02, which is equivalent to a mean return period of 50 years.

Differently, in some Building Codes the basic wind speed is defined as the 3-second gust speed, at 10 meters above ground in an open situation, estimated to be exceeded on the average once in 50 years.

Therefore, the basic wind velocity depends on the height above the terrain, the terrain roughness and orography. Many meteorological stations are located such that recorded wind speeds need corrections for non-standard conditions in terms of exposure, anemometer heights and topographic effects. The methods in ESDU 91043 (ESDU, 1991)allow to convert the mean wind speeds over hills and other topography whereas those in ESDU 84011 (ESDU, 1984) allow to convert wind speed profiles over terrain with roughness changes. Other instructions were provided by Miller et al. (Miller, et al., 1998) for calibration of the exposure of UK anemographs. In fact, the design wind speeds have to be calculated using a base wind speed which is then multiplied by a series of factor, which together define the exposure of the site in terms of the effects of the surrounding topography, the ground roughness and the height above sea level. The heterogeneous nature of actual terrain involves that the exposure of any site is likely to vary significantly with the wind direction and, therefore, different directional factors have to be defined to convert recorded wind speeds. The correction can be done following this procedure:

- calculation of the friction (or shear) velocity, u_*, by means of the logarithmic wind speed profile:

$$u(z) = \frac{1}{k} u_* \ln\left(\frac{z}{z_0}\right) \tag{2.21}$$

Where $u(z)$ is the wind speed at height z above the ground, k (~0.41) is the von Karman's constant, z_0 is the roughness length;

- calculation of the geostrophic wind speed, V_g, by the geostrophic drag law:

$$V_g = \frac{u_*}{k}\left[\ln\left(\frac{u_*}{f z_0}\right) + 1\right] \tag{2.22}$$

Where f is the Coriolis parameter;

- conversion of the geostrophic wind speed to the friction velocity associated to different roughness length by the Eq. (2.22).
- calculation of the surface wind speed at a height of 10 m by the Eq. (2.21).

For directional assessment of wind speeds it is worth pointing out that the terrain roughness to be used for a given wind direction depends on the ground roughness and the distance with uniform terrain roughness in an angular sector around the wind direction. Small areas (less than 10% of the area under consideration) with deviating roughness may be ignored, as shown in the Figure 2.1.

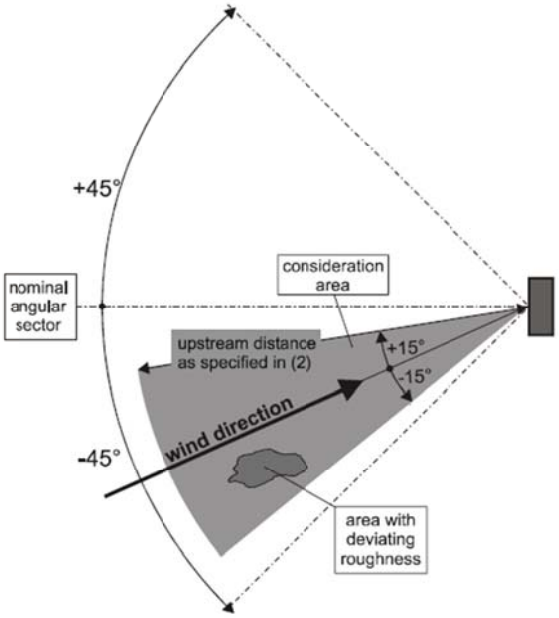

Figure 2.1 Assessment of terrain roughness (captured from Eurocode 1-4 (CEN, 2005))

2.7 Directional and seasonal assessment

The analysis of extreme winds can exhibit a strong directionality or seasonality and, therefore, a refined analysis of these characteristic can involve estimates of extreme wind speeds associated to the same return period very different sector by sector or season by season. The seasonal factor is of use in the design of temporary structures and the optimization of phased construction. Furthermore, many structures behaves differently to winds from different directions, therefore, the treatment of recorded data with respect to direction allows to obtain more reliable values of design wind speeds and, of course, to optimize the orientation of the structure. However, extreme wind speeds occurring in different sectors of wind directions are not physically independent phenomena and, therefore, the probability of having at a specific site a strong storm hour within a certain sector of wind directions has to be given with the conditional probability. The extreme value

analysis of the strong wind climate has to be based on independent and mutually excluding storm phenomena (Gomes , et al., 1977). An arbitrary sorting of observed extreme wind speeds for different sectors into separate ensembles violates this demand. There is no theory that allows recombining the results of such statistics. Nevertheless, Cook (Cook, 1983) showed that the characteristic product of the Type I distribution, that is the ratio between the mode and the dispersion of fitted distribution, does not vary significantly with direction allowing to consider sets of data not correlated each other.

However, when a separate analysis of extreme wind speeds by direction sector has been carried out, the directional coefficient can be defined as the ratio between the wind speed with a certain annual probability of exceedence at a specific sector and the overall wind speed with the same probability of exceedence:

$$c_{dir} = \frac{v(Tr50, \theta)}{v(Tr50)} \tag{2.23}$$

Where $v(Tr50, \theta)$ is the 50-year return period wind speed for a given direction θ and $v(Tr50)$ is the 50-year return period wind speed irrespective of direction.

On the contrary, extremes from different periods of time are independent and exclusive and the classical models for prediction of extreme events can be applied without any further considerations. The seasonal coefficient can be defined as:

$$c_{sea} = \frac{v(Tr50, t)}{v(Tr50)} \tag{2.24}$$

Where $v(Tr50, t)$ is the 50-year return period wind speed for a given period of time t and $v(Tr50)$ is the 50-year return period wind speed obtained from all data.

2.7.1 Handling statistical combination of directional wind speeds

When a separate analysis of extreme wind speeds by direction sector has been carried out, the relationship between the probability of exceedence of a specified

wind speed from all direction sectors and that from direction sector θ_i has to be defined.

Under the assumption that the i direction sectors are mutually exclusive, the probability of non-exceeding a specific wind speed can be obtained by the following expression, known as Bayes' rule:

$$P(v \leq v^*) = \sum_{i=1}^{n} P(v \leq v^* | \theta_i) \cdot P(\theta_i) \tag{2.25}$$

Where the symbol θ_i is the i-th direction sector in which the data have been disaggregated, $P(v \leq v^*)$ is the probability that a wind speed v is not exceeded for all wind direction, $P(v \leq v^* | \theta_i)$ is the probability that a wind speed v is not exceeded for i-th direction sector and $P(\theta_i)$ is the probability that the wind blows from i-th direction sector. The assumption that the i direction sectors are mutually exclusive is quite strong and, typically, is not verified; in fact when, for a specific year, the annual maximum is referred to more than one direction the value is referred to events that are not mutually exclusive.

Supposing that events are statistically independent of each other, an alternative approach allows to obtain the exceedence probability of a specific wind speed level considering i directional events by the following equation:

$$P(v \leq v^*) = \prod_{i=1}^{n} P(v \leq v^* | \theta_i) \tag{2.26}$$

In the Figure 2.2 a comparison between the directional (gray lines) and omnidirectional (blue thick line) cdfs is shown; in the same figure, the cdf obtained by means of Eq. (2.26) is shown, validating the consistency of the presented approach for evaluating aggregated probability of non-excedeence, once the directional one are known. The Figure 2.2 is referred to LIRP station; in the

appendix 2 the same comparison is presented for all the station analyzed in the present work.

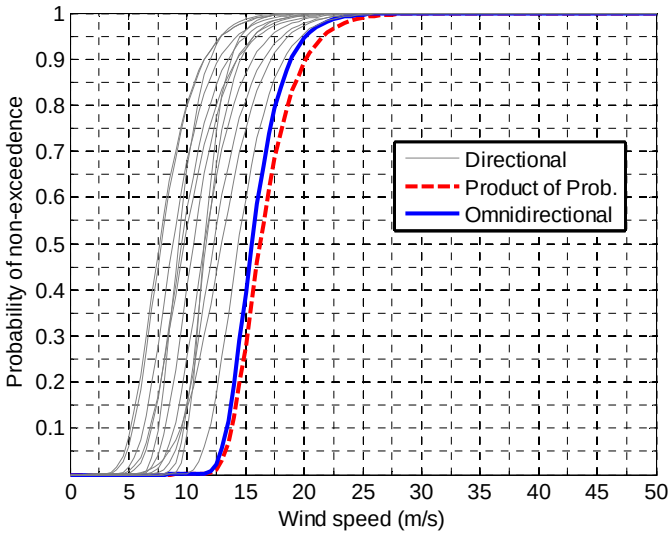

Figure 2.2 Comparison between directional, omnidirectional and calculated cdfs

When the hypothesis of statistically independence is not demonstrated, the correlation has be taken into account applying the rules of probability. In this case, the product of cdfs isn't appropriate and it is necessary to consider the pdfs and their terms of correlation.

2.7.2 Handling statistical dependence of seasonal wind speeds

When a separate analysis of extreme wind speeds by season has been carried out, the relationship between the probability of exceedence of a specified wind speed from all seasons and that from season t has to be defined. Following the approach presented in the previous section and supposing that events are statistically independent of each other, the probability of non-exceedence a specific wind speed level considering t seasonal events is obtained by the following equation:

$$P(v \leq v^*) = \prod_{t=1}^{n} P(v \leq v^*|t) \tag{2.27}$$

For the LIRP station, a comparison between the seasonal (gray lines) and omnidirectional (blue thick line) cdfs is shown in the Figure 2.3; the function obtained by applying the Eq. (2.27) is depicted by a red dashed line.

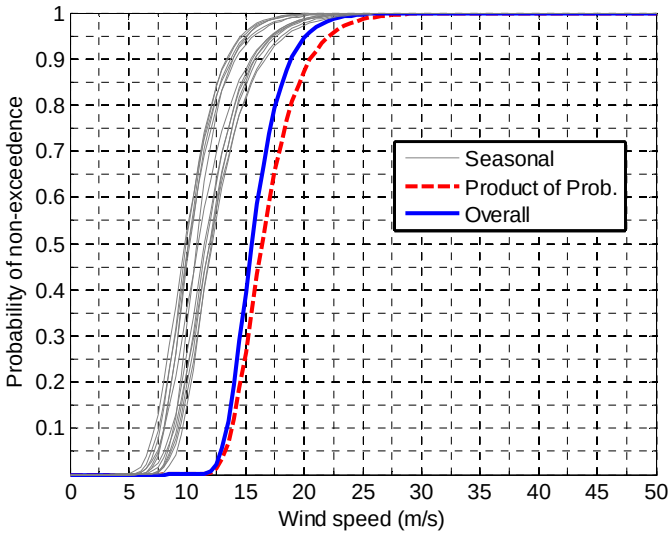

Figure 2.3 Comparison between seasonal, overall and calculated cdfs

It's worth pointing out that a good estimation by applying the Eq. (2.27) is found. In the appendix 2 the same comparison is presented for all the station analyzed in the present work.

2.8 Effect of the daily number of measurements on the statistics of extreme wind speeds

Typically, the data recorded over a large number of years are characterized by different sampling periods. Although the wind speed associated to a specific return period is conventionally calculated on basis of the annual maxima of consecutive 10-minute averages, very often the averages are saved with a temporal spacing of

several hours. Indeed, sometimes they are available only at three-hour interval (that are eight daily measurements of the ten-minute averaged wind speeds) and very seldom they are available at one-hour sampling period or less during all time interval. Therefore, the statistical treatment of data can be based on heterogeneous recorded data, i.e. the present extreme wind map of Italy was built based on both hourly recorded data and three-hour interval recoded data. In (Chiodi, et al., 2011), this effect is called "downsampling" whereas Larsen et al. (Larsen, et al., 2006) called it disjunct sampling.

It is obviously that for the Extreme Value analysis to be accurate, the ten-minute averaged wind speed would need to be measured with a sampling period of 10 minutes, that is 144 times a day. As said, such data is very seldom available but a rather lower number of measurements per day are usually taken. It seems reasonably to understand and quantify the effect of this downsampling of the data; as shown in the following, this downsampling has the effect of reducing the maxima, therefore giving a non-conservative estimate of the design wind speed. The peak wind speeds, which would be captured by contiguous record, may fall in the gaps between consecutive samples and therefore be missed (Figure 2.4).

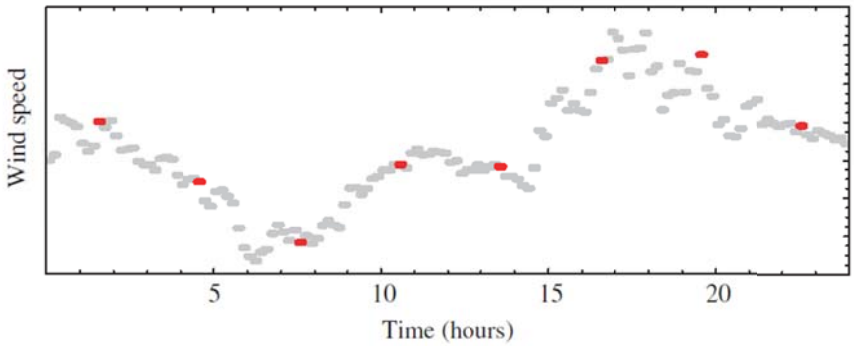

Figure 2.4 Illustration of concept of downsampling referred to 3-hour sampling period of 10-minute averaged wind speeds, depicted with dark short lines (Larsén and Mann, 2006)

(Larsen, et al., 2006) investigated the effects of the downsampling (or disjunct sampling, as they called it) on the attenuation of the extreme wind estimation by means of a simple theoretical approach as well as measurements. The proposed methodology assumed that the time series is a Gaussian Markov chain and the average annual wind maxima at different sampling intervals were calculated. In the present work, the issue was investigated empirically with the following procedure. The hourly measurements of the ten-minute averaged wind speed were used to evaluate the 50-year return periods wind speeds v50 with different methods. The original data were then artificially downsampled to two hours; two records were obtained, which were used to evaluate the models' parameters and the 50-year return period wind speeds. The original data were then downsampled to three hours; three records were obtained, which were used to evaluate the models' parameters and the 50-year return period wind speeds. The procedure was repeated to four, six, eight, twelve and twenty-four hours downsampling. The resulting 50-year return period wind speeds were plotted against the sampling period ΔT. An example of the results obtained for the LIBA meteorological station is shown in the Figure 2.5.

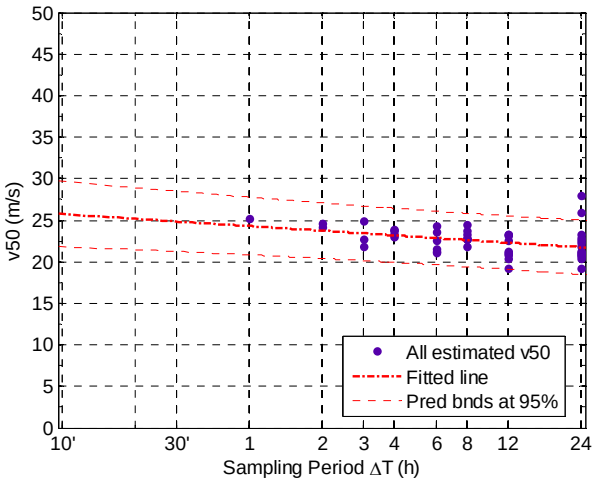

Figure 2.5 Artificial downsampling of recorded data for LIBA meteorological station

The dash-dot line denotes the best fitted line whereas the dashed red lines represent the upper and lower 95% prediction bounds.

For each sampling period ΔT, the median values of estimated 50-year return period wind speeds were calculated and plotted against the sampling period ΔT, as shown in the Figure 2.6.

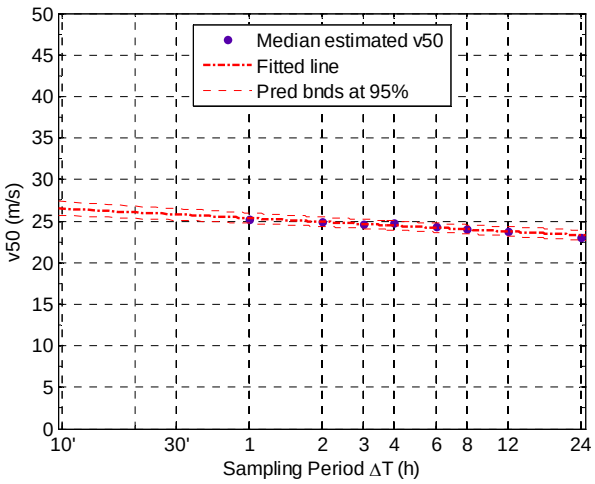

Figure 2.6 Artificial downsampling of recorded data for LIBA meteorological station (estimated median v50)

The dash-dot line denotes the best fitted line whereas the dashed red lines represent the upper and lower 95% prediction bounds. In particular, the interpolation of the points obtained with the procedure above would allow an empirical correction of data with sampling periods greater than ten minutes. In particular, a natural logarithm law represents the best fit of data:

$$v_{50}(\Delta T) = a \cdot \ln(\Delta T) + b \qquad (2.28)$$

Where $v_{50}(\Delta T)$ is the 50-year return period wind speed function of sampling period ΔT anda and b represent model unknown parameters.

For ΔT=1 hour, $\ln(\Delta T) = 0$ and $v_{50}(\Delta T = 1\ hour) = b$; in other words, the parameter b represents the 50-year return period wind speed associated to a hourly

sampling period and it's almost the same of that estimated with statistical treatment of recorded data. Therefore, the Eq. (2.27) can be rewritten as:

$$v_{50}(\Delta T) = a \cdot \ln(\Delta T) + v_{50}(\Delta T = 1) \tag{2.29}$$

As shown in the Figure 2.6, the Eq. (2.28) looks as a straight line with a negative slope in a logarithmic chart, revealing that the downsampling has the effect of reducing the estimated wind speeds for design purposes.

The Eq. (2.27) can also be normalized with respect to the averaging time T of 10 minutes, obtaining the following expressions:

$$v_{50}(\tau) = a' \cdot \ln(\tau) + b' \tag{2.30}$$

$$\tau = \frac{\Delta T}{T = 10'} \tag{2.31}$$

In such way the constants a and b have the dimensions of a velocity and, in particular, when τ=1 and, hence, ΔT=10', $\ln(\tau) = 0$ and $v_{50}(\Delta T = 10') = b'$. Therefore, the parameter b' represents the 50-year return period wind speed associated to a theoretically sampling period of 10 minutes.

The results obtained for the LIBA station are presented in the Table 2.2 Part of the results of downsampling of data referred to the LIBA station.

Table 2.2 Part of the results of downsampling of data referred to the LIBA station

Station	Interval		$v_{50}(\Delta T=1)$ (m/s)	a (m/s/h)	$v_{50}(\Delta T=10')$ (m/s)	ρ_1	ρ_2	ρ_3	ρ_4
LIBA	1959	2010	25,37	-0,72	26,67	1,03	1,05	1,09	1,16

Column 7, 8, 9 and 10 of the Table 2.2 Part of the results of downsampling of data referred to the LIBA station contain the ratios between 50-year return period wind speeds obtained at 10-minute sampling period and those obtained at 30-minute, 1-hour, 3-hour and 24-hour sampling period, respectively. In fact, the ratios are defined as follows:

$$\rho_1 = \frac{v_{50}(\Delta T = 10')}{v_{50}(\Delta T = 30')} \tag{2.31}$$

$$\rho_2 = \frac{v_{50}(\Delta T = 10')}{v_{50}(\Delta T = 1hr)} \tag{2.32}$$

$$\rho_3 = \frac{v_{50}(\Delta T = 10')}{v_{50}(\Delta T = 3hr)} \tag{2.33}$$

$$\rho_4 = \frac{v_{50}(\Delta T = 10')}{v_{50}(\Delta T = 24hr)} \tag{2.34}$$

These coefficients can be used to manually correct the maxima used to predicting wind speed-return period laws; furthermore, they can also be used to standardize data sets sampled at different sampling periods. For instance, as illustrated in the section 3.4.1, most of the recorded data are available at three-hour intervals from 1951 to 1972 and at one-hour intervals from 1973 to 2010. Once the wind speeds are standardized in terms of sampling period, a more accurate statistical analysis can be performed.

3 WIND HAZARD

The characterization of extreme wind speeds is the basic step towards the investigation of the performance of wind-exposed structures in the framework of multihazard assessment. In the chapter, an historical evolution of Italian regulations on wind action on structures is presented; in fact, the knowledge of the hypotheses about wind actions at the design epoch can provide interesting information for assessment of existing structures. Furthermore, the statistical methods presented in the previous chapter are applied to the recorded data at the stations belonging to the Italian Air Force meteorological network. The results of the analyses allow to estimate the annual frequency of exceeding a specific maximum velocity level; the maximum wind speed can be adopted as the measure that reflects the wind intensity.

3.1 Historical evolution of Italian regulations on wind actions on structures

In the last hundred years, a lot of guidelines and codes have been published in Italy (Bartoli, et al., 2011) (Chiodi, et al., 2011). The first ones didn't deal with wind actions that are firstly discussed from forties in the documents published by the National Research Council of Italy and Associazione Costruttori Acciaio Italiani (CNR-ACAI, 1946). Later, the Italian regulations on the wind loading on structures have had a rather complex evolution with a parallel diffusion of mandatory and recommended standards; the guidelines published by the National Research Council of Italy (CNR, 1964) (CNR, 1967) (CNR, 1981) (CNR, 1985) (CNR, 2008) have been only recommended specifications whereas the Codes issued by the Ministry of Infrastructures (M.LL.PP., 1978) (M.LL.PP., 1982) (M.LL.PP., 1996) (NTC, 2008) have been adopted as mandatory regulations for

design purposes. At present, when designing wind exposed structures, Italian Designers can chose between three different options, i.e. complying with the Code issued by the Ministry of Infrastructures and Transports (NTC, 2008), with Eurocode 1 (CEN, 2005) or with the CNR Guidelines (CNR, 2008). A brief review of the main Italian regulations about wind loading on structures can be an useful tool to understand the design assumptions and actions adopted at the epoch of construction, and to predict the possible structural vulnerabilities due to obsolete design approaches and/or codes' specifications.

3.1.1 CNR-ACAI 1946 Recommendations

CNR-ACAI 1946 Recommendations were written as rules for steel constructions but the load on structures represented an important part of them. Regarding wind actions, the following values of reference velocity pressure referred to a flat and open country terrain are adopted:

- $80\ \mathrm{kg/m^2}$ ($\cong 800\ MPa$) for h ≤ 20 m above ground level;
- $110\ \mathrm{kg/m^2}$ ($\cong 1000\ MPa$) for 20 < h ≤ 80 m above ground level;
- $130\ \mathrm{kg/m^2}$ ($\cong 1300\ MPa$) for h > 80 m from above ground level.

The wind pressure was assumed to be the peak velocity pressure in the sense of present Codes; in fact no design specifications were provided for the exposure factors and the terrain roughness that were implicitly considered into the definition of the velocity pressure profile.

3.1.2 CNR 1964 and CNR 1967 Recommendations

CNR 1964 and CNR 1967 Recommendations introduced, for the first time, a wind map of Italy (Figure 3.1) that divided it into five zones, named from A to E.

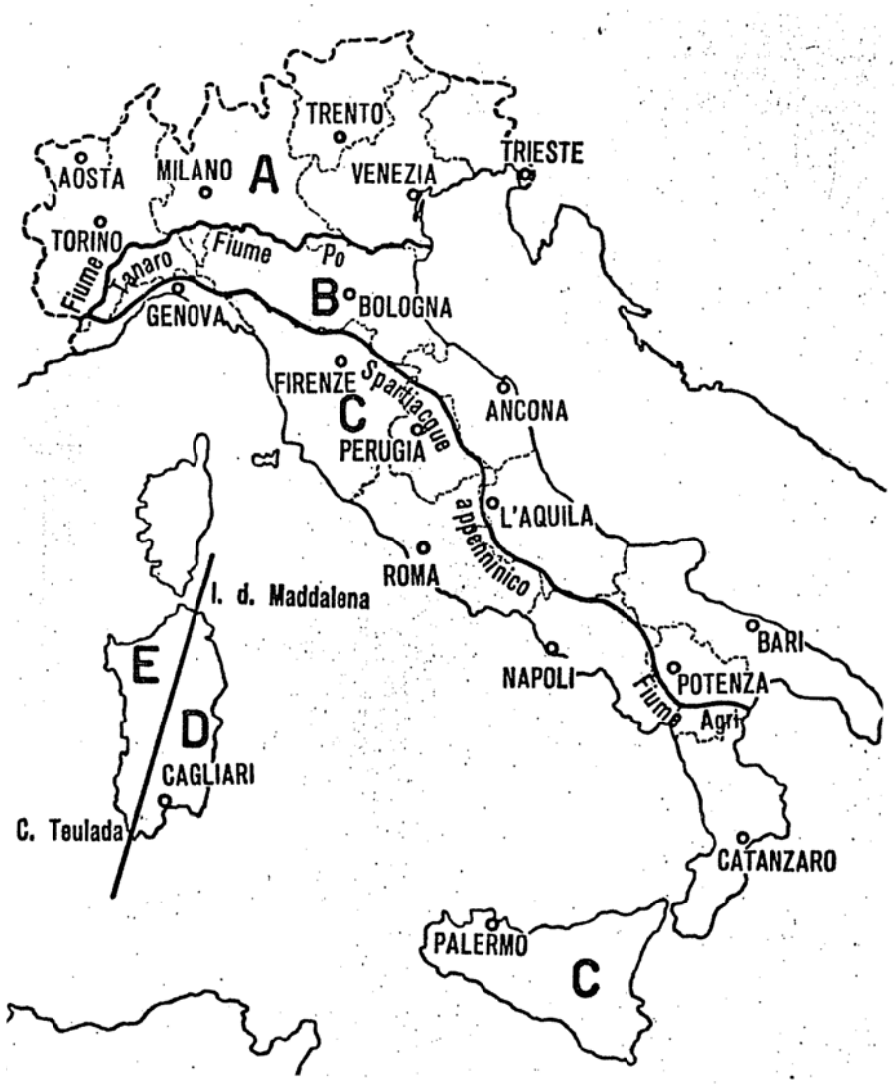

Figure 3.1 Wind map of Italy provided by (CNR, 1964) (CNR, 1967)

Combining this wind map with the altitude and the distance from the sea (Figure 3.2), four other zones were defined whose provided values of reference velocity pressure referred to a flat and open country terrain at 20 m above ground level were:

- 60 kg/m^2 ($\cong 600\ MPa$) for zone 1;
- 80 kg/m^2 ($\cong 800\ MPa$) for zone 2;

- $100\ \mathrm{kg/m^2}$ ($\cong 1000\ MPa$) for zone 3;
- $120\ \mathrm{kg/m^2}$ ($\cong 1200\ MPa$) for zone 4.

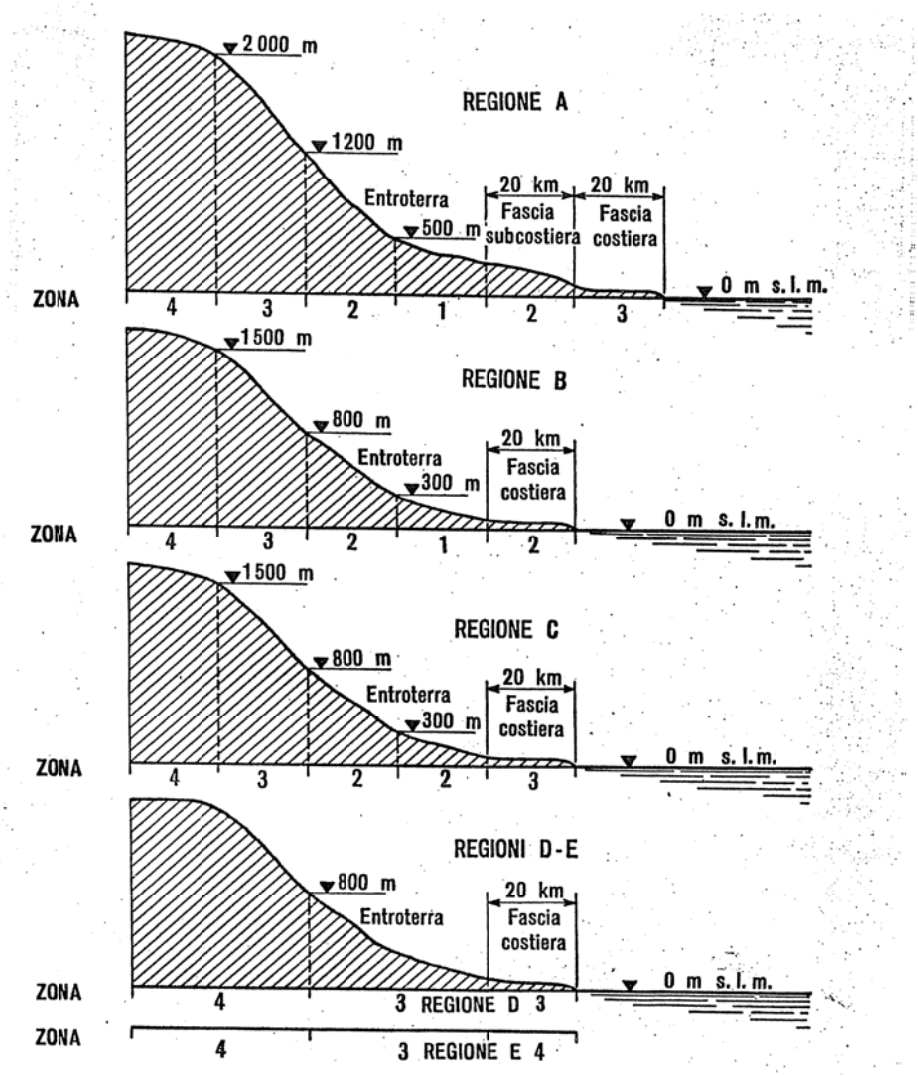

Figure 3.2 Subclassification based on the altitude and the distance from the sea (CNR 1964-1967)

CNR 1964 and CNR 1967 Recommendations also provided four wind profile laws, shown in the Figure 3.3.

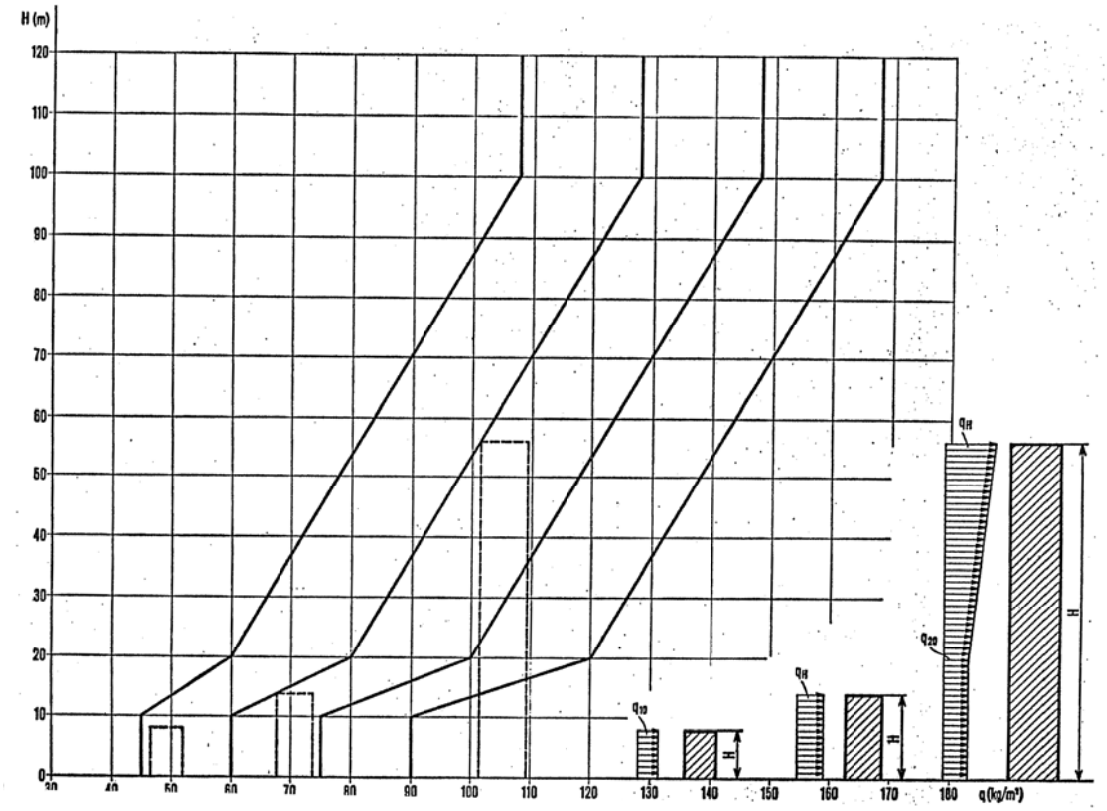

Figure 3.3 Wind pressure profiles (CNR 1964-1967)

Although more detailed and refined with respect to the CNR-ACAI Recommendations, the CNR 1964 and CNR 1967 Guidelines didn't consider either the terrain orography nor the terrain roughness and, therefore, the effects of the wind turbulence. In this framework, the wind pressure was assumed to be the peak velocity pressure in the sense of present Codes and it was (wrongly) assumed to be very different from the actual physical behavior, i.e. for the assumption that it is constant between the ground level and the height of 10 m above it. It is worth pointing out that the peak velocity pressures provided by Recommendations correspond to wind velocities at 10 m above ground of terrain category II (as defined by the present Codes) of about 18, 21, 24 and 26 m/s (Bartoli, et al., 2011).

3.1.3 Building Code 1978 and 1982

Although the CNR Recommendations had been an important tool for purpose design for many years, they hadn't ever been mandatory rules. The first mandatory Italian regulation on the the wind loading of structures was the Building Code of 1978 (M.LL.PP., 1978), that included all updated criteria provided by CNR 1964 and 1967 Recommendations. The Building Code of 1982 (M.LL.PP., 1982) represented the updated version of the Building Code 1978 but no further specifications about wind actions on structures were provided, despite the improvements introduced by the CNR 1981 Recommendations, which will be discussed in the next paragraph.

3.1.4 CNR 1981 Recommendations

CNR 1981 Recommendations (CNR, 1981) introduced a lot of updated criteria concerning, for instance, the basic wind velocity, the terrain roughness and orography and the return period coefficient. Hence, for the first time, the wind actions on the structures were calculated based on the basic wind velocity, defined as the 10-minute averaged wind velocity with an annual risk of being exceeded of 0.02 (that means a 50-year return period), irrespective of wind direction, at a height of 10 m above flat open country terrain. The basic wind velocity was set equal to 32 m/s everywhere, a very high value if compared with the previous values established by the CNR 1964 and 1967 Recommendations and also the present values; the logarithm wind profile was adopted and the Type I extreme value distribution was considered in order to estimate the wind velocities associated to return periods different from the standard value of 50 years.

3.1.5 CNR Recommendations 1985

CNR Recommendations 1985 (CNR, 1985) were characterized by some important improvements about the gust factors, the exposure factors and the basic

wind velocity which was set equal to 30 m/s everywhere. This choice was too much conservative for low wind-exposed zones of Italy and, mainly, the lack of a wind map of Italy didn't allow a consistent and refined definition of realistic wind actions on structures. This last issue had been investigated for many years in the late eighties and in the early nineties and a wind map of Italy was then proposed (Ballio, et al., 1991a) (Ballio, et al., 1991b) (Ballio, et al., 1999).

3.1.6 Building Code 1996

The Building Code 1996 (M.LL.PP., 1996) replaced the Building Code 1982 and introduced the wind map of Italy shown in the Figure 3.4. As stated in the previous chapter, the map divides Italy into nine zones, to which different values of the reference wind velocity is associated, in the range of 25 to 31 m/s. This is defined as the ten-minute averaged omnidirectional wind velocity at 10 m of height in flat open country (corresponding to a roughness length z_o=0.05m), associated with a return period of 50 years. Furthermore, with respect to the CNR Recommendations published in the eighties, an alternative characterization of the exposure factors and the topography factors was provided.

3.1.7 Eurocode 1, Building Code 2008 and CNR Guidelines 207-2008

At present, when designing wind exposed structures, Italian Engineers can chose between three different options, i.e. complying with the Building Code 2008 (NTC, 2008), with Eurocode 1 (CEN, 1994) (CEN, 2005), or with the CNR Guidelines 207-2008 (CNR, 2008). The CNR Guidelines 207 seems to be the most updated and detailed specifications whereas the Building Code 2008 doesn't include a lot of improvements in the field of Wind Engineering. In particular, the Building Code 2008 refers to the pressure coefficients provided by the CNR 1964 Recommendations, which are clearly obsolete and, in many cases, unconservative. Additionally, no mention is given for directional and seasonal factors which are

instead introduced by the Eurocode 1, although in the national Annex they are set equal to 1.

3.2 Present Italian extreme wind map

An extreme wind map of Italy was derived in the nineties, which has then been used by Italian Building Codes (M.LL.PP., 1996) (NTC, 2008), by Eurocode 1 (CEN, 1994) (CEN, 2005) and by the National Research Council Guidelines (CNR, 2008). The map was built based on eight daily measurements of the ten-minute averaged wind speeds recorded by 42 meteorological stations of the Italian Air Force over a large number of years, and of the continuous measurement of the ten-minute averaged wind speeds at 27 meteorological stations belonging to the Italian Electrical Company (ENEL) over a limited number of years. The former where used for extreme value analysis; the latter for process analysis (Ballio, et al., 1991a) (Ballio, et al., 1991b) (Ballio, et al., 1999).The map divides Italy into nine zones, to which different values of the reference wind velocity is associated, in the range of 25 to 31 m/s. This is defined as the ten-minute averaged omnidirectional wind velocity at 10 m of height in flat open country (corresponding to a roughness length z_o=0.05m), associated with a return period of 50 years.

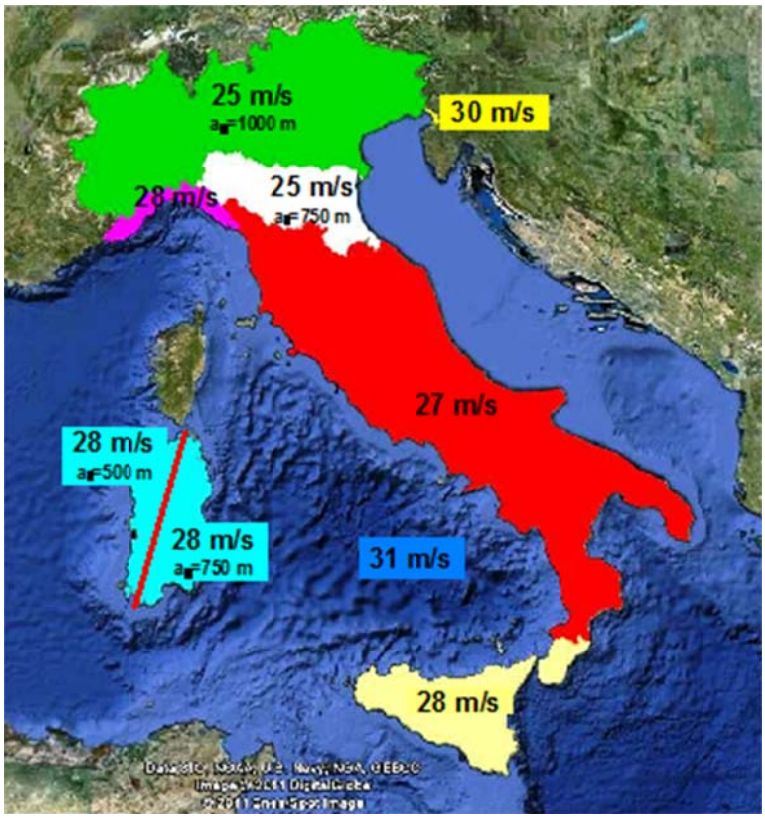

Figure 3.4 Present extreme wind map of Italy (©Google)

In addition, for each zone the variation law of the reference wind velocity with altitude is given. Furthermore, the parameters of the logarithmic mean wind profile are given, as a function of the zone, of the distance from the sea and of the terrain roughness. For design return periods other than 50 years, return coefficients are given based on a Type I Extreme Value (Gumbel) distribution.

More recently, updated criteria for the definition of the return law were presented (Pagnini , et al., 2009), a modified version of which has also been incorporated in the National Research Council Guidelines (CNR, 2008). The analyses are based on eight daily measurements of the ten-minute averaged wind speeds recorded by 39 meteorological stations of the Italian Air Force over about 50 years. It is postulated that process analysis is more reliable that extreme value

analysis and it is therefore applied to the data. There results that the return coefficient is only function of the shape parameter of the Weibull distribution of the mean wind speed.

Notwithstanding the reliability of the existing approaches, which indeed allow a consistent implementation in the design procedures, it is clear that there are several issues needing deeper investigation. First of all, larger the database of wind velocities available, the better the possibilities of obtaining reliable estimates of the design wind velocities. However, the larger the database in terms of measurement stations and number of years of acquisition, the greater the inconsistencies it reveals. This issue, also pointed out by Pagnini and Solari (Pagnini , et al., 2009), is related to the improvement of measurement techniques and data storage, to the use of data deriving from inhomogeneous instrumentations and setups and affected by possible long term climate changes (data drift). Second, Italy is a 1200 Km long country, spanning more than 10º of latitude, with 7500 km of coastline and featuring nearly 5000 m high mountains. This causes a very inhomogeneous and often mixed wind climate, in many cases dominated by local effects and with many cases of microclimates. Variability of the extreme values of the wind velocity form one site to another can be very large, also for sites not too far apart. A zoning of the design wind velocity to a scale smaller than the one available would be desirable, but clearly very difficult to obtain. Finally, though considered by Eurocode 1 no provision is given for directional and season factors. The former, in particular, may play a quite strong role in the evaluation of the reliability of a structure, or in its optimisation.

Furthermore, it is reasonable to expect that the national design wind speed maps for Europe should match along borders and that the relative magnitude between neighboring countries' design wind speeds is low. However, the current design wind speed maps for Europe don't match at borders, resulting in a variation of up

to 100 % in the design wind load within relatively short distances (Gatey, et al., 2007).

With the aim of trying to fill some of the existing gaps, the analysis of the huge database containing the measurements taken over a period of about 60 years at the meteorological stations of the Italian Air Force has been undertaken, and is currently being carried out. In the following, the information on the criteria and on the procedures used and preliminary results of the analyses are presented.

3.3 Towards an update extreme wind map of Italy

3.3.1 The database

The database considered in the present study consists of 119 stations for ground level measurements, located as shown in Figure 3.5. Most of them belongs to the Italian Air Force meteorological network. About 55 stations are located at an altitude of more than 500 m above sea level and 25 of them at an altitude of more than 1000 m, allowing some (but not complete) analysis of the variation of the extreme wind velocities with altitude.

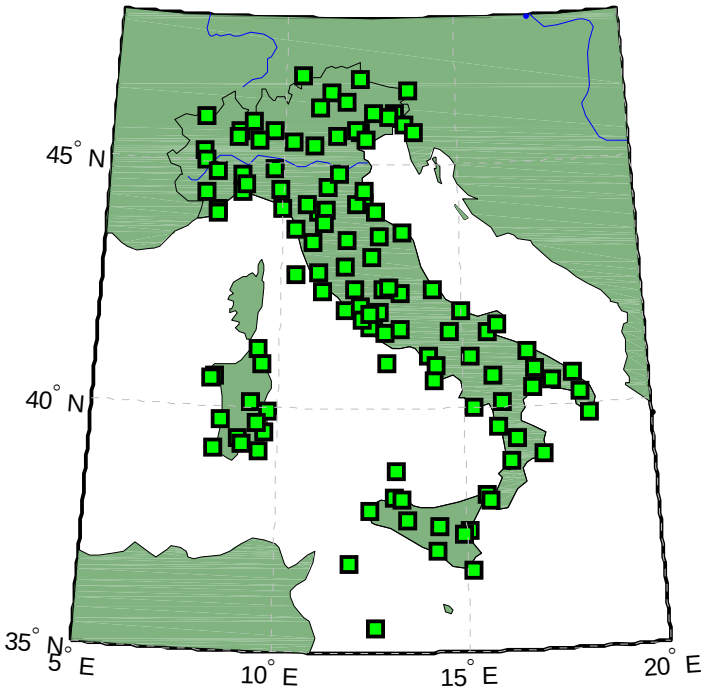

Figure 3.5 Meteorological stations considered in this study

Measurements of temperature, wind speed and direction, rainfall, barometric pressure and other meteorological parameters are taken at the stations. The Air Force meteorological service also gathers data coming from stations belonging to other Administrations. Data collected starting from 1951 has been digitized into an electronic database. All the data comply with the WMO (World Meteorological Organization) and ICAO (International Civil Aviation Organization) standards.

For this research ten-minute averaged wind speeds have been considered; most of the data are available at three-hour intervals from 1951 to 1972 and at one-hour intervals from 1973 to 2010. Only a minor portion of the data comes from measurements at half-hour intervals, usually referred to the period from 2000 to 2010. In addition, the daily maxima were available, and were used to cross-check possible errors, especially extremely high mean values. Most of the stations are located within airports, therefore feature almost uniform surroundings in terms of

orography and roughness. Some others, especially those located at high altitude, may feature pronounced local effects. The anemometers are located at an elevation of 10 m above the ground, and some of them have been replaced over the years with more sophisticated ones, having different specifications; in particular, a variation of the onset threshold over the years is evident, and must be properly accounted for.

The availability, besides wind speeds, of other meteorological data allows not only a cross-check for error detection, but also a better definition of the local climate. This may lead to the detection of cases of mixed wind climates, and gives the possibility to account for these in the definition of the basic wind velocity and in the return, directional and season coefficients.

3.3.2 Statistical treatment of the wind data

As a first step, for each station the time series of the mean wind speed was checked for errors. Each ten-minute averaged wind speed was checked to be smaller than the daily maximum three-second gust speed, also available in the database. When the latter was unavailable, the ten-minute averaged wind speed was automatically compared with the preceding and subsequent values, and a manual check was then performed when significant differences were found; the value was accepted otherwise. For all the cases not fulfilling the requirements above, wind data where cross-checked with pressure data and ignored only if not corresponding to a abrupt change in pressure. All the erroneous data were removed, and a table was built containing a synthesis of the available information for each year of measurement: number of measurements per day, total number of measurements available, lowest measured wind speed (as an estimate of the anemometer onset speed) number of wind calms, duration of the longest calm. The latter parameter was used to point out potential failures of the anemometer (false calms). In case of very long calms (usually in the order of a day, depending on the anemometer onset

speed), the data were carefully analysed in order to assess whether there were reasons to consider the calm as a false one. The conclusions drawn were recorded in a worksheet. The data were then divided into 12 sectors of 30º each (345º-15º, 15º-45º, …) for directional analysis, and into 12 months for seasonal analysis. The parameters of the omnidirectional and of the directional Weibull distributions of the mean values were estimated and, furthermore, the time series were used to calculate the parameters of the omnidirectional and of the directional Extreme Value distributions of the annual maxima (Fisher, et al., 1928) (Gumbel, 1958) (Lagomarsino , et al., 1992) and monthly maxima. In particular, the parameters of the Type I (Gumbel) Extreme value distribution were calculated using Gringorten's formula and those of the Generalised Extreme Value (GEV) distribution were calculated with the Maximum Likelihood Method. Finally, the fifty-year return period omnidirectional and directional wind speeds were calculated from the Gumbel and GEV distributions. In addition, POT analysis was carried out allowing to compare and check the results obtained with asymptotic analysis. Presently process analysis (Gomes , et al., 1977) is also being applied to the data. In the following part of the research an attempt will also be made towards the definition of mixed wind climates, through the crossing of the different meteorological parameters measured at each station.

Although, some of the recoded data needed correction for roughness and for orography, it must be emphasized that the results are not corrected for roughness conditions, topography and height of the anemometer different from the standard. Many times the anemometers are placed in airports and therefore it is reasonable that they should not be corrected; in other cases the corrections can give rise to significant variations with respect to 50-year return period wind speeds. In other words, although the results are obtained from a rigorous methodology, some of them still require a post-processing correction before the use for design purposes.

In Table 3.1 Part of the results for the 119 stations some of the results obtained from the omnidirectional analyses of 119 stations are presented whereas detailed results are presented in the Appendix 2.

In particular, columns 1 and 2 contain the denomination and the ICAO code of each station whereas columns 3, 4 and 5 contain the latitude, the longitude and the altitude above sea level, respectively; columns 6 and 7 denote the time interval of the available data. Column 8, 9 and 10 give the main statistical information about the population of the data and, in particular, column 8 contains the percentage of wind calms, ranging between 7.3% and 68.3%, with an average of 30.0% and a standard deviation of 15.5%. Columns 9 and 10 contain the Weibull c and k parameters of the ten-minute averaged wind speeds, as evaluated through the Least Square Method of the entire sample after removal of the calms. The evaluation of the Weibull parameters was also done using the Maximum Likelihood Method and the Method of Moments, and it was noted that, though the c values never differ more than 3% when calculated with the three methods, the k values vary up to 30%. In more detail, the Least Square Method underestimates the c values and overestimates the k values with respect to the other methods. Differences on the k parameter are translated into modifications in the tail of the distribution; therefore play a significant role when process analysis is applied for evaluating the distribution of the extremes.

Table 3.1 Part of the results for the 119 stations

Station	ICAO Code	Lat.	Long.	Alt.	Interval		Population			Annual maxima							
							wind calms	Weibull		Gringorten			GEV		Weibull		
								c	k	μ	a	v50	k	Δv50	c	k	Δv50
		(°N)	(°E)	(m)			(%)	(m/s)		(m/s)	(m/s)	(m/s)		(%)	(m/s)		(%)
Albenga (SV)	LIMG	44.04	8.13	45	1951	2005	44.7	4.5	1.8	13.9	2.5	23.7	-0.14	6.5	16.6	5.4	-4.0
Alghero (SS)	LIEA	40.63	8.29	27	1951	2005	26.7	4.8	1.9	15.8	1.9	23.4	-0.37	10.0	17.9	8.3	0.2
Ancona Falconara	LIPY	43.62	13.36	16	1960	2005	36.1	3.8	2.1	14.2	2.4	23.6	-0.22	9.0	16.8	6.0	-1.9
Arezzo	LIQB	43.46	11.85	249	1957	2010	54.3	4.1	2.1	13.0	2.5	22.9	0.03	0.7	15.7	4.5	-6.9
Aviano (PN)	LIPA	46.03	12.60	126	1951	2010	35.8	2.8	2.2	10.8	2.3	19.9	0.16	-6.6	13.3	4.3	-16.3
Bari Palese	LIBD	41.14	16.77	54	1951	2005	16.5	4.2	2.2	14.3	2.3	23.2	0.26	-12.3	16.8	5.7	-22.1
Bergamo Orio al Serio	LIME	45.67	9.70	239	1951	2005	42.1	2.6	2.1	11.8	2.3	20.8	-0.10	5.0	14.2	4.9	-5.0
Bologna Borgo Panigale	LIPE	44.53	11.29	38	1951	2005	39.5	3.0	2.2	11.7	2.0	19.6	-0.18	6.8	13.9	5.6	-3.1
Bolzano	LIPB	46.46	11.33	241	1951	2005	66.1	3.1	1.6	10.9	1.5	16.9	-0.11	3.7	12.6	6.2	-3.3
Brescia Ghedi	LIPL	45.44	10.27	102	1951	2010	45.1	2.7	1.8	13.1	3.0	24.9	0.04	3.3	16.2	3.7	-2.8
Brindisi	LIBR	40.66	17.95	15	1951	2010	17.8	5.4	2.3	16.0	3.1	28.2	0.08	-1.4	19.4	4.4	-8.2
Cagliari Decimomannu	LIED	39.35	8.97	24	1962	2010	30.3	5.3	1.9	15.2	2.0	23.1	0.03	2.2	17.4	6.0	-3.1
Cagliari Elmas	LIEE	39.25	9.06	5	1951	2010	14.6	4.9	2.0	16.3	2.2	25.0	-0.36	10.2	18.7	7.6	-0.2
Cameri (NO)	LIMN	45.53	8.67	178	1957	2010	56.9	2.4	1.8	11.3	2.8	22.4	0.06	0.1	14.2	3.8	-9.8
Campobasso	LIBS	41.57	14.65	793	1958	2009	32.9	5.4	1.8	20.6	2.8	31.7	-0.38	10.8	23.6	8.0	-0.9
Capo Bellavista (OG)	LIEB	39.93	9.72	150	1951	2010	13.9	5.1	1.9	20.1	3.7	34.6	-0.29	10.1	24.1	5.6	-1.3
Capo Bonifati (CS)	LIBW	39.58	15.88	484	1960	2010	33.3	5.6	1.7	20.7	3.6	34.7	-0.13	5.0	24.6	5.3	-3.7
Capo Caccia (SS)	LIEH	40.57	8.17	204	1975	2010	11.1	5.6	1.9	20.8	2.7	31.4	-0.12	4.9	23.7	6.9	-3.1
Capo Carbonara (CA)	LIEC	39.10	9.52	118	1951	2010	11.4	7.4	1.9	21.3	6.2	45.3	-0.40	17.8	27.5	4.0	3.9
Capo Frasca (CA)	LIEF	39.75	8.47	95	1962	2010	10.5	6.2	2.2	19.8	2.4	29.0	-0.31	9.0	22.4	8.4	-0.3
Capo Mele (SV)	LIMU	43.95	8.17	220	1963	2010	13.4	5.9	1.7	21.9	3.0	33.6	-0.24	8.2	25.1	7.2	-1.6
Capo Palinuro (SA)	LIQK	40.02	15.28	184	1951	2009	18.6	4.5	1.8	19.9	3.6	34.0	-0.17	6.7	23.7	5.3	-3.3

Station	ICAO Code	Lat.	Long.	Alt.	Interval		Population			Annual maxima							
							wind calms	Weibull		Gringorten			GEV		Weibull		
								c	k	μ	a	v50	k	Δv50	c	k	Δv50
		(°N)	(°E)	(m)			(%)	(m/s)		(m/s)	(m/s)	(m/s)		(%)	(m/s)		(%)
Capo S. Lorenzo (CA)	LIEL	39.50	9.63	5	1953	2006	36.4	4.3	2.2	13.5	2.0	21.3	-0.20	7.0	15.6	6.5	-2.6
Capri (NA)	LIQC	40.55	14.20	160	1951	2009	20.7	3.5	1.7	15.4	4.2	31.8	-0.08	5.0	19.7	3.7	-5.8
Carloforte (CI)	LIEZ	39.13	8.32	15	1951	1996	15.1	7.0	2.1	16.6	3.9	31.7	0.15	-4.0	20.5	4.2	-15.9
Catania Fontanarossa	LICC	37.47	15.06	12	1951	2005	26.7	4.2	2.2	14.6	2.3	23.5	-0.11	3.8	17.0	5.5	-3.4
Catania Sigonella	LICZ	37.40	14.92	29	1961	2010	22.1	5.2	2.1	16.5	1.7	23.0	-0.28	6.3	18.3	9.3	-1.9
Cervia (RA)	LIPC	44.22	12.30	6	1968	2010	22.4	3.6	1.9	14.7	2.3	23.7	-0.33	10.4	17.1	6.6	-1.1
Civitavecchia (RM)	LIQJ	42.03	11.82	3	1951	2010	14.8	4.1	1.9	15.6	2.8	26.5	-0.14	7.8	18.6	5.8	-4.3
Cozzo Spadaro (SR)	LICO	36.68	15.13	51	1951	2010	13.2	4.6	1.9	16.2	3.0	27.9	-0.03	2.5	19.4	5.4	-8.7
Crotone	LIBC	39.00	17.08	159	1951	2005	23.6	5.3	2.2	15.4	2.4	24.9	-0.24	8.8	18.0	6.3	-1.7
Dobbiaco (BZ)	LIVD	46.73	12.22	1222	1953	2010	63.2	3.8	2.0	9.9	2.2	18.3	-0.07	3.8	12.2	4.3	-5.7
Elba Monte Calamita (LI)	LIRX	42.73	10.40	396	1961	2009	15.0	5.4	2.0	18.0	2.9	29.2	-0.01	2.8	21.0	6.3	-8.6
Enna	LICE	37.57	14.27	1000	1951	2010	21.1	5.6	2.1	15.8	2.8	26.7	0.15	-5.9	18.9	5.1	-14.6
Ferrara	LIPF	44.82	11.61	9	1951	2009	22.8	2.8	2.2	9.5	1.6	15.9	-0.45	14.6	11.2	6.6	1.3
Firenze Peretola	LIRQ	43.80	11.20	44	1951	2005	56.9	3.5	1.7	13.5	2.7	23.9	0.05	-0.8	16.3	4.6	-9.4
Foggia Amendola	LIBA	41.54	15.71	60	1959	2010	18.9	4.7	1.9	16.1	2.3	24.9	-0.06	2.8	18.6	6.0	-4.0
Fonni (NU)	LIEN	40.12	9.25	1000	1951	2006	33.5	4.4	2.2	14.0	3.2	26.7	-0.13	6.8	17.4	4.3	-4.1
Forli	LIPK	44.19	12,0685	32	1969	2005	45.6	3.0	1.6	13.2	2.8	24.3	0.19	-7.3	16.2	4.3	-17.3
Frontone (PU)	LIVF	43.52	12.72	570	1954	2010	29.9	4.2	1.8	17.1	3.1	29.2	-0.12	4.8	20.5	5.1	-4.0
Frosinone	LIRH	41.63	13.28	193	1951	2010	44.7	3.0	1.5	13.2	2.8	24.2	-0.25	11.4	16.1	5.0	-1.2
Gela (CL)	LICL	37.07	14.22	65	1965	2010	20.4	4.4	1.8	15.4	3.2	27.9	-0.56	18.0	18.7	5.4	4.8
Genova	LIMJ	44.41	8.84	2	1962	2005	18.1	5.1	1.7	16.9	1.8	23.8	0.05	1.4	18.9	7.2	-2.8
Gioia del Colle (BA)	LIBV	40.77	16.93	352	1959	2010	25.6	5.8	2.2	18.5	2.4	27.7	-0.14	3.9	21.1	6.7	-2.9
Govone (CN)	LIMQ	44.80	8.10	300	1951	1985	56.4	3.5	2.2	13.6	4.5	31.2	0.07	-0.7	18.0	3.1	-12.4
Grazzanise (CE)	LIRM	41.06	14.08	9	1962	2009	36.7	4.0	2.0	15.7	1.8	22.6	-0.03	1.9	17.6	7.6	-5.0
Grosseto	LIRS	42.77	11.07	7	1951	2009	28.0	4.2	1.7	15.5	2.2	24.1	-0.11	4.2	17.9	6.3	-3.8

Station	ICAO Code	Lat.	Long.	Alt.	Interval		Population			Annual maxima							
							wind calms	Weibull		Gringorten			GEV		Weibull		
								c	k	μ	a	v50	k	Δv50	c	k	Δv50
		(°N)	(°E)	(m)			(%)	(m/s)		(m/s)	(m/s)	(m/s)		(%)	(m/s)		(%)
Grottaglie (TA)	LIBG	40.52	17.40	69	1960	2005	41.9	4.7	2.3	14.6	2.1	22.8	0.00	1.5	16.9	6.5	-8.0
Guardiavecchia (SS)	LIEG	41.22	9.40	170	1951	1999	11.2	8.0	2.0	21.1	4.8	39.7	-0.64	21.7	25.8	6.0	4.2
Guidonia (RM)	LIRG	41.98	12.74	88	1951	2010	56.9	4.0	2.1	12.3	2.0	20.1	-0.06	2.7	14.5	5.5	-5.6
Lamezia Terme (CZ)	LICA	38.91	16.24	12	1978	1999	23.2	4.4	1.8	15.7	2.1	23.7	0.03	1.5	17.9	6.4	-5.3
Lampedusa (AG)	LICD	35.50	12.61	21	1959	2005	11.6	6.1	2.3	16.2	2.7	26.6	-0.21	7.8	19.0	6.0	-2.5
L'Aquila Preturo	LIQI	42.37	13.30	665	1954	1999	38.7	6.0	1.8	16.6	6.4	41.5	-0.16	11.4	22.7	3.0	-2.4
Latina	LIRL	41.55	12.91	25	1961	2010	47.3	3.3	1.6	13.2	2.1	21.3	-0.18	7.5	15.4	6.2	-2.8
Latronico (PZ)	LIBU	40.08	16.02	888	1951	2010	23.3	6.1	1.8	20.2	4.3	36.9	-0.35	13.2	24.6	5.1	0.5
Lecce Galatina	LIBN	40.24	18.13	53	1951	2010	21.6	5.1	2.0	15.8	2.2	24.4	-0.06	2.6	18.3	6.1	-4.0
Marina di Ginosa (TA)	LIBH	40.40	16.85	1	1968	2010	10.6	4.7	2.3	18.2	2.1	26.5	-0.32	8.2	20.4	8.6	-1.4
Messina	LICF	38.20	15.55	54	1951	2010	22.3	3.6	2.1	13.3	1.8	20.5	-0.06	2.6	15.3	6.3	-4.4
Milano Linate	LIML	45.45	9.28	108	1951	1999	53.4	2.8	2.0	12.6	2.5	22.4	-0.28	11.0	15.2	5.1	-0.5
Milano Malpensa	LIMC	45.63	8.72	234	1951	1999	55.9	2.7	1.8	14.0	2.9	25.3	-0.06	3.8	17.0	4.6	-6.3
Mondovi (CN)	LIMY	44.38	7.82	500	1951	2010	52.9	3.1	2.2	11.8	2.8	22.6	-0.20	9.3	14.7	4.3	-2.3
Monte Argentario (GR)	LIQO	42.38	11.17	631	1961	2009	10.8	5.9	1.7	18.6	4.0	34.2	0.08	-0.3	22.8	4.2	-8.3
Monte Bisbino (CO)	LIMO	45.87	9.07	1322	1952	1998	43.4	3.7	1.7	15.0	2.1	23.2	-0.34	10.6	17.3	7.5	-0.1
Monte Cimone (MO)	LIVC	44.18	10.70	2165	1951	2010	18.2	8.3	1.9	26.7	6.1	50.5	-0.21	8.6	33.1	4.5	-2.9
Monte S. Angelo (FG)	LIBE	41.70	15.95	838	1951	2009	10.5	6.5	1.9	21.8	4.9	40.7	-0.24	10.3	26.9	4.6	-1.2
Monte Scuro (CS)	LIBQ	39.33	16.40	1669	1952	2010	21.4	4.8	1.9	17.5	3.6	31.4	-0.32	12.4	21.3	5.2	0.4
Monte Terminillo (RI)	LIRK	42.47	12.98	1874	1951	2007	23.1	6.5	1.9	21.9	6.5	47.1	-0.02	1.8	28.5	3.4	-8.9
Napoli Capodichino	LIRN	40.88	14.29	90	1951	2005	36.7	3.7	1.8	15.1	2.6	25.2	-0.14	5.3	17.9	5.4	-3.4
Novi Ligure (AL)	LIMR	44.77	8.78	189	1951	1998	43.5	2.6	1.9	10.5	1.4	16.1	-0.12	4.8	12.0	6.8	-4.1
Olbia (OT)	LIEO	40.90	9.52	11	1969	2005	27.2	5.1	1.8	16.1	1.8	23.1	-0.28	8.3	18.1	9.0	-0.8
Paganella (TN)	LIVP	46.15	11.03	2125	1951	2010	32.6	5.7	1.9	17.6	3.5	31.4	-0.27	10.5	21.3	5.1	-0.9
Palermo Boccadifalco	LICP	38.12	13.32	120	1951	2008	20.0	4.3	2.1	14.5	2.9	25.8	0.13	-5.7	17.6	4.8	-16.7

Station	ICAO Code	Lat.	Long.	Alt.	Interval		Population			Annual maxima							
							wind calms	Weibull		Gringorten			GEV		Weibull		
								c	k	μ	a	v50	k	Δv50	c	k	Δv50
		(°N)	(°E)	(m)			(%)	(m/s)		(m/s)	(m/s)	(m/s)		(%)	(m/s)		(%)
Palermo Punta Raisi	LICJ	38.18	13.10	20	1960	2005	20.7	5.4	1.8	18.8	1.8	25.7	-0.20	5.0	20.8	9.6	-1.9
Pantelleria (TP)	LICG	36.82	11.97	198	1951	2010	8.3	6.4	2.1	19.9	3.8	34.7	-0.16	6.2	23.9	5.0	-3.4
Passo dei Giovi (GE)	LIMV	44.55	8.93	488	1951	2010	7.3	5.6	2.4	13.1	2.9	24.4	0.17	5.3	16.1	3.8	-0.1
Passo della Cisa (MS)	LIMT	44.47	9.93	1039	1951	2009	14.2	6.5	2.2	17.9	2.5	27.6	-0.15	4.6	20.7	6.4	-2.9
Passo Porretta (PT)	LIQD	44.02	11.00	1314	1951	2002	30.7	6.1	1.9	17.4	4.8	36.0	0.05	-1.0	22.3	3.8	-13.5
Passo Rolle (TN)	LIVR	46.30	11.78	2004	1951	2009	49.1	4.0	2.1	13.9	2.4	23.4	-0.36	12.3	16.5	5.9	0.8
Perdasdefogu (OG)	LIEP	39.67	9.43	608	1961	2007	16.2	5.5	2.0	17.5	2.5	27.4	-0.48	14.0	20.1	7.8	1.7
Perugia S. Egidio	LIRZ	43.10	12.51	208	1967	2005	43.0	3.9	1.8	13.6	1.6	20.0	-0.03	2.3	15.4	7.0	-4.4
Pescara	LIBP	42.44	14.19	10	1951	2005	43.5	3.5	1.8	15.2	2.7	25.7	-0.06	3.2	18.1	5.3	-5.9
Piacenza	LIMS	44.91	9.72	138	1951	2010	46.3	3.3	2.1	12.4	2.4	21.6	-0.02	1.7	15.0	4.8	-6.5
Pisa S.Giusto	LIRP	43.68	10.38	6	1951	2010	29.4	3.6	1.7	14.9	1.8	21.9	-0.19	5.2	16.9	7.4	-2.3
Plateau Rosa (AO)	LIMH	45.93	7.70	3480	1951	2010	14.9	7.5	1.7	23.3	4.8	42.1	-0.47	16.8	28.2	5.9	1.4
Ponza (LT)	LIQZ	40.92	12.95	184	1951	2010	11.5	5.5	1.9	19.4	3.3	32.3	-0.29	9.4	22.9	6.0	-1.8
Potenza	LIBZ	40.63	15.80	845	1951	2007	34.3	5.4	2.1	15.7	2.6	25.9	-0.12	4.8	18.5	5.6	-4.2
Prizzi (PA)	LICX	37.72	13.43	1034	1951	2010	13.3	4.6	2.2	15.0	2.6	25.3	0.04	0.2	17.8	5.0	-7.5
Punta Marina (RA)	LIVM	44.47	12.28	2	1951	2010	24.7	3.8	2.0	14.1	3.0	26.0	-0.09	5.1	17.3	4.6	-5.9
Radicofani (SI)	LIQR	42.90	11.77	816	1951	2010	25.0	4.8	1.8	14.0	4.4	31.3	-0.07	6.5	18.4	3.5	-7.0
Reggio Calabria	LICR	38.07	15.65	11	1951	2005	16.7	5.4	2.0	15.2	2.5	24.9	-0.32	10.3	17.8	6.3	-1.0
Rieti	LIQN	42.43	12.85	390	1973	2005	51.4	3.3	2.0	10.3	0.8	13.5	-0.45	8.8	11.2	13.0	0.5
Rifredo Mugello (FI)	LIQM	44.06	11.24	887	1961	1982	12.3	7.6	1.9	20.8	4.1	36.7	-1.10	20.4	24.9	6.1	6.4
Rimini	LIPR	44.03	12.61	13	1951	2010	29.8	3.6	1.8	14.5	2.2	23.1	-0.08	3.1	16.9	5.6	-3.8
Roma Ciampino	LIRA	41.80	12.60	129	1951	2010	26.4	3.7	1.8	15.9	2.3	24.8	-0.05	2.2	18.5	6.0	-4.7
Roma Fiumicino	LIRF	41.81	12.25	5	1958	1999	19.0	4.5	1.9	15.8	2.2	24.5	-0.07	3.3	18.2	6.0	-3.5
Roma Pratica di Mare	LIRE	41.65	12.45	22	1960	2009	17.3	4.4	1.9	14.7	2.0	22.3	-0.14	4.5	16.8	6.7	-3.2
Roma Urbe	LIRU	41.96	12.50	19	1951	2005	42.8	4.1	1.7	13.0	1.8	20.1	-0.10	4.5	15.0	6.6	-4.4

Station	ICAO Code	Lat.	Long.	Alt.	Interval		Population			Annual maxima							
							wind calms	Weibull		Gringorten			GEV		Weibull		
								c	k	μ	a	v50	k	Δv50	c	k	Δv50
		(°N)	(°E)	(m)			(%)	(m/s)		(m/s)	(m/s)	(m/s)		(%)	(m/s)		(%)
Ronchi dei Legionari (GO)	LIPQ	45.83	13.47	17	1967	2005	42.1	3.2	1.6	15.6	2.8	26.7	-0.13	6.0	18.6	5.3	-4.0
S. Maria di Leuca (LE)	LIBY	39.82	18.35	104	1951	2010	8.5	5.3	2.1	16.2	2.3	25.2	-0.30	8.8	18.7	6.9	-1.0
S.Valentino alla Muta (BZ)	LIVE	46.80	10.50	1459	1951	2010	35.1	4.3	2.3	11.4	3.0	23.1	0.11	-1.1	14.5	3.7	-10.6
Sarzana Luni (SP)	LIQW	44.09	9.99	13	1970	2010	20.0	3.0	2.0	12.9	1.9	20.1	-0.04	4.4	14.9	6.5	-4.9
Tarvisio (UD)	LIVO	46.50	13.58	777	1951	2010	53.8	2.5	1.8	9.9	2.4	19.1	-0.07	4.6	12.3	4.2	-6.8
Termoli (CB)	LIBT	42.00	15.00	16	1951	2009	20.3	5.9	1.8	20.3	3.3	33.1	-0.54	15.5	23.7	7.4	1.9
Torino Bric Della Croce	LIMK	45.03	7.72	709	1952	2010	48.6	3.5	2.1	12.8	2.7	23.5	-0.14	5.4	15.7	4.5	-4.2
Torino Caselle	LIMF	45.20	7.65	302	1951	2005	68.3	2.4	1.9	11.7	2.6	22.0	-0.06	4.7	14.5	4.1	-4.4
Trapani Birgi	LICT	37.92	12.49	7	1962	2010	21.2	5.7	2.0	19.9	2.6	30.2	0.00	0.9	22.8	6.4	-6.1
Trevico (AV)	LIRT	41.05	15.23	1085	1952	2009	10.7	6.6	2.2	18.6	3.4	31.9	-0.19	8.6	22.2	5.5	-2.5
Treviso Istrana	LIPS	45.68	12.08	42	1951	2009	42.0	2.9	1.9	12.9	1.8	20.0	-0.26	7.6	14.8	6.8	-2.0
Treviso S. Angelo	LIPH	45.65	12.20	18	1955	2009	49.0	2.3	1.7	11.7	2.4	21.1	-0.02	2.9	14.2	4.1	-3.8
Trieste	LIVT	45.67	13.75	3	1951	2010	36.9	3.5	1.6	15.3	2.6	25.3	-0.12	5.4	18.0	5.7	-4.6
Udine Campoformido	LIPD	46.03	13.19	94	1951	1978	50.5	3.6	1.9	13.3	2.2	21.8	-0.14	7.3	15.6	6.3	-4.1
Udine Rivolto	LIPI	45.98	13.03	52	1969	2010	37.2	3.0	1.8	13.5	2.1	21.8	-0.42	13.3	15.7	6.8	2.0
Ustica (PA)	LICU	38.70	13.18	243	1951	2010	12.1	6.5	1.9	20.6	5.2	40.9	-0.05	3.7	26.0	4.0	-8.1
Venezia Tessera	LIPZ	45.51	12.35	2	1961	2005	36.5	3.4	1.9	15.3	2.1	23.4	0.03	2.7	17.6	5.8	-2.2
Verona Villafranca	LIPX	45.38	10.88	73	1951	2010	46.3	2.7	1.7	13.8	2.9	25.1	0.01	1.7	16.9	4.2	-5.3
Vicenza	LIPT	45.57	11.53	38	1951	2008	64.8	2.7	1.9	10.2	1.8	17.2	0.25	-7.9	12.1	4.8	-15.3
Vigna di Valle (RM)	LIRB	42.08	12.22	266	1951	2009	16.3	4.2	1.9	15.0	2.1	23.3	0.21	-9.2	17.3	6.5	-19.3
Viterbo	LIRV	42.43	12.06	307	1955	2010	14.6	4.6	1.9	15.6	2.3	24.5	-0.10	3.8	18.1	6.2	-4.2
Volterra (PI)	LIQV	43.40	10.87	555	1961	1998	19.7	5.4	1.8	17.9	3.0	29.8	-0.31	11.6	21.0	6.4	-1.3

Columns 11, 12 and 13 contain the Gumbel μ and a parameters (estimated with Gringorten's method) and the corresponding 50-year return period wind speed v_{50}, while columns 14 and 15 contain the shape parameter k of the GEV distribution and the percentage difference between v_{50} calculated from the Gumbel and GEV distributions (the μ and a parameters of the GEV distribution are shown in the Appendix 2). Columns 14 and 15 give an idea of the accuracy associated with the use of a Type I Extreme Value distribution. In particular, the shape parameter of the GEV distribution tends to zero when the data are Gumbel distributed, while it is positive or negative when a Frechet or a reversed Weibull distribution is more appropriate, respectively. Furthermore, the goodness of fit of Weibull distribution to annual maxima is evaluated in order to do a comparison with Gumbel and GEV distributions. Columns 16, 17 and 18 contain the Weibull c and k parameters (estimated with the Maximum Likelihood Method) referred to the annual maxima and the percentage difference between v_{50} calculated from the Weibull and GEV distributions. It is noted the v_{50} calculated with the Gumbel distribution is typically larger than the corresponding value calculated with the GEV distribution; in other words, the Gumbel distribution tends to overestimate the 50-year return period wind speed v_{50} with respect to the GEV distribution. Vice versa the Weibull distribution tends to underestimate the 50-year return period wind speeds v_{50} with respect to the GEV distribution. In the Figure 3.6, the percentage differences between the values of v50 calculated with the Gumbel and GEV distributions are plotted as a function of the GEV parameter k. It is noted that, although there is an outlier (station of Rifredo Mugello, indicated as its ICAO code LIQM), there is a fairly good linear correlation between the values (equation is shown in the figure).

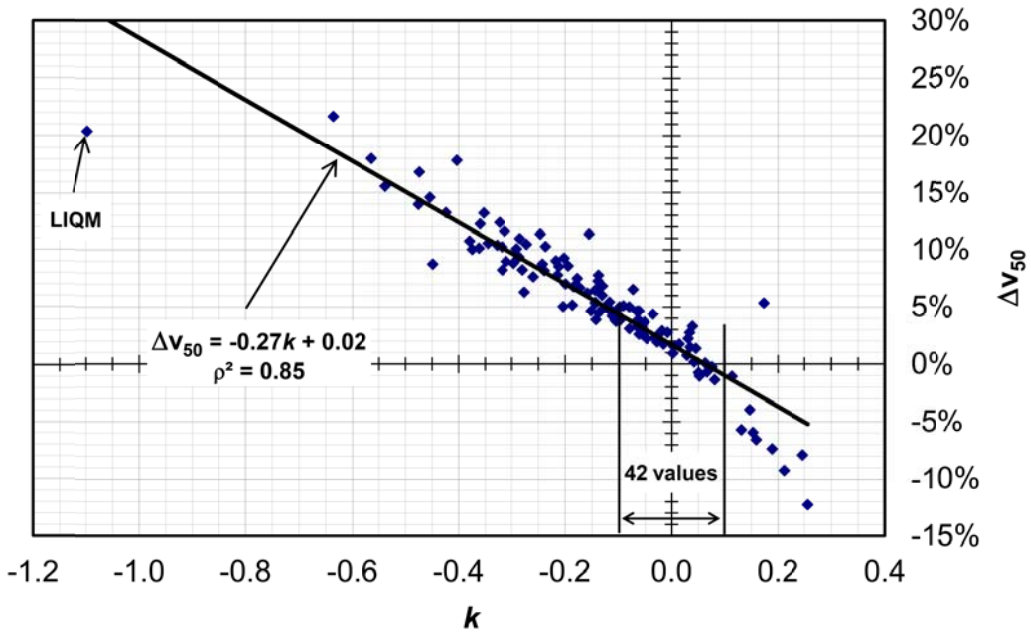

Figure 3.6 Difference between the v50 values evaluated with the Gumbel and GEV distributions

It is also observed that about 35% of the values (42/119) of the GEV parameter *k* fall within the range of -0.1 to 0.1, whereas about 65% of them (77/119) fall within the range of -0.2 to 0.2. Furthermore, it's interesting noting that about 78% of the values (93/119) of the GEV parameter *k* are lower than 0, suggesting once again that the Gumbel distribution tends to overestimate the 50-year return period wind speed v_{50} with respect to the GEV distribution. On average, the Gumbel distribution provides 50-year return period wind speeds v_{50} larger than those evaluated with GEV distribution by more than 5%, with a maximum of 21.7%.

In Figure 3.7, the percentage differences between the values of v50 calculated with the Weibull and GEV distributions are plotted as a function of the GEV parameter *k*. It is noted that, although there is an outlier (station of Rifredo Mugello, indicated as its ICAO code LIQM), there is a good linear correlation

between the values (equation is shown in the figure), although less accurate than the previous case.

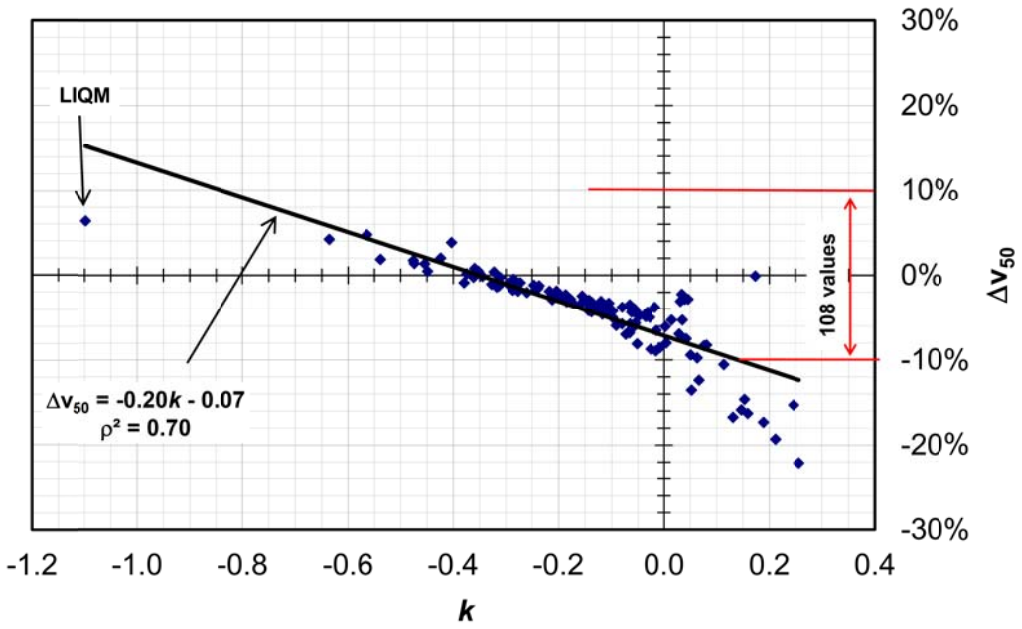

Figure 3.7 Difference between the v50 values evaluated with the Weibull and GEV distributions

On average, the Weibull distribution provides 50-year return period wind speeds v_{50} smaller than those evaluated with GEV distribution by more than 4%, with a maximum of 22.1%. It's worth noting that, in 78% of the cases (93/119), the percentage differences between the values of v50 calculated with the Weibull and GEV distributions fall within the range of -0.1% to 0.1%.

3.3.3 Directionality and seasonality of the Italian wind climate

The directional features of the Italian wind climate are being investigated through the ratio of the directional and omnidirectional 50-year maximum wind speed, which is by definition the directional coefficient.

The directional coefficients are calculated for sectors of 30º. The values obtained range between 0.37 and 1.10, and are rather scattered on the Italian territory. Notice that, though usually lower than one, the directional coefficient can take values slightly larger than one. This occurs when for one particular direction the standard deviation of the annual directional maxima is significantly larger than that of the omnidirectional maxima. A polar diagram of directional coefficients referred to the LIRP station is shown in the

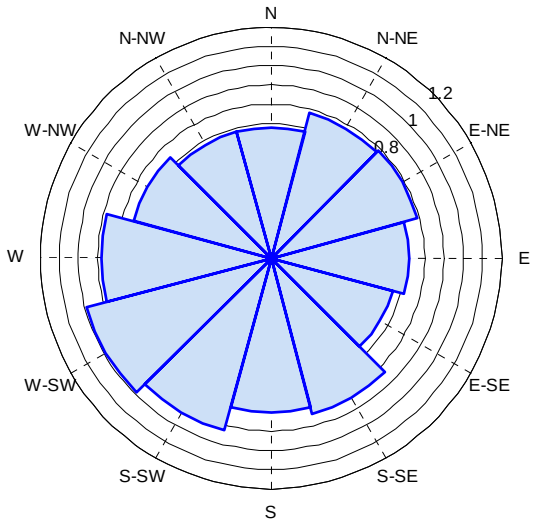

Figure 3.8 Polar diagram of directional coefficients (LIRP station)

Figure 3.8 shows that the directional coefficients assume values ranging from 0.65 to 1.00 with the maximum values associated to South-West directional sectors. Detailed results about directional behaviour of wind climate are presented in the appendix 2 (polar diagrams) and 4 (tables) for all the 119 stations.

The seasonal features of the Italian wind climate are being investigated through the ratio of the monthly and overall 50-year maximum wind speed, which is by definition the seasonal coefficient. The values obtained range between 0.47 and 1.09: typically, the higher values correspond to the winter whereas the lower to the

summer. A diagram of seasonal coefficients referred to the LIRP station is shown in the Figure 3.9.

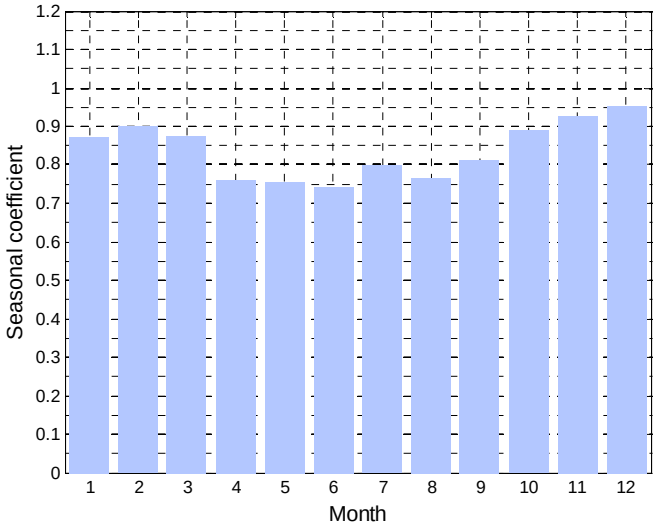

Figure 3.9 Diagram of seasonal coefficients (LIRP station)

Detailed results about seasonal behaviour of wind climate are presented in the appendix 2 (diagrams) and 5 (tables) for all the 119 stations.

4 STRUCTURAL VULNERABILITY

Vulnerability is a measure of the intrinsic ability of a structure or entity to withstand the forces produced by a hazardous phenomenon. It is commonly expressed as the degree of damage that can be expected to result from the occurrence of a particular hazardous event of a given magnitude. The structural characteristics of entities exposed to hazardous phenomena therefore determines their vulnerability. Recent earthquake and hurricanes have highlighted the importance and the urgency of rehabilitating deficient structures to achieve an acceptable level of performance. This can be achieved either reducing the load effect input to the existing structure, or improving strength, stiffness and/or ductility. In comparison to the design of a new structure, one of the biggest consequences of assessing an existing structure is that the structural and the material information need to be estimated.

With respect to wind hazard, the vulnerability of the most common building types is basically determined by the roof type and the type of openings. Typically buildings with concrete slab roofs and protected openings are characterized by low vulnerability; otherwise, existing steel buildings can be very vulnerable because of, for instance, obsolete design specifications and aging of the structure. In particular, steel hangar structures, that are characterized by large spans and very large wind-exposed surfaces, exhibit several failure mechanisms as clearly shown during last extreme wind events. Furthermore, the wartime hangars have inherent weakness in their structural strength and their strength fall below current standards for design and loadings. The degree of shortcomings in the hangar's strength depended on its location within Italy as this determined the wind and snow loadings applied to it.

Many of these hangars are subject to maintenance, repair and refurbishment works depending upon the condition of a particular hangar, its current and future use and predicted life time. In the absence of original steel certificates or design calculations, the interpretation of permissible design stresses applied at the time requires sound engineering decision coupled with knowledge of developments in iron and steel construction during last century. Therefore, the historical design codes, steels and connections are covered. The significance of dominant openings in a hangar building due to door and window openings and the building's permeability is also explained. Due to concerns about weakness in the structural strength of wartime hangars, sometimes operational constraints had to be put in force. For instance, the main hangar doors could have to be kept shut and the structure put under observation during adverse weather conditions of snowfall and high winds. The chapter provides a brief review of properties of materials, structural details and structural types adopted in the past for steel hangars. The first ones were built at the beginning of the 20th century in the early development of the aviation industry and, therefore, a dissertation about oldest materials used in the construction of metal buildings is essential to understand the behavior of historic structures.

4.1 Historical evolution of materials and connections

Iron and steel have been used in the construction of buildings for centuries. Cast iron has a relatively high carbon content (more than 1.5%) along with silicon and sulphur. As a result, cast iron is hard and brittle, with limited tensile strength. It is difficult to work, so it must normally be used in cast assemblies. Because of its availability and fairly good compressive strength, it was used quite extensively for columns in buildings built in the early to middle 19th century (FEMA, 1997). Engineers preferred not to use cast iron in components that were either part of a

lateral load system or developed significant bending or tension, because of brittle and dramatic failures of cast iron components in bridges and other structures. Cast iron continued to be used into the early part of the 20th century, but wrought iron became the more dominant material in the late 19th century, and steel overtook both in the early 1900s. Wrought iron is much more workable than cast iron; it is more ductile and has better tensile capacity. As a result, it was a more versatile construction material than the cast iron that preceded it. However, for columns, cast iron was still viewed as the most economical material until very late in the 1800s. Steel was largely made possible by the development of the Bessemer process combined with the open hearth furnace (FEMA, 1997). A number of tests for steel and structural steel components are reported during the 1890s. Examination of the reported test results suggests that the properties of this early steel were not very different from steel used in the 1950s and 1960s. However, in Italy only few steel structures were built before 1950s because of the shortage of raw material and use for military purposes of what was available. Riveted connections were the primary method for connecting steel members whereas welding techniques were first developed around 1915 and used in a few structures in the 1920s and 1930s, but usage was limited due to poor quality. Mild steel bolts also had limited usage during this period. By the mid-1960s, the use of riveted connections was abandoned as high-strength bolts and electric arc welding became the standard connection technique. Around this time, a good improvement of performance of steel was reached and higher-strength steels were also introduced during this period.

As stated, cast iron was used extensively throughout the 19th century, but its use was primarily for columns, which carried compression with no significant tension or bending. Cast iron performed poorly when it was subjected to these alternate stress states, and wrought iron had filled in as an alternate construction material for these other applications in the second half of the 1800s.

Wrought iron and cast iron were largely replaced by steel at the turn of the century. Wrought iron and steel were more ductile than cast iron and more easily worked, and a wide range of field and shop modifications was possible. These wrought iron and steel buildings had some common attributes, but in general, the members and connections were unique. Engineers made extensive use of riveted built-up steel and wrought iron members with riveted connections.

The members were commonly built up from plates, angles, and channels. These built up members used tie plates and lacing, and the large number of rivets made them labor-intensive. Connections were formed with haunches, knee braces, and large gusset plates. In the 1920s, use of the unique, complex built-up members began to be phased out, and standard I and H-shapes replaced them as the standard for member design. Partially restrained (PR) connections, such as the riveted T-stub and clip angle connections, became the normal connection. Because the clip angle connections were weaker and more flexible, they were used as the beam column connections in shorter buildings or in the top stories of taller buildings. The T-stub connection was stiffer and stronger, and it was used in the lower floors of taller buildings where the connection moments were larger. Stiffened angle or T-stub connections were often used to provide a beam connection to the weak axis of the column. It should be noted that all buildings constructed during this era used relatively simple design calculations compared to modern buildings. Bolts and welding were sometimes used, but rivets were clearly the dominant connection. Significant changes began to appear from 1950s. The use of rivets was discontinued in favor of high-strength bolts and welding. In the very first structures, bolts were merely used to replace the rivets in connections such as the clip angle and T-stub connection. However, flange plate and end plate connections were used more frequently. Increased use of and confidence in welding made these connections possible. By using these connections, engineers were often able to develop greater connection strength and stiffness with less labor. significant

differences began to evolve in the way buildings were designed for regions of high seismic activity, and for other regions. These regional differences were developed because regions with significant seismic design requirements had to deal with larger lateral forces, but also because of the increased emphasis on ductility in seismic design procedures. In less seismically active zones, the weaker, more flexible connections were retained for a longer period of time, while in the seismically active zones the fully restrained FR connection began to evolve. Also, braced frames and alternate structural systems were used because they could often achieve much greater strength and ductility with less steel and more economical connections. The trends established in the 1960s continued into the following period. There was increased emphasis on ductility in seismic design, and extensive rules, intended to assure ductility for moment frames, braced frames, and other structural systems, were established. These rules undoubtedly had some substantial benefit, but compliance was often expensive, and there was a distinct tendency toward using structures with less redundancy, since these less-redundant structures required satisfaction of the ductility criteria at fewer locations. This reduced redundancy also resulted in larger member and connection sizes. This separation of the practice between regions with significant seismic design requirements, and those with little or no seismic design requirements, continued to widen. The less seismically active regions sometimes retained more flexible connections with greater redundancy in the overall structure. Moreover, the steel and construction processes themselves were also changing. There was a significant increase in steel produced by reprocessing scrap metal in an electric furnace. As a result, the yield stress of standard steels increased, while the tensile stress remained relatively stable. Welding evolved from the relatively expensive stick welding shielded arc process to the quicker and more economical flux core, gas shield, and dual shield processes. High-strength bolts were increasingly used as slip-critical friction bolts; however, quality control variations caused by tightening and installation became a

major concern. These changes in turn produced changes in the ductility and behavior of many steel structures.

4.1.1 1916 Specifications

At the beginning of the 19th century two main metal structural typologies can be distinguished: the large span roofing structures and the structure for bridges, mostly for railway use. Hence, the first specifications about the mechanical properties of steel were for Railway Engineering and they were published by the Italian Railways Institution. However, Italian Government published some specifications in 1916 in which the nominal ultimate strength was set equal to $33\ \mathrm{kg/mm^2}$ ($\cong 330\ MPa$) whereas the nominal ultimate strain was set equal to 9%.

4.1.2 UNI 743/1938 Specifications

Many years later, in 1938, the Italian National Standards Body (UNI) published the 743 Specification in which the types of steel shown in the Figure 4.1 were introduced.

Materiale	Tabella UNI	Designazione convenzionale della qualità dell'acciaio	Prova di trazione				Prova di resilienza K	Osservazioni
			Carico unit. di rottura R Kg/mmq	Allungamento minimo % A 5	Allungamento minimo % A 10	Carico unit. di snervam. S Kg/mmq	Kgm/cmq	
Profilati, barre e larghi piatti (1)	UNI 743	A 00 UNI 743	< 50	—	—	—	—	
		A 37 » »	37÷45	25	20	—	6	
		Aq 34 » »	34÷42	30	25	—	10	acciaio di qualità
		Aq 42 » »	42÷50	25	20	23	7	» »
		Aq 50 » »	50÷60	22	18	17	4	» »
		(Aq 60 » »)	60÷70	17	14	31	3	» »
Lamiere (2)	UNI 815	A 00 UNI 815	—	—	—	—	—	
		(A 34 » »)	34÷42	25	20	—	8	
		A 42 » »	42÷50	22	18	—	5	
		(Aq 34 » »)	34÷44	32	26	19	15	acciaio di qualità
		Aq 42 » »	42÷50	27	22	23	9	» »
		Aq 48 » »	48÷55	23	19	26	7	» »
		Aq 53 » »	53÷63	20	16	29	5 0	» »
Tubi	UNI 663	(A 00 UNI 663)	—	—	—	—	—	
		Aq 35 » »	35÷45	28	23	21	—	acciaio di qualità
		(Aq 45 » »)	45÷55	23	19	24	—	» »
		Aq 55 » »	55÷65	17	14	29	—	» »
		(Aq 65 » »)	65÷75	12	10	33	—	» »

Figure 4.1 Types of steel defined by the UNI 1938 Specifications

It's worth pointing out that different steel qualities were defined and, for each of them, both the nominal yielding strength and nominal ultimate strength were provided.

4.1.3 CNR-ACAI 1946 Recommendations

The CNR-ACAI Recommendations 1946 (CNR-ACAI, 1946) didn't introduce any further improvements and cited the UNI 743/1938 Specifications regarding the metal materials and their mechanical properties that had to be used; however, in the framework of admissible stresses method, the admissible strength and the elastic moduli were fixed, as shown in the Figure 4.2.

	Qualità del materiale	σ_{am} Kg/mm²	E t/cm²	G t/cm²
1	Ferro agglomerato o ferro colato di fabbricazione antecedente al 1895	9	2000	770
2	Acciaio in verghe A 37 UNI 743, lamiere A 42 UNI 815 e in tubi A 35 UNI 663	14	2100	810
3	Acciaio in verghe Aq 42 UNI 743, lamiere Aq 48 UNI 815	16	2100	810
4	Acciaio in verghe Aq 50 UNI 743 lamiere Aq 53 UNI 815 e in tubi A 55 UNI 663	18	2100	810
5	Acciaio in verghe e in lamiere, speciale ad alto limite elastico As 52	0.55 del limite di snervamento σ_s	2100	810

Figure 4.2 Admissible mechanical properties fixed by the CNR-ACAI 1946 Specifications

Further limits were introduced for riveted and bolted connections; in particular, it's worth noting that the admissible shear strength of the rivets and the bolts had to be less than 10 kg/mm^2 and 13 kg/mm^2 for Aq 34 steel type and As 44 steel type, respectively.

4.2 Effects of fatigue

The steel long-span roofing may be vulnerable to the effects of the fatigue under wind loading. Fatigue damage appears in the form of fatigue cracks and can occur in primary loaded or secondary elements. Since fatigue failure is depending on the load spectra over the service life, consequently, existing steel structures suffer more from fatigue and accumulate more damage the older the structures are (Kühn, et al., 2008). Another aspect is the acceptability of a fatigue crack with regard to the consequence of failure related to the main structure. For instance, a fatigue crack initiated in a secondary element, e.g. caused by restraint, is usually not of major

importance for a hazard scenario of structure. Fatigue cracks in main elements, as longitudinal, cross and main girders, may be of high risk for a break down of a structure and for the safety of people being on or in these structures.

With respect to wind actions, the susceptibility of the structures to stress variations can be due to (Kühn, et al., 2008):

- Fatigue resulting from stresses induced by wind action spectra;
- Fatigue resulting from stresses induced by vortex excitation or other aerodynamic excitation mechanisms (under constant wind action);
- Combination of both.

In addition to quasi-statically effects due to a slowly varying load, there are also some dynamic effects due to the rate of the change of load.

The Eurocode 3 part. 1-9 (CEN, 2003) and Eurocode 1 part. 1-4 (CEN, 2005) provide some criteria for evaluating if the effects of fatigue may become relevant and need to be investigated and also give methods for the assessment of fatigue resistance of members, connections and joints subjected to fatigue loading.

4.3 Steel aircraft hangars: main structural types

Aircraft hangars are characterized by large spans and exhibit, in some cases, design solutions typical of industrial buildings. A review of main structural types and their historical evolution is shown. The oldest ones were built before the first world war but no information about them is available. Some hangars were built around World War II, during 1930s, and are still in use. Typically, they are characterized by 35 meters long span trusses and structure type number 1 and 2, as shown in the Figure 4.3 and Figure 4.4. Many of the war time hangars were erected as temporary structures in anticipation of a short design life. They were produced in order to provide a fast, economical solution to a need for hangars before and during World War II. They were built quickly and over a short period of time and,

perhaps, the predicted short time exposure to wind and snow loading would have allowed smaller loadings to be considered than is the case for long term exposure as the magnitude of the design load is dependent upon the life of the structure (DWS, 1995). In dealing with any hangar works, it is vital that the hangar type is correctly identified, especially due to that some hangars differ each other only for few structural details. To the best knowledge of the author, the following structural types can be recognized:

- Structural type named 1 (ST1) characterized by roof trusses supported on main longitudinal truss, in turn rests on the middle transversal truss, as shown in Fig. 5.19;

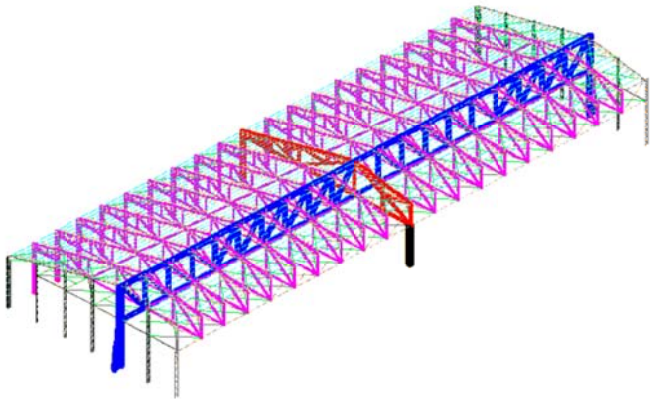

Figure 4.3 Structural Type 1

It's worth pointing out that ST1 suffers from a problem of instability of the support under the middle transversal truss; as shown below, this issue was the reason of the failure happened in Pratica di Mare in 2001.

- Structural type named 2 (ST2) characterized by roof trusses supported on main longitudinal truss, in turn rests on the middle transversal portal frame, as shown in Fig. 5.20;

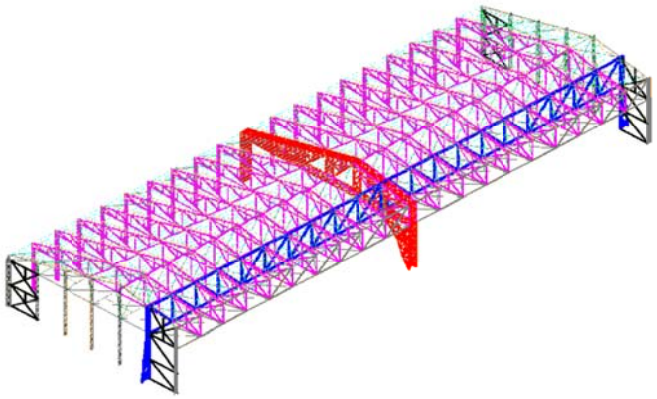

Figure 4.4 Structural Type 2

With respect to wind, the ST2 seems to be less vulnerable than ST1 due to the presence of the middle transversal portal frame, both in terms of instability of middle support and upinflection of the longitudinal truss guidance of the doors.

- Structural type named 3 (ST3) characterized by two longitudinal Pratt trusses that realize the support for transversal trusses, as shown in the Figure 4.5;

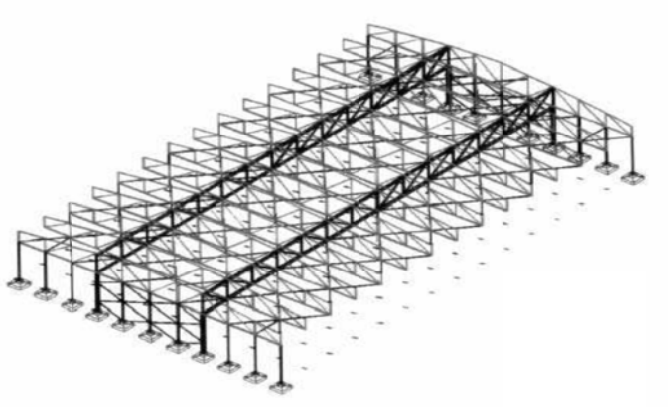

Figure 4.5 Structural Type 3

The main characteristic of the Pratt truss is that diagonal members are only in tension for gravity load effects. This allows these members to be used

more efficiently, as slenderness effects related to buckling under compression loads will typically not control the design. However, such feature may represent the most vulnerable point of the oldest hangars, that are typically not design for suction effects on the roofing.

- The Structural Type 4 (TP4) is a lightweight structure made from steel lattice portal frames in which the doors run level with the top of the side panelling. Each gable end has six sliding doors allowing an opening the full width of the hangar to be formed. Some hangars may now have operational doors on one end only, the other end with doors permanently locked.

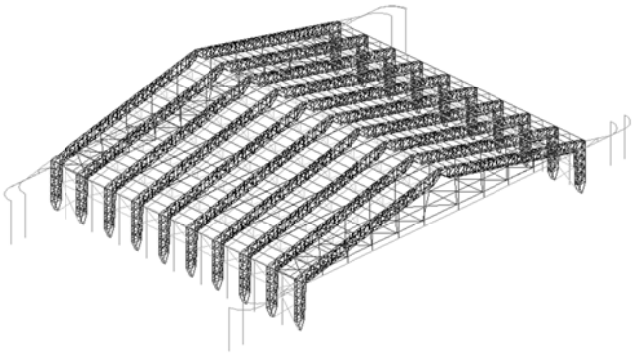

Figure 4.6 Structural Type 4

Longitudinal stability of the hangar is provided by bracing the frames at roof level and in the side walls at three locations, one at each end and one in the middle of the building.

- The Structural Type 5 (TP5) is characterized by a space frame truss, whose space truss consisting of tetrahedron shape, supported on RC columns.
- The Structural Type 6 (TP6) is characterized by a double series of trusses, one in the transversal direction and the other in the orthogonal one, as shown in the Figure 4.7; typically, the roofing is supported on four circular steel-concrete composite columns. It should be noted the presence of the portal frame in front of the hangar whose function is to support the doors.

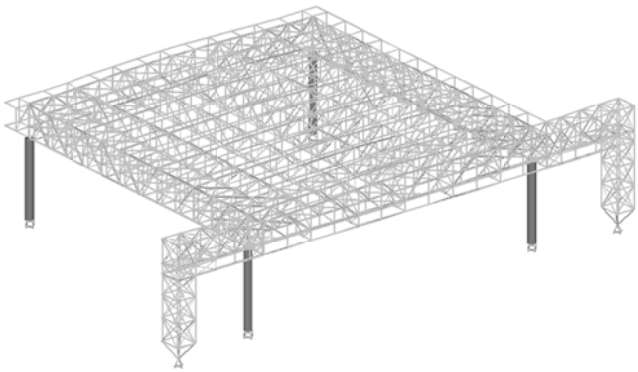

Figure 4.7 Structural Type 6

- The Structural Type 7 (TP7) is designed as an "assembly" of two TP6 and, therefore, is characterized by a double series of trusses, one in the transversal direction and the other in the orthogonal one, as shown in the Figure 4.8;

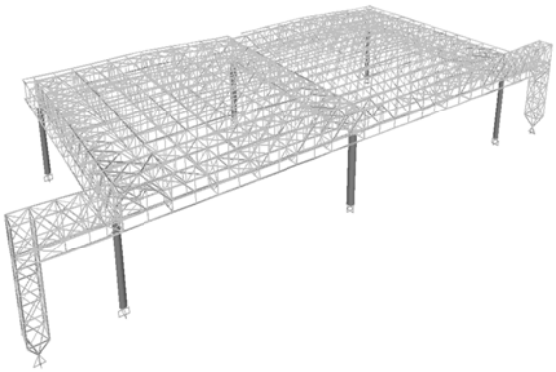

Figure 4.8 Structural Type 7

Unlike the previous one, the roofing of the ST7 is supported on six circular steel-concrete composite columns, whose middle ones are, obviously, larger than the perimeter ones. It's worth pointing out that all structural types have

doors on only one side, except for ST3 and ST4 that can have doors on both sides. Typically, ST7 presents 40x40 m or 60x60 m wide truss gratings.
The most modern structural type is shown in the Figure 4.9 and it is named as ST8.

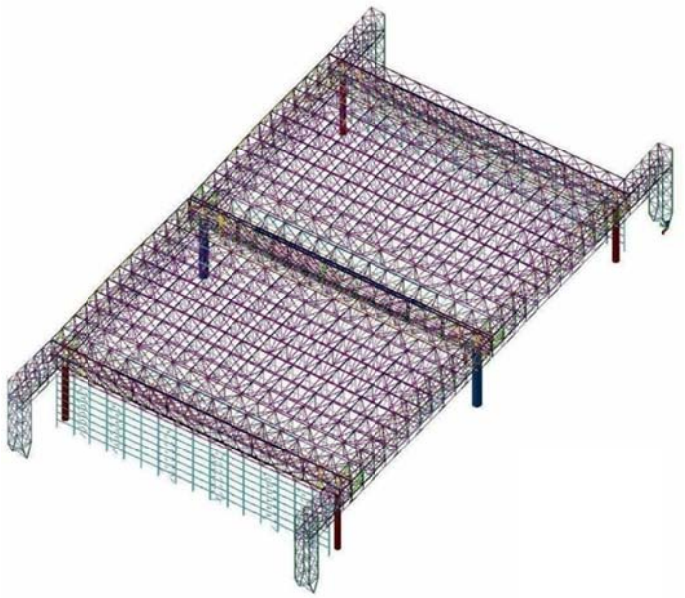

Figure 4.9 Structural Type 8

The main element of innovation compared to previous similar structural patterns (ST6 and ST7) is the double opening. Typically, ST8 presents two 80x60 m wide truss gratings that means 120x80 m wide hangar.

4.4 Failures due to extreme events

Although still in service, only a few existing steel hangars are damage free, usually due to the lack of systematic maintenance and/or to structural deficiencies. Furthermore, an inadequate knowledge and maturity about typical aspects of design of steel structures at the epoch of construction can be a critical aspect with respect to buckling phenomena and connection details. After a study about the main causes of decay and structural inadequacy of ancient metallic large span structures,

D'Aniello (D'Aniello, et al., 2009) recognized that a significant source of structural deficiency could be found in the old rivet connections. Typical damage occurred during last extreme wind events or earthquakes include buckled braces and failure of connections.

During the 1994 Northridge, California earthquake, over two hundred buildings experienced fractured beam-column or column-baseplate connections. The reasons for this poor performance are complex, and still under investigation. One significant factor was lack of quality control of the entire welding process, in combination with the use of weld filler that has almost no notch toughness. Other factors contributed to this poor behavior, such as the thickness of the column and beam flanges, the stiffness and strength of the panel zones, triaxial stress effects, high confinement of the joints, and poor welding procedures, for example, high heat input, rapid cool down, and conditions allowing hydrogen embrittlement.

With regard to hurricanes, it is useful to distinguish between local and global failures. The most frequent type of global failure observed was the uplift of the roofings due to lack of adequate supports, typically not designed to lifting actions, or to local failures such as local buckling phenomena, buckling of truss elements and failure of connections. In this regard, an important role can be played by the roofing type. Some truss types, such as Pratt trusses, are inherent vulnerable to uplift of roofing; in fact, the diagonal members are in tension only for gravity load effects and they can exhibit buckling phenomena for moderate uplift loads. Another important issue concern the typical design approach used in the past when a truss is usually modeled as a two-dimensional plane frame without taking into account out-of-plane loads whose effects on members considerably reduce frames' capacity. Furthermore, the stripping away of the roofing (i.e. corrugated metal sheeting) is another source of vulnerability, even if not related to structural behavior of the buildings. Windows were also shown to be weak points in the building envelope

and the breaking down of them can strongly modify the interaction between external and internal pressure, increasing the risk of uplift of roofing.

In the following, some failure cases due to extreme wind events occurred in Italy are presented. The damage that affected some steel aircraft hangars during extreme wind phenomena reported in recent years are briefly discussed with the aim of identifying some elements of vulnerabilities and, at the same time, developing the knowledge to design those technical devices for the reduction of the inherent weaknesses of the existing structures.

4.4.1.1 Pratica di Mare 2001

On November 19th, 2001 a violent storm occurred on the Pratica di Mare Airport (near Rome) causing the structural collapse of a hangar and significant damages to another one. In detail, the collapsed hangar was built in 1936 and was 100x36.8 m wide and a height equal to 9 and 16 m on the front and at the peak, respectively. It was also characterized by Structural Type 1, as shown in the Figure 4.3, and transversal axis oriented in the direction E-W. The doors were located only on the west side and, as clearly shown in the Figure 4.3, the structural system was designed in order to have only one column on the west side. The 36-meter long transversal trusses were placed at a 5-meter distance (Figure 4.10) whereas the longitudinal truss was 9-meter spaced from the front side of the hangar (Figure 4.11).

Figure 4.10 Roof planimetry

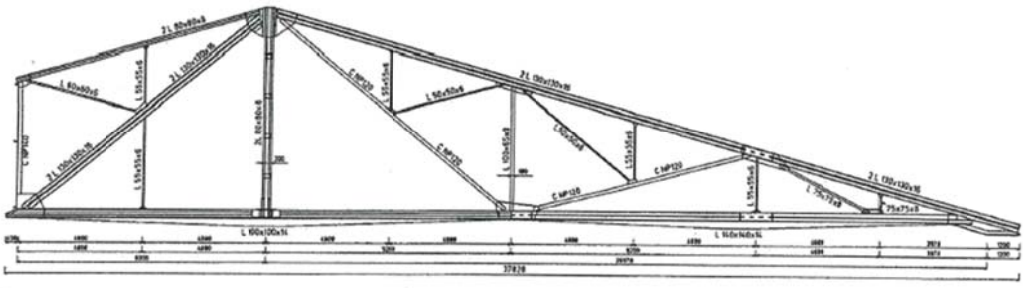

Figure 4.11 Main middle truss

The pictures taken after the collapse show the sensational effects of wind actions on structures (Figure 4.12).

Figure 4.12 The collapse of hangar occurred at Pratica di Mare Airport on 2001

From the investigations it was found that, under the action of wind, the roof was raised and rotated counterclockwise, if viewed in plan. The middle transversal truss, after having raised and rotated, in the back down it lost the support of the column at the center of the front and collapsed, taking with it the longitudinal truss and all the transversal trusses resting on it. Therefore, the failure of the hangar was caused by the suction action of the wind on the roof whose supports were not adequately designed with respect to lifting actions (Chiodi, et al., 2011)

These considerations are consistent with the anemometer record that showed a nearly orthogonal to the incident direction of the wind at the front of the hangar and a component that would justify the rotation. The daily maximum wind speed, recorded by the weather station located inside the airport, was characterized by the parameters of engineering interest shown in the Table 2.1, where v_3 denotes the 3-second gust wind speed.

Table 4.1 Daily maximum wind speed recorded at Pratica di Mare (2001-11-18)

Time	Direction (°)	v_3 (m/s)
16:10	300	26.8

For a comparison, the hourly 10-minute averaged wind speeds v_{600} are also reported in Table 4.2.

Table 4.2 Hourly wind speeds and barometric pressures recorded at Pratica di Mare (2001-11-18)

Time	Direction (°)	v_{600} (m/s)	Barometric pressure (hPa)
15:00	110	6.7	1016
16:00	110	10.3	1014
17:00	320	2.1	1016

Some further considerations can be outlined; during the event, the doors were closed, suggesting that the effects could have been more severe if the doors were opened. Furthermore, looking at the position of the doors after the collapse, it may be assumed that, before the loss of the middle support, the longitudinal truss of driving doors was raised by an amount such that the loss of the top rail of doors can occurred. In this sense, it is interesting to report the detail of the top rail of the doors, shown in the Figure 4.13.

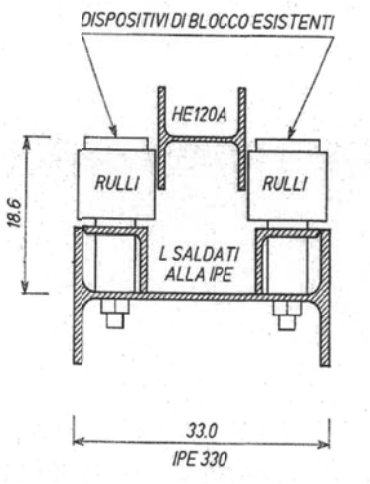

Figure 4.13 Detail of the top rail of the doors

Moreover, with respect to the shape of the hangar and the size and the position of the openings, it is interesting to simulate the wind actions adopted by different Building Codes during the last century in order to study the evolution of ratio between the uplift design actions and structural weight; the results are summarized in the Figure 4.14.

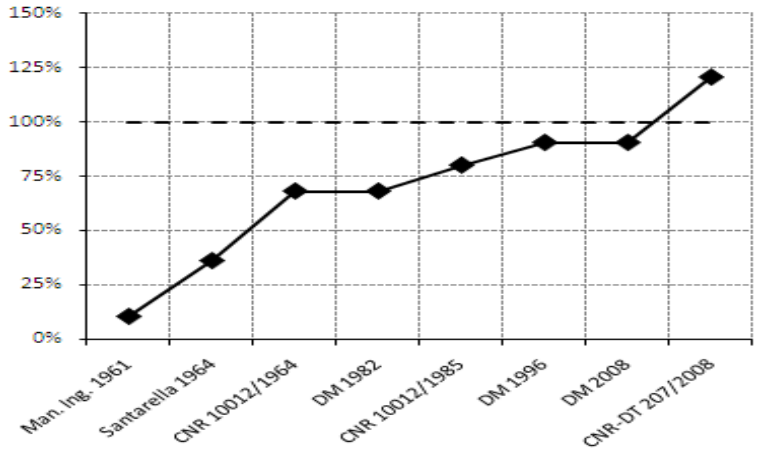

Figure 4.14 Evolution of uplift actions (building with uniform leakage)

It is clear that the oldest design approaches led to unconservative estimation of wind actions and, therefore, it's reasonably that the oldest supports were not designed with respect to the uplift of the roof.

A further reflection concerns the analysis of anemometer records; as evidently shown by the Table 4.1 and Table 4.2, the ratio between the 3-s gust wind speed and the 10-minute averaged wind speed was very high and, moreover, the 10-minute averaged wind speed was of only 10.3 m/s; this could be due to the downsampling, as extensively illustrated in the section 2.8.

4.4.1.2 Lecce 2006

The September 26th, 2006 a violent storm occurred at Lecce Airport and caused extensive damage over the entire airport area and the surrounding areas.

The most damaged hangar was the so called no 29; this hangar is characterized by a 52x32 m wide rectangular plan and the structural scheme number 3, as defined in the previous section.

Figure 4.15 Damages at Lecce Airport on 2006 (1/2)

Figure 4.16 Damages at Lecce Airport on 2006 (2/2)

As shown in the Figure 4.16, six of the ten doors lost the upper guide and they were reversed inside the hangar and many steel frames collapsed or yielded, as shown in the Figure 4.17, 4.19, 4.20 and 4.21 (Camarda, 2006).

Figure 4.17 Yielded frame (Lecce 2006)

Figure 4.18 Collapsed frame (Lecce 2006)

Figure 4.19 Buckling of a frame

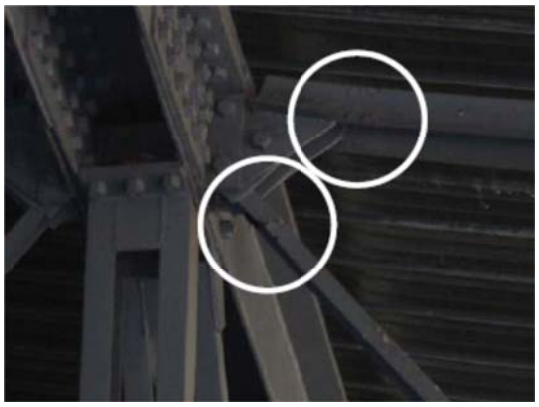

Figure 4.20 Plastic hinges at joints

The cantilever trusses, shown below, are divided into three meshes with beams, designed to absorb only the tensile stresses due to the dead loads and the load of the beam of the top rail of the portals. Due to wind actions, it is likely that the beams declined up with an inflection at the top rail of doors enough to untie themselves and to reverse them (Figure 4.21). The beams, designed to tensile stresses, have subjected to a compressive force greater than the critical one, so as to determine the buckling and, in one case, even the collapse (Camarda, 2006).

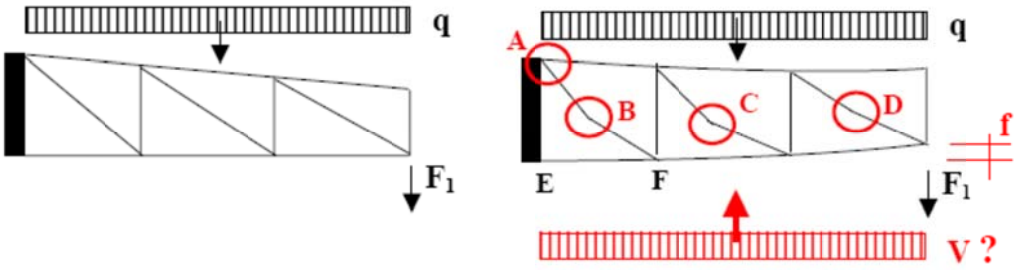

Figure 4.21 Cantilever truss and loading conditions

The daily maximum wind speed, recorded by the weather station located inside the airport, was characterized by the parameters of engineering interest shown in Table 4.3, where v_3 denotes the 3-second gust wind speed.

Table 4.3 Daily maximum wind speed recorded at Lecce (2006-09-26)

Time	Direction (°)	v_3 (m/s)
11:00	120	40.1

For a comparison, the hourly 10-minute averaged wind speeds v_{600} are also reported in Table 4.4.

Table 4.4 Hourly wind speeds and barometric pressures recorded at Lecce (2006-09-26)

Time	Direction (°)	v_{600} (m/s)	Barometric pressure (hPa)
10:00	100	13.4	1000
11:00	90	20.8	990
12:00	260	17.0	997

Therefore, it is clear that the wind blew from a directional orthogonal to the doors, as shown in the following figure.

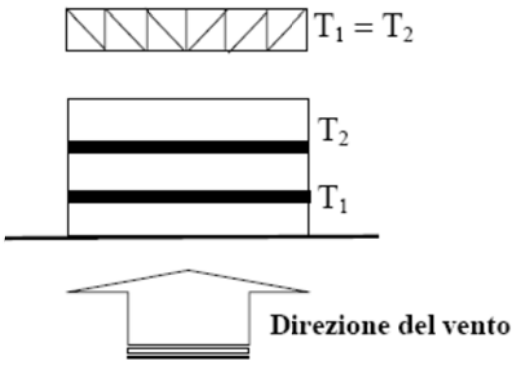

Figure 4.22 Wind direction with respect to the building orientation

4.4.1.3 Lecce 2009

On days 4th – 6th of March an extended meteorological phenomena, associated with a very active cold air core coming from North Atlantic, has affected all areas of central and western Europe and the Mediterranean Sea; heavy rainfall, snowfall, strong winds and sea storm occurred over the crossed areas. The winds, reinforced by the cold air advection, have intensified and veered to the west over Tyrrhenian regions while persisted from south over southern Adriatic and Ionian regions. On March 05th, 2009 there have been gusts from the south-west up to 80 Kts at Lecce Galatina airport. The comparison with the pre-event pictures shows that the phenomenon caused much more devastating consequences with respect to the event occurred on September 2006, although in both cases the weather instrumentation had reached the maximum value, equal to an instantaneous speed of about 40-41 m/s. In the Figure 4.23 and Figure 4.24, the anemograph and the barometric pressure graph are shown (Camarda, 2009).

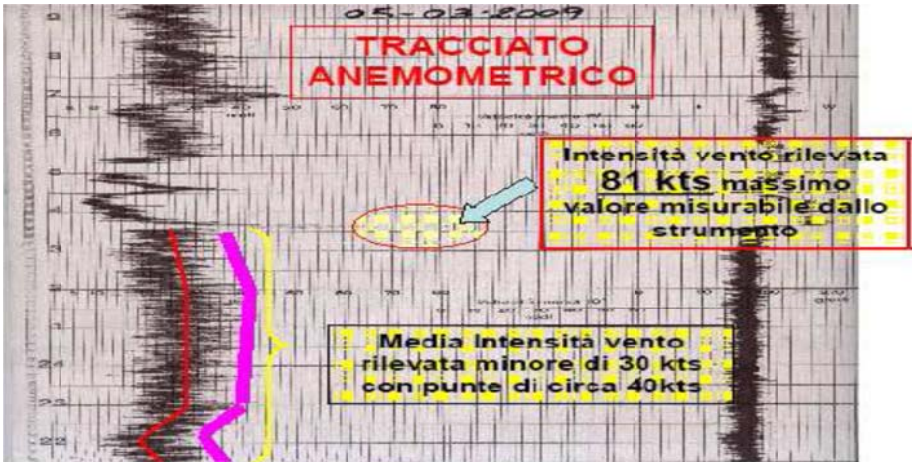

Figure 4.23 Anemogram at Lecce airport (2009-03-05)

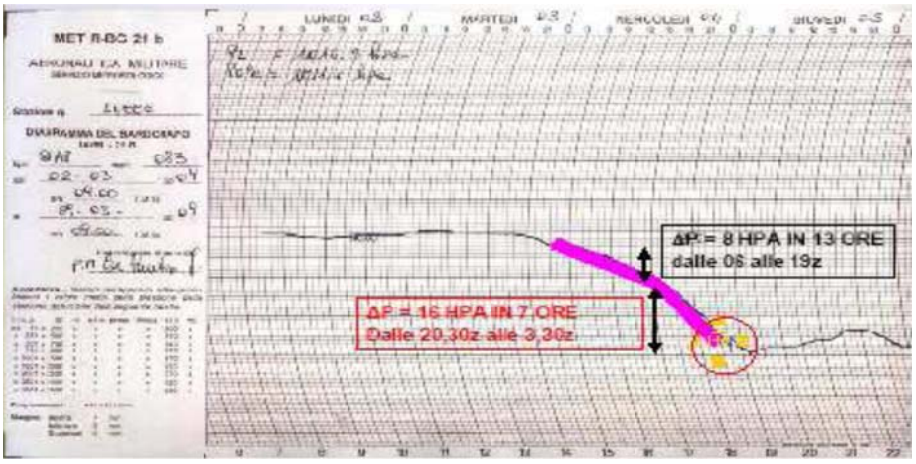

Figure 4.24 Barometric pressure graph

The most important damage to infrastructure were recorded again at the hangar no 29. Differently from the event of 2006, the most intense event blew from a not perfectly orthogonal direction with respect to larger building dimension (Figure 4.25).

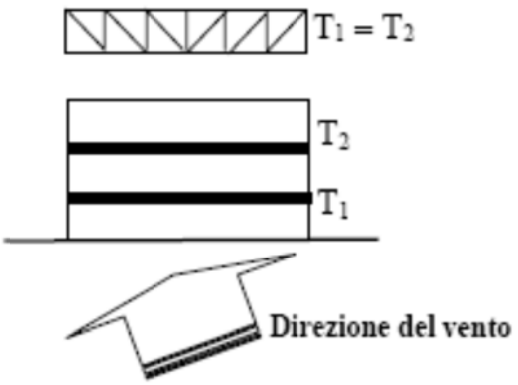

Figure 4.25 Wind direction with respect to building orientation

Upon the passage of the tornado, the structure had two opened doors, as shown in the Figure 4.26, and this caused important damages to the hangar (Figure 4.27).

Figure 4.26 The hangar no 29 before the event (Lecce 05-03-2009)

Figure 4.27 The hangar no 29 after the event (Lecce 05-03-2009)

The extreme event caused upward inflection of the roof, estimated in several centimeters, and this inflection caused the plasticization of several nodes and frames (Camarda, 2009), as shown in Figure 4.28, 4.30, 4.31 and 4.32.

Figure 4.28 Buckling of a steel frame

Figure 4.29 Structural damage to roof

Figure 4.30 Damages to the doors

Figure 4.31 Damages to column base connection

The Figure 4.30 shows the overturning of the doors due to the uplift of the roof and, maybe, to the too small distance security of the top rail of the doors, shown in the Figure 4.32

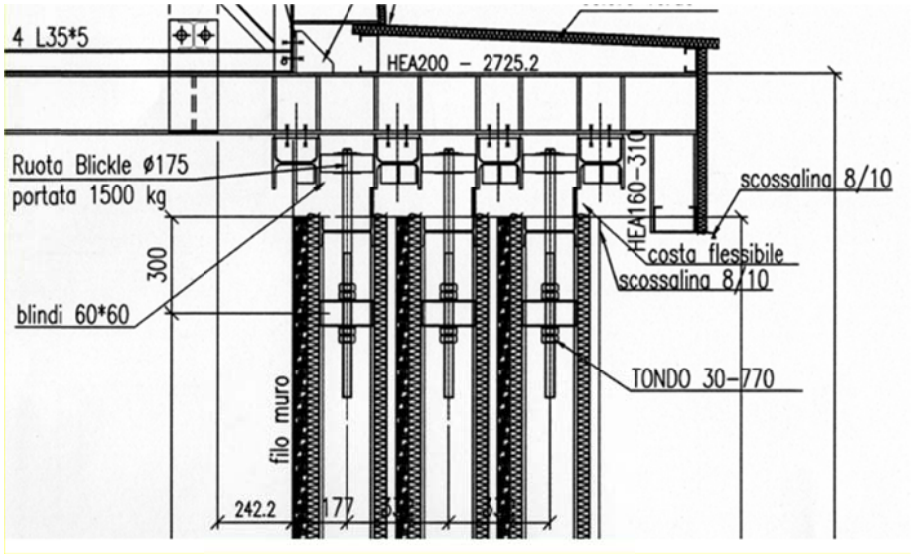

Figure 4.32 Detail of the top rail of the doors (Chiodi, et al., 2011)

Similarly to what was done previously, with respect to the shape of the hangar and the size and the position of the openings, it is interesting to simulate the ratio between the wind actions adopted by different Building Codes during the last

century and the structural weight, in order to study the evolution of the uplift actions (Figure 4.33)

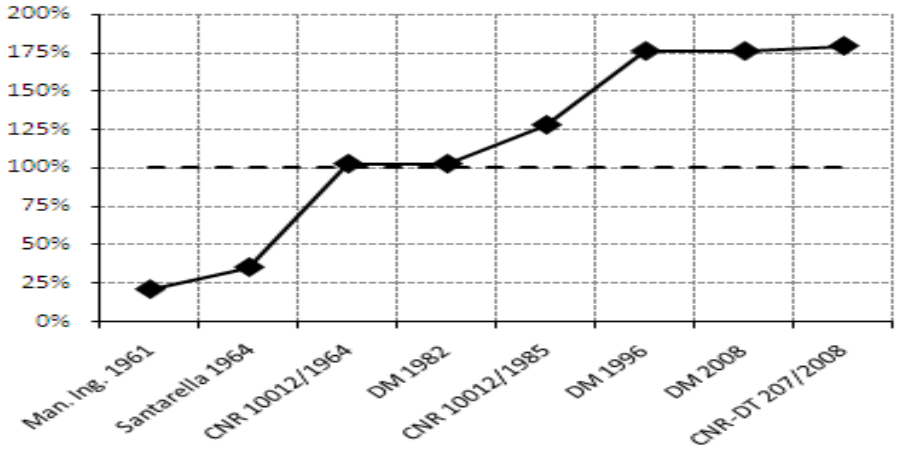

Figure 4.33 Evolution of uplift actions (building with a dominant opening)

5 AERODYNAMIC INTERACTION

Wind flow generates a spatially and temporally varying external pressure distribution on the external surface of a building. The pressure inside the building is dependent on this external surface pressure, the position and the size of all openings and the effective volume of the building. In conventional buildings, openings in the external skin tend to be small and distributed over all faces, unless there is a dominant opening; due to their particular use, the steel aircraft hangars have a dominant opening that allows increased internal pressures to occur. The study of the interaction between the internal pressures, external pressures and the building structural behavior can be very complex, and it is often impossible to determine some of the governing parameters with a high level of accuracy. In particular, the location and size of the openings significantly affect the flow characteristics of air through the structure envelope. In order to simplify the problem and to outline a model that describes pressures inside a building, it can be reasonable to consider some hypotheses about the distribution and size of the openings and to exclude the theoretical case of completely rigid and sealed buildings. Under these assumptions, one can identify two limiting cases: buildings, rigid or flexible, with uniform leakage and buildings, rigid or flexible, with a dominant opening. If a building has an opening area greater than or equal to three times the sum of areas of the remaining openings, then this can be considered as dominant opening with respect to the others. Under this condition, to assess the pressure inside the building, the contribution of inertia of the flow through the large opening has to be considered. It was demonstrated that a building with a single volume and a single opening behaves like a Helmholtz resonator in acoustics. Vice versa for uniform leakage, there is a large number of openings; but, provided these

are uniformly distributed, an approximate solution can be obtained by lumping them into two groups; one group with a total area including all openings on the windward surfaces (having positive external pressures), while the second group with a total area including all openings on the leeward and side surfaces (having negative pressures). With regard to flexibility of buildings, although for non-rigid buildings it is quite impossible to model the exact structural behavior, it may however be reasonable to consider a single component of the building such the roof to be flexible. Depending on degree of flexibility, real structures may behave in either a quasi-static or a dynamic manner. The first of these simplified but near real situations is considered next.

5.1 Internal pressure

Internal pressures, produced by wind action, are dependent on the external pressure field and the position and size of all openings connecting the exterior to the interior, and the effective volume of the building. The internal pressure in a nominally sealed building is generally small in magnitude compared to external pressures. However, the failure of a door or window in such a building will create a dominant opening and can generate large internal pressures in strong winds, and in combination with large external pressures acting in the same direction will result in large net pressures across the envelope causing failures. In many other cases, such as for industrial buildings or hangars for airport facilities, wind loads due to a dominant opening have to be taken into account because of typical large openings related to the use of the buildings. Holmes (Holmes, 1979) and Vickery and Bloxham (Vickery, et al., 1992) studied internal pressures in buildings with large openings. Ginger et al. (Ginger, et al., 1997) carried out full scale studies on internal pressure, and showed that the results compared favorably with theoretical analysis. Holmes (Holmes, 1979) described correct scaling requirements for model

studies, by applying dimensional analysis techniques. The non-dimensional parameters were used by Ginger and Kim (Ginger, et al., 2009) to derive relationships between fluctuating internal pressures and the external pressure at a dominant wall opening in terms of the sizes of volume and dominant opening. Further experimental studies at model scale were carried out by Ginger et al. (Ginger, et al., 2009), and indicated a range of values of discharge coefficient, k, for fluctuating flow through an opening, a critical parameter for the theoretical prediction of internal pressures. Internal pressure data specified in design standards are based on studies from a limited range of opening sizes and volumes, and a simple quasi-steady theoretical analysis. In most cases, reduced internal pressures are specified for designing large buildings without due consideration given to the sizes of potential dominant openings.

5.1.1 Rigid Buildings with a dominant opening

Internal pressure fluctuations in a nominally sealed building are generally small in magnitude compared to external pressures. However, the failure of a door or window on the building can create a dominant opening and generate large internal pressures in strong winds that contribute a significant proportion to the total design wind loads. Indeed, a dominant opening in a windward wall will generate large positive internal pressures during windstorms, which, in combination with large suction pressures on the roof, commonly causes building failures and is hence a governing design criterion for both cladding and structural components of a building. The fluctuating (and peak) internal pressures are dependent on the external pressure and the size of the opening and the size of the building volume. Holmes (Holmes, 1979), Vickery (Vickery, 1986), Vickery and Bloxham (Vickery, et al., 1992), and Stathopoulos et al. (Stathopoulos, 1984) studied the mean and the fluctuating internal pressures in buildings with windward and leeward openings using theoretical techniques and wind tunnel tests. In more detail, Holmes

approached the case of a single windward opening as a damped Helmholtz resonator. Inertia effects were found to produce resonance amplification in the response of the internal pressure to turbulent external pressures and to a step change in external pressure. Furthermore, Sharma and Richards (Sharma, et al., 2003) showed that Helmholtz resonance depends on wind flow direction and, in particular, that Helmholtz resonance under oblique wind flow produces an extremely strong response in internal pressure fluctuations, in comparison with that obtained under normal onset flow. However, these effects are unlikely to be of much practical significance except for the case of a sudden large opening occurring in a relatively rigid building.

The response of pressure inside a building is related to the external pressures and the air flow in and out of openings in the envelope. The unsteady discharge equation relates the flow Q through an opening of area A and the pressure drop Δp across the opening in the following equation:

$$\Delta p = \frac{1}{2} C_L \rho U_O^2 + C_I \rho \frac{\partial U_O}{\partial t} \sqrt{A} \tag{5.1}$$

Here $U_O = (Q/A)$ is the area-averaged velocity through the opening. The first term on the right hand side of Equation (5.1) represents the pressure drop due to separation while the second is that required to accelerate the flow through the opening. The loss coefficient C_L is equivalent to $1/k\text{^}2$, where k is the discharge coefficient used by (Holmes, 1979), and C_I is the inertial coefficient. The effective length of the slug of air accelerated through the opening is $\mathrm{l_e} = \mathrm{C_I}\sqrt{\mathrm{A}}$.

Vickery and Bloxham (Vickery, et al., 1992) indicated that C_L and C_I can only be theoretically determined for limited situations such as a sharp edged circular opening connecting two large volumes, where potential flow theory gives $C_L = ((\pi + 2)/\pi)\text{^}2 = 2.68$ and $C_I = \sqrt{\pi/4} = 0.89$.

An opening in the building envelope can be considered to be dominant if it is larger than the total background leakage area (i.e., porosity resulting from gaps in the envelope). A dominant opening can arise from an open window or from a breached wall panel. If the ratio of size of the dominant opening to total background leakage area exceeds 9:1, Vickery (Vickery, 1986) (Vickery, et al., 1992) showed that internal pressure fluctuations are not significantly influenced by the leakage, and a reasonable approach is to study the pressure in a sealed building with a single opening. In such cases, previous studies by Holmes and Ginger et al. have shown that the mean internal pressure equals the mean external pressure at the opening.

Holmes and Vickery derived the following equation, which describes the pressures in a Helmholtz resonator, to relate the variation of internal pressure in a building $C_{p_i}$with a dominant opening of area A, in termsof external pressure at the opening, C_{p_e}:

$$\frac{\rho C_I V_{IE}}{n\sqrt{A}p_0}\ddot{C_{p_\iota}} + \left[\frac{\rho V_{IE}\overline{U_h}}{2nkAp_0}\right]^2 \dot{C_{p_\iota}}\left|\dot{C_{p_\iota}}\right| + C_{p_i} = C_{p_e} \tag{5.2}$$

Where p_0 is the atmosphericpressure, n is the ratio of specific heats of air, V_{IE} is the effective internal volume of the building which also accounts for flexibility of the building envelope, and $\overline{U_h}$ is the mean wind speed at roof height, h.

The above equation can also be written in the following form (Vickery, et al., 1992):

$$\frac{1}{\omega_H^2}\ddot{C_{p_\iota}} + \left[\frac{\beta}{\omega_H}\right]^2 \dot{C_{p_\iota}}\left|\dot{C_{p_\iota}}\right| + C_{p_i} = C_{p_e} \tag{5.3}$$

Where

$$\omega_H^2 = \frac{n\sqrt{A}p_0}{\rho C_I V_{IE}} = \frac{a_s^2\sqrt{A}}{C_I V_{IE}} \tag{5.4}$$

$$\beta \approx \frac{1}{2}\sqrt{\frac{C_L}{C_I}}\cdot\frac{\overline{U_h}}{a_s}\cdot\sqrt{\frac{V_{IE}}{A^{3/2}}} \tag{5.5}$$

Here, $a_s = \sqrt{n \cdot p_0/\rho}$ is the speed of sound with $n = 1.4$ for an adiabatic process. The un-damped Helmholtz frequency is:

$$f_H^2 = \left(\frac{\omega_H}{2\pi}\right)^2 = \frac{1}{4\pi^2}\cdot\frac{a_s^2\sqrt{A}}{C_I V_{IE}} \tag{5.6}$$

5.1.2 Flexible building with a dominant opening

When the structural frequency of the building components (e.g. the roof) is considerably higher than the frequencies over the energy containing region of onset wind turbulence, the structure will respond in a quasi-static manner to applied loading (i.e. to envelope external and internal pressure). That is structural deflections can be assumed to be linearly related to the applied loading. Assuming that the flexibility of a typical building is concentrated in the roof, then the change in non-dimensional internal volume and its time derivatives can be represented by:

$$\upsilon = \frac{\Delta V}{V_0} = \frac{V - V_0}{V_0} = \frac{V}{V_0} - 1 = \frac{q}{k_b}\left(C_{p_i} - C_{p_{er}}\right) \tag{5.7}$$

$$\dot{\upsilon} = \frac{q}{k_b}\left(\dot{C_{p_\iota}} - \dot{C_{p_{er}}}\right) \tag{5.8}$$

$$\ddot{\upsilon} = \frac{q}{k_b}\left(\ddot{C_{p_\iota}} - \ddot{C_{p_{er}}}\right) \tag{5.9}$$

in which $C_{p_{er}}$ is the area-averaged fluctuating external roof pressure coefficient, and k_b isthe building bulk modulus defined as the ratio of increase in net pressure loading to volumetric strain. For an increase in internal pressure, Δq, Vickery (Vickery, 1986) estimated the bulk modulus of the building as:

$$k_b = \frac{\Delta q}{\frac{\Delta V}{V_0}} = \frac{unit\ pressure}{volumetric\ strain} = \frac{N}{\alpha}\left[\frac{q_V}{\frac{S_C}{H} + 2\left(\frac{S_F}{B} + \frac{S_F}{L}\right)\frac{q_V}{q_L}}\right] \tag{5.10}$$

Where S_C,S_F, B, H and L are shown in the Figure 5.1, q_V is the vertical live load, q_L is the lateral live load, $\alpha \cong 0.6$ is a deflection shape factor, $N \cong 180 \div 360$ for unfinished and finished buildings, respectively.

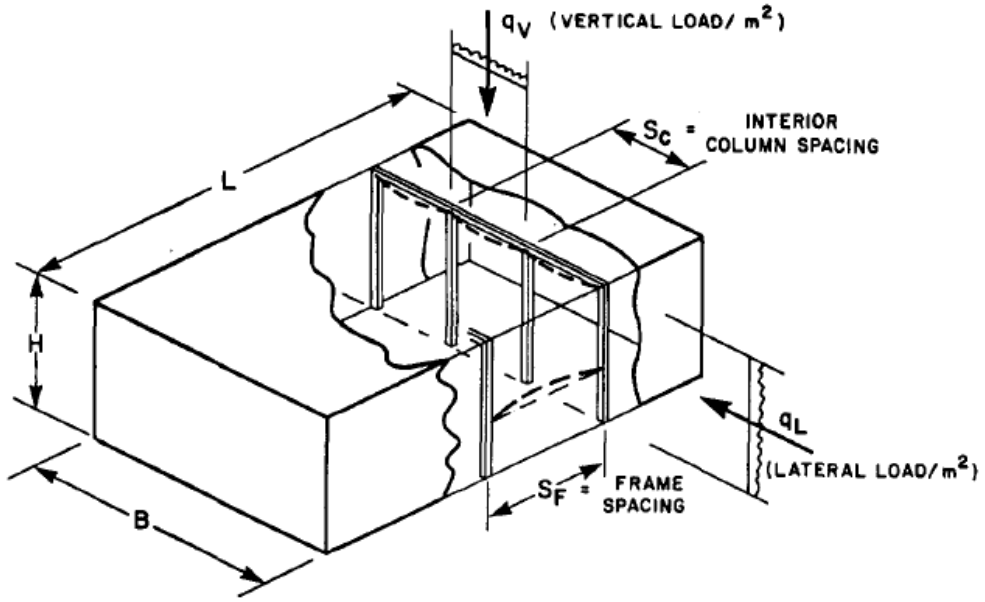

Figure 5.1 Definition of building dimensions and loads (Vickery, 1986)

The ratio of the building bulk modulus, k_b, to the bulk modulus of air, k_a, is:

$$\frac{k_b}{k_a} = \frac{N}{\alpha}\left[\frac{q_V}{\frac{S_C}{H} + 2\left(\frac{S_F}{B} + \frac{S_F}{L}\right)\frac{q_V}{q_L}}\right]\frac{1}{np_0} \tag{5.11}$$

The ratio can vary between 5 for stiff structures to 0.2 for flexible large span roof structures. Therefore, for buildings characterized by closely spaced columns, the influence of building flexibility is small since the pressure/volume relationship is determined primarily by the compressibility of the contained air. Vice versa the

dynamics of large span flexible roof systems are significantly influenced by the internal pressure.

If a building has an opening with a total area equal or greater than about twice the background leakage area then the internal pressure is very strongly dependent upon the external pressure at the opening. In this case a more satisfactory approach is to examine the equation of motion for a sealed building with a single opening. On these assumptions, following the quasi-static approach, the response of internal pressure in any flexible building can be shown to be governed by the equation (Sharma, 2008):

$$\begin{aligned}\frac{\rho C_I V_{IE}}{n\sqrt{A}p_0}\left(1+\frac{k_a}{k_b}\right)\left(\ddot{C}_{p_\iota}-\frac{k_a}{k_b+k_a}\ddot{C}_{p_{er}}\right)\\ +\left[\frac{\rho V_{IE}\overline{U_h}}{2nkAp_0}\left(1+\frac{k_a}{k_b}\right)\right]^2\left(\dot{C}_{p_\iota}\right.\\ \left.-\frac{k_a}{k_b+k_a}\ddot{C}_{p_{er}}\right)\left|C_{p_\iota}-\frac{\dot{k}_a}{k_b+k_a}\ddot{C}_{p_{er}}\right|+C_{p_i}=C_{p_e}\end{aligned} \tag{5.12}$$

This result describes the response of building internal pressure to a sudden opening when the roof structure responds in a quasi-static manner. It is different from the results obtained by Vickery and Sharma and Richards because the effects of external pressure on the flexible component have been included. The un-damped Helmholtz frequency f_H' can be obtained from the Eq. (5.4):

$$f_H'=\frac{\omega_H}{2\pi}=\frac{1}{2\pi}\frac{a_s\sqrt[4]{A}}{\sqrt{C_I V_{IE}}}\frac{1}{\sqrt{1+\frac{k_a}{k_b}}}=\frac{f_H}{\sqrt{1+\frac{k_a}{k_b}}} \tag{5.13}$$

Where f_H is the Helmholtz frequency for a corresponding rigid building. It can be pointed out that an increase of building flexibility results in a decrease in the

Helmholtz resonance frequency. However, an increase of building flexibility also means an increase of damping in the system.

When the effects of external pressure on the flexible component are not considered, the above equation becomes:

$$\frac{\rho C_I V_{IE}}{n\sqrt{A}p_0}\left(1+\frac{k_a}{k_b}\right)\ddot{C_{p_\iota}}+\left[\frac{\rho V_{IE}\overline{U_h}}{2nkAp_0}\left(1+\frac{k_a}{k_b}\right)\right]^2\dot{C_{p_\iota}}\left|\dot{C_{p_\iota}}\right|+C_{p_i}=C_{p_e} \qquad (5.14)$$

That is the formulation obtained by Vickery (1986).

5.1.3 Rigid leaky building

Vickery (Vickery, 1986) and Harris (Harris, 1990) analyzed the case of the nominally sealed building and showed that the external pressure fluctuations at frequencies above a characteristic frequency f_C are attenuated and not passed effectively into the building. Moreover, Vickery showed that the attenuation of internal pressures can result in a significantly reduced internal pressure gust factor compared to external pressure gust factors. Openings in nominally sealed conventional building envelopes tend to be small and uniformly distributed, and the inertia term is negligible compared with the damping term in Eq. (5.14). The mean internal pressure coefficient inside a building with total areas of windward openings, A_W, and leeward openings, A_L, can be derived by assuming the orifice flow relationship in and out of the openings and considering mass conservation:

$$\overline{C_{p_\iota}}=\frac{\overline{p_\iota}-p_0}{q}=\frac{\overline{C_{p_W}}}{1+\left(\frac{A_L}{A_W}\right)^2}+\frac{\overline{C_{p_L}}}{1+\left(\frac{A_W}{A_L}\right)^2} \qquad (5.15)$$

Where p_0 is the reference static (atmospheric) pressure, $\overline{C_{p_W}}$ and $\overline{C_{p_L}}$ are the external pressure coefficients at the windward and leeward openings, respectively, and

$$q = \frac{1}{2}\rho\overline{u^2} \tag{5.16}$$

is the reference dynamic pressure, with ρ density of air.

The response of internal pressure to changes in external pressure can be described by a characteristic frequency fc (Ginger, et al., 1997):

$$f_C = \frac{1}{2\pi}\cdot\left(\frac{np_0\sqrt{(A_W^2 + A_L^2)^2}}{\rho\sqrt{C_L}V_{IE}\overline{U_h}A_W A_L\sqrt{\Delta\overline{C_p}}}\right) \tag{5.17}$$

Here, area A_W includes all openings on the surfaces having higher pressures thanthe interior, area A_L includes all openings on the surfaces having lower pressures thanthe interior and $\Delta\overline{C_p} = \overline{C_{p_W}} - \overline{C_{p_L}}$ is the net mean pressure difference between thesewindward and leeward surfaces.

5.1.4 Flexible leaky building

The response of internal pressure to changes in external pressure can be described by a characteristic frequency fc (Vickery, 1986):

$$f_C = \frac{1}{2\pi}\cdot\frac{k_a}{1+\frac{k_a}{k_b}}\left(\frac{np_0\sqrt{(A_W^2 + A_L^2)^2}}{\rho\sqrt{C_L}V_{IE}\overline{U_h}A_W A_L\sqrt{\Delta\overline{C_p}}}\right) \tag{5.18}$$

The physical interpretation of the above equation is that external pressures with frequencies above f_C are attenuated and not passed effectively into the building through the leakage paths. Conversely, frequencies below f_C are transmitted through the skin but are attenuated if the bulk modulus of the building k_b is large compared to k_a.

5.2 Historical evolution of pressure coefficients

5.2.1 CNR-ACAI 1946 Reccomendations

The wind pressure was assumed to act statically in a direction normal to the surface of the structure or element and the internal and external pressure coefficients were given in Figure 5.2, captured from the Recommendations.

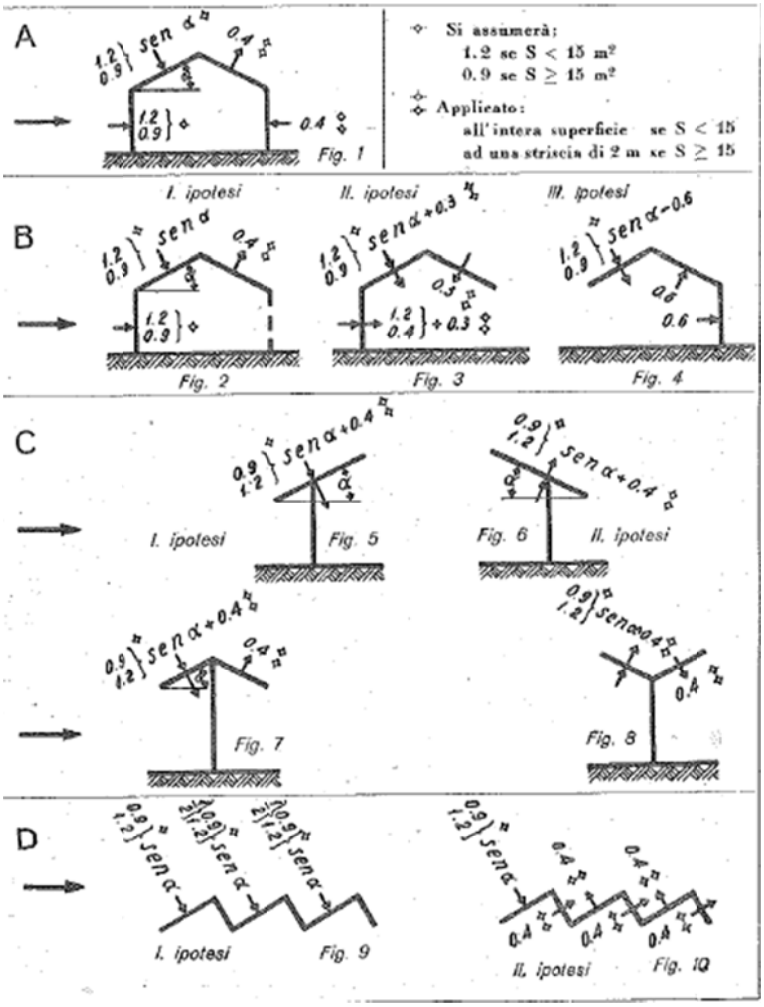

Figure 5.2 Pressure coefficients by CNR-ACAI (1946)

As partially shown in the Figure 5.2, some limit cases were defined corresponding to sealed buildings, buildings with a dominant opening, roofings and

others. Furthermore, the combined snow and wind loads condition had to be considered for design purposes.

5.2.2 CNR 1964-1967 Recommendations

An important improvement with respect to previous regulations was the better characterization of internal and external pressure coefficients, shown in the Figure 5.3.

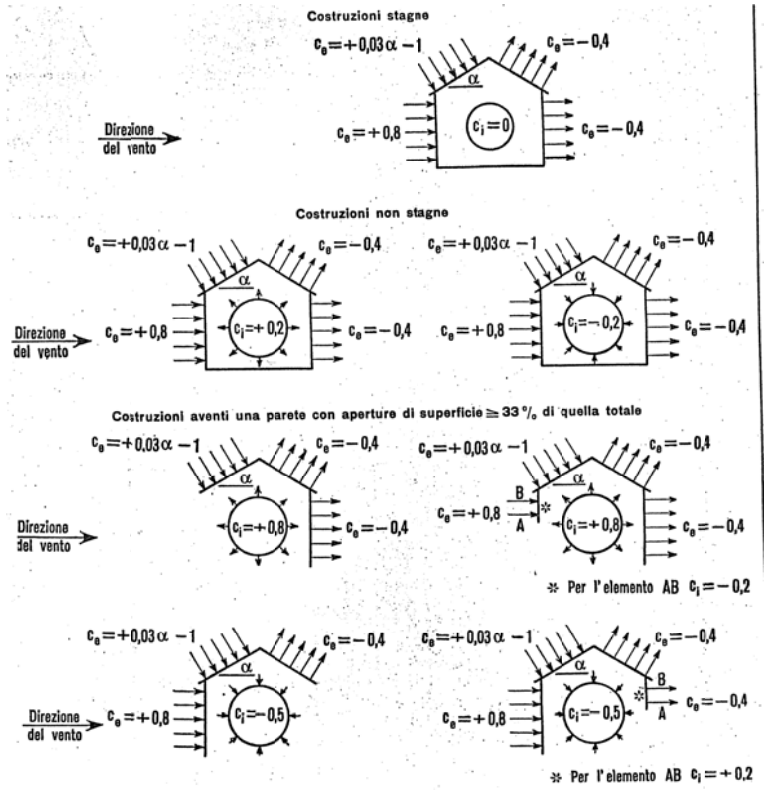

Figure 5.3 Internal and external pressure coefficients (CNR 1964-1967)

5.3 Design/assessment assisted by wind tunnel testing

The combination of tests and calculations is increasingly used due to the sophisticated architectural shapes and the absence of corresponding reliable fluid-dynamics models. Typically, the wind tunnel testing is used to check the

assumptions made in the design, especially with respect to complex aeroelastic phenomena, such as the lock-in, the flutter, the rain-wind induced vibration, etc. (Majowiecki, et al., 2010). However, it can also represent an useful tool for assessment of the existing structures, especially when these are historical buildings or strategic structures.

5.3.1 Proper Orthogonal Decomposition (POD)

The Proper Orthogonal Decomposition (POD) is a statistical method particularly suitable for dealing with many problems concerning wind engineering. The POD has been applied to optimally approximate the multi-variate random fields through use of low-order orthogonal vectors from modal decomposition of either zero-time-lag covariance matrix or cross spectral density one of this multi-variate random field (Hoa, 2009). According to type of basic matrix in the modal decomposition, the POD has been branched by either the Covariance Proper Transformation or the Spectral Proper Transformation. Main advantage of the POD is that the multi-variate random fields can be decomposed and described in such simplified way as a combination of a few low-order dominant eigenvectors (modes) and omitting higher-order ones that is convenient for order-reduced representation of the random fields, random force modeling and stochastic response prediction. In particular, the covariance matrix-branched POD and its transformation have been applied for analysis and synthesis of the random field, especially of dynamic surface field around low-rise and high-rise buildings as well as bridge girders. In fact, the structural response can be determined by separately evaluating the mean, the quasi-steady and the resonant response. The first term takes into account the mean pressure distributions, the second one is obtained by performing a classical covariance proper orthogonal decomposition and the third one takes into account the dynamic amplification of a suitable number of structural vibration modes, each one being excited by the unsteady wind pressures.

5.3.2 Covariance proper transformation

The multi-variate random fields can be represented in terms of a zero-time-lag covariance matrix, which are determined as follow:

$$R_v = \left[R_{v_j v_k}(0)\right] = \begin{bmatrix} R_{v_1 v_1}(0) & \cdots & R_{v_1 v_N}(0) \\ \vdots & \cdots & \vdots \\ R_{v_N v_1}(0) & \cdots & R_{v_N v_N}(0) \end{bmatrix} \tag{5.19}$$

Where R_v is the zero-time-lag covariance matrix, $R_{v_j v_k}(0)$ are the elements of the covariance matrix between $v_j(t)$ and $v_k(t)$ at nodes j, k, that are determined as follows:

$$R_{v_j v_k}(0) = E\left[v_j(t) v_k^T(t)\right] \tag{5.20}$$

Where E[] and T denote the expectation and transpose operators.

It is worth pointing out that the zero-time-lag covariance matrix is symmetric, real and positive definite.

The covariance matrix-based orthogonal vectors are found as the eigenvector solution of the eigen problem of the zero-time-lag covariance matrix R_v of the N-variate correlated random process $v(t)$:

$$R_v \Phi_v = \Gamma_v \Phi_v \tag{5.21}$$

$$\Gamma_v = \begin{bmatrix} \gamma_{v1} & 0 & 0 \\ 0 & \ddots & 0 \\ 0 & 0 & \gamma_{vN} \end{bmatrix} \tag{5.22}$$

$$\Phi_v = [\Phi_{v1} \quad \Phi_{v2} \quad \Phi_{v3}] = \begin{bmatrix} \phi_{v11} & \cdots & \phi_{vN1} \\ \vdots & \cdots & \vdots \\ \phi_{v1N} & \cdots & \phi_{vNN} \end{bmatrix} \tag{5.23}$$

Where Γ_v is the covariance matrix-based eigenvalue matrix, whose eigenvalues are $\gamma_{v1}, \ldots, \gamma_{vN}$, and Φ_v is the eigenvector matrix, whose columns are the eigenvectors $\Phi_{v1}, \ldots, \Phi_{vN}$.

Due to symmetric, real, positive-definite covariance matrix, thus the covariance eigenvalues are real and positive, and the covariance eigenvectors (also called as covariance modes) are also real, satisfy the orthogonal conditions:

$$\Phi_v \Phi_v^T = I \tag{5.24}$$

$$\Phi_v R_v \Phi_v^T = \Gamma_v \tag{5.25}$$

Then, the multi-variate correlated random process and its covariance matrix can be reconstructed approximately using i-order truncated number of low-order eigenvalues, eigenvectors as follows:

$$v(t) = \Phi_v x_v(t) \approx \sum_{i=1}^{\bar{N}} \phi_{vi} x_{vi}(t) \tag{5.26}$$

$$R_v = \Phi_v \Gamma_v \Phi_v^T \approx \sum_{i=1}^{\bar{N}} \phi_{vi} \gamma_{vi} \phi_{vi}^T \tag{5.27}$$

Where $x_v(t) = \{x_{v1}(t), \dots, x_{v\bar{N}}(t)\}^T$ is the low-order covariance principal coordinates as uncorrelated random subprocesses, $\bar{N} < N$ is the number of truncated covariance modes.

Finally, the covariance principal coordinates can be determined from observed data as follows:

$$x_v(t) = \Phi_v^{-1} v(t) = v(t) \Phi_v = \sum_{i=1}^{N} v_i(t) \phi_{vi} \tag{5.28}$$

6 PROPOSED METHODOLOGY FOR ESTIMATING WIND RISK

A methodology for estimating the annual risk of failure of steel structures under wind loads has already been proposed by (Duthinh, et al., 2008); this methodology accounts in a detailed and rigorous manner for nonlinear structural behavior and for the directionality of the wind speeds and the aerodynamic effects. The methodology uses databases of wind tunnel pressure, nonlinear finite-element analysis, and directional wind speeds from the National Institute of Standards and Technology (NIST) hurricane database augmented by statistical techniques. However, Duthin's methodology doesn't consider uncertainties with respect to the parameters governing wind loading and material performance and, moreover, the methodology has not been applied in a multihazard framework. A multihazard perspective allows to investigate more comprehensively the performance of structure and to optimize the design or the assessment. In this context, a probabilistic framework seems to be the more suitable tool to examine the performances under different and increasing levels of actions and, furthermore, it allows to numerically compare the behavior for many limit states.

The chapter focuses on wind risk assessment and, in order to perform a reliable multi-risk assessment or design, a review of Performance-Based Engineering is presented. In particular, the recent developments in the field of Performance-Based Wind Engineering can be an useful tool for performing probabilistic wind risk assessment. Accordingly to PBE approaches, a methodology for estimating wind risk in a probabilistic framework is then proposed.

6.1 Performance-Based Engineering

It is widely recognized that the most rational way of assessing and reducing the risks of buildings and infrastructures subjected to natural and man-made hazards is Performance-Based Design (PBD) or Performance-Based Engineering (PBE). The basic concepts of PBE have been formalized and applied in earthquake engineering and later they have been extended to other engineering fields, such as blast engineering, fire engineering and, more recently, wind engineering. The central objective of any procedure for Performance-Based design is the assessment of the adequacy of the structure through the probabilistic description of a set of decision variables DV. Each DV is a (quantitative) measure of a specific structural performance, that can be defined in terms of interest of the stakeholder or of the society in general.

Performance-based earthquake engineering aims at improving seismic risk decision-making through assessment and design methods that have a strong scientific basis and that express options in terms that enable stakeholders to make informed decisions. A visualization of performance-based earthquake engineering is shown in the Figure 6.1, where relations between structural response, performance-oriented descriptions (e.g. limit state such as Immediate Occupacy, Life Safety and Collapse Prevention) and loss estimation are outlined.

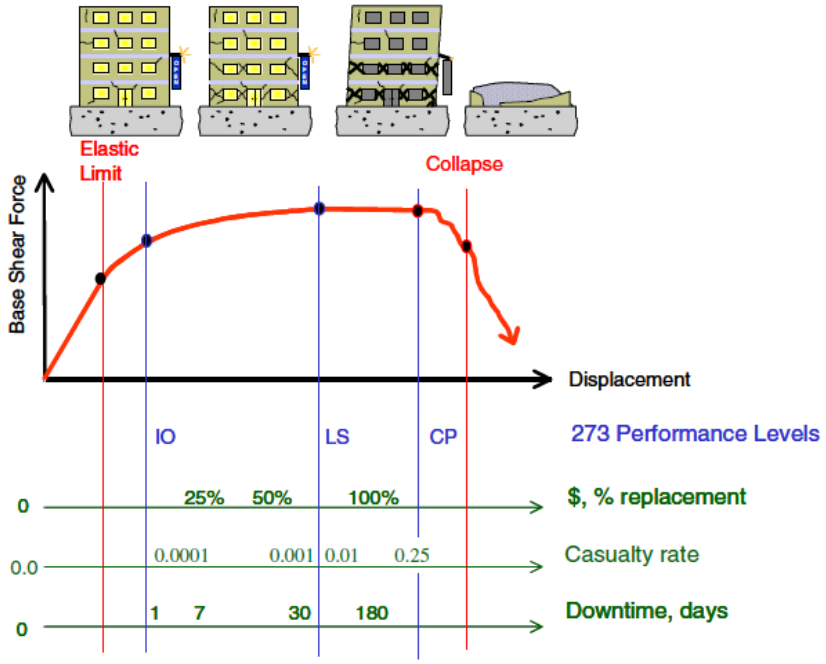

Figure 6.1 A visualization of PBEE (Moehle, et al., 2004)

A robust methodology for performance-based earthquake engineering has been developed by researchers at the Pacific Earthquake Engineering Research (PEER) Center (Cornell, et al., 2000) (Moehle, et al., 2004). Given the uncertainty and variability in seismic response, the PEER's framework is formalized within a probabilistic basis. Referring to Figure 6.2, PEER's probabilistic assessment framework is described in terms of four main analysis steps: hazard analysis, structural/nonstructural analysis, damage analysis and loss analysis. The outcome of each step is mathematically characterized by one of four generalized variables: Intensity Measure (IM), Engineering Demand Parameter (EDP), Damage Measure (DM) and Decision Variable (DV).

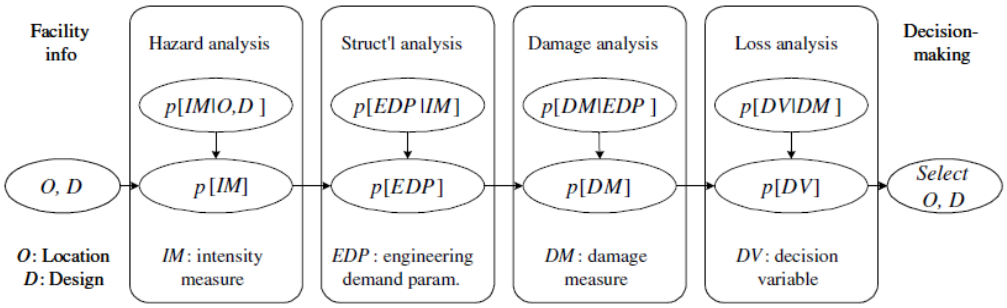

Figure 6.2 – PEER's framework for PBEE (Moehle, et al., 2004)

Recognizing the uncertainties involved, these variables are expressed in a probabilistic sense as conditional probabilities of exceedance by the formula:

$$\lambda(DV) = \int_{DM}\int_{EDP}\int_{IM} G(DV/DM)|dG(DM|EDP)||dG(EDP|IM)||d\lambda(IM)| \quad (6.1)$$

where IM denotes an intensity measure (e.g. the peak ground acceleration or the spectral acceleration at a selected period), EDP denotes an engineering demand parameter (e.g. an interstory drift), DM denotes a damage measure (e.g. the accumulated plastic rotation at a joint), DV denotes a decision variable (e.g. economic loss, duration of downtime), $G(x|y) = P(x < X|Y = y)$ denotes the conditional complementary cumulative distribution function (CCDF) of random variable X given Y =y, and$\lambda(x)$ denotes the mean rate of $\{x < X\}$events per year. Furthermore, similar formulas can be written for each of the intermediate measures. Specifically:

$$\lambda(DM) = \int_{EDP}\int_{IM} G(DM|EDP)|dG(EDP|IM)||d\lambda(IM)| \quad (6.2)$$

Gives the mean rate of the events $\{dm < DM\}$ in time, whereas:

$$\lambda(EDP) = \int_{DM} G(EDP|IM)|d\lambda(IM)| \tag{6.3}$$

Gives the mean rate of the events $\{edp < EDP\}$ in time. Implicit in these formulas is not only the stochastic nature of earthquakes, but also random and epistemic uncertainties present in describing the model of the structure and its environment.

Previous formulas are statements of the total probability theorem for the mean number of $\{dv < DV\}$, $\{dm < DM\}$, and $\{edp < EDP\}$ events per year, respectively. They are exact as long as the relevant conditional distributions shown in these formulas are identical for successive earthquake events. This implicitly assumes that the structure does not deteriorate and that it is instantaneously restored to its original state after each damaging earthquake. An important advantage of this approach is that it decomposes the task of assessing earthquake effects into the subtasks of seismic hazard analysis, $\lambda(IM)$, structural fragility analysis, $G(EDP|IM)$, damage analysis, $G(DM|EDP)$, and loss analysis, $G(DV|DM)$, each of which may be handled by a different group of experts. Although it is shown that the use of the formula to compute previous probabilities could lead to errors when non-ergodic variables (random or epistemic) are present (Der Kiureghian, 2005), the formula can be a very useful tool for design and assessment of structures. Indeed it can be used both for computing the mean annual rate of a performance measure exceeding a specific threshold and for computing the probability that a performance measure will exceed a specific threshold during a given period of time.

The first assessment step entails a hazard analysis, through which one evaluates one or more ground motion Intensity Measures (IM). For standard earthquake intensity measures (such as peak ground acceleration or spectral acceleration) IM is obtained through conventional probabilistic seismic hazard analyses. Typically, IM

is described as a mean annual probability of exceedance, $p(IM)$, which is specific to the location (O) and design characteristics (D) of the facility. In addition to determining IM, the hazard analysis involves characterization of appropriate ground motion input records for response history analyses.

Given IM and input ground motions, the next step is to perform structural simulations to calculate Engineering Demand Parameters (EDP), which characterize the response in terms of deformations, accelerations, induced forces, or other appropriate quantities. For buildings, the most common EDPs are interstory drift ratios, inelastic component deformations and strains, and floor acceleration spectra. Relationships between EDP and IM are typically obtained through inelastic simulations, which rely on models and simulation tools in the fields of structural engineering, geotechnical engineering, SSFI (soil-structure-foundation-interaction), and non-structural component and system response. PEER has developed various approaches, such as the incremented dynamic analysis technique (Vamvatsikos, et al., 2002), to systematize procedures for characterizing the conditional probability, $p(EDP|IM)$, which can then be integrated with the $p(IM)$, to calculate mean annual probabilities of exceeding the EDPs.

The next step in the process is to perform a damage analysis, which relates the EDPs to Damage Measures, DM. The DMs include quantitative descriptions of damage to structural elements, non-structural elements, and contents. This quantification must be relevant and in sufficient detail to enable subsequent quantification of the necessary repairs, disruption of function, and safety hazards.

The final step in the methodology is to calculate Decision Variables, DV, in terms that are useful to decision makers.

6.2 Performance-Based Wind Engineering (PBWE)

The procedure for Performance-Based Wind Engineering hereafter illustrated is an extension of framework developed at PEER Center and originally applied for PBEE. As stated in the introduction to the chapter, in the framework of Performance Based Engineering, decision variables DV have to be identified and estimated. In Wind Engineering examples of decision variables are the number of lives lost during windstorms, the economic losses resulting from windstorms, the exceeding of a (collapse or serviceability) limit state, the discomfort of the occupants, the length of the out-of-service time, etc.

The starting points of the procedure are the relationships, expressed in probabilistic terms, between the performances specific to the considered construction (collapse prevention, occupant safety, accessibility, full functionality, limited displacements or accelerations, etc.) and different intensities of the wind action, associated to different mean return periods. With reference to a specific performance, usually the structural risk is conventionally measured by the probability of exceeding a relevant value of the corresponding DV, and this probability of exceedance is expressed in terms of a mean annual frequency, that is evaluated by taking into account the wind hazard (i.e. the frequency of occurrence of wind actions of specified intensity and characteristics at the site), the structural response and damages, and the correlation between the attained damage level and the relevant DV. The structural design should be optimized by applying a decisional strategy to the risk analyses, with the objective of minimizing the total risk or of maximizing an utility function.

Alan G. Davenport's wind loading chain (Isyumova, 2011) is a good basis for formalization of Performance-Based Wind Engineering: the chain, shown in the Fig. 2.7, was in recognition that the evaluation of the wind loading and its effects relies on several interconnected considerations, each of which requires scrutiny and systematic assessment.

Figure 6.3 – Alan G. Davenport's wind loading chain

His approach was based on the chain of thought which recognized that the wind loading experienced by a particular building or structure is determined by the combined effects of the local wind climate, which must be described in statistical terms; the local wind exposure, which is influenced by terrain roughness and topography; the aerodynamics characteristics of the building shape; and the potential for load increases due possible wind-induced resonant vibrations (Isyumova, 2011). He also recognized that clear criteria must be in place for judging the importance of the consequences of the predicted wind action. This included the effects of wind on the integrity of the structure and the exterior envelope and various serviceability considerations, such as the control of the wind-induced drift, the effects of building motions on occupants and the usability of outdoor areas at and near particular buildings and structures. The chain approach permits systematic estimates of the statistical variability of the predicted wind action and, following Davenport's approach, a procedure of PBWE should consist of several steps aimed at:

1) defining the wind hazard at the site, in terms of wind intensity associated to different mean return periods and parameters of the wind velocity field taking into account terrain roughness and topography;
2) defining the models of the interaction phenomena and the relevant interaction parameters (aerodynamic response);
3) analyzing the structural response, mainly in the context of stochastic dynamics;
4) defining and evaluating indicators of the structural damage (intended as an unacceptable performance), considering performances related to safety and functionality or comfort;

5) defining the decisional variables that are appropriate to quantify the performances required for the structure, in terms of consequences of damage (personal damages, restoration costs, costs due to loss or deterioration of service, alterations of users comfort, etc.);
6) evaluating the structural risk by the probabilistic characterization of the decision variables;
7) optimizing design, that is minimizing risk, by appropriate techniques of decision analysis.

Ciampoli et al. (Ciampoli, et al., 2011) focused on a general presentation of the probabilistic procedure for the application of Performance-Based Design concepts to Wind Engineering and outlined the following steps:

1) The assessment of the wind hazard requires the use of efficient techniques for modeling wind actions and the choice of the intensity parameter vector IM whose stochastic characteristics are sufficient to describe satisfactorily and efficiently the Aeolian hazard at the site.
2) The probabilistic modeling of the interaction phenomena implies the choice and probabilistic characterization of a set of parameters, that allow to take into account the relevant aspects of the interaction between the environment and the structure.
3) The probabilistic modeling of the structural response requires the choice of the relevant engineering demand parameter vector EDP (accelerations and velocities of selected points, stresses and displacements, uplift of the roof, etc.).
4) The damage evaluation requires the choice (and probabilistic characterization) of the damage parameter vector DM, that is able to quantify the structural damage due to wind actions in relation to the considered performances. The choices of EDP and DM are strongly dependent on the considered structural type and performances. Different parameters can be assumed as DM: they can be defined by one or a combination of relevant EDPs, or by other parameters,

representing, for example for industrial buildings, exceeding of a specific threshold referred to uplift of the roof.

5) The decision variable DVs, that quantify the performances, must distinguish between low and high performance levels: the former (low performances) imply possible consequences on structural and personal safety (e.g. partial or total collapse, permanent damages); the latter (high performances) affect only serviceability and comfort (e.g. small displacements, limited vibrations, wind discomfort, also in the area around the structures). For low performances, the significant DV can be identified with the cost necessary to restore the construction to the undamaged state (or rebuild it in case of collapse); correspondingly, DM is the set of damages to be restored, and the EDP are the most significant response parameters for the specific case (peak displacement or acceleration at the building top, overall action at the base, local pressure, etc.). High performances are related to the users' comfort/discomfort and, in case of buildings, to inconvenient alterations of the wind field in pedestrian areas around the construction. Using the "limit states" approach (i.e. quantifying the structural risk by the probability of exceeding a limit state), ultimate limit states (ULS) are related to low performances (examples are the attainment of the capacity of any significant part of the structure, the fatigue collapse of some elements, the instability of parts or of the whole structure, etc.) while serviceability limit states (SLS) are related to high performances (examples are excessive deformations or vibrations compromising the use of the structure or its function in service).

   Appropriate relationships between any DM and the relevant EDP allow to evaluate the damage states corresponding to given values of the response parameter EDP, and also the resulting losses, taking into consideration the relationships between DM and DV. According to the usual definition of risk as the convolution of hazard, vulnerability and exposure, the relationships

between DM and DV take into account the exposure, that reflects the consequences of damage.

6.3 Effect of wind direction on structural reliability

There are many structures which are very sensitive to wind direction and, therefore, the wind direction has to be taken into account. For instance, Indeed, the wind direction for which the response to wind is most unfavorable does not necessarily coincide with the wind direction for which the wind speeds are strongest. Of course, the direction effect is most important when the structural resistance is highly direction-dependent or the winds show strong directionality, or both. However, wind loads depends on both the extreme wind speeds and the extremes of the wind-induced actions or action effects. For instance, external pressures coefficients strongly depend on flow wind direction; Generally, the complex interaction of the corresponding directionalities does not allow separating the two variables.

The effect of wind direction on structural reliability is studied by (Wen, 1984) as a problem of a vector wind force process outcrossing a structural resistance boundary which may be direction-dependent. In fact, if the structure resistance is direction dependent, it is necessary to treat the two horizontal components of the wind velocity as a vector process. Furthermore, (Rojiani, et al., 1980) established that the random dynamic oscillation contributes only a relatively small part in the overall uncertainty if compared with those due to mean wind velocity variation and structural and wind velocity environment parameter variabilities. Hence, the dynamic behavior can be neglected and the reliability problem can be formulated in the load (or mean wind velocity) space and is analytically much more tractable. In this approach the reliability is the direction-dependent resistance boundary not being outcrossed by the mean velocity process over a given period of time.

Davenport (Davenport, 1983) studied the effect of wind direction based on such an outcrossing analysis and concluded that there is a significant reduction in risk failure for direction sensitive structures compared with results based on a "worst direction" assumption commonly used in practice. The same conclusion was reached by Wen (Wen, 1984).

Three main methods are applicable to the estimation of wind directionality effects. They are (Vega-Ávila, 2008):

- the method of the one-dimensional sample of largest yearly wind effects;
- the sector-by-sector approach;
- the out-crossing of the limit-state boundary method;

The one-dimensional sample of largest yearly wind effects method is considered a simple yet rigorous estimation procedure in the calculation of extreme wind load effects based on directional properties of extreme winds, building aerodynamics and given building orientation. The method is based on the creation of a wind effect time-series from annual directional maxima wind speeds that have been previously allocated to directional sectors and allocation of a peak (or pseudo-steady) pressure coefficient to respective sectors for a predefined building orientation. After selection of peak (or pseudo-steady) loading coefficients C_p for each direction from wind-tunnel or full-scale measurements and extraction of wind speed annual maxima V for each direction from meteorological records that contain a large number of years (typically in the order of more than 20 years), the wind load effect can be calculated as a function of direction for a given building orientation. Then only maxima (or minima) wind load effect from all directions in each extreme wind event is extracted converting the multidimensional analysis into a "one-dimensional sample of largest wind effects"; the extreme value analysis is then rendered using such sample of wind effects to predict wind effect or speed at longer return periods used for design. A hidden limitation of the method is that it does not consider variations in the peak or pseudo-steady loading coefficients within a given sector and assumes deterministic

values (although for various directions) that assume the extreme wind speed occurs simultaneously with the maximum loading coefficient ever recorded. This consideration then opens the door to another possibility; namely for the second highest, or M-highest, wind speed in a year to occur with a higher loading coefficient, which in turn could produce a load effect unaccounted in the original method.

The second method, the sector-by-sector approach, is conceptually similar to the first one with the exception that extreme value analysis is done for each direction separately assuming data allocated in sectors is independent. The previous method, named 'one-dimensional sample of wind effects', only takes the maximum (positive) and minimum (negative) wind load effect to create two one-dimensional samples from where inferences are drawn directly for higher mean recurrence intervals irrespective of wind direction. The sector-by-sector approach retains the multi-dimensional information provided by the directionality of extreme winds and loading coefficients. In essence, it creates n number of one-dimensional samples where n is the number of sectors defined (often defined by limitations imposed by the data resolution).

In the third method, the out-crossing of the limit-state boundary method, the reliability is the direction dependent resistance boundary not being outcrossed by the mean velocity (vector) process over a given period of time. Davenport (Davenport, 1977) studied the effect of wind direction based on such an out-crossing analysis and concluded that there is a significant reduction in response level (or risk failure) for direction sensitive structures compared with the results based on a worst direction assumption commonly used in practice. Based on data on wind and wind pressure on buildings, (Simiu, et al., 1981) studied wind direction effects on cladding loads and found that the so-called worst direction approach may overestimate the design cladding load by a factor of two or more, and that an indiscriminate use of a factor of 0.8 for direction effect is not appropriate. The critical aspect of the out-crossing method is in the estimation of

the mean out-crossing rate. Determination of this rate requires a sound definition of the joint probability distribution of wind speed and direction and its derivatives in time (or alternatively knowledge of its frequency spectrum). If the joint probability distribution function of wind speed and direction is defined for the extreme winds and its derivative can be estimated as a function of time (based on independent events) then the method would be promising. Otherwise, the method as of right now uses information of the mean wind vector assuming it is a random stationary process. The current version of this method creates the joint probability density function of mean wind speed and direction from continuous records (i.e. also known as parent wind data), or using records that are strongly correlated in time. This method, without allowance for correlated data, has been compared to those derived from the theory of extremes and measurements, indicating that unacceptable discrepancies are found (Wen, 1984). Unless a sound validation of the method is given showing that extremes in the region are in fact defined from the parent population, this method is generally regarded as un-conservative and is not recommended according to (Simiu, et al., 2006).

In a probabilistic framework, the directional behavior of a structures can be investigated by using the total probability theorem; in fact, under the assumption of exclusiveness of events, the overall probability of failure P_f can be obtained by the following expression:

$$P_f = \sum_{\theta} P(EDP > DM|\theta) \cdot P(\theta) \tag{6.4}$$

Where $P(\theta)$ is the relative frequency of the wind events from the direction θ.

6.4 Probabilistic approach for multi risk assessment

The best way to characterize the randomness (variability) associated to physical processes is to perform a probabilistic analysis. In this framework, the probabilities

of the events are quantified probabilistically, i.e. using probability density distributions that reflect the uncertainty regarding the actual probability of the events. In other words, the uncertainty is a measure of the limited state of knowledge referred to the events. The development of scenarios introduces model assumptions and model parameters that are based on what is currently known about the physics of the relevant processes and the behavior of system under given conditions. It is important that both natural variability of physical processes (i.e. random or stochastic uncertainty) and the uncertainties in knowledge of these processes (i.e. epistemic or state of knowledge uncertainty) are properly accounted for. Important tools for developing quantitative approach to estimation of risk are Bayes' Theorem, which shows how to update a prior distribution over basic event probability to reflect new evidence or information, and Total Probability Theorem, which permits the decomposition of a specific probability into more tractable variable. In particular, the probability of failure P_f or $P(C)$ can be written as:

$$P_f = \sum_A P(C|A) \cdot P(A) \tag{6.5}$$

where A stands for a critical event, such as earthquake, wind, fire, blast, etc., $P(A)$is the probability of occurrence of event A and $P(C|A)$ is the probability of collapse due to A. Equation (6.5) is written, according to total probability theorem, assuming that the critical events A are mutually exclusive (i.e., they cannot occur simultaneously) and collectively exhaustive (i.e., all potential events A are considered). Terms in Equation (6.5) can be neglected if the rate of occurrence associated with the corresponding events is negligible. The de minimis risk v_{dm}, which defines the acceptable risk, is in the order of 10^{-7}/year (Paté-Cornell, 1994). Therefore, if the annual risk of occurrence of any critical event A is considerably less than the de minimis level, this event can be neglected. Hence, the multi-hazard acceptance criteria can be written as following:

$$P_f = \sum_A P(C|A) \cdot P(A) \leq v_{dm} \tag{6.6}$$

The above-mentioned criterion can be used for both probability based design and assessment of structures for collapse limit state. In particular, the methodology can take into account both wind and earthquake hazards.

The use of the load coincidence method for the analysis of structural reliability under the combination of multiple loads has been examined in (Pearce, et al., 1984). The authors stated that, for a general stationary stochastic process, an upper bound to the probability of failure in the interval (0,T) is given by:

$$P_f(T) \leq P_f(0) + \nu T \tag{6.7}$$

in which $P_f(0)$ is the probability of failure at t=0 and ν is the mean crossing rate of the failure surface. Under the assumption of Poisson's process, for two events, the probability of a given threshold being exceeded is expressed in the form:

$$P_f(T) \approx 1 - exp\{-(\lambda_1 P_1 + \lambda_2 P_2 + \lambda_{12} P_{12})T\} \tag{6.8}$$

in which λ_i is the mean rate of occurrences of *i*-th event, λ_{12} is the mean coincidence rate of occurrences of events, P_i is the conditional probability of the threshold being exceeded given the occurrence of *i*-th event and P_{12} is the conditional probability of exceeding the threshold given that two events happen. The rate λ_{12} for coincident wind and earthquake is small, therefore wind and earthquake may be treated as mutually exclusive and the Eq. (6.8) can be simplified. Under these assumptions, the annual frequency of collapse can be calculated by the expression:

$$P_f = \sum_E P(C|E)P(E) + \sum_W P(C|W)P(W) \tag{6.9}$$

where P_f stands for the annual rate of collapse,$P(E)$ and$P(W)$stand for the annual rates of occurrence of earthquake intensities and wind speeds, respectively. $P(C|E)$ and $P(C|W)$ represent seismic and wind fragilities. The summations used in Equation (6.9) refer to the disaggregation of both earthquake and wind hazard into different class of events. In particular, assuming the spectral acceleration Sa as the intensity measure of earthquake, the seismic contribution to total probability of failure is given by the expression:

$$P_f^E = P(E_D > E_C) = \sum_{Sa} P(E_D > E_C|E_D = Sa) \cdot P(E_D = Sa) \tag{6.10}$$

where E_D represents the seismic demand whereas E_C the seismic capacity.

With the same approach, assuming the wind speed Ws as the intensity measure of wind events, the wind contribution to total probability of failure is given by the expression:

$$P_f^W = P(W_D > W_C) = \sum_{Ws} P(W_D > W_C|W_D = Ws) \cdot P(W_D = Ws) \tag{6.11}$$

where W_D represents the wind demand whereas W_C the wind capacity.

The fragility of a structural system commonly is modeled using a lognormal distribution:

$$Fr(x) = \Phi\left[\frac{\ln(x) - \lambda_R}{\xi_R}\right] \tag{6.12}$$

where $\Phi[\blacksquare]$represents the standard normal cumulative distribution function, λ_R is the logarithmic median of capacity R and ξ_R is the logarithmic standard deviation of capacity R.

Although the seismic and the actions can be considered mutually exclusive and collectively exhaustive, some questions need to be raised. First of all, the risk consistency in the multihazard design aiming at estimation of reliable combined

probability of failure has to be investigated, in particular for design purposes. In this context, Duthinh and Simiu (Duthinh, et al., 2010) have determined that ASCE 7 Standard provisions on design of structures in regions subjected to strong winds and earthquakes can be unconservative. Moreover, another question of interest concerns the structural vulnerability; the issue of synergistic designs under multiple hazards was examined by Hayes et al. , who found that strengthening of the structure for seismic loads can improve performance under blast loads and progressive collapse resistance. On the other hand, Crosti et al. (Crosti, et al., 2011) have shown that the use of ductile connections, which improves performance under seismic loads, does not affect performance under strong winds.

6.5 Vulnerability and fragility curves

The structural vulnerability can be defined as the conditional probability of failure for a given set of input variables therefore vulnerability and fragility curves are both indicators of the capacity of a specified structure to withstand the actions. To develop each type of curve, the level of damage or damage state must be defined. For instance, with respect to wind vulnerability, one could identify damage states involving roof failure, doors failure, or some other type of failure. As stated, first of all, the Intensity Measures (IMs), the Engineering Demand Parameters (EDPs) and the Damage Measure (DMs) have to be defined. Once the distribution of damage is known over a range of intensity measures, the vulnerability for that type of structure can be determined. With respect to wind vulnerability, the Figure 6.4 shows the process of vulnerability curve generation from individual PDF sassociated with particular wind speeds.

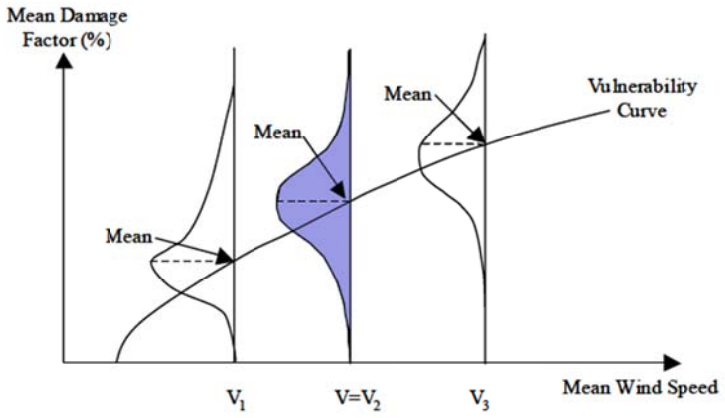

Figure 6.4 Vulnerability Curve (captured from (Cope, 2004))

Instead, the fragility curve provides the probability that a certain level of damage will be exceeded at a given wind speed and, therefore, it is calculated from the Vulnerability Curve shown above. The Figure 6.5 and Figure 6.6 allow to understand the generation of the fragility curves from the vulnerability curve.

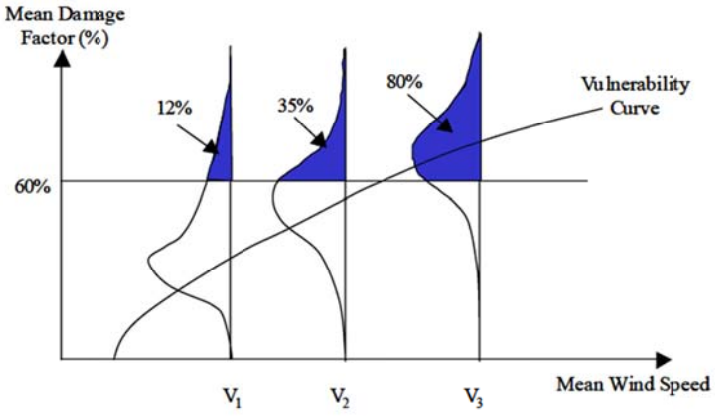

Figure 6.5 Fragility curve generation for 60% structural damage (captured from (Cope, 2004))

At each wind speed, the one's complement of the cumulative distribution functions (shaded areas in the Figure 6.5) become the data points for the fragility curve (Figure 6.6).

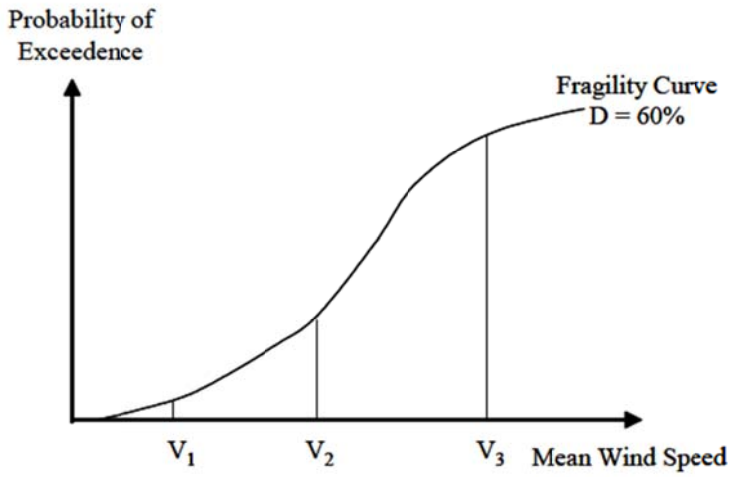

Figure 6.6 Fragility curve for 60% structural damage (captured from (Cope, 2004))

6.6 Overview of the proposed methodology

As widely mentioned previously, the shape, the openings and the structural type of a building can change significantly the aerodynamic interaction between the environment and the construction. Therefore, the knowledge of all these features is a necessary prerequisite for the use of the methodology as important as statistical treatment of recorded wind data. In this dissertation a methodology for assessing wind risk is proposed aiming at the evaluation of the annual probability of achievement a fixed limit state due to wind actions. In a multihazard framework, the resulting value can be compared with the same probability referred to seismic actions obtained by applying the IDA approach. The proposed methodology involves the following steps, each one associated to a particular ring of the Davenport's wind loading chain, as shown in the Figure 6.7:

1. Analysis of recorded data and correction to taking into account non-standard conditions in terms of roughness, orography and height of anemometer; this correction can be done by methods presented in the section 2.7;

2. When the recorded data are available in the form of 10-minute averaged wind speed, the directional statistical treatment is performed by means of methods illustrated in the Chapter 2; sometimes the data need correction in order to taking into account the effect of dowsampling, as illustrated in the section 2.9;
3. Estimation of peak wind speeds by means of Monte Carlo simulation; in fact, The peak wind velocity can be expressed as the sum of the mean velocity and the fluctuating time-dependent velocity by the expression:

$$v_p(t) = v_m + v'(t) \tag{6.13}$$

where $v_p(t)$ is the peak velocity, v_m is the mean velocity calculated by estimated weibull parameters, $v'(t)$ is the fluctuating time-dependent velocity, characterized by a normal distribution having mean 0 and variance:

$$\sigma_{v'} = v_m \cdot I_V \tag{6.14}$$

where I_V is the turbulence intensity.

4. Performing wind tunnel tests, the pressure fields around the building are obtained for all directions and configurations; the peak pressure coefficients can be estimated by means of the Cook and Mayne approach (Cook, 1990);
5. Approximation of the pressure fields by means of Proper Orthogonal Decomposition (POD), as illustrated in the section 5.3; in such way, the random fields can be decomposed and described as a combination of a few low-order dominant eigenvectors (modes);
6. Calculation of peak loads, each of them associated to a particular peak wind speed;
7. Definition of EDPs of interest;
8. Definition of DMs for each EDP defined;

9. Using non-linear finite element analysis, the wind speeds associated to the limit states of interest are calculated;
10. The fragility and vulnerability curves are obtained by count of the number of events associated to the achievement of the DMs for each EDPs; the fragility and vulnerability curves have to be evaluated for each directional wind speed;
11. The wind risk is obtained by the convolution of the hazard curves, estimated from steps 1 and 2, and the fragility curves, estimated by means of the steps from 3 to 10.

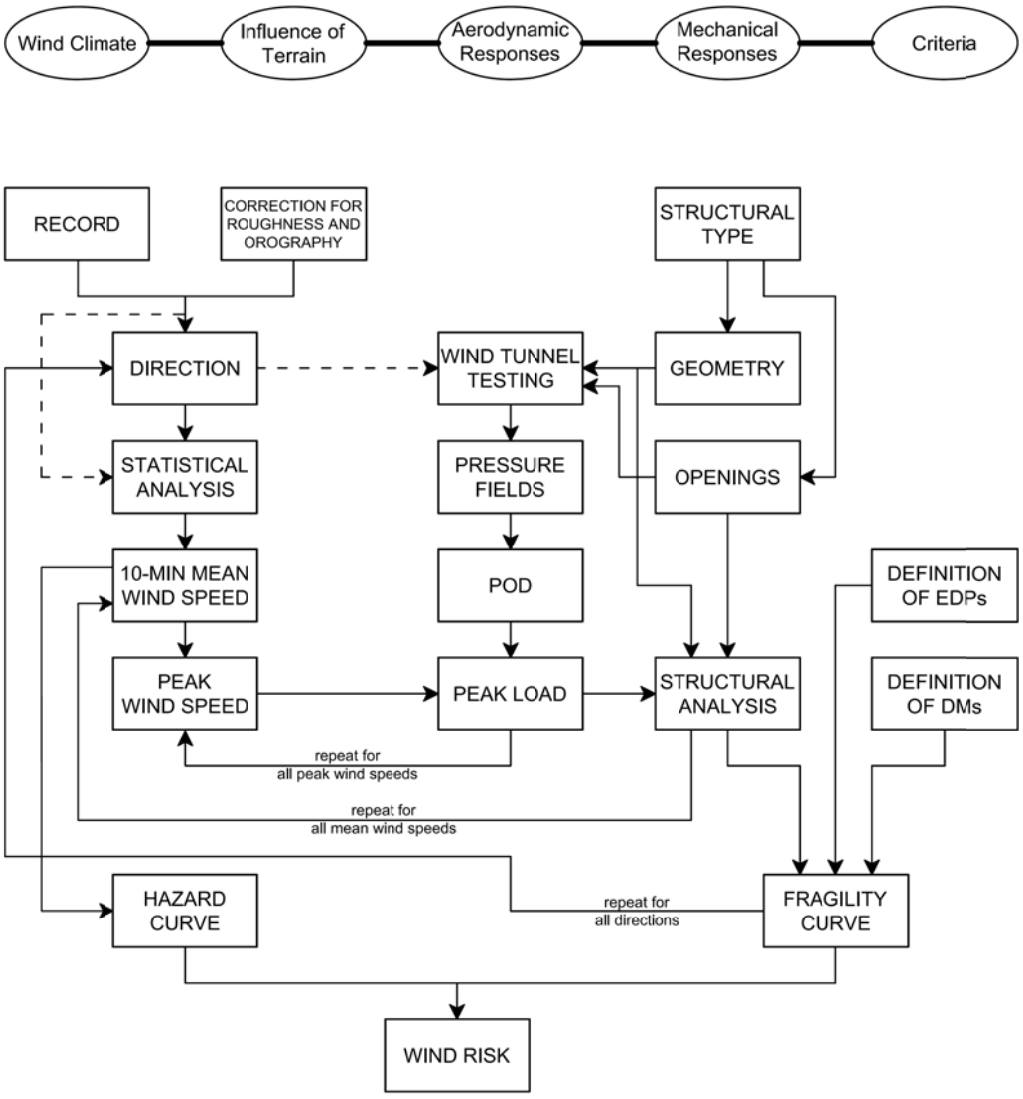

Figure 6.7 Methodology for evaluation of wind risk

The methodology can be subdivided into three main areas: one, on the left side of the Figure 6.7, refers to the estimation of wind hazard; another, on the right side, refers to the structural behavior of the structure; the last one, in the middle, denotes the interaction between the structure and the environment and contributes to the estimation of structural fragility. The summation of the products between the hazard and the fragility curves allow to estimate the annual risk associated to the

achievement of a specific limit state due to wind actions, as stated in the previous sections.

With respect to the “hazard area”, using the time series of the wind speed and direction, the methodology involves the steps described in the Chapter 2.

With respect to the “vulnerability area”, the structural type and the geometry are considered known information; they can be identified between those typologies defined in the section 4.3. The size and the location of openings significantly affect the behavior of structure and also the pressure fields. For this reason and in order to statistically evaluate the distribution of both external and internal pressures, the wind tunnel testing can be performed. Of course, the wind tunnel testing and POD technique allow to characterize the pressure fields and, therefore, to estimate wind loads as input for the structural analyses. In the framework of PBWE, Engineering Demand Parameters (EDPs) have to be defined, possibly related to the geometry and distribution of openings. For each of them, damage measures (DMs) that define different levels of performance have to be defined in order to estimate probability of failure associated to a specific wind speed.

7 APPLICATION OF THE METHODOLOGY TO A CASE STUDY

A possible application of the methodology described in the previous chapters can refer to steel hangars located in seismic zones. With respect to steel hangars located in Italy, the Country is one of the most seismic countries in the Mediterranean area, both in terms of frequency and intensity of earthquake occurrences; on the other hand, it's worth pointing out that the Italian wind climate is characterized by rather low annual average wind velocity, and moderately high extremes. In such situation, the contribution of the wind risk to the total probability associated to a specific limit state can be as important as the seismic risk. As discussed above, these events have to be examined to define a reliable prediction of extreme loads, and a probabilistic multi-hazard approach can be employed to investigate the performance of a structure under critical events and to ensure its acceptable performance during its entire lifetime. The seismic fragility is calculated by implementing an incremental dynamic analysis (IDA) using the method of multiple-stripe analysis (MSA) whereas the wind fragility is calculated by implementing an incremental static analysis by taking into account all possible failure mechanism induced by wind loads.

7.1 Case study 1

The calculation of annual seismic risk of collapse of a steel hangar belonging to Italian Air Force located in Rome Ciampino Airport is here presented. The hangar is characterized by six 12 m high circular steel-concrete composite columns and two 40x40 m wide truss gratings. Non-linearity is referred only to columns that are

divided into five parts, each one characterized by a specific moment-curvature relationship, depending on the axial force (Mander, et al., 1988). In the Figure 7.1 the refined finite element model of the structure in which steel trusses are modeled as frames is depicted. However, in this study, in order to evaluate the seismic fragility, the top floor has been modeled as a rigid diaphragms (Figure 7.2).

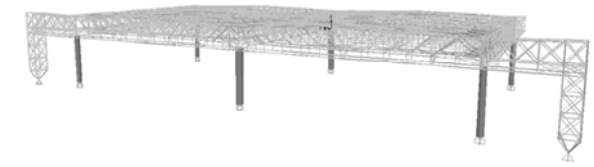

Figure 7.1 Model for determination of linear dynamic properties

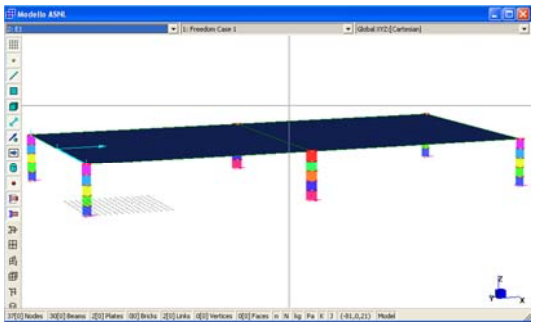

Figure 7.2 Model for non-linear response history analysis

7.1.1 Seismic hazard

The current zoning of the Italian territory in terms of seismic hazard has been defined starting from the criteria set up by Italian regulations; they establish that seismic areas are classified into 4 classes defined according to the maximum ground acceleration (a_{max}) having a 10% probability of being exceeded in 50 years. It also established the responsibility of the Regional Governments to modify the details of the distribution of the seismic hazard in each Region with respect to the

national map provided by the Italian Civil Protection Department. The responsibility for the National seismic hazard map has been given to INGV (Istituto Nazionale di Geofisica e Vulcanologia). The new seismic classification of the Italian territory has been compiled in terms of value of a_{max} referred to sites on rocks or very rigid soil (characterized by values of Vs30>800 m/s, including possible shallow altered layers with maximum thickness of 5 m). Conversely, identification of possible amplifications of ground acceleration due to local effects, is under the responsibility of the Regional Governments. The basic database used for the compilation of the new map of seismic hazard has been the Catalogue of Italian earthquakes (CPTI). The most recent version of such a catalog (CPTI2) was produced during the activity of the INGV Working Group, updating the older one with the inclusion of all the instrumental data available since 1999. Homogeneous values of magnitude were determined (Msp) for all the events in the Catalogue; these data were used in combination with empirical laws of energy attenuation with epicentral distance for the Italian territory (Sabetta, et al., 1996) to calculate expected ground acceleration in a given site. As required by the Italian regulations, evaluations of a_{max} were carried out using a grid of points with intervals of 0.05°; the results were given in units gravity acceleration (g), and represented by color strips with intervals of 0.025 g. The map representing the 90th percentile of the peak ground acceleration in the next 50 years is reported in Figure 7.3. It gives an overall picture of seismic hazard in the whole Italian territory where a_{max} ranges from a minimum of 0.03 g to a maximum of approximately 0.3 g.

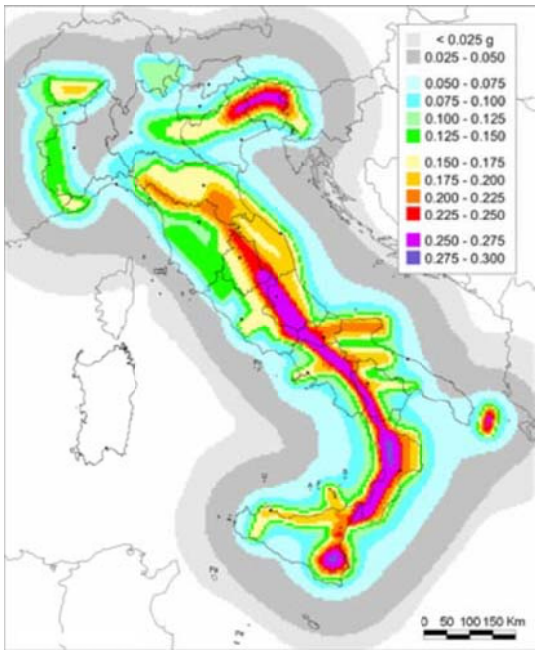

Figure 7.3 Seismic map of Italy representing the 90th percentile of the peak ground acceleration in the next 50 years

Seismic hazard has been characterized as the mean annual frequency of exceeding a given level of spectral acceleration at the fundamental period of structure. The hazard values are taken from the tabulated values in INGV, Italian National Institute of Geophysics and Volcanology, in which, the mean annual rate of exceeding an earthquake event of interest has been calculated using probabilistic seismic hazard analysis (PSHA) for the site of the structure. INGV has evaluated probabilistic seismic hazard foreach node of a regular 5 km spacing grid that cover the whole Italian territory with over 13000 nodes (Meletti, et al., 2007). The results are provided in hazard curves in terms of PGA and spectral acceleration, Sa(T), for ten different periods from 0.1 to 2 s. Hazard curves are lumped in nine probabilities of exceedance in 50 years (from 2 to 81%); all data can be accessed at http://esse1-gis.mi.ingv.it. These design spectra practically coincide with uniform hazard spectra (UHS) on rock for the site in question. In IDA approach the seismic motion

has been represented in terms of ground acceleration time-histories. Recorded accelerograms have been used provided that the samples are adequately qualified with regard to the seismogenetic features of the sources and to the soil conditions of the site. Their values are scaled from 0,1 g to 2 g and, in particular, a combination of seven accelerograms (Figure 7.4) compatible in the average with the reference spectra according to code criteria discussed above has been considered by using software REXEL (Iervolino, et al., 2009).

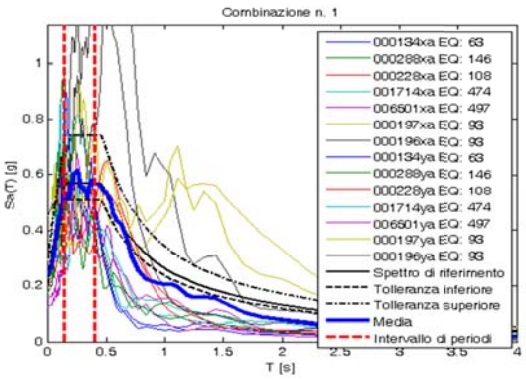

Figure 7.4 Selected Accelograms

7.1.2 Seismic vulnerability

Incremental Dynamic Analysis have been performed and the results in terms of multiple stripe and fragility curve are showed in the Figure 7.5 and Figure 7.6. The Figure 7.5 is plotted in log-log scale whereas the Figure 7.6 is plotted in linear scale. The maximum drift associated to the limit state of collapse is calculated by integrating the moment-curvature relationships and it is equal to 0,085 m, as denoted by black dashed line in Figure 7.6.

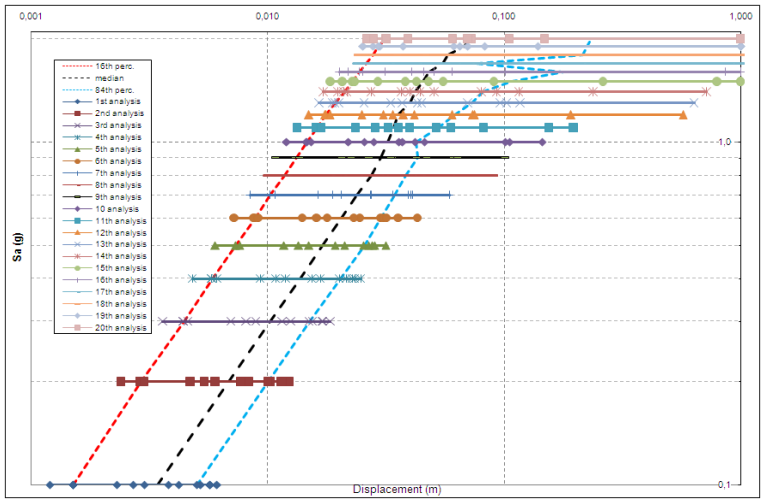

Figure 7.5 Results of IDA in terms of Multiple-Stripes

The black dashed line in Figure 7.5 denotes the median values of the stripes whereas the red and blue ones the 16th percentile and 84th percentile, respectively.

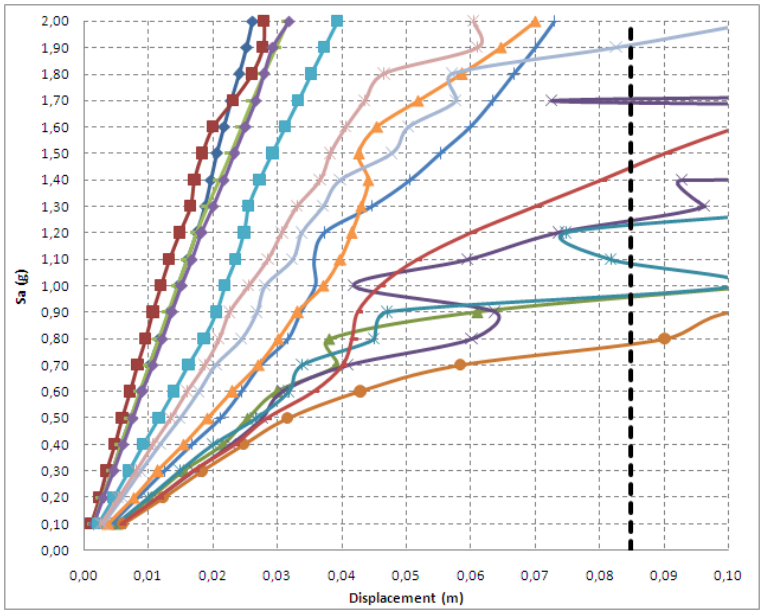

Figure 7.6 Results of IDA in terms of Accelograms

In Figure 7.6 each line represents the analyses performed for each accelerogram from 0,1 g to 2 g. It can be noted that some of them do not have a monotonically increasing trend and some others do not reach the maximum drift threshold.

Seismic fragility is depicted in Figure 7.7, where the blue line and red line are referred to the cases in which the median value and the mean value have been assumed as stripe parameter, respectively.

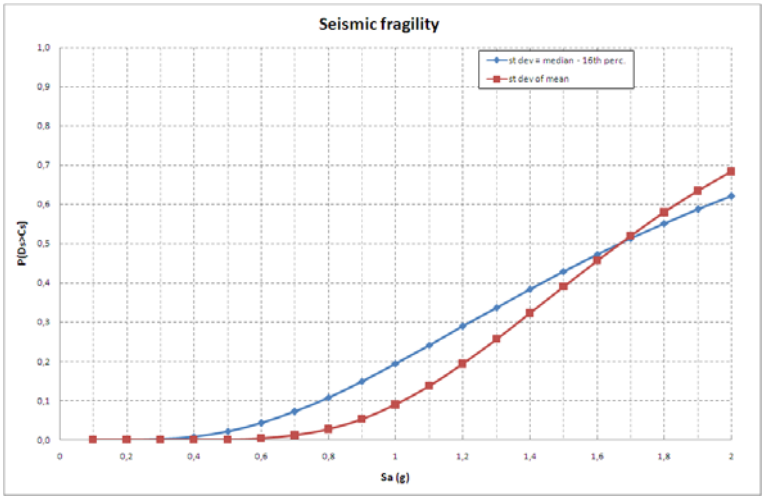

Figure 7.7 Seismic fragility

Integrating the seismic fragility curve and the seismic hazard curve, the annual frequency of collapse referred to seismic risk for the structure has been calculated and it is equal to $7{,}9*10^{-5}$, assuming the median value of stripe.

7.2 Case study 2

The framework for estimation of the annual wind risk of collapse of a steel hangar belonging to Italian Air Force located at Pisa Airport is here presented. The steel aircraft hangar is characterized by a structural type 2, as defined in the section 4.3. The hangar was built in forties and is 102x36 m wide and it has a height equal to 13.5 and 16 m on front and at the peak, respectively. The doors are 9 m high.

7.2.1 Wind hazard

The hourly wind speed data for the period 1951-2010 (60 years) recorded by Climate Department CNMCA of Italian Air Force are adopted herein to calculate the more reasonable value of wind loads at the site of the structure. The anemometer position has been constant throughout that period and the height of the anemometer head has always been the standard meteorological value of 10 m. The probabilistic approach has been conducted with the asymptotic analysis (Lagomarsino , et al., 1992) considering the annual maxima according to the Gringorten method. The results of the omnidirectional analysis with Gringorten method are shown in terms of probability of exceedance for different values of wind speed in Figure 7.8.

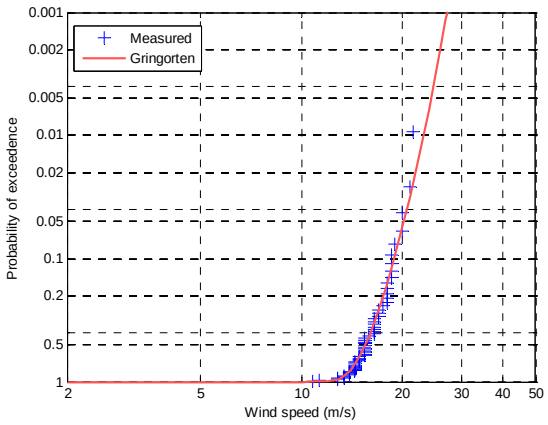

Figure 7.8 Omnidirectional wind hazard for Pisa Airport

Further information for a refined estimation of the directional wind risk can be found in the appendixes.

7.2.2 Wind vulnerability

In order to complete the calculation of the wind contribution to the risk of collapse, the failure mechanism induced by wind loads have to be analyzed. In fact wind loads can induce collapse for instance by the uplift of the roof, by the yielding of the steel frames or by the failure of the steel joints. Following the methodology proposed in this work, the results of wind tunnel testing are needed. The experimental tests have been performed in

the boundary layer wind tunnel of CRIACIV, in Prato, Italy. This is an open circuit wind tunnel with a working cross section 2.4 m wide and 1.6 m high and total length 11 m. The model has been realized in 1:200 scale and different arrangements have been used to simulate the dominat opening and the uniform leakage (Figure 7.9 and Figure 7.10).

Figure 7.9 Model tested without openings

Figure 7.10 Model tested with a dominant opening

For example, the external pressure fields for the model tested with a dominant opening and without openings are shown in the Figure 7.11 and Figure 7.12, respectively.

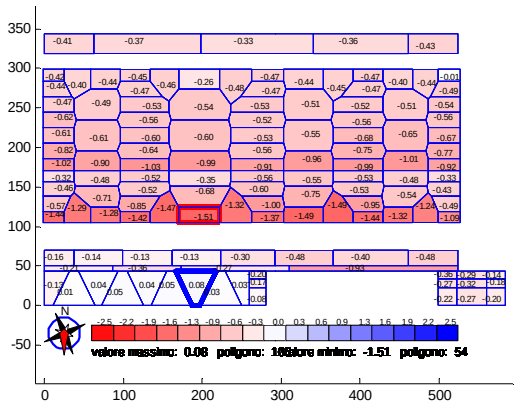

Figure 7.11 Example of the external pressure fields for model with a dominant opening

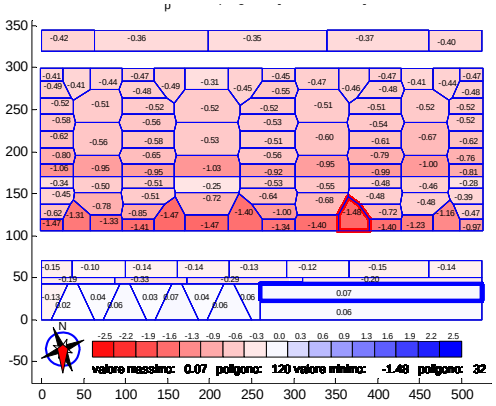

Figure 7.12 Example of the external pressure fields for model without openings

Once the pressure fields are known, the POD technique can be performed and the wind risk can be evaluated.

8 CONCLUSIONS

A general methodology for calculating the annual wind risk associated to different limit states is proposed. The methodology can be employed in a multihazard perspective in order to investigate the performance of a structure under critical events and to ensure its acceptable performance during its entire lifetime. In particular, this thesis focuses on the case of steel aircraft hangars subjected to both seismic and wind actions. This is so true in Italy that is one of the most seismic countries in the Mediterranean area, both in terms of frequency and intensity of earthquake; on the other hand, the wind climate is characterized by rather low annual average wind velocity and moderately high extremes. These actions can reasonably considered uncorrelated and, therefore, the design can be carried out separately. The problem is approached in a probabilistic framework due that the uncertainties affect the wind field, the structural response and also the aerodynamic interaction between the environment and the structure. A preliminary (and not complete) statistical treatment of recorded data on the whole Italian country is performed by using the most common criteria adopted in wind engineering; if integrated with correction for non-standard condition in terms of orography, roughness and height of the anemometer, the results of statistical treatment of recorded data could form the basis for an upgrade of the present Italian extreme wind map. However, the work still represent the basis for risk assessment and wind hazard. From the preliminary results presented here, it's worth pointing out that the sampling period of the mean wind speed affects the parameters of the Gumbel distribution of the maxima, therefore of the design wind speed, and an underestimation of extreme wind speeds is observed. Furthermore, it's clear that

the Gumbel distribution is conservative for the evaluation of the design wind speeds and, in most of the cases, it overestimates it by a small percentage, but the error is in some cases greater than 20%, if compared with the results of the GEV distribution. On the other hand, the Weibull distribution is not conservative for the evaluation of the design wind speeds. Moreover, the directional and seasonal characteristics of the wind climate are evident, that it would be desirable to take into account when evaluating the design wind speed.

The structural vulnerability is examined reviewing properties of materials, structural details and structural types adopted in the past for steel hangars, that are considered as representative wind-exposed structures. The attention is focused on historical evolution of structural types and adopted design standards; some failure cases which occurred during the last years due to extreme wind events are illustrated. Hence the main elements of vulnerability are discussed.

Furthermore, the aerodynamic interaction is investigated; the role of the location and size of the openings is outlined and, in particular, the main theories about the propagation of the internal pressure due to a dominant opening are examined. The proposed methodology involves the characterization by wind tunnel testing and some results are briefly mentioned in the Chapter 7, where two applications of multihazard framework are presented.

Finally, by integrating the structural fragility and the hazard for the site, the methodology gives a numerical evaluation of the probability of achievement a specific limit state or threshold and, hence, provides a tool for assessment and retrofit of existing structures and for design of new structures.

REFERENCES

An Ying e Pandey M.D. A comparison of methods of extreme wind speed estimation [Rivista] // Journal of Wind Engineering and Industrial Aerodynamics, vol. 93. - 2005.

Augusti Giuliano e Ciampoli Marcello Performance-Based Design in risk assessment and reduction [Rivista] // Probabilistic Engineering Mechanics vol.23. - 2008. - p. 496–508.

Augusti Giuliano, Borri Claudio e Niemann Hans-Jurgen Is Aeolian risk as significant as other environmental risks? [Rivista] // Reliability Engineering and System Safety, vol. 74. - 2001. - p. 227-237.

Ballio Giulio [et al.] A first step towards a map of Italian extreme winds. Part 1: General Principles and analysis methodology [Rivista] // Costruzioni Metalliche, vol. 3. - 1991a. - p. 147-17.

Ballio Giulio [et al.] A first step towards a map of Italian extreme winds. Part 2: Results, ripercussion on standards, design implications. [Rivista] // Costruzioni Metalliche, vol. 4. - 1991b. - p. 209-242.

Ballio Giulio [et al.] Probabilistic analysis of Italian extreme winds: Reference velocity and return criterion [Rivista] // Wind and Structures, vol. 2. - 1999. - p. 51-68.

Bartoli Gianni, Ricciardelli Francesco e Solari Giovanni Historical evolution of Italian Regulations on wind actions on structures and its implication on the design of steel structures [Atti di convegno] // XXIII Congresso C.T.A. - Le giornate italiane della costruzione in acciaio. - Lacco Ameno, Ischia (NA), Italy : [s.n.], 2011.

Camarda Donato 61° Stormo Lecce - Eventi meteorici eccezionali del 26-9-2006. Relazione manufatto n.29 di P.G. [Rapporto]. - 2006.

Camarda Donato B.A. Lecce - Eventi meteorologici eccezionali del 5 marzo 2009 (in Italian) [Rapporto]. - 2009.

CEN Eurocode 1: Actions on structures - Part 1-4: General actions – Wind actions. EN 1991-1-4:2005 [Rapporto]. - 2005.

CEN Eurocode 1: Basis of design and actions on structures - Part 2-4: Actions on structures – Wind Actions. ENV 1991-2-4:1994 [Rapporto]. - 1994.

CEN Eurocode 3: Design of steel structures - Part 1-9: Fatigue. prEN 1993-1-9 [Rapporto]. - 2003.

Chen Xinzhong e Kareem Ahsan Proper Orthogonal Decomposition-Based Modeling,Analysis, and Simulation of Dynamic Wind Load Effects on Structures [Rivista] // Journal of Engineering Mechanics, Vol. 131. - 2005. - p. 325-339.

Chiodi Remo [et al.] Steel hangar structures belonging to Air Force and vulnerability to wind actions [Atti di convegno] // XXIII Congresso C.T.A. - Le giornate italiane della costruzione in acciaio. - Lacco Ameno, Ischia (NA), Italy : [s.n.], 2011.

Chiodi Remo [et al.] Updated statistical analysis of Italian extreme wind speeds [Atti di convegno] // 13th International Conference on Wind Engineering. - Amsterdam, The Netherlands : [s.n.], 2011.

Ciampoli M., Petrini F. e Augusti G. Performance-Based Wind Engineering: Towards a general procedure [Rivista] // Structural Safety vol. 33. - 2011. - p. 367-378.

CNR Istruzioni per la valutazione delle azioni e degli effetti del vento sulle costruzioni. CNR-DT 207/2008 [Rapporto]. - 2008.

CNR Istruzioni per la valutazione delle azioni e degli effetti del vento sulle costruzioni. CNR-DT 207/2008 [Rapporto]. - 2008.

CNR Norme CNR 10012 - Azioni sulle costruzioni (in Italian) [Rapporto]. - 1981.

CNR Norme CNR 10012 - Istruzioni per la valutazione delle azioni sulle costruzioni (in Italian) [Rapporto]. - 1985.

CNR Norme CNR-UNI 10012 - Ipotesi di carico sulle costruzioni (in Italian) [Rapporto]. - 1964.

CNR Norme CNR-UNI 10012 - Ipotesi di carico sulle costruzioni (in Italian) [Rapporto]. - 1967.

CNR-ACAI Istruzioni per il calcolo, l'esecuzione e la manutenzione delle costruzioni metalliche (in Italian) [Rapporto]. - Milano, Italy : Associazione fra i Costruttori in Acciaio Italiani, 1946.

Coffman Bradley F. [et al.] Wind Effects on Low-Rise Metal Buildings:Database-Assisted Design versus ASCE 7-05 Standard Estimates [Rivista] // Journal of Structural Engineering, Vol. 136. - 2010. - p. 744-748.

Cook N.J. Note on directional and seasonal assessment of extreme winds for design [Rivista] // Journal of Wind Engineering and Industrial Aerodynamics, vol. 112. - 1983. - p. 365-372.

Cook N.J. The designer's guide to wind loading of building structures. Part 2: Static structures [Libro]. - London : Butterworths, 1990.

Cook N.J. Towards better estimation of extreme winds [Rivista] // Journal of Wind Engineering and Industrial Aerodynamics, vol. 9. - 1982. - p. 295-323.

Cook Nicholas J. Confidence limits for extreme wind speeds in mixed climates [Rivista] // Journal of Wind Engineering and Industrial Aerodynamics, vol. 92. - 2004. - p. 41–51.

Cook Nicholas J., Harris R. Ian e Whiting Richard Extreme wind speeds in mixed climates revisited [Rivista] // Journal of Wind Engineering and Industrial Aerodynamics, vol. 91. - 2003. - p. 403–422.

Cope Anne D. Predicting the vulnerability of typical residential buildings to hurricane damage [Libro]. - 2004.

Cornell C.A. e Krawinkler H. Progress and challenges in seismic performance assessment. [Online] // PEER Center News, Spring. - 2000. - http://peer.berkeley.edu/news/2000spring/index.html.

Crosti Chiara, Duthin Dat e Simiu Emil Risk Consistency and Sinergy in Multihazard Design [Rivista] // Journal of Structural Engineering, vol. 137. - 2011. - p. 844-849.

D'Aniello Mario [et al.] Experimental analysis of riveted connection in historic metallic structures. [Sezione di libro] // Protection of Historical BUildings, PROHITECH 09 / aut. libro Mazzolani. - London : Taylor & Francis Group, 2009.

Davenport A.G. On the assessment of the reliability of wind loading on low buildings [Rivista] // Journal of Wind Engineering and Industrial Aerodynamics, vol. 11. - 1983. - p. 21-37.

Davenport A.G. The prediction of risk under wind loading [Atti di convegno] // 2nd International Conference on Structural Safety and Reliability. - Munich, Germany : [s.n.], 1977.

Davison A.C. e Smith R.L. Models of exceedances over high thresholds [Rivista] // Journal of the Royal Statistical Society. - 1990.

Der Kiureghian Armen Non-ergodicity and PEER's framework formula [Rivista] // Earthquake Engng Struct. Dyn., vol.34. - 2005. - p. 1643–1652.

Durham Ken Treating the Rsiks in Cairns [Rivista] // Natural Hazards, vol. 30. - 2003. - p. 251-261.

Duthinh D. [et al.] Low-Rise Steel Structures under Directional Winds: Mean Recurrence Interval of Failure [Rivista] // Journal of Structural Engineering, Vol. 134. - 2008. - p. 1383-1388.

Duthinh Dat e Fritz William P. Safety Evaluation of Low-Rise Steel Structures under Wind Loads by Nonlinear Database-Assisted Technique [Rivista] // Journal of Structural Engineering, Vol. 133. - 2007. - p. 587-594.

Duthinh Dat e Simiu Emil Safety of Structures in Strong Winds and Earthquakes: Multihazard Considerations [Rivista] // Journal of Structural Engineering, vol. 136. - 2010. - p. 330-333.

DWS Guide to World War II Hangars [Rapporto]. - [s.l.] : Defence Works Services, 1995.

ESDU Mean wind speeds over hills and other topography [Libro]. - [s.l.] : Item 91043., 1991.

ESDU Wind speed profiles over terrain with roughness changes. Item 84011 [Rapporto]. - 1984.

FEMA NEHRP Commentary on the Guidelines for the seismic rehabilitation of buildings. FEMA 274 [Rapporto]. - 1997.

Fisher R.A. e Tippett L.H.C. Limiting forms of the frequency distribution of the largest or smaller [Rivista] // Proc. Cambridge Phil. Soc. 24. - 1928.

Galambos J. The asymptotic theory of extreme order statistics [Libro]. - New York : Wiley, 1978.

Galambos Janos e Macri Nicholas Classical extreme value model and prediction of extreme winds [Rivista] // Journal of Structural Engineering, vol. 125. - 1999. - p. 792-794.

Gatey D.A. e Miller C.A. An investigation into 50-year return period wind speed differences for Europe [Rivista] // Journal of Wind Engineering and Industrial Aerodynamics, vol. 95. - 2007. - p. 1040–1052.

Ghobarah Ahmed Performance-based design in earthquake engineering: state of development [Rivista] // Engineering Structures, vol. 23. - 2001. - p. 878–884.

Ginger J. D., Holmes J. D. e Kim P. Y. Variation of Internal Pressure with Varying Sizes of Dominant Openings and Volumes [Rivista] // Journal of structural engineering, vol. 136. - 2010. - p. 1319-1326.

Ginger J.D. e Letchford C.W. Net pressures on a low-rise full-scale building [Rivista] // Journal of Wind Engineering and Industrial Aerodynamics, vol. 83. - 1999. - p. 239-250.

Ginger J.D., Mehta K.C. e Yeatts B.B. Internal pressures in a low-rise full-scale building [Rivista] // Journal of Wind Engineering and Industrial Aerodynamics, vol. 72. - 1997. - p. 163 174.

Ginger John e Kim Peter Variation of internal pressure wiyh size of dominant operning and volume [Atti di convegno] // The Seventh Asia-Pacific Conference on Wind Engineering. - Taipei, Taiwan : [s.n.], 2009.

Gioffre` Massimiliano [et al.] Wind-induced peak bending moments in low-rise building frames [Rivista] // Journal of Engineering Mechanics, vol. 126. - 2000. - p. 879-881.

Gomes L. e Vickery B.J. On the prediction of extreme winds speeds from the parent distribution [Rivista] // J.Ind. Aero., vol. 2. - 1977. - p. 21-36.

Goulet Christine A. [et al.] Evaluation of the seismic performance of a code-conforming reinforced-concrete frame building—from seismic hazard to collapse safety and economic losses [Rivista] // Earthquake Engng Struct. Dyn., vol. 36. - 2007. - p. 1973–1997.

Grigoriu Mircea Estimates of extreme windsfrom short records [Rivista] // Journal of Structural Engineering, vol. 110. - 1984. - p. 1467-1484.

Gringorten I.I. A plotting rule for extreme probability paper [Rivista] // J. Geophysical Res., vol. 68. - 1963. - p. 813-14.

Gross John [et al.] Novel extreme value estimation procedures: application to extreme wind data [Sezione di libro] // Extreme Value Theory and Applications / aut. libro Galambos J.. - [s.l.] : Kluwer Academic Publishers, 1994.

Gumbel E.J. Statistics of Extremes [Libro]. - New York : Columbia University Press, 1958.

Ham Hee J. [et al.] Pod-based identification of modal parameters from wind-induced structural response [Atti di convegno] // BBAA VI International Colloquium on: Bluff Bodies Aerodynamics & Applications. - Milano, Italy : [s.n.], 2008.

Hanzlik Petr [et al.] Building Orientation and Wind Effects Estimation [Rivista] // Journal of Engineering Mechanics. - 2005. - p. 254-258.

Harris Ian Generalised Pareto methods for wind extremes. Useful tool or mathematical mirage? [Rivista] // Journal of Wind Engineering and Industrial Aerodynamics, vol. 93. - 2005. - p. 341-360.

Harris R. Ian A new direct version of the Cook–Mayne method for wind pressure probabilities in temperate storms [Rivista] // Journal of Wind Engineering and Industrial Aerodynamics, vol. 93. - 2005. - p. 581–600.

Harris R.I. Improvements to the "Method of Independent Storms" [Rivista] // Journal of Wind Engineering and Industrial Aerodynamics, vol. 80 . - 1999. - p. 1-30.

Harris R.I. Gumbel re-visited - a new look at extreme value statistics applied to wind speeds [Rivista] // Journal of Wind Engineering and Industrial Aerodynamics, vol. 59. - 1996. - p. 1-22.

Harris R.I. The accuracy of design values predicted from extreme value analysis [Rivista] // Journal of Wind Engineering and Industrial Aerodynamics, vol. 89. - 2001. - p. 153-164.

Harris R.I. The propagation of internal pressures in buildings [Rivista] // Journal of Wind Engineering and Industrial Aerodynamics, vol. 34. - 1990. - p. 169-184.

Hoa Le Thai Proper orthogonal decomposition and recent advanced topics in wind engineering [Rivista] // Journal of Science, Mathematics - Physics, vol. 25. - 2009. - p. 21-38.

Holmes J. D. Mean and fluctuating internal pressures induced by wind [Atti di convegno] // 5th International Conference on Wind Engineering. - Fort Collins, Colorado, USA : [s.n.], 1979.

Holmes J.D. e Moriarty W.W. Application of the generalized Pareto distribution to extreme value analysis in wind engineering [Rivista] // Journal of Wind Engineering and Industrial Aerodynamics, vol. 83. - 1999. - p. 1-10.

Holmes J.D. Fatigue life under along-wind loading — closed-form solutions [Rivista] // Engineering Structures, vol. 24. - 2002. - p. 109-114.

Holmes J.D. Analysis and synthesis of pressure fluctuations on bluff bodies using eigenvectors [Rivista] // Journal o[Wind Engineering and Industrial Aerodynamics, vol. 33. - 1990. - p. 219-230.

Holmes J.D. Distribution of peak wind loads on a low-rise building [Rivista] // Journal of Wind Engineering and Industrial Aerodynamics, vol. 29. - 1988. - p. 59-67.

Holmes J.D. e Ginger J.D. Codification of internal pressures for building [Atti di convegno] // The Seventh Asia-Pacific Conference on Wind Engineering. - Taipei, Taiwan : [s.n.], 2009.

Holmes J.D. Mean and fluctuating internal pressures induced by wind [Atti di convegno] // 5th International Conference on Wind Engineering. - Fort Collins, Colorado, USA : [s.n.], 1979.

Iervolino I., Galasso C. e Cosenza E. REXEL: computer aided record selection for code-based seismic structural analysis [Rivista] // Bull. Earthquake Engineering. - 2009.

Isyumova Nicholas Alan G. Davenport's mark on wind engineering [Atti di convegno] // 13th International Conference on Wind Engineering. - Amsterdam, The Netherlands : [s.n.], 2011.

Jenkinson A.F. The frequency distribution of the annual maximum (or minimum) values of meteorological elements [Rivista] // Quarterly Journal of the Royal Meteorological Society, vol. 81. - 1955. - p. 158-171.

Kareem Ahsan Numerical simulation of wind effects: A probabilistic perspective [Rivista] // Journal of Wind Engineering and Industrial Aerodynamics, vol. 96. - 2008. - p. 1472-1497.

Kasperski M. Design wind loads for a low-rise building taking into account directional effects [Rivista] // Journal of Wind Engineering and Industrial Aerodynamics, vol. 95. - 2007. - p. 1125-1144.

Kasperski Michael Estimation of the design wind speed based on uncertain parametres of the wind climate [Atti di convegno] // The Seventh Asia-Pacific Conference on Wind Engineering. - Taipei, Taiwan : [s.n.], 2009.

Kasperski Michael Influence of the direction change during a storm on the exceedance probability of the design wind load [Atti di convegno] // 13th International Conference on Wind Engineering. - Amsterdam, The Netherlands : [s.n.], 2011.

Khanduri A.C. e Morrow G.C. Vulnerability of buildings to windstorms and insurance loss estimation [Rivista] // Journal of Wind Engineering and Industrial Aerodynamics, vol. 91. - 2003. - p. 455–467.

Kühn B. [et al.] Assessment of Existing Steel Structures: Recommendations for Estimation of Remaining Fatigue Life [Rapporto]. - [s.l.] : G. Sedlacek, F. Bijlaard, M. Géradin, A. Pinto and S. Dimova, 2008.

Lagomarsino S., Piccardo G. e Solari G. Statistical analysis of high return period wind speeds [Rivista] // J.Wind Eng. Ind. Aero.,vol. 41-44. - 1992. - p. 485-496.

Larsen Xiaoli Guo e Mann Jakob The effects of disjunct sampling and averaging time on maximum mean wind speeds [Rivista] // Journal of Wind Engineering and Industrial Aerodynamics, vol. 94. - 2006. - p. 581–602.

Lechner James A., Leigh Stefan D. e Simiu Emil Recent Approaches to Extreme Value Estimation with Application to Wind Speeds,. Part I: the Pickands Method [Rivista] // Journal of Wind Engineering and Industrial Aerodynamics, vol. 41-44. - 1992. - p. 509-519.

Lee Kyung Ho e Rosowsky David V. Fragility assessment for roof sheathing failure in high wind regions [Rivista] // Engineering Structures, vol. 27. - 2005. - p. 857-868.

Lombardo Franklin T. e Simiu Emil Extreme wind speed estimation: Issues and improvements [Atti di convegno] // 13th International Conference on Wind Engineering. - Amsterdam, The Netherlands : [s.n.], 2011.

M.LL.PP. Aggiornamento delle normative tecniche relative ai "Criteri generali per la verifica della sicurezza delle costruzioni e dei carichi e sovraccarichi" (in Italian) [Rapporto]. - 1982.

M.LL.PP. Criteri generali per la verifica della sicurezza delle costruzioni e dei carichi e sovraccarichi (in Italian) [Rapporto]. - 1978.

M.LL.PP. Norme tecniche relative ai Criteri generali per la verifica di sicurezza delle costruzioni e dei carichi e sovraccarichi. D.M.LL.PP.16/01/1996 (in Italian) [Rapporto]. - 1996.

Majowiecki Massimo e Cosentino Nicola Design Assisted By Wind Tunnel Testing [Atti di convegno] // 34th International Symposium on Bridge and Structural Engineering. Large Structures and Infrastructures for Environmentally Constrained and Urbanised Areas. - Venice, Italy : [s.n.], 2010.

Makkonen Lasse Problems in the extreme value analysis [Rivista] // Structural Safety, vol. 30. - 2008. - p. 405–419.

Mander J.B., Priestley J.N. e Park R. Theoretical Stress-Strain Model for Confined Concrete [Rivista] // Journal of Structural Engineering, vol. 114. - 1988.

Marzocchi W. [et al.] Principles of multi-risk assessment. Interaction amongst natural and man-induced risks. [Rapporto]. - 2009.

Meletti C. e Montaldo V. Stime di pericolosità sismica per diverse probabilità di superamento in 50 anni: valori di ag. Progetto DPC-INGV S1, Deliverable S1 (in Italian) [Rapporto]. - 2007.

Miller C.A., Cook N.J. e Barnard R.H. Calibration of the exposure of UK anemographs [Rivista] // Journal of Wind Engineering and Industrial Aerodynamics, voll. 74-76. - 1998. - p. 153-161.

Miller Craig A once in 50-year wind speed map for Europe derived from mean sea level pressure measurements [Rivista] // Journal of Wind Engineering and Industrial Aerodynamics, vol. 91. - 2003. - p. 1813–1826.

Moehle Jack e Deierlein Gregory G. A framework methodology for performance-based earthquake engineering [Atti di convegno] // 13th World Conference on Earthquake Engineering. - Vancouver, B.C., Canada : [s.n.], 2004.

Moriarty W.W. The implications for extreme gust estimations of the variable frequencies of directional winds 1.Theoretical considerations [Rivista] // Journal of Wind Engineering and Industrial Aerodynamics, vol. 25. - 1987. - p. 307-318.

Moriarty W.W. The implications for extreme gust estimations of the variable frequencies of directional winds [Rivista] // Journal of Wind Engineering and IndustriaI Aerodynamics, vol. 25. - 1987. - p. 319-334.

Munich RE TOPICS GEO Natural catastrophes 2010 Analyses, assessments, positions [Rapporto] : Annual Report. - 2010.

Murlidharan T.L. e Durgaprasad J. Knowledge-based expert system for damage assessment and vulnerability analysis of structures subjected to cyclones [Rivista] // Journal of Wind Engineering and Industrial Aerodynamics, vol.72. - 1997. - p. 479-491.

Naess A. e Gaidai O. Estimation of extreme values from sampled time series [Rivista] // Structural Safety, vol. 31. - 2009. - p. 325–334.

NTC Nuove norme tecniche per le costruzioni. D.M.14/01/2008 [Rapporto]. - 2008.

Pagnini L.C. e Solari G. Preliminary elements for an innovative wind map of Italy [Atti di convegno] // 5th European African Conference on Wind Engineering. - Florence, Italy : [s.n.], 2009.

Pandey M.D. An adaptive exponential model for extreme wind speed estimation [Rivista] // Journal of Wind Engineering and Industrial Aerodynamics, vol. 90. - 2002. - p. 839-866.

Paté-Cornell E. Quantitative safety goals for risk management of industrial facilities [Rivista] // Structural facilietis, vol. 13. - 1994. - p. 145-157.

Pearce H.T. e Wen Y.K. Stochastic combination of load effects [Rivista] // Journal of Structural Engineering, vol. 110. - 1984. - p. 1613-1629.

Rigato Antonio , Chang Peter e Simiu Emil Database-assisted design, standardization, and wind direction effects [Rivista] // Journal of Structural Engineering, vol. 127. - 2001. - p. 853-860.

Robertson A.P. , Holmes J.D. e Smith B.W. Verification of closed-form solutions of fatigue life under along-wind loading [Rivista] // Engineering Structures, vol. 26. - 2004. - p. 1381–1387.

Rojiani Kamal B. e Wen Yi-Kwei Effect of estimation and sampling errors in distributions of extreme winds on structural reliability [Rivista] // Engineering Structures, vol. 2. - 1980. - p. 237-243.

Sabetta Fabio e Pugliese Antonio Estimation of Response Spectra and Simulation of Nonstationary Earthquake Ground Motions [Rivista] // Bulletin of the Seismological Society of America, vol. 86. - 1996. - p. 337-352.

Sadek Fahim [et al.] Sampling Errors in the Estimation of Peak Wind-Induced Internal Forces in Low-Rise Structures [Rivista] // Journal of Engineering Mechanics, vol. 130. - 2004. - p. 235-239.

Sharma R.N. Internal and net envelope pressures in a building having quasi-static flexibility and a dominant opening [Rivista] // Journal of Wind Engineering and Industrial Aerodynamics, vol. 96. - 2008. - p. 1074–1083.

Sharma R.N. e Richards P.J. The influence of Helmholtz resonance on internal pressures in a low-rise building [Rivista] // Journal of Wind Engineering and Industrial Aerodynamics, vol. 91. - 2003. - p. 807-828.

Simiu E. e Filliben J.J. Wind direction effects on cladding and structural loads [Rivista] // Engineering Structures, vol. 3. - 1981. - p. 181-186.

Simiu E. e Heckert N.A. Extreme Wind Distribution Tails: a "Peaks over Threshold" approach [Rivista] // Journal of Structural Engineering, vol. 122. - 1996. - p. 539-547.

Simiu E. e Miyata T. Design of buildings and bridges for wind: a practical guide for ASCE-7 standard users and designers of special structures [Libro]. - New Jersey : John Wiley & Sons, 2006.

Simiu E., Filliben J.J. e Shaver J.R. Short-term Records and Extreme Wind Speeds [Rivista] // Journal of the Structural Division, vol. 108. - 1982. - p. 2571-2577.

Simiu Emil e Lechner James A. Discussion of ‘‘Classical Extreme Value Model and Prediction of Extreme Winds,’’ by Janos Galambos and Nicholas Macri [Rivista] // Journal of structural engineering. - 2002. - p. 271-272.

Simiu Emil e Stathopoulos Theodore Codification of wind loads on buildings using bluff body aerodynamics and climatological data bases [Rivista] // Journal of Wind Engineering and Industrial Aerodynamics, voll. 69-71. - 1997. - p. 497-506.

Simiu Emil, Filliben J. J. e Biétry J. Sampling errors in the estimation of extreme wind speeds [Rivista] // Journal of the Structural Division, vol. 104. - 1978. - p. 491-501.

Solari Giovanni e Carassale Luigi Modal transformation tools in structural dynamics and wind engineering [Rivista] // Wind and Structures, vol. 3. - 2000. - p. 221-241.

Song Fang-Fang e Ou Jin-Ping Wind hazard damage estimation of industrial buildings [Atti di convegno] // The Seventh Asia-Pacific Conference on Wind Engineering. - Taipei, Taiwan : [s.n.], 2009.

Stathopoulos Ted Wind loads on low buildings: in the wake of Alan Davenport's contributions [Rivista] // Journal of Wind Engineering and Industrial Aerodynamics, vol. 91. - 2003. - p. 1565–1585.

Stathopoulos Theodore Wind loads on low-rise buildings: a review of the state of the art [Rivista] // Engineering Structures, vol. 6. - 1984. - p. 119-135.

Takle E. S. e Brown J. M. Note on the Use Weibull Statistics to Characterize Wind-Speed Data [Rivista] // Journal of Applied Meteorology, vol. 17. - 1978. - p. 556-559.

Tamura Y. e Suganuma S. Proper orthogonal decomposition of random wind pressure field [Rivista] // Journal of Fluids and Structures, vol.13. - 1999. - p. 1069-1095.

Tamura Yukio e Cao Shuyang International Group for Wind-Related Disaster Risk Reduction (IG-WRDRR) [Atti di convegno] // 13th International Conference on Wind Engineering. - Amsterdam, The Netherlands : [s.n.], 2011.

Tieleman Henry W. Wind tunnel simulation of wind loading on low-rise structures: a review [Rivista] // Journal of Wind Engineering and Industrial Aerodynamics, vol. 91. - 2003. - p. 1627-1649.

Tutkun Murat , Johansson Peter B. V. e George William K. Three-Component Vectorial Proper Orthogonal Decomposition of Axisymmetric Wake Behind a Disk [Rivista] // AIAA Journal, vol. 46. - 2008. - p. 1118-1134.

Vamvatsikos Dimitrios e Cornell C. Allin Incremental dynamic analysis [Rivista] // Earthquake Engng Struct. Dyn., vol. 31. - 2002. - p. 491–514.

Vega-Ávila Rolando E. Wind directionality: A reliability-based approach [Libro]. - 2008.

Vickery B.J. e Bloxham C. Internal pressure dynamics with a dominant opening [Rivista] // Journal of Wind Engineering and Industrial Aerodynamics, vol. 41-44. - 1992. - p. 193-204.

Vickery B.J. Gust-factors for internal-pressures in low rise buildings [Rivista] // Journal of Wind Engineering and Industrial Aerodynamics, vol. 23. - 1986. - p. 259--271.

Vickery B.J. e Georgiou P.N. A simplified approach to the determination of the influence of internal pressures on the dynamics of large span roofs [Rivista] // Journal of Wind Engineering and Industrial Aerodynamics, vol. 38. - 1991. - p. 357-369.

Wen Yi-Kwei Wind direction and structural reliability [Rivista] // Journal of Structural Engineering, vol. 109. - 1983. - p. 1028-1041.

Wen Yi-Kwei Wind direction and structural reliability: II [Rivista] // Journal of Structural Engineering, vol.110. - 1984. - p. 1253-1264.

Wijnant I.L. [et al.] Severe wind gust thresholds for Meteoalarm derived from uni-uniform return periods in ECA&D [Atti di convegno] // 13th International Conference on Wind Engineering. - Amsterdam, The Netherlands : [s.n.], 2011.

Yang T. Y. [et al.] Seismic Performance Evaluation of Facilities: Methodology and Implementation [Rivista] // Journal of structural engineering, vol. 135. - 2009. - p. 1146-1154.

APPENDIX 1 – DENOMINATION AND LOCATION OF STATIONS

In this appendix the denomination (also with the ICAO Code) and location in terms of Latitude (°North), Longitude (°East) and Altitude (in meters) of the 119 meteorological stations considered in this study are presented.

Table 5 Denomination and location of meteorological stations considered in this study

Station	ICAO Code	Lat. (°N)	Long. (°E)	Alt. (m)
Albenga (SV)	LIMG	44.04	8.13	45
Alghero (SS)	LIEA	40.63	8.29	27
Ancona Falconara	LIPY	43.62	13.36	16
Arezzo	LIQB	43.46	11.85	249
Aviano (PN)	LIPA	46.03	12.60	126
Bari Palese	LIBD	41.14	16.77	54
Bergamo Orio al Serio	LIME	45.67	9.70	239
Bologna Borgo Panigale	LIPE	44.53	11.29	38
Bolzano	LIPB	46.46	11.33	241
Brescia Ghedi	LIPL	45.44	10.27	102
Brindisi	LIBR	40.66	17.95	15
Cagliari Decimomannu	LIED	39.35	8.97	24
Cagliari Elmas	LIEE	39.25	9.06	5
Cameri (NO)	LIMN	45.53	8.67	178
Campobasso	LIBS	41.57	14.65	793
Capo Bellavista (OG)	LIEB	39.93	9.72	150
Capo Bonifati (CS)	LIBW	39.58	15.88	484
Capo Caccia (SS)	LIEH	40.57	8.17	204
Capo Carbonara (CA)	LIEC	39.10	9.52	118
Capo Frasca (CA)	LIEF	39.75	8.47	95
Capo Mele (SV)	LIMU	43.95	8.17	220
Capo Palinuro (SA)	LIQK	40.02	15.28	184
Capo S. Lorenzo (CA)	LIEL	39.50	9.63	5
Capri (NA)	LIQC	40.55	14.20	160
Carloforte (CI)	LIEZ	39.13	8.32	15

Station	ICAO Code	Lat. (°N)	Long. (°E)	Alt. (m)
Catania Fontanarossa	LICC	37.47	15.06	12
Catania Sigonella	LICZ	37.40	14.92	29
Cervia (RA)	LIPC	44.22	12.30	6
Civitavecchia (RM)	LIQJ	42.03	11.82	3
Cozzo Spadaro (SR)	LICO	36.68	15.13	51
Crotone	LIBC	39.00	17.08	159
Dobbiaco (BZ)	LIVD	46.73	12.22	1222
Elba Monte Calamita (LI)	LIRX	42.73	10.40	396
Enna	LICE	37.57	14.27	1000
Ferrara	LIPF	44.82	11.61	9
Firenze Peretola	LIRQ	43.80	11.20	44
Foggia Amendola	LIBA	41.54	15.71	60
Fonni (NU)	LIEN	40.12	9.25	1000
Forli	LIPK	44.19	12,0685	32
Frontone (PU)	LIVF	43.52	12.72	570
Frosinone	LIRH	41.63	13.28	193
Gela (CL)	LICL	37.07	14.22	65
Genova	LIMJ	44.41	8.84	2
Gioia del Colle (BA)	LIBV	40.77	16.93	352
Govone (CN)	LIMQ	44.80	8.10	300
Grazzanise (CE)	LIRM	41.06	14.08	9
Grosseto	LIRS	42.77	11.07	7
Grottaglie (TA)	LIBG	40.52	17.40	69
Guardiavecchia (SS)	LIEG	41.22	9.40	170
Guidonia (RM)	LIRG	41.98	12.74	88
Lamezia Terme (CZ)	LICA	38.91	16.24	12
Lampedusa (AG)	LICD	35.50	12.61	21
L'Aquila Preturo	LIQI	42.37	13.30	665
Latina	LIRL	41.55	12.91	25
Latronico (PZ)	LIBU	40.08	16.02	888
Lecce Galatina	LIBN	40.24	18.13	53
Marina di Ginosa (TA)	LIBH	40.40	16.85	1
Messina	LICF	38.20	15.55	54
Milano Linate	LIML	45.45	9.28	108
Milano Malpensa	LIMC	45.63	8.72	234
Mondovi (CN)	LIMY	44.38	7.82	500
Monte Argentario (GR)	LIQO	42.38	11.17	631
Monte Bisbino (CO)	LIMO	45.87	9.07	1322
Monte Cimone (MO)	LIVC	44.18	10.70	2165
Monte S. Angelo (FG)	LIBE	41.70	15.95	838

Station	ICAO Code	Lat. (°N)	Long. (°E)	Alt. (m)
Monte Scuro (CS)	LIBQ	39.33	16.40	1669
Monte Terminillo (RI)	LIRK	42.47	12.98	1874
Napoli Capodichino	LIRN	40.88	14.29	90
Novi Ligure (AL)	LIMR	44.77	8.78	189
Olbia (OT)	LIEO	40.90	9.52	11
Paganella (TN)	LIVP	46.15	11.03	2125
Palermo Boccadifalco	LICP	38.12	13.32	120
Palermo Punta Raisi	LICJ	38.18	13.10	20
Pantelleria (TP)	LICG	36.82	11.97	198
Passo dei Giovi (GE)	LIMV	44.55	8.93	488
Passo della Cisa (MS)	LIMT	44.47	9.93	1039
Passo Porretta (PT)	LIQD	44.02	11.00	1314
Passo Rolle (TN)	LIVR	46.30	11.78	2004
Perdasdefogu (OG)	LIEP	39.67	9.43	608
Perugia S. Egidio	LIRZ	43.10	12.51	208
Pescara	LIBP	42.44	14.19	10
Piacenza	LIMS	44.91	9.72	138
Pisa S.Giusto	LIRP	43.68	10.38	6
Plateau Rosa (AO)	LIMH	45.93	7.70	3480
Ponza (LT)	LIQZ	40.92	12.95	184
Potenza	LIBZ	40.63	15.80	845
Prizzi (PA)	LICX	37.72	13.43	1034
Punta Marina (RA)	LIVM	44.47	12.28	2
Radicofani (SI)	LIQR	42.90	11.77	816
Reggio Calabria	LICR	38.07	15.65	11
Rieti	LIQN	42.43	12.85	390
Rifredo Mugello (FI)	LIQM	44.06	11.24	887
Rimini	LIPR	44.03	12.61	13
Roma Ciampino	LIRA	41.80	12.60	129
Roma Fiumicino	LIRF	41.81	12.25	5
Roma Pratica di Mare	LIRE	41.65	12.45	22
Roma Urbe	LIRU	41.96	12.50	19
Ronchi dei Legionari (GO)	LIPQ	45.83	13.47	17
S. Maria di Leuca (LE)	LIBY	39.82	18.35	104
S.Valentino alla Muta (BZ)	LIVE	46.80	10.50	1459
Sarzana Luni (SP)	LIQW	44.09	9.99	13
Tarvisio (UD)	LIVO	46.50	13.58	777
Termoli (CB)	LIBT	42.00	15.00	16
Torino Bric Della Croce	LIMK	45.03	7.72	709
Torino Caselle	LIMF	45.20	7.65	302

Station	ICAO Code	Lat. (°N)	Long. (°E)	Alt. (m)
Trapani Birgi	LICT	37.92	12.49	7
Trevico (AV)	LIRT	41.05	15.23	1085
Treviso Istrana	LIPS	45.68	12.08	42
Treviso S. Angelo	LIPH	45.65	12.20	18
Trieste	LIVT	45.67	13.75	3
Udine Campoformido	LIPD	46.03	13.19	94
Udine Rivolto	LIPI	45.98	13.03	52
Ustica (PA)	LICU	38.70	13.18	243
Venezia Tessera	LIPZ	45.51	12.35	2
Verona Villafranca	LIPX	45.38	10.88	73
Vicenza	LIPT	45.57	11.53	38
Vigna di Valle (RM)	LIRB	42.08	12.22	266
Viterbo	LIRV	42.43	12.06	307
Volterra (PI)	LIQV	43.40	10.87	555

APPENDIX 2 – DETAILED RESULTS OF STATISTICAL TREATMENT OF WIND RECORDS

The detailed (numerical and graphical) results of the statistical treatment of wind records are presented. First of all, the numerical results are explained and after the graphical ones. Most of the symbols are introduced in the chapter 3; the only ones that have not already been introduced are Dn that represents the test statistic of the Kolmogorov-Smirnov test; it represents the maximum "distance" between the recorded data and the fitted distribution. The test also return the p-value that is shown for each fitted distribution on the columns 11, 17 and 22.

ICAO Code	PARENT DISTRIBUTION						EXTREME VALUE DISTRIBUTIONS															
	Weibull LSM		Weibull MLE		Weibull MOM		Gringorten					GEV						WEIBULL				
	c (m/s)	k	c (m/s)	k	c (m/s)	k	μ (m/s)	a (m/s)	Dn	p-value	v50 (m/s)	k	μ (m/s)	σ (m/s)	Dn	p-value	v50 (m/s)	c (m/s)	k	Dn	p-value	v50 (m/s)
LIBA	4.69	1.91	4.74	1.75	4.71	1.70	16.1	2.3	0.10	0.71	24.9	-0.06	16.1	2.3	0.09	0.79	24.2	18.6	6.0	0.13	0.34	23.3
LIBC	5.35	2.18	5.43	1.91	5.40	1.85	15.4	2.4	0.14	0.27	24.9	-0.24	15.7	2.8	0.11	0.59	22.7	18.0	6.3	0.14	0.27	22.3
LIBD	4.23	2.24	4.29	1.93	4.27	1.89	14.3	2.3	0.12	0.47	23.2	0.26	14.1	1.8	0.13	0.40	26.0	16.8	5.7	0.20	0.03	21.3
LIBE	6.50	1.87	6.61	1.64	6.55	1.56	21.8	4.9	0.09	0.67	40.7	-0.24	22.4	5.6	0.09	0.78	36.5	26.9	4.6	0.12	0.37	36.1
LIBG	4.71	2.35	4.79	1.99	4.76	1.94	14.6	2.1	0.12	0.60	22.8	0.00	14.6	2.0	0.11	0.65	22.5	16.9	6.5	0.20	0.07	20.8
LIBH	4.74	2.30	4.82	1.90	4.79	1.84	18.2	2.1	0.13	0.50	26.5	-0.32	18.5	2.6	0.09	0.83	24.3	20.4	8.6	0.12	0.56	24.0
LIBN	5.07	1.96	5.13	1.79	5.10	1.75	15.8	2.2	0.10	0.64	24.4	-0.06	15.9	2.3	0.09	0.75	23.7	18.3	6.1	0.16	0.10	22.8
LIBP	3.46	1.80	3.53	1.52	3.46	1.41	15.2	2.7	0.12	0.45	25.7	-0.06	15.3	2.7	0.12	0.46	24.8	18.1	5.3	0.15	0.20	23.5
LIBQ	4.76	1.90	4.84	1.64	4.79	1.56	17.5	3.6	0.15	0.16	31.4	-0.32	18.1	4.2	0.12	0.40	27.5	21.3	5.2	0.13	0.28	27.7
LIBR	5.40	2.27	5.48	1.97	5.45	1.92	16.0	3.1	0.09	0.70	28.2	0.08	16.0	2.7	0.10	0.51	28.6	19.4	4.4	0.16	0.08	26.4
LIBS	5.41	1.76	5.52	1.52	5.43	1.43	20.6	2.8	0.16	0.14	31.7	-0.38	21.2	3.5	0.09	0.85	28.3	23.6	8.0	0.09	0.78	28.0
LIBT	5.94	1.83	6.05	1.62	5.99	1.55	20.3	3.3	0.22	0.01	33.1	-0.54	21.4	4.1	0.11	0.51	28.0	23.7	7.4	0.11	0.53	28.5
LIBU	6.08	1.83	6.17	1.62	6.11	1.56	20.2	4.3	0.15	0.19	36.9	-0.35	21.0	5.2	0.08	0.87	32.0	24.6	5.1	0.07	0.94	32.2
LIBV	5.77	2.16	5.86	1.88	5.83	1.82	18.5	2.4	0.11	0.49	27.7	-0.14	18.7	2.7	0.08	0.90	26.7	21.1	6.7	0.13	0.29	25.9
LIBW	5.58	1.72	5.70	1.46	5.58	1.35	20.7	3.6	0.08	0.93	34.7	-0.13	20.9	3.9	0.08	0.95	33.0	24.6	5.3	0.13	0.40	31.8
LIBY	5.32	2.13	5.38	1.93	5.36	1.89	16.2	2.3	0.11	0.45	25.2	-0.30	16.5	2.8	0.08	0.87	23.0	18.7	6.9	0.11	0.49	22.7
LIBZ	5.39	2.09	5.47	1.83	5.43	1.77	15.7	2.6	0.12	0.37	25.9	-0.12	15.8	2.8	0.10	0.64	24.6	18.5	5.6	0.10	0.60	23.6
LICA	4.40	1.82	4.44	1.71	4.42	1.67	15.7	2.1	0.10	0.97	23.7	0.03	15.7	1.8	0.11	0.94	23.3	17.9	6.4	0.17	0.48	22.1
LICC	4.23	2.22	4.30	1.91	4.27	1.86	14.6	2.3	0.14	0.28	23.5	-0.11	14.7	2.5	0.11	0.54	22.6	17.0	5.5	0.15	0.19	21.8
LICD	6.15	2.30	6.23	2.05	6.20	2.02	16.2	2.7	0.16	0.26	26.6	-0.21	16.5	3.0	0.12	0.59	24.5	19.0	6.0	0.10	0.82	23.9
LICE	5.61	2.14	5.69	1.90	5.66	1.85	15.8	2.8	0.12	0.42	26.7	0.15	15.7	2.4	0.09	0.73	28.3	18.9	5.1	0.17	0.07	24.7
LICF	3.61	2.06	3.66	1.82	3.64	1.76	13.3	1.8	0.09	0.68	20.5	-0.06	13.4	1.9	0.09	0.68	19.9	15.3	6.3	0.17	0.07	19.1
LICG	6.41	2.09	6.49	1.86	6.46	1.82	19.9	3.8	0.09	0.68	34.7	-0.16	20.1	4.3	0.07	0.94	32.6	23.9	5.0	0.09	0.73	31.5

ICAO Code	PARENT DISTRIBUTION						EXTREME VALUE DISTRIBUTIONS															
	Weibull LSM		Weibull MLE		Weibull MOM		Gringorten					GEV						WEIBULL				
	c	k	c	k	c	k	μ	a	Dn	p-value	v50	k	μ	σ	Dn	p-value	v50	c	k	Dn	p-value	v50
	(m/s)		(m/s)		(m/s)		(m/s)	(m/s)			(m/s)		(m/s)	(m/s)			(m/s)	(m/s)				(m/s)
LICJ	5.45	1.80	5.52	1.65	5.48	1.60	18.8	1.8	0.11	0.67	25.7	-0.20	19.0	2.0	0.11	0.68	24.4	20.8	9.6	0.15	0.27	24.0
LICL	4.41	1.79	4.49	1.54	4.42	1.45	15.4	3.2	0.17	0.18	27.9	-0.56	16.4	4.1	0.12	0.55	22.9	18.7	5.4	0.11	0.67	24.0
LICO	4.55	1.91	4.63	1.64	4.58	1.55	16.2	3.0	0.09	0.66	27.9	-0.03	16.2	3.0	0.10	0.55	27.2	19.4	5.4	0.13	0.31	25.0
LICP	4.29	2.10	4.36	1.77	4.32	1.68	14.5	2.9	0.13	0.43	25.8	0.13	14.3	2.5	0.13	0.44	27.3	17.6	4.8	0.17	0.17	23.4
LICR	5.44	1.96	5.46	1.91	5.45	1.90	15.2	2.5	0.14	0.28	24.9	-0.32	15.6	3.0	0.09	0.86	22.4	17.8	6.3	0.07	0.96	22.2
LICT	5.72	2.04	5.81	1.77	5.77	1.71	19.9	2.6	0.09	0.77	30.2	0.00	19.9	2.6	0.10	0.70	29.9	22.8	6.4	0.14	0.32	28.2
LICU	6.53	1.88	6.65	1.63	6.58	1.55	20.6	5.2	0.10	0.61	40.9	-0.05	20.7	5.3	0.10	0.61	39.4	26.0	4.0	0.11	0.43	36.4
LICX	4.65	2.22	4.73	1.86	4.69	1.79	15.0	2.6	0.10	0.67	25.3	0.04	15.0	2.4	0.10	0.69	25.2	17.8	5.0	0.18	0.06	23.4
LICZ	5.19	2.10	5.26	1.91	5.23	1.86	16.5	1.7	0.16	0.17	23.0	-0.28	16.7	2.0	0.10	0.73	21.6	18.3	9.3	0.13	0.40	21.2
LIEA	4.76	1.87	4.79	1.78	4.77	1.75	15.8	1.9	0.18	0.08	23.4	-0.37	16.2	2.4	0.12	0.46	21.0	17.9	8.3	0.10	0.65	21.1
LIEB	5.11	1.95	5.21	1.61	5.13	1.50	20.1	3.7	0.15	0.17	34.6	-0.29	20.7	4.5	0.08	0.84	31.1	24.1	5.6	0.07	0.95	30.7
LIEC	7.36	1.93	7.49	1.70	7.43	1.63	21.3	6.2	0.16	0.20	45.3	-0.40	22.7	7.4	0.14	0.36	37.2	27.5	4.0	0.14	0.32	38.7
LIED	5.27	1.94	5.30	1.90	5.29	1.89	15.2	2.0	0.15	0.21	23.1	0.03	15.3	1.8	0.16	0.16	22.6	17.4	6.0	0.20	0.04	21.9
LIEE	4.89	1.98	4.95	1.81	4.92	1.77	16.3	2.2	0.16	0.08	25.0	-0.36	16.8	2.7	0.08	0.81	22.4	18.7	7.6	0.08	0.78	22.4
LIEF	6.20	2.16	6.30	1.88	6.26	1.82	19.8	2.4	0.13	0.50	29.0	-0.31	20.2	2.7	0.11	0.68	26.4	22.4	8.4	0.12	0.52	26.3
LIEG	8.04	2.02	8.13	1.86	8.10	1.82	21.1	4.8	0.27	0.00	39.7	-0.64	22.9	5.6	0.14	0.35	31.1	25.8	6.0	0.19	0.11	32.4
LIEH	5.58	1.88	5.68	1.65	5.62	1.58	20.8	2.7	0.10	0.94	31.4	-0.12	21.0	2.8	0.12	0.86	29.8	23.7	6.9	0.17	0.46	28.9
LIEL	4.32	2.20	4.38	1.91	4.35	1.85	13.5	2.0	0.17	0.53	21.3	-0.20	13.7	2.2	0.12	0.84	19.8	15.6	6.5	0.17	0.51	19.3
LIEN	4.41	2.17	4.46	1.90	4.44	1.86	14.0	3.2	0.13	0.60	26.7	-0.13	14.2	3.5	0.16	0.36	24.8	17.4	4.3	0.20	0.12	23.9
LIEO	5.06	1.78	5.07	1.75	5.07	1.74	16.1	1.8	0.12	0.69	23.1	-0.28	16.4	2.0	0.11	0.80	21.2	18.1	9.0	0.12	0.70	21.1
LIEP	5.52	2.00	5.61	1.75	5.57	1.68	17.5	2.5	0.15	0.73	27.4	-0.48	18.2	3.0	0.16	0.72	23.5	20.1	7.8	0.16	0.69	24.0
LIEZ	6.98	2.13	7.03	1.94	7.01	1.92	16.6	3.9	0.17	0.55	31.7	0.15	16.4	3.1	0.18	0.47	33.0	20.5	4.2	0.20	0.34	28.5
LIMC	2.65	1.76	2.69	1.46	2.62	1.31	14.0	2.9	0.13	0.36	25.3	-0.06	14.1	3.0	0.13	0.38	24.4	17.0	4.6	0.13	0.36	22.9
LIME	2.63	2.06	2.66	1.74	2.63	1.66	11.8	2.3	0.09	0.78	20.8	-0.10	11.9	2.4	0.11	0.56	19.8	14.2	4.9	0.17	0.12	18.8
LIMF	2.43	1.95	2.47	1.57	2.42	1.42	11.7	2.6	0.14	0.27	22.0	-0.06	11.9	2.6	0.13	0.36	21.0	14.5	4.1	0.16	0.15	20.1

ICAO Code	PARENT DISTRIBUTION						EXTREME VALUE DISTRIBUTIONS															
	Weibull LSM		Weibull MLE		Weibull MOM		Gringorten					GEV						WEIBULL				
	c	k	c	k	c	k	μ	a	Dn	p-value	v50	k	μ	σ	Dn	p-value	v50	c	k	Dn	p-value	v50
	(m/s)		(m/s)		(m/s)		(m/s)	(m/s)			(m/s)		(m/s)	(m/s)			(m/s)	(m/s)				(m/s)
LIMG	4.51	1.84	4.57	1.64	4.52	1.56	13.9	2.5	0.14	0.32	23.7	-0.14	14.0	2.7	0.12	0.49	22.2	16.6	5.4	0.13	0.39	21.3
LIMH	7.51	1.71	7.61	1.59	7.56	1.55	23.3	4.8	0.22	0.02	42.1	-0.47	24.6	5.8	0.12	0.47	35.0	28.2	5.9	0.12	0.41	35.5
LIMJ	5.14	1.74	5.17	1.70	5.16	1.69	16.9	1.8	0.12	0.58	23.8	0.05	16.9	1.5	0.10	0.81	23.5	18.9	7.2	0.19	0.11	22.8
LIMK	3.52	2.07	3.58	1.71	3.53	1.60	12.8	2.7	0.15	0.16	23.5	-0.14	13.0	3.1	0.11	0.43	22.2	15.7	4.5	0.11	0.50	21.3
LIML	2.78	2.03	2.82	1.65	2.78	1.53	12.6	2.5	0.12	0.49	22.4	-0.28	12.9	3.0	0.08	0.93	19.9	15.2	5.1	0.10	0.70	19.8
LIMN	2.38	1.85	2.41	1.54	2.36	1.40	11.3	2.8	0.11	0.77	22.4	0.06	11.3	2.5	0.10	0.87	22.3	14.2	3.8	0.17	0.24	20.4
LIMO	3.72	1.68	3.79	1.46	3.72	1.36	15.0	2.1	0.18	0.12	23.2	-0.34	15.4	2.5	0.12	0.57	20.7	17.3	7.5	0.12	0.50	20.7
LIMQ	3.51	2.23	3.56	1.75	3.53	1.64	13.6	4.5	0.08	0.98	31.2	0.07	13.6	4.0	0.09	0.90	31.4	18.0	3.1	0.12	0.69	27.9
LIMR	2.63	1.85	2.67	1.57	2.62	1.45	10.5	1.4	0.12	0.65	16.1	-0.12	10.5	1.5	0.13	0.53	15.3	12.0	6.8	0.15	0.39	14.7
LIMS	3.28	2.10	3.33	1.78	3.30	1.70	12.4	2.4	0.08	0.88	21.6	-0.02	12.5	2.3	0.08	0.84	21.3	15.0	4.8	0.16	0.11	20.0
LIMT	6.45	2.20	6.55	1.93	6.52	1.88	17.9	2.5	0.14	0.24	27.6	-0.15	18.1	2.8	0.11	0.57	26.3	20.7	6.4	0.14	0.26	25.6
LIMU	5.87	1.70	5.96	1.53	5.90	1.46	21.9	3.0	0.10	0.91	33.6	-0.24	22.2	3.4	0.10	0.88	30.8	25.1	7.2	0.12	0.72	30.4
LIMV	5.59	2.37	5.60	2.32	5.60	2.31	13.1	2.9	0.19	0.05	24.4	0.17	13.4	1.8	0.12	0.49	23.1	16.1	3.8	0.21	0.02	23.1
LIMY	3.15	2.19	3.19	1.83	3.16	1.75	11.8	2.8	0.15	0.48	22.6	-0.20	12.1	3.1	0.11	0.82	20.5	14.7	4.3	0.12	0.74	20.1
LIPA	2.75	2.23	2.79	1.84	2.77	1.77	10.8	2.3	0.11	0.52	19.9	0.16	10.7	1.9	0.10	0.60	21.2	13.3	4.3	0.18	0.05	18.2
LIPB	3.09	1.59	3.12	1.48	3.09	1.43	10.9	1.5	0.14	0.28	16.9	-0.11	11.0	1.6	0.11	0.51	16.2	12.6	6.2	0.13	0.32	15.7
LIPC	3.57	1.93	3.62	1.72	3.59	1.65	14.7	2.3	0.16	0.23	23.7	-0.33	15.1	2.8	0.09	0.85	21.3	17.1	6.6	0.11	0.71	21.1
LIPD	3.64	1.92	3.70	1.60	3.64	1.48	13.3	2.2	0.15	0.50	21.8	-0.14	13.5	2.2	0.17	0.37	20.2	15.6	6.3	0.16	0.45	19.4
LIPE	3.04	2.20	3.08	1.90	3.06	1.84	11.7	2.0	0.14	0.26	19.6	-0.18	11.9	2.3	0.11	0.56	18.3	13.9	5.6	0.08	0.86	17.7
LIPF	2.77	2.16	2.81	1.84	2.78	1.76	9.5	1.6	0.23	0.01	15.9	-0.45	9.9	2.0	0.17	0.15	13.6	11.2	6.6	0.17	0.12	13.7
LIPH	2.30	1.73	2.33	1.49	2.28	1.37	11.7	2.4	0.12	0.42	21.1	-0.02	11.8	2.3	0.12	0.44	20.5	14.2	4.1	0.14	0.22	19.8
LIPI	2.96	1.80	3.01	1.53	2.96	1.41	13.5	2.1	0.12	0.71	21.8	-0.42	14.0	2.6	0.13	0.59	18.9	15.7	6.8	0.13	0.58	19.3
LIPK	2.98	1.65	3.02	1.47	2.97	1.39	13.2	2.8	0.11	0.82	24.3	0.19	13.1	2.3	0.11	0.77	26.1	16.2	4.3	0.16	0.37	22.2
LIPL	2.70	1.80	2.74	1.55	2.69	1.44	13.1	3.0	0.13	0.27	24.9	0.04	13.2	2.6	0.11	0.46	24.1	16.2	3.7	0.19	0.02	23.4
LIPQ	3.16	1.64	3.22	1.40	3.14	1.28	15.6	2.8	0.12	0.68	26.7	-0.13	15.8	3.0	0.10	0.87	25.1	18.6	5.3	0.16	0.35	24.1

ICAO Code	PARENT DISTRIBUTION						EXTREME VALUE DISTRIBUTIONS															
	Weibull LSM		Weibull MLE		Weibull MOM		Gringorten					GEV						WEIBULL				
	c	k	c	k	c	k	μ	a	Dn	p-value	v50	k	μ	σ	Dn	p-value	v50	c	k	Dn	p-value	v50
	(m/s)		(m/s)		(m/s)		(m/s)	(m/s)			(m/s)		(m/s)	(m/s)			(m/s)	(m/s)				(m/s)
LIPR	3.65	1.75	3.68	1.64	3.66	1.59	14.5	2.2	0.13	0.29	23.1	-0.08	14.6	2.3	0.11	0.49	22.4	16.9	5.6	0.11	0.48	21.6
LIPS	2.90	1.94	2.94	1.64	2.90	1.53	12.9	1.8	0.14	0.21	20.0	-0.26	13.1	2.2	0.10	0.64	18.5	14.8	6.8	0.13	0.28	18.1
LIPT	2.72	1.91	2.71	1.68	2.67	1.57	10.2	1.8	0.17	0.07	17.2	0.25	10.1	1.3	0.15	0.14	18.5	12.1	4.8	0.22	0.01	16.1
LIPX	2.73	1.67	2.77	1.43	2.70	1.30	13.8	2.9	0.10	0.59	25.1	0.01	13.9	2.7	0.08	0.83	24.7	16.9	4.2	0.15	0.15	23.4
LIPY	3.85	2.12	3.90	1.81	3.87	1.74	14.2	2.4	0.11	0.79	23.6	-0.22	14.5	2.6	0.11	0.76	21.5	16.8	6.0	0.14	0.52	21.1
LIPZ	3.35	1.89	3.41	1.58	3.36	1.47	15.3	2.1	0.19	0.13	23.4	0.03	15.4	1.8	0.17	0.21	22.8	17.6	5.8	0.20	0.09	22.3
LIQB	4.08	2.13	4.15	1.80	4.11	1.72	13.0	2.5	0.09	0.86	22.9	0.03	13.0	2.4	0.08	0.92	22.7	15.7	4.5	0.16	0.14	21.3
LIQC	3.47	1.73	3.54	1.40	3.42	1.24	15.4	4.2	0.08	0.93	31.8	-0.08	15.5	4.4	0.07	0.98	30.2	19.7	3.7	0.12	0.50	28.6
LIQD	6.09	1.86	6.18	1.66	6.13	1.59	17.4	4.8	0.11	0.73	36.0	0.05	17.3	4.4	0.12	0.62	36.3	22.3	3.8	0.13	0.58	32.0
LIQI	5.97	1.77	6.10	1.50	5.99	1.39	16.6	6.4	0.17	0.18	41.5	-0.16	17.1	6.7	0.18	0.14	36.8	22.7	3.0	0.19	0.11	35.9
LIQJ	4.08	1.90	4.15	1.65	4.10	1.56	15.6	2.8	0.13	0.83	26.5	-0.14	15.8	2.9	0.14	0.72	24.5	18.6	5.8	0.18	0.45	23.4
LIQK	4.46	1.85	4.54	1.58	4.48	1.49	19.9	3.6	0.16	0.19	34.0	-0.17	20.2	4.1	0.12	0.52	31.7	23.7	5.3	0.13	0.42	30.7
LIQM	7.62	1.91	7.69	1.78	7.65	1.74	20.8	4.1	0.12	0.88	36.7	-1.10	23.1	6.8	0.15	0.65	29.2	24.9	6.1	0.11	0.94	31.2
LIQN	3.28	2.02	3.32	1.84	3.30	1.79	10.3	0.8	0.16	0.47	13.5	-0.45	10.5	1.0	0.18	0.28	12.3	11.2	13.0	0.19	0.24	12.4
LIQO	5.86	1.73	5.92	1.59	5.88	1.54	18.6	4.0	0.12	0.49	34.2	0.08	18.6	3.5	0.10	0.69	34.3	22.8	4.2	0.18	0.10	31.6
LIQR	4.83	1.85	4.92	1.58	4.84	1.47	14.0	4.4	0.13	0.40	31.3	-0.07	14.2	4.4	0.15	0.28	29.2	18.4	3.5	0.20	0.06	27.3
LIQV	5.37	1.83	5.46	1.62	5.41	1.55	17.9	3.0	0.18	0.65	29.8	-0.31	18.5	3.5	0.14	0.90	26.4	21.0	6.4	0.13	0.93	26.0
LIQW	3.04	2.03	3.06	1.84	3.05	1.80	12.9	1.9	0.13	0.96	20.1	-0.04	13.0	1.7	0.12	0.98	19.3	14.9	6.5	0.21	0.54	18.4
LIQZ	5.48	1.94	5.56	1.73	5.52	1.67	19.4	3.3	0.22	0.02	32.3	-0.29	19.9	4.0	0.15	0.18	29.3	22.9	6.0	0.13	0.33	28.8
LIRA	3.73	1.75	3.78	1.55	3.73	1.47	15.9	2.3	0.09	0.69	24.8	-0.05	16.0	2.3	0.08	0.77	24.3	18.5	6.0	0.13	0.25	23.2
LIRB	4.22	1.90	4.28	1.67	4.25	1.60	15.0	2.1	0.12	0.43	23.3	0.21	14.8	1.8	0.11	0.47	25.5	17.3	6.5	0.16	0.11	21.4
LIRE	4.39	1.95	4.42	1.82	4.41	1.79	14.7	2.0	0.11	0.54	22.3	-0.14	14.8	2.2	0.09	0.81	21.3	16.8	6.7	0.13	0.42	20.7
LIRF	4.48	1.87	4.54	1.69	4.51	1.64	15.8	2.2	0.13	0.44	24.5	-0.07	15.9	2.2	0.11	0.62	23.7	18.2	6.0	0.16	0.20	22.9
LIRG	4.01	2.10	4.06	1.88	4.04	1.83	12.3	2.0	0.10	0.58	20.1	-0.06	12.4	2.1	0.09	0.65	19.6	14.5	5.5	0.13	0.24	18.5
LIRH	2.97	1.55	3.00	1.40	2.96	1.32	13.2	2.8	0.11	0.92	24.2	-0.25	13.6	3.1	0.13	0.83	21.4	16.1	5.0	0.15	0.70	21.2

ICAO Code	PARENT DISTRIBUTION						EXTREME VALUE DISTRIBUTIONS															
	Weibull LSM		Weibull MLE		Weibull MOM		Gringorten					GEV						WEIBULL				
	c (m/s)	k	c (m/s)	k	c (m/s)	k	μ (m/s)	a (m/s)	Dn	p-value	v50 (m/s)	k	μ (m/s)	σ (m/s)	Dn	p-value	v50 (m/s)	c (m/s)	k	Dn	p-value	v50 (m/s)
LIRK	6.50	1.95	6.59	1.71	6.54	1.64	21.9	6.5	0.10	0.56	47.1	-0.02	21.9	6.4	0.10	0.56	46.3	28.5	3.4	0.09	0.68	42.5
LIRL	3.32	1.64	3.34	1.55	3.32	1.51	13.2	2.1	0.11	0.83	21.3	-0.18	13.4	2.3	0.13	0.68	19.7	15.4	6.2	0.16	0.42	19.2
LIRM	3.97	1.95	4.03	1.69	3.99	1.61	15.7	1.8	0.14	0.49	22.6	-0.03	15.7	1.8	0.14	0.43	22.2	17.6	7.6	0.15	0.35	21.1
LIRN	3.68	1.84	3.74	1.61	3.70	1.52	15.1	2.6	0.11	0.58	25.2	-0.14	15.3	2.9	0.09	0.76	23.9	17.9	5.4	0.14	0.26	23.1
LIRP	3.55	1.68	3.60	1.54	3.56	1.48	14.9	1.8	0.10	0.59	21.9	-0.19	15.0	2.1	0.13	0.26	20.7	16.9	7.4	0.16	0.07	20.3
LIRQ	3.54	1.74	3.59	1.56	3.55	1.49	13.5	2.7	0.12	0.48	23.9	0.05	13.4	2.5	0.11	0.53	24.1	16.3	4.6	0.14	0.27	22.0
LIRS	4.19	1.73	4.26	1.53	4.21	1.46	15.5	2.2	0.10	0.67	24.1	-0.11	15.6	2.4	0.07	0.92	23.1	17.9	6.3	0.13	0.31	22.2
LIRT	6.60	2.21	6.70	1.92	6.67	1.88	18.6	3.4	0.11	0.83	31.9	-0.19	18.9	3.7	0.14	0.55	29.1	22.2	5.5	0.16	0.39	28.4
LIRU	4.10	1.72	4.12	1.69	4.11	1.67	13.0	1.8	0.12	0.49	20.1	-0.10	13.1	1.9	0.12	0.53	19.2	15.0	6.6	0.13	0.40	18.4
LIRV	4.61	1.95	4.66	1.75	4.63	1.69	15.6	2.3	0.13	0.36	24.5	-0.10	15.7	2.4	0.11	0.57	23.5	18.1	6.2	0.15	0.21	22.6
LIRX	5.40	1.97	5.47	1.76	5.44	1.71	18.0	2.9	0.11	0.94	29.2	-0.01	18.0	2.7	0.13	0.87	28.4	21.0	6.3	0.14	0.81	26.1
LIRZ	3.85	1.77	3.90	1.62	3.87	1.57	13.6	1.6	0.10	0.89	20.0	-0.03	13.6	1.6	0.10	0.86	19.5	15.4	7.0	0.16	0.34	18.7
LIVC	8.27	1.89	8.41	1.65	8.33	1.58	26.7	6.1	0.13	0.28	50.5	-0.21	27.3	7.1	0.08	0.82	46.2	33.1	4.5	0.09	0.75	44.9
LIVD	3.77	2.05	3.83	1.78	3.80	1.71	9.9	2.2	0.13	0.26	18.3	-0.07	10.0	2.2	0.12	0.37	17.6	12.2	4.3	0.13	0.28	16.7
LIVE	4.30	2.26	4.37	1.84	4.34	1.77	11.4	3.0	0.11	0.55	23.1	0.11	11.4	2.4	0.08	0.84	23.3	14.5	3.7	0.17	0.07	21.1
LIVF	4.24	1.81	4.32	1.51	4.23	1.39	17.1	3.1	0.10	0.59	29.2	-0.12	17.3	3.4	0.08	0.87	27.8	20.5	5.1	0.12	0.44	26.7
LIVM	3.83	1.99	3.89	1.67	3.84	1.57	14.1	3.0	0.15	0.17	26.0	-0.09	14.2	3.2	0.14	0.22	24.6	17.3	4.6	0.13	0.28	23.3
LIVO	2.49	1.76	2.50	1.60	2.48	1.53	9.9	2.4	0.11	0.75	19.1	-0.07	9.9	2.4	0.11	0.75	18.2	12.3	4.2	0.12	0.70	17.1
LIVP	5.73	1.89	5.81	1.69	5.77	1.63	17.6	3.5	0.13	0.26	31.4	-0.27	18.1	4.2	0.07	0.92	28.1	21.3	5.1	0.08	0.85	27.9
LIVR	4.02	2.11	4.07	1.83	4.04	1.77	13.9	2.4	0.13	0.31	23.4	-0.36	14.4	3.0	0.12	0.50	20.6	16.5	5.9	0.13	0.39	20.7
LIVT	3.54	1.57	3.61	1.35	3.52	1.23	15.3	2.6	0.14	0.17	25.3	-0.12	15.4	2.7	0.14	0.18	23.9	18.0	5.7	0.14	0.21	22.9

Each station is identified by its ICAO code and the figures are illustrated in the following table, as example.

ICAO Code

Wind rose of the Parent distribution	Empirical pdf of the Parent distribution and fitted Weibull distributions (parameters estimated through MLE, MOM and LSM)
Wind rose of the annual maxima	Gumbel probability plot of the annual maxima (Gringorten's method)
Wind rose of the monthly maxima	Gumbel probability plot of the monthly maxima (Gringorten's method)

page i

Wind speed-return period relationships evaluated by different methods based on the annual maxima	Wind speed-return period relationships evaluated by different methods based on the monthly maxima
Comparison between directional, omnidirectional and estimated (by product of probalities) cdfs	Polar diagram of directional coefficients
Comparison between seasonal, overall and estimated (by product of probalities) cdfs	Histogram of seasonal coefficients
Artificial downsampling of recorded data (all estimated v50 values)	Artificial downsampling of recorded data (median estimated v50)

page i+1

LIBA

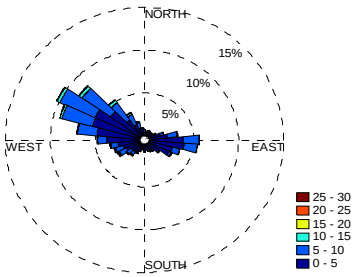
NORTH
15%
10%
5%
WEST
EAST
SOUTH
25 - 30
20 - 25
15 - 20
10 - 15
5 - 10
0 - 5

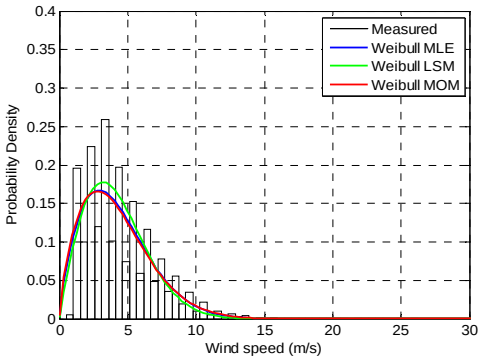
Measured
Weibull MLE
Weibull LSM
Weibull MOM
Probability Density
Wind speed (m/s)

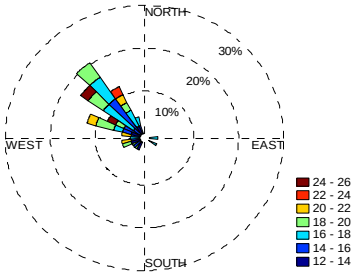
NORTH
30%
20%
10%
WEST
EAST
SOUTH
24 - 26
22 - 24
20 - 22
18 - 20
16 - 18
14 - 16
12 - 14

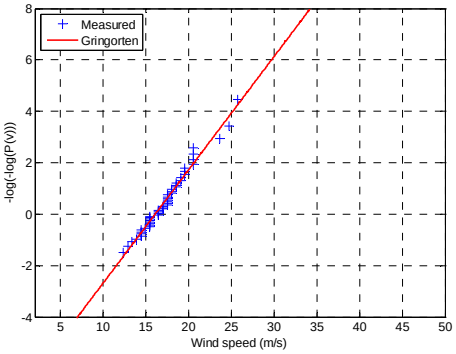
Measured
Gringorten
-log(-log(P(v)))
Wind speed (m/s)

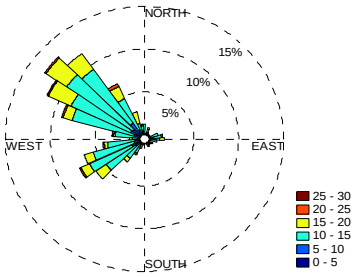
NORTH
15%
10%
5%
WEST
EAST
SOUTH
25 - 30
20 - 25
15 - 20
10 - 15
5 - 10
0 - 5

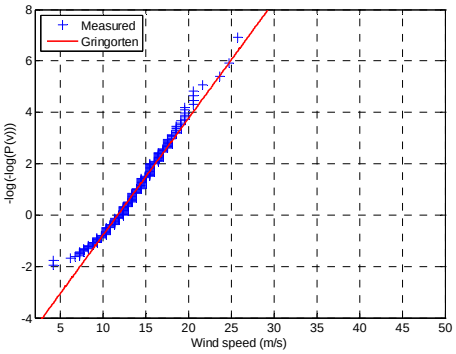
Measured
Gringorten
-log(-log(P(v)))
Wind speed (m/s)

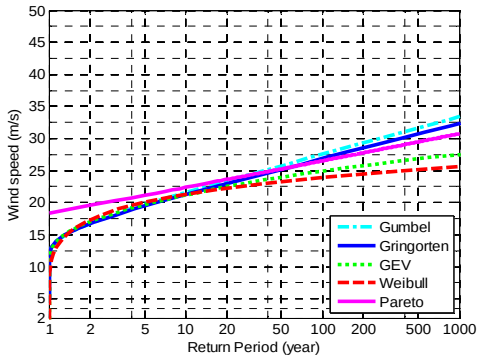
Wind speed (m/s)
Return Period (year)
Gumbel
Gringorten
GEV
Weibull
Pareto

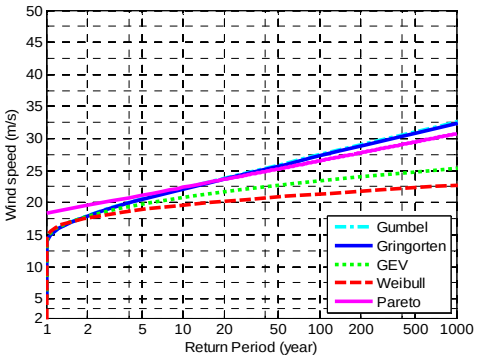
Wind speed (m/s)
Return Period (year)
Gumbel
Gringorten
GEV
Weibull
Pareto

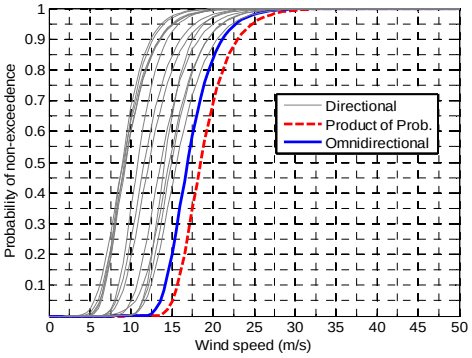
Probability of non-exceedence
Wind speed (m/s)
Directional
Product of Prob.
Omnidirectional

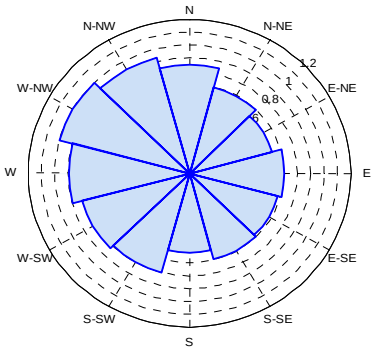
N
N-NE
E-NE
E
E-SE
S-SE
S
S-SW
W
W-NW
N-NW

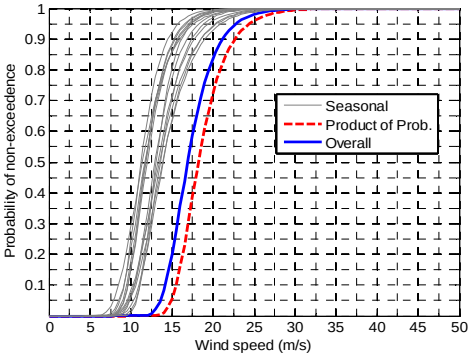
Probability of non-exceedence
Wind speed (m/s)
Seasonal
Product of Prob.
Overall

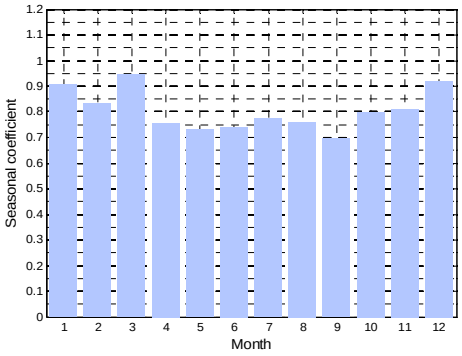
Seasonal coefficient
Month

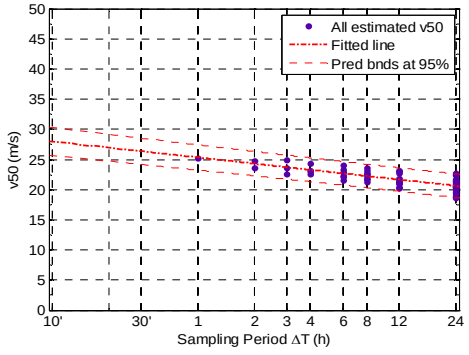
v50 (m/s)
Sampling Period ΔT (h)
All estimated v50
Fitted line
Pred bnds at 95%

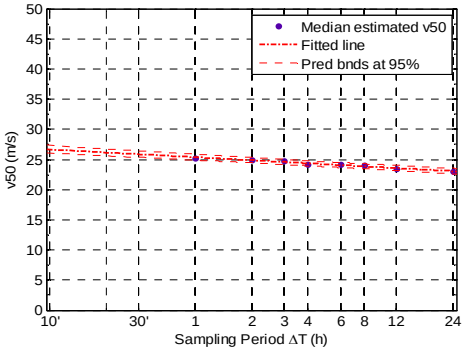
v50 (m/s)
Sampling Period ΔT (h)
Median estimated v50
Fitted line
Pred bnds at 95%

LIBC

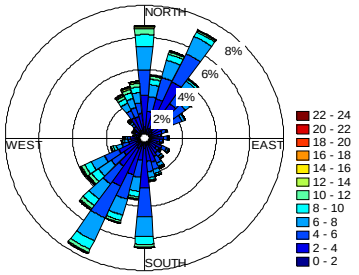
NORTH
EAST
SOUTH
WEST
8%
6%
4%
2%
22 - 24
20 - 22
18 - 20
16 - 18
14 - 16
12 - 14
10 - 12
8 - 10
6 - 8
4 - 6
2 - 4
0 - 2

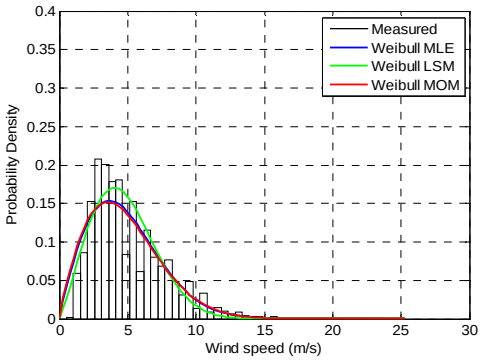
Measured
Weibull MLE
Weibull LSM
Weibull MOM
Probability Density
Wind speed (m/s)

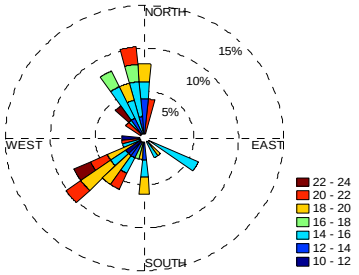
NORTH
EAST
SOUTH
WEST
15%
10%
5%
22 - 24
20 - 22
18 - 20
16 - 18
14 - 16
12 - 14
10 - 12

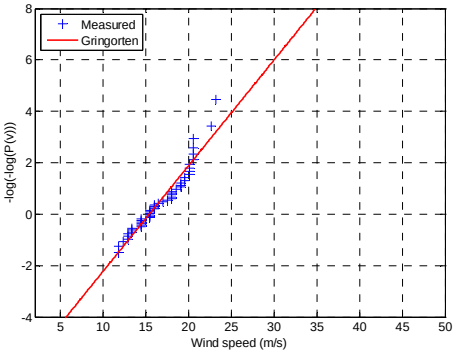
Measured
Gringorten
-log(-log(P(v)))
Wind speed (m/s)

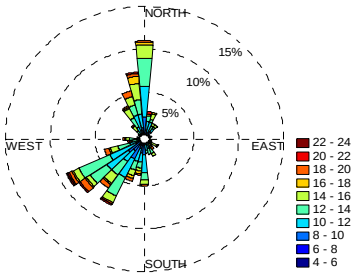
NORTH
EAST
SOUTH
WEST
15%
10%
5%
22 - 24
20 - 22
18 - 20
16 - 18
14 - 16
12 - 14
10 - 12
8 - 10
6 - 8
4 - 6

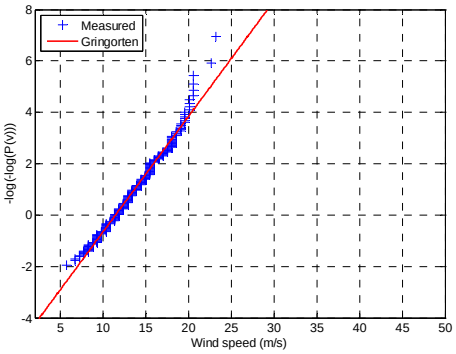
Measured
Gringorten
-log(-log(P(v)))
Wind speed (m/s)

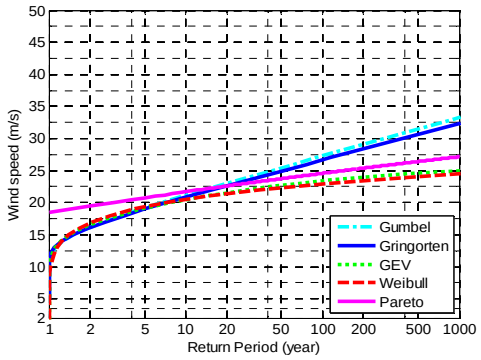
Wind speed (m/s)
Return Period (year)
Gumbel
Gringorten
GEV
Weibull
Pareto

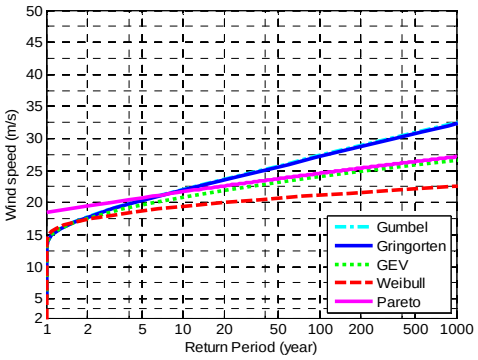
Wind speed (m/s)
Return Period (year)
Gumbel
Gringorten
GEV
Weibull
Pareto

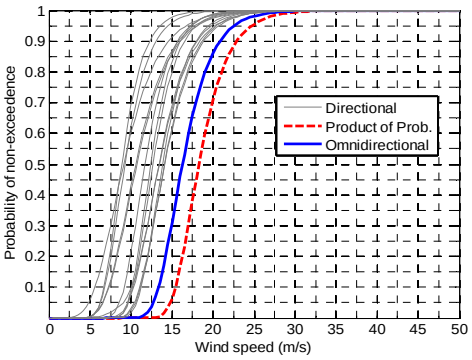
Probability of non-exceedence
Wind speed (m/s)
Directional
Product of Prob.
Omnidirectional

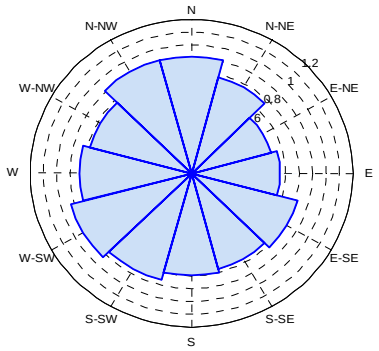
N
N-NE
E-NE
E
E-SE
S-SE
S
S-SW
W
W-NW
N-NW

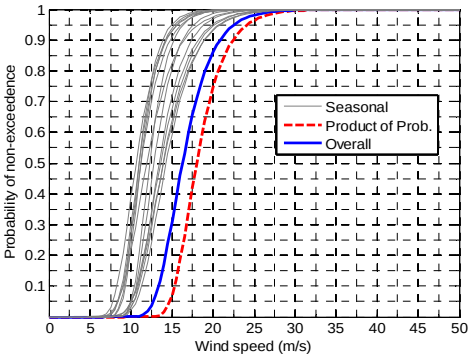
Probability of non-exceedence
Wind speed (m/s)
Seasonal
Product of Prob.
Overall

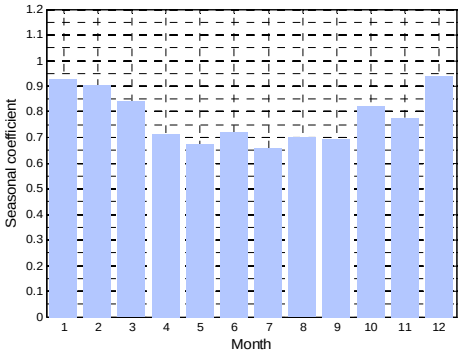
Seasonal coefficient
Month

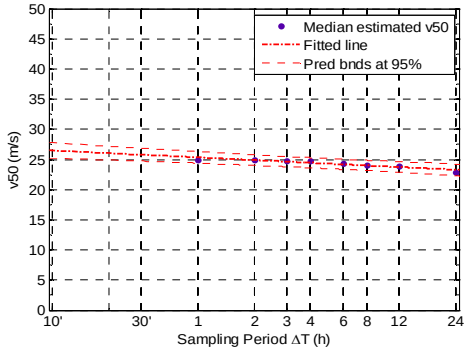
v50 (m/s)
Sampling Period ΔT (h)
Median estimated v50
Fitted line
Pred bnds at 95%

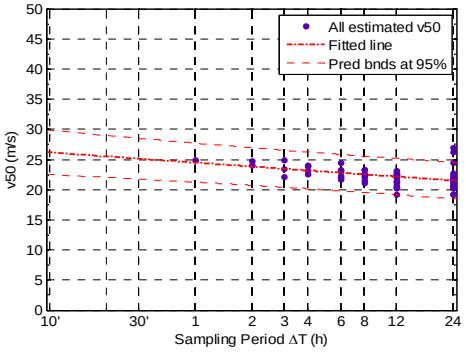
v50 (m/s)
Sampling Period ΔT (h)
All estimated v50
Fitted line
Pred bnds at 95%

LIBD

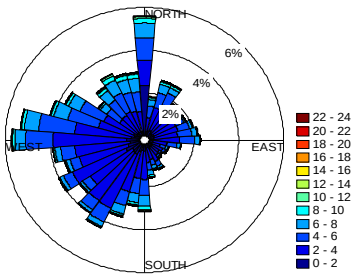
NORTH
6%
4%
2%
WEST
EAST
SOUTH
22 - 24
20 - 22
18 - 20
16 - 18
14 - 16
12 - 14
10 - 12
8 - 10
6 - 8
4 - 6
2 - 4
0 - 2

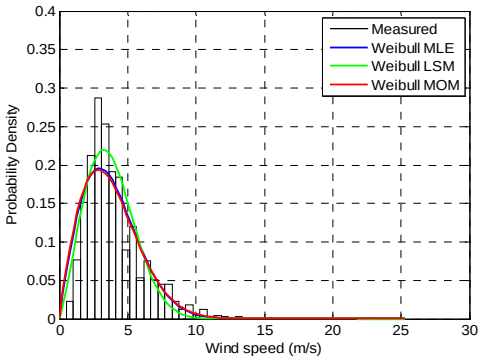
Measured
Weibull MLE
Weibull LSM
Weibull MOM
Probability Density
Wind speed (m/s)

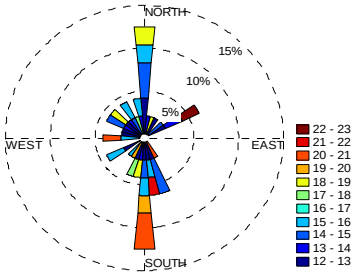
NORTH
15%
10%
5%
WEST
EAST
SOUTH
22 - 23
21 - 22
20 - 21
19 - 20
18 - 19
17 - 18
16 - 17
15 - 16
14 - 15
13 - 14
12 - 13

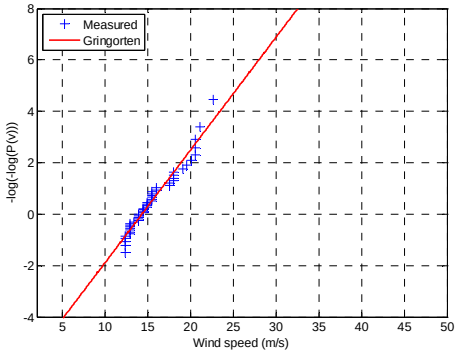
Measured
Gringorten
-log(-log(P(v)))
Wind speed (m/s)

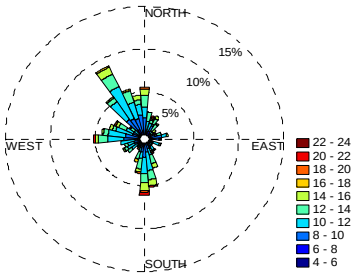
NORTH
15%
10%
5%
WEST
EAST
SOUTH
22 - 24
20 - 22
18 - 20
16 - 18
14 - 16
12 - 14
10 - 12
8 - 10
6 - 8
4 - 6

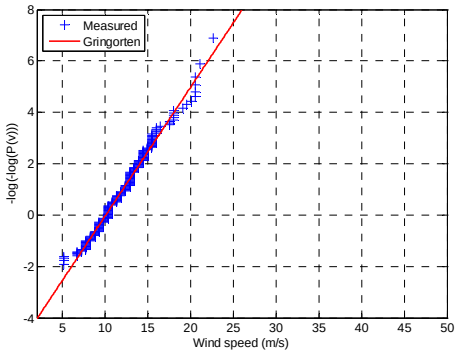
Measured
Gringorten
-log(-log(P(v)))
Wind speed (m/s)

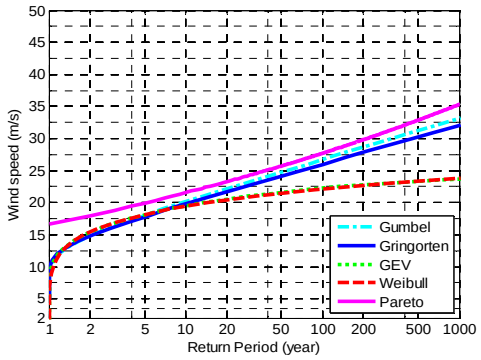
Wind speed (m/s)
Return Period (year)
Gumbel
Gringorten
GEV
Weibull
Pareto

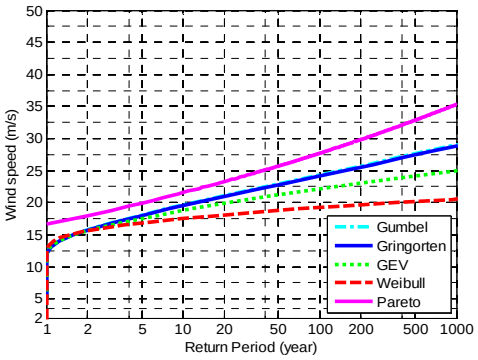
Wind speed (m/s)
Return Period (year)
Gumbel
Gringorten
GEV
Weibull
Pareto

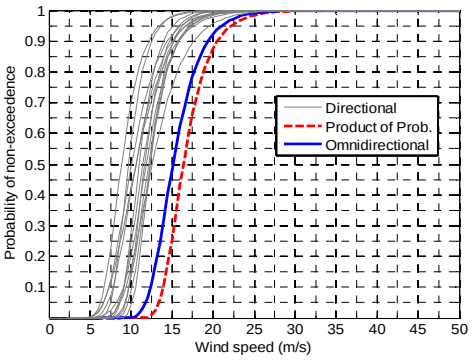
Probability of non-exceedence
Wind speed (m/s)
Directional
Product of Prob.
Omnidirectional

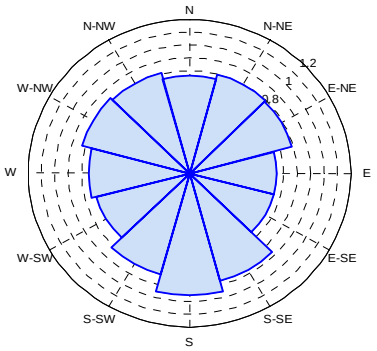
N
N-NE
E-NE
E
E-SE
S-SE
S
S-SW
W
W-NW
N-NW

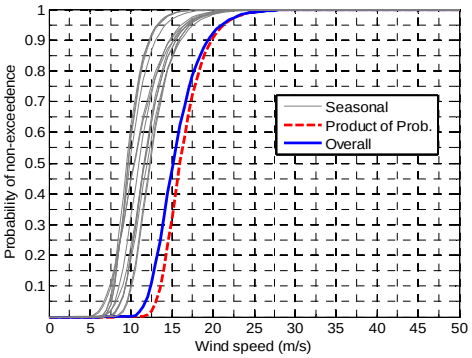
Probability of non-exceedence
Wind speed (m/s)
Seasonal
Product of Prob.
Overall

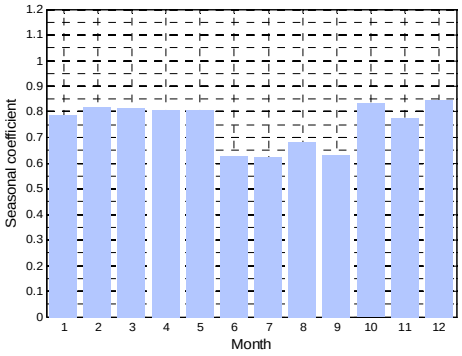
Seasonal coefficient
Month

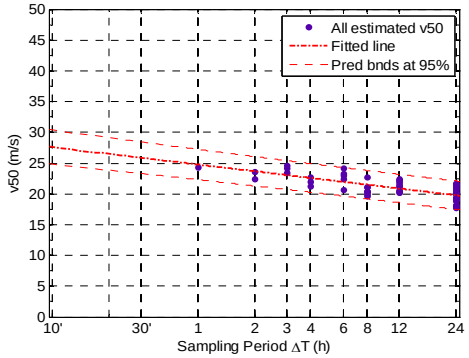
v50 (m/s)
Sampling Period ΔT (h)
All estimated v50
Fitted line
Pred bnds at 95%

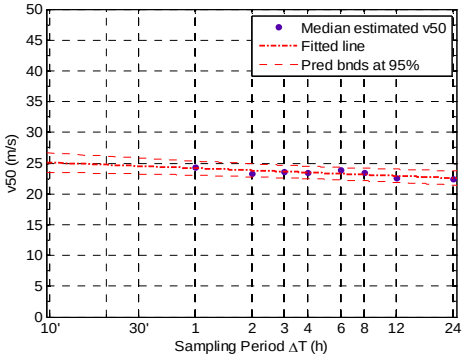
v50 (m/s)
Sampling Period ΔT (h)
Median estimated v50
Fitted line
Pred bnds at 95%

LIBE

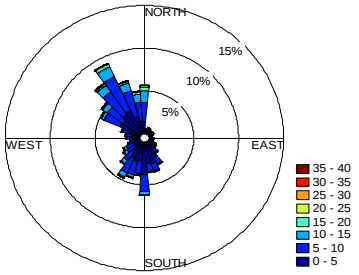
NORTH
15%
10%
5%
WEST
EAST
SOUTH
35 - 40
30 - 35
25 - 30
20 - 25
15 - 20
10 - 15
5 - 10
0 - 5

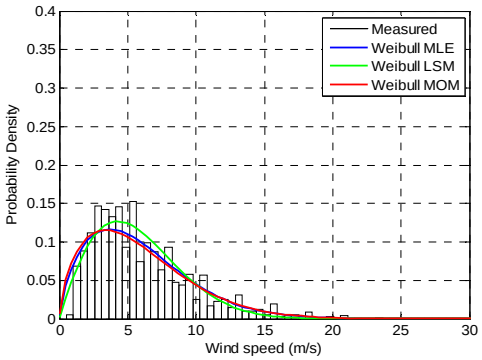
Measured
Weibull MLE
Weibull LSM
Weibull MOM
Probability Density
Wind speed (m/s)

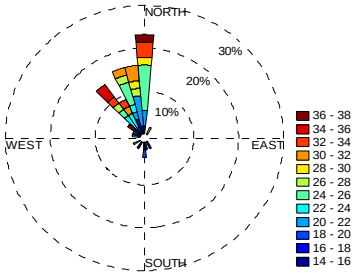
NORTH
30%
20%
10%
WEST
EAST
SOUTH
36 - 38
34 - 36
32 - 34
30 - 32
28 - 30
26 - 28
24 - 26
22 - 24
20 - 22
18 - 20
16 - 18
14 - 16

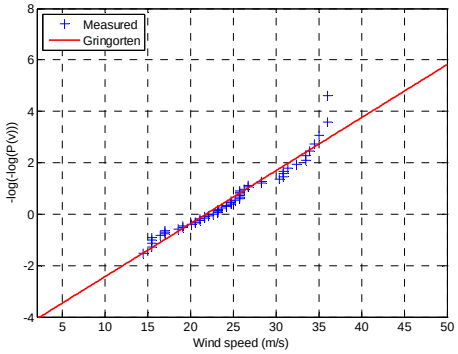
Measured
Gringorten
-log(-log(P(v)))
Wind speed (m/s)

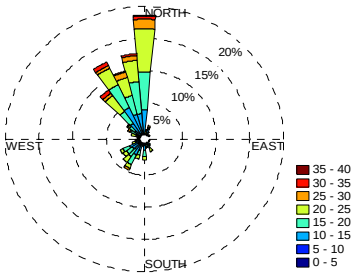
NORTH
20%
15%
10%
5%
WEST
EAST
SOUTH
35 - 40
30 - 35
25 - 30
20 - 25
15 - 20
10 - 15
5 - 10
0 - 5

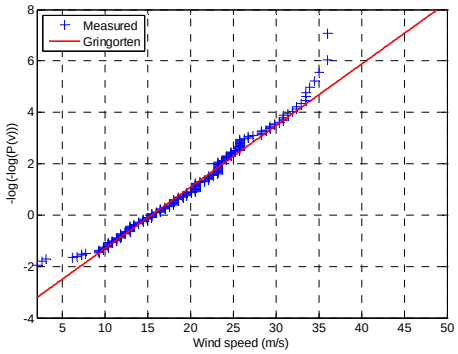
Measured
Gringorten
-log(-log(P(v)))
Wind speed (m/s)

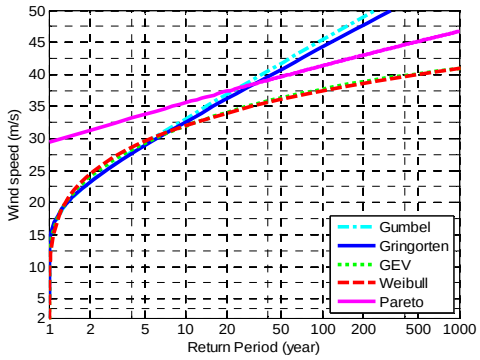
Wind speed (m/s)
Return Period (year)
Gumbel
Gringorten
GEV
Weibull
Pareto

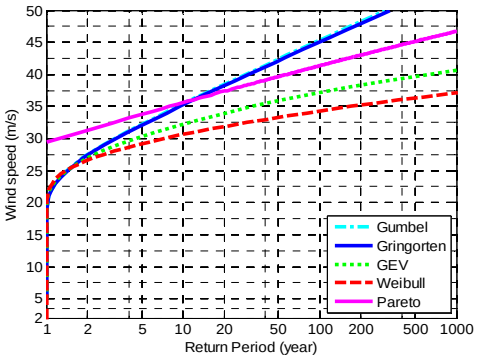
Wind speed (m/s)
Return Period (year)
Gumbel
Gringorten
GEV
Weibull
Pareto

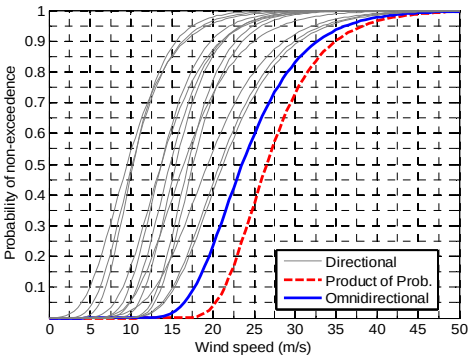
Probability of non-exceedence
Wind speed (m/s)
Directional
Product of Prob.
Omnidirectional

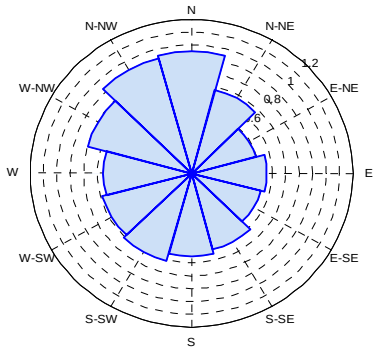
N
N-NE
E-NE
E
E-SE
S-SE
S
S-SW
W
W-NW
N-NW

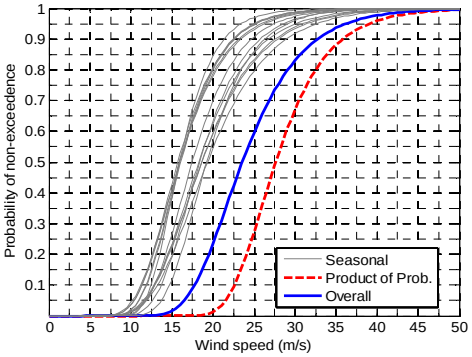
Probability of non-exceedence
Wind speed (m/s)
Seasonal
Product of Prob.
Overall

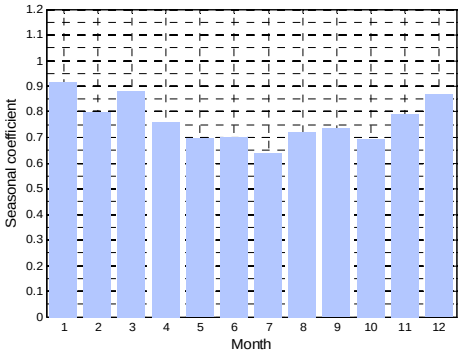
Seasonal coefficient
Month

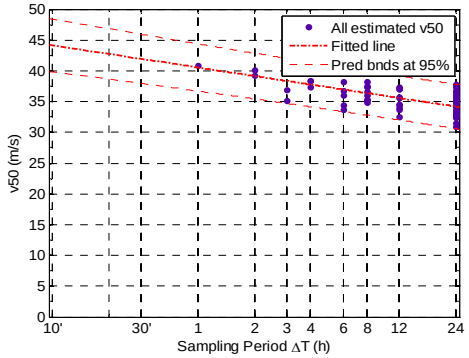
v50 (m/s)
Sampling Period ΔT (h)
All estimated v50
Fitted line
Pred bnds at 95%

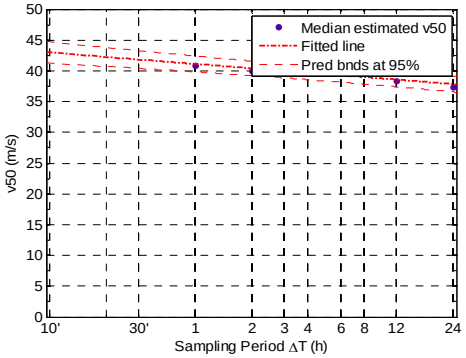
v50 (m/s)
Sampling Period ΔT (h)
Median estimated v50
Fitted line
Pred bnds at 95%

LIBG

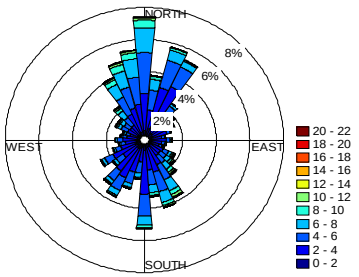
NORTH
8%
6%
4%
2%
WEST
EAST
SOUTH
20 - 22
18 - 20
16 - 18
14 - 16
12 - 14
10 - 12
8 - 10
6 - 8
4 - 6
2 - 4
0 - 2

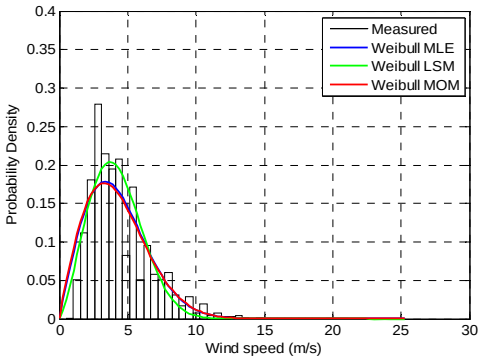
Measured
Weibull MLE
Weibull LSM
Weibull MOM
Probability Density
Wind speed (m/s)

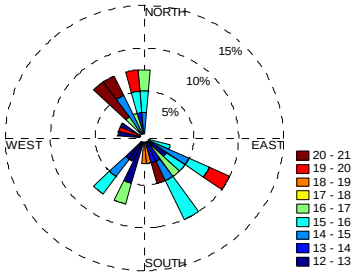
NORTH
15%
10%
5%
WEST
EAST
SOUTH
20 - 21
19 - 20
18 - 19
17 - 18
16 - 17
15 - 16
14 - 15
13 - 14
12 - 13

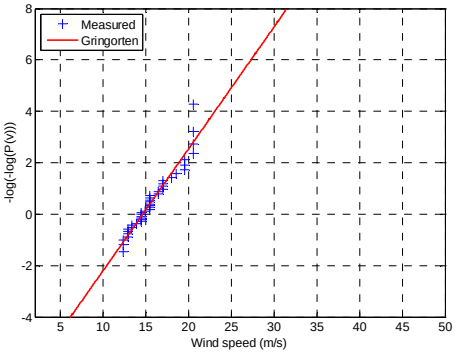
Measured
Gringorten
-log(-log(P(v)))
Wind speed (m/s)

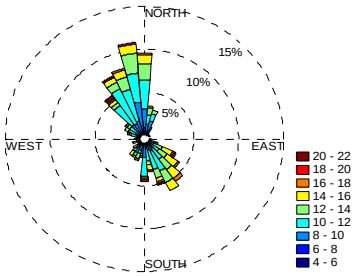
NORTH
15%
10%
5%
WEST
EAST
SOUTH
20 - 22
18 - 20
16 - 18
14 - 16
12 - 14
10 - 12
8 - 10
6 - 8
4 - 6

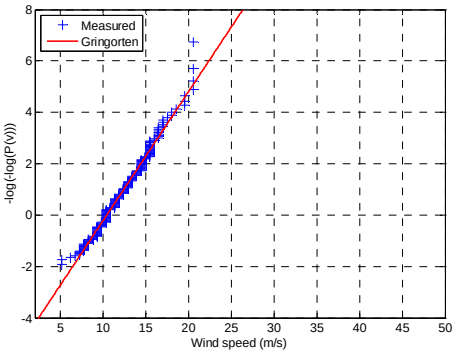
Measured
Gringorten
-log(-log(P(v)))
Wind speed (m/s)

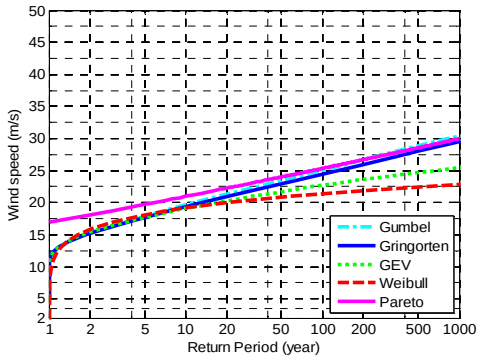
Wind speed (m/s)
Return Period (year)
Gumbel
Gringorten
GEV
Weibull
Pareto

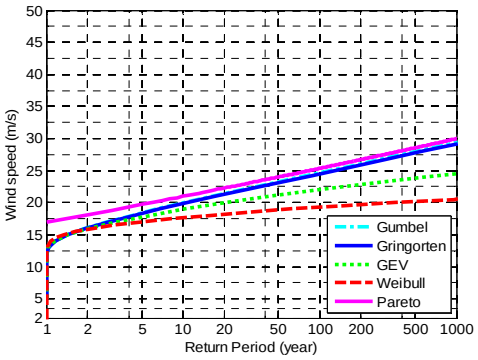
Wind speed (m/s)
Return Period (year)
Gumbel
Gringorten
GEV
Weibull
Pareto

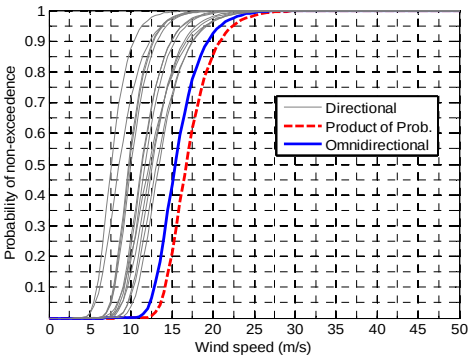
Probability of non-exceedence
Wind speed (m/s)
Directional
Product of Prob.
Omnidirectional

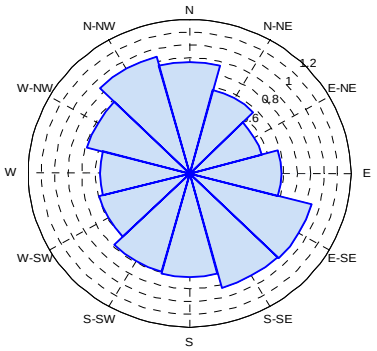
N
N-NE
E-NE
E
E-SE
S-SE
S
S-SW
W
W-NW
N-NW

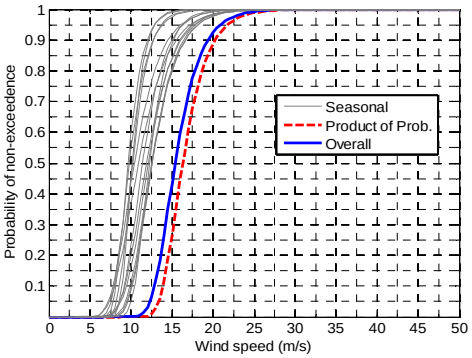
Probability of non-exceedence
Wind speed (m/s)
Seasonal
Product of Prob.
Overall

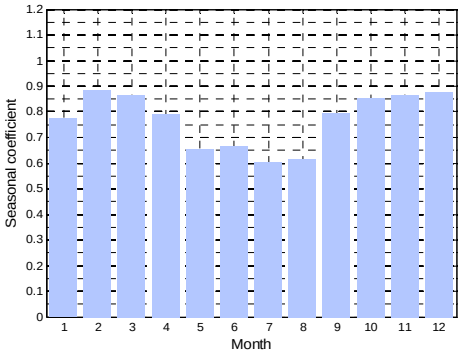
Seasonal coefficient
Month

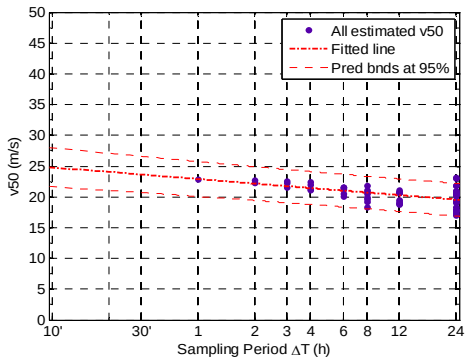
v50 (m/s)
Sampling Period ΔT (h)
All estimated v50
Fitted line
Pred bnds at 95%

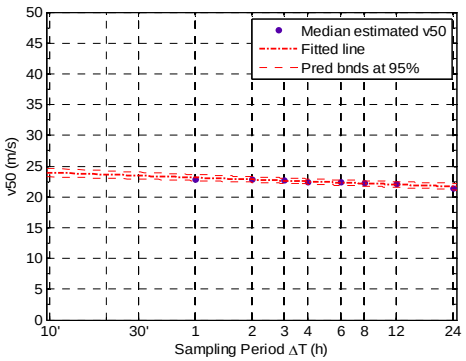
v50 (m/s)
Sampling Period ΔT (h)
Median estimated v50
Fitted line
Pred bnds at 95%

LIBH

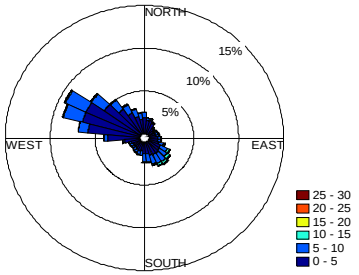
NORTH
15%
10%
5%
WEST
EAST
SOUTH
25 - 30
20 - 25
15 - 20
10 - 15
5 - 10
0 - 5

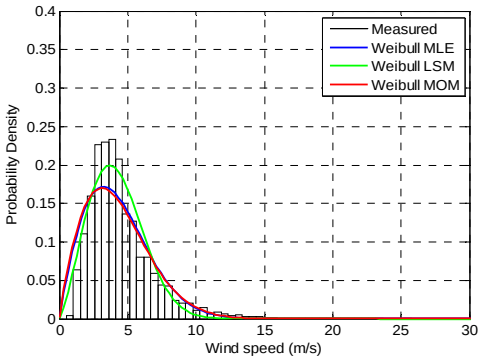
Measured
Weibull MLE
Weibull LSM
Weibull MOM
Probability Density
Wind speed (m/s)

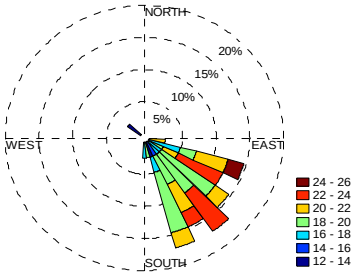
NORTH
20%
15%
10%
5%
WEST
EAST
SOUTH
24 - 26
22 - 24
20 - 22
18 - 20
16 - 18
14 - 16
12 - 14

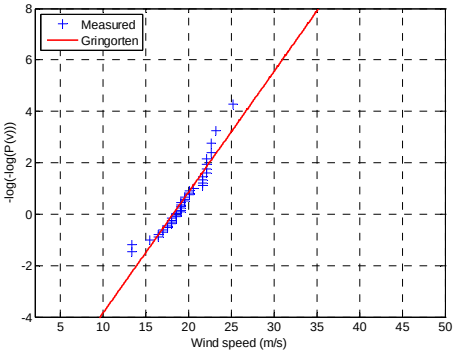
Measured
Gringorten
-log(-log(P(v)))
Wind speed (m/s)

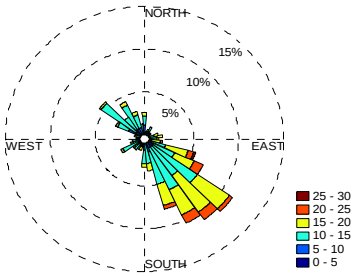
NORTH
15%
10%
5%
WEST
EAST
SOUTH
25 - 30
20 - 25
15 - 20
10 - 15
5 - 10
0 - 5

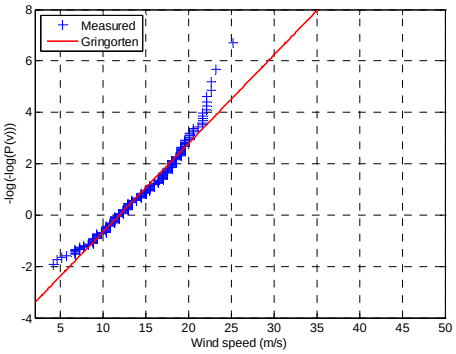
Measured
Gringorten
-log(-log(P(v)))
Wind speed (m/s)

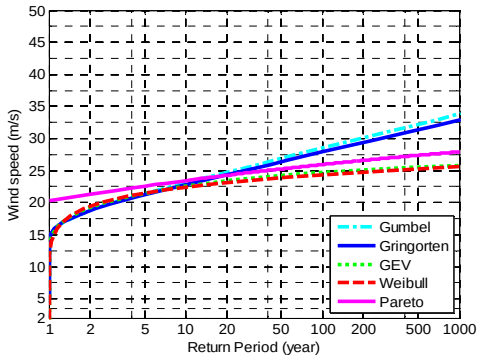
Wind speed (m/s)
Return Period (year)
Gumbel
Gringorten
GEV
Weibull
Pareto

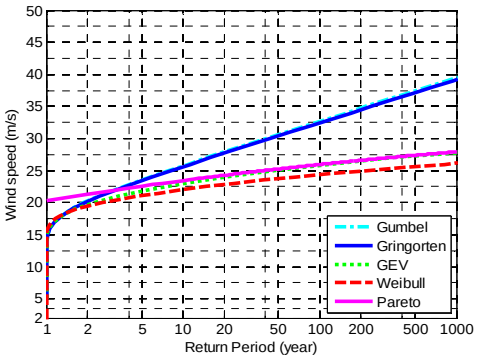
Wind speed (m/s)
Return Period (year)
Gumbel
Gringorten
GEV
Weibull
Pareto

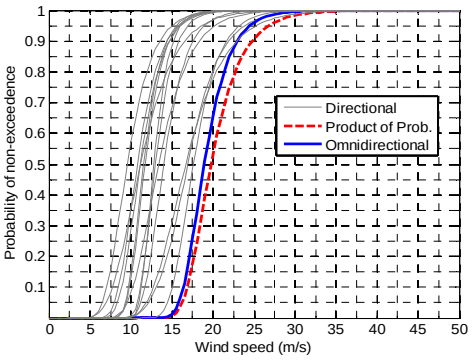
Probability of non-exceedence
Wind speed (m/s)
Directional
Product of Prob.
Omnidirectional

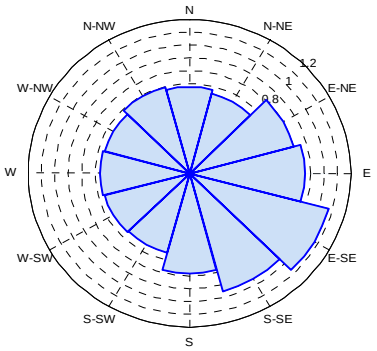
N
N-NE
E-NE
E
E-SE
S-SE
S
S-SW
W
W-NW
N-NW

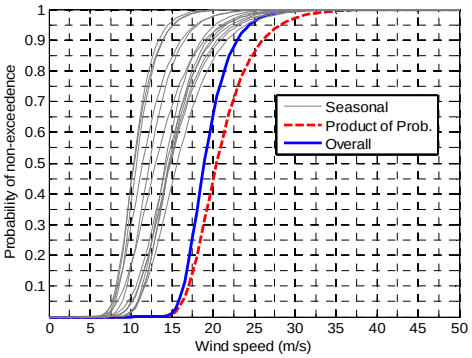
Probability of non-exceedence
Wind speed (m/s)
Seasonal
Product of Prob.
Overall

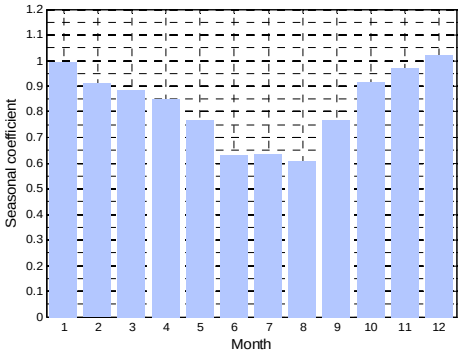
Seasonal coefficient
Month

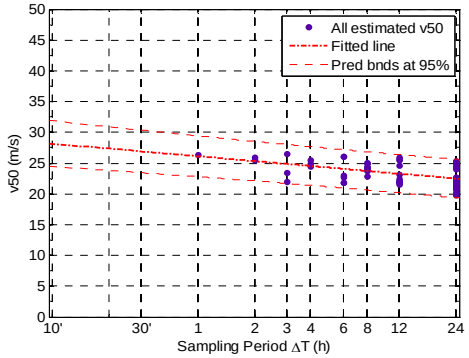
v50 (m/s)
Sampling Period ΔT (h)
All estimated v50
Fitted line
Pred bnds at 95%

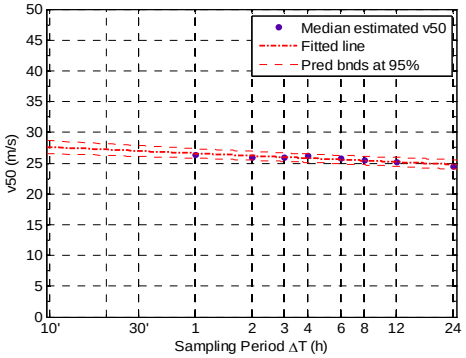
v50 (m/s)
Sampling Period ΔT (h)
Median estimated v50
Fitted line
Pred bnds at 95%

LIBN

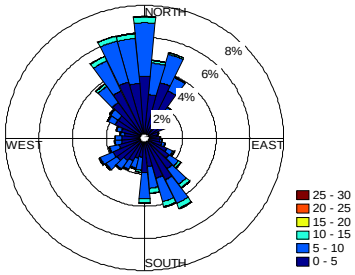
NORTH
8%
6%
4%
2%
WEST
EAST
SOUTH
25 - 30
20 - 25
15 - 20
10 - 15
5 - 10
0 - 5

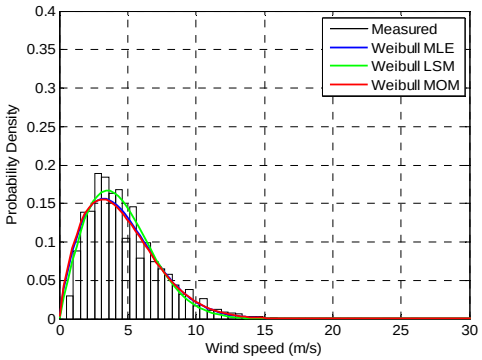
Measured
Weibull MLE
Weibull LSM
Weibull MOM
Probability Density
Wind speed (m/s)

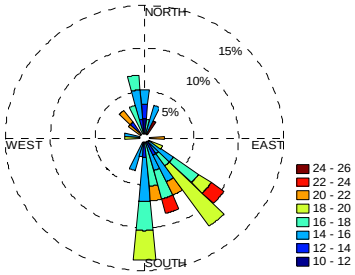
NORTH
15%
10%
5%
WEST
EAST
SOUTH
24 - 26
22 - 24
20 - 22
18 - 20
16 - 18
14 - 16
12 - 14
10 - 12

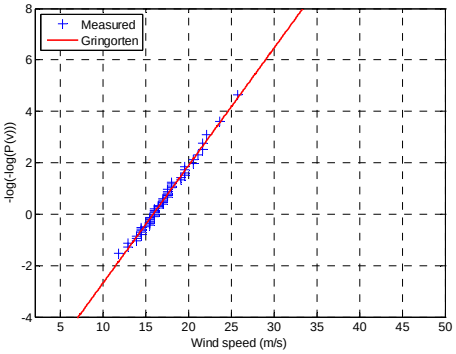
Measured
Gringorten
-log(-log(P(v)))
Wind speed (m/s)

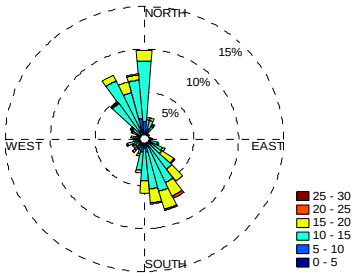
NORTH
15%
10%
5%
WEST
EAST
SOUTH
25 - 30
20 - 25
15 - 20
10 - 15
5 - 10
0 - 5

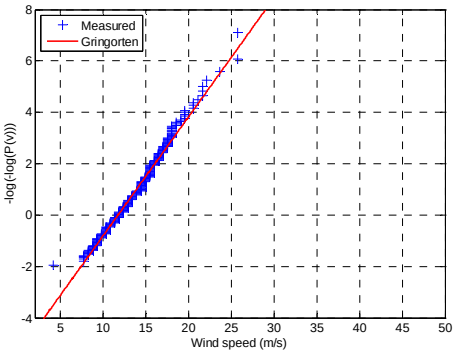
Measured
Gringorten
-log(-log(P(v)))
Wind speed (m/s)

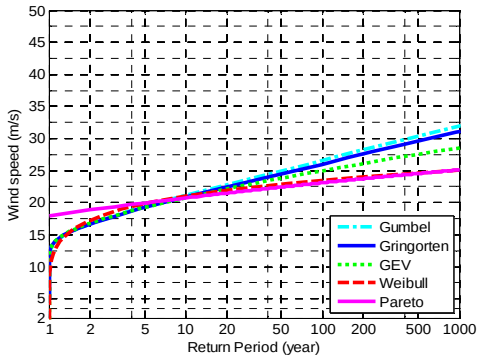
Wind speed (m/s)
Return Period (year)
Gumbel
Gringorten
GEV
Weibull
Pareto

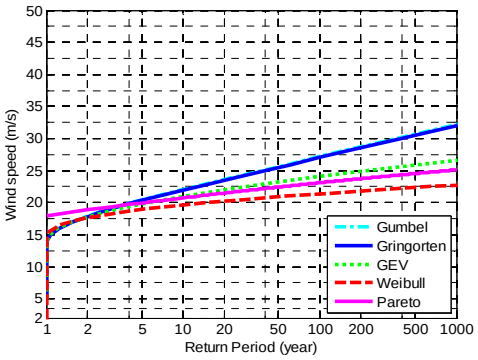
Wind speed (m/s)
Return Period (year)
Gumbel
Gringorten
GEV
Weibull
Pareto

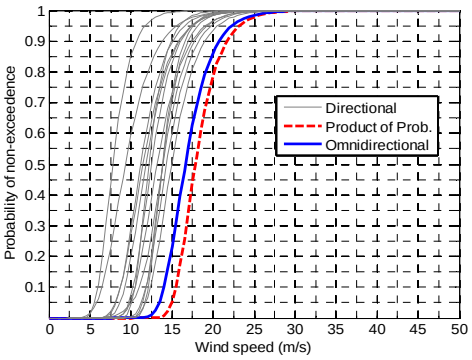
Probability of non-exceedence
Wind speed (m/s)
Directional
Product of Prob.
Omnidirectional

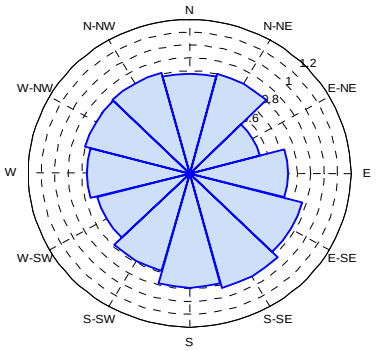
N
N-NE
E-NE
E
E-SE
S-SE
S
S-SW
W
W-NW
N-NW

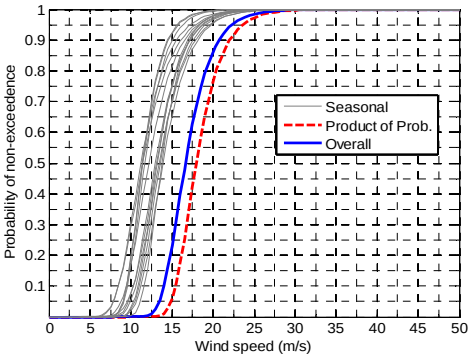
Probability of non-exceedence
Wind speed (m/s)
Seasonal
Product of Prob.
Overall

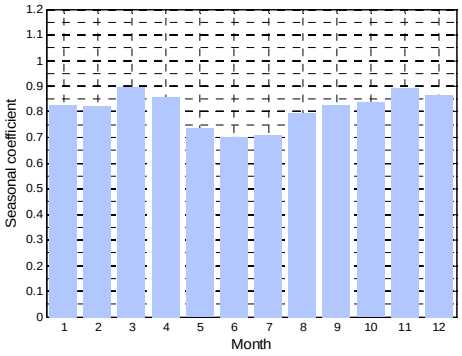
Seasonal coefficient
Month

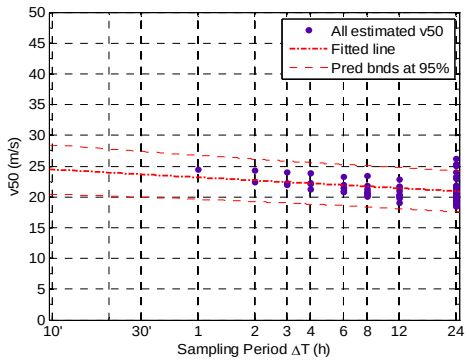
v50 (m/s)
Sampling Period ΔT (h)
All estimated v50
Fitted line
Pred bnds at 95%

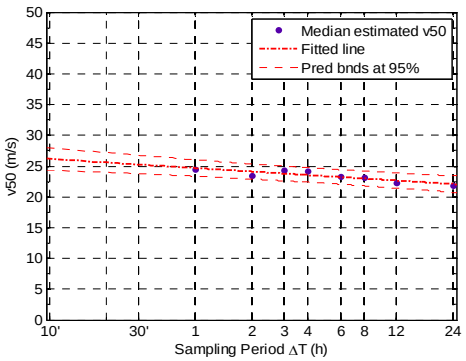
v50 (m/s)
Sampling Period ΔT (h)
Median estimated v50
Fitted line
Pred bnds at 95%

LIBP

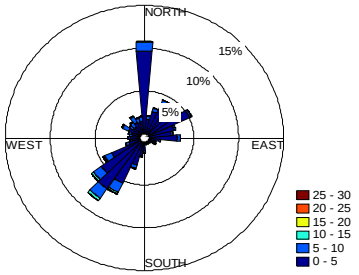
NORTH
15%
10%
5%
WEST
EAST
SOUTH
25 - 30
20 - 25
15 - 20
10 - 15
5 - 10
0 - 5

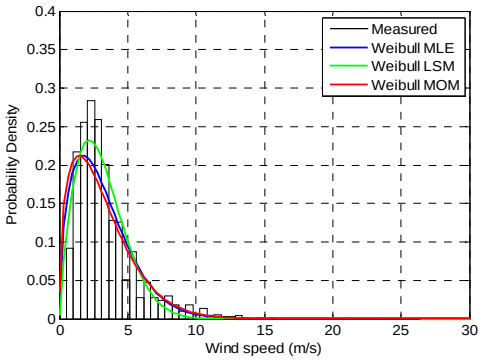
Measured
Weibull MLE
Weibull LSM
Weibull MOM
Probability Density
Wind speed (m/s)

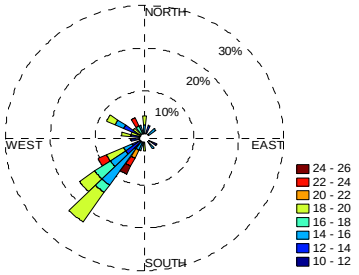
NORTH
30%
20%
10%
WEST
EAST
SOUTH
24 - 26
22 - 24
20 - 22
18 - 20
16 - 18
14 - 16
12 - 14
10 - 12

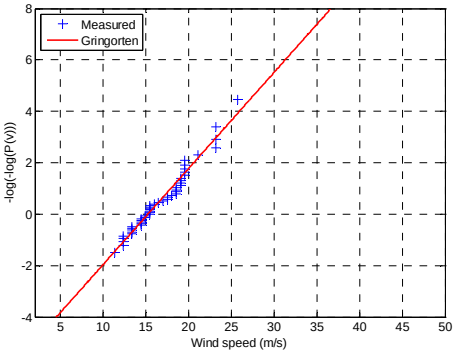
Measured
Gringorten
-log(-log(P(v)))
Wind speed (m/s)

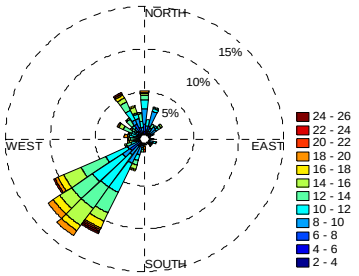
NORTH
15%
10%
5%
WEST
EAST
SOUTH
24 - 26
22 - 24
20 - 22
18 - 20
16 - 18
14 - 16
12 - 14
10 - 12
8 - 10
6 - 8
4 - 6
2 - 4

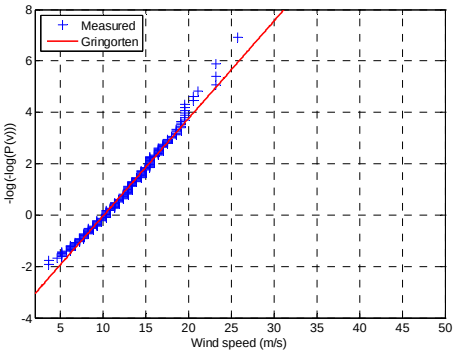
Measured
Gringorten
-log(-log(P(v)))
Wind speed (m/s)

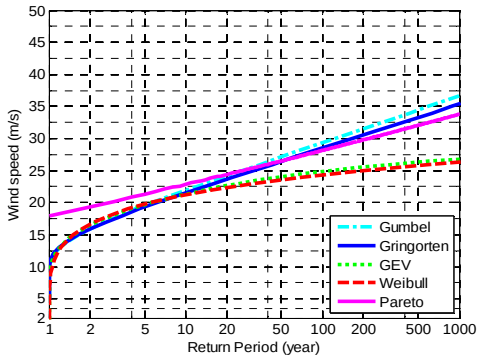
Wind speed (m/s)
Return Period (year)
Gumbel
Gringorten
GEV
Weibull
Pareto

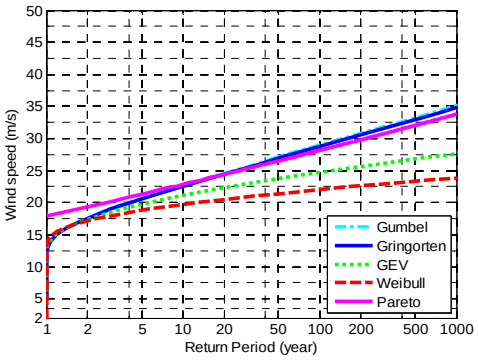
Wind speed (m/s)
Return Period (year)
Gumbel
Gringorten
GEV
Weibull
Pareto

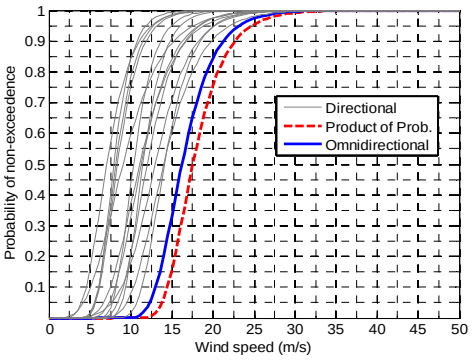
Probability of non-exceedence
Wind speed (m/s)
Directional
Product of Prob.
Omnidirectional

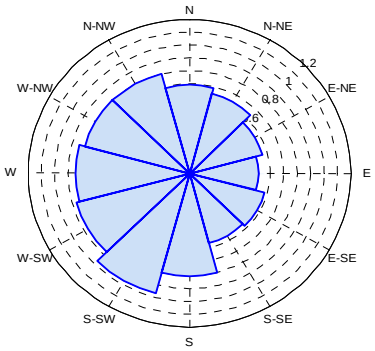
N
N-NE
E-NE
E
E-SE
S-SE
S
S-SW
W
W-NW
N-NW

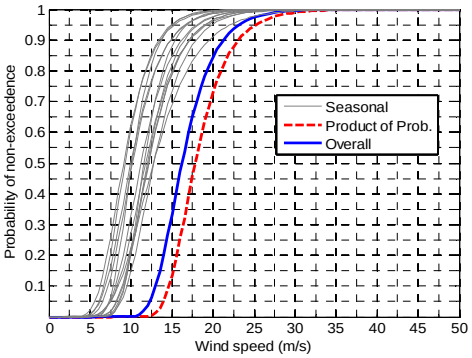
Probability of non-exceedence
Wind speed (m/s)
Seasonal
Product of Prob.
Overall

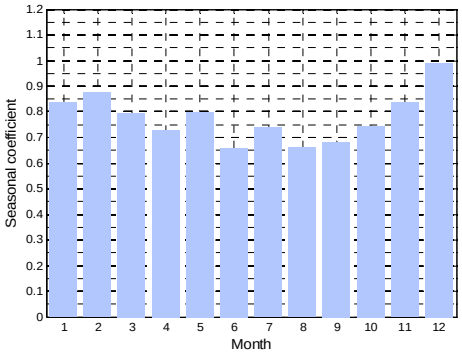
Seasonal coefficient
Month

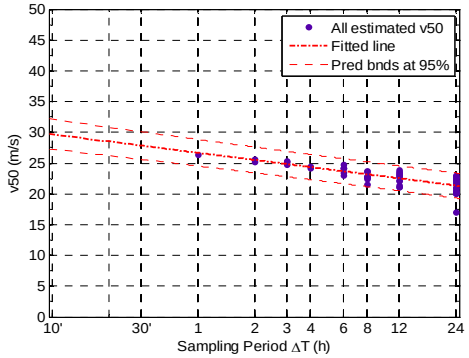
v50 (m/s)
Sampling Period ΔT (h)
All estimated v50
Fitted line
Pred bnds at 95%

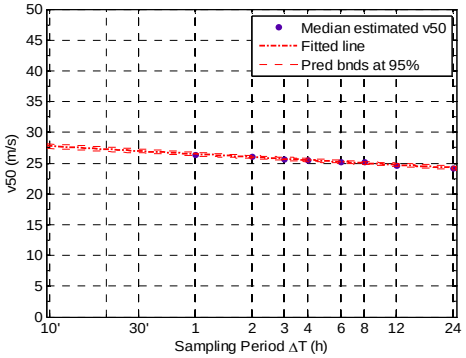
v50 (m/s)
Sampling Period ΔT (h)
Median estimated v50
Fitted line
Pred bnds at 95%

LIBQ

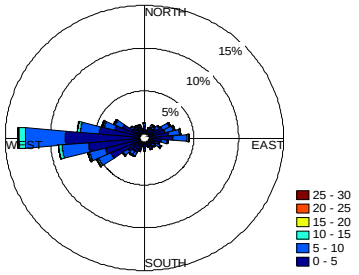
NORTH
15%
10%
5%
WEST
EAST
SOUTH
25 - 30
20 - 25
15 - 20
10 - 15
5 - 10
0 - 5

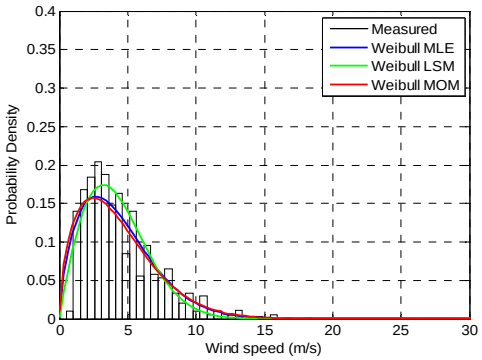
Measured
Weibull MLE
Weibull LSM
Weibull MOM
Probability Density
Wind speed (m/s)

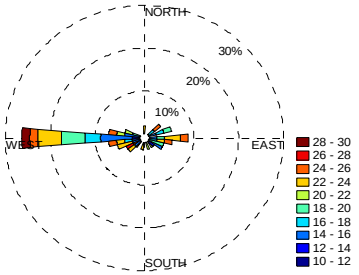
NORTH
30%
20%
10%
WEST
EAST
SOUTH
28 - 30
26 - 28
24 - 26
22 - 24
20 - 22
18 - 20
16 - 18
14 - 16
12 - 14
10 - 12

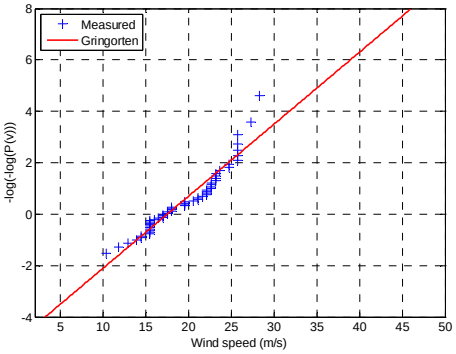
Measured
Gringorten
-log(-log(P(v)))
Wind speed (m/s)

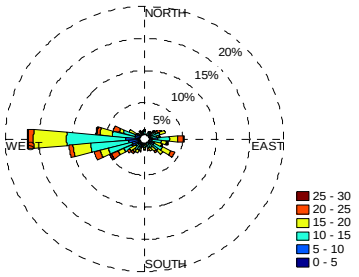
NORTH
20%
15%
10%
5%
WEST
EAST
SOUTH
25 - 30
20 - 25
15 - 20
10 - 15
5 - 10
0 - 5

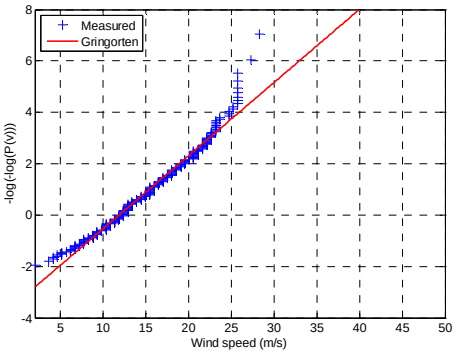
Measured
Gringorten
-log(-log(P(v)))
Wind speed (m/s)

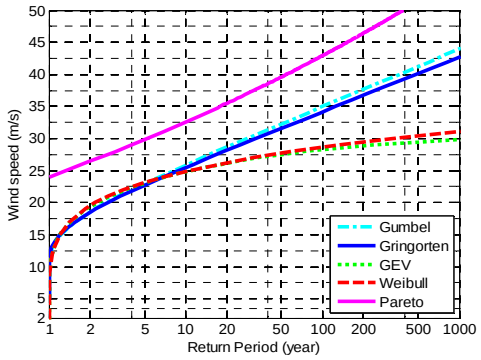
Wind speed (m/s)
Return Period (year)
Gumbel
Gringorten
GEV
Weibull
Pareto

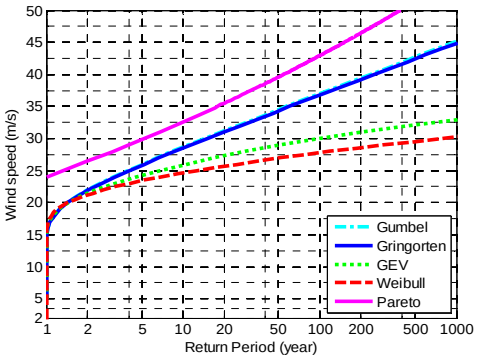
Wind speed (m/s)
Return Period (year)
Gumbel
Gringorten
GEV
Weibull
Pareto

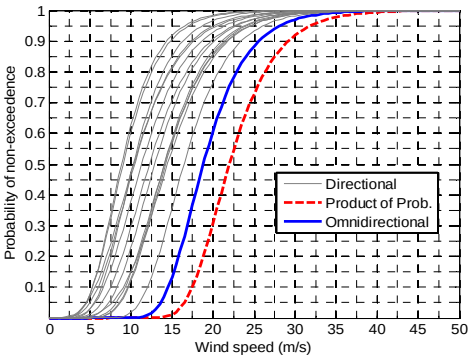
Probability of non-exceedence
Wind speed (m/s)
Directional
Product of Prob.
Omnidirectional

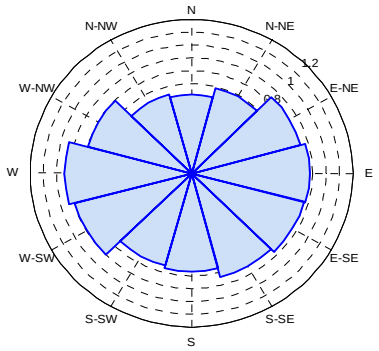
N
N-NE
E-NE
E
E-SE
S-SE
S
S-SW
W
W-NW
N-NW

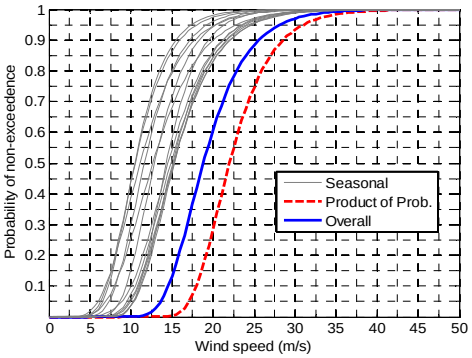
Probability of non-exceedence
Wind speed (m/s)
Seasonal
Product of Prob.
Overall

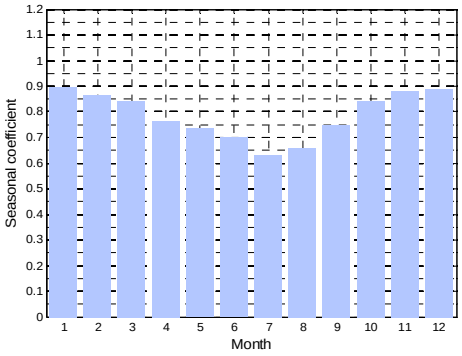
Seasonal coefficient
Month

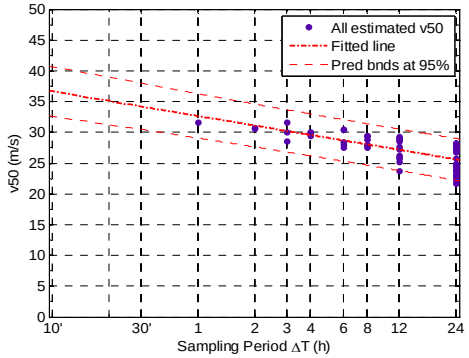
v50 (m/s)
Sampling Period ΔT (h)
All estimated v50
Fitted line
Pred bnds at 95%

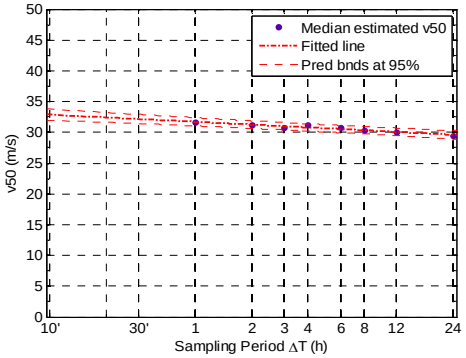
v50 (m/s)
Sampling Period ΔT (h)
Median estimated v50
Fitted line
Pred bnds at 95%

LIBR

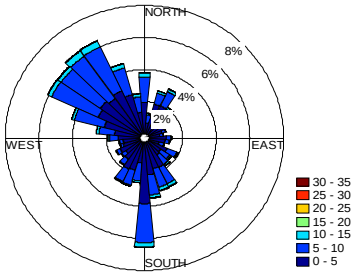
NORTH
8%
6%
4%
2%
WEST
EAST
SOUTH
30 - 35
25 - 30
20 - 25
15 - 20
10 - 15
5 - 10
0 - 5

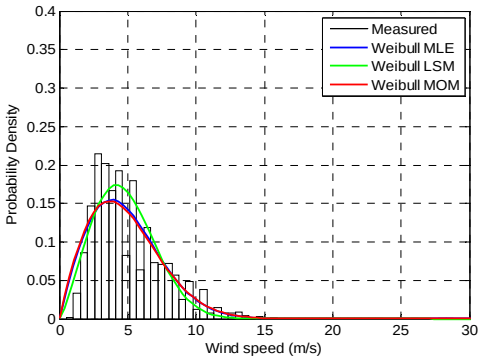
Measured
Weibull MLE
Weibull LSM
Weibull MOM
Probability Density
Wind speed (m/s)

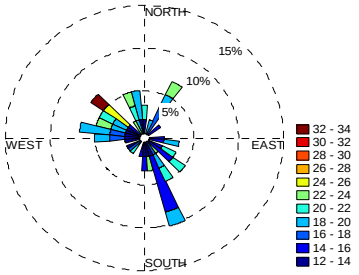
NORTH
15%
10%
5%
WEST
EAST
SOUTH
32 - 34
30 - 32
28 - 30
26 - 28
24 - 26
22 - 24
20 - 22
18 - 20
16 - 18
14 - 16
12 - 14

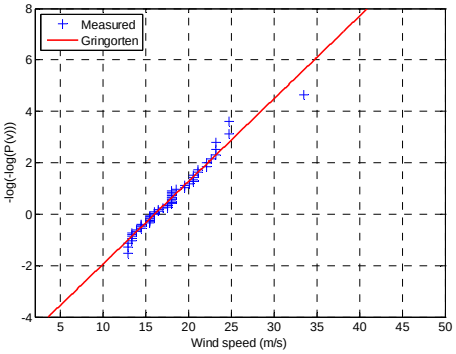
Measured
Gringorten
-log(-log(P(v)))
Wind speed (m/s)

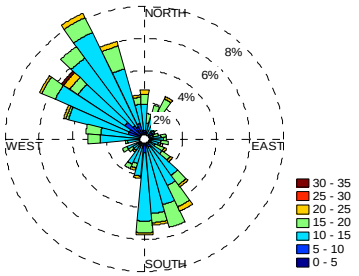
NORTH
8%
6%
4%
2%
WEST
EAST
SOUTH
30 - 35
25 - 30
20 - 25
15 - 20
10 - 15
5 - 10
0 - 5

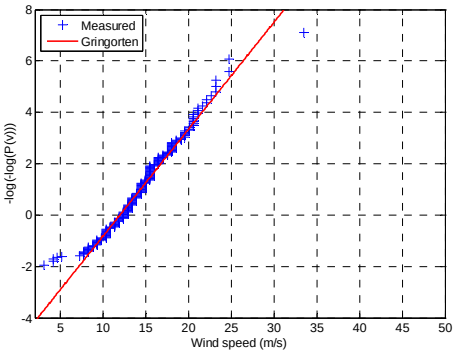
Measured
Gringorten
-log(-log(P(v)))
Wind speed (m/s)

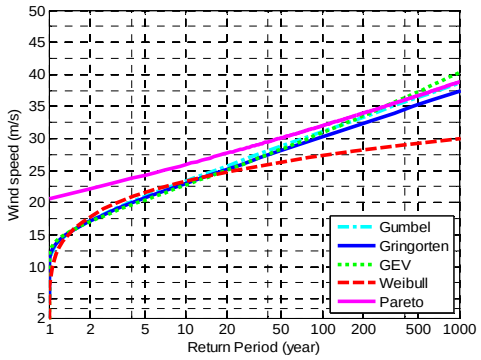
Wind speed (m/s)
Return Period (year)
Gumbel
Gringorten
GEV
Weibull
Pareto

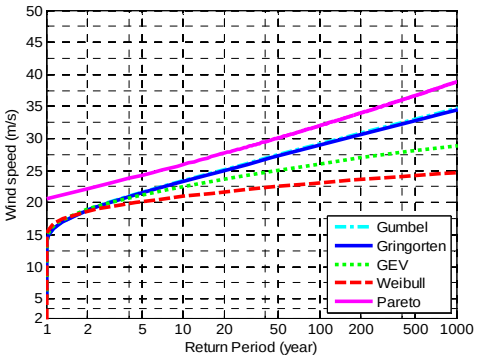
Wind speed (m/s)
Return Period (year)
Gumbel
Gringorten
GEV
Weibull
Pareto

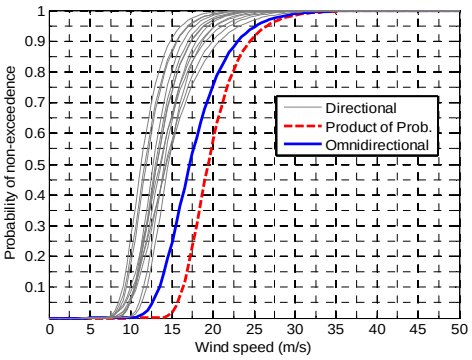
Probability of non-exceedence
Wind speed (m/s)
Directional
Product of Prob.
Omnidirectional

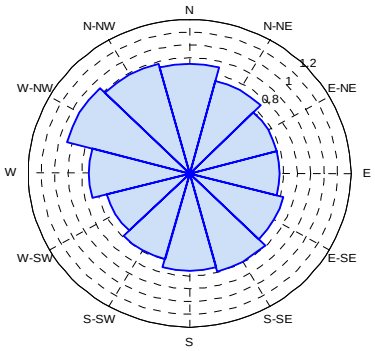
N
N-NE
E-NE
E
E-SE
S-SE
S
S-SW
W
W-NW
N-NW

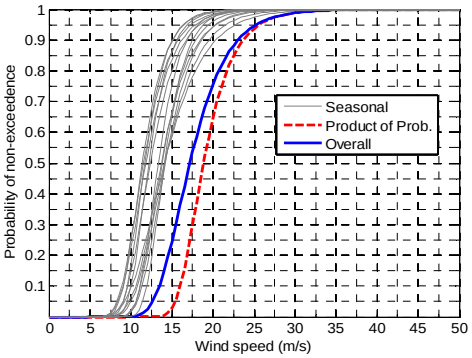
Probability of non-exceedence
Wind speed (m/s)
Seasonal
Product of Prob.
Overall

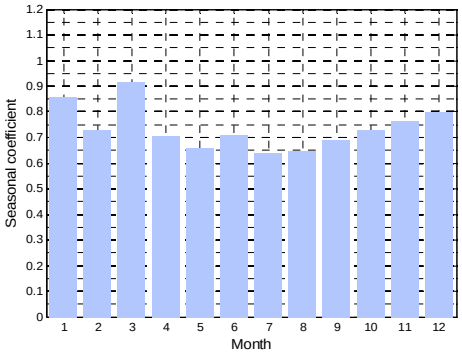
Seasonal coefficient
Month

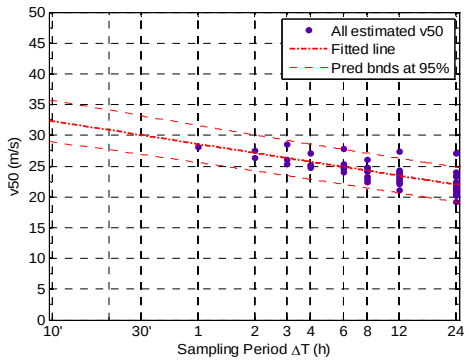
v50 (m/s)
Sampling Period ΔT (h)
All estimated v50
Fitted line
Pred bnds at 95%

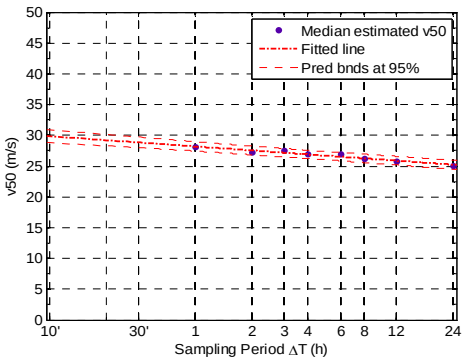
v50 (m/s)
Sampling Period ΔT (h)
Median estimated v50
Fitted line
Pred bnds at 95%

LIBS

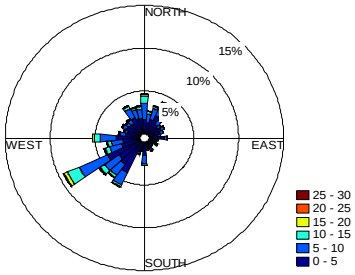
NORTH
15%
10%
5%
WEST
EAST
SOUTH
25 - 30
20 - 25
15 - 20
10 - 15
5 - 10
0 - 5

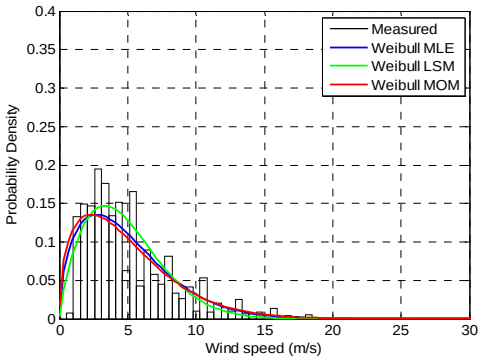
Measured
Weibull MLE
Weibull LSM
Weibull MOM
Probability Density
Wind speed (m/s)

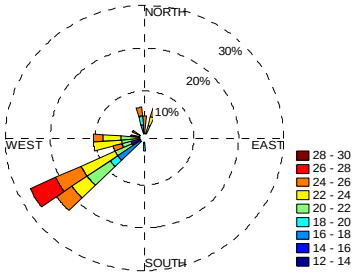
NORTH
30%
20%
10%
WEST
EAST
SOUTH
28 - 30
26 - 28
24 - 26
22 - 24
20 - 22
18 - 20
16 - 18
14 - 16
12 - 14

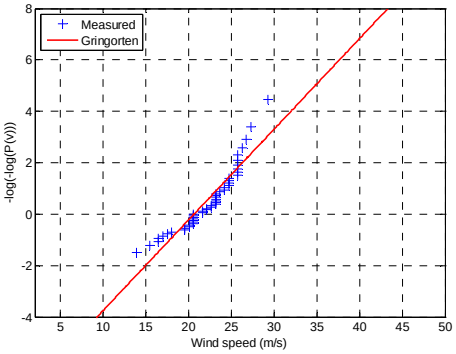
Measured
Gringorten
-log(-log(P(v)))
Wind speed (m/s)

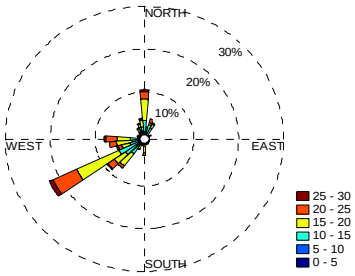
NORTH
30%
20%
10%
WEST
EAST
SOUTH
25 - 30
20 - 25
15 - 20
10 - 15
5 - 10
0 - 5

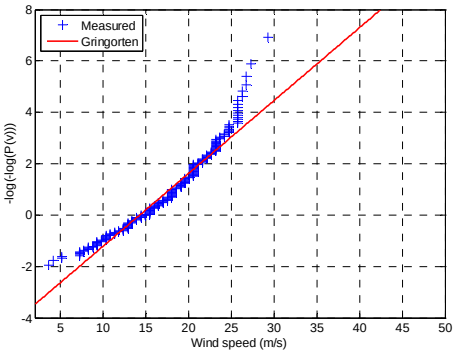
Measured
Gringorten
-log(-log(P(v)))
Wind speed (m/s)

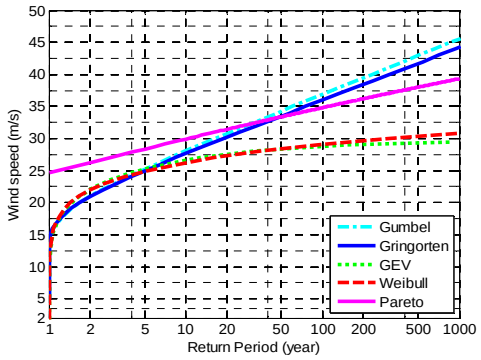
Wind speed (m/s)
Return Period (year)
Gumbel
Gringorten
GEV
Weibull
Pareto

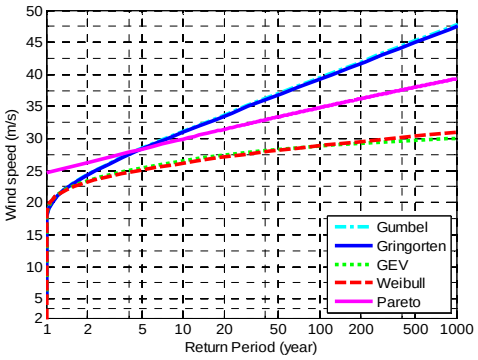
Wind speed (m/s)
Return Period (year)
Gumbel
Gringorten
GEV
Weibull
Pareto

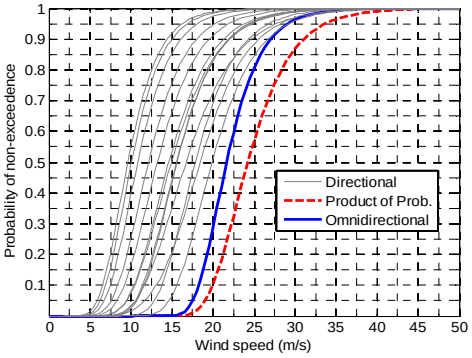
Probability of non-exceedence
Wind speed (m/s)
Directional
Product of Prob.
Omnidirectional

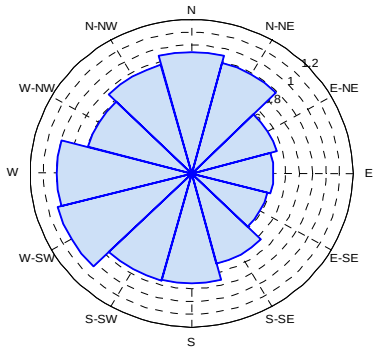
N
N-NE
E-NE
E
E-SE
S-SE
S
S-SW
W
W-NW
N-NW

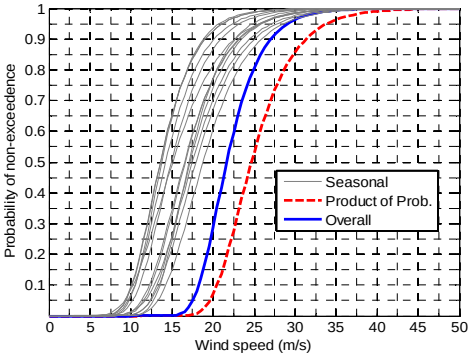
Probability of non-exceedence
Wind speed (m/s)
Seasonal
Product of Prob.
Overall

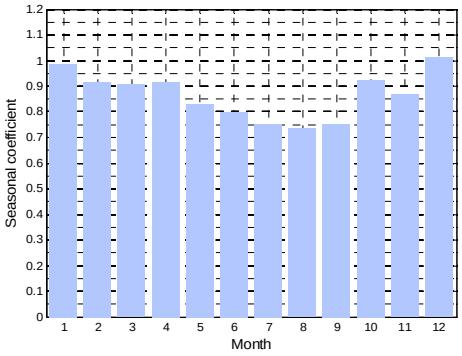
Seasonal coefficient
Month

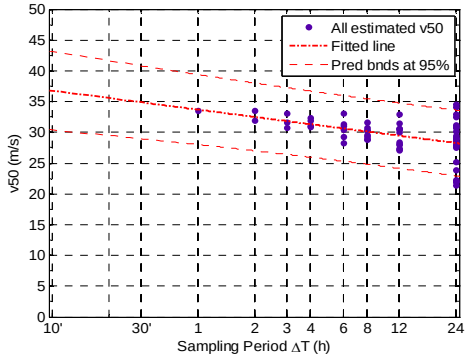
v50 (m/s)
Sampling Period ΔT (h)
All estimated v50
Fitted line
Pred bnds at 95%

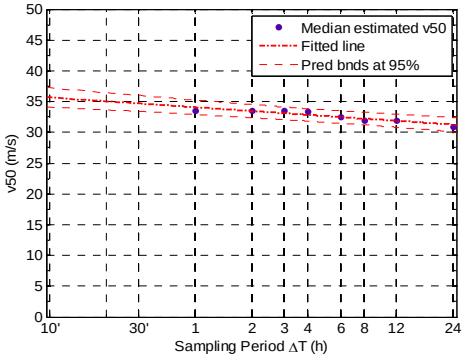
v50 (m/s)
Sampling Period ΔT (h)
Median estimated v50
Fitted line
Pred bnds at 95%

LIBT

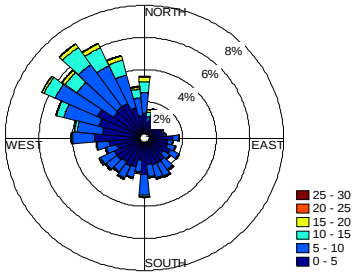
NORTH
8%
6%
4%
2%
WEST
EAST
SOUTH
25 - 30
20 - 25
15 - 20
10 - 15
5 - 10
0 - 5

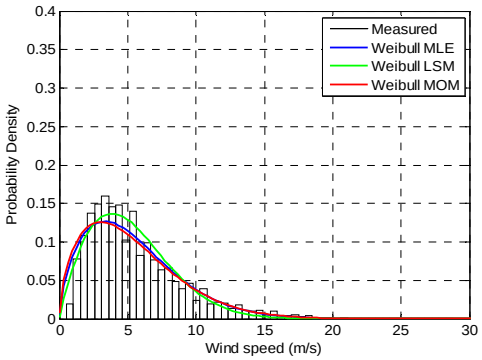
Measured
Weibull MLE
Weibull LSM
Weibull MOM
Probability Density
Wind speed (m/s)

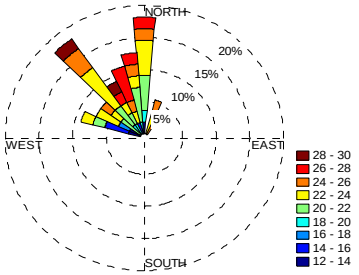
NORTH
20%
15%
10%
5%
WEST
EAST
SOUTH
28 - 30
26 - 28
24 - 26
22 - 24
20 - 22
18 - 20
16 - 18
14 - 16
12 - 14

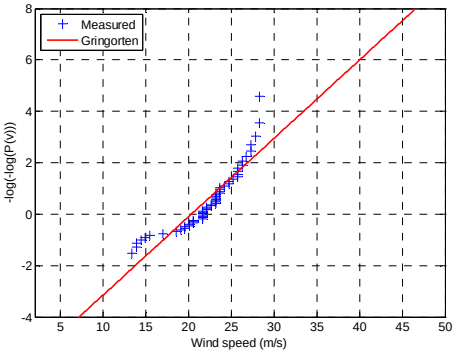
Measured
Gringorten
-log(-log(P(v)))
Wind speed (m/s)

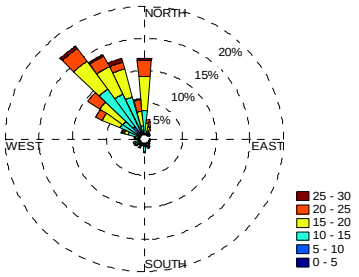
NORTH
20%
15%
10%
5%
WEST
EAST
SOUTH
25 - 30
20 - 25
15 - 20
10 - 15
5 - 10
0 - 5

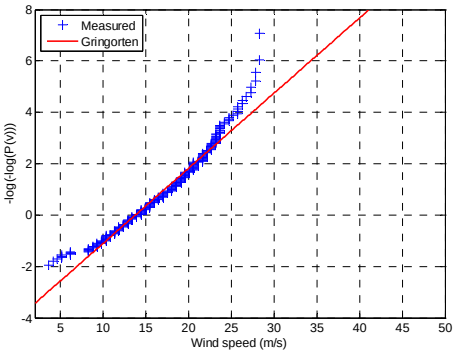
Measured
Gringorten
-log(-log(P(v)))
Wind speed (m/s)

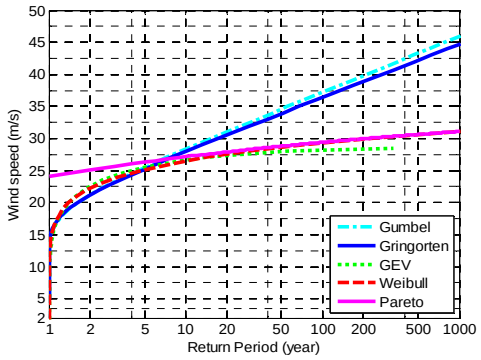
Wind speed (m/s)
Return Period (year)
Gumbel
Gringorten
GEV
Weibull
Pareto

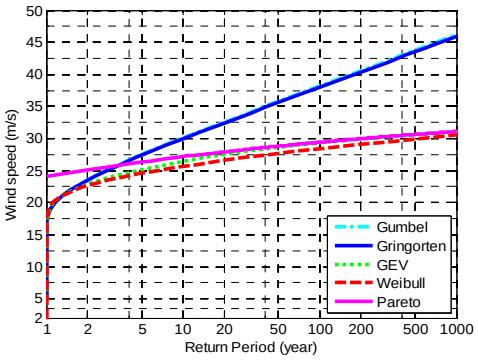
Wind speed (m/s)
Return Period (year)
Gumbel
Gringorten
GEV
Weibull
Pareto

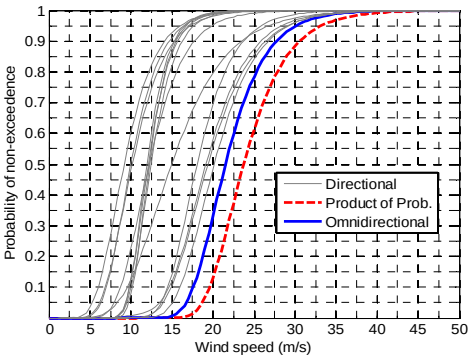
Probability of non-exceedence
Wind speed (m/s)
Directional
Product of Prob.
Omnidirectional

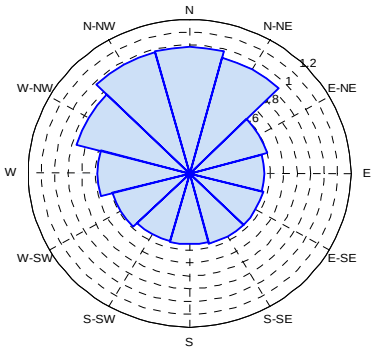
N
N-NE
E-NE
E
E-SE
S-SE
S
S-SW
W
W-NW
N-NW

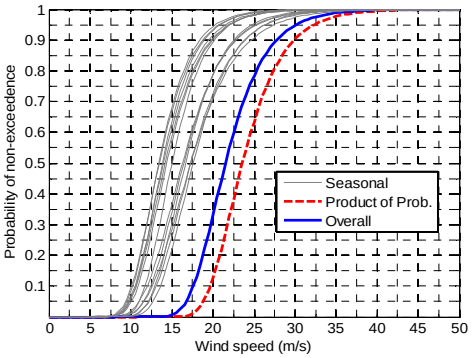
Probability of non-exceedence
Wind speed (m/s)
Seasonal
Product of Prob.
Overall

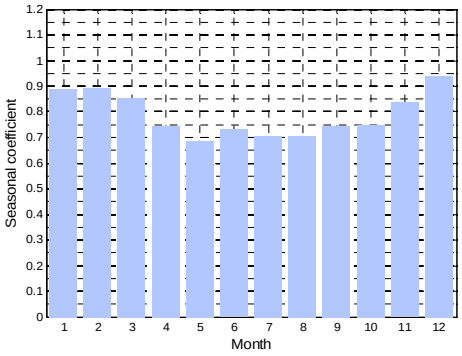
Seasonal coefficient
Month

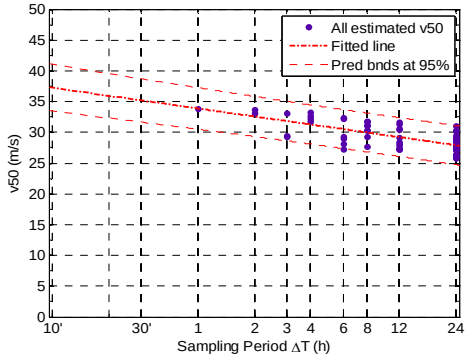
v50 (m/s)
Sampling Period ΔT (h)
All estimated v50
Fitted line
Pred bnds at 95%

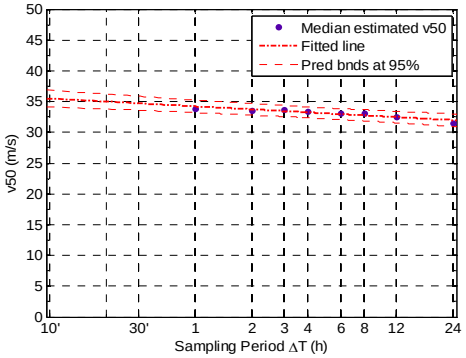
v50 (m/s)
Sampling Period ΔT (h)
Median estimated v50
Fitted line
Pred bnds at 95%

LIBU

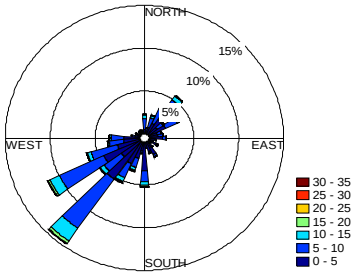
NORTH
15%
10%
5%
WEST
EAST
SOUTH
30 - 35
25 - 30
20 - 25
15 - 20
10 - 15
5 - 10
0 - 5

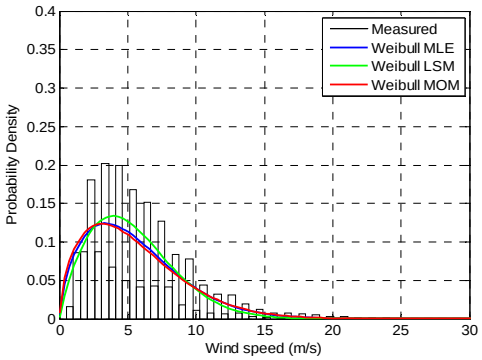
Measured
Weibull MLE
Weibull LSM
Weibull MOM
Probability Density
Wind speed (m/s)

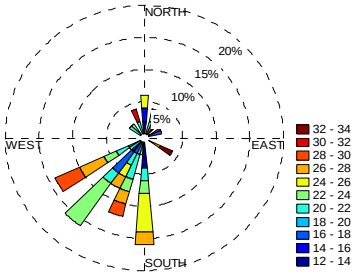
NORTH
20%
15%
10%
5%
WEST
EAST
SOUTH
32 - 34
30 - 32
28 - 30
26 - 28
24 - 26
22 - 24
20 - 22
18 - 20
16 - 18
14 - 16
12 - 14

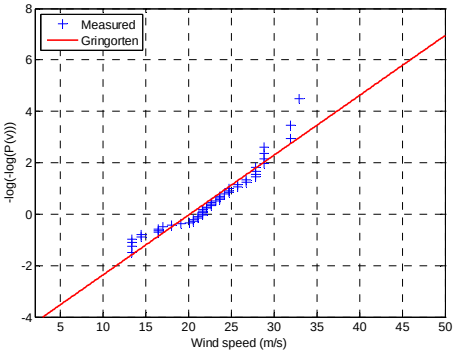
Measured
Gringorten
-log(-log(P(v)))
Wind speed (m/s)

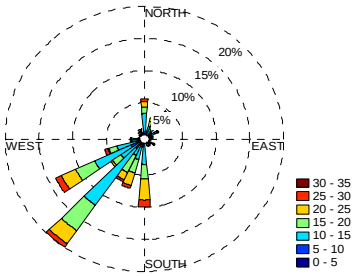
NORTH
20%
15%
10%
5%
WEST
EAST
SOUTH
30 - 35
25 - 30
20 - 25
15 - 20
10 - 15
5 - 10
0 - 5

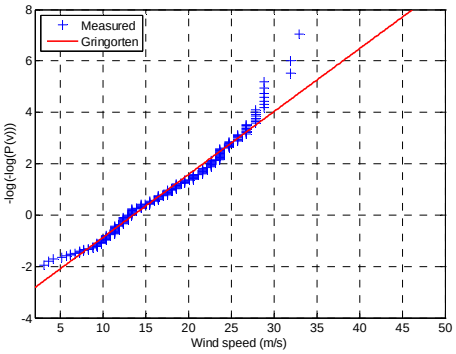
Measured
Gringorten
-log(-log(P(v)))
Wind speed (m/s)

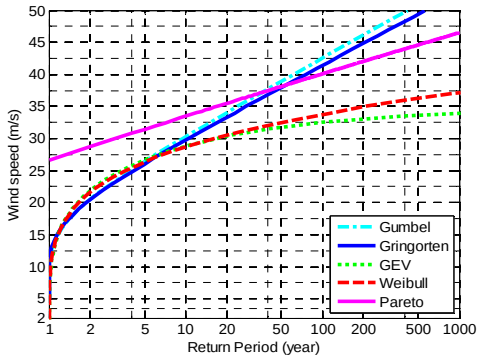
Wind speed (m/s)
Return Period (year)
Gumbel
Gringorten
GEV
Weibull
Pareto

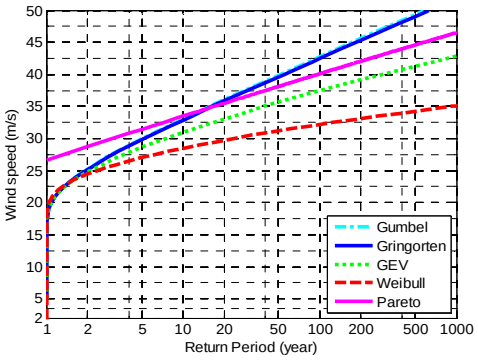
Wind speed (m/s)
Return Period (year)
Gumbel
Gringorten
GEV
Weibull
Pareto

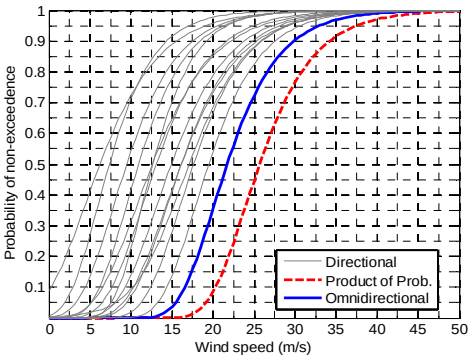
Probability of non-exceedence
Wind speed (m/s)
Directional
Product of Prob.
Omnidirectional

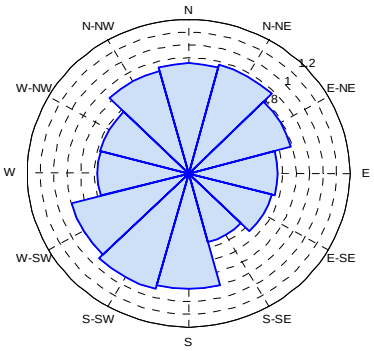
N
N-NE
E-NE
E
E-SE
S-SE
S
S-SW
W
W-NW
N-NW

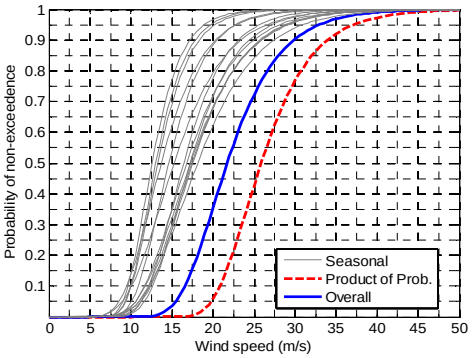
Probability of non-exceedence
Wind speed (m/s)
Seasonal
Product of Prob.
Overall

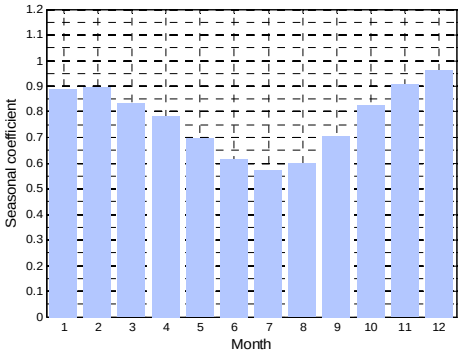
Seasonal coefficient
Month

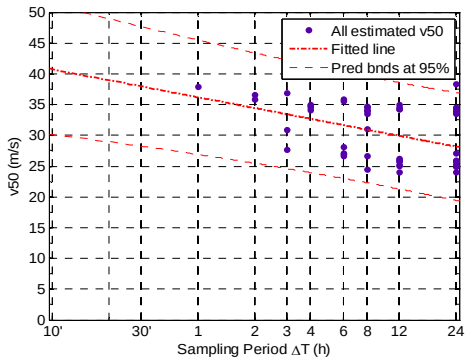
v50 (m/s)
Sampling Period ΔT (h)
All estimated v50
Fitted line
Pred bnds at 95%

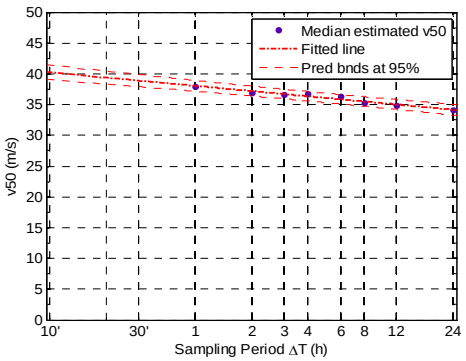
v50 (m/s)
Sampling Period ΔT (h)
Median estimated v50
Fitted line
Pred bnds at 95%

LIBV

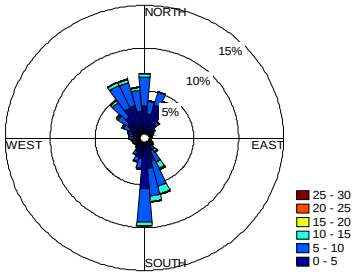
NORTH
15%
10%
5%
WEST
EAST
SOUTH
25 - 30
20 - 25
15 - 20
10 - 15
5 - 10
0 - 5

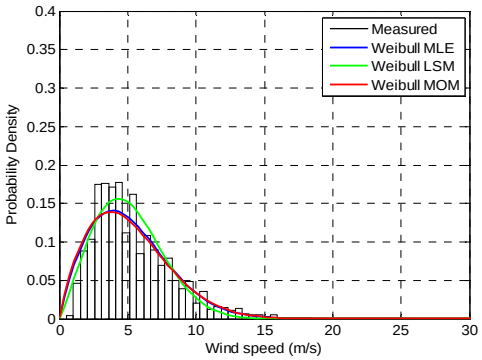
Measured
Weibull MLE
Weibull LSM
Weibull MOM
Probability Density
Wind speed (m/s)

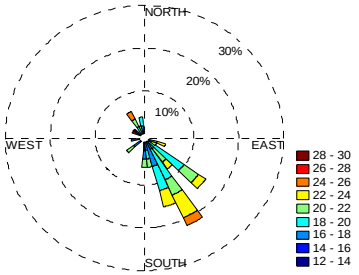
NORTH
30%
20%
10%
WEST
EAST
SOUTH
28 - 30
26 - 28
24 - 26
22 - 24
20 - 22
18 - 20
16 - 18
14 - 16
12 - 14

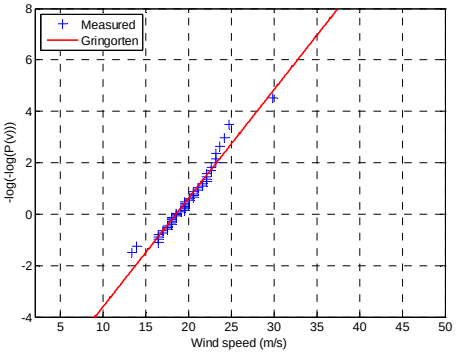
Measured
Gringorten
-log(-log(P(v)))
Wind speed (m/s)

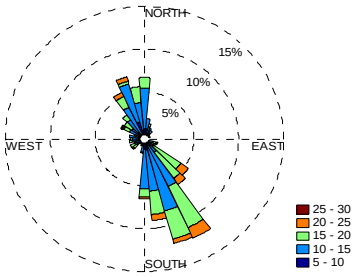
NORTH
15%
10%
5%
WEST
EAST
SOUTH
25 - 30
20 - 25
15 - 20
10 - 15
5 - 10

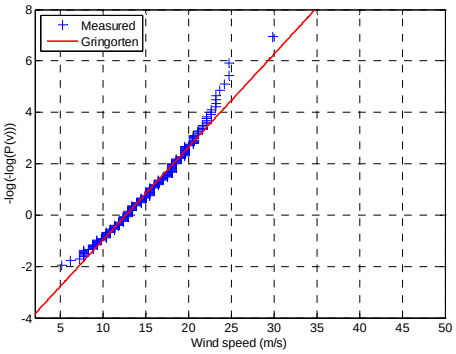
Measured
Gringorten
-log(-log(P(v)))
Wind speed (m/s)

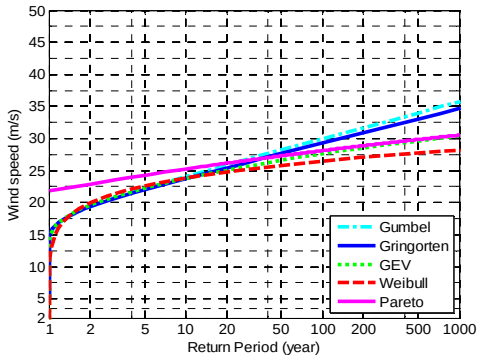
Wind speed (m/s)
Return Period (year)
Gumbel
Gringorten
GEV
Weibull
Pareto

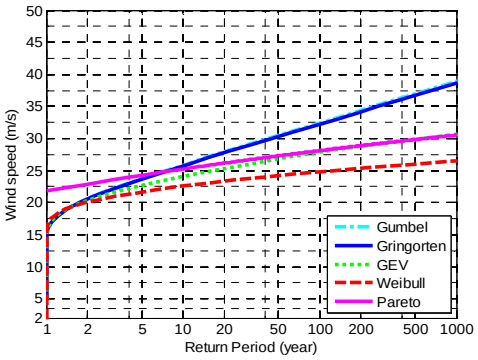
Wind speed (m/s)
Return Period (year)
Gumbel
Gringorten
GEV
Weibull
Pareto

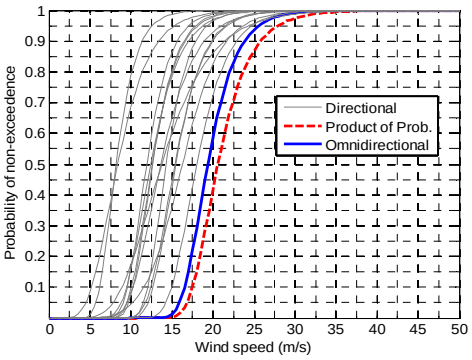
Probability of non-exceedence
Wind speed (m/s)
Directional
Product of Prob.
Omnidirectional

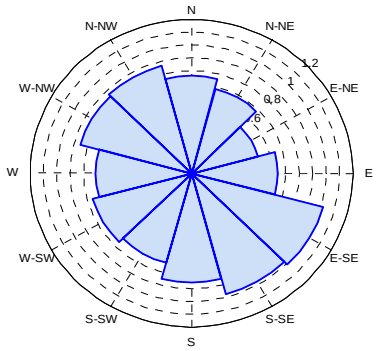
N
N-NE
E-NE
E
E-SE
S-SE
S
S-SW
W
W-NW
N-NW

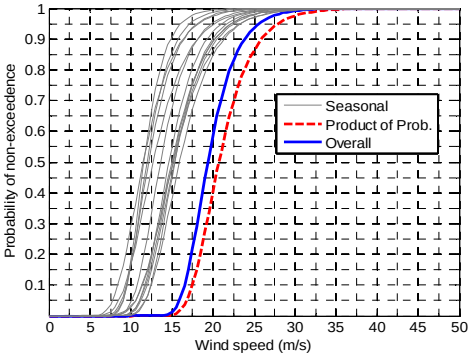
Probability of non-exceedence
Wind speed (m/s)
Seasonal
Product of Prob.
Overall

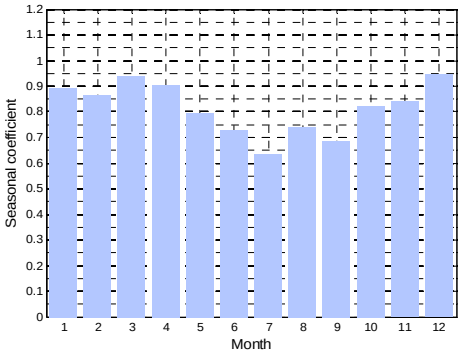
Seasonal coefficient
Month

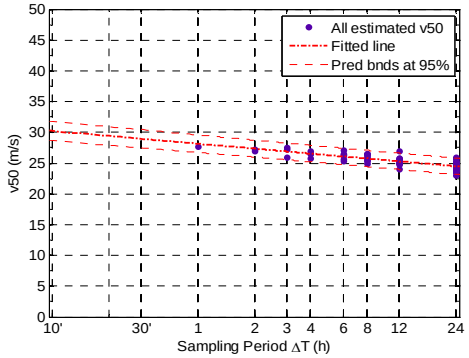
v50 (m/s)
Sampling Period ΔT (h)
All estimated v50
Fitted line
Pred bnds at 95%

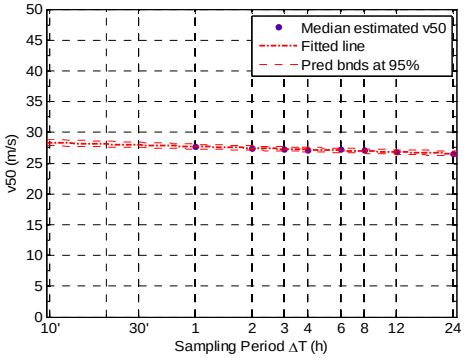
v50 (m/s)
Sampling Period ΔT (h)
Median estimated v50
Fitted line
Pred bnds at 95%

LIBW

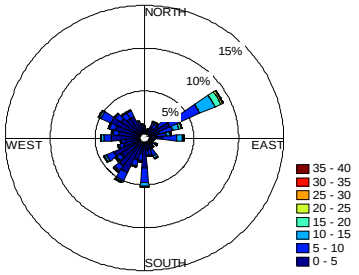
NORTH
15%
10%
5%
WEST
EAST
SOUTH
35 - 40
30 - 35
25 - 30
20 - 25
15 - 20
10 - 15
5 - 10
0 - 5

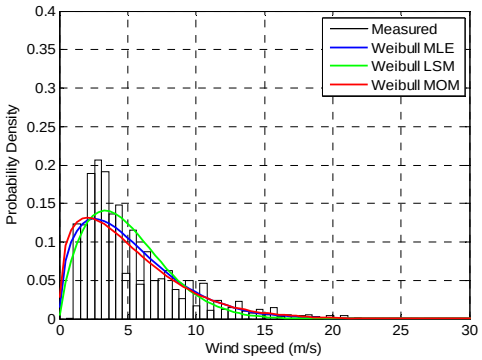
Measured
Weibull MLE
Weibull LSM
Weibull MOM
Probability Density
Wind speed (m/s)

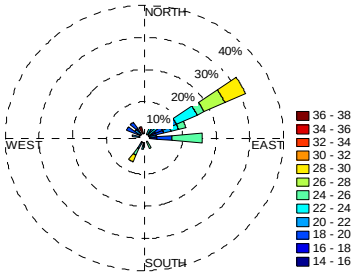
NORTH
40%
30%
20%
10%
WEST
EAST
SOUTH
36 - 38
34 - 36
32 - 34
30 - 32
28 - 30
26 - 28
24 - 26
22 - 24
20 - 22
18 - 20
16 - 18
14 - 16

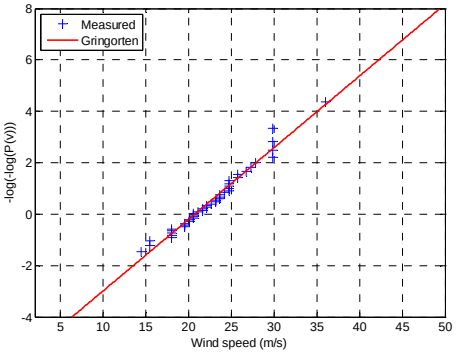
Measured
Gringorten
-log(-log(P(v)))
Wind speed (m/s)

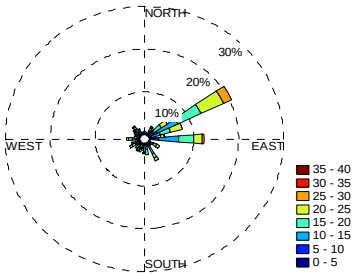
NORTH
30%
20%
10%
WEST
EAST
SOUTH
35 - 40
30 - 35
25 - 30
20 - 25
15 - 20
10 - 15
5 - 10
0 - 5

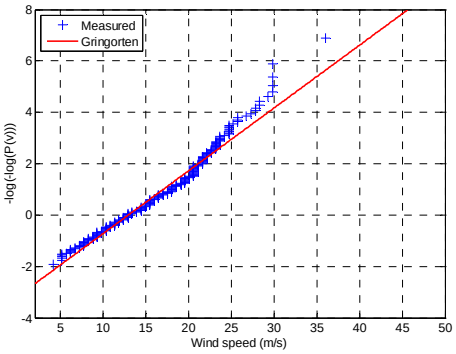
Measured
Gringorten
-log(-log(P(v)))
Wind speed (m/s)

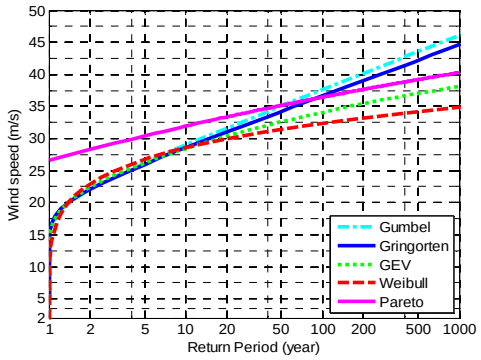
Wind speed (m/s)
Return Period (year)
Gumbel
Gringorten
GEV
Weibull
Pareto

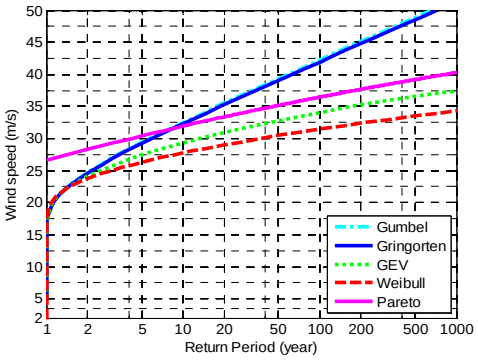
Wind speed (m/s)
Return Period (year)
Gumbel
Gringorten
GEV
Weibull
Pareto

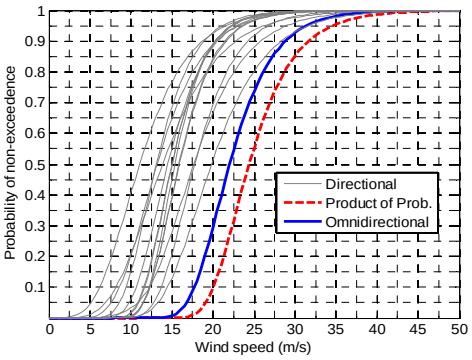
Probability of non-exceedence
Wind speed (m/s)
Directional
Product of Prob.
Omnidirectional

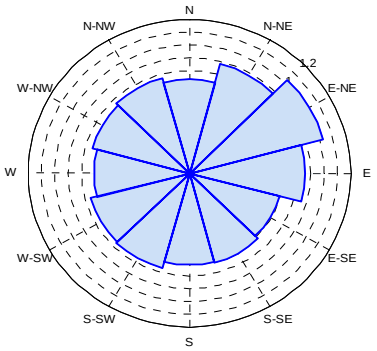
N
N-NE
E-NE
E
E-SE
S-SE
S
S-SW
W
W-NW
N-NW

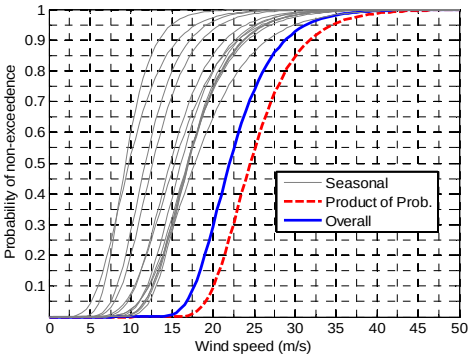
Probability of non-exceedence
Wind speed (m/s)
Seasonal
Product of Prob.
Overall

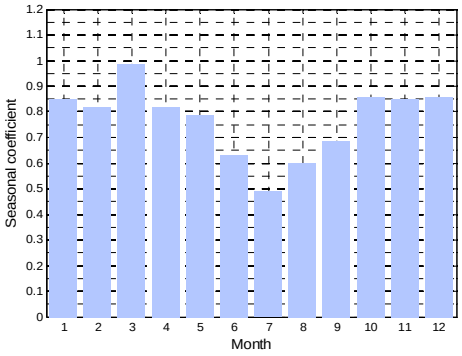
Seasonal coefficient
Month

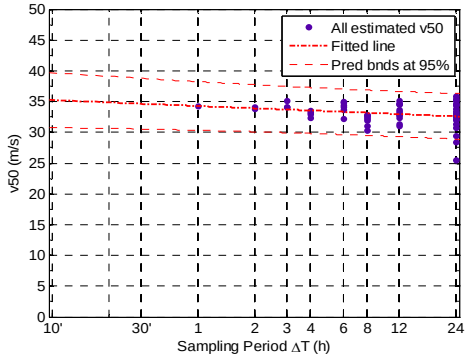
v50 (m/s)
Sampling Period ΔT (h)
All estimated v50
Fitted line
Pred bnds at 95%

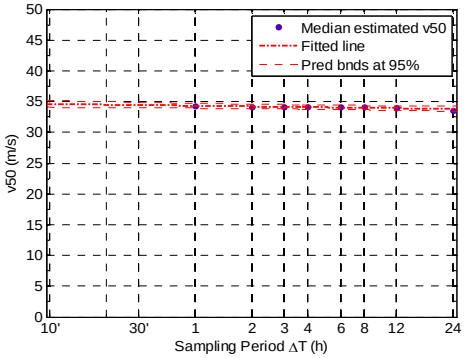
v50 (m/s)
Sampling Period ΔT (h)
Median estimated v50
Fitted line
Pred bnds at 95%

LIBY

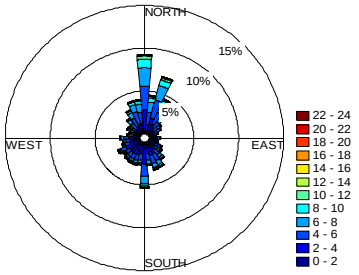
NORTH
15%
10%
5%
WEST
EAST
SOUTH
22 - 24
20 - 22
18 - 20
16 - 18
14 - 16
12 - 14
10 - 12
8 - 10
6 - 8
4 - 6
2 - 4
0 - 2

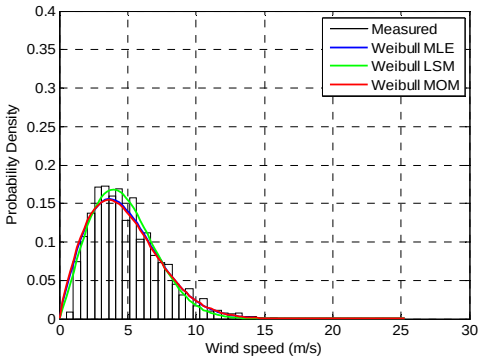
Measured
Weibull MLE
Weibull LSM
Weibull MOM
Probability Density
Wind speed (m/s)

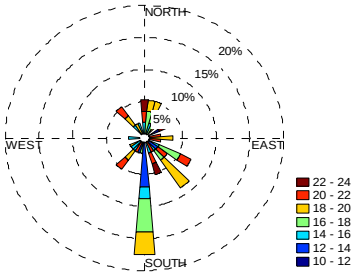
NORTH
20%
15%
10%
5%
WEST
EAST
SOUTH
22 - 24
20 - 22
18 - 20
16 - 18
14 - 16
12 - 14
10 - 12

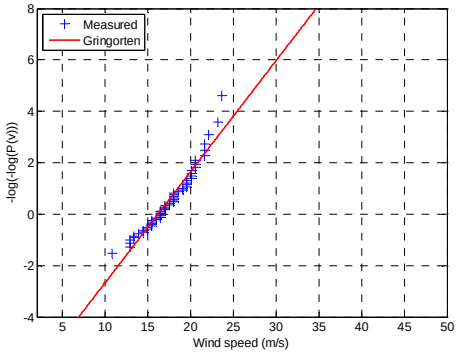
Measured
Gringorten
-log(-log(P(v)))
Wind speed (m/s)

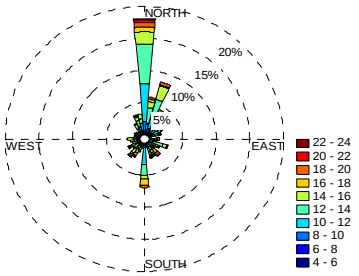
NORTH
20%
15%
10%
5%
WEST
EAST
SOUTH
22 - 24
20 - 22
18 - 20
16 - 18
14 - 16
12 - 14
10 - 12
8 - 10
6 - 8
4 - 6

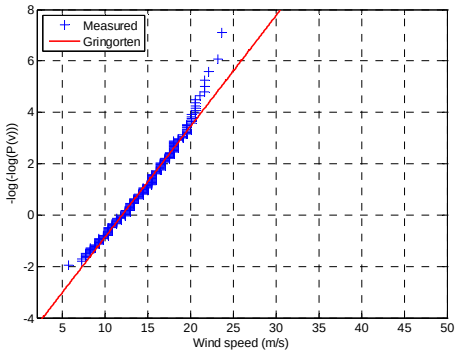
Measured
Gringorten
-log(-log(P(v)))
Wind speed (m/s)

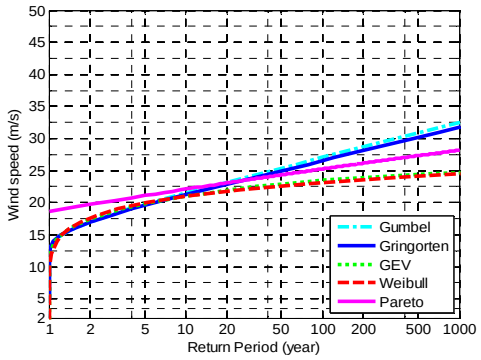
Wind speed (m/s)
Return Period (year)
Gumbel
Gringorten
GEV
Weibull
Pareto

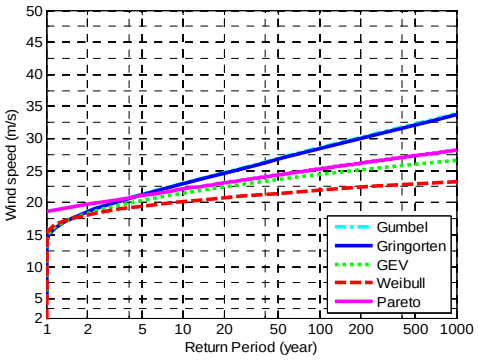
Wind speed (m/s)
Return Period (year)
Gumbel
Gringorten
GEV
Weibull
Pareto

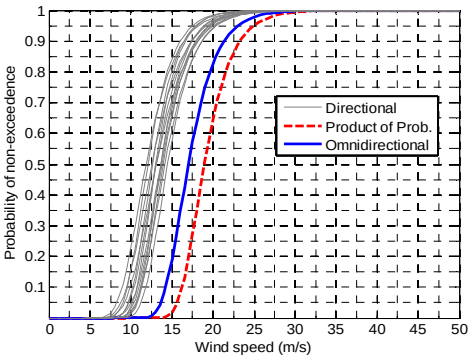
Probability of non-exceedence
Wind speed (m/s)
Directional
Product of Prob.
Omnidirectional

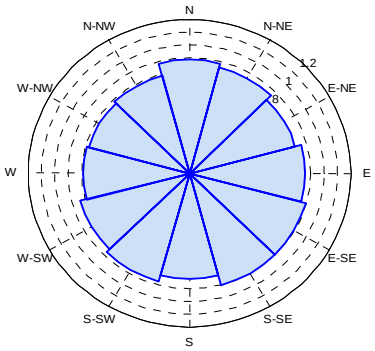
N
N-NE
E-NE
E
E-SE
S-SE
S
S-SW
W
W-NW
N-NW

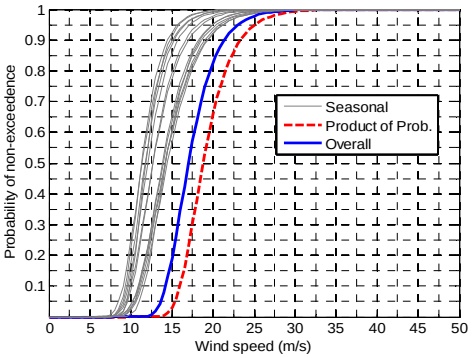
Probability of non-exceedence
Wind speed (m/s)
Seasonal
Product of Prob.
Overall

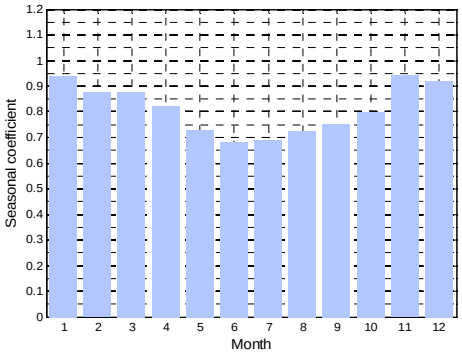
Seasonal coefficient
Month

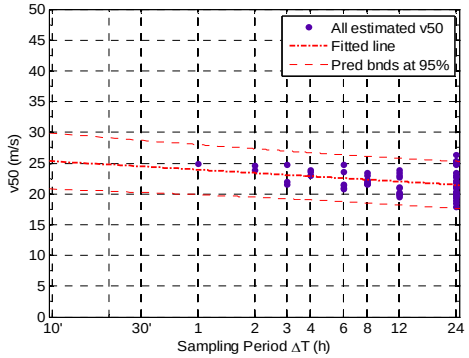
v50 (m/s)
Sampling Period ΔT (h)
All estimated v50
Fitted line
Pred bnds at 95%

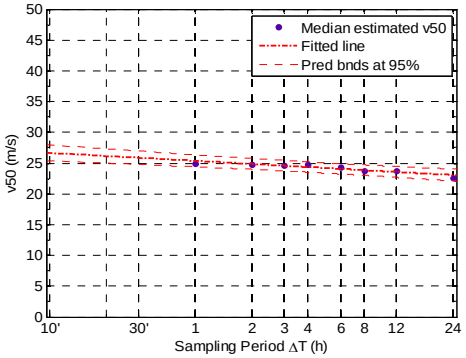
v50 (m/s)
Sampling Period ΔT (h)
Median estimated v50
Fitted line
Pred bnds at 95%

LIBZ

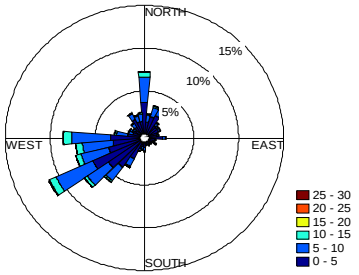
NORTH
15%
10%
5%
WEST
EAST
SOUTH
25 - 30
20 - 25
15 - 20
10 - 15
5 - 10
0 - 5

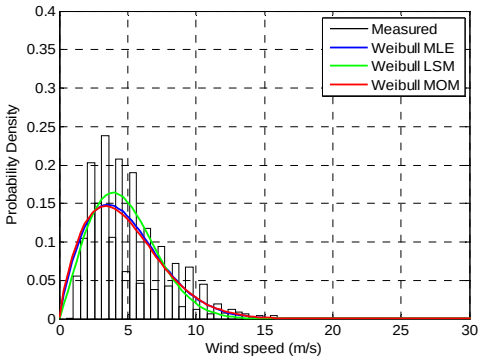
Measured
Weibull MLE
Weibull LSM
Weibull MOM
Probability Density
Wind speed (m/s)

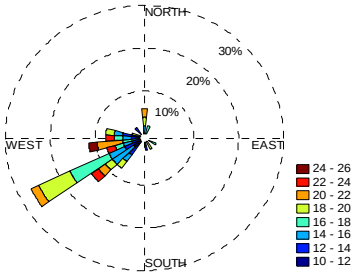
NORTH
30%
20%
10%
WEST
EAST
SOUTH
24 - 26
22 - 24
20 - 22
18 - 20
16 - 18
14 - 16
12 - 14
10 - 12

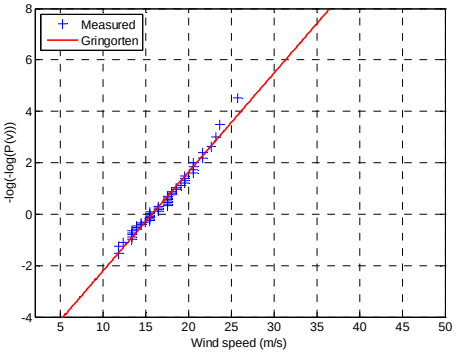
Measured
Gringorten
-log(-log(P(v)))
Wind speed (m/s)

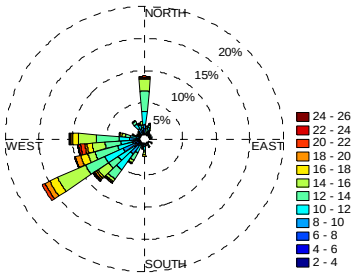
NORTH
20%
15%
10%
5%
WEST
EAST
SOUTH
24 - 26
22 - 24
20 - 22
18 - 20
16 - 18
14 - 16
12 - 14
10 - 12
8 - 10
6 - 8
4 - 6
2 - 4

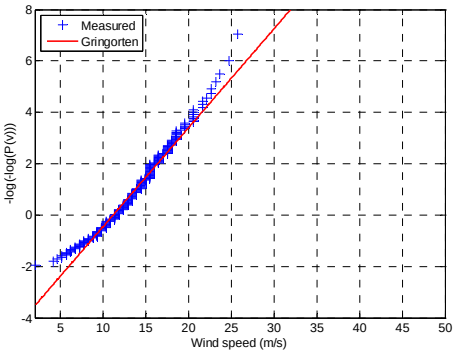
Measured
Gringorten
-log(-log(P(v)))
Wind speed (m/s)

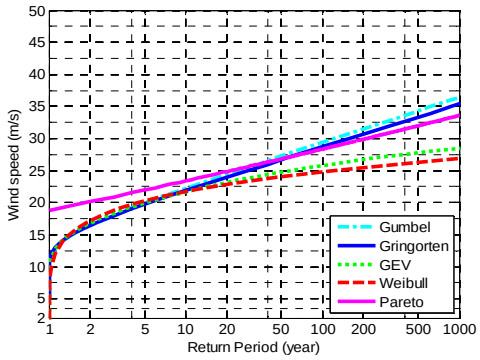
Wind speed (m/s)
Return Period (year)
Gumbel
Gringorten
GEV
Weibull
Pareto

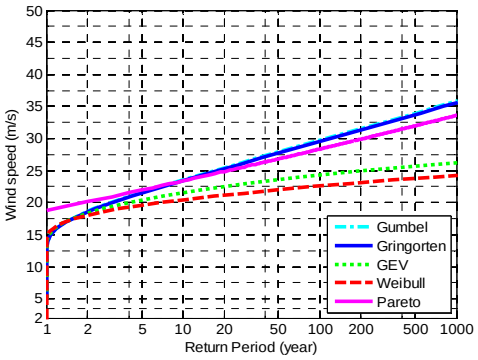
Wind speed (m/s)
Return Period (year)
Gumbel
Gringorten
GEV
Weibull
Pareto

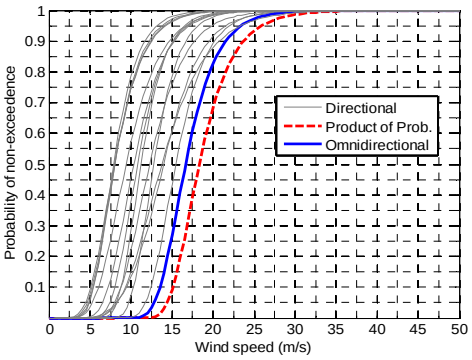
Probability of non-exceedence
Wind speed (m/s)
Directional
Product of Prob.
Omnidirectional

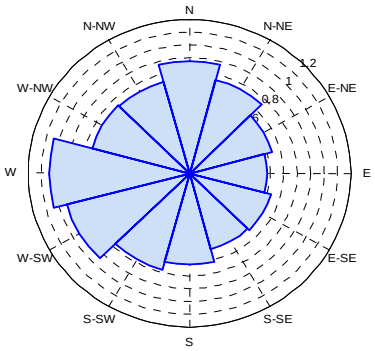
N
N-NE
E-NE
E
E-SE
S-SE
S
S-SW
W
W-NW
N-NW

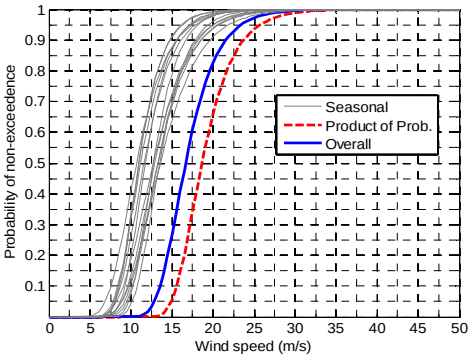
Probability of non-exceedence
Wind speed (m/s)
Seasonal
Product of Prob.
Overall

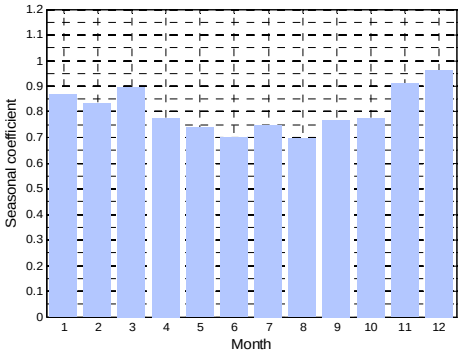
Seasonal coefficient
Month

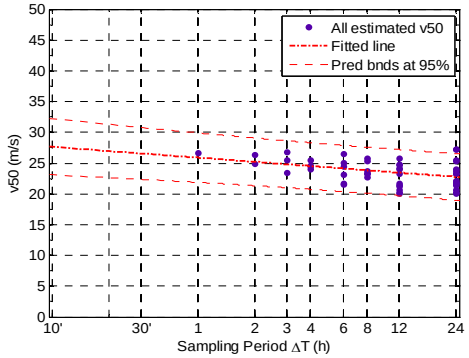
v50 (m/s)
Sampling Period ΔT (h)
All estimated v50
Fitted line
Pred bnds at 95%

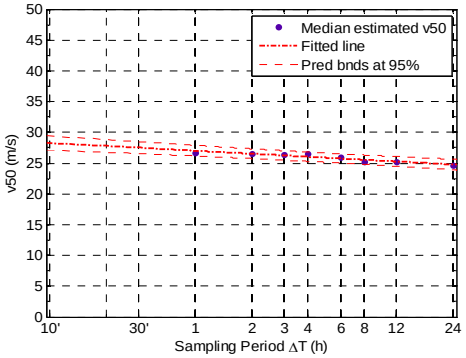
v50 (m/s)
Sampling Period ΔT (h)
Median estimated v50
Fitted line
Pred bnds at 95%

LICA

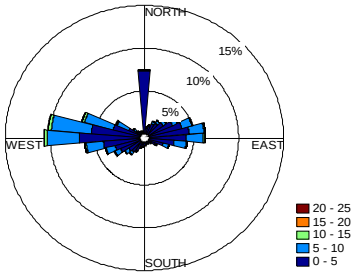
NORTH
15%
10%
5%
WEST
EAST
SOUTH
20 - 25
15 - 20
10 - 15
5 - 10
0 - 5

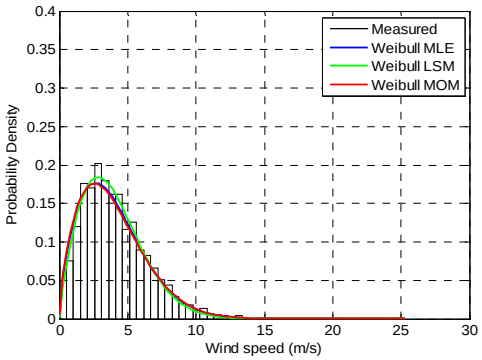
Measured
Weibull MLE
Weibull LSM
Weibull MOM
Probability Density
Wind speed (m/s)

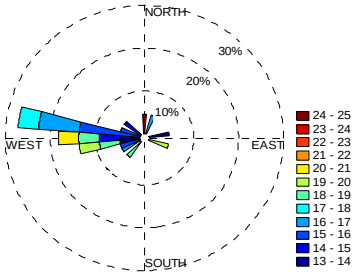
NORTH
30%
20%
10%
WEST
EAST
SOUTH
24 - 25
23 - 24
22 - 23
21 - 22
20 - 21
19 - 20
18 - 19
17 - 18
16 - 17
15 - 16
14 - 15
13 - 14

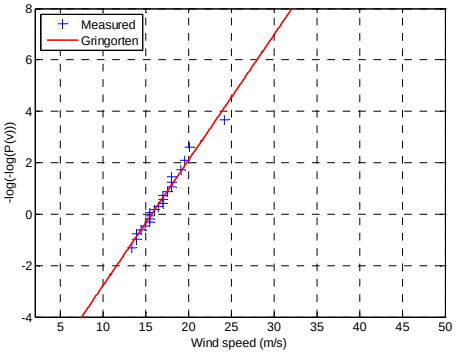
Measured
Gringorten
-log(-log(P(v)))
Wind speed (m/s)

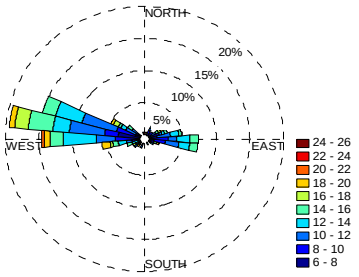
NORTH
20%
15%
10%
5%
WEST
EAST
SOUTH
24 - 26
22 - 24
20 - 22
18 - 20
16 - 18
14 - 16
12 - 14
10 - 12
8 - 10
6 - 8

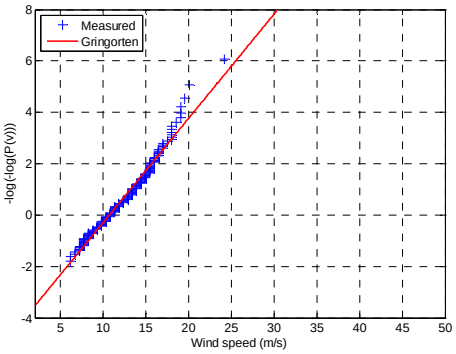
Measured
Gringorten
-log(-log(P(v)))
Wind speed (m/s)

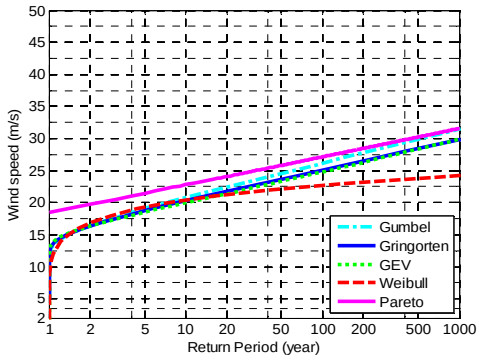
Wind speed (m/s)
Return Period (year)
Gumbel
Gringorten
GEV
Weibull
Pareto

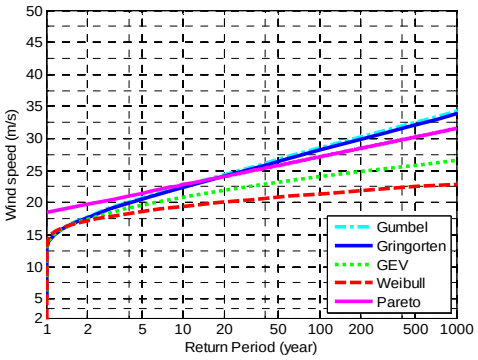
Wind speed (m/s)
Return Period (year)
Gumbel
Gringorten
GEV
Weibull
Pareto

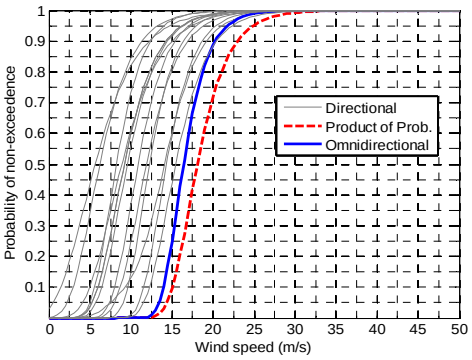
Probability of non-exceedence
Wind speed (m/s)
Directional
Product of Prob.
Omnidirectional

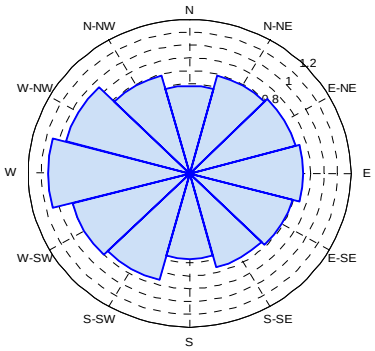
N
N-NE
E-NE
E
E-SE
S-SE
S
S-SW
W
W-NW
N-NW

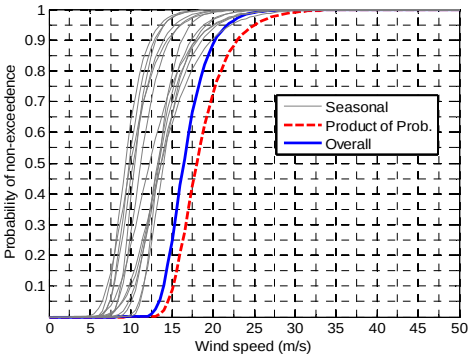
Probability of non-exceedence
Wind speed (m/s)
Seasonal
Product of Prob.
Overall

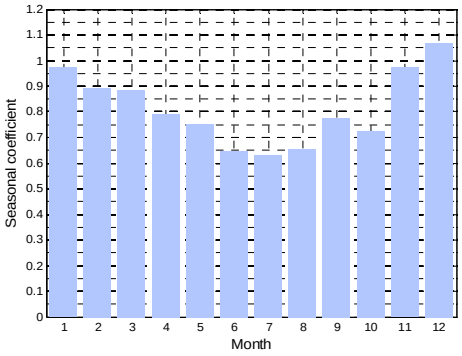
Seasonal coefficient
Month

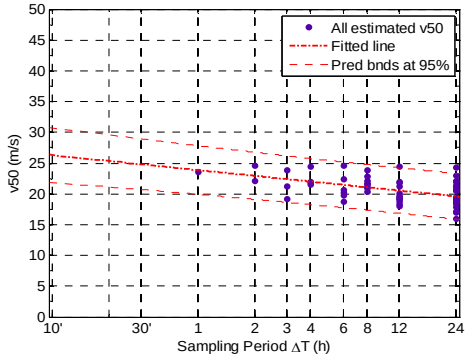
v50 (m/s)
Sampling Period ΔT (h)
All estimated v50
Fitted line
Pred bnds at 95%

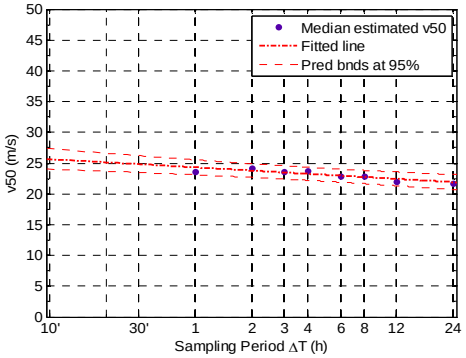
v50 (m/s)
Sampling Period ΔT (h)
Median estimated v50
Fitted line
Pred bnds at 95%

LICC

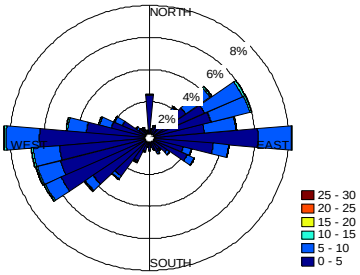
NORTH
8%
6%
4%
2%
WEST
EAST
SOUTH
25 - 30
20 - 25
15 - 20
10 - 15
5 - 10
0 - 5

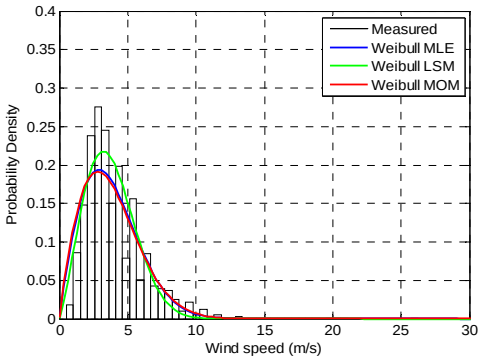
Measured
Weibull MLE
Weibull LSM
Weibull MOM
Probability Density
Wind speed (m/s)

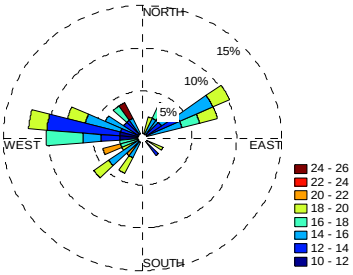
NORTH
15%
10%
5%
WEST
EAST
SOUTH
24 - 26
22 - 24
20 - 22
18 - 20
16 - 18
14 - 16
12 - 14
10 - 12

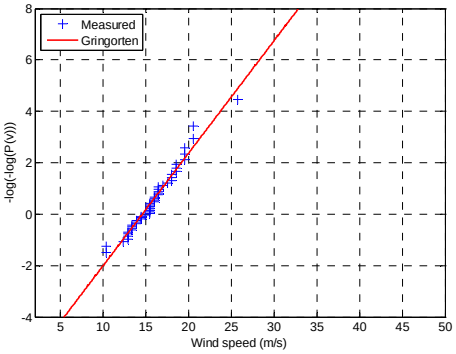
Measured
Gringorten
-log(-log(P(v)))
Wind speed (m/s)

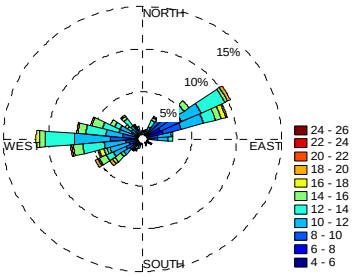
NORTH
15%
10%
5%
WEST
EAST
SOUTH
24 - 26
22 - 24
20 - 22
18 - 20
16 - 18
14 - 16
12 - 14
10 - 12
8 - 10
6 - 8
4 - 6

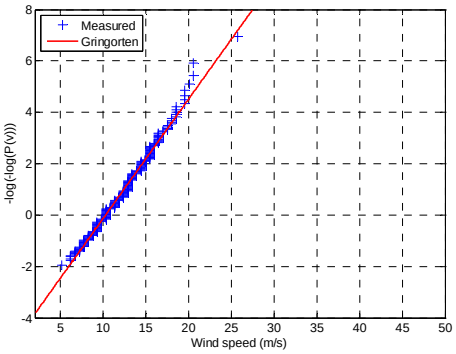
Measured
Gringorten
-log(-log(P(v)))
Wind speed (m/s)

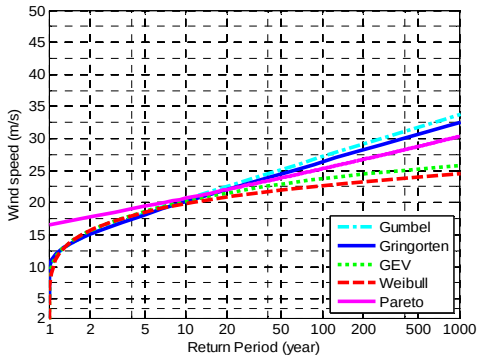
Wind speed (m/s)
Return Period (year)
Gumbel
Gringorten
GEV
Weibull
Pareto

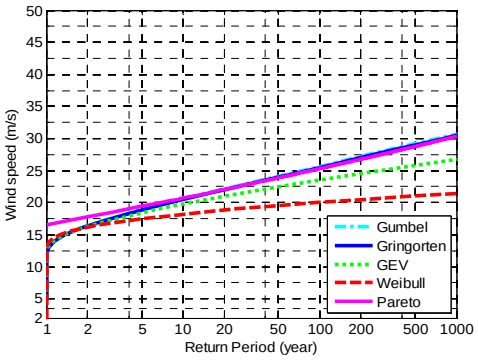
Wind speed (m/s)
Return Period (year)
Gumbel
Gringorten
GEV
Weibull
Pareto

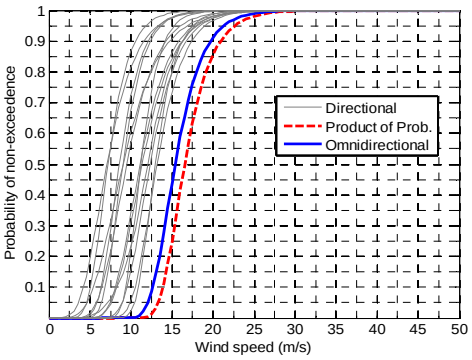
Probability of non-exceedence
Wind speed (m/s)
Directional
Product of Prob.
Omnidirectional

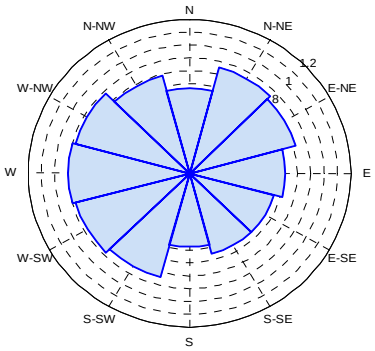
N
N-NE
E-NE
E
E-SE
S-SE
S
S-SW
W
W-NW
N-NW

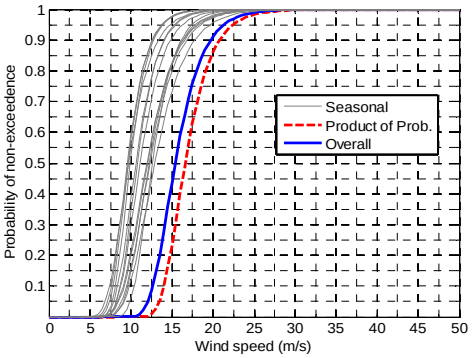
Probability of non-exceedence
Wind speed (m/s)
Seasonal
Product of Prob.
Overall

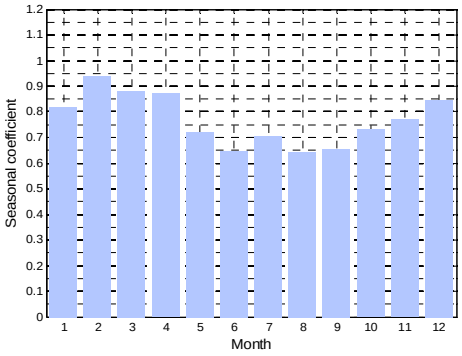
Seasonal coefficient
Month

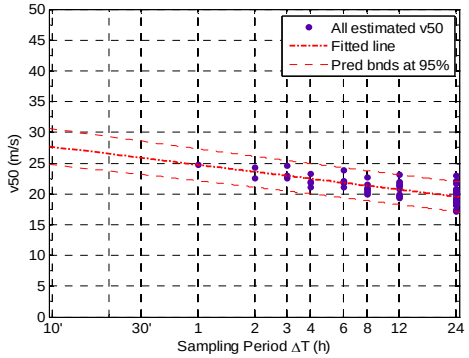
v50 (m/s)
Sampling Period ΔT (h)
All estimated v50
Fitted line
Pred bnds at 95%

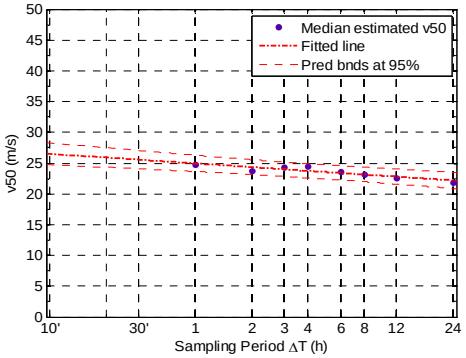
v50 (m/s)
Sampling Period ΔT (h)
Median estimated v50
Fitted line
Pred bnds at 95%

LICD

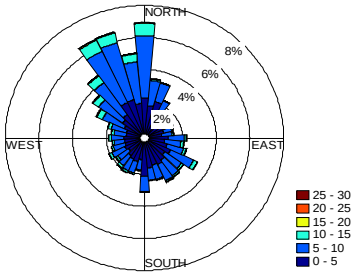
NORTH
8%
6%
4%
2%
WEST
EAST
SOUTH
25 - 30
20 - 25
15 - 20
10 - 15
5 - 10
0 - 5

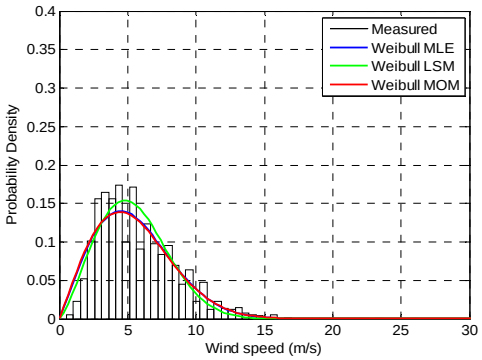
Measured
Weibull MLE
Weibull LSM
Weibull MOM
Probability Density
Wind speed (m/s)

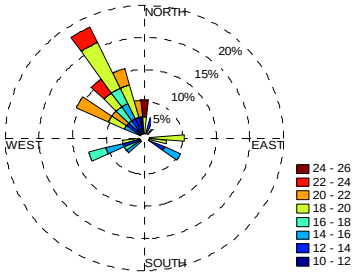
NORTH
20%
15%
10%
5%
WEST
EAST
SOUTH
24 - 26
22 - 24
20 - 22
18 - 20
16 - 18
14 - 16
12 - 14
10 - 12

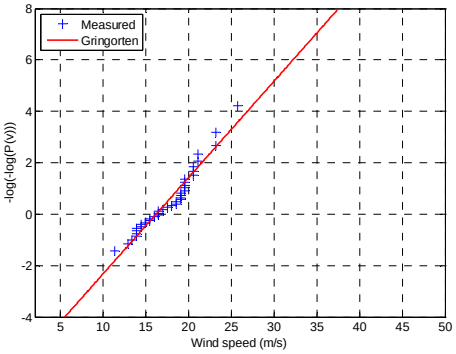
Measured
Gringorten
-log(-log(P(v)))
Wind speed (m/s)

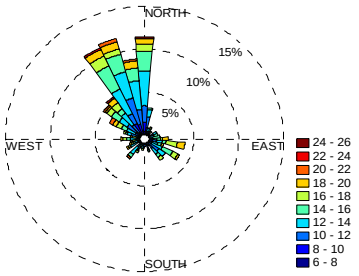
NORTH
15%
10%
5%
WEST
EAST
SOUTH
24 - 26
22 - 24
20 - 22
18 - 20
16 - 18
14 - 16
12 - 14
10 - 12
8 - 10
6 - 8

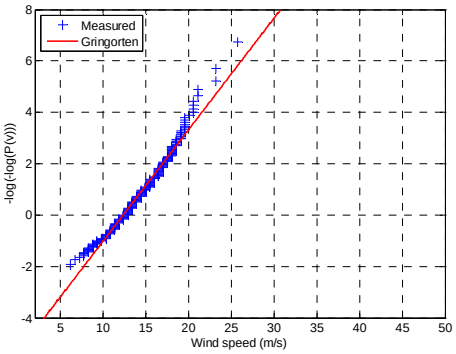
Measured
Gringorten
-log(-log(P(v)))
Wind speed (m/s)

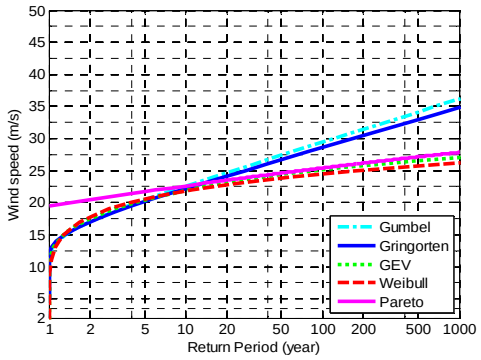
Wind speed (m/s)
Return Period (year)
Gumbel
Gringorten
GEV
Weibull
Pareto

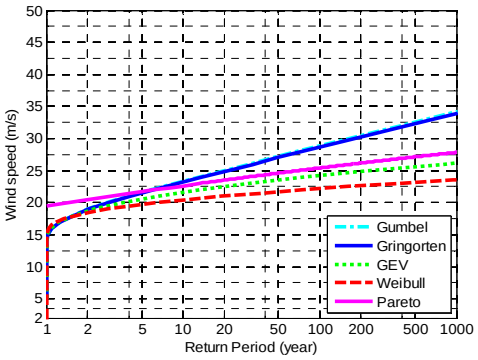
Wind speed (m/s)
Return Period (year)
Gumbel
Gringorten
GEV
Weibull
Pareto

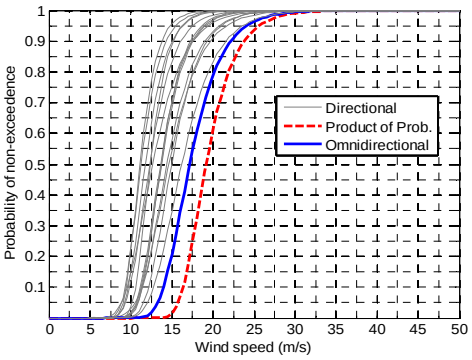
Probability of non-exceedence
Wind speed (m/s)
Directional
Product of Prob.
Omnidirectional

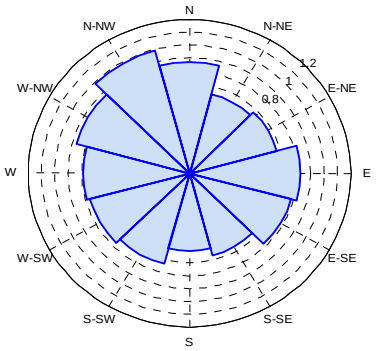
N
N-NE
E-NE
E
E-SE
S-SE
S
S-SW
W
W-NW
N-NW

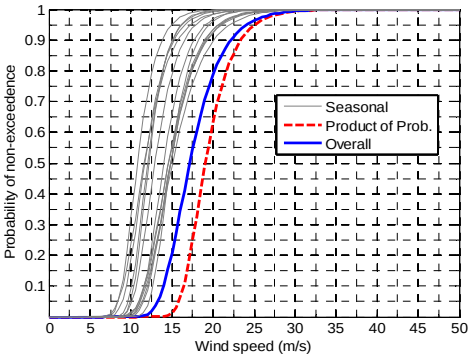
Probability of non-exceedence
Wind speed (m/s)
Seasonal
Product of Prob.
Overall

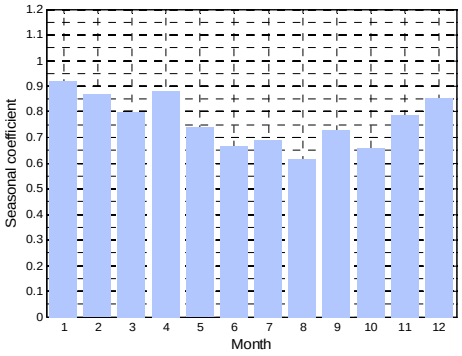
Seasonal coefficient
Month

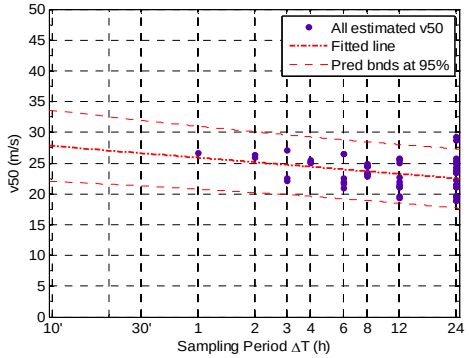
v50 (m/s)
Sampling Period ΔT (h)
All estimated v50
Fitted line
Pred bnds at 95%

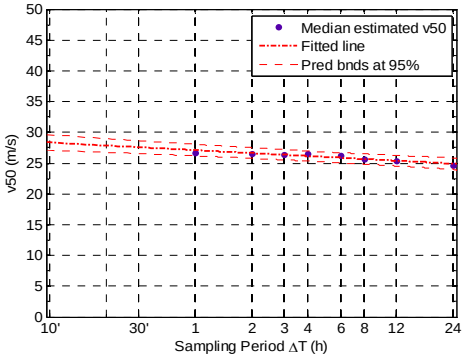
v50 (m/s)
Sampling Period ΔT (h)
Median estimated v50
Fitted line
Pred bnds at 95%

LICE

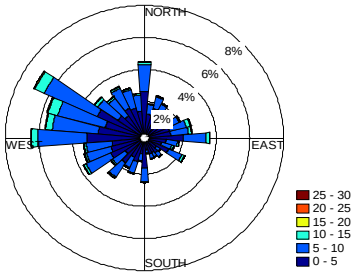
NORTH
8%
6%
4%
2%
WEST
EAST
SOUTH
25 - 30
20 - 25
15 - 20
10 - 15
5 - 10
0 - 5

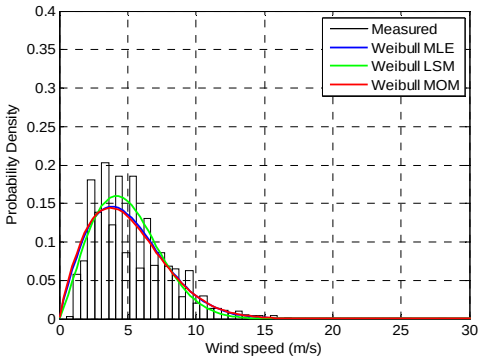
Measured
Weibull MLE
Weibull LSM
Weibull MOM
Probability Density
Wind speed (m/s)

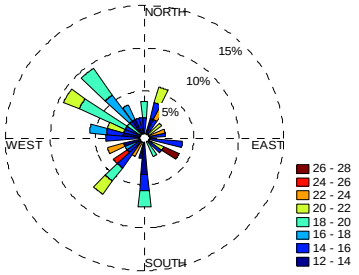
NORTH
15%
10%
5%
WEST
EAST
SOUTH
26 - 28
24 - 26
22 - 24
20 - 22
18 - 20
16 - 18
14 - 16
12 - 14

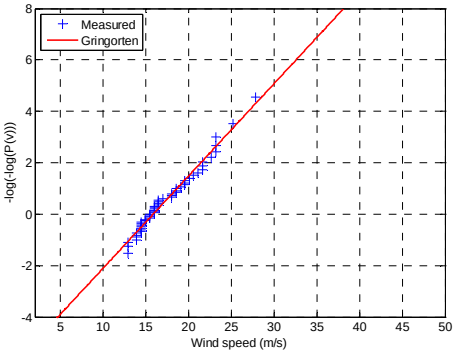
Measured
Gringorten
-log(-log(P(v)))
Wind speed (m/s)

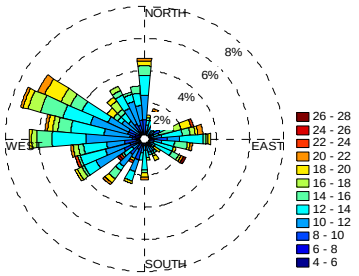
NORTH
8%
6%
4%
2%
WEST
EAST
SOUTH
26 - 28
24 - 26
22 - 24
20 - 22
18 - 20
16 - 18
14 - 16
12 - 14
10 - 12
8 - 10
6 - 8
4 - 6

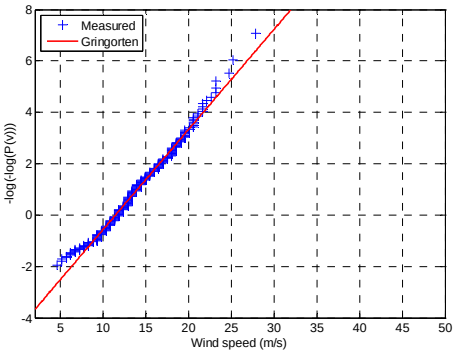
Measured
Gringorten
-log(-log(P(v)))
Wind speed (m/s)

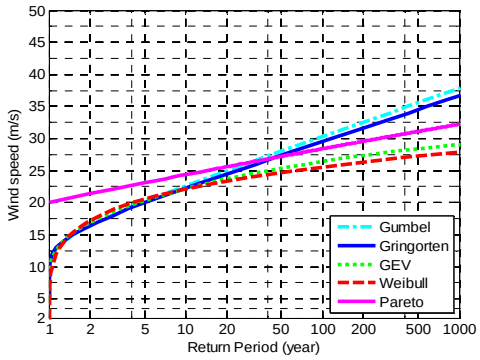
Wind speed (m/s)
Return Period (year)
Gumbel
Gringorten
GEV
Weibull
Pareto

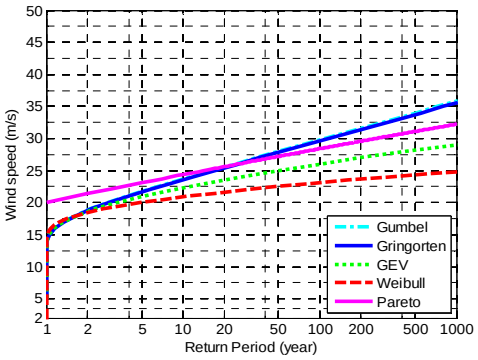
Wind speed (m/s)
Return Period (year)
Gumbel
Gringorten
GEV
Weibull
Pareto

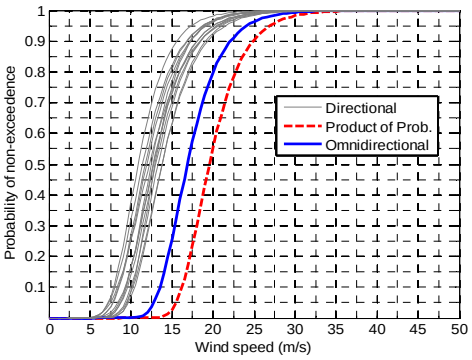
Probability of non-exceedence
Wind speed (m/s)
Directional
Product of Prob.
Omnidirectional

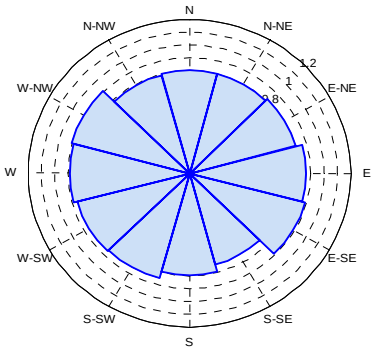
N
N-NE
E-NE
E
E-SE
S-SE
S
S-SW
W
W-NW
N-NW

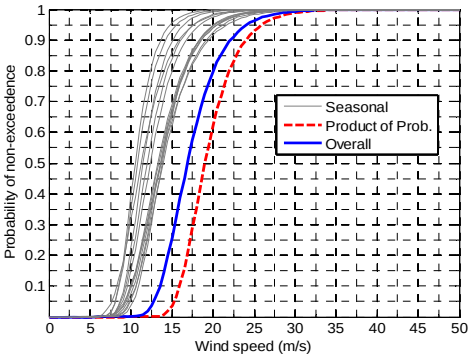
Probability of non-exceedence
Wind speed (m/s)
Seasonal
Product of Prob.
Overall

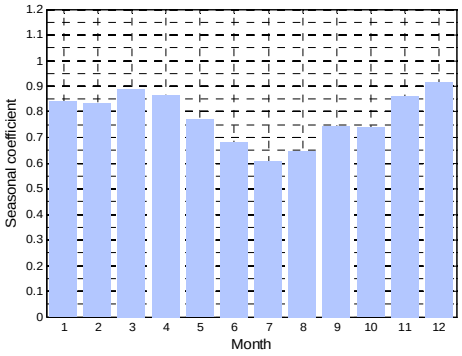
Seasonal coefficient
Month

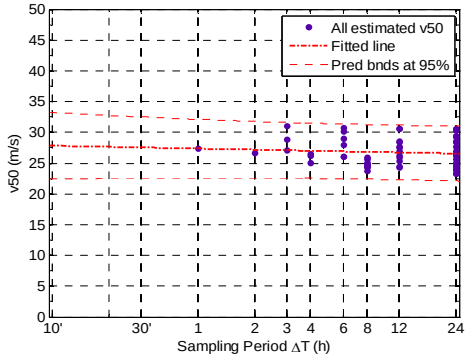
v50 (m/s)
Sampling Period ΔT (h)
All estimated v50
Fitted line
Pred bnds at 95%

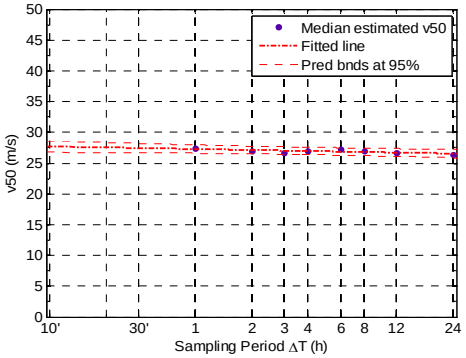
v50 (m/s)
Sampling Period ΔT (h)
Median estimated v50
Fitted line
Pred bnds at 95%

LICF

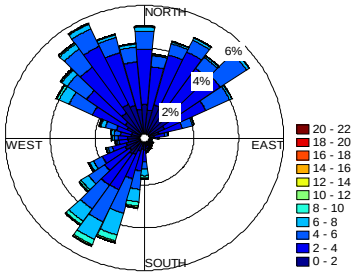
NORTH
EAST
SOUTH
WEST
6%
4%
2%
20 - 22
18 - 20
16 - 18
14 - 16
12 - 14
10 - 12
8 - 10
6 - 8
4 - 6
2 - 4
0 - 2

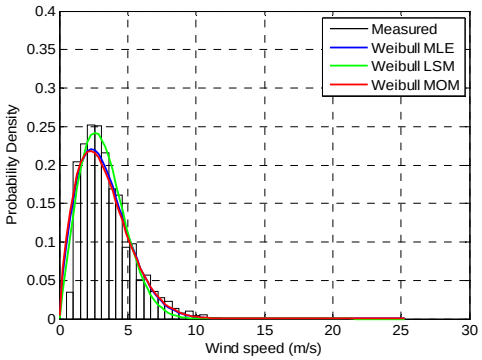
Measured
Weibull MLE
Weibull LSM
Weibull MOM
Probability Density
Wind speed (m/s)

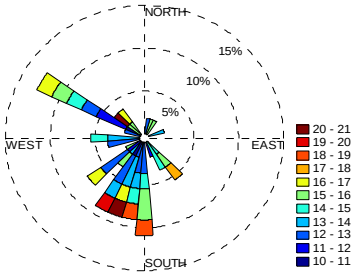
NORTH
EAST
SOUTH
WEST
15%
10%
5%
20 - 21
19 - 20
18 - 19
17 - 18
16 - 17
15 - 16
14 - 15
13 - 14
12 - 13
11 - 12
10 - 11

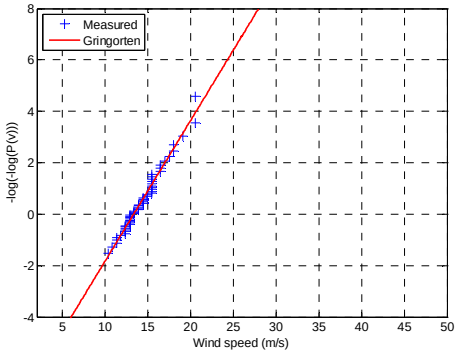
Measured
Gringorten
-log(-log(P(v)))
Wind speed (m/s)

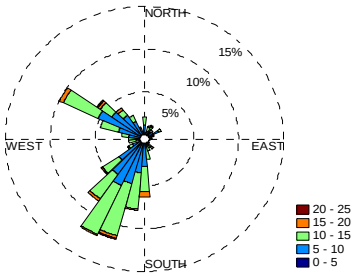
NORTH
EAST
SOUTH
WEST
15%
10%
5%
20 - 25
15 - 20
10 - 15
5 - 10
0 - 5

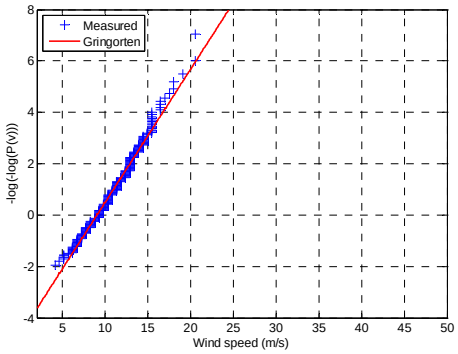
Measured
Gringorten
-log(-log(P(v)))
Wind speed (m/s)

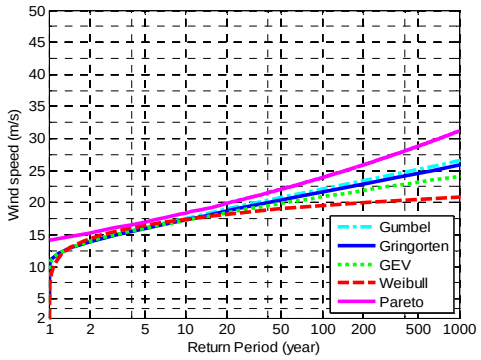
Wind speed (m/s)
Return Period (year)
Gumbel
Gringorten
GEV
Weibull
Pareto

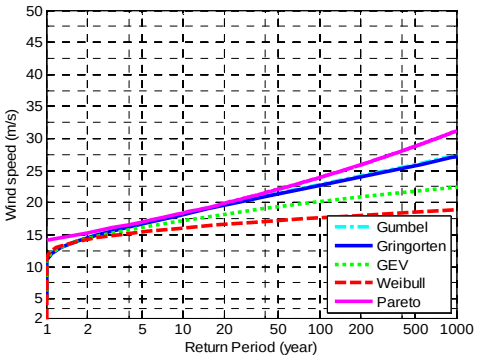
Wind speed (m/s)
Return Period (year)
Gumbel
Gringorten
GEV
Weibull
Pareto

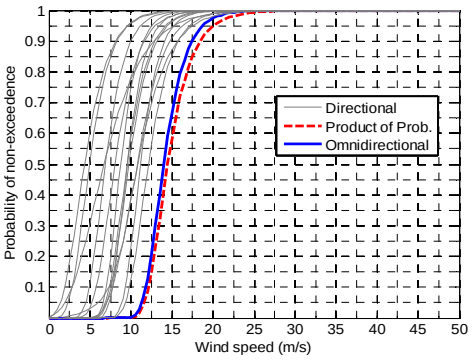
Probability of non-exceedence
Wind speed (m/s)
Directional
Product of Prob.
Omnidirectional

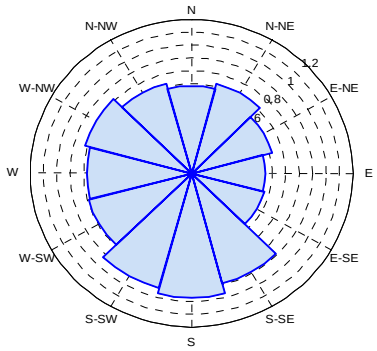
N
N-NE
E-NE
E
E-SE
S-SE
S
S-SW
W
W-NW
N-NW

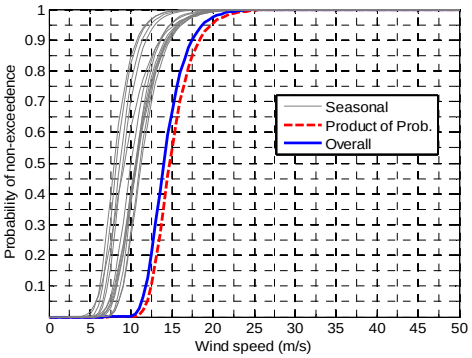
Probability of non-exceedence
Wind speed (m/s)
Seasonal
Product of Prob.
Overall

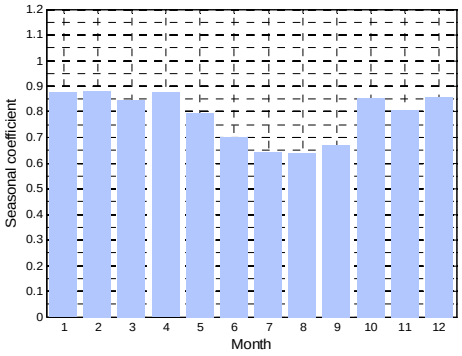
Seasonal coefficient
Month

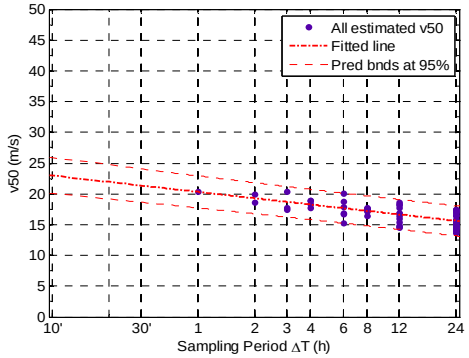
v50 (m/s)
Sampling Period ΔT (h)
All estimated v50
Fitted line
Pred bnds at 95%

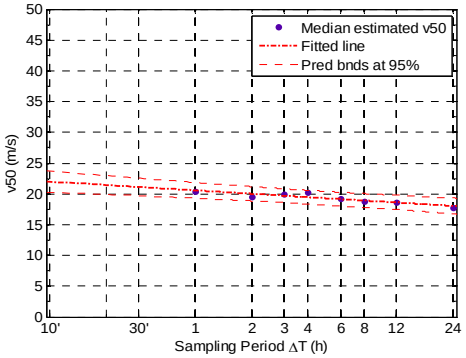
v50 (m/s)
Sampling Period ΔT (h)
Median estimated v50
Fitted line
Pred bnds at 95%

LICG

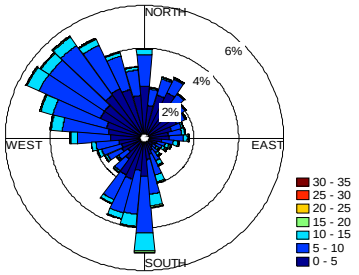
NORTH
6%
4%
2%
WEST
EAST
SOUTH
30 - 35
25 - 30
20 - 25
15 - 20
10 - 15
5 - 10
0 - 5

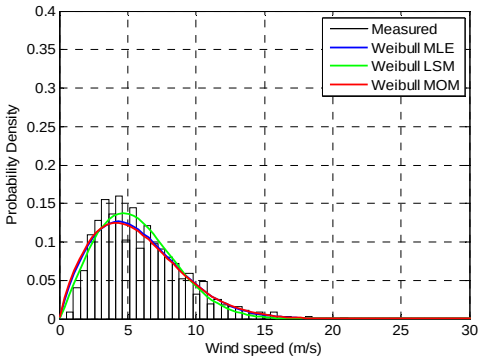
Measured
Weibull MLE
Weibull LSM
Weibull MOM
Probability Density
Wind speed (m/s)

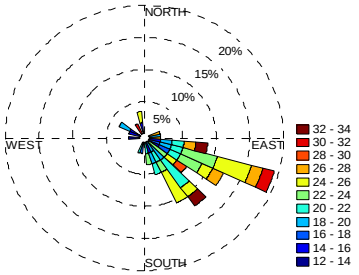
NORTH
20%
15%
10%
5%
WEST
EAST
SOUTH
32 - 34
30 - 32
28 - 30
26 - 28
24 - 26
22 - 24
20 - 22
18 - 20
16 - 18
14 - 16
12 - 14

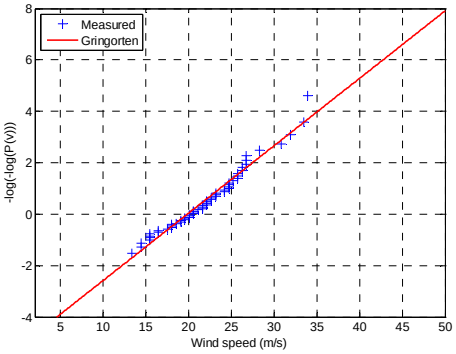
Measured
Gringorten
-log(-log(P(v)))
Wind speed (m/s)

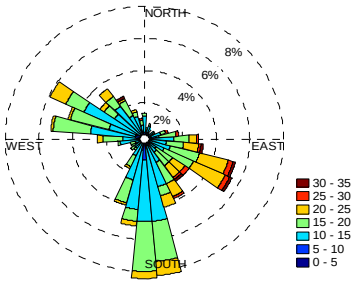
NORTH
8%
6%
4%
2%
WEST
EAST
SOUTH
30 - 35
25 - 30
20 - 25
15 - 20
10 - 15
5 - 10
0 - 5

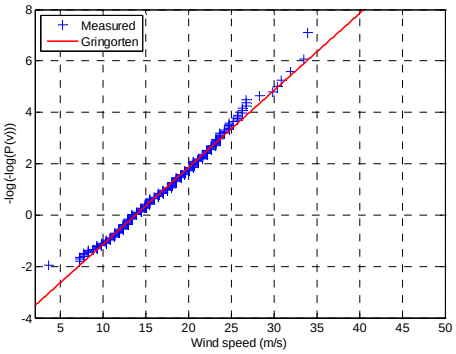
Measured
Gringorten
-log(-log(P(v)))
Wind speed (m/s)

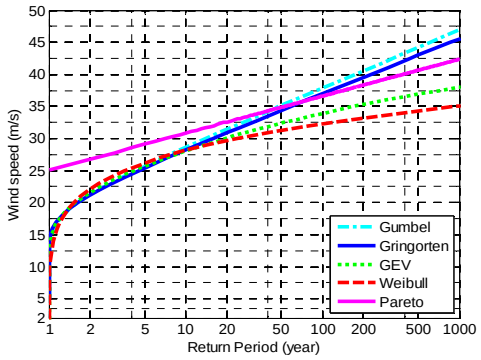
Wind speed (m/s)
Return Period (year)
Gumbel
Gringorten
GEV
Weibull
Pareto

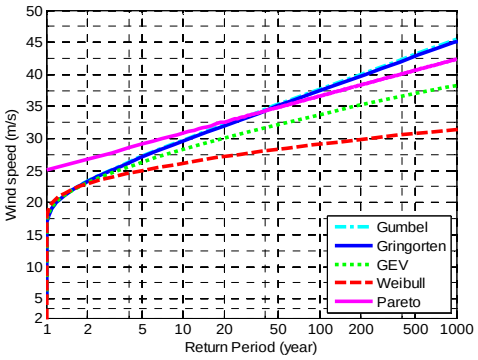
Wind speed (m/s)
Return Period (year)
Gumbel
Gringorten
GEV
Weibull
Pareto

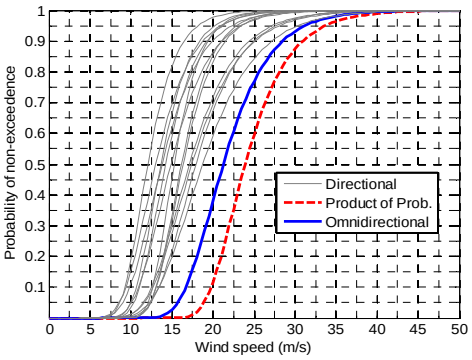
Probability of non-exceedence
Wind speed (m/s)
Directional
Product of Prob.
Omnidirectional

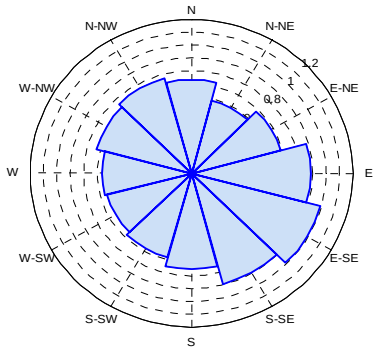
N
N-NE
E-NE
E
E-SE
S-SE
S
S-SW
W
W-NW
N-NW

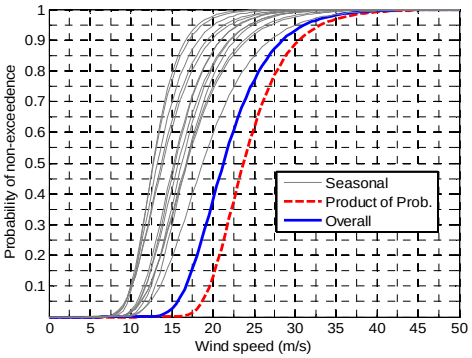
Probability of non-exceedence
Wind speed (m/s)
Seasonal
Product of Prob.
Overall

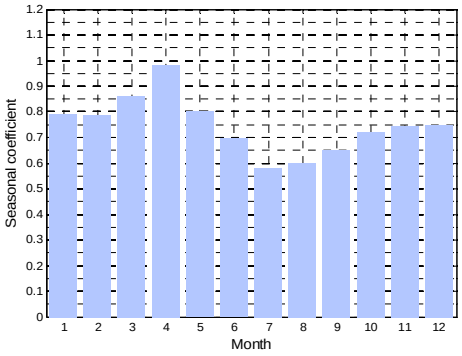
Seasonal coefficient
Month

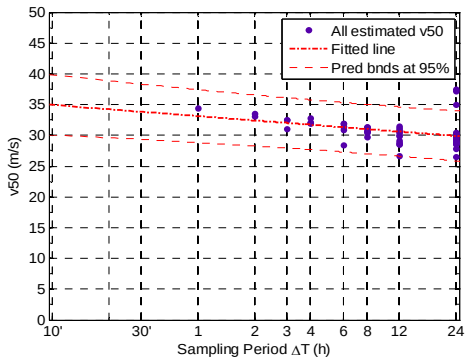
v50 (m/s)
Sampling Period ΔT (h)
All estimated v50
Fitted line
Pred bnds at 95%

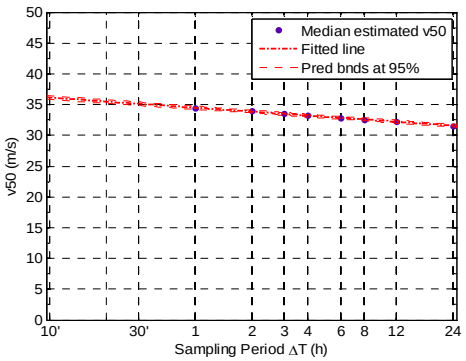
v50 (m/s)
Sampling Period ΔT (h)
Median estimated v50
Fitted line
Pred bnds at 95%

LICJ

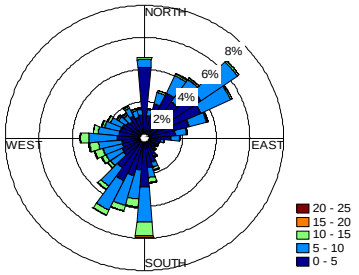
NORTH
EAST
SOUTH
WEST
8%
6%
4%
2%
20 - 25
15 - 20
10 - 15
5 - 10
0 - 5

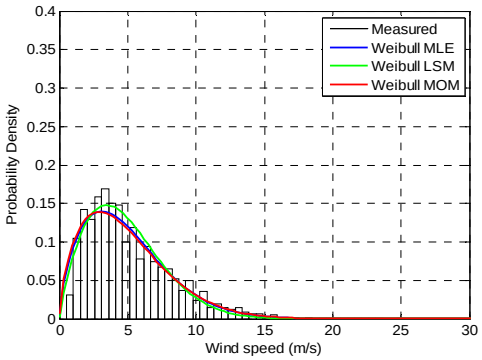
Measured
Weibull MLE
Weibull LSM
Weibull MOM
Probability Density
Wind speed (m/s)

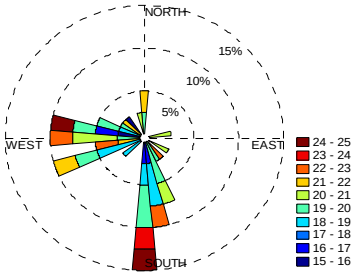
NORTH
EAST
SOUTH
WEST
15%
10%
5%
24 - 25
23 - 24
22 - 23
21 - 22
20 - 21
19 - 20
18 - 19
17 - 18
16 - 17
15 - 16

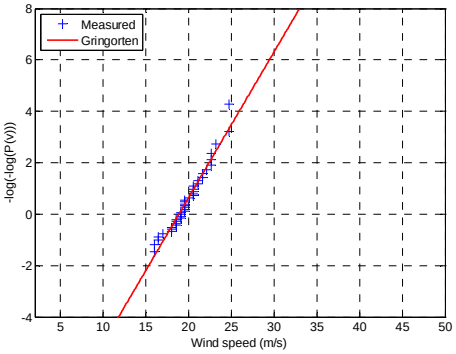
Measured
Gringorten
-log(-log(P(v)))
Wind speed (m/s)

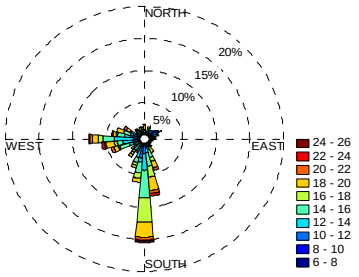
NORTH
EAST
SOUTH
WEST
20%
15%
10%
5%
24 - 26
22 - 24
20 - 22
18 - 20
16 - 18
14 - 16
12 - 14
10 - 12
8 - 10
6 - 8

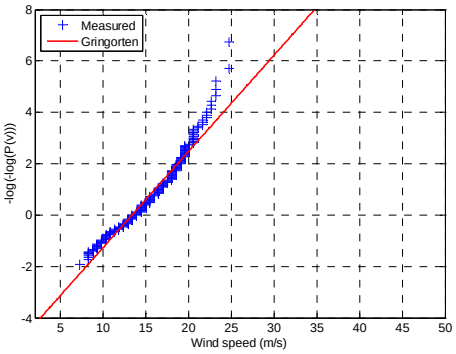
Measured
Gringorten
-log(-log(P(v)))
Wind speed (m/s)

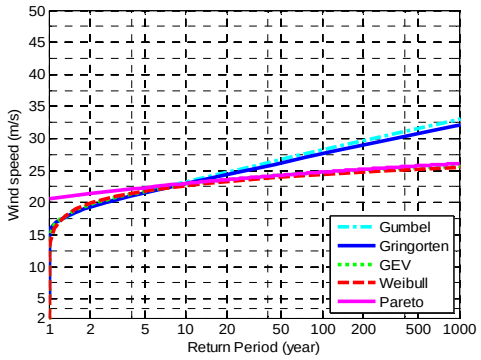
Wind speed (m/s)
Return Period (year)
Gumbel
Gringorten
GEV
Weibull
Pareto

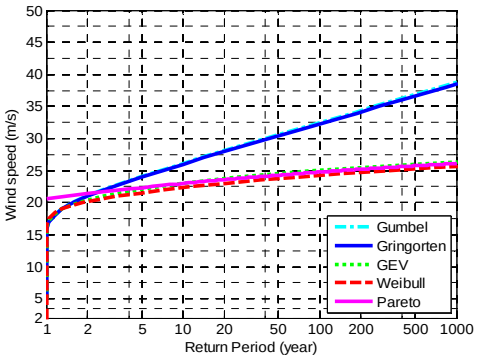
Wind speed (m/s)
Return Period (year)
Gumbel
Gringorten
GEV
Weibull
Pareto

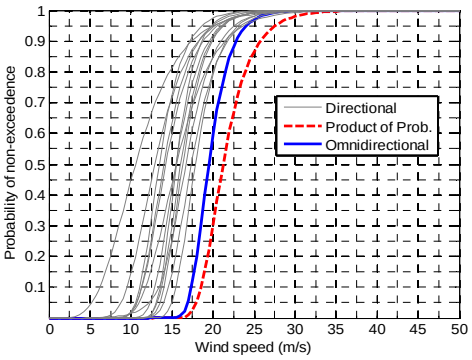
Probability of non-exceedence
Wind speed (m/s)
Directional
Product of Prob.
Omnidirectional

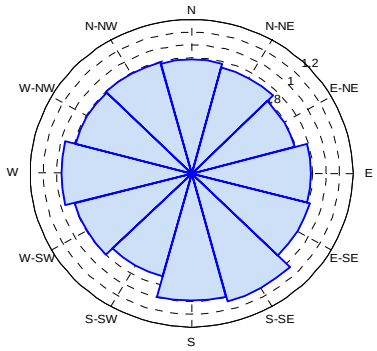
N
N-NE
E-NE
E
E-SE
S-SE
S
S-SW
W
W-NW
N-NW

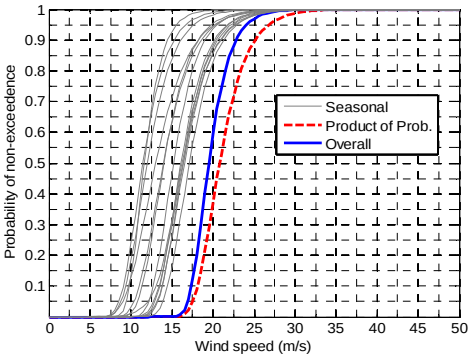
Probability of non-exceedence
Wind speed (m/s)
Seasonal
Product of Prob.
Overall

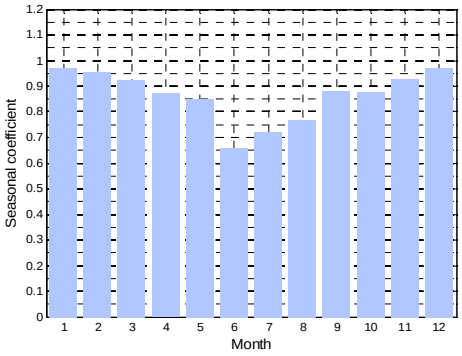
Seasonal coefficient
Month

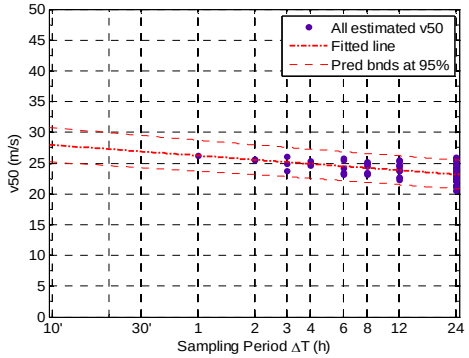
v50 (m/s)
Sampling Period ΔT (h)
All estimated v50
Fitted line
Pred bnds at 95%

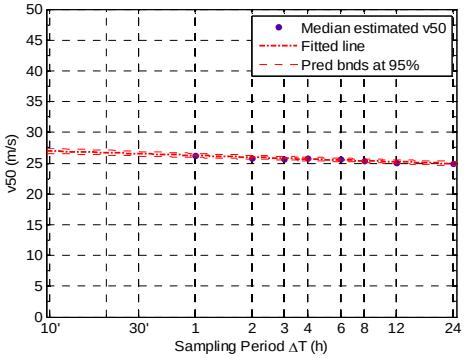
v50 (m/s)
Sampling Period ΔT (h)
Median estimated v50
Fitted line
Pred bnds at 95%

LICL

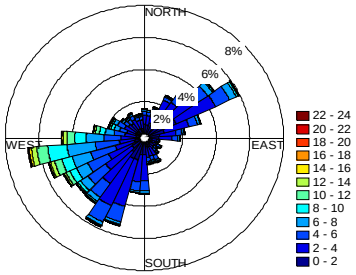
NORTH
8%
6%
4%
2%
WEST
EAST
SOUTH
22 - 24
20 - 22
18 - 20
16 - 18
14 - 16
12 - 14
10 - 12
8 - 10
6 - 8
4 - 6
2 - 4
0 - 2

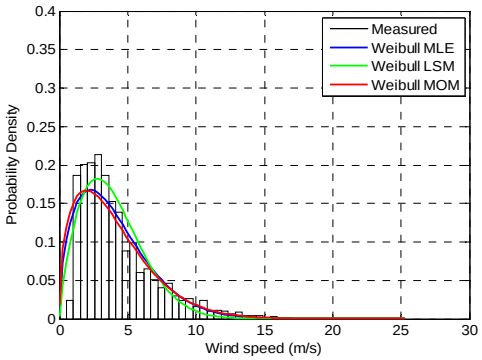
Measured
Weibull MLE
Weibull LSM
Weibull MOM
Probability Density
Wind speed (m/s)

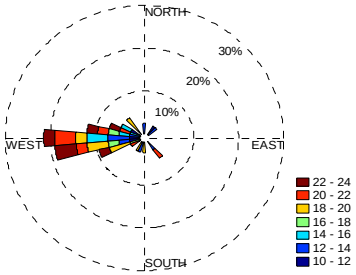
NORTH
30%
20%
10%
WEST
EAST
SOUTH
22 - 24
20 - 22
18 - 20
16 - 18
14 - 16
12 - 14
10 - 12

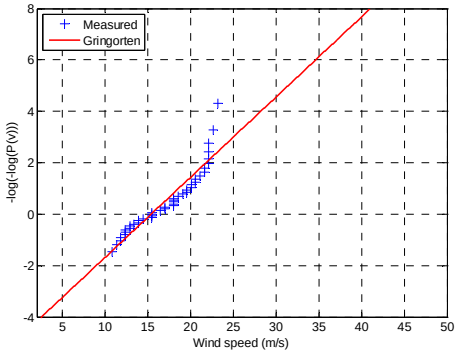
Measured
Gringorten
-log(-log(P(v)))
Wind speed (m/s)

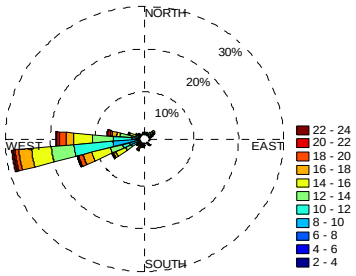
NORTH
30%
20%
10%
WEST
EAST
SOUTH
22 - 24
20 - 22
18 - 20
16 - 18
14 - 16
12 - 14
10 - 12
8 - 10
6 - 8
4 - 6
2 - 4

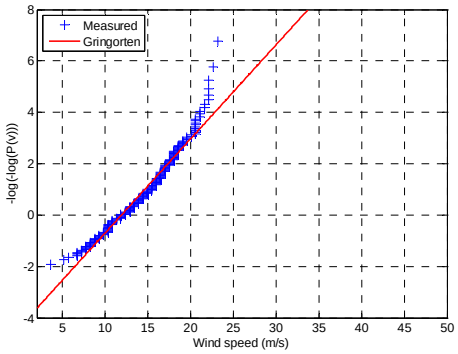
Measured
Gringorten
-log(-log(P(v)))
Wind speed (m/s)

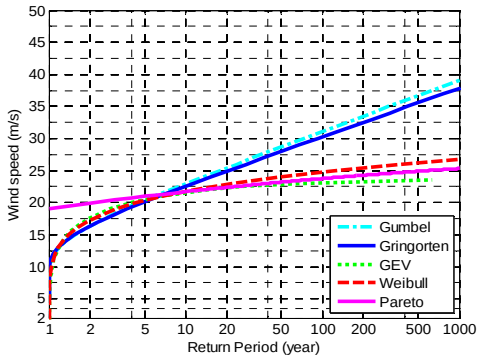
Wind speed (m/s)
Return Period (year)
Gumbel
Gringorten
GEV
Weibull
Pareto

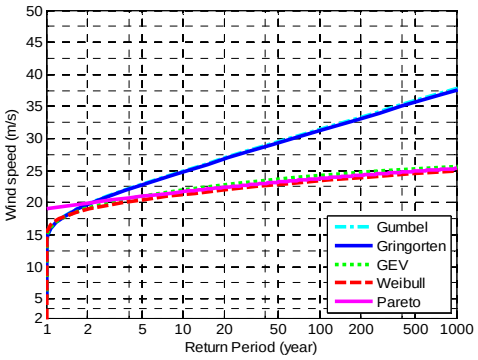
Wind speed (m/s)
Return Period (year)
Gumbel
Gringorten
GEV
Weibull
Pareto

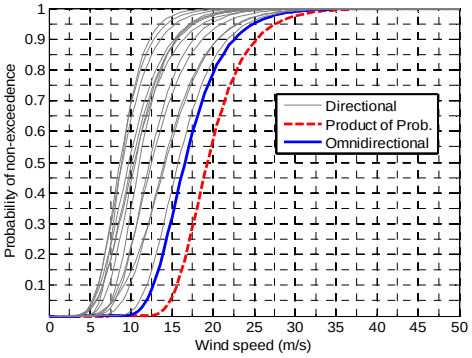
Probability of non-exceedence
Wind speed (m/s)
Directional
Product of Prob.
Omnidirectional

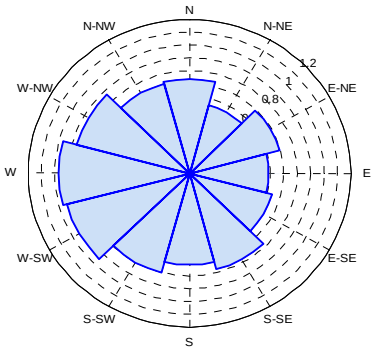
N
N-NE
E-NE
E
E-SE
S-SE
S
S-SW
W
W-NW
N-NW

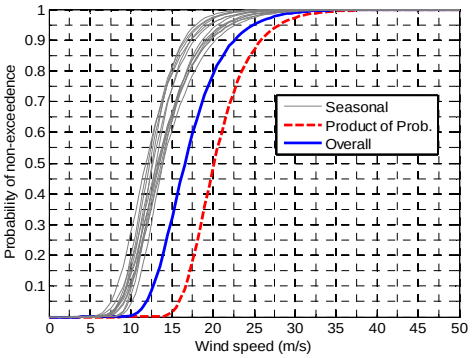
Probability of non-exceedence
Wind speed (m/s)
Seasonal
Product of Prob.
Overall

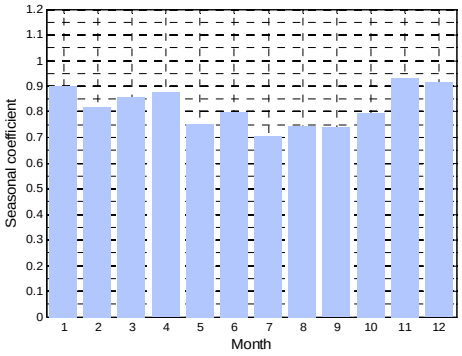
Seasonal coefficient
Month

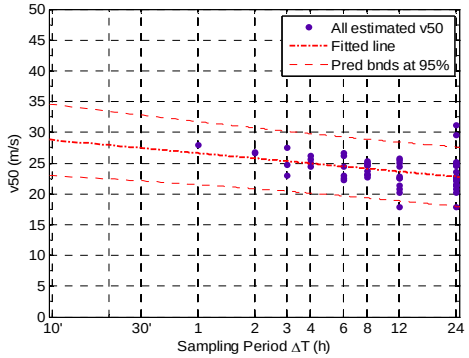
v50 (m/s)
Sampling Period ΔT (h)
All estimated v50
Fitted line
Pred bnds at 95%

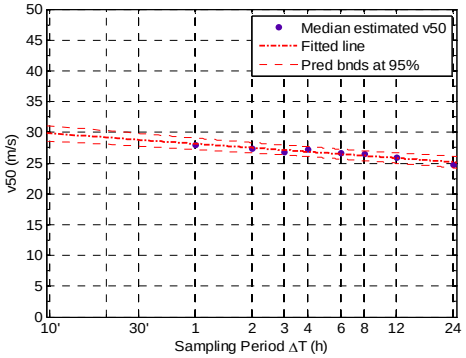
v50 (m/s)
Sampling Period ΔT (h)
Median estimated v50
Fitted line
Pred bnds at 95%

LICO

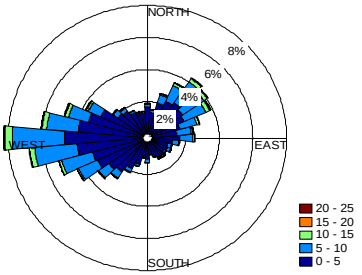
NORTH
8%
6%
4%
2%
WEST
EAST
SOUTH
20 - 25
15 - 20
10 - 15
5 - 10
0 - 5

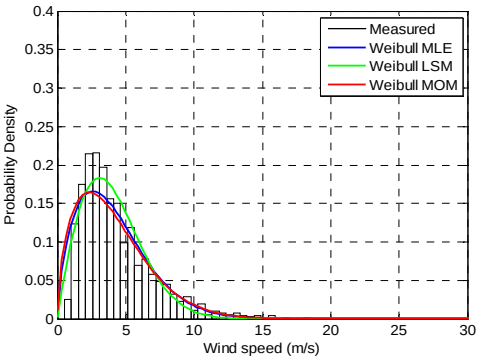
Measured
Weibull MLE
Weibull LSM
Weibull MOM
Probability Density
Wind speed (m/s)

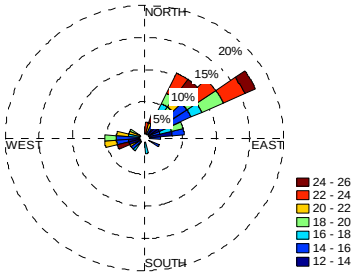
NORTH
20%
15%
10%
5%
WEST
EAST
SOUTH
24 - 26
22 - 24
20 - 22
18 - 20
16 - 18
14 - 16
12 - 14

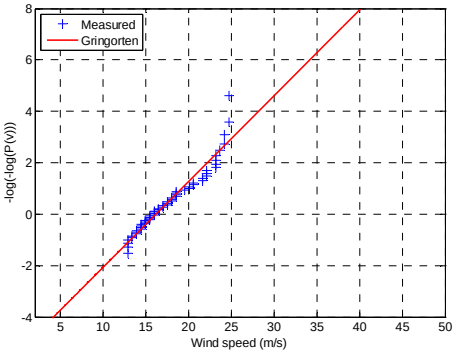
Measured
Gringorten
-log(-log(P(v)))
Wind speed (m/s)

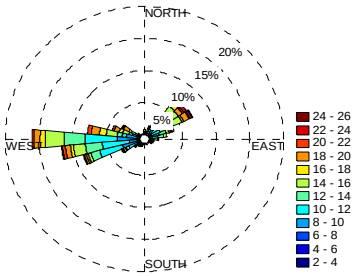
NORTH
20%
15%
10%
5%
WEST
EAST
SOUTH
24 - 26
22 - 24
20 - 22
18 - 20
16 - 18
14 - 16
12 - 14
10 - 12
8 - 10
6 - 8
4 - 6
2 - 4

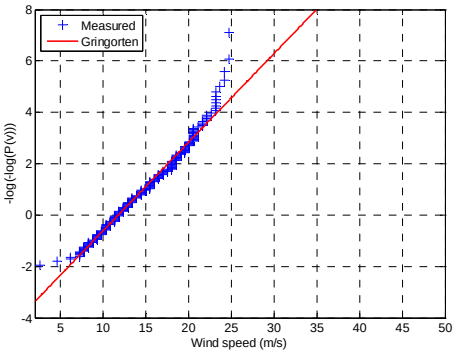
Measured
Gringorten
-log(-log(P(v)))
Wind speed (m/s)

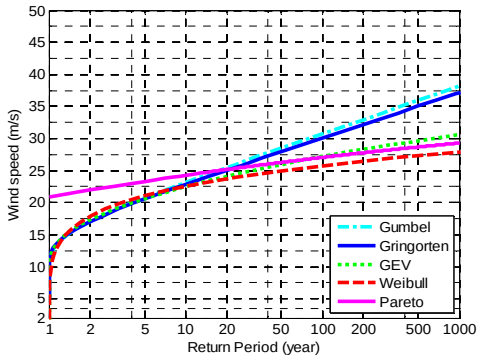
Wind speed (m/s)
Return Period (year)
Gumbel
Gringorten
GEV
Weibull
Pareto

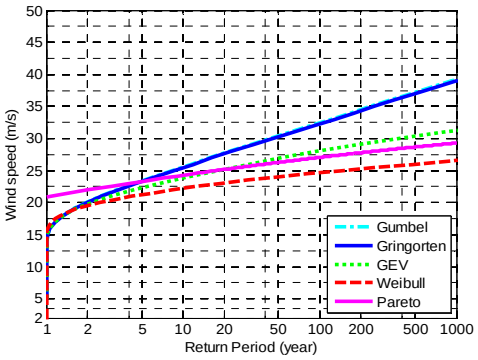
Wind speed (m/s)
Return Period (year)
Gumbel
Gringorten
GEV
Weibull
Pareto

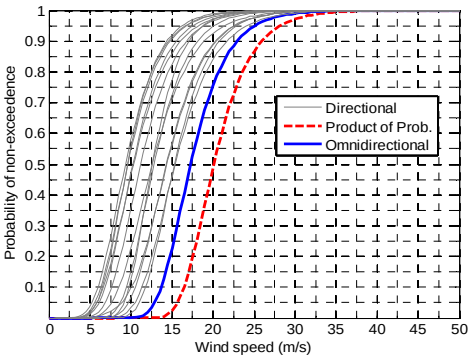
Probability of non-exceedence
Wind speed (m/s)
Directional
Product of Prob.
Omnidirectional

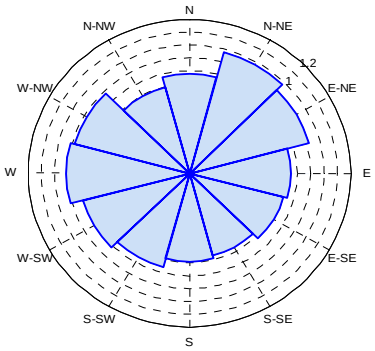
N
N-NE
E-NE
E
E-SE
S-SE
S
S-SW
W
W-NW
N-NW

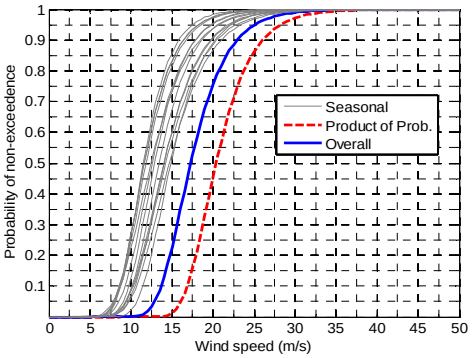
Probability of non-exceedence
Wind speed (m/s)
Seasonal
Product of Prob.
Overall

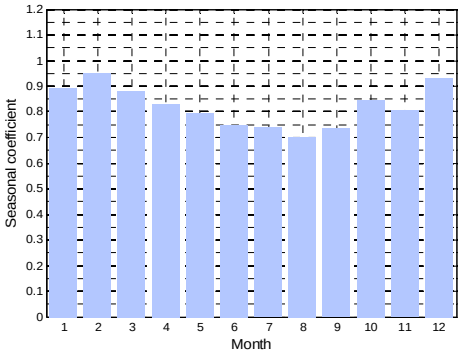
Seasonal coefficient
Month

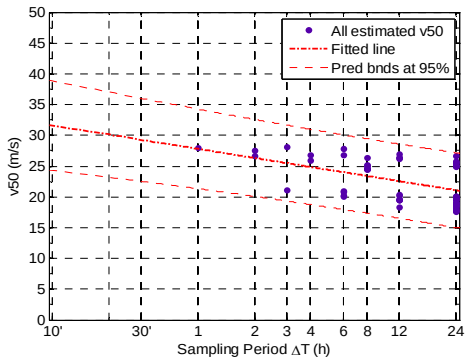
v50 (m/s)
Sampling Period ΔT (h)
All estimated v50
Fitted line
Pred bnds at 95%

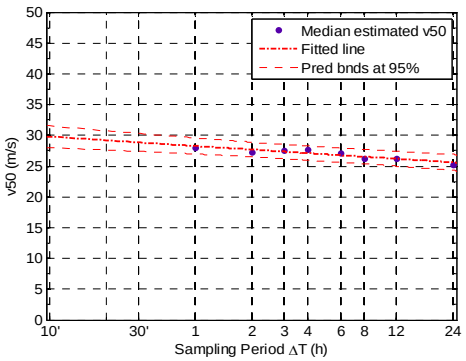
v50 (m/s)
Sampling Period ΔT (h)
Median estimated v50
Fitted line
Pred bnds at 95%

LICP

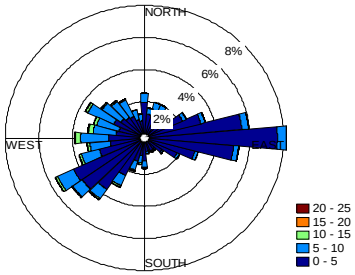
NORTH
8%
6%
4%
2%
WEST
EAST
SOUTH
20 - 25
15 - 20
10 - 15
5 - 10
0 - 5

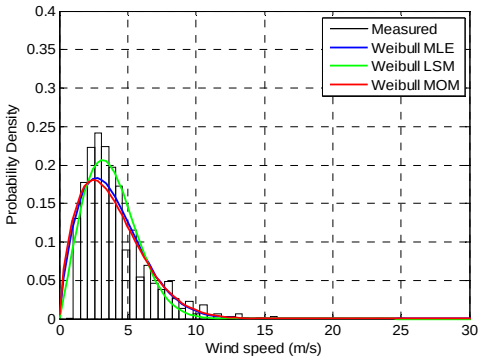
Measured
Weibull MLE
Weibull LSM
Weibull MOM
Probability Density
Wind speed (m/s)

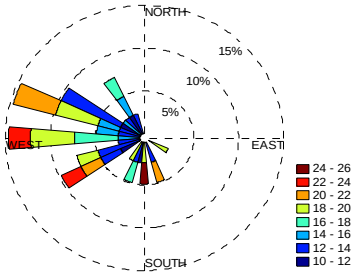
NORTH
15%
10%
5%
WEST
EAST
SOUTH
24 - 26
22 - 24
20 - 22
18 - 20
16 - 18
14 - 16
12 - 14
10 - 12

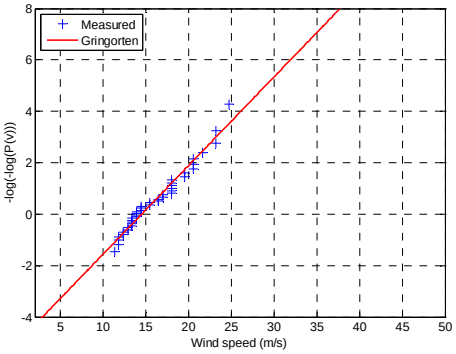
Measured
Gringorten
-log(-log(P(v)))
Wind speed (m/s)

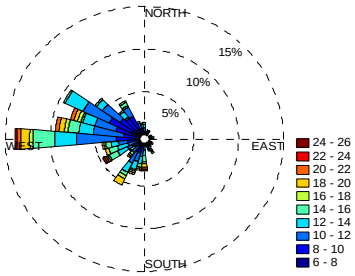
NORTH
15%
10%
5%
WEST
EAST
SOUTH
24 - 26
22 - 24
20 - 22
18 - 20
16 - 18
14 - 16
12 - 14
10 - 12
8 - 10
6 - 8

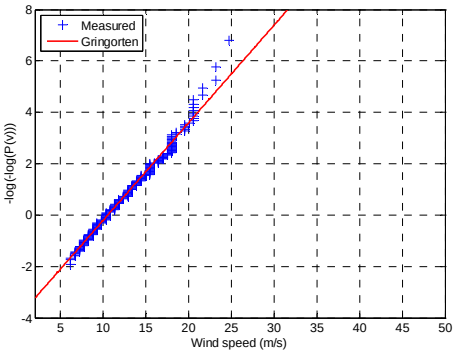
Measured
Gringorten
-log(-log(P(v)))
Wind speed (m/s)

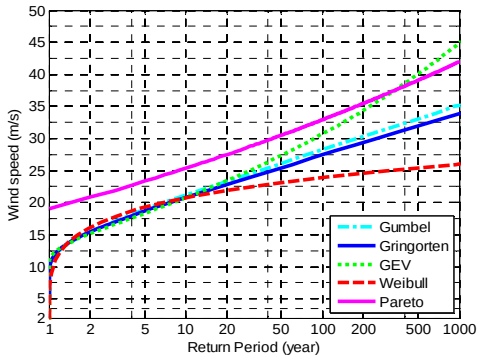
Wind speed (m/s)
Return Period (year)
Gumbel
Gringorten
GEV
Weibull
Pareto

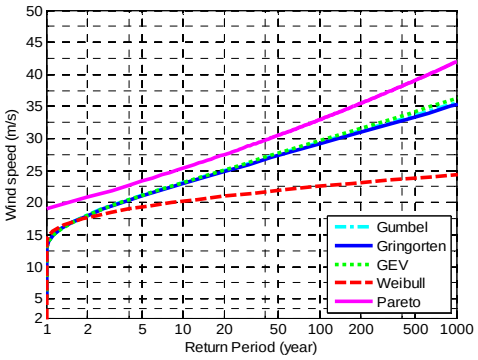
Wind speed (m/s)
Return Period (year)
Gumbel
Gringorten
GEV
Weibull
Pareto

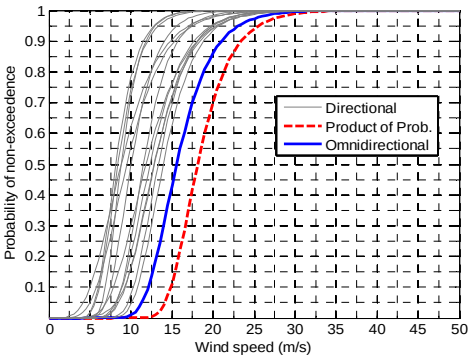
Probability of non-exceedence
Wind speed (m/s)
Directional
Product of Prob.
Omnidirectional

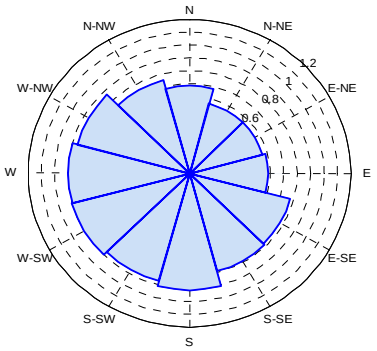
N
N-NE
E-NE
E
E-SE
S-SE
S
S-SW
W
W-NW
N-NW

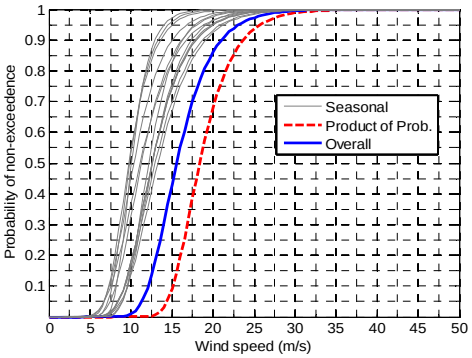
Probability of non-exceedence
Wind speed (m/s)
Seasonal
Product of Prob.
Overall

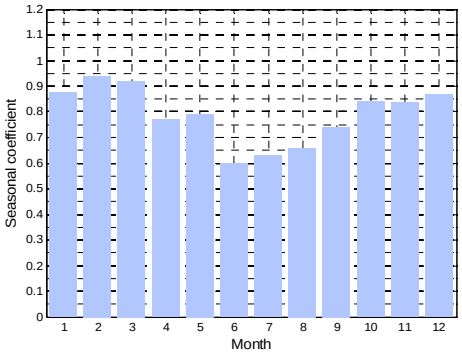
Seasonal coefficient
Month

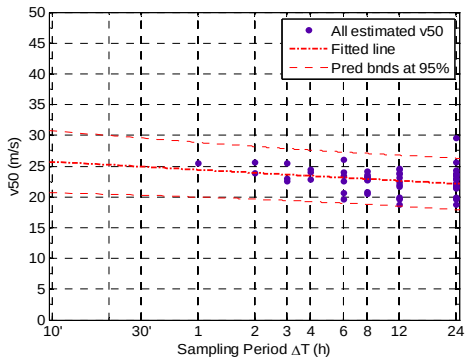
v50 (m/s)
Sampling Period ΔT (h)
All estimated v50
Fitted line
Pred bnds at 95%

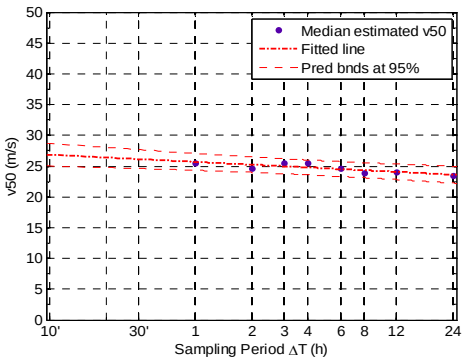
v50 (m/s)
Sampling Period ΔT (h)
Median estimated v50
Fitted line
Pred bnds at 95%

LICR

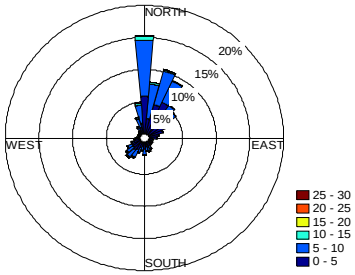
NORTH
20%
15%
10%
5%
WEST
EAST
SOUTH
25 - 30
20 - 25
15 - 20
10 - 15
5 - 10
0 - 5

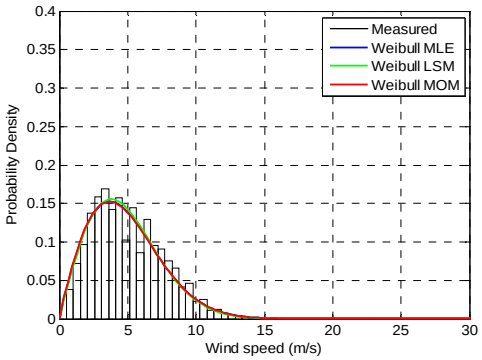
Measured
Weibull MLE
Weibull LSM
Weibull MOM
Probability Density
Wind speed (m/s)

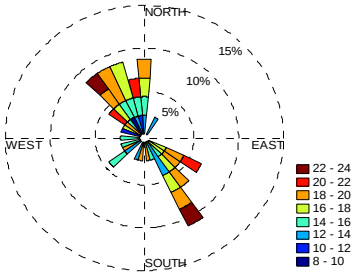
NORTH
15%
10%
5%
WEST
EAST
SOUTH
22 - 24
20 - 22
18 - 20
16 - 18
14 - 16
12 - 14
10 - 12
8 - 10

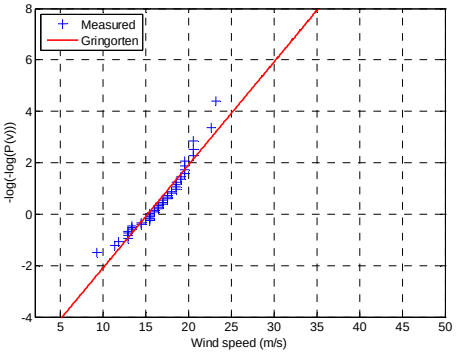
Measured
Gringorten
-log(-log(P(v)))
Wind speed (m/s)

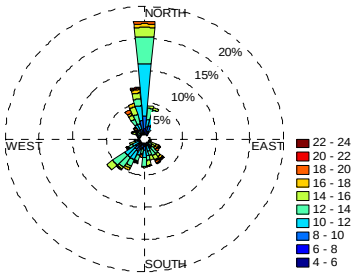
NORTH
20%
15%
10%
5%
WEST
EAST
SOUTH
22 - 24
20 - 22
18 - 20
16 - 18
14 - 16
12 - 14
10 - 12
8 - 10
6 - 8
4 - 6

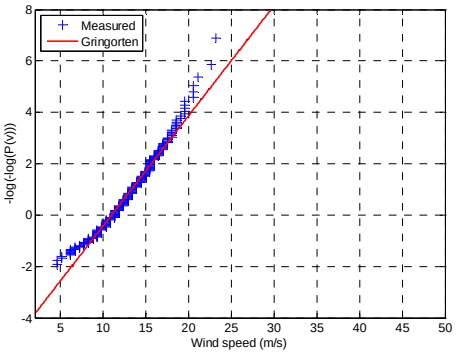
Measured
Gringorten
-log(-log(P(v)))
Wind speed (m/s)

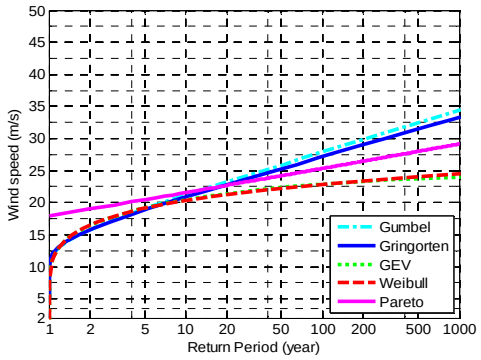
Wind speed (m/s)
Return Period (year)
Gumbel
Gringorten
GEV
Weibull
Pareto

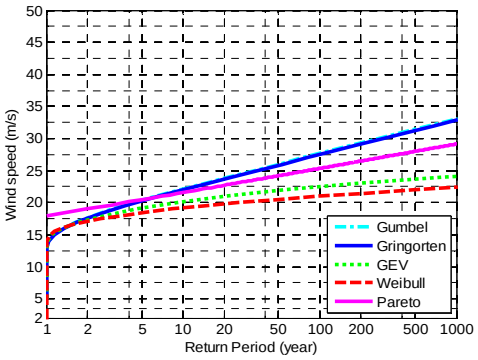
Wind speed (m/s)
Return Period (year)
Gumbel
Gringorten
GEV
Weibull
Pareto

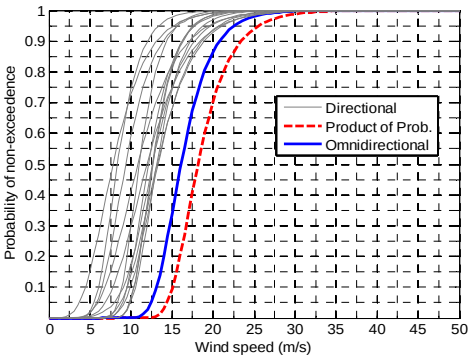
Probability of non-exceedence
Wind speed (m/s)
Directional
Product of Prob.
Omnidirectional

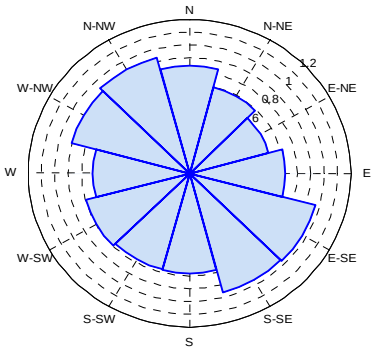
N
N-NE
E-NE
E
E-SE
S-SE
S
S-SW
W
W-NW
N-NW

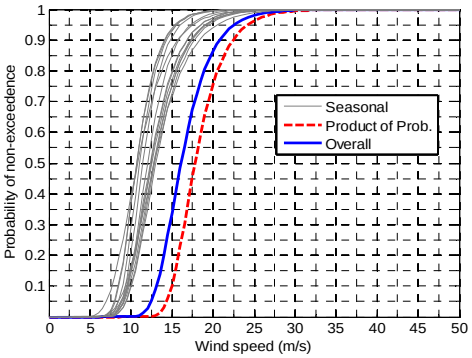
Probability of non-exceedence
Wind speed (m/s)
Seasonal
Product of Prob.
Overall

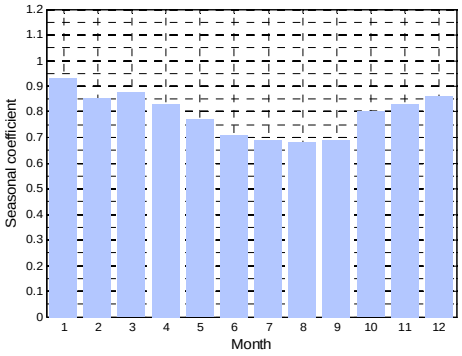
Seasonal coefficient
Month

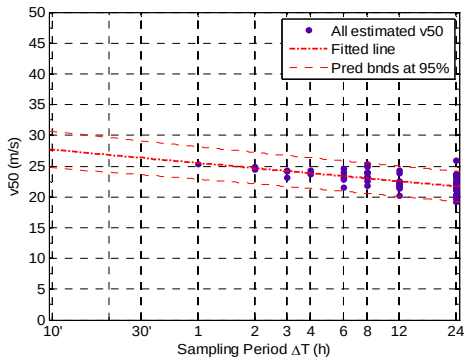
v50 (m/s)
Sampling Period ΔT (h)
All estimated v50
Fitted line
Pred bnds at 95%

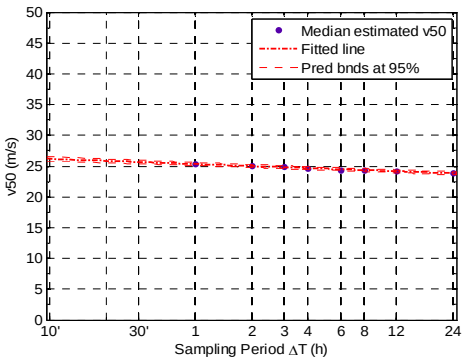
v50 (m/s)
Sampling Period ΔT (h)
Median estimated v50
Fitted line
Pred bnds at 95%

LICT

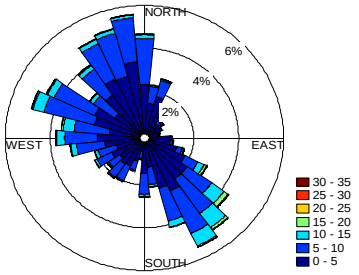
NORTH
6%
4%
2%
WEST
EAST
SOUTH
30 - 35
25 - 30
20 - 25
15 - 20
10 - 15
5 - 10
0 - 5

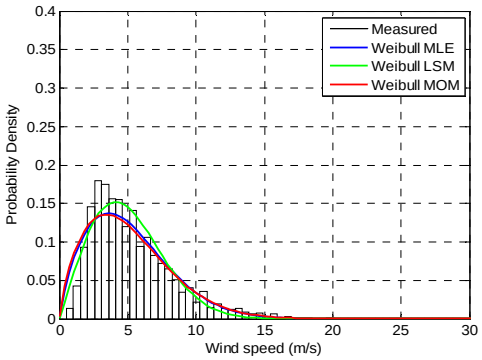
Measured
Weibull MLE
Weibull LSM
Weibull MOM
Probability Density
Wind speed (m/s)

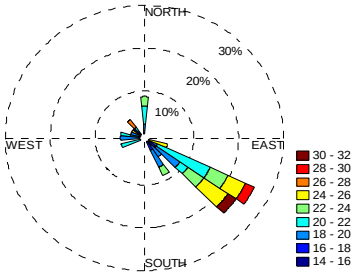
NORTH
30%
20%
10%
WEST
EAST
SOUTH
30 - 32
28 - 30
26 - 28
24 - 26
22 - 24
20 - 22
18 - 20
16 - 18
14 - 16

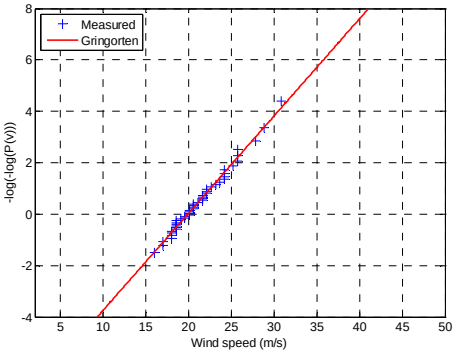
Measured
Gringorten
-log(-log(P(v)))
Wind speed (m/s)

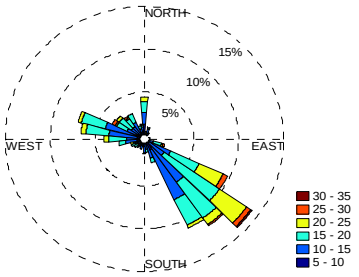
NORTH
15%
10%
5%
WEST
EAST
SOUTH
30 - 35
25 - 30
20 - 25
15 - 20
10 - 15
5 - 10

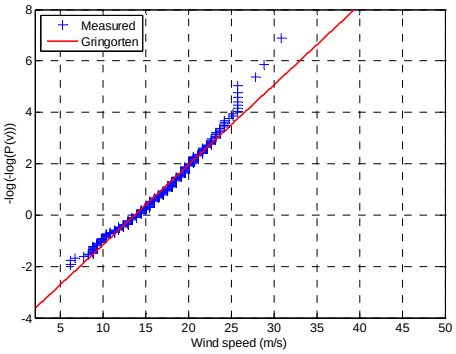
Measured
Gringorten
-log(-log(P(v)))
Wind speed (m/s)

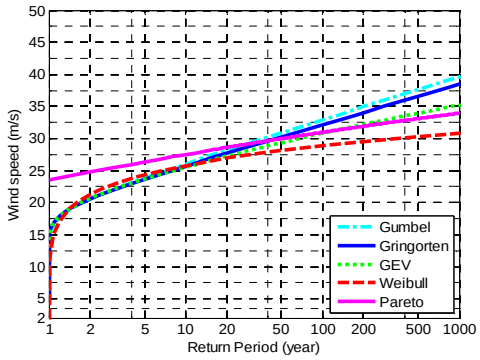
Wind speed (m/s)
Return Period (year)
Gumbel
Gringorten
GEV
Weibull
Pareto

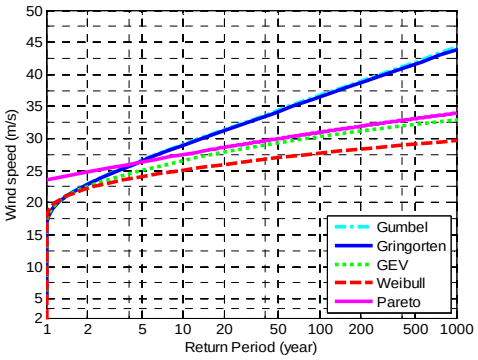
Wind speed (m/s)
Return Period (year)
Gumbel
Gringorten
GEV
Weibull
Pareto

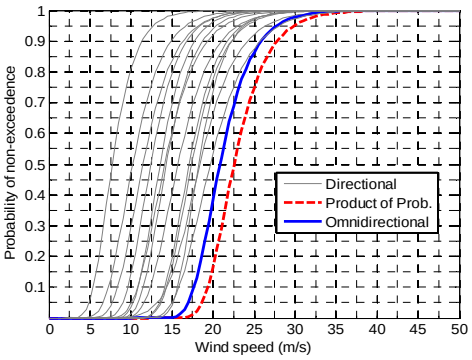
Probability of non-exceedence
Wind speed (m/s)
Directional
Product of Prob.
Omnidirectional

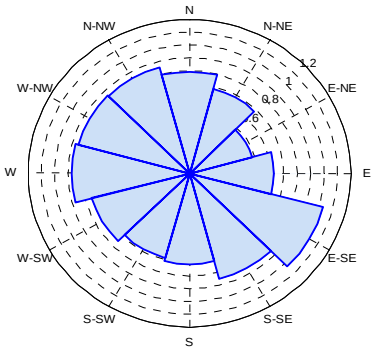
N
N-NE
E-NE
E
E-SE
S-SE
S
S-SW
W
W-NW
N-NW

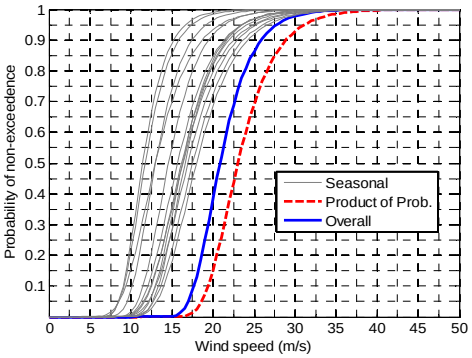
Probability of non-exceedence
Wind speed (m/s)
Seasonal
Product of Prob.
Overall

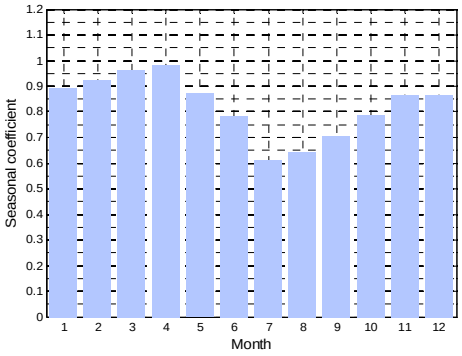
Seasonal coefficient
Month

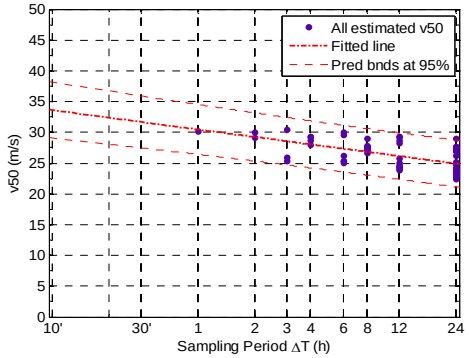
v50 (m/s)
Sampling Period ΔT (h)
All estimated v50
Fitted line
Pred bnds at 95%

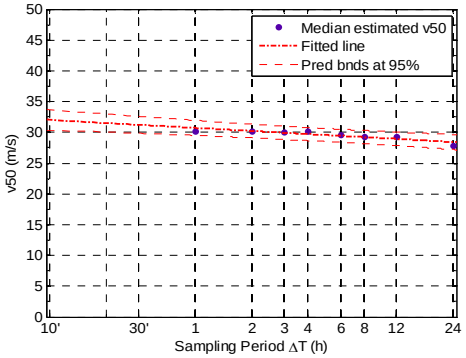
v50 (m/s)
Sampling Period ΔT (h)
Median estimated v50
Fitted line
Pred bnds at 95%

LICU

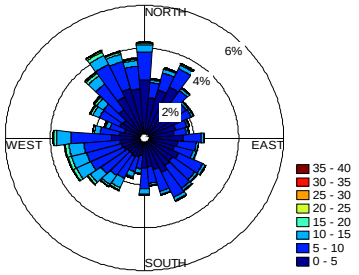
NORTH
6%
4%
2%
WEST
EAST
SOUTH
35 - 40
30 - 35
25 - 30
20 - 25
15 - 20
10 - 15
5 - 10
0 - 5

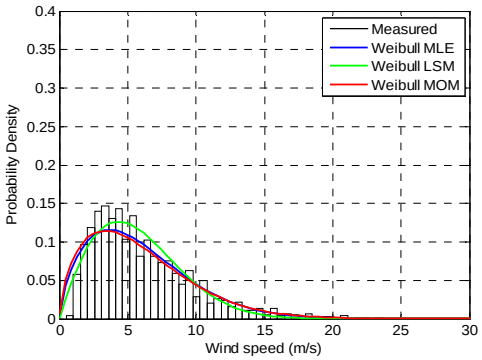
Measured
Weibull MLE
Weibull LSM
Weibull MOM
Probability Density
Wind speed (m/s)

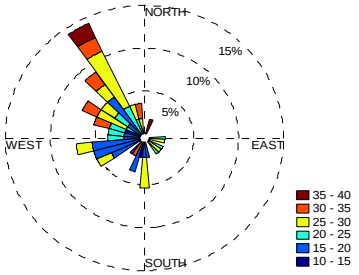
NORTH
15%
10%
5%
WEST
EAST
SOUTH
35 - 40
30 - 35
25 - 30
20 - 25
15 - 20
10 - 15

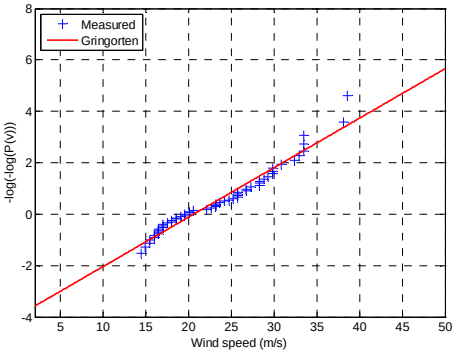
Measured
Gringorten
-log(-log(P(v)))
Wind speed (m/s)

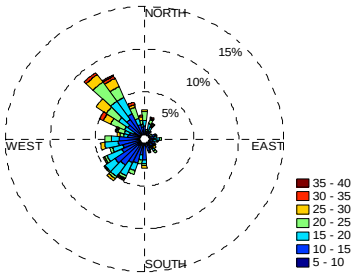
NORTH
15%
10%
5%
WEST
EAST
SOUTH
35 - 40
30 - 35
25 - 30
20 - 25
15 - 20
10 - 15
5 - 10

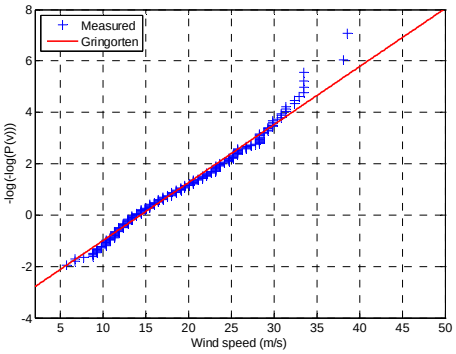
Measured
Gringorten
-log(-log(P(v)))
Wind speed (m/s)

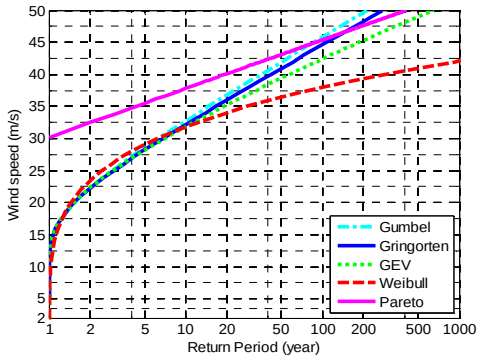
Wind speed (m/s)
Return Period (year)
Gumbel
Gringorten
GEV
Weibull
Pareto

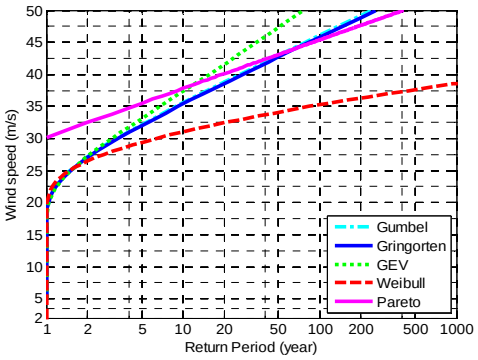
Wind speed (m/s)
Return Period (year)
Gumbel
Gringorten
GEV
Weibull
Pareto

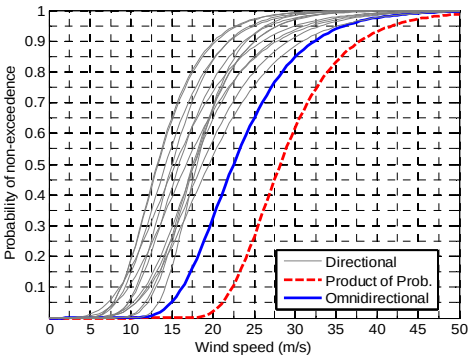
Probability of non-exceedence
Wind speed (m/s)
Directional
Product of Prob.
Omnidirectional

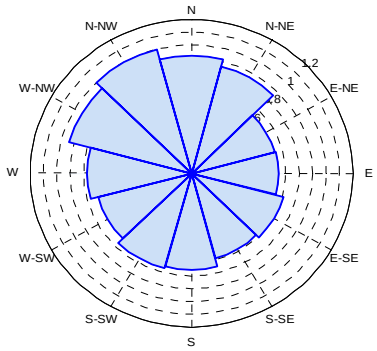
N
N-NE
E-NE
E
E-SE
S-SE
S
S-SW
W
W-NW
N-NW

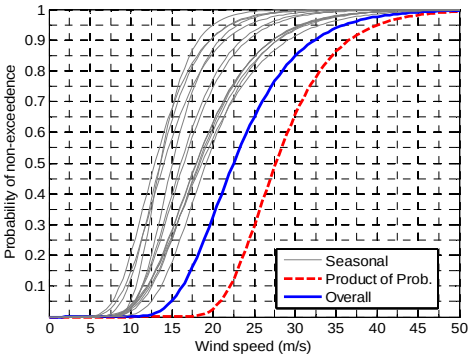
Probability of non-exceedence
Wind speed (m/s)
Seasonal
Product of Prob.
Overall

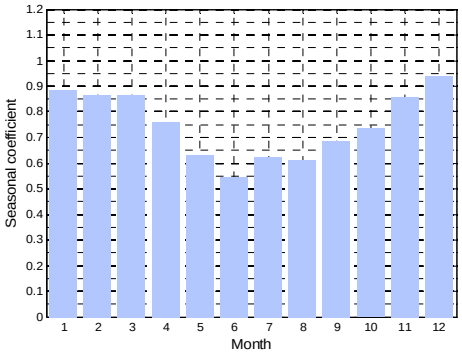
Seasonal coefficient
Month

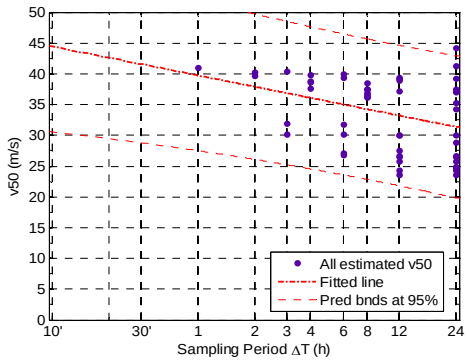
v50 (m/s)
Sampling Period ΔT (h)
All estimated v50
Fitted line
Pred bnds at 95%

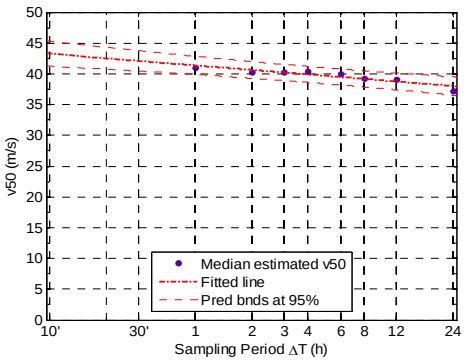
v50 (m/s)
Sampling Period ΔT (h)
Median estimated v50
Fitted line
Pred bnds at 95%

LICX

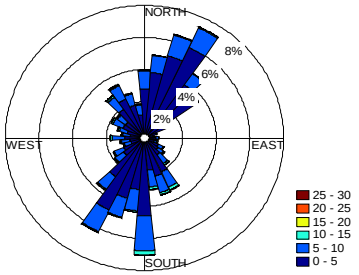
NORTH
8%
6%
4%
2%
WEST
EAST
SOUTH
25 - 30
20 - 25
15 - 20
10 - 15
5 - 10
0 - 5

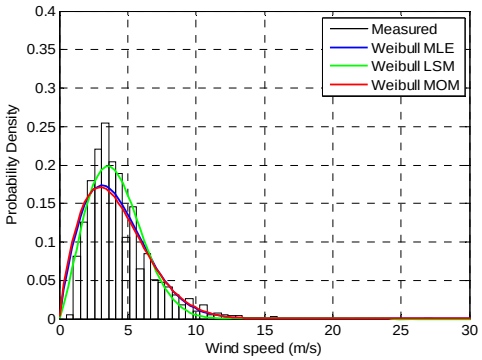
Measured
Weibull MLE
Weibull LSM
Weibull MOM
Probability Density
Wind speed (m/s)

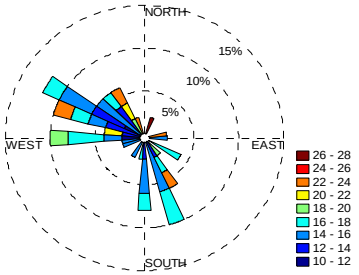
NORTH
15%
10%
5%
WEST
EAST
SOUTH
26 - 28
24 - 26
22 - 24
20 - 22
18 - 20
16 - 18
14 - 16
12 - 14
10 - 12

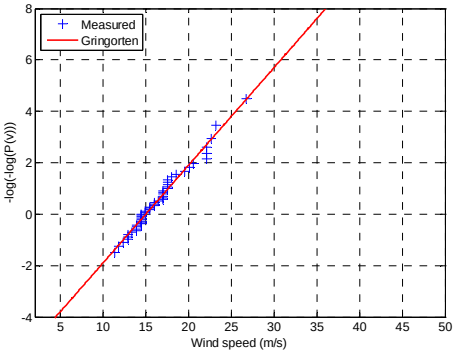
Measured
Gringorten
-log(-log(P(v)))
Wind speed (m/s)

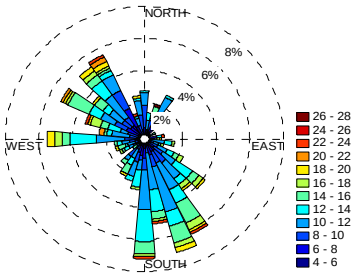
NORTH
8%
6%
4%
2%
WEST
EAST
SOUTH
26 - 28
24 - 26
22 - 24
20 - 22
18 - 20
16 - 18
14 - 16
12 - 14
10 - 12
8 - 10
6 - 8
4 - 6

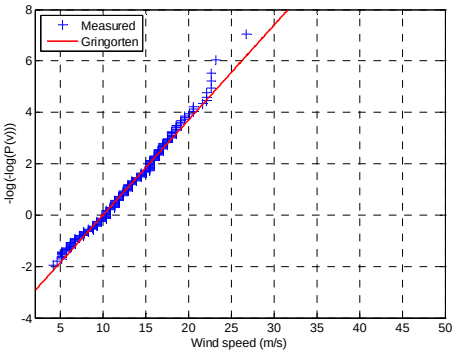
Measured
Gringorten
-log(-log(P(v)))
Wind speed (m/s)

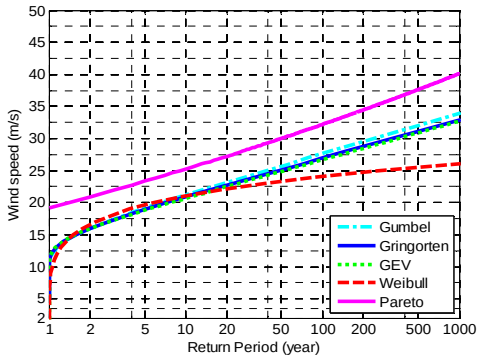
Wind speed (m/s)
Return Period (year)
Gumbel
Gringorten
GEV
Weibull
Pareto

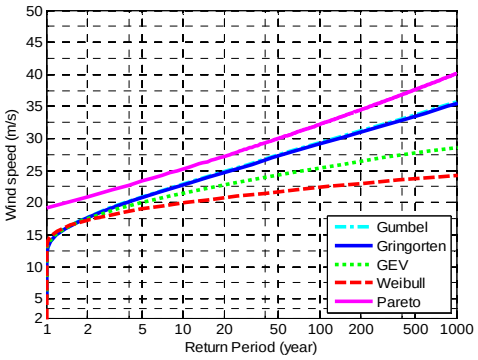
Wind speed (m/s)
Return Period (year)
Gumbel
Gringorten
GEV
Weibull
Pareto

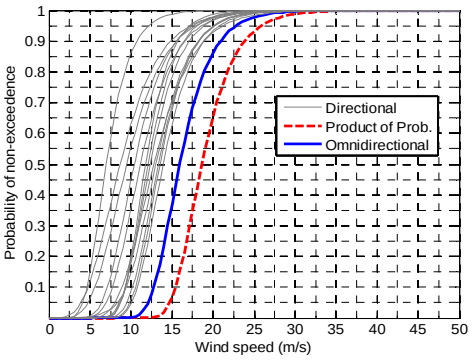
Probability of non-exceedence
Wind speed (m/s)
Directional
Product of Prob.
Omnidirectional

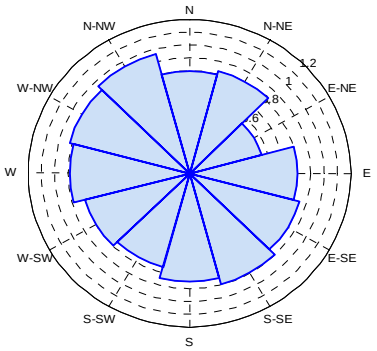
N
N-NE
E-NE
E
E-SE
S-SE
S
S-SW
W
W-NW
N-NW

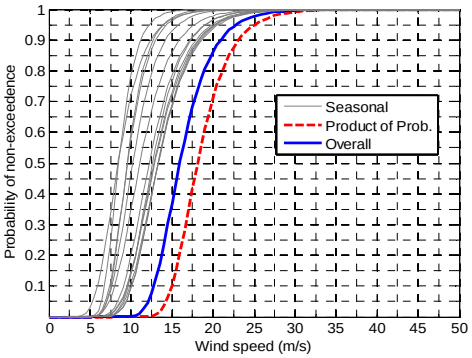
Probability of non-exceedence
Wind speed (m/s)
Seasonal
Product of Prob.
Overall

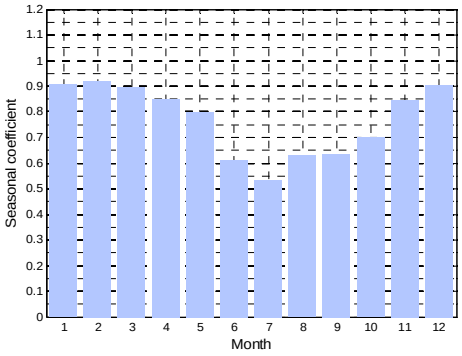
Seasonal coefficient
Month

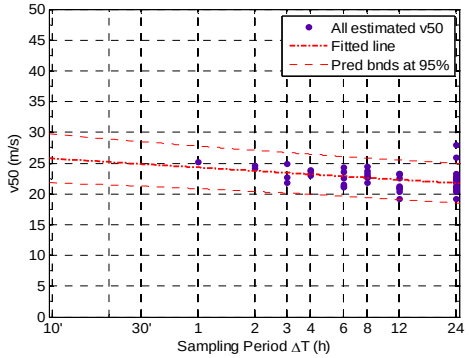
v50 (m/s)
Sampling Period ΔT (h)
All estimated v50
Fitted line
Pred bnds at 95%

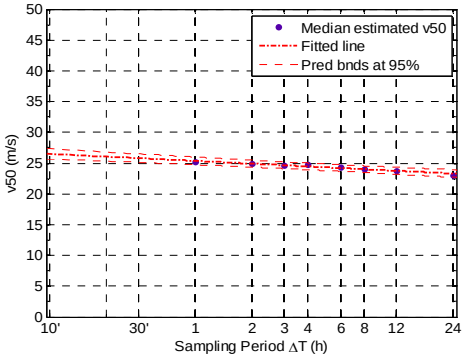
v50 (m/s)
Sampling Period ΔT (h)
Median estimated v50
Fitted line
Pred bnds at 95%

LICZ

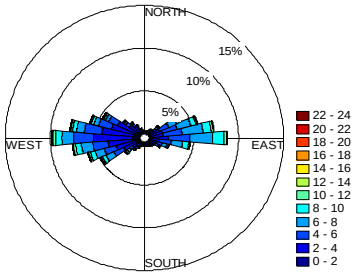
NORTH
15%
10%
5%
WEST
EAST
SOUTH
22 - 24
20 - 22
18 - 20
16 - 18
14 - 16
12 - 14
10 - 12
8 - 10
6 - 8
4 - 6
2 - 4
0 - 2

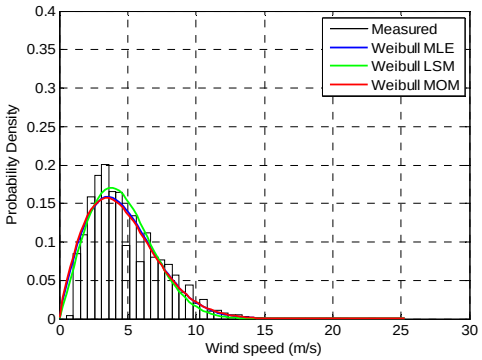
Measured
Weibull MLE
Weibull LSM
Weibull MOM
Probability Density
Wind speed (m/s)

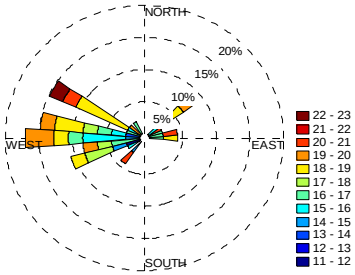
NORTH
20%
15%
10%
5%
WEST
EAST
SOUTH
22 - 23
21 - 22
20 - 21
19 - 20
18 - 19
17 - 18
16 - 17
15 - 16
14 - 15
13 - 14
12 - 13
11 - 12

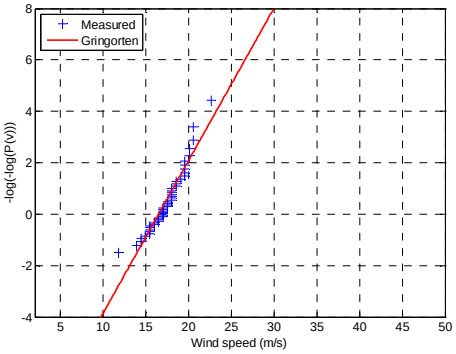
Measured
Gringorten
-log(-log(P(v)))
Wind speed (m/s)

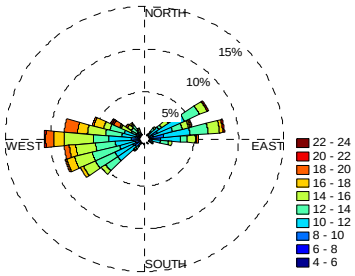
NORTH
15%
10%
5%
WEST
EAST
SOUTH
22 - 24
20 - 22
18 - 20
16 - 18
14 - 16
12 - 14
10 - 12
8 - 10
6 - 8
4 - 6

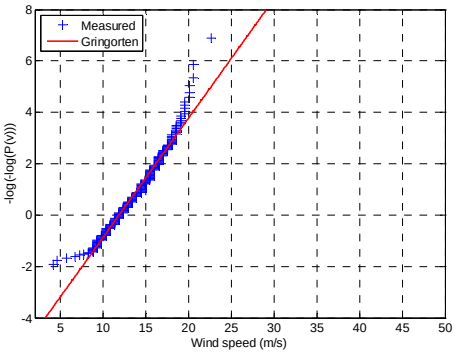
Measured
Gringorten
-log(-log(P(v)))
Wind speed (m/s)

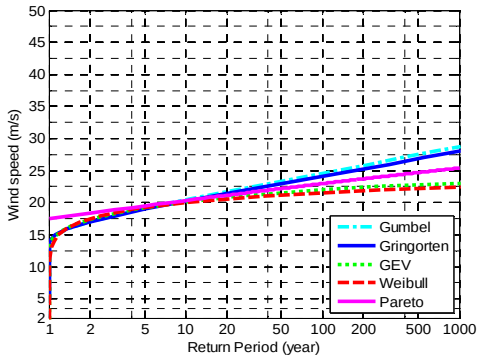
Wind speed (m/s)
Return Period (year)
Gumbel
Gringorten
GEV
Weibull
Pareto

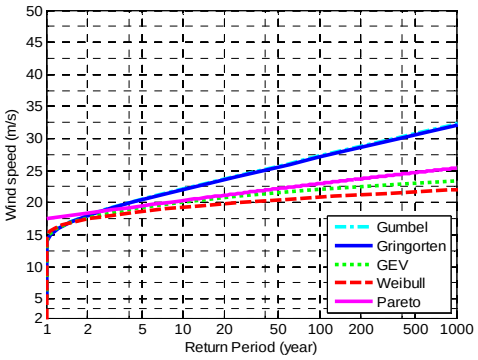
Wind speed (m/s)
Return Period (year)
Gumbel
Gringorten
GEV
Weibull
Pareto

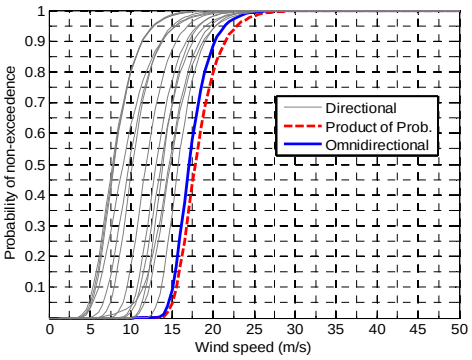
Probability of non-exceedence
Wind speed (m/s)
Directional
Product of Prob.
Omnidirectional

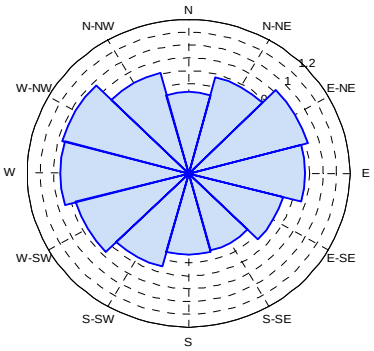
N
N-NE
E-NE
E
E-SE
S-SE
S
S-SW
W
W-NW
N-NW

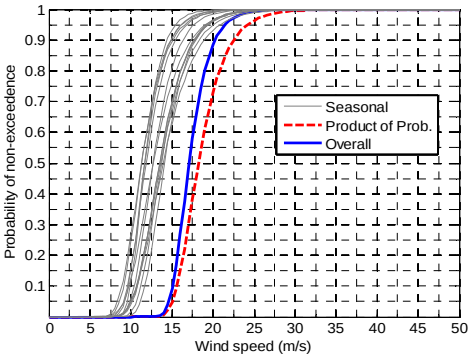
Probability of non-exceedence
Wind speed (m/s)
Seasonal
Product of Prob.
Overall

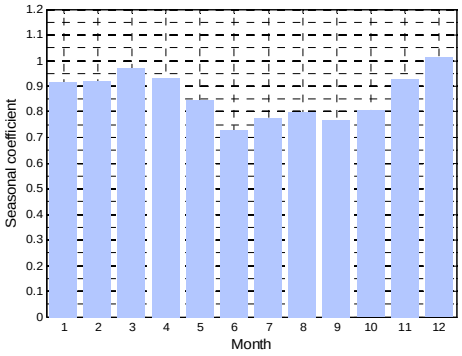
Seasonal coefficient
Month

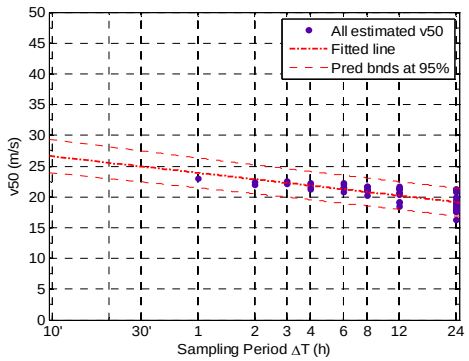
v50 (m/s)
Sampling Period ΔT (h)
All estimated v50
Fitted line
Pred bnds at 95%

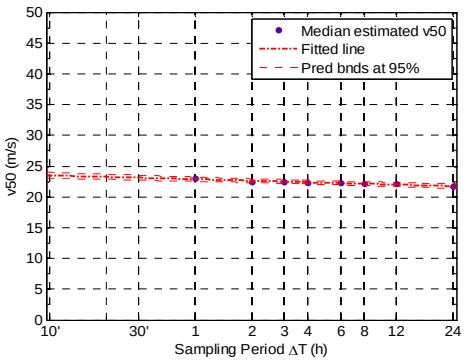
v50 (m/s)
Sampling Period ΔT (h)
Median estimated v50
Fitted line
Pred bnds at 95%

LIEA

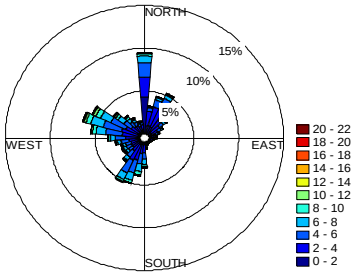
NORTH
15%
10%
5%
WEST
EAST
SOUTH
20 - 22
18 - 20
16 - 18
14 - 16
12 - 14
10 - 12
8 - 10
6 - 8
4 - 6
2 - 4
0 - 2

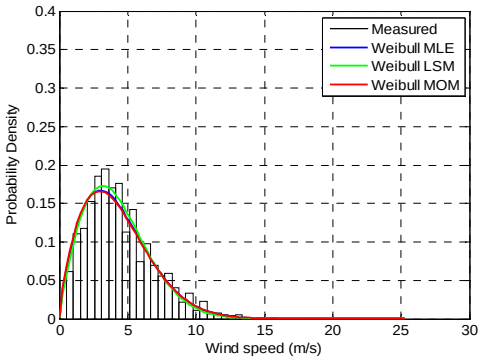
Measured
Weibull MLE
Weibull LSM
Weibull MOM
Probability Density
Wind speed (m/s)

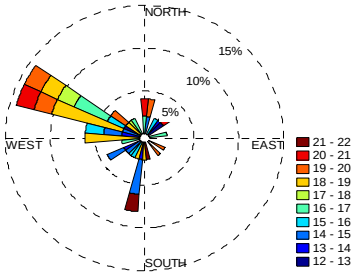
NORTH
15%
10%
5%
WEST
EAST
SOUTH
21 - 22
20 - 21
19 - 20
18 - 19
17 - 18
16 - 17
15 - 16
14 - 15
13 - 14
12 - 13

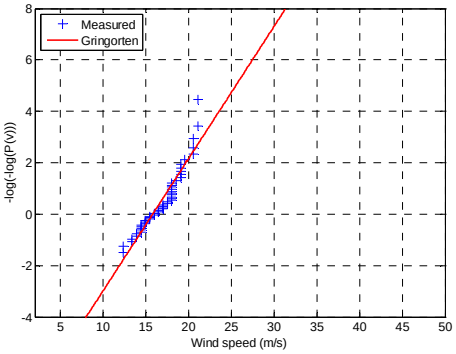
Measured
Gringorten
-log(-log(P(v)))
Wind speed (m/s)

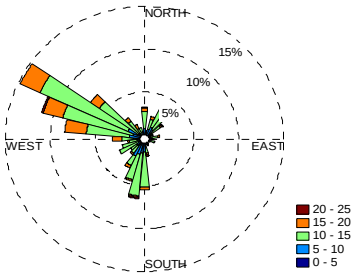
NORTH
15%
10%
5%
WEST
EAST
SOUTH
20 - 25
15 - 20
10 - 15
5 - 10
0 - 5

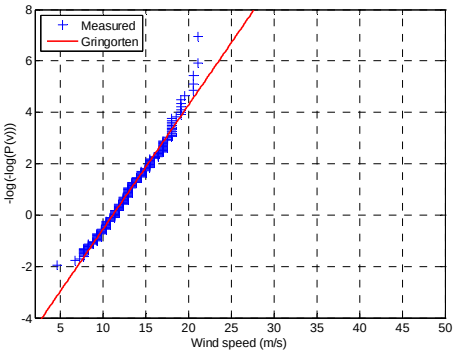
Measured
Gringorten
-log(-log(P(v)))
Wind speed (m/s)

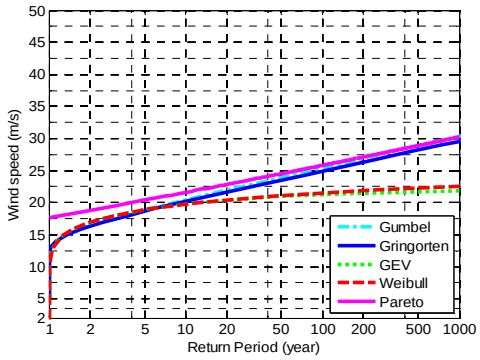
Wind speed (m/s)
Return Period (year)
Gumbel
Gringorten
GEV
Weibull
Pareto

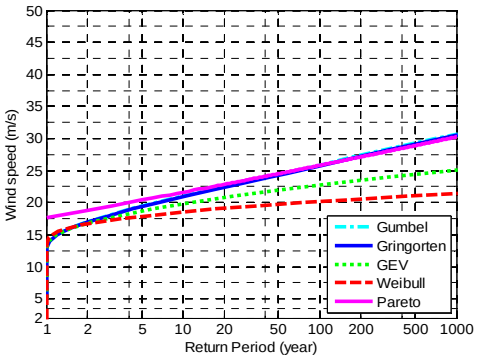
Wind speed (m/s)
Return Period (year)
Gumbel
Gringorten
GEV
Weibull
Pareto

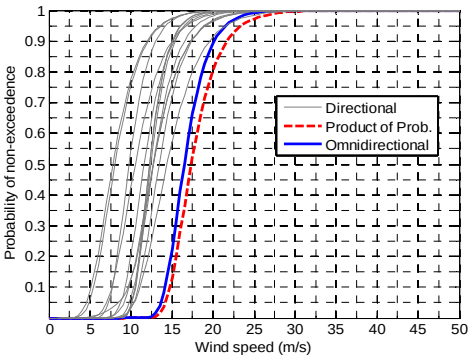
Probability of non-exceedence
Wind speed (m/s)
Directional
Product of Prob.
Omnidirectional

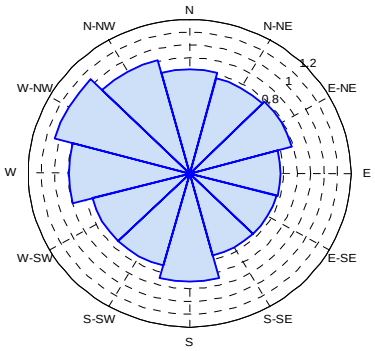
N
N-NE
E-NE
E
E-SE
S-SE
S
S-SW
W
W-NW
N-NW

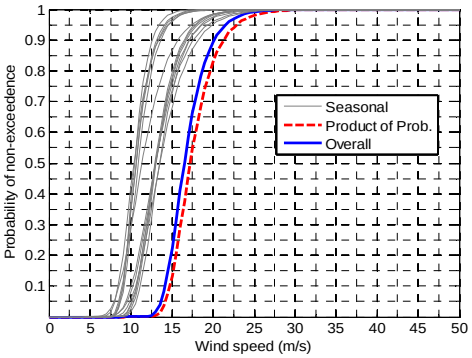
Probability of non-exceedence
Wind speed (m/s)
Seasonal
Product of Prob.
Overall

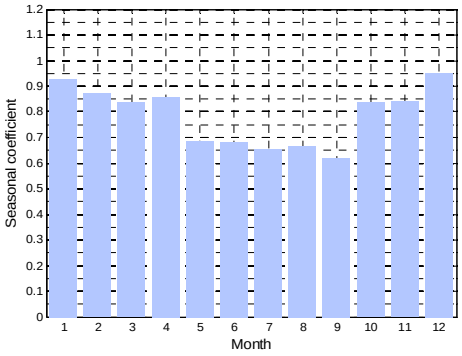
Seasonal coefficient
Month

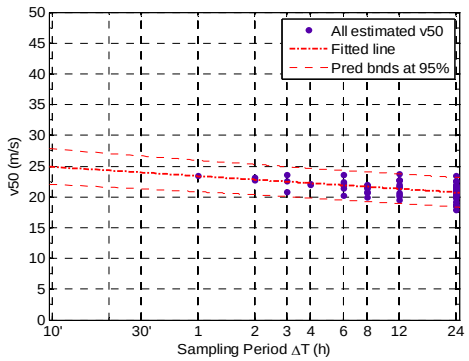
v50 (m/s)
Sampling Period ΔT (h)
All estimated v50
Fitted line
Pred bnds at 95%

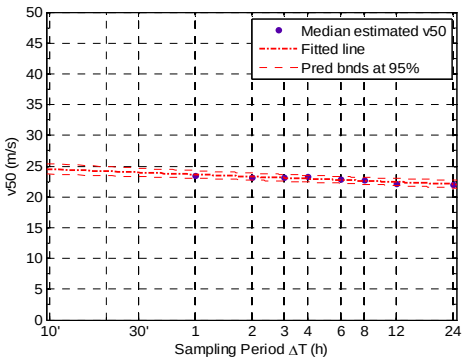
v50 (m/s)
Sampling Period ΔT (h)
Median estimated v50
Fitted line
Pred bnds at 95%

LIEB

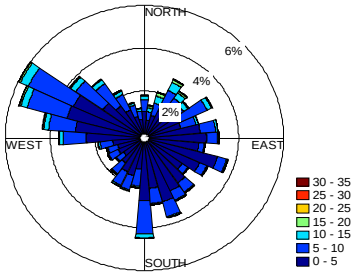
NORTH
6%
4%
2%
WEST
EAST
SOUTH
30 - 35
25 - 30
20 - 25
15 - 20
10 - 15
5 - 10
0 - 5

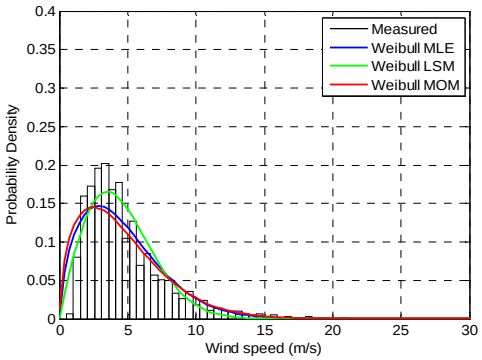
Measured
Weibull MLE
Weibull LSM
Weibull MOM
Probability Density
Wind speed (m/s)

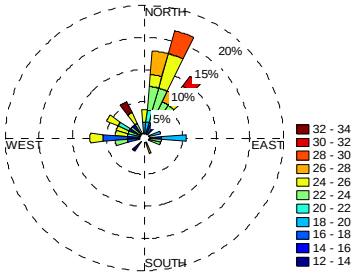
NORTH
20%
15%
10%
5%
WEST
EAST
SOUTH
32 - 34
30 - 32
28 - 30
26 - 28
24 - 26
22 - 24
20 - 22
18 - 20
16 - 18
14 - 16
12 - 14

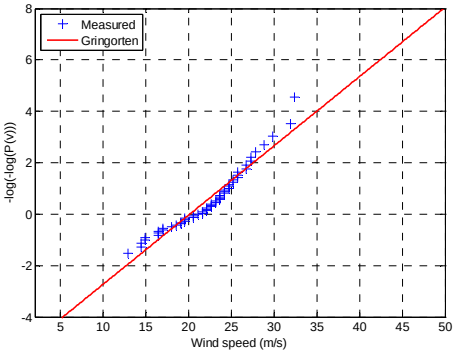
Measured
Gringorten
-log(-log(P(v)))
Wind speed (m/s)

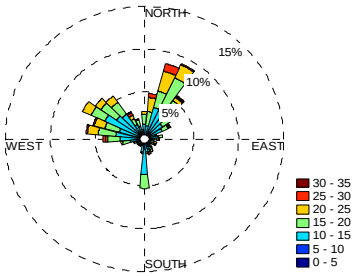
NORTH
15%
10%
5%
WEST
EAST
SOUTH
30 - 35
25 - 30
20 - 25
15 - 20
10 - 15
5 - 10
0 - 5

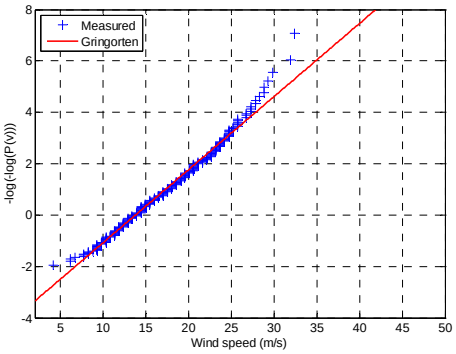
Measured
Gringorten
-log(-log(P(v)))
Wind speed (m/s)

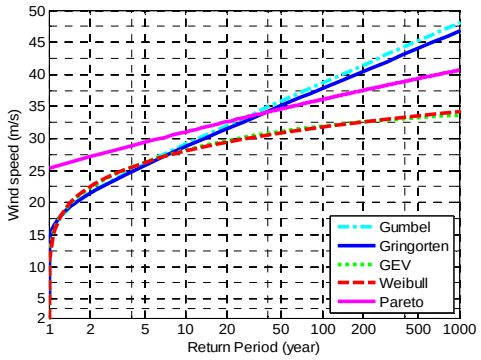
Wind speed (m/s)
Return Period (year)
Gumbel
Gringorten
GEV
Weibull
Pareto

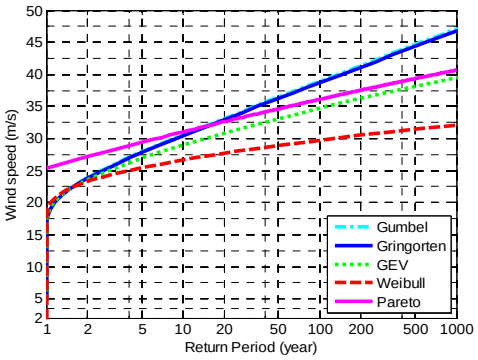
Wind speed (m/s)
Return Period (year)
Gumbel
Gringorten
GEV
Weibull
Pareto

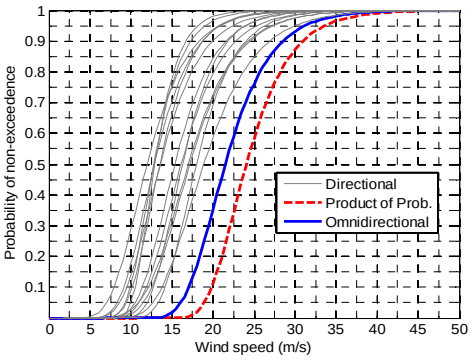
Probability of non-exceedence
Wind speed (m/s)
Directional
Product of Prob.
Omnidirectional

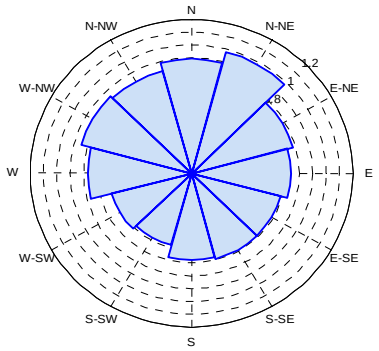
N
N-NE
E-NE
E
E-SE
S-SE
S
S-SW
W
W-NW
N-NW

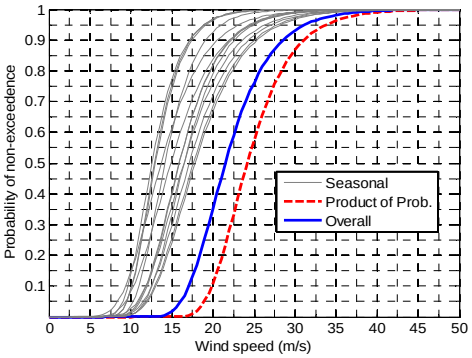
Probability of non-exceedence
Wind speed (m/s)
Seasonal
Product of Prob.
Overall

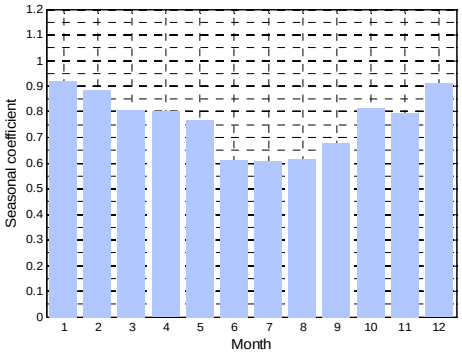
Seasonal coefficient
Month

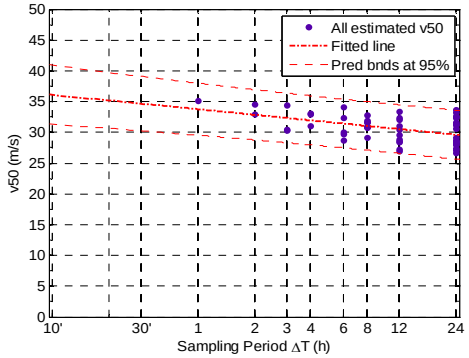
v50 (m/s)
Sampling Period ΔT (h)
All estimated v50
Fitted line
Pred bnds at 95%

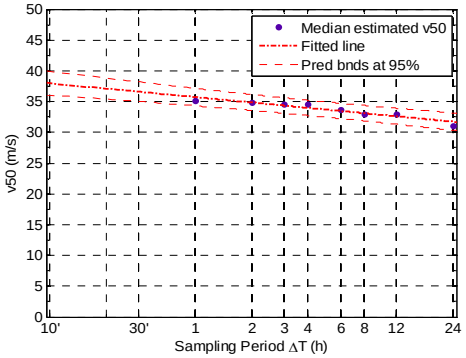
v50 (m/s)
Sampling Period ΔT (h)
Median estimated v50
Fitted line
Pred bnds at 95%

LIEC

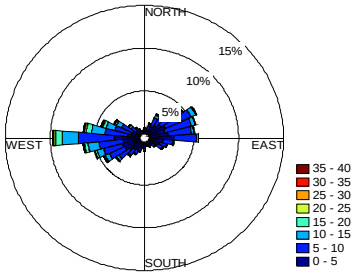
NORTH
15%
10%
5%
WEST
EAST
SOUTH
35 - 40
30 - 35
25 - 30
20 - 25
15 - 20
10 - 15
5 - 10
0 - 5

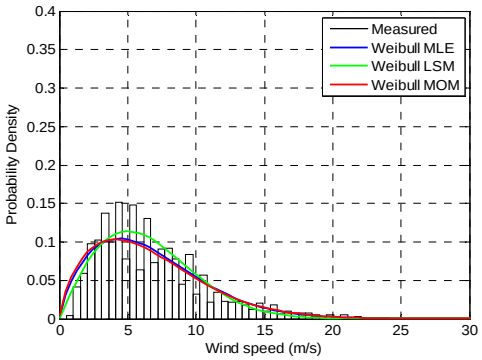
Measured
Weibull MLE
Weibull LSM
Weibull MOM
Probability Density
Wind speed (m/s)

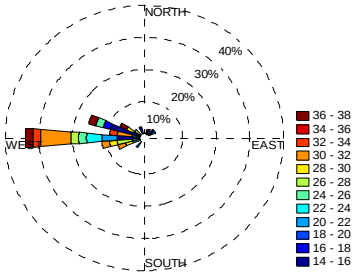
NORTH
40%
30%
20%
10%
WEST
EAST
SOUTH
36 - 38
34 - 36
32 - 34
30 - 32
28 - 30
26 - 28
24 - 26
22 - 24
20 - 22
18 - 20
16 - 18
14 - 16

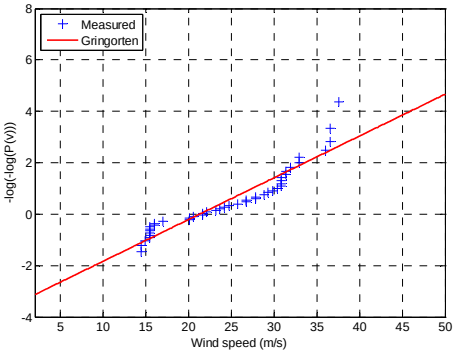
Measured
Gringorten
-log(-log(P(v)))
Wind speed (m/s)

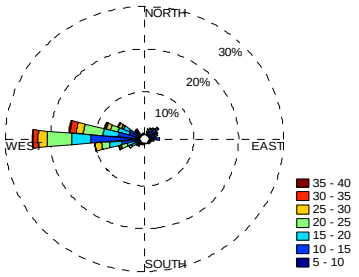
NORTH
30%
20%
10%
WEST
EAST
SOUTH
35 - 40
30 - 35
25 - 30
20 - 25
15 - 20
10 - 15
5 - 10

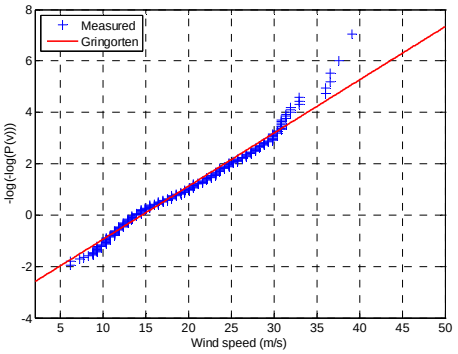
Measured
Gringorten
-log(-log(P(v)))
Wind speed (m/s)

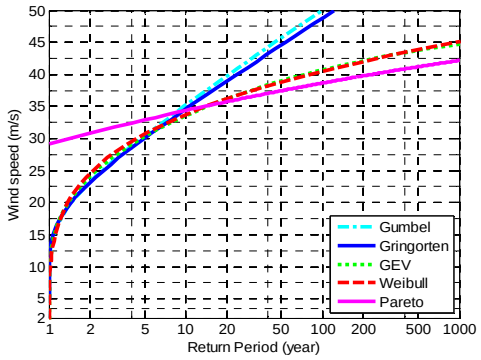
Wind speed (m/s)
Return Period (year)
Gumbel
Gringorten
GEV
Weibull
Pareto

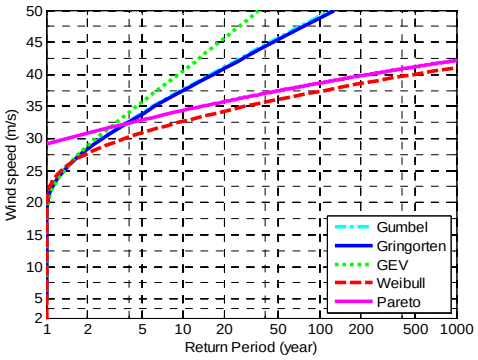
Wind speed (m/s)
Return Period (year)
Gumbel
Gringorten
GEV
Weibull
Pareto

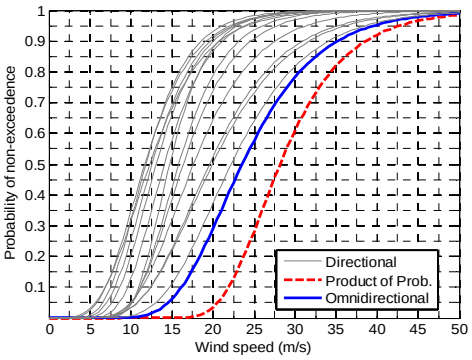
Probability of non-exceedence
Wind speed (m/s)
Directional
Product of Prob.
Omnidirectional

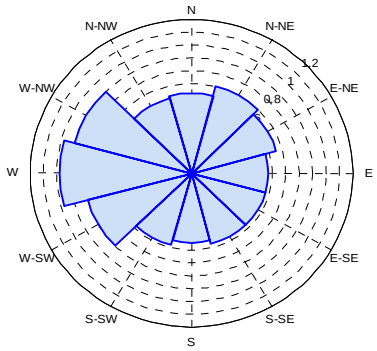
N
N-NE
E-NE
E
E-SE
S-SE
S
S-SW
W
W-NW
N-NW

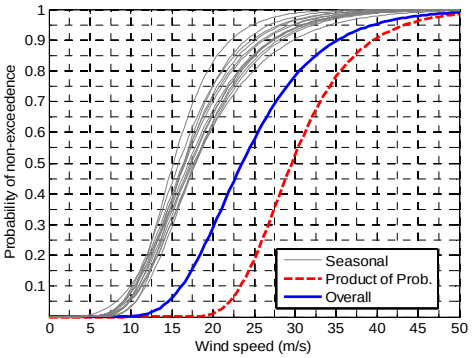
Probability of non-exceedence
Wind speed (m/s)
Seasonal
Product of Prob.
Overall

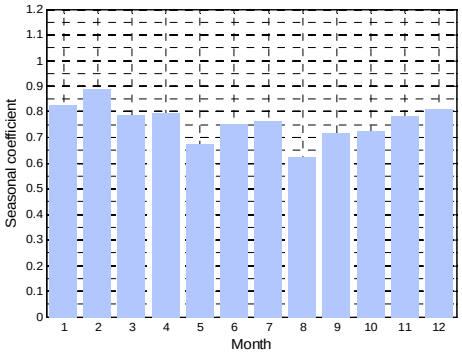
Seasonal coefficient
Month

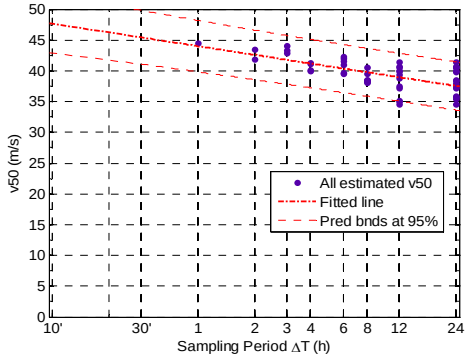
v50 (m/s)
Sampling Period ΔT (h)
All estimated v50
Fitted line
Pred bnds at 95%

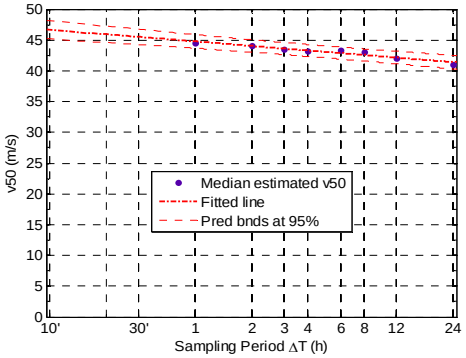
v50 (m/s)
Sampling Period ΔT (h)
Median estimated v50
Fitted line
Pred bnds at 95%

LIED

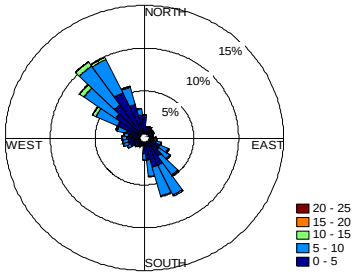
NORTH
15%
10%
5%
WEST
EAST
SOUTH
20 - 25
15 - 20
10 - 15
5 - 10
0 - 5

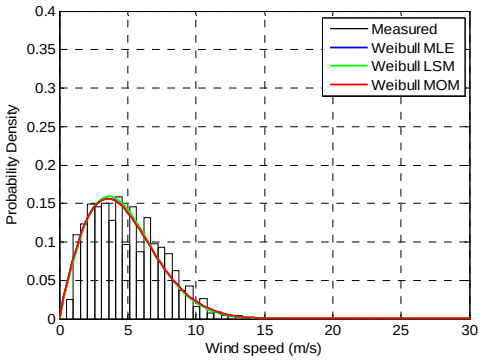
Measured
Weibull MLE
Weibull LSM
Weibull MOM
Probability Density
Wind speed (m/s)

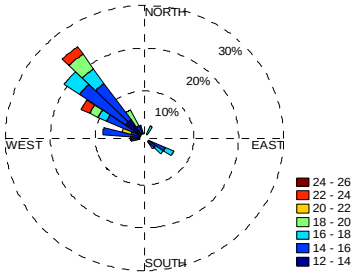
NORTH
30%
20%
10%
WEST
EAST
SOUTH
24 - 26
22 - 24
20 - 22
18 - 20
16 - 18
14 - 16
12 - 14

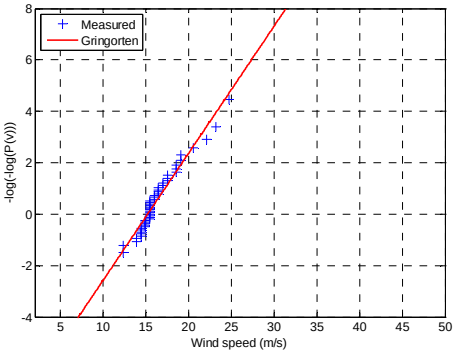
Measured
Gringorten
-log(-log(P(v)))
Wind speed (m/s)

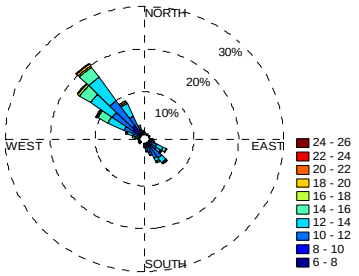
NORTH
30%
20%
10%
WEST
EAST
SOUTH
24 - 26
22 - 24
20 - 22
18 - 20
16 - 18
14 - 16
12 - 14
10 - 12
8 - 10
6 - 8

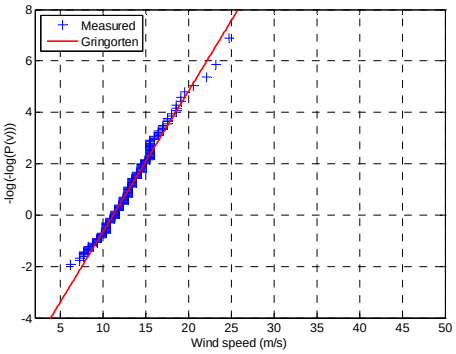
Measured
Gringorten
-log(-log(P(v)))
Wind speed (m/s)

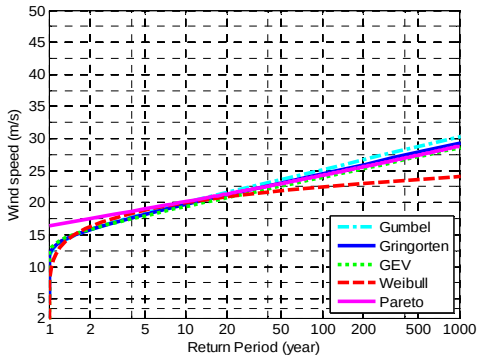
Wind speed (m/s)
Return Period (year)
Gumbel
Gringorten
GEV
Weibull
Pareto

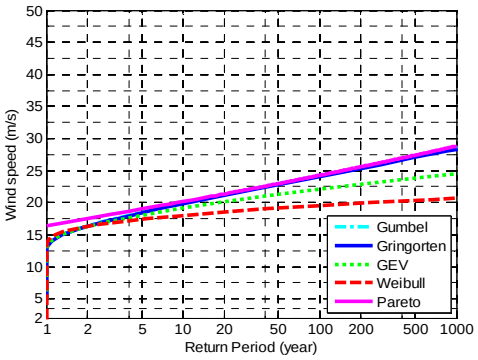
Wind speed (m/s)
Return Period (year)
Gumbel
Gringorten
GEV
Weibull
Pareto

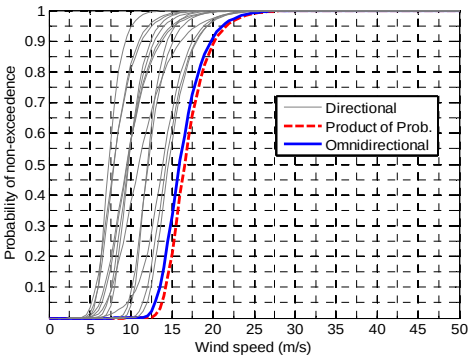
Probability of non-exceedence
Wind speed (m/s)
Directional
Product of Prob.
Omnidirectional

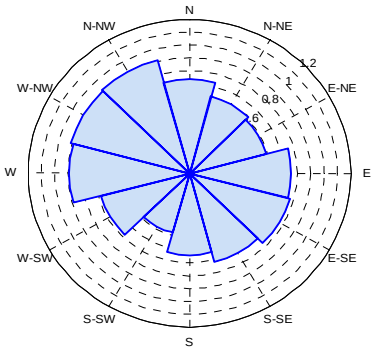
N
N-NE
E-NE
E
E-SE
S-SE
S
S-SW
W
W-NW
N-NW

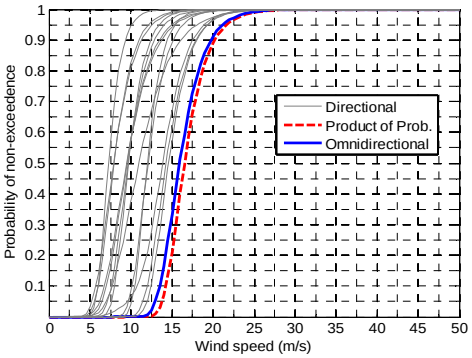
Probability of non-exceedence
Wind speed (m/s)
Directional
Product of Prob.
Omnidirectional

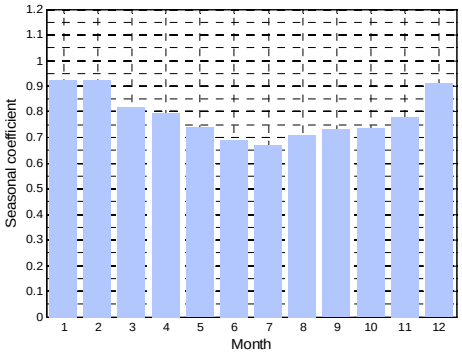
Seasonal coefficient
Month

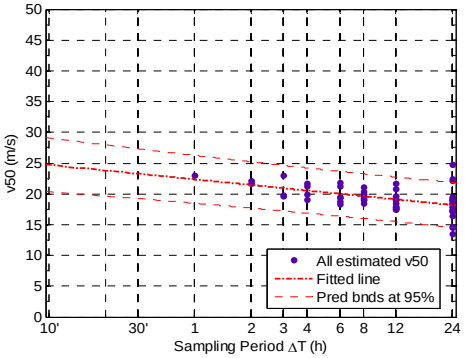
v50 (m/s)
Sampling Period ΔT (h)
All estimated v50
Fitted line
Pred bnds at 95%

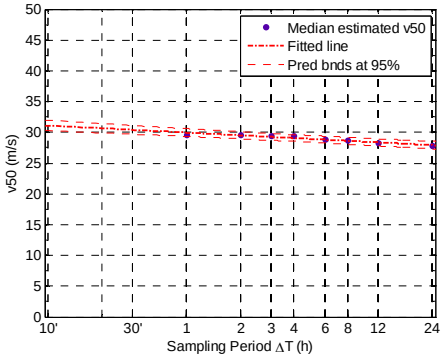
v50 (m/s)
Sampling Period ΔT (h)
Median estimated v50
Fitted line
Pred bnds at 95%

LIEE

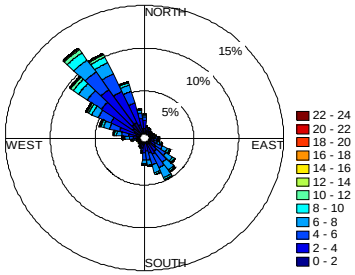
NORTH
15%
10%
5%
WEST
EAST
SOUTH
22 - 24
20 - 22
18 - 20
16 - 18
14 - 16
12 - 14
10 - 12
8 - 10
6 - 8
4 - 6
2 - 4
0 - 2

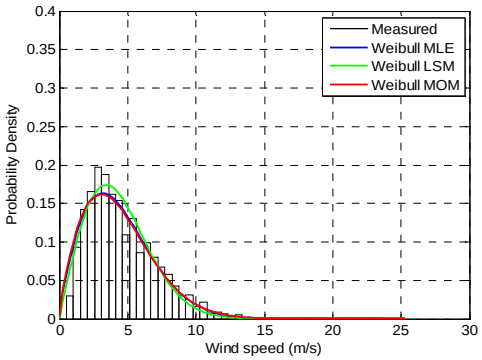
Measured
Weibull MLE
Weibull LSM
Weibull MOM
Probability Density
Wind speed (m/s)

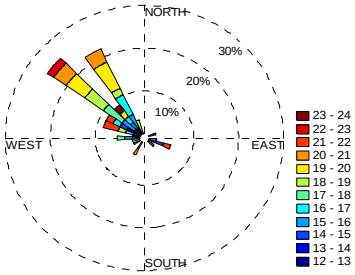
NORTH
30%
20%
10%
WEST
EAST
SOUTH
23 - 24
22 - 23
21 - 22
20 - 21
19 - 20
18 - 19
17 - 18
16 - 17
15 - 16
14 - 15
13 - 14
12 - 13

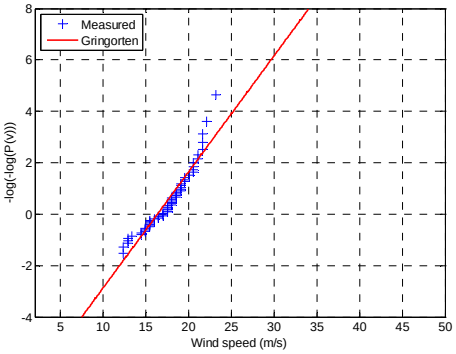
Measured
Gringorten
-log(-log(P(v)))
Wind speed (m/s)

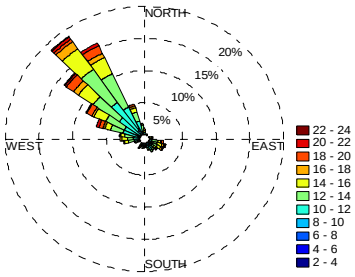
NORTH
20%
15%
10%
5%
WEST
EAST
SOUTH
22 - 24
20 - 22
18 - 20
16 - 18
14 - 16
12 - 14
10 - 12
8 - 10
6 - 8
4 - 6
2 - 4

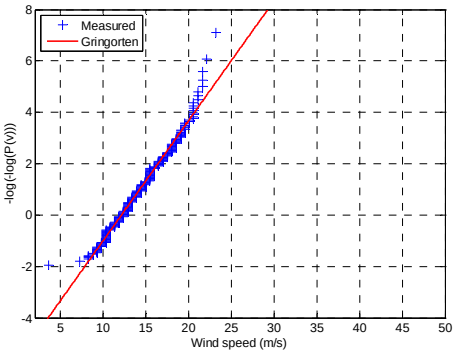
Measured
Gringorten
-log(-log(P(v)))
Wind speed (m/s)

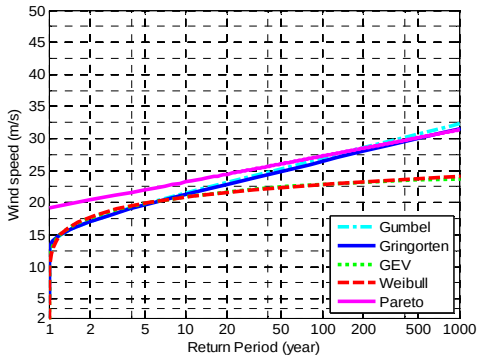
Wind speed (m/s)
Return Period (year)
Gumbel
Gringorten
GEV
Weibull
Pareto

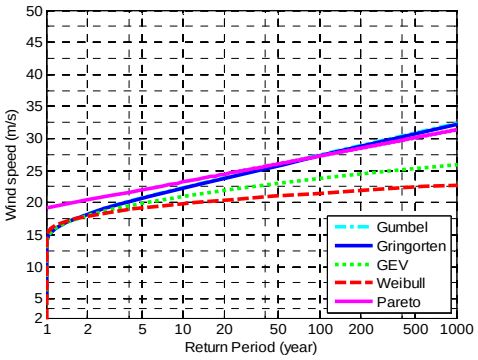
Wind speed (m/s)
Return Period (year)
Gumbel
Gringorten
GEV
Weibull
Pareto

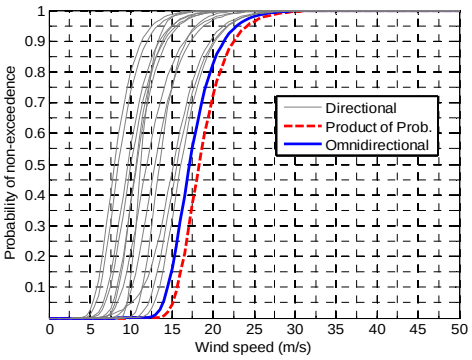
Probability of non-exceedence
Wind speed (m/s)
Directional
Product of Prob.
Omnidirectional

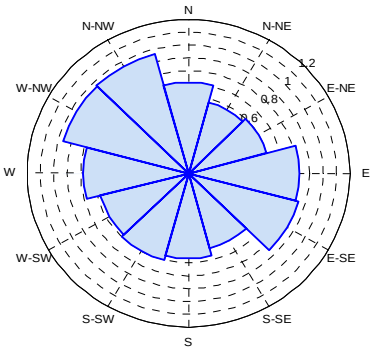
N
N-NE
E-NE
E
E-SE
S-SE
S
S-SW
W
W-NW
N-NW

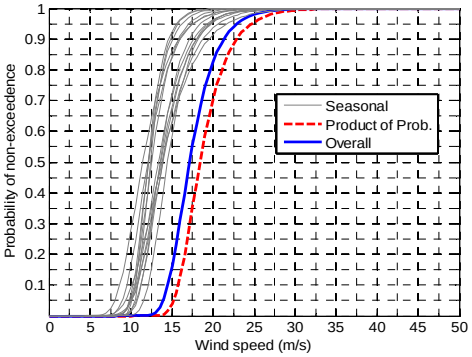
Probability of non-exceedence
Wind speed (m/s)
Seasonal
Product of Prob.
Overall

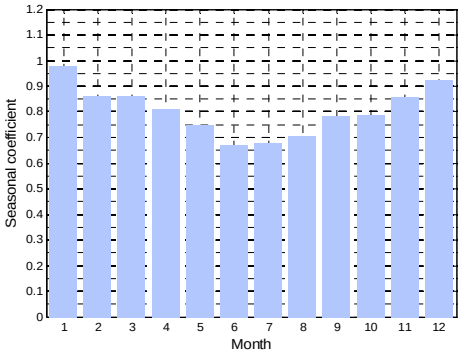
Seasonal coefficient
Month

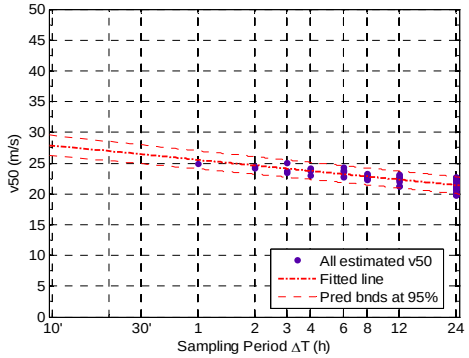
v50 (m/s)
Sampling Period ΔT (h)
All estimated v50
Fitted line
Pred bnds at 95%

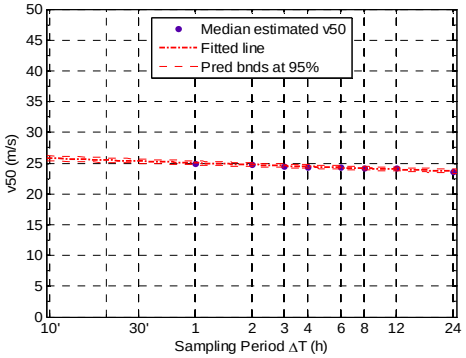
v50 (m/s)
Sampling Period ΔT (h)
Median estimated v50
Fitted line
Pred bnds at 95%

LIEF

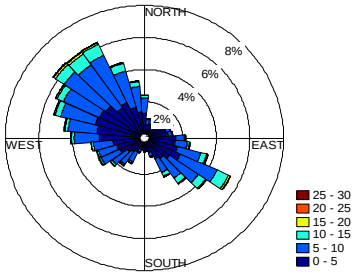
NORTH
8%
6%
4%
2%
WEST
EAST
SOUTH
25 - 30
20 - 25
15 - 20
10 - 15
5 - 10
0 - 5

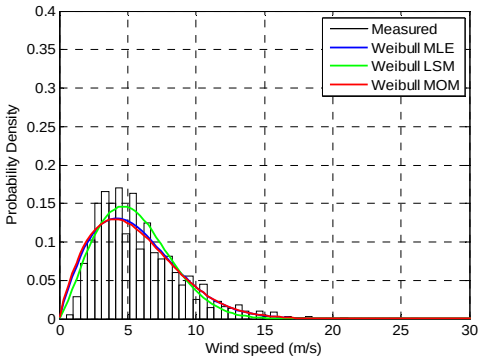
Measured
Weibull MLE
Weibull LSM
Weibull MOM
Probability Density
Wind speed (m/s)

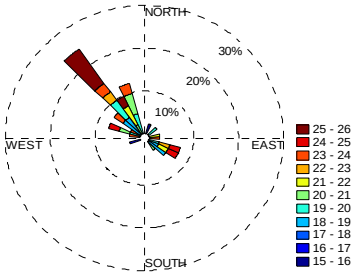
NORTH
30%
20%
10%
WEST
EAST
SOUTH
25 - 26
24 - 25
23 - 24
22 - 23
21 - 22
20 - 21
19 - 20
18 - 19
17 - 18
16 - 17
15 - 16

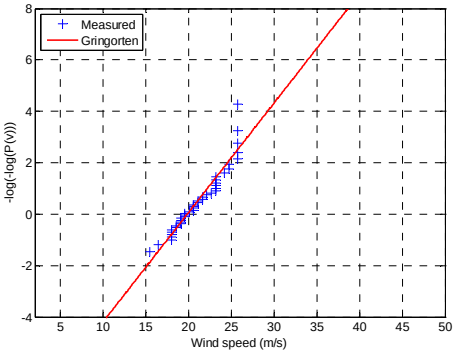
Measured
Gringorten
-log(-log(P(v)))
Wind speed (m/s)

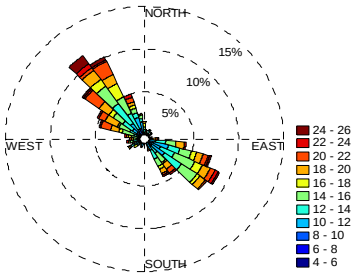
NORTH
15%
10%
5%
WEST
EAST
SOUTH
24 - 26
22 - 24
20 - 22
18 - 20
16 - 18
14 - 16
12 - 14
10 - 12
8 - 10
6 - 8
4 - 6

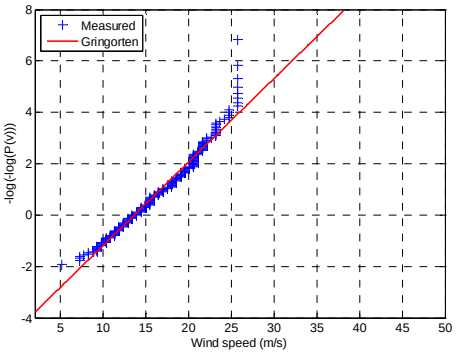
Measured
Gringorten
-log(-log(P(v)))
Wind speed (m/s)

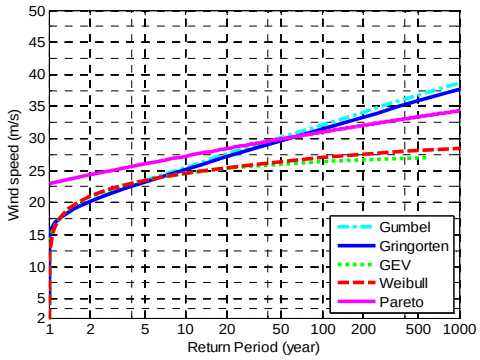
Wind speed (m/s)
Return Period (year)
Gumbel
Gringorten
GEV
Weibull
Pareto

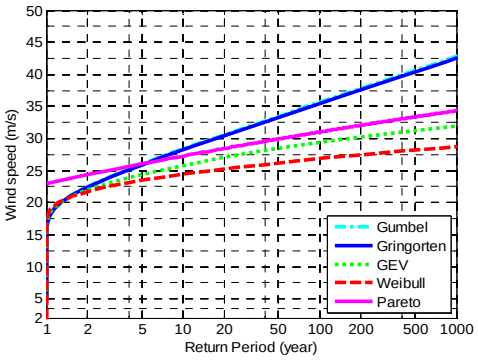
Wind speed (m/s)
Return Period (year)
Gumbel
Gringorten
GEV
Weibull
Pareto

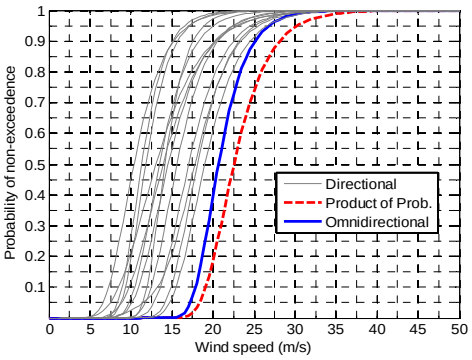
Probability of non-exceedence
Wind speed (m/s)
Directional
Product of Prob.
Omnidirectional

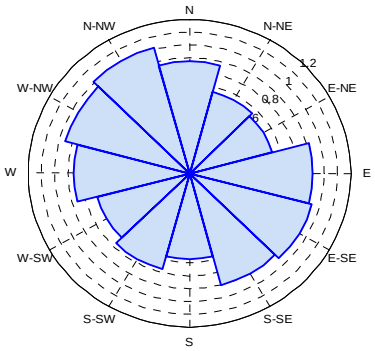
N
N-NE
E-NE
E
E-SE
S-SE
S
S-SW
W
W-NW
N-NW

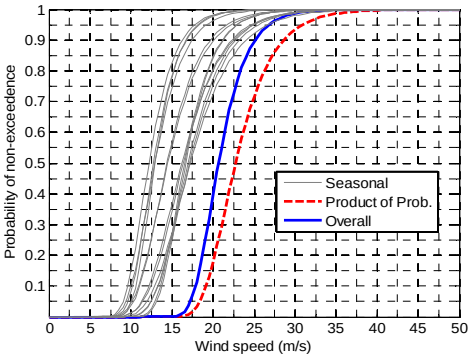
Probability of non-exceedence
Wind speed (m/s)
Seasonal
Product of Prob.
Overall

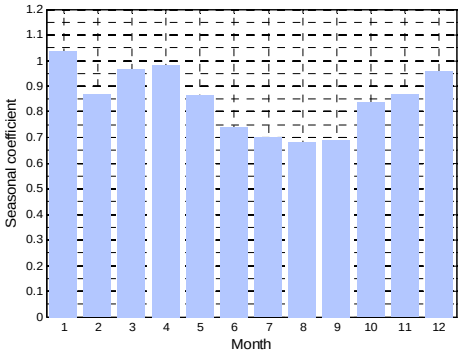
Seasonal coefficient
Month

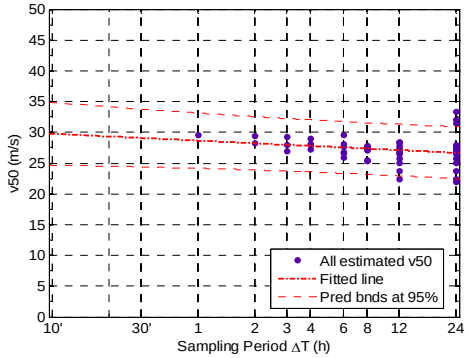
v50 (m/s)
Sampling Period ΔT (h)
All estimated v50
Fitted line
Pred bnds at 95%

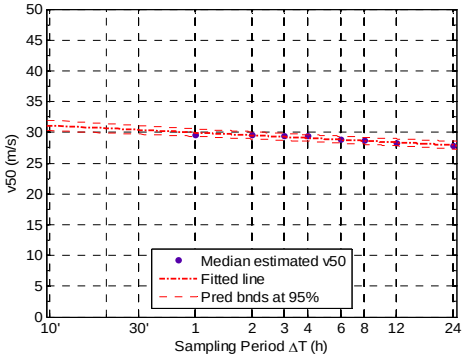
v50 (m/s)
Sampling Period ΔT (h)
Median estimated v50
Fitted line
Pred bnds at 95%

LIEG

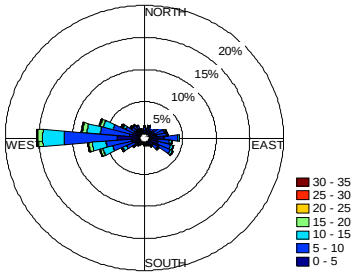
NORTH
20%
15%
10%
5%
WEST
EAST
SOUTH
30 - 35
25 - 30
20 - 25
15 - 20
10 - 15
5 - 10
0 - 5

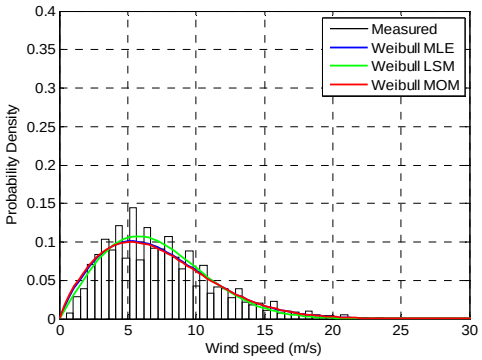
Measured
Weibull MLE
Weibull LSM
Weibull MOM
Probability Density
Wind speed (m/s)

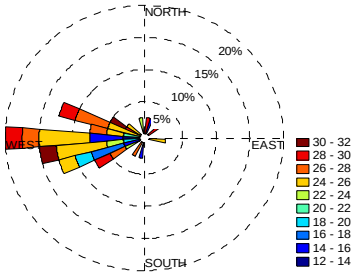
NORTH
20%
15%
10%
5%
WEST
EAST
SOUTH
30 - 32
28 - 30
26 - 28
24 - 26
22 - 24
20 - 22
18 - 20
16 - 18
14 - 16
12 - 14

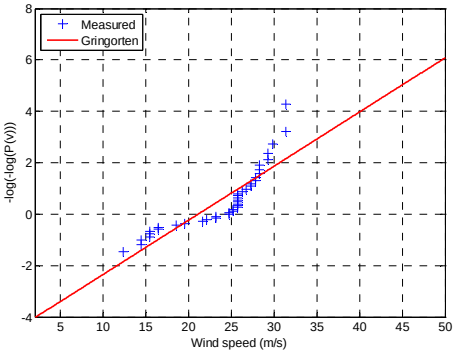
Measured
Gringorten
-log(-log(P(v)))
Wind speed (m/s)

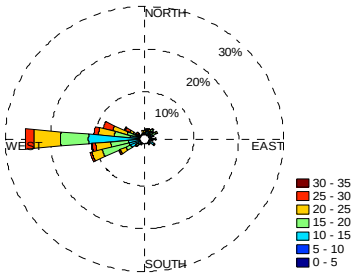
NORTH
30%
20%
10%
WEST
EAST
SOUTH
30 - 35
25 - 30
20 - 25
15 - 20
10 - 15
5 - 10
0 - 5

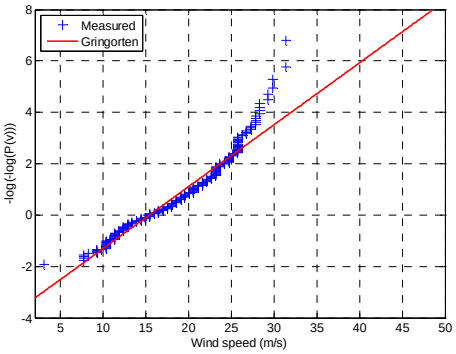
Measured
Gringorten
-log(-log(P(v)))
Wind speed (m/s)

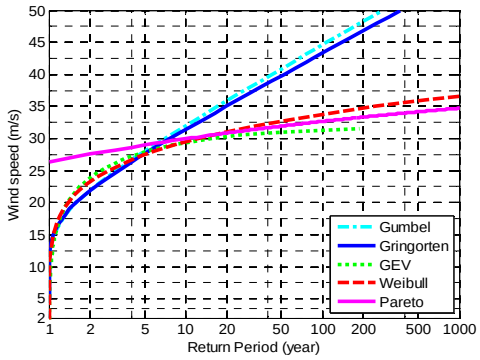
Wind speed (m/s)
Return Period (year)
Gumbel
Gringorten
GEV
Weibull
Pareto

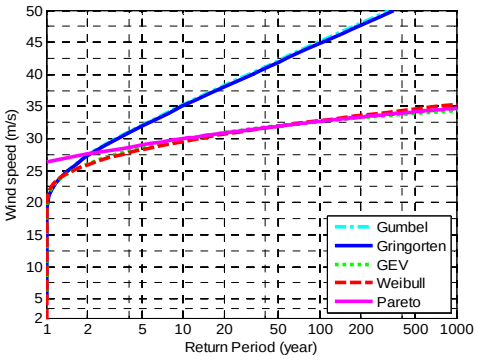
Wind speed (m/s)
Return Period (year)
Gumbel
Gringorten
GEV
Weibull
Pareto

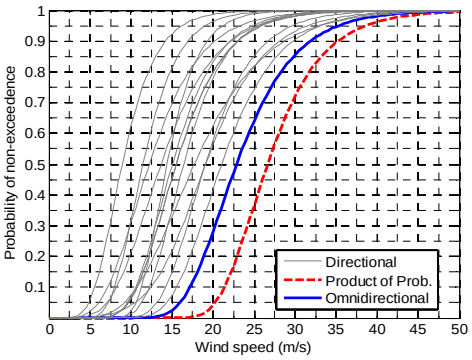
Probability of non-exceedence
Wind speed (m/s)
Directional
Product of Prob.
Omnidirectional

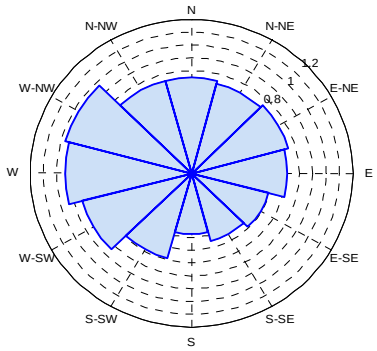
N
N-NE
E-NE
E
E-SE
S-SE
S
S-SW
W
W-NW
N-NW

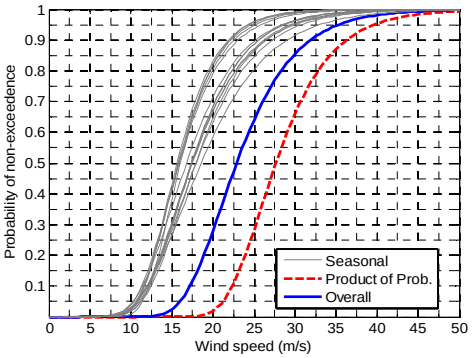
Probability of non-exceedence
Wind speed (m/s)
Seasonal
Product of Prob.
Overall

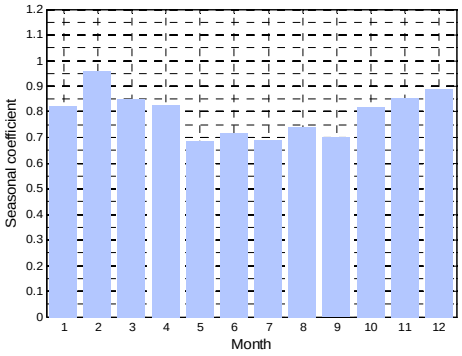
Seasonal coefficient
Month

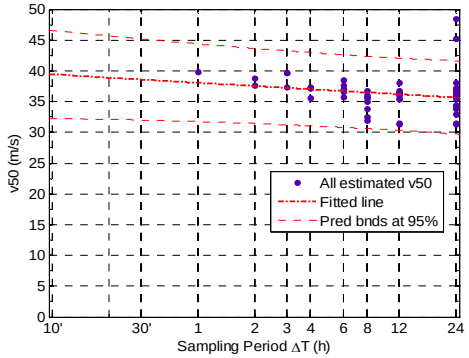
v50 (m/s)
Sampling Period ΔT (h)
All estimated v50
Fitted line
Pred bnds at 95%

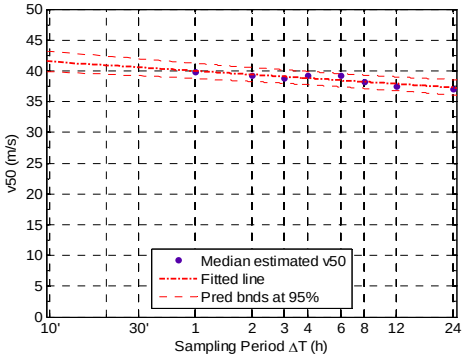
v50 (m/s)
Sampling Period ΔT (h)
Median estimated v50
Fitted line
Pred bnds at 95%

LIEH

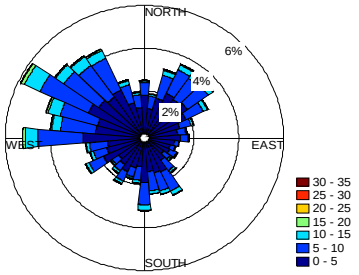
NORTH
6%
4%
2%
WEST
EAST
SOUTH
30 - 35
25 - 30
20 - 25
15 - 20
10 - 15
5 - 10
0 - 5

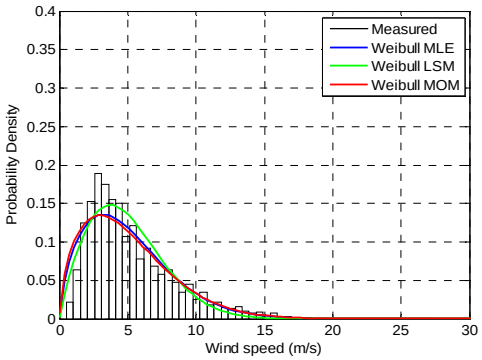
Measured
Weibull MLE
Weibull LSM
Weibull MOM
Probability Density
Wind speed (m/s)

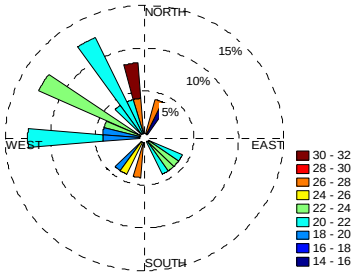
NORTH
15%
10%
5%
WEST
EAST
SOUTH
30 - 32
28 - 30
26 - 28
24 - 26
22 - 24
20 - 22
18 - 20
16 - 18
14 - 16

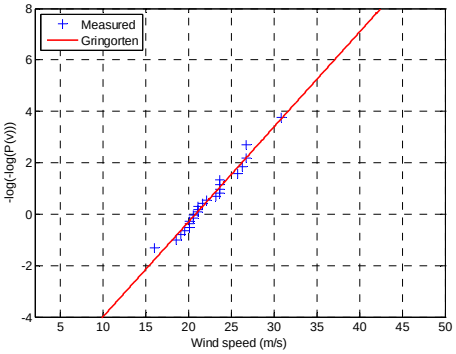
Measured
Gringorten
-log(-log(P(v)))
Wind speed (m/s)

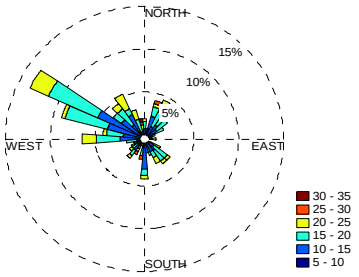
NORTH
15%
10%
5%
WEST
EAST
SOUTH
30 - 35
25 - 30
20 - 25
15 - 20
10 - 15
5 - 10

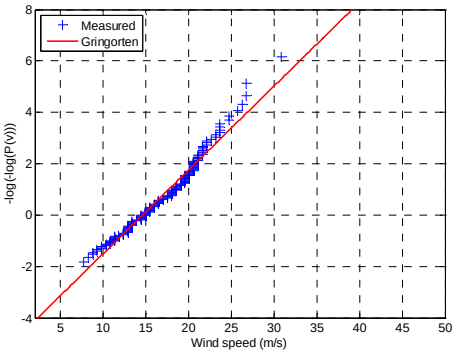
Measured
Gringorten
-log(-log(P(v)))
Wind speed (m/s)

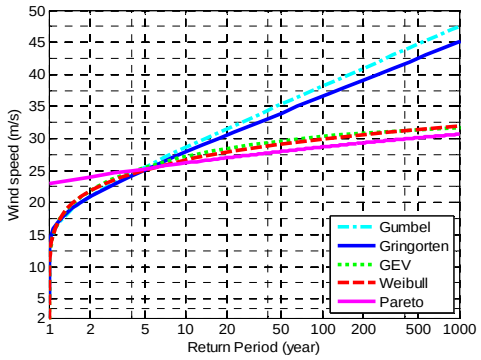
Wind speed (m/s)
Return Period (year)
Gumbel
Gringorten
GEV
Weibull
Pareto

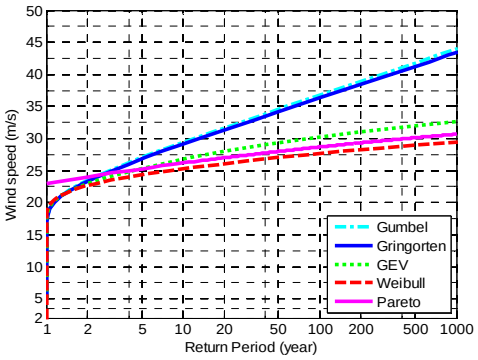
Wind speed (m/s)
Return Period (year)
Gumbel
Gringorten
GEV
Weibull
Pareto

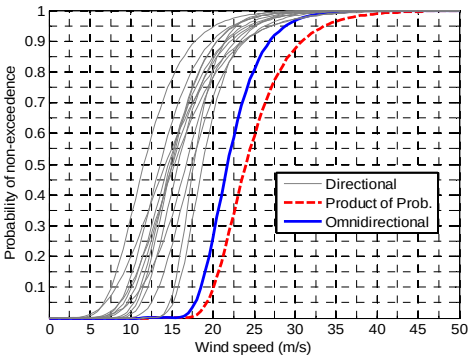
Probability of non-exceedence
Wind speed (m/s)
Directional
Product of Prob.
Omnidirectional

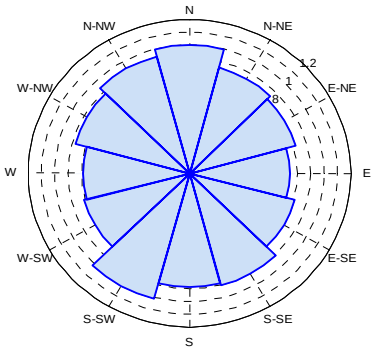
N
N-NE
E-NE
E
E-SE
S-SE
S
S-SW
W
W-NW
N-NW

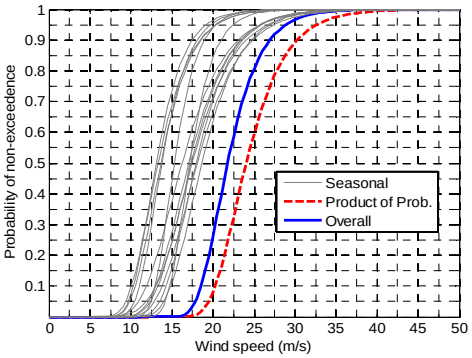
Probability of non-exceedence
Wind speed (m/s)
Seasonal
Product of Prob.
Overall

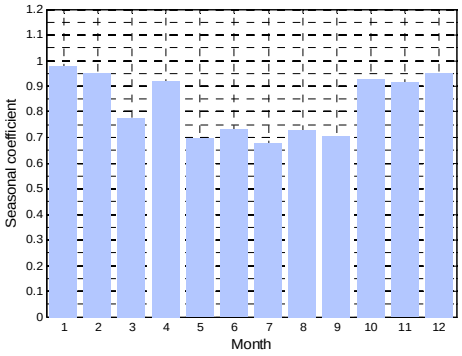
Seasonal coefficient
Month

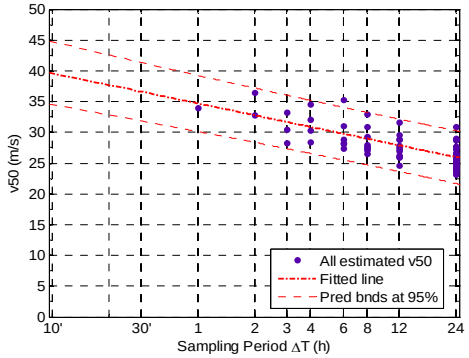
v50 (m/s)
Sampling Period ΔT (h)
All estimated v50
Fitted line
Pred bnds at 95%

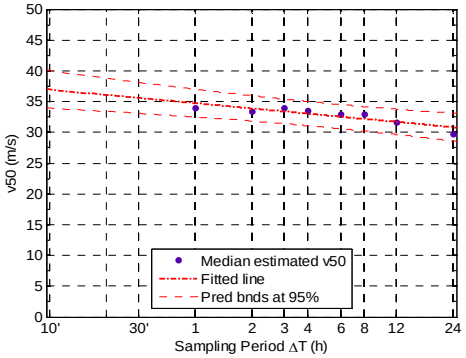
v50 (m/s)
Sampling Period ΔT (h)
Median estimated v50
Fitted line
Pred bnds at 95%

LIEL

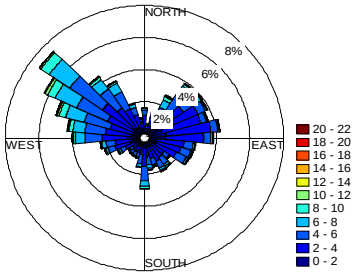
NORTH
8%
6%
4%
2%
WEST
EAST
SOUTH
20 - 22
18 - 20
16 - 18
14 - 16
12 - 14
10 - 12
8 - 10
6 - 8
4 - 6
2 - 4
0 - 2

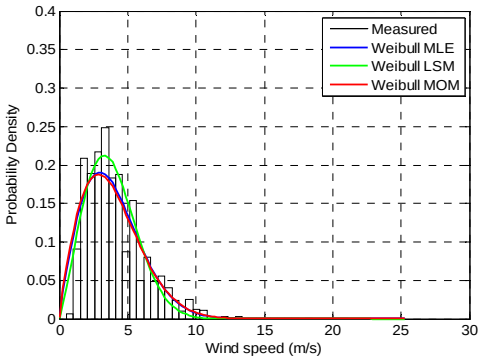
Measured
Weibull MLE
Weibull LSM
Weibull MOM
Probability Density
Wind speed (m/s)

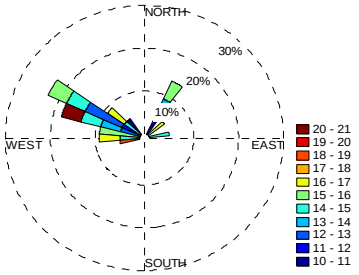
NORTH
30%
20%
10%
WEST
EAST
SOUTH
20 - 21
19 - 20
18 - 19
17 - 18
16 - 17
15 - 16
14 - 15
13 - 14
12 - 13
11 - 12
10 - 11

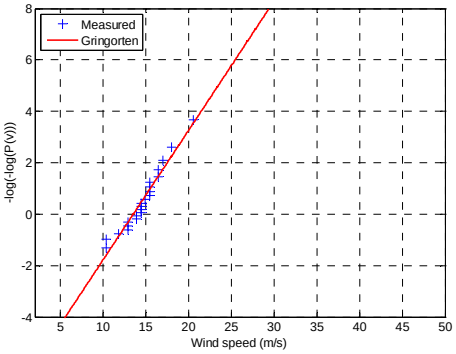
Measured
Gringorten
-log(-log(P(v)))
Wind speed (m/s)

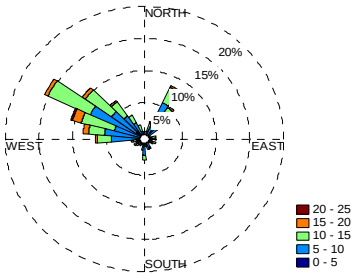
NORTH
20%
15%
10%
5%
WEST
EAST
SOUTH
20 - 25
15 - 20
10 - 15
5 - 10
0 - 5

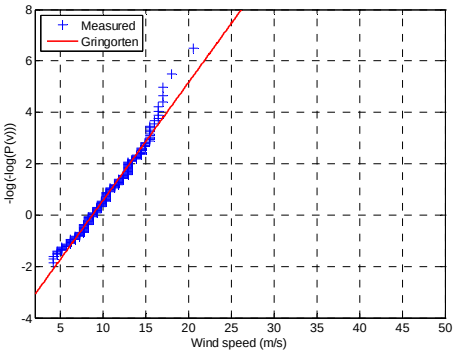
Measured
Gringorten
-log(-log(P(v)))
Wind speed (m/s)

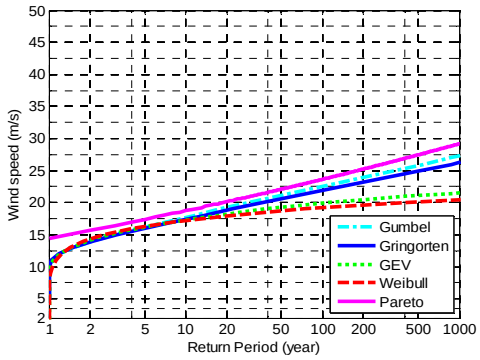
Wind speed (m/s)
Return Period (year)
Gumbel
Gringorten
GEV
Weibull
Pareto

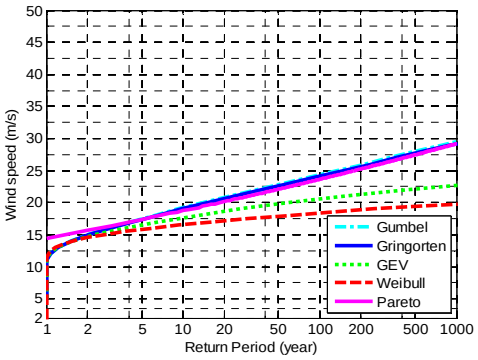
Wind speed (m/s)
Return Period (year)
Gumbel
Gringorten
GEV
Weibull
Pareto

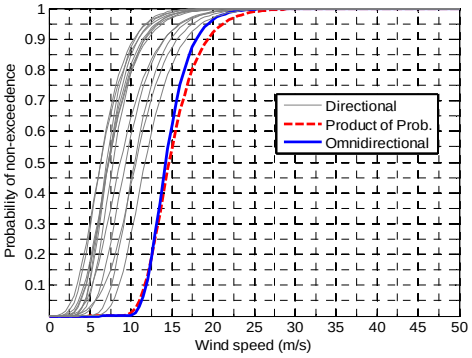
Probability of non-exceedence
Wind speed (m/s)
Directional
Product of Prob.
Omnidirectional

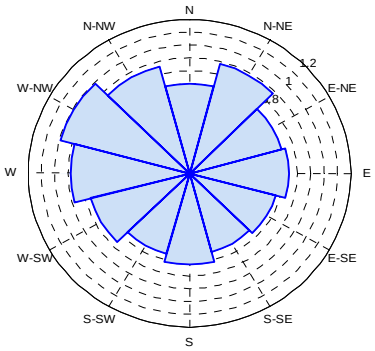
N
N-NE
E-NE
E
E-SE
S-SE
S
S-SW
W
W-NW
N-NW

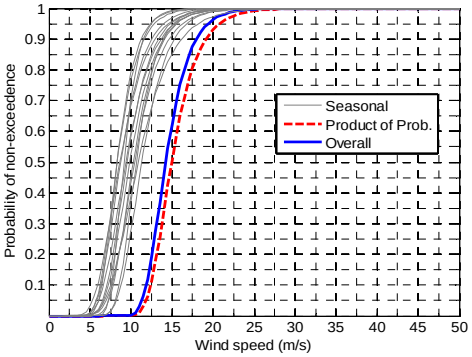
Probability of non-exceedence
Wind speed (m/s)
Seasonal
Product of Prob.
Overall

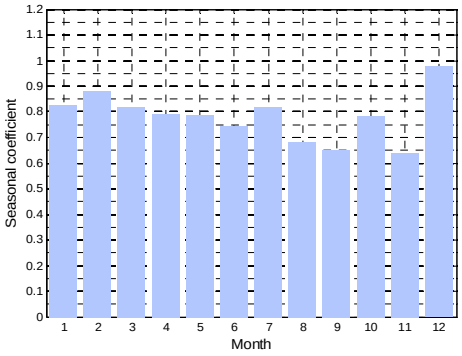
Seasonal coefficient
Month

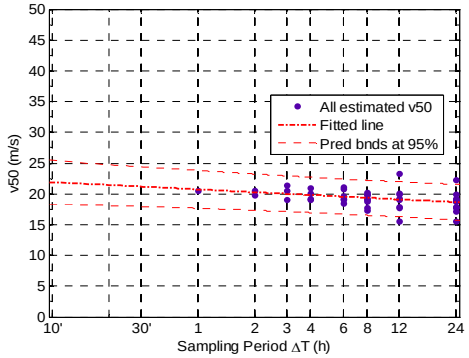
v50 (m/s)
Sampling Period ΔT (h)
All estimated v50
Fitted line
Pred bnds at 95%

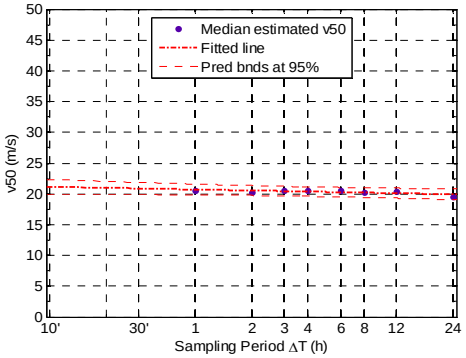
v50 (m/s)
Sampling Period ΔT (h)
Median estimated v50
Fitted line
Pred bnds at 95%

LIEN

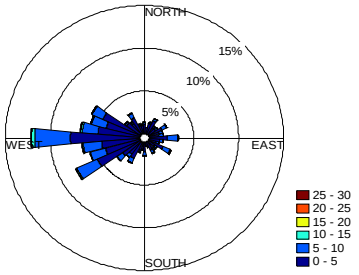
NORTH
15%
10%
5%
WEST
EAST
SOUTH
25 - 30
20 - 25
15 - 20
10 - 15
5 - 10
0 - 5

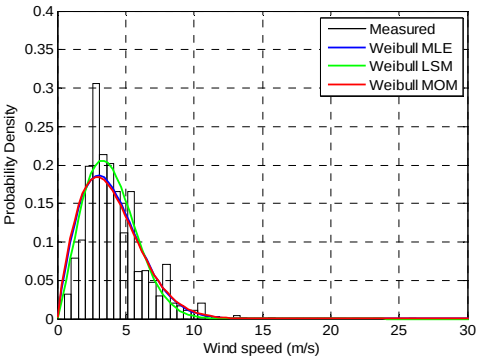
Measured
Weibull MLE
Weibull LSM
Weibull MOM
Probability Density
Wind speed (m/s)

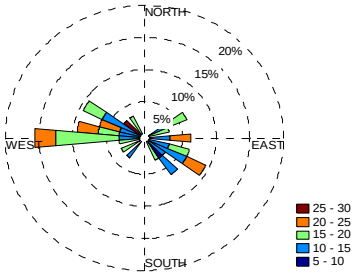
NORTH
20%
15%
10%
5%
WEST
EAST
SOUTH
25 - 30
20 - 25
15 - 20
10 - 15
5 - 10

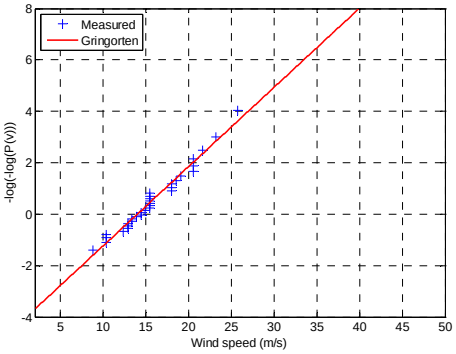
Measured
Gringorten
-log(-log(P(v)))
Wind speed (m/s)

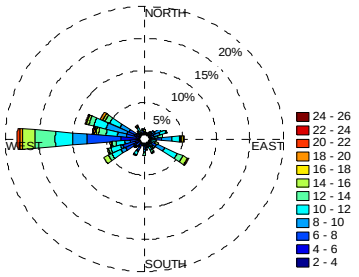
NORTH
20%
15%
10%
5%
WEST
EAST
SOUTH
24 - 26
22 - 24
20 - 22
18 - 20
16 - 18
14 - 16
12 - 14
10 - 12
8 - 10
6 - 8
4 - 6
2 - 4

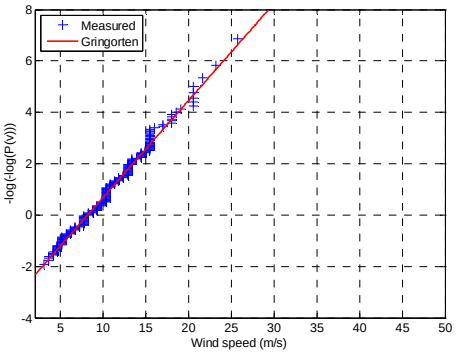
Measured
Gringorten
-log(-log(P(v)))
Wind speed (m/s)

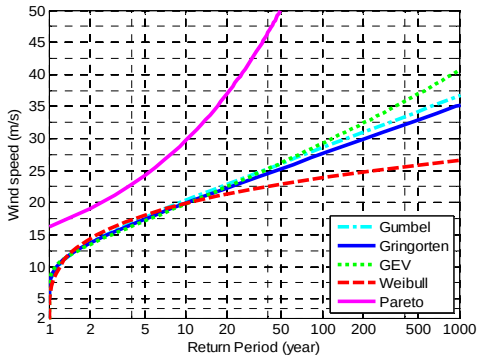
Wind speed (m/s)
Return Period (year)
Gumbel
Gringorten
GEV
Weibull
Pareto

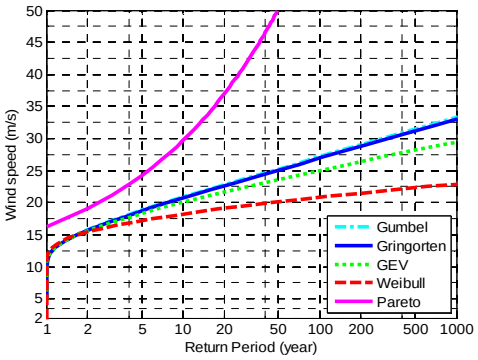
Wind speed (m/s)
Return Period (year)
Gumbel
Gringorten
GEV
Weibull
Pareto

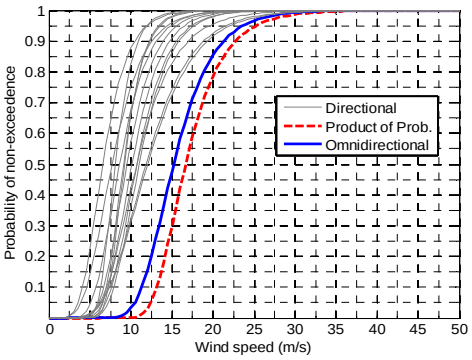
Probability of non-exceedence
Wind speed (m/s)
Directional
Product of Prob.
Omnidirectional

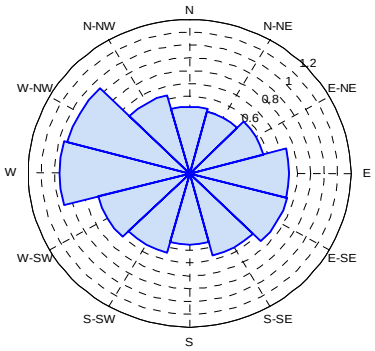
N
N-NE
E-NE
E
E-SE
S-SE
S
S-SW
W
W-NW
N-NW

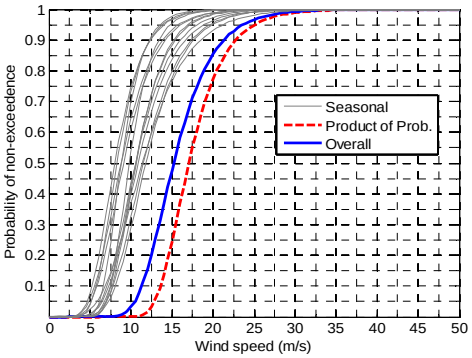
Probability of non-exceedence
Wind speed (m/s)
Seasonal
Product of Prob.
Overall

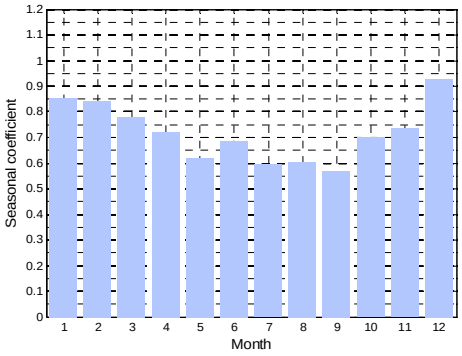
Seasonal coefficient
Month

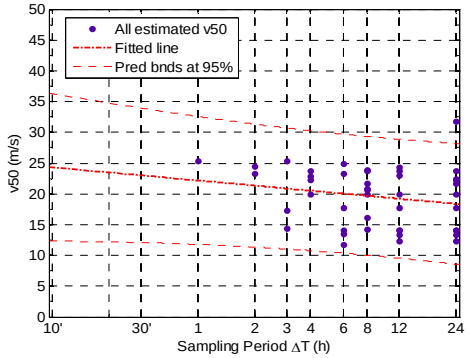
v50 (m/s)
Sampling Period ΔT (h)
All estimated v50
Fitted line
Pred bnds at 95%

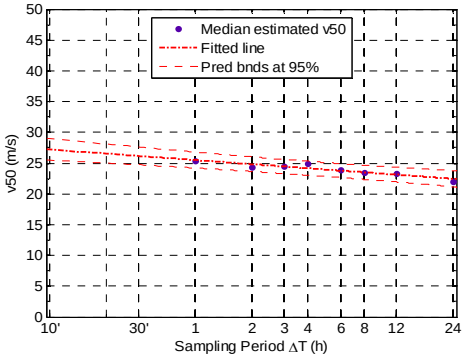
v50 (m/s)
Sampling Period ΔT (h)
Median estimated v50
Fitted line
Pred bnds at 95%

LIEO

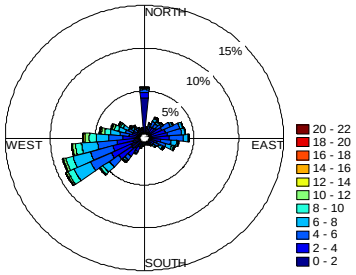
NORTH
15%
10%
5%
WEST
EAST
SOUTH
20 - 22
18 - 20
16 - 18
14 - 16
12 - 14
10 - 12
8 - 10
6 - 8
4 - 6
2 - 4
0 - 2

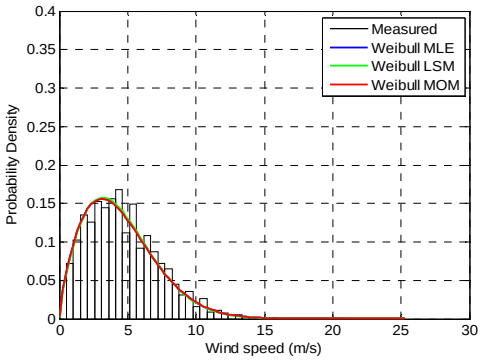
Measured
Weibull MLE
Weibull LSM
Weibull MOM
Probability Density
Wind speed (m/s)

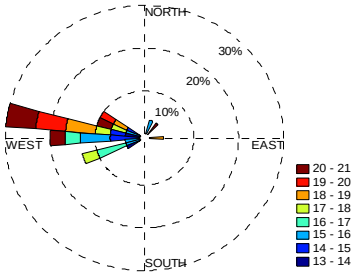
NORTH
30%
20%
10%
WEST
EAST
SOUTH
20 - 21
19 - 20
18 - 19
17 - 18
16 - 17
15 - 16
14 - 15
13 - 14

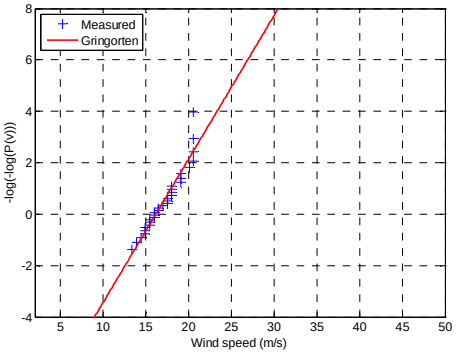
Measured
Gringorten
-log(-log(P(v)))
Wind speed (m/s)

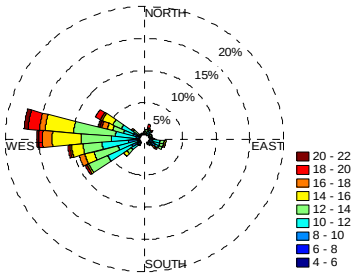
NORTH
20%
15%
10%
5%
WEST
EAST
SOUTH
20 - 22
18 - 20
16 - 18
14 - 16
12 - 14
10 - 12
8 - 10
6 - 8
4 - 6

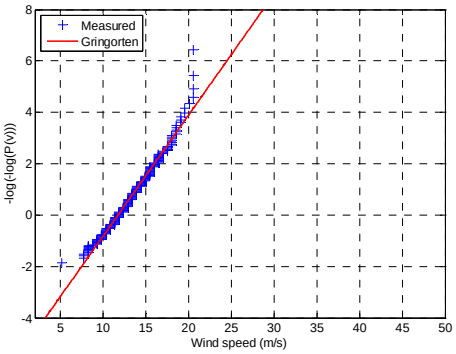
Measured
Gringorten
-log(-log(P(v)))
Wind speed (m/s)

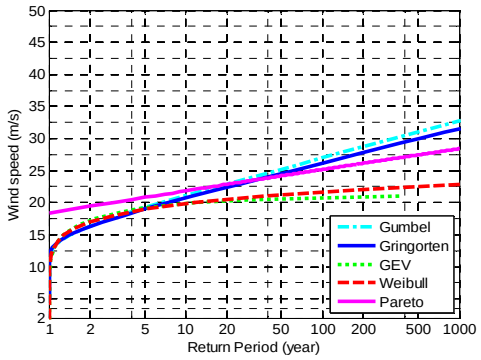
Wind speed (m/s)
Return Period (year)
Gumbel
Gringorten
GEV
Weibull
Pareto

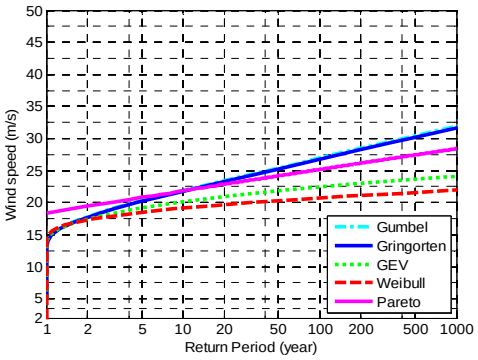
Wind speed (m/s)
Return Period (year)
Gumbel
Gringorten
GEV
Weibull
Pareto

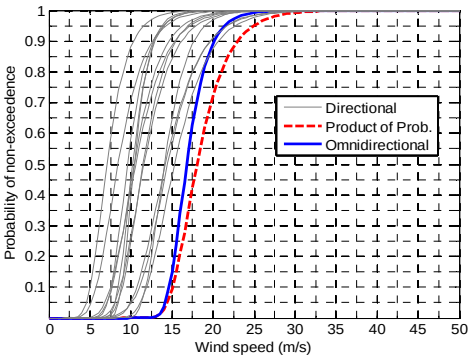
Probability of non-exceedence
Wind speed (m/s)
Directional
Product of Prob.
Omnidirectional

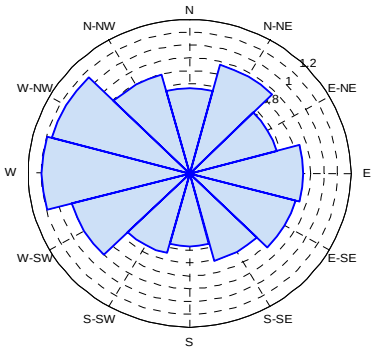
N
N-NE
E-NE
E
E-SE
S-SE
S
S-SW
W
W-NW
N-NW

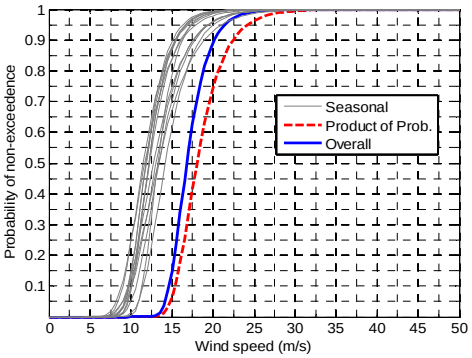
Probability of non-exceedence
Wind speed (m/s)
Seasonal
Product of Prob.
Overall

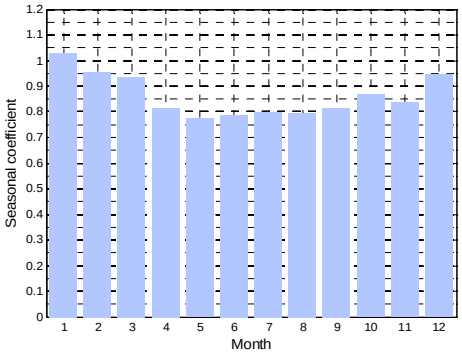
Seasonal coefficient
Month

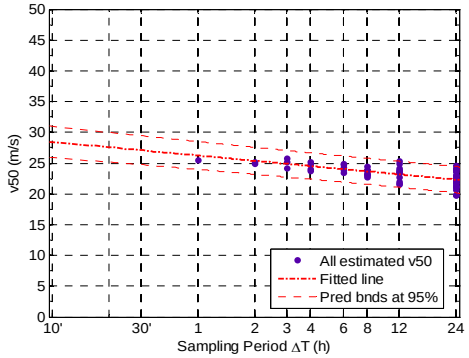
v50 (m/s)
Sampling Period ΔT (h)
All estimated v50
Fitted line
Pred bnds at 95%

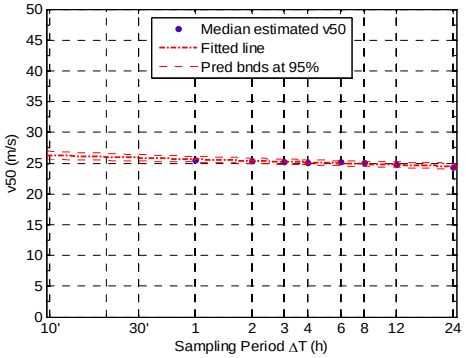
v50 (m/s)
Sampling Period ΔT (h)
Median estimated v50
Fitted line
Pred bnds at 95%

LIEP

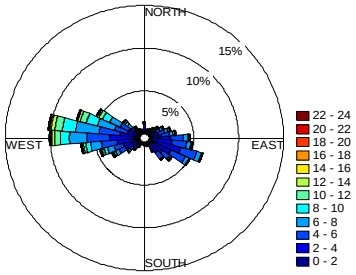
NORTH
15%
10%
5%
WEST
EAST
SOUTH
22 - 24
20 - 22
18 - 20
16 - 18
14 - 16
12 - 14
10 - 12
8 - 10
6 - 8
4 - 6
2 - 4
0 - 2

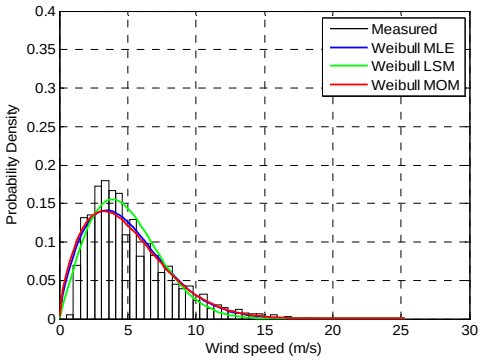
Measured
Weibull MLE
Weibull LSM
Weibull MOM
Probability Density
Wind speed (m/s)

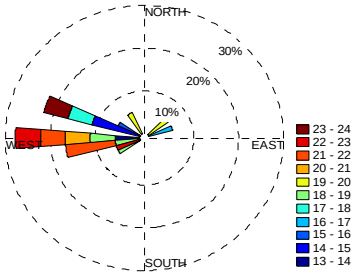
NORTH
30%
20%
10%
WEST
EAST
SOUTH
23 - 24
22 - 23
21 - 22
20 - 21
19 - 20
18 - 19
17 - 18
16 - 17
15 - 16
14 - 15
13 - 14

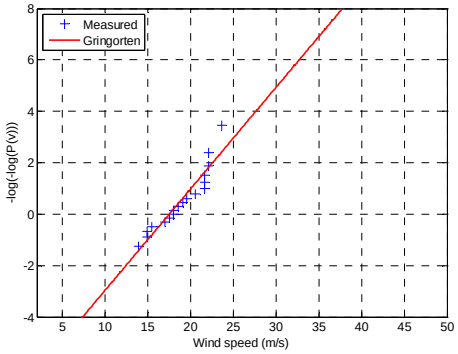
Measured
Gringorten
-log(-log(P(v)))
Wind speed (m/s)

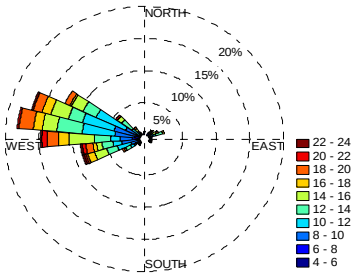
NORTH
20%
15%
10%
5%
WEST
EAST
SOUTH
22 - 24
20 - 22
18 - 20
16 - 18
14 - 16
12 - 14
10 - 12
8 - 10
6 - 8
4 - 6

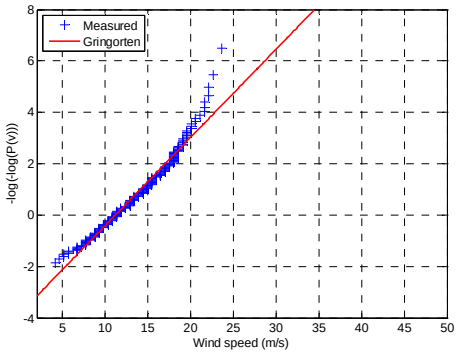
Measured
Gringorten
-log(-log(P(v)))
Wind speed (m/s)

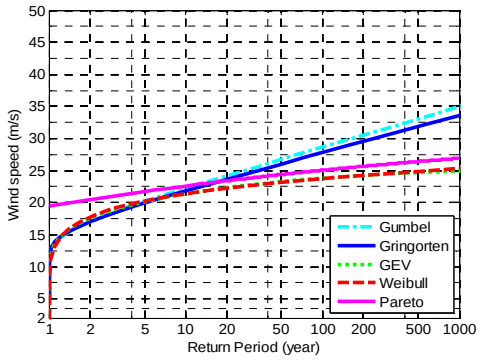
Wind speed (m/s)
Return Period (year)
Gumbel
Gringorten
GEV
Weibull
Pareto

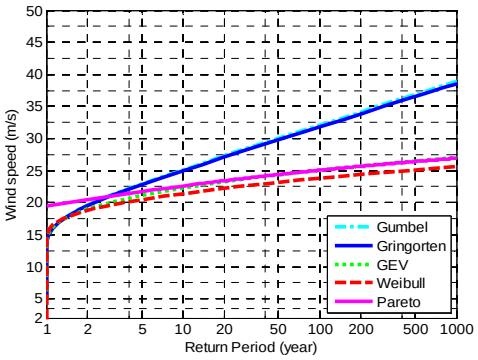
Wind speed (m/s)
Return Period (year)
Gumbel
Gringorten
GEV
Weibull
Pareto

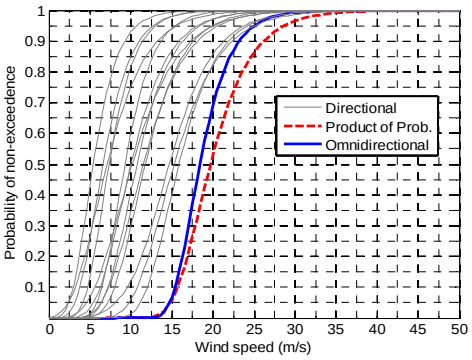
Probability of non-exceedence
Wind speed (m/s)
Directional
Product of Prob.
Omnidirectional

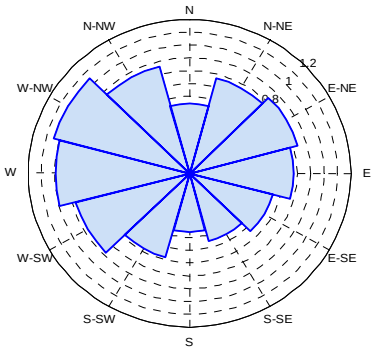
N
N-NE
E-NE
E
E-SE
S-SE
S
S-SW
W
W-NW
N-NW

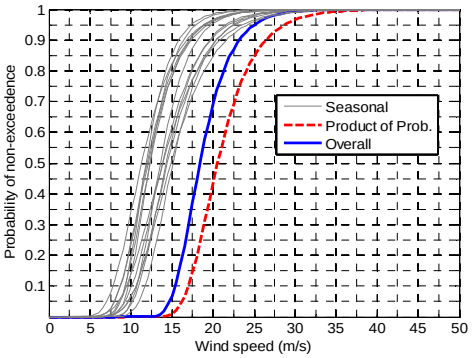
Probability of non-exceedence
Wind speed (m/s)
Seasonal
Product of Prob.
Overall

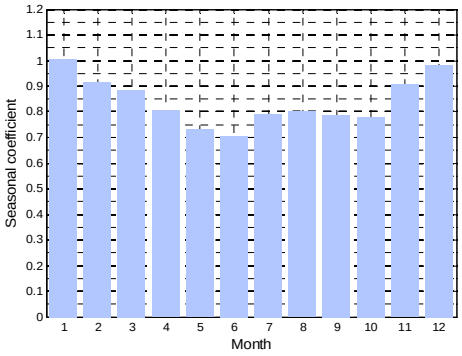
Seasonal coefficient
Month

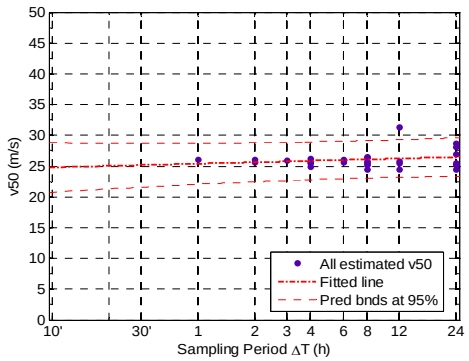
v50 (m/s)
Sampling Period ΔT (h)
All estimated v50
Fitted line
Pred bnds at 95%

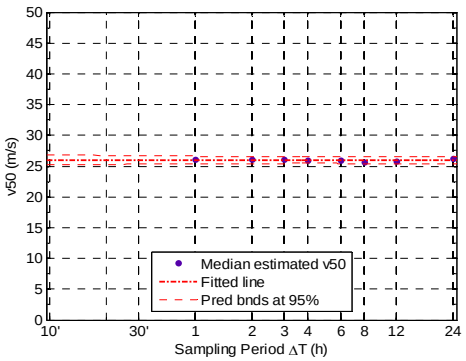
v50 (m/s)
Sampling Period ΔT (h)
Median estimated v50
Fitted line
Pred bnds at 95%

LIEZ

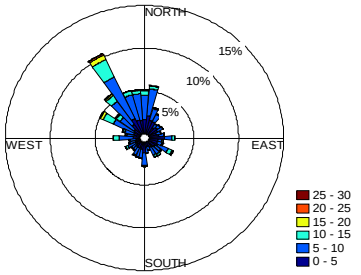
NORTH
15%
10%
5%
WEST
EAST
SOUTH
25 - 30
20 - 25
15 - 20
10 - 15
5 - 10
0 - 5

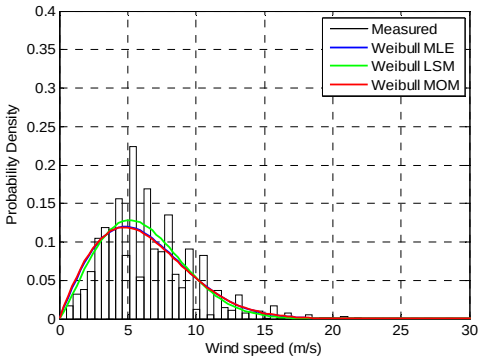
Measured
Weibull MLE
Weibull LSM
Weibull MOM
Probability Density
Wind speed (m/s)

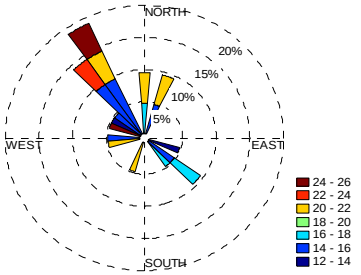
NORTH
20%
15%
10%
5%
WEST
EAST
SOUTH
24 - 26
22 - 24
20 - 22
18 - 20
16 - 18
14 - 16
12 - 14

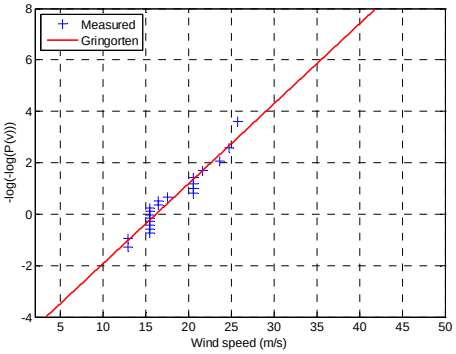
Measured
Gringorten
-log(-log(P(v)))
Wind speed (m/s)

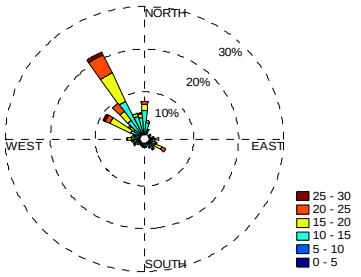
NORTH
30%
20%
10%
WEST
EAST
SOUTH
25 - 30
20 - 25
15 - 20
10 - 15
5 - 10
0 - 5

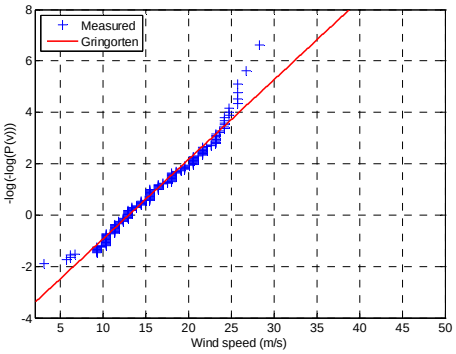
Measured
Gringorten
-log(-log(P(v)))
Wind speed (m/s)

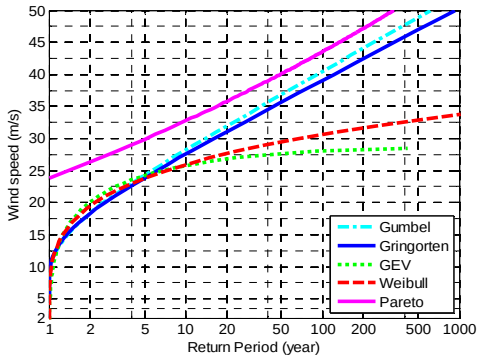
Wind speed (m/s)
Return Period (year)
Gumbel
Gringorten
GEV
Weibull
Pareto

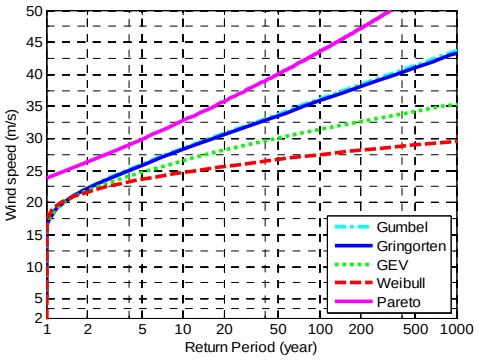
Wind speed (m/s)
Return Period (year)
Gumbel
Gringorten
GEV
Weibull
Pareto

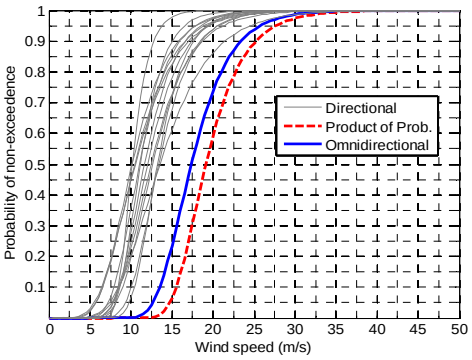
Probability of non-exceedence
Wind speed (m/s)
Directional
Product of Prob.
Omnidirectional

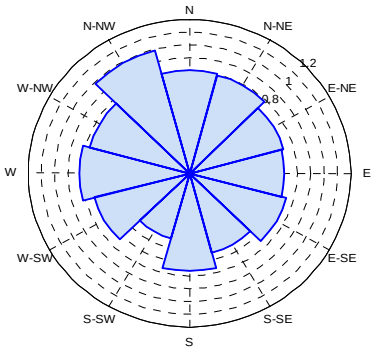
N
N-NE
E-NE
E
E-SE
S-SE
S
S-SW
W
W-NW
N-NW

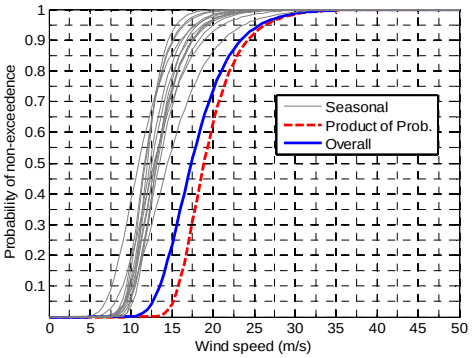
Probability of non-exceedence
Wind speed (m/s)
Seasonal
Product of Prob.
Overall

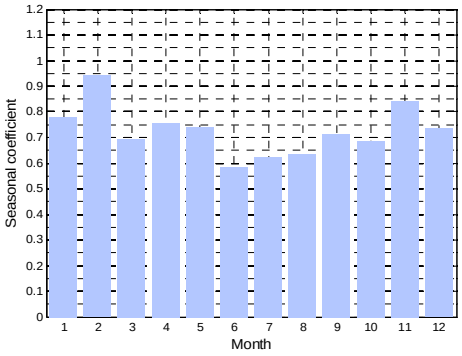
Seasonal coefficient
Month

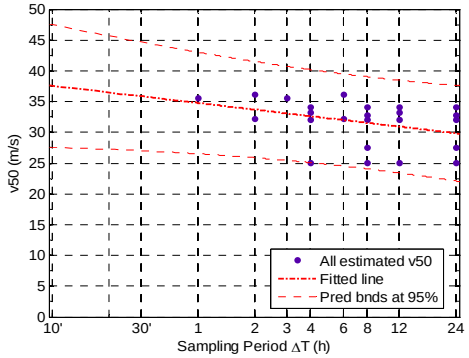
v50 (m/s)
Sampling Period ΔT (h)
All estimated v50
Fitted line
Pred bnds at 95%

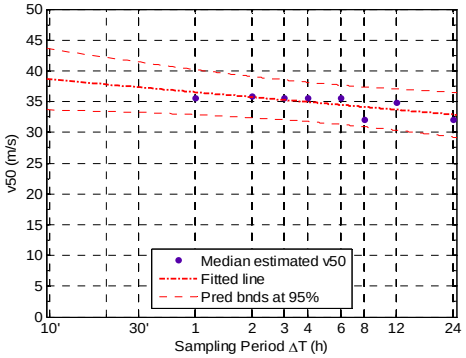
v50 (m/s)
Sampling Period ΔT (h)
Median estimated v50
Fitted line
Pred bnds at 95%

LIMC

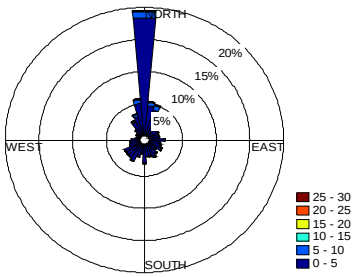
NORTH
20%
15%
10%
5%
WEST
EAST
SOUTH
25 - 30
20 - 25
15 - 20
10 - 15
5 - 10
0 - 5

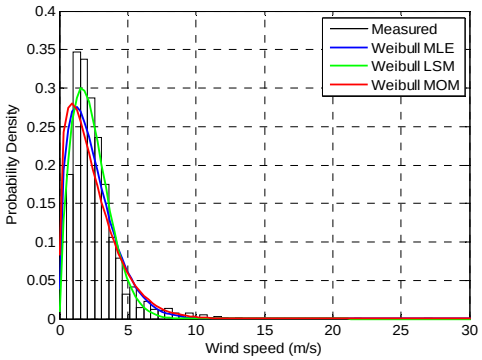
Measured
Weibull MLE
Weibull LSM
Weibull MOM
Probability Density
Wind speed (m/s)

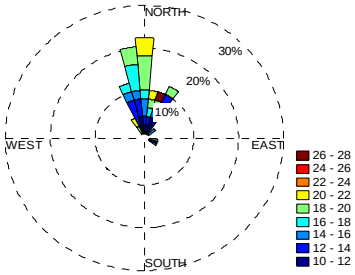
NORTH
30%
20%
10%
WEST
EAST
SOUTH
26 - 28
24 - 26
22 - 24
20 - 22
18 - 20
16 - 18
14 - 16
12 - 14
10 - 12

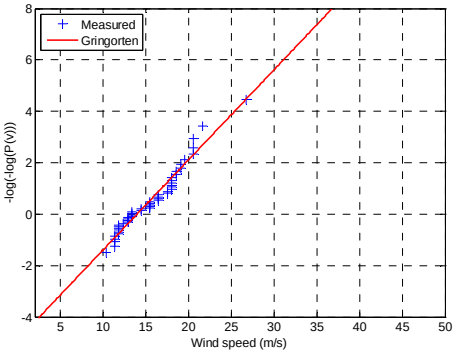
Measured
Gringorten
-log(-log(P(v)))
Wind speed (m/s)

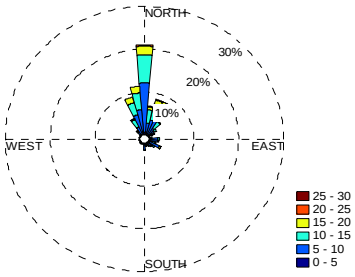
NORTH
30%
20%
10%
WEST
EAST
SOUTH
25 - 30
20 - 25
15 - 20
10 - 15
5 - 10
0 - 5

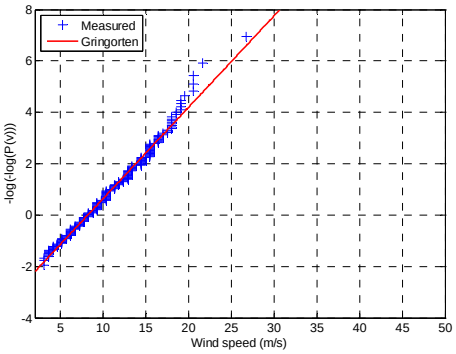
Measured
Gringorten
-log(-log(P(v)))
Wind speed (m/s)

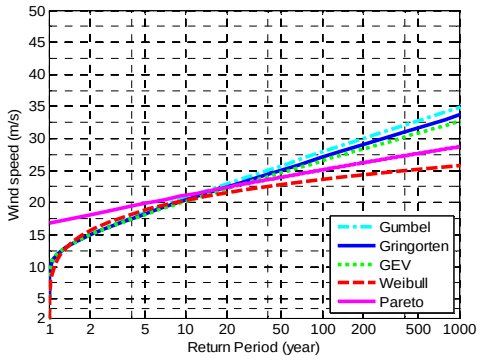
Wind speed (m/s)
Return Period (year)
Gumbel
Gringorten
GEV
Weibull
Pareto

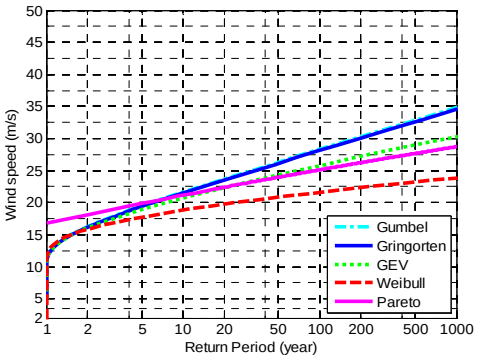
Wind speed (m/s)
Return Period (year)
Gumbel
Gringorten
GEV
Weibull
Pareto

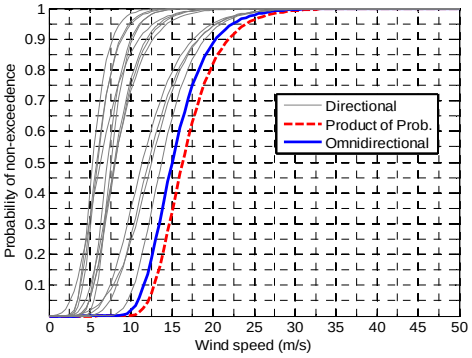
Probability of non-exceedence
Wind speed (m/s)
Directional
Product of Prob.
Omnidirectional

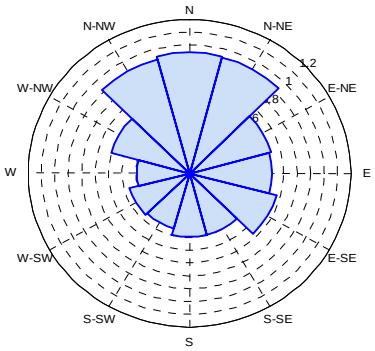
N
N-NE
E-NE
E
E-SE
S-SE
S
S-SW
W
W-NW
N-NW

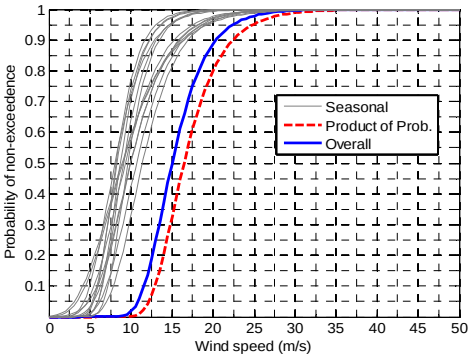
Probability of non-exceedence
Wind speed (m/s)
Seasonal
Product of Prob.
Overall

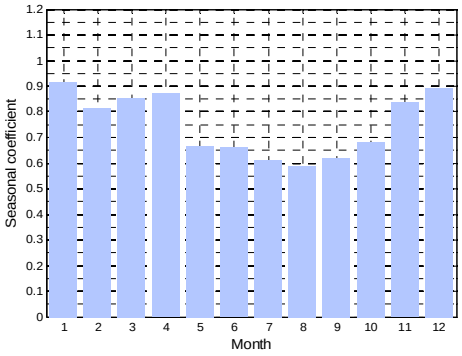
Seasonal coefficient
Month

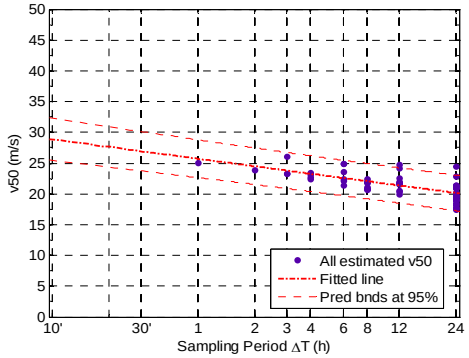
v50 (m/s)
Sampling Period ΔT (h)
All estimated v50
Fitted line
Pred bnds at 95%

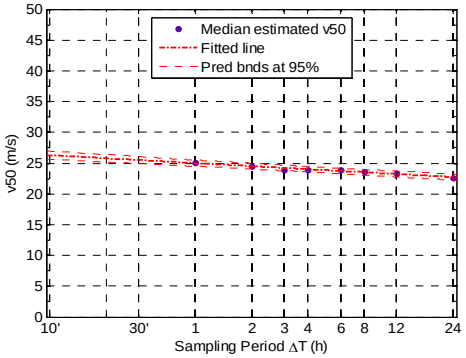
v50 (m/s)
Sampling Period ΔT (h)
Median estimated v50
Fitted line
Pred bnds at 95%

LIME

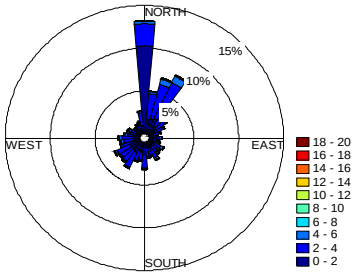
NORTH
15%
10%
5%
WEST
EAST
SOUTH
18 - 20
16 - 18
14 - 16
12 - 14
10 - 12
8 - 10
6 - 8
4 - 6
2 - 4
0 - 2

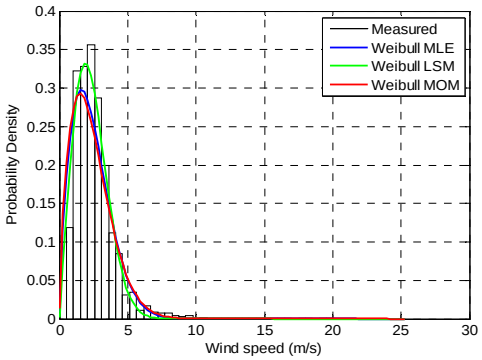
Measured
Weibull MLE
Weibull LSM
Weibull MOM
Probability Density
Wind speed (m/s)

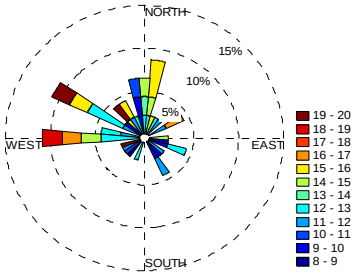
NORTH
15%
10%
5%
WEST
EAST
SOUTH
19 - 20
18 - 19
17 - 18
16 - 17
15 - 16
14 - 15
13 - 14
12 - 13
11 - 12
10 - 11
9 - 10
8 - 9

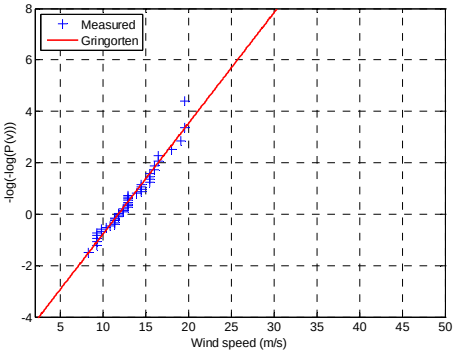
Measured
Gringorten
-log(-log(P(v)))
Wind speed (m/s)

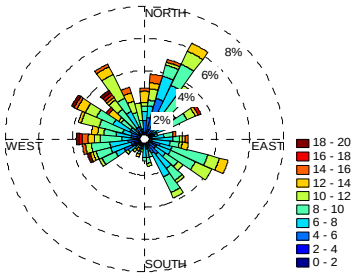
NORTH
8%
6%
4%
2%
WEST
EAST
SOUTH
18 - 20
16 - 18
14 - 16
12 - 14
10 - 12
8 - 10
6 - 8
4 - 6
2 - 4
0 - 2

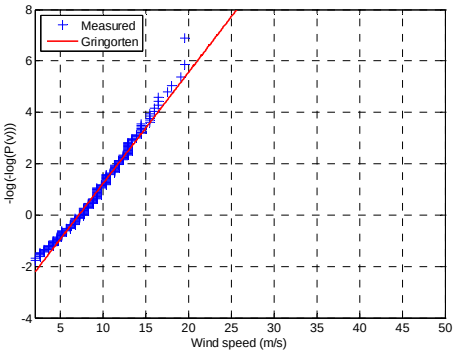
Measured
Gringorten
-log(-log(P(v)))
Wind speed (m/s)

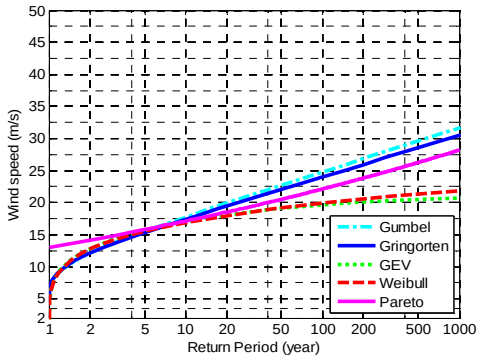
Wind speed (m/s)
Return Period (year)
Gumbel
Gringorten
GEV
Weibull
Pareto

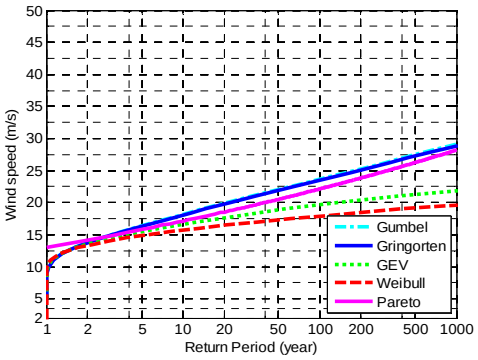
Wind speed (m/s)
Return Period (year)
Gumbel
Gringorten
GEV
Weibull
Pareto

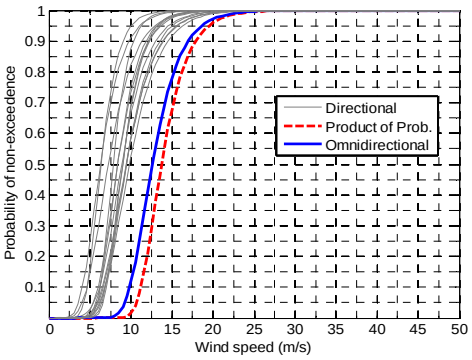
Probability of non-exceedence
Wind speed (m/s)
Directional
Product of Prob.
Omnidirectional

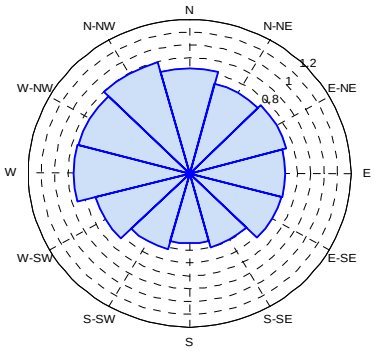
N
N-NE
E-NE
E
E-SE
S-SE
S
S-SW
W
W-NW
N-NW

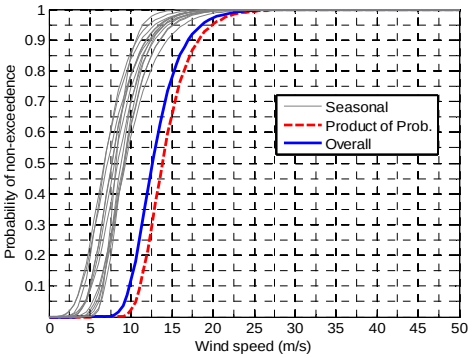
Probability of non-exceedence
Wind speed (m/s)
Seasonal
Product of Prob.
Overall

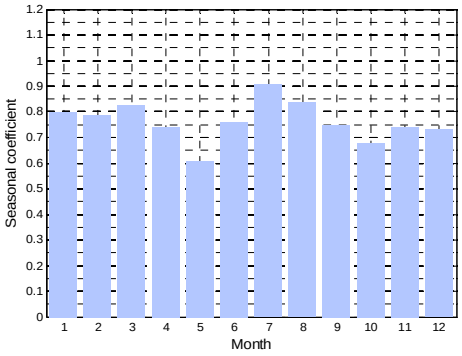
Seasonal coefficient
Month

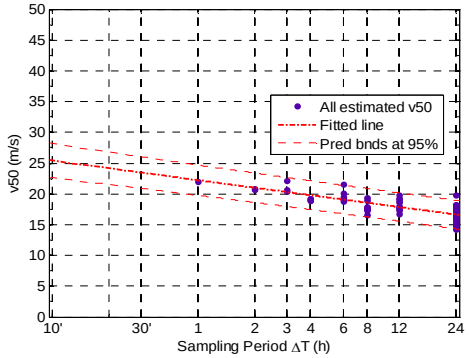
v50 (m/s)
Sampling Period ΔT (h)
All estimated v50
Fitted line
Pred bnds at 95%

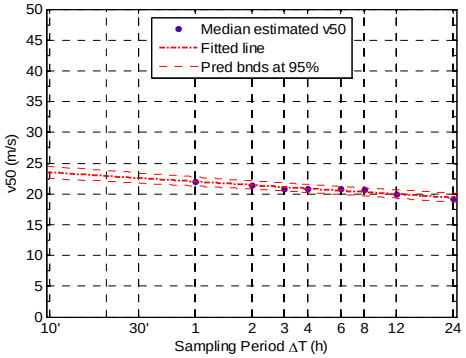
v50 (m/s)
Sampling Period ΔT (h)
Median estimated v50
Fitted line
Pred bnds at 95%

LIMF

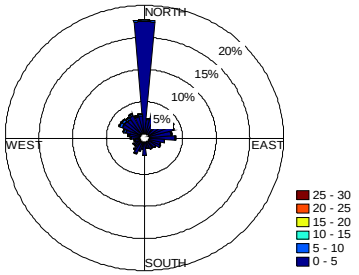
NORTH
20%
15%
10%
5%
WEST
EAST
SOUTH
25 - 30
20 - 25
15 - 20
10 - 15
5 - 10
0 - 5

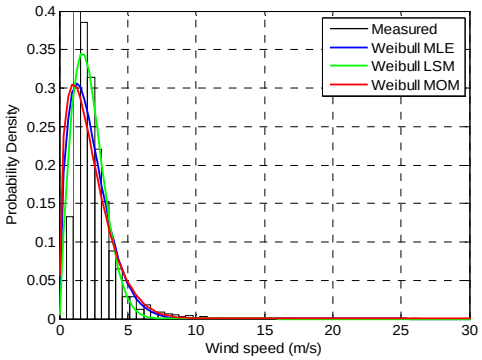
Measured
Weibull MLE
Weibull LSM
Weibull MOM
Probability Density
Wind speed (m/s)

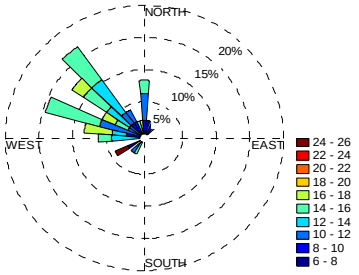
NORTH
20%
15%
10%
5%
WEST
EAST
SOUTH
24 - 26
22 - 24
20 - 22
18 - 20
16 - 18
14 - 16
12 - 14
10 - 12
8 - 10
6 - 8

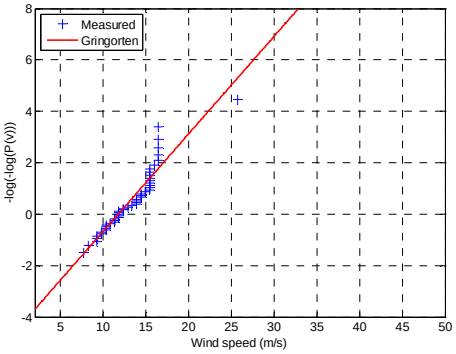
Measured
Gringorten
-log(-log(P(v)))
Wind speed (m/s)

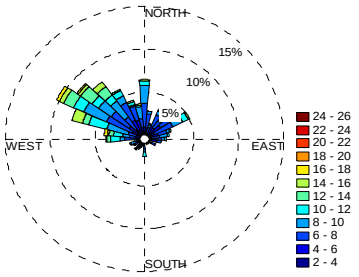
NORTH
15%
10%
5%
WEST
EAST
SOUTH
24 - 26
22 - 24
20 - 22
18 - 20
16 - 18
14 - 16
12 - 14
10 - 12
8 - 10
6 - 8
4 - 6
2 - 4

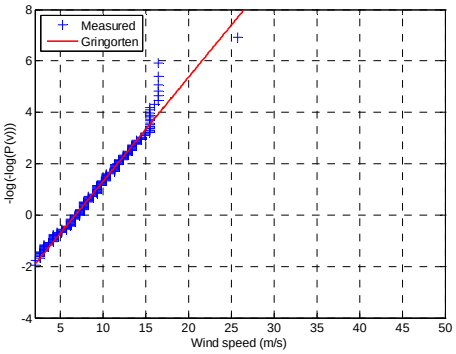
Measured
Gringorten
-log(-log(P(v)))
Wind speed (m/s)

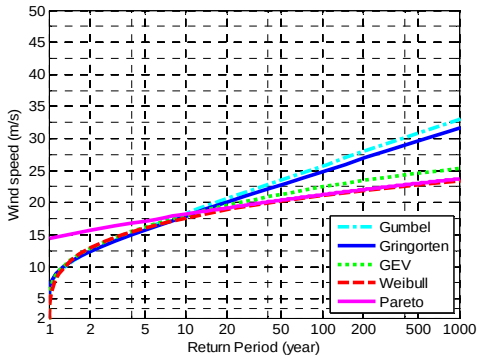
Wind speed (m/s)
Return Period (year)
Gumbel
Gringorten
GEV
Weibull
Pareto

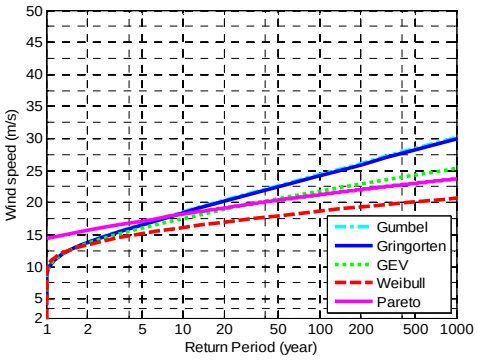
Wind speed (m/s)
Return Period (year)
Gumbel
Gringorten
GEV
Weibull
Pareto

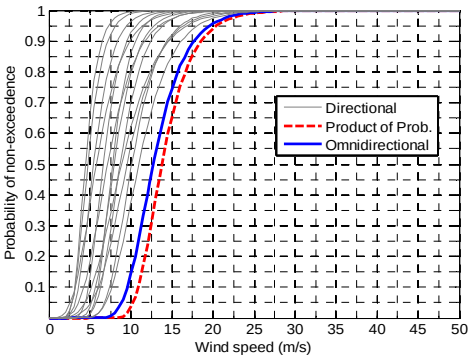
Probability of non-exceedence
Wind speed (m/s)
Directional
Product of Prob.
Omnidirectional

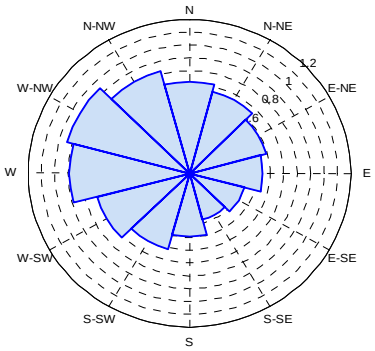
N
N-NE
E-NE
E
E-SE
S-SE
S
S-SW
W
W-NW
N-NW

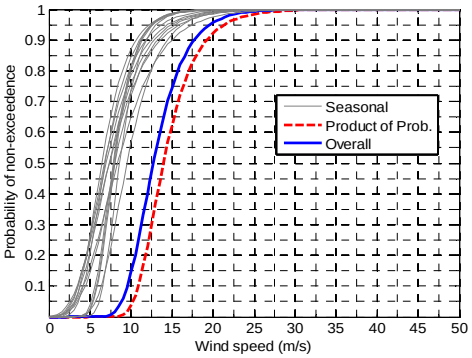
Probability of non-exceedence
Wind speed (m/s)
Seasonal
Product of Prob.
Overall

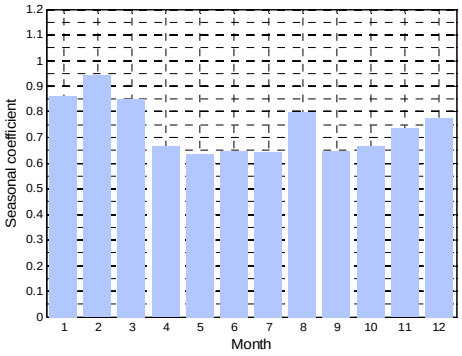
Seasonal coefficient
Month

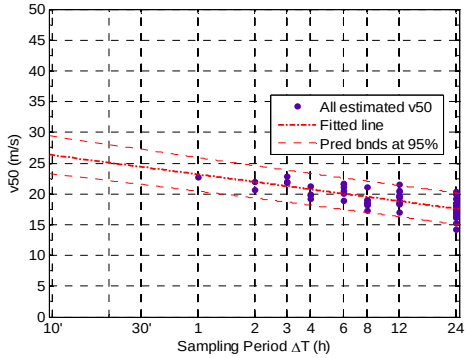
v50 (m/s)
Sampling Period ΔT (h)
All estimated v50
Fitted line
Pred bnds at 95%

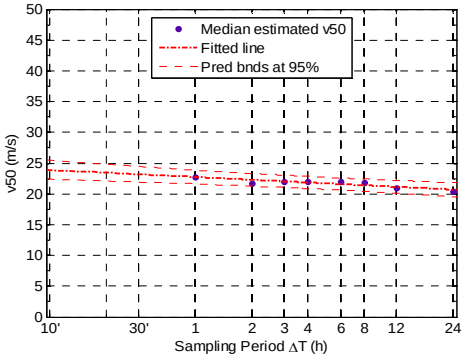
v50 (m/s)
Sampling Period ΔT (h)
Median estimated v50
Fitted line
Pred bnds at 95%

LIMG

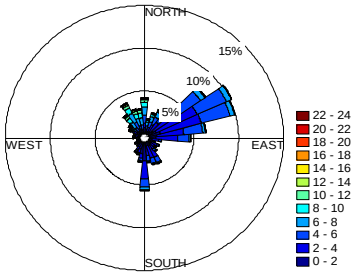
NORTH
15%
10%
5%
WEST
EAST
SOUTH
22 - 24
20 - 22
18 - 20
16 - 18
14 - 16
12 - 14
10 - 12
8 - 10
6 - 8
4 - 6
2 - 4
0 - 2

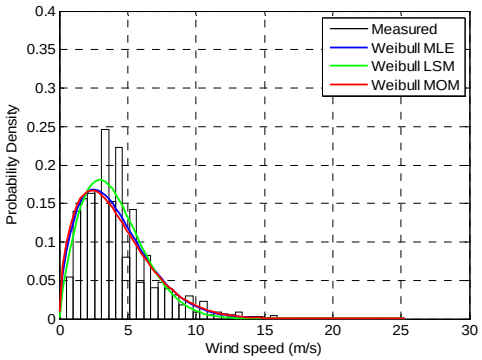
Measured
Weibull MLE
Weibull LSM
Weibull MOM
Probability Density
Wind speed (m/s)

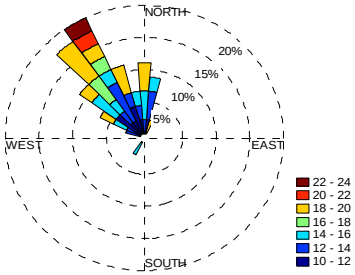
NORTH
20%
15%
10%
5%
WEST
EAST
SOUTH
22 - 24
20 - 22
18 - 20
16 - 18
14 - 16
12 - 14
10 - 12

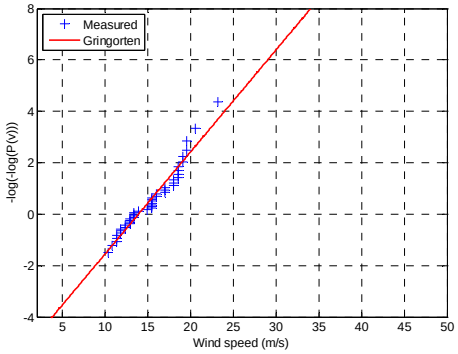
Measured
Gringorten
-log(-log(P(v)))
Wind speed (m/s)

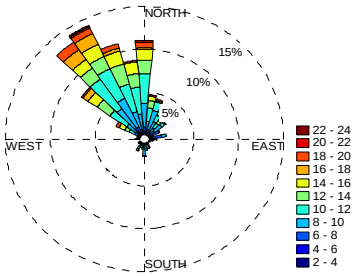
NORTH
15%
10%
5%
WEST
EAST
SOUTH
22 - 24
20 - 22
18 - 20
16 - 18
14 - 16
12 - 14
10 - 12
8 - 10
6 - 8
4 - 6
2 - 4

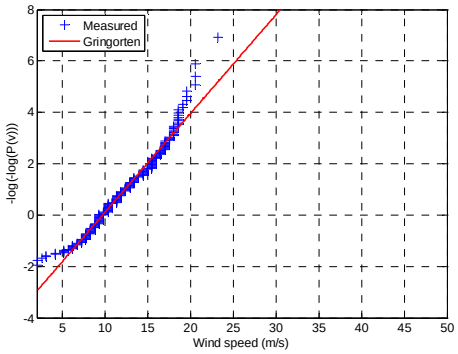
Measured
Gringorten
-log(-log(P(v)))
Wind speed (m/s)

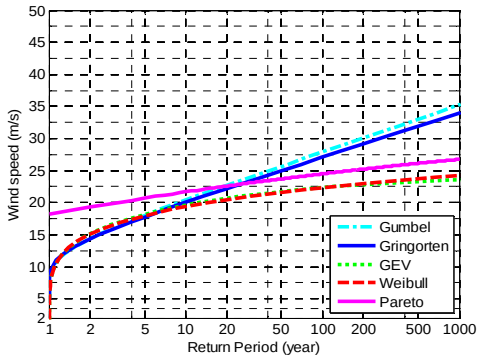
Wind speed (m/s)
Return Period (year)
Gumbel
Gringorten
GEV
Weibull
Pareto

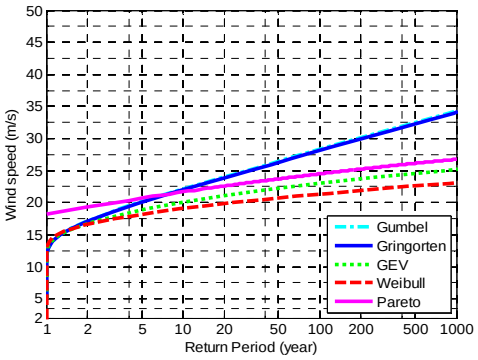
Wind speed (m/s)
Return Period (year)
Gumbel
Gringorten
GEV
Weibull
Pareto

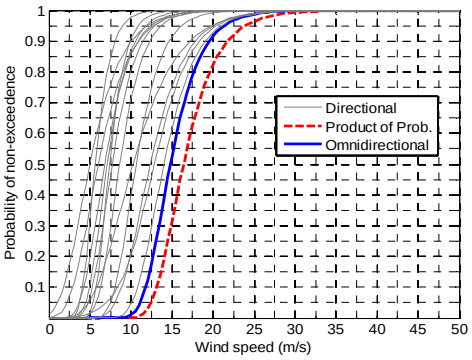
Probability of non-exceedence
Wind speed (m/s)
Directional
Product of Prob.
Omnidirectional

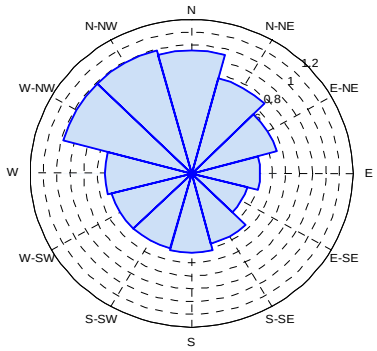
N
N-NE
E-NE
E
E-SE
S-SE
S
S-SW
W
W-NW
N-NW

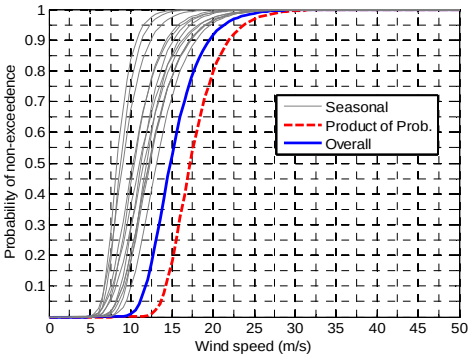
Probability of non-exceedence
Wind speed (m/s)
Seasonal
Product of Prob.
Overall

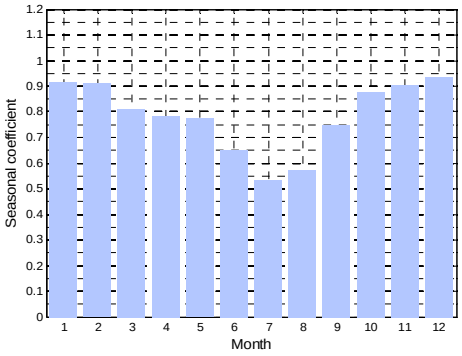
Seasonal coefficient
Month

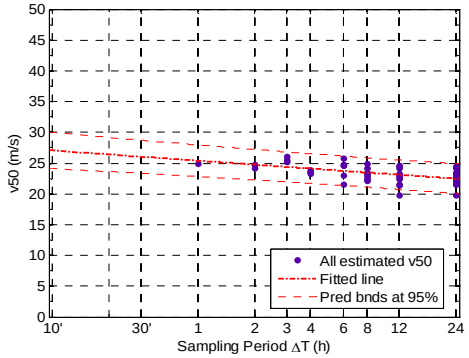
v50 (m/s)
Sampling Period ΔT (h)
All estimated v50
Fitted line
Pred bnds at 95%

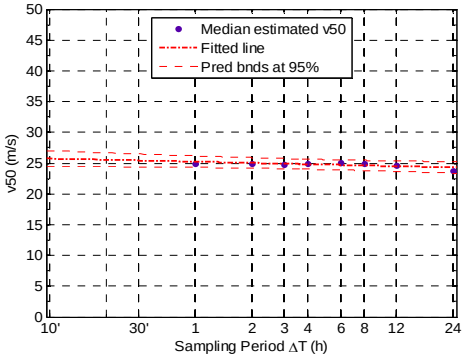
v50 (m/s)
Sampling Period ΔT (h)
Median estimated v50
Fitted line
Pred bnds at 95%

LIMH

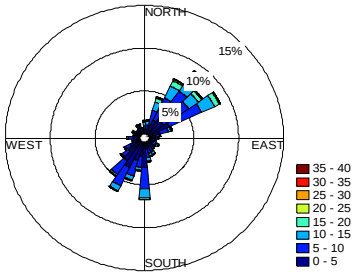
NORTH
15%
10%
5%
WEST
EAST
SOUTH
35 - 40
30 - 35
25 - 30
20 - 25
15 - 20
10 - 15
5 - 10
0 - 5

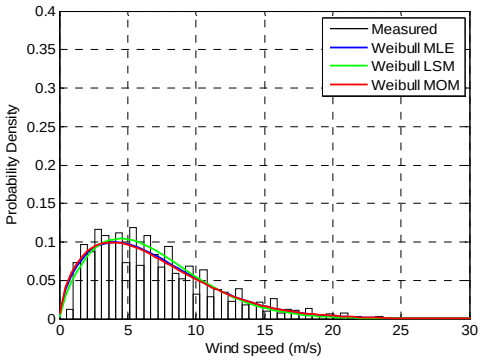
Measured
Weibull MLE
Weibull LSM
Weibull MOM
Probability Density
Wind speed (m/s)

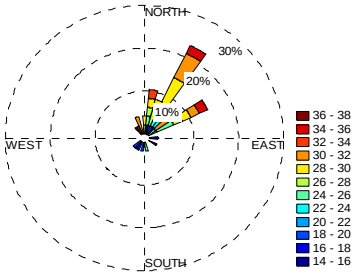
NORTH
30%
20%
10%
WEST
EAST
SOUTH
36 - 38
34 - 36
32 - 34
30 - 32
28 - 30
26 - 28
24 - 26
22 - 24
20 - 22
18 - 20
16 - 18
14 - 16

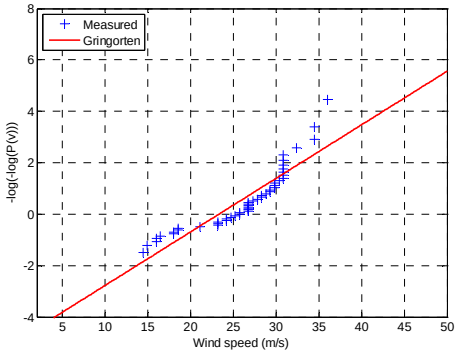
Measured
Gringorten
-log(-log(P(v)))
Wind speed (m/s)

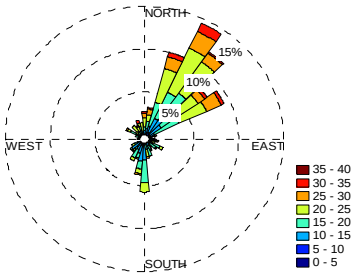
NORTH
15%
10%
5%
WEST
EAST
SOUTH
35 - 40
30 - 35
25 - 30
20 - 25
15 - 20
10 - 15
5 - 10
0 - 5

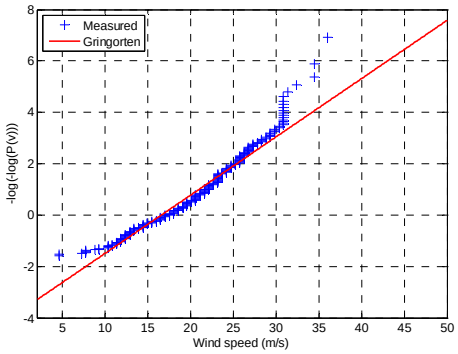
Measured
Gringorten
-log(-log(P(v)))
Wind speed (m/s)

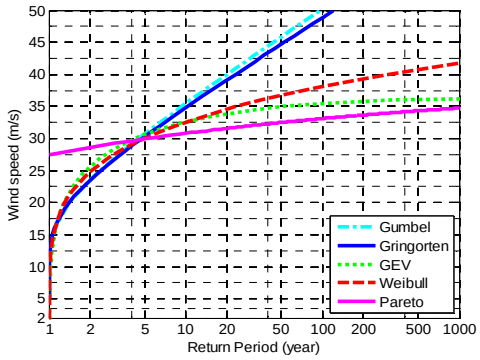
Wind speed (m/s)
Return Period (year)
Gumbel
Gringorten
GEV
Weibull
Pareto

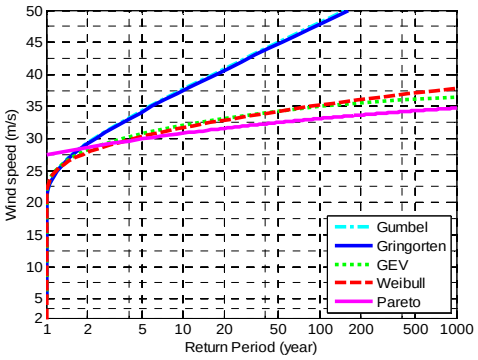
Wind speed (m/s)
Return Period (year)
Gumbel
Gringorten
GEV
Weibull
Pareto

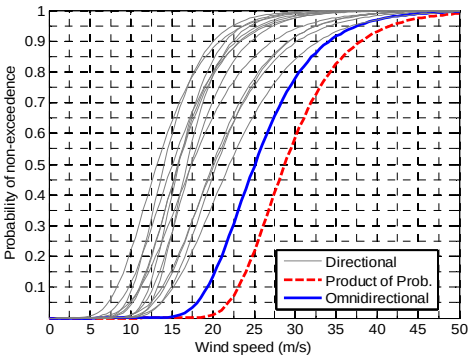
Probability of non-exceedence
Wind speed (m/s)
Directional
Product of Prob.
Omnidirectional

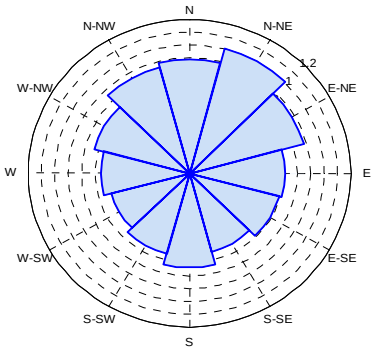
N
N-NE
E-NE
E
E-SE
S-SE
S
S-SW
W
W-NW
N-NW

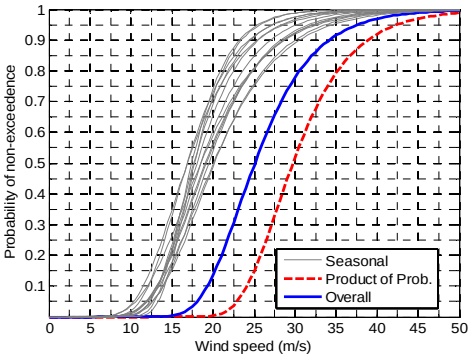
Probability of non-exceedence
Wind speed (m/s)
Seasonal
Product of Prob.
Overall

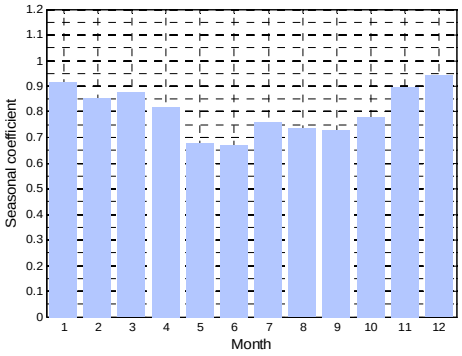
Seasonal coefficient
Month

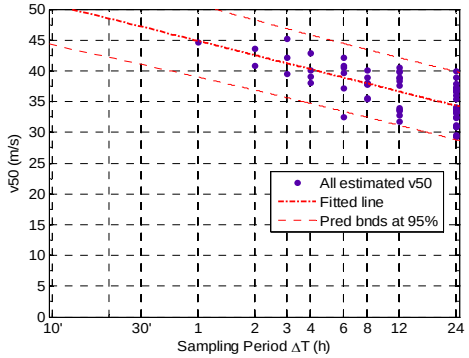
v50 (m/s)
Sampling Period ΔT (h)
All estimated v50
Fitted line
Pred bnds at 95%

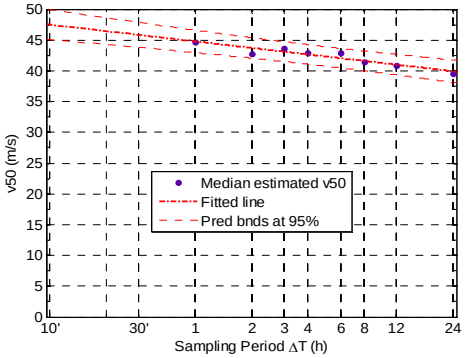
v50 (m/s)
Sampling Period ΔT (h)
Median estimated v50
Fitted line
Pred bnds at 95%

LIMJ

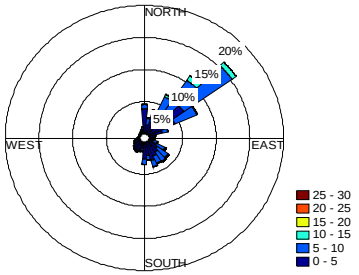
NORTH
EAST
SOUTH
WEST
20%
15%
10%
5%
25 - 30
20 - 25
15 - 20
10 - 15
5 - 10
0 - 5

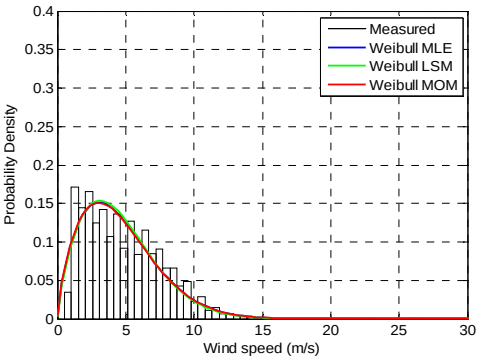
Measured
Weibull MLE
Weibull LSM
Weibull MOM
Probability Density
Wind speed (m/s)

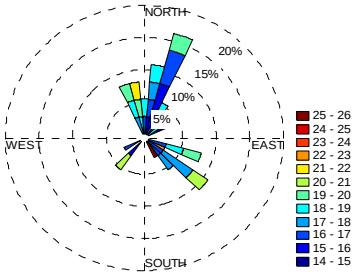
NORTH
EAST
SOUTH
WEST
20%
15%
10%
5%
25 - 26
24 - 25
23 - 24
22 - 23
21 - 22
20 - 21
19 - 20
18 - 19
17 - 18
16 - 17
15 - 16
14 - 15

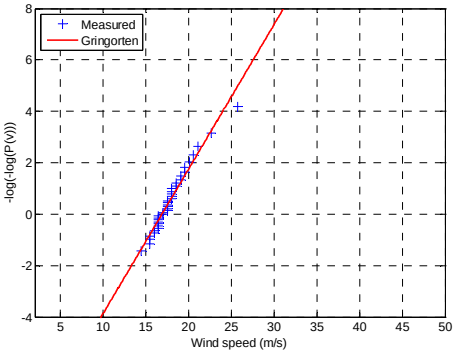
Measured
Gringorten
-log(-log(P(v)))
Wind speed (m/s)

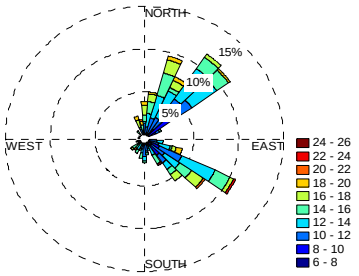
NORTH
EAST
SOUTH
WEST
15%
10%
5%
24 - 26
22 - 24
20 - 22
18 - 20
16 - 18
14 - 16
12 - 14
10 - 12
8 - 10
6 - 8

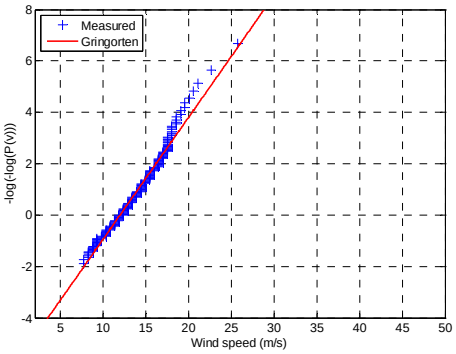
Measured
Gringorten
-log(-log(P(v)))
Wind speed (m/s)

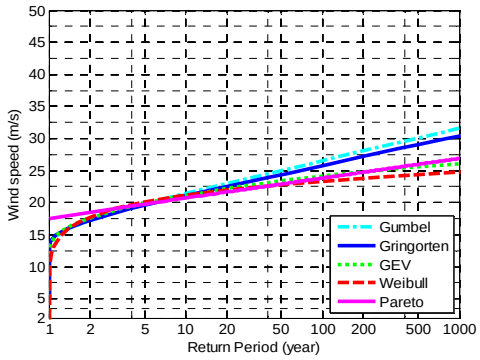
Wind speed (m/s)
Return Period (year)
Gumbel
Gringorten
GEV
Weibull
Pareto

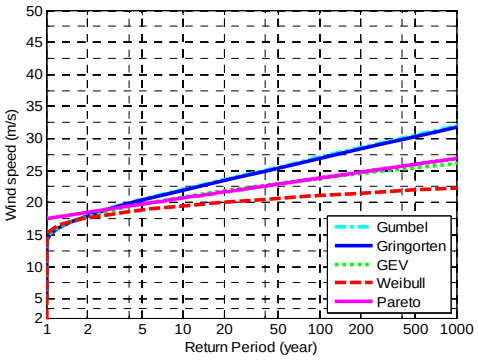
Wind speed (m/s)
Return Period (year)
Gumbel
Gringorten
GEV
Weibull
Pareto

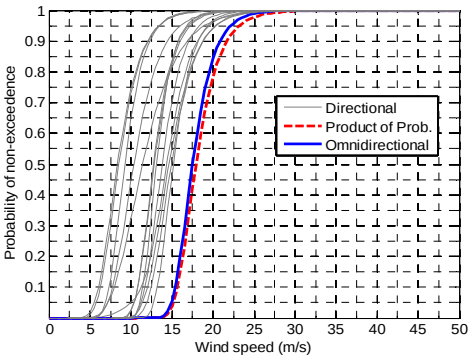
Probability of non-exceedence
Wind speed (m/s)
Directional
Product of Prob.
Omnidirectional

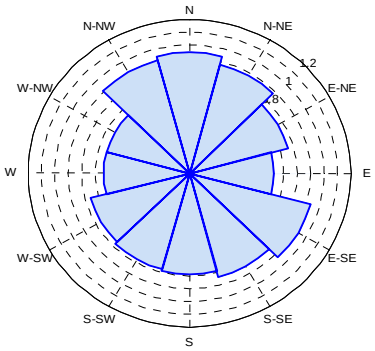
N
N-NE
E-NE
E
E-SE
S-SE
S
S-SW
W
W-NW
N-NW

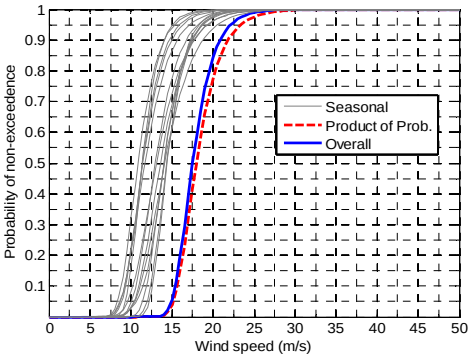
Probability of non-exceedence
Wind speed (m/s)
Seasonal
Product of Prob.
Overall

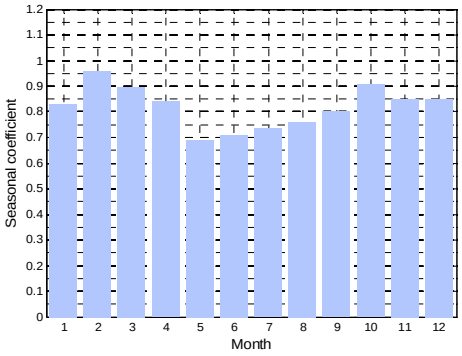
Seasonal coefficient
Month

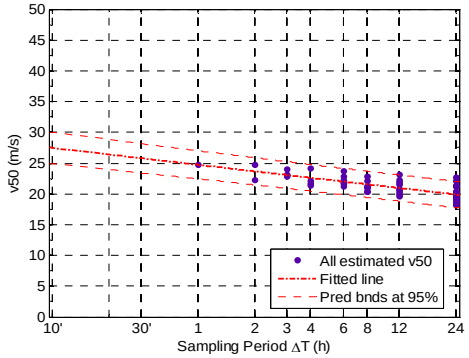
v50 (m/s)
Sampling Period ΔT (h)
All estimated v50
Fitted line
Pred bnds at 95%

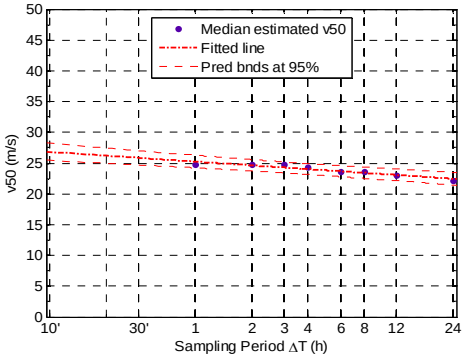
v50 (m/s)
Sampling Period ΔT (h)
Median estimated v50
Fitted line
Pred bnds at 95%

LIMK

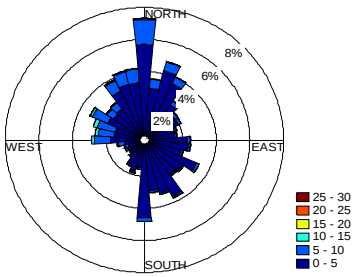
NORTH
8%
6%
4%
2%
WEST
EAST
SOUTH
25 - 30
20 - 25
15 - 20
10 - 15
5 - 10
0 - 5

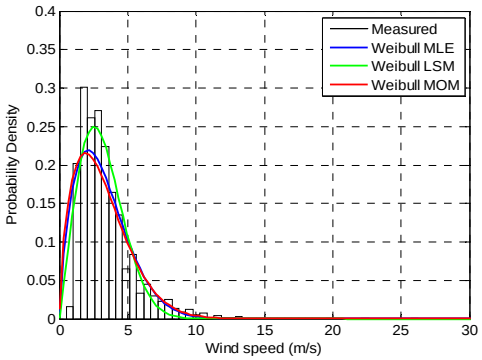
Measured
Weibull MLE
Weibull LSM
Weibull MOM
Probability Density
Wind speed (m/s)

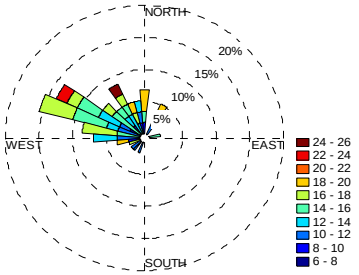
NORTH
20%
15%
10%
5%
WEST
EAST
SOUTH
24 - 26
22 - 24
20 - 22
18 - 20
16 - 18
14 - 16
12 - 14
10 - 12
8 - 10
6 - 8

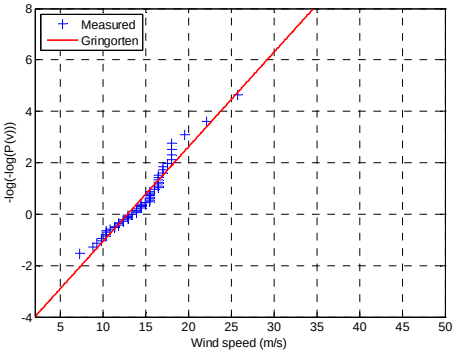
Measured
Gringorten
-log(-log(P(v)))
Wind speed (m/s)

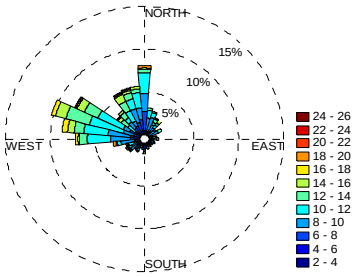
NORTH
15%
10%
5%
WEST
EAST
SOUTH
24 - 26
22 - 24
20 - 22
18 - 20
16 - 18
14 - 16
12 - 14
10 - 12
8 - 10
6 - 8
4 - 6
2 - 4

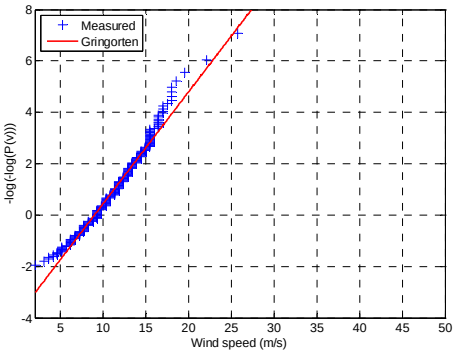
Measured
Gringorten
-log(-log(P(v)))
Wind speed (m/s)

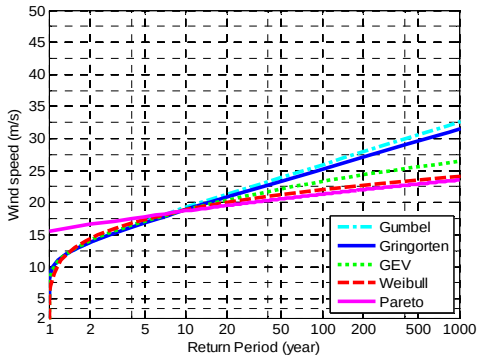
Wind speed (m/s)
Return Period (year)
Gumbel
Gringorten
GEV
Weibull
Pareto

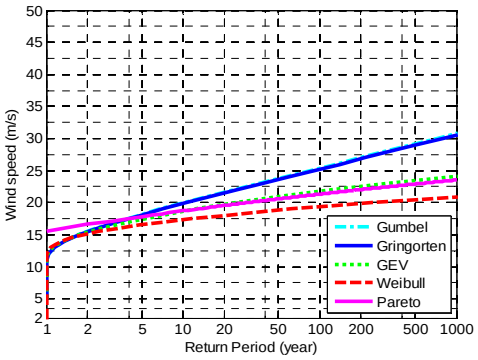
Wind speed (m/s)
Return Period (year)
Gumbel
Gringorten
GEV
Weibull
Pareto

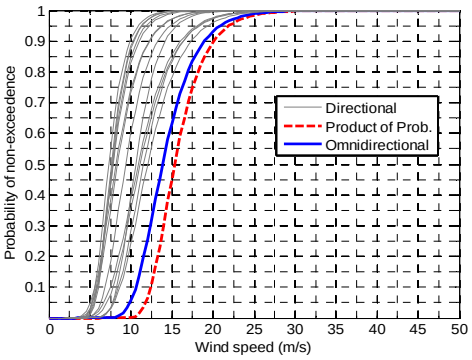
Probability of non-exceedence
Wind speed (m/s)
Directional
Product of Prob.
Omnidirectional

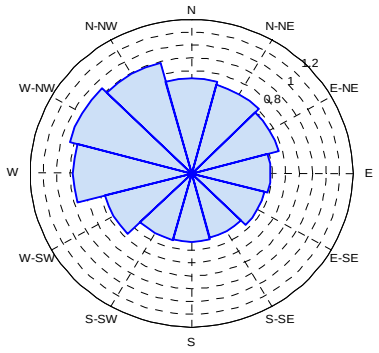
N
N-NE
E-NE
E
E-SE
S-SE
S
S-SW
W
W-NW
N-NW

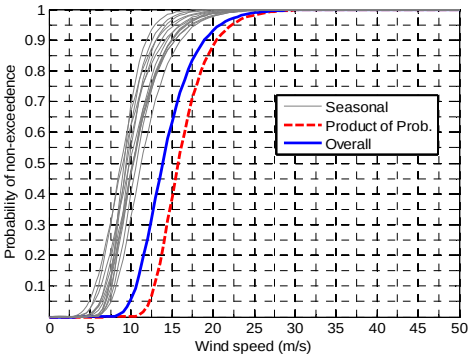
Probability of non-exceedence
Wind speed (m/s)
Seasonal
Product of Prob.
Overall

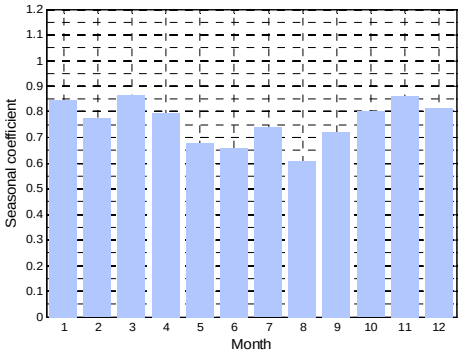
Seasonal coefficient
Month

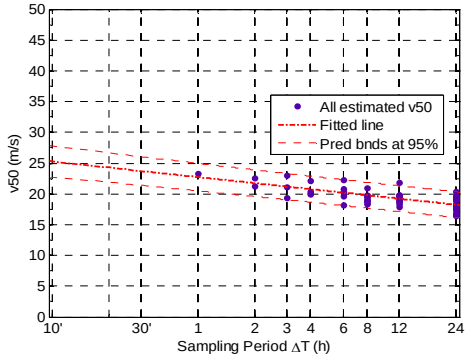
v50 (m/s)
Sampling Period ΔT (h)
All estimated v50
Fitted line
Pred bnds at 95%

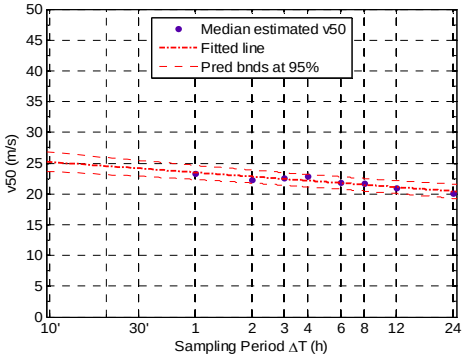
v50 (m/s)
Sampling Period ΔT (h)
Median estimated v50
Fitted line
Pred bnds at 95%

LIML

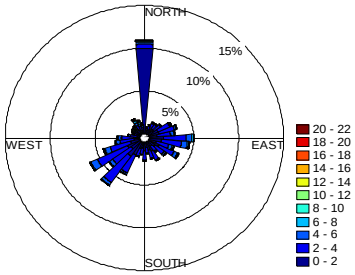
NORTH
15%
10%
5%
WEST
EAST
SOUTH
20 - 22
18 - 20
16 - 18
14 - 16
12 - 14
10 - 12
8 - 10
6 - 8
4 - 6
2 - 4
0 - 2

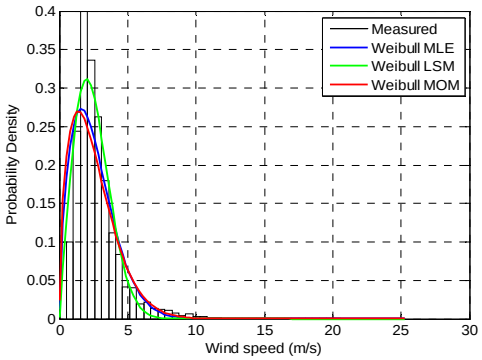
Measured
Weibull MLE
Weibull LSM
Weibull MOM
Probability Density
Wind speed (m/s)

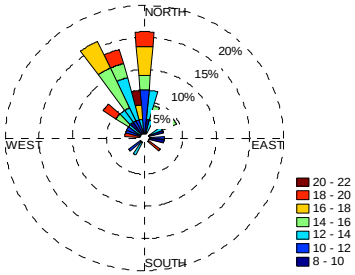
NORTH
20%
15%
10%
5%
WEST
EAST
SOUTH
20 - 22
18 - 20
16 - 18
14 - 16
12 - 14
10 - 12
8 - 10

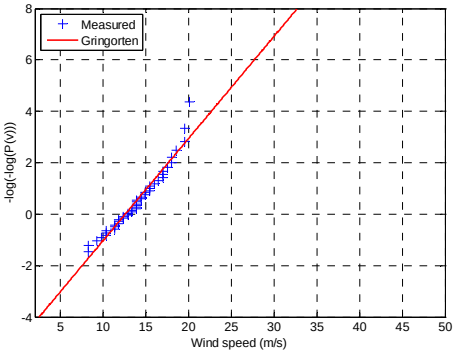
Measured
Gringorten
-log(-log(P(v)))
Wind speed (m/s)

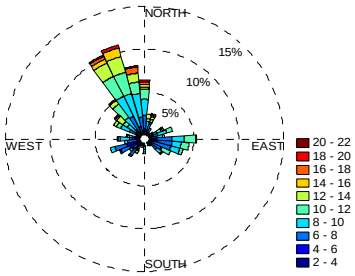
NORTH
15%
10%
5%
WEST
EAST
SOUTH
20 - 22
18 - 20
16 - 18
14 - 16
12 - 14
10 - 12
8 - 10
6 - 8
4 - 6
2 - 4

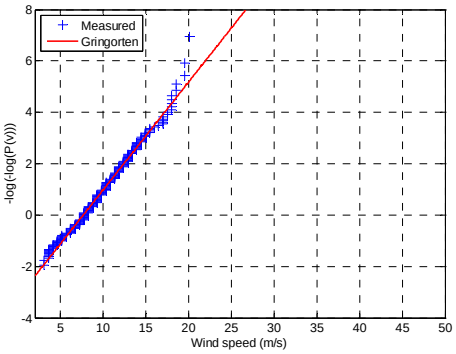
Measured
Gringorten
-log(-log(P(v)))
Wind speed (m/s)

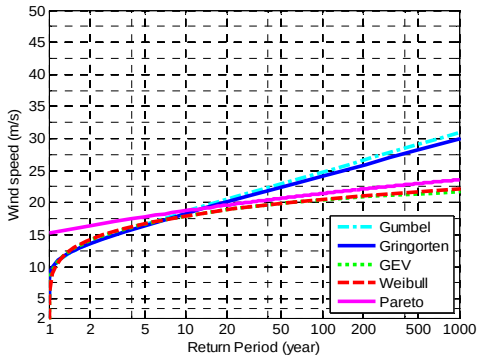
Wind speed (m/s)
Return Period (year)
Gumbel
Gringorten
GEV
Weibull
Pareto

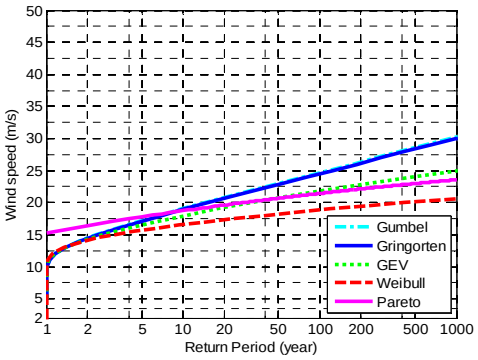
Wind speed (m/s)
Return Period (year)
Gumbel
Gringorten
GEV
Weibull
Pareto

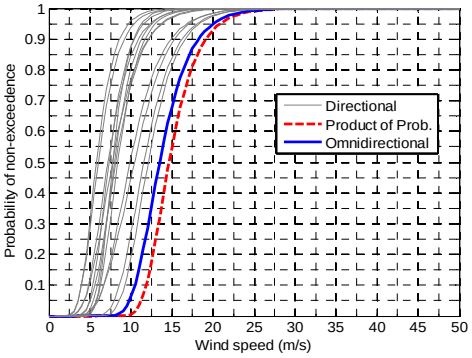
Probability of non-exceedence
Wind speed (m/s)
Directional
Product of Prob.
Omnidirectional

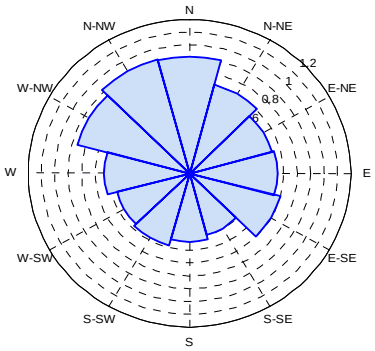
N
N-NE
E-NE
E
E-SE
S-SE
S
S-SW
W
W-NW
N-NW

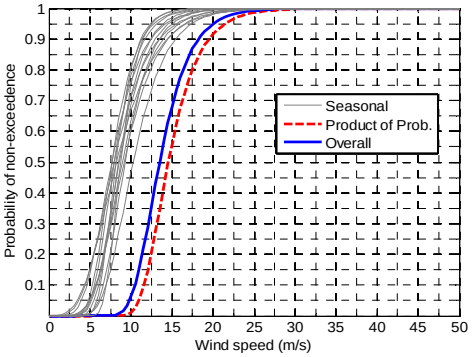
Probability of non-exceedence
Wind speed (m/s)
Seasonal
Product of Prob.
Overall

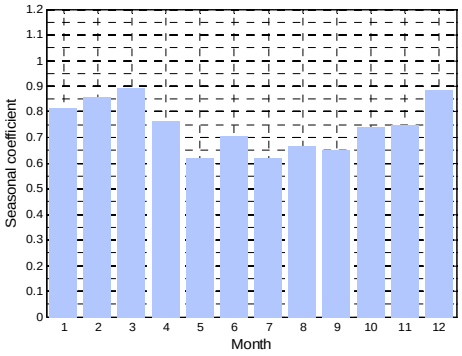
Seasonal coefficient
Month

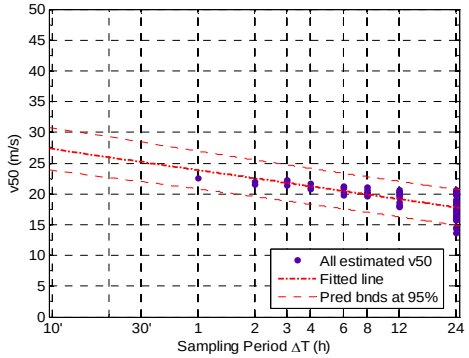
v50 (m/s)
Sampling Period ΔT (h)
All estimated v50
Fitted line
Pred bnds at 95%

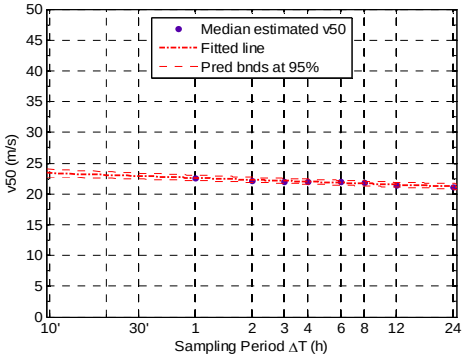
v50 (m/s)
Sampling Period ΔT (h)
Median estimated v50
Fitted line
Pred bnds at 95%

LIMN

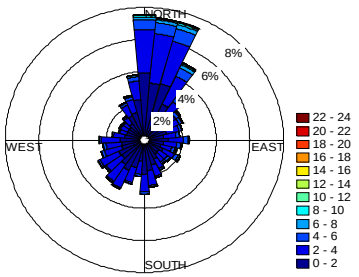
NORTH
8%
6%
4%
2%
WEST
EAST
SOUTH
22 - 24
20 - 22
18 - 20
16 - 18
14 - 16
12 - 14
10 - 12
8 - 10
6 - 8
4 - 6
2 - 4
0 - 2

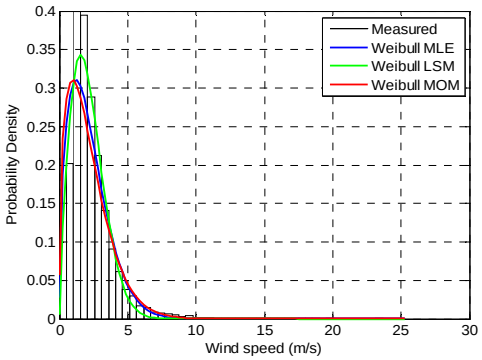
Measured
Weibull MLE
Weibull LSM
Weibull MOM
Probability Density
Wind speed (m/s)

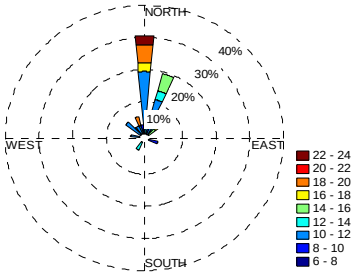
NORTH
40%
30%
20%
10%
WEST
EAST
SOUTH
22 - 24
20 - 22
18 - 20
16 - 18
14 - 16
12 - 14
10 - 12
8 - 10
6 - 8

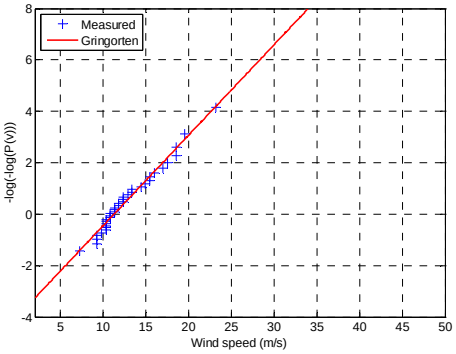
Measured
Gringorten
-log(-log(P(v)))
Wind speed (m/s)

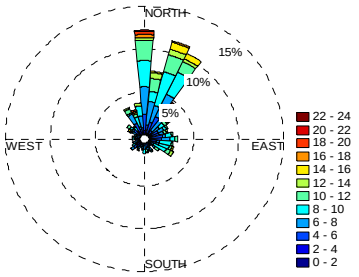
NORTH
15%
10%
5%
WEST
EAST
SOUTH
22 - 24
20 - 22
18 - 20
16 - 18
14 - 16
12 - 14
10 - 12
8 - 10
6 - 8
4 - 6
2 - 4
0 - 2

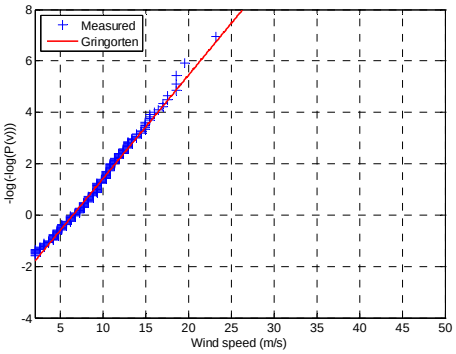
Measured
Gringorten
-log(-log(P(v)))
Wind speed (m/s)

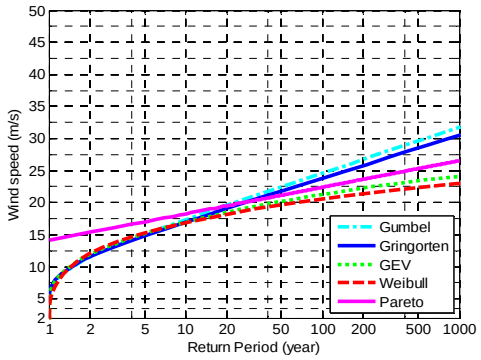
Wind speed (m/s)
Return Period (year)
Gumbel
Gringorten
GEV
Weibull
Pareto

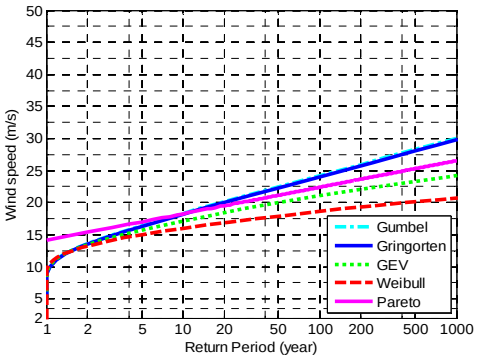
Wind speed (m/s)
Return Period (year)
Gumbel
Gringorten
GEV
Weibull
Pareto

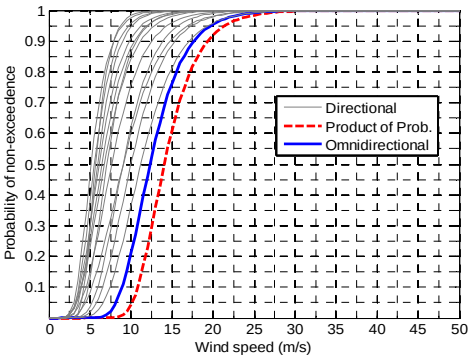
Probability of non-exceedence
Wind speed (m/s)
Directional
Product of Prob.
Omnidirectional

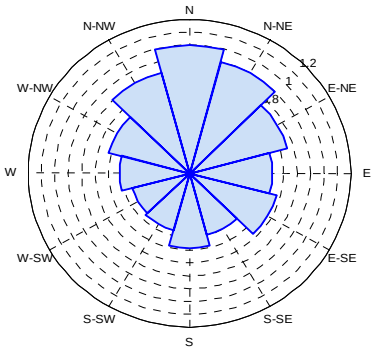
N
N-NE
E-NE
E
E-SE
S-SE
S
S-SW
W
W-NW
N-NW

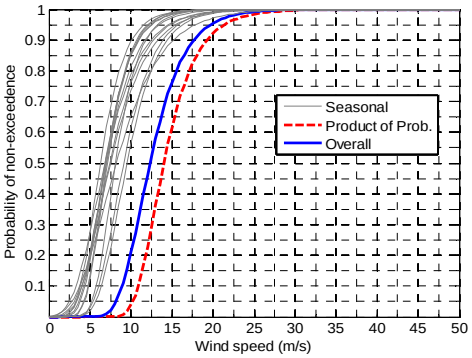
Probability of non-exceedence
Wind speed (m/s)
Seasonal
Product of Prob.
Overall

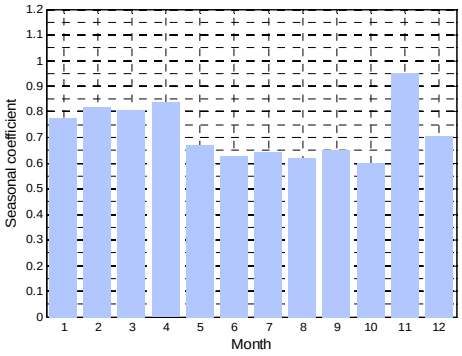
Seasonal coefficient
Month

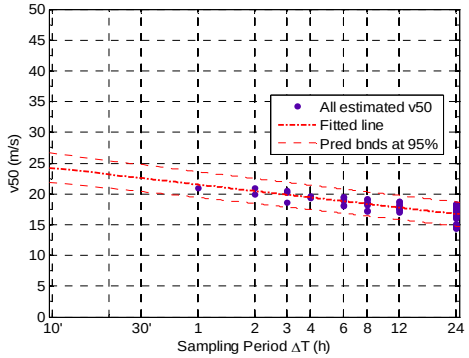
v50 (m/s)
Sampling Period ΔT (h)
All estimated v50
Fitted line
Pred bnds at 95%

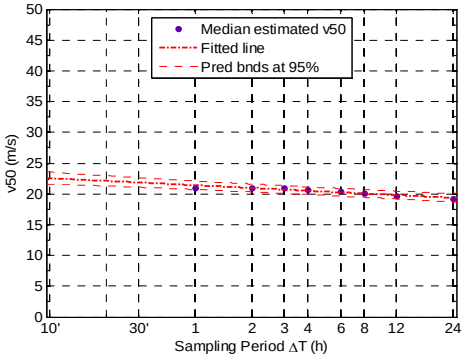
v50 (m/s)
Sampling Period ΔT (h)
Median estimated v50
Fitted line
Pred bnds at 95%

LIMO

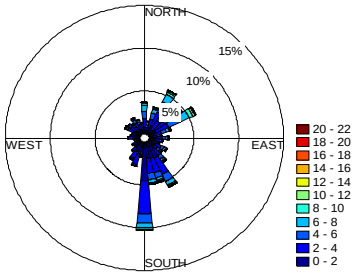
NORTH
15%
10%
5%
WEST
EAST
SOUTH
20 - 22
18 - 20
16 - 18
14 - 16
12 - 14
10 - 12
8 - 10
6 - 8
4 - 6
2 - 4
0 - 2

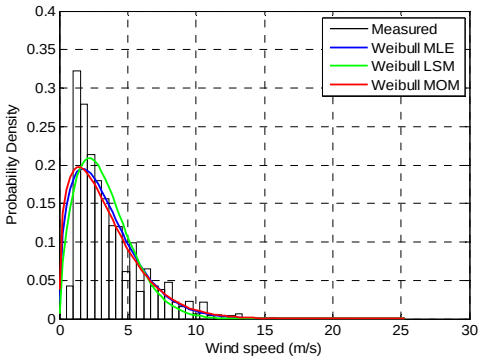
Measured
Weibull MLE
Weibull LSM
Weibull MOM
Probability Density
Wind speed (m/s)

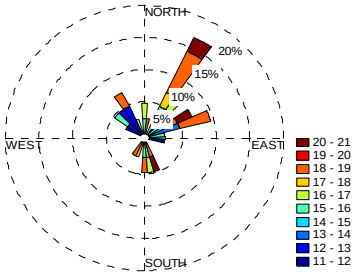
NORTH
20%
15%
10%
5%
WEST
EAST
SOUTH
20 - 21
19 - 20
18 - 19
17 - 18
16 - 17
15 - 16
14 - 15
13 - 14
12 - 13
11 - 12

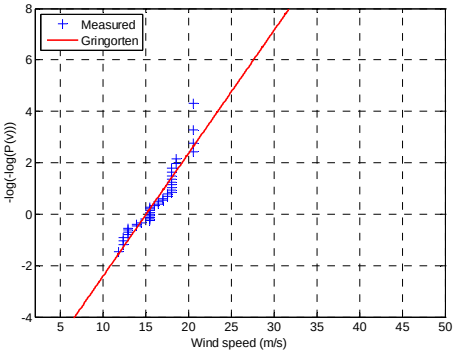
Measured
Gringorten
-log(-log(P(v)))
Wind speed (m/s)

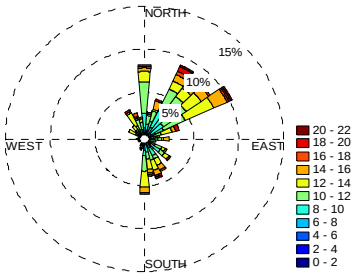
NORTH
15%
10%
5%
WEST
EAST
SOUTH
20 - 22
18 - 20
16 - 18
14 - 16
12 - 14
10 - 12
8 - 10
6 - 8
4 - 6
2 - 4
0 - 2

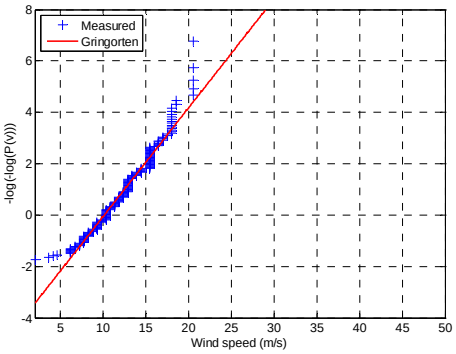
Measured
Gringorten
-log(-log(P(v)))
Wind speed (m/s)

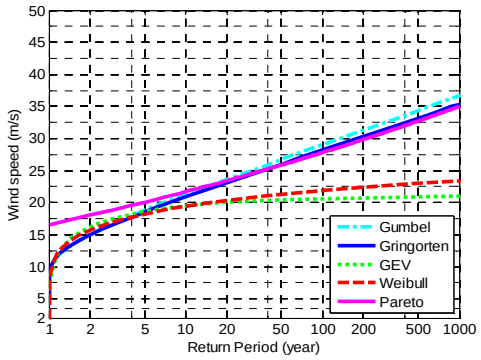
Wind speed (m/s)
Return Period (year)
Gumbel
Gringorten
GEV
Weibull
Pareto

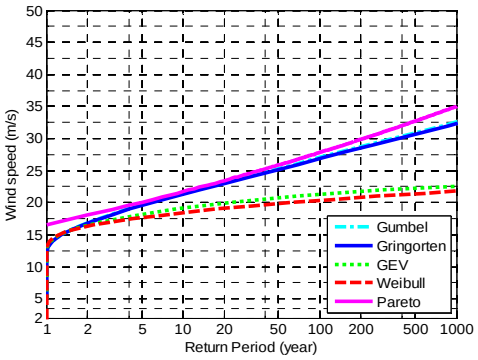
Wind speed (m/s)
Return Period (year)
Gumbel
Gringorten
GEV
Weibull
Pareto

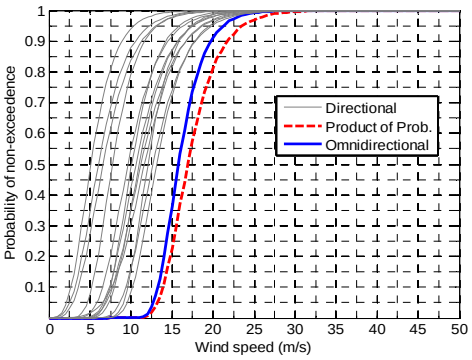
Probability of non-exceedence
Wind speed (m/s)
Directional
Product of Prob.
Omnidirectional

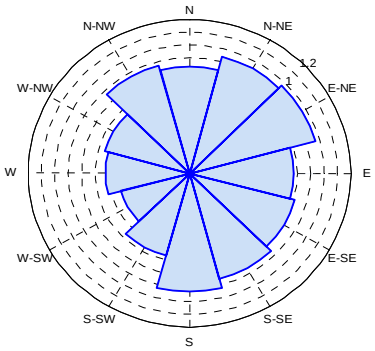
N
N-NE
E-NE
E
E-SE
S-SE
S
S-SW
W
W-NW
N-NW

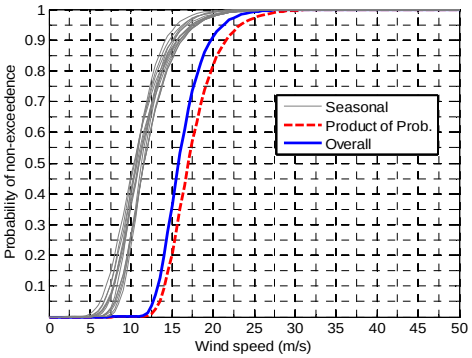
Probability of non-exceedence
Wind speed (m/s)
Seasonal
Product of Prob.
Overall

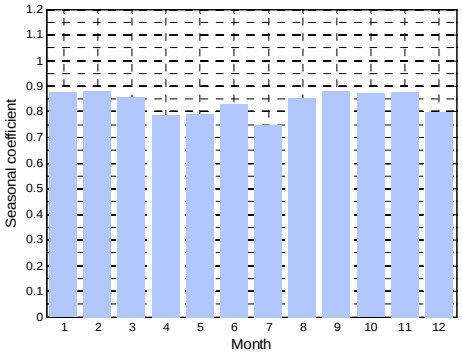
Seasonal coefficient
Month

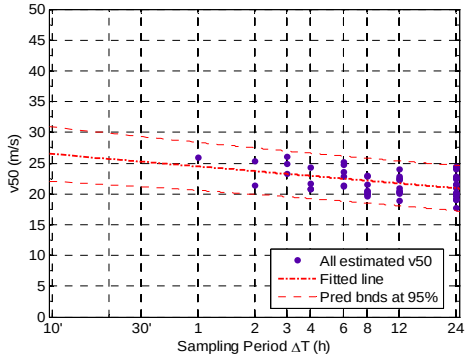
v50 (m/s)
Sampling Period ΔT (h)
All estimated v50
Fitted line
Pred bnds at 95%

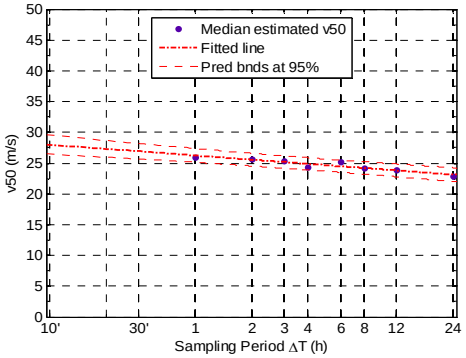
v50 (m/s)
Sampling Period ΔT (h)
Median estimated v50
Fitted line
Pred bnds at 95%

LIMQ

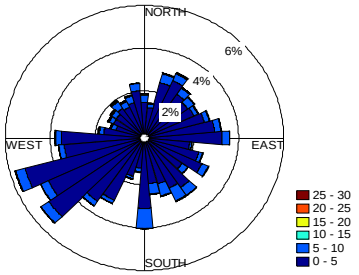
NORTH
6%
4%
2%
WEST
EAST
SOUTH
25 - 30
20 - 25
15 - 20
10 - 15
5 - 10
0 - 5

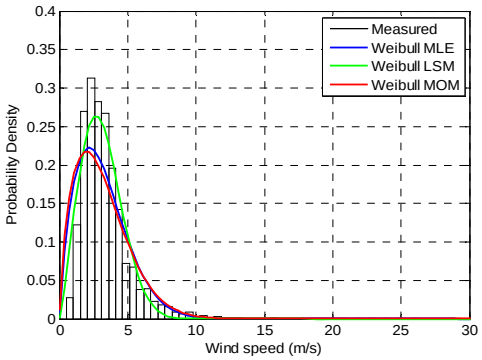
Measured
Weibull MLE
Weibull LSM
Weibull MOM
Probability Density
Wind speed (m/s)

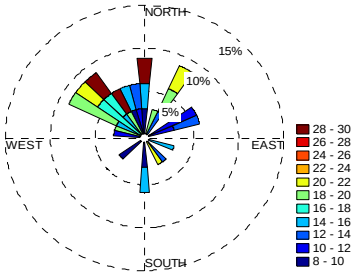
NORTH
15%
10%
5%
WEST
EAST
SOUTH
28 - 30
26 - 28
24 - 26
22 - 24
20 - 22
18 - 20
16 - 18
14 - 16
12 - 14
10 - 12
8 - 10

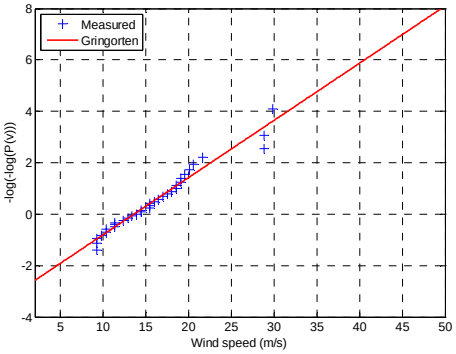
Measured
Gringorten
-log(-log(P(v)))
Wind speed (m/s)

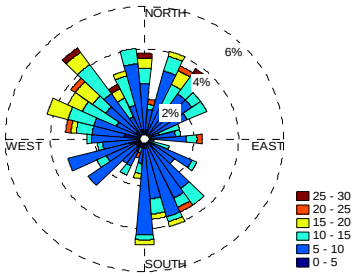
NORTH
6%
4%
2%
WEST
EAST
SOUTH
25 - 30
20 - 25
15 - 20
10 - 15
5 - 10
0 - 5

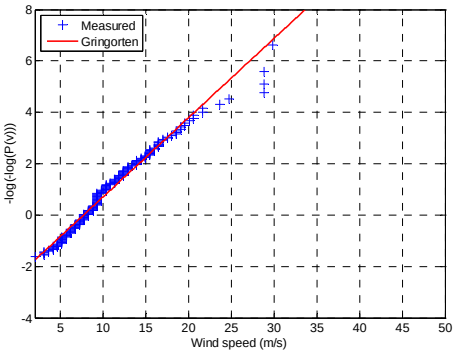
Measured
Gringorten
-log(-log(P(v)))
Wind speed (m/s)

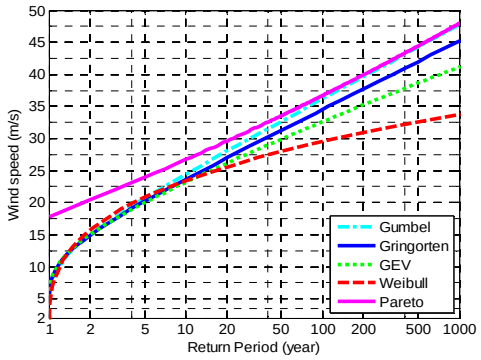
Wind speed (m/s)
Return Period (year)
Gumbel
Gringorten
GEV
Weibull
Pareto

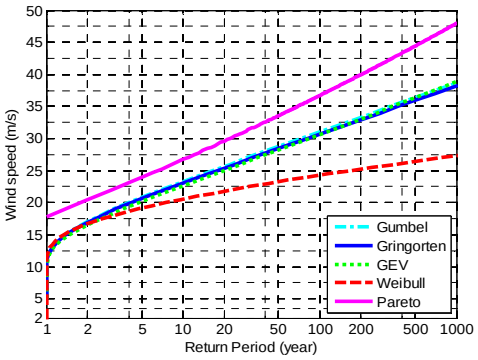
Wind speed (m/s)
Return Period (year)
Gumbel
Gringorten
GEV
Weibull
Pareto

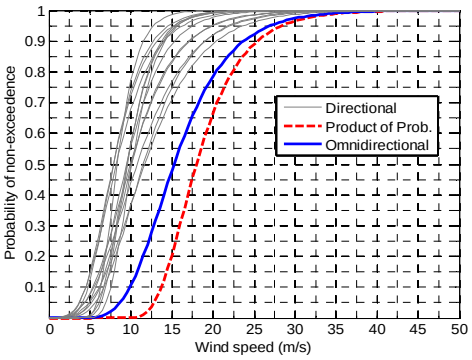
Probability of non-exceedence
Wind speed (m/s)
Directional
Product of Prob.
Omnidirectional

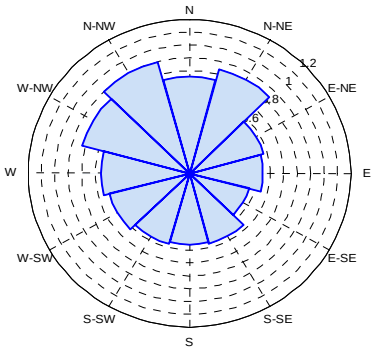
N
N-NE
E-NE
E
E-SE
S-SE
S
S-SW
W
W-NW
N-NW

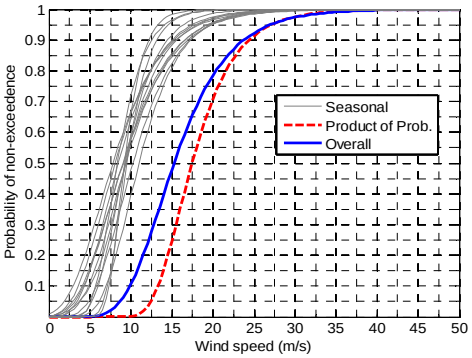
Probability of non-exceedence
Wind speed (m/s)
Seasonal
Product of Prob.
Overall

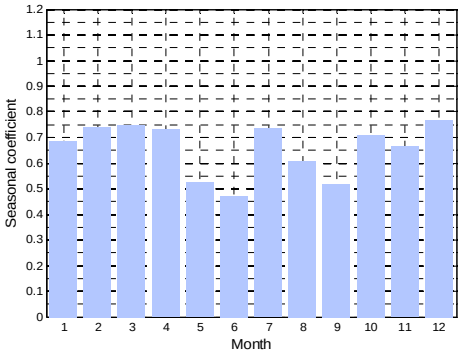
Seasonal coefficient
Month

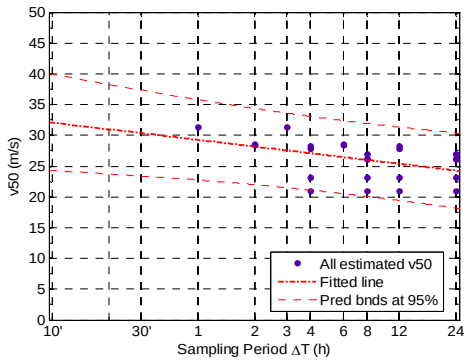
v50 (m/s)
Sampling Period ΔT (h)
All estimated v50
Fitted line
Pred bnds at 95%

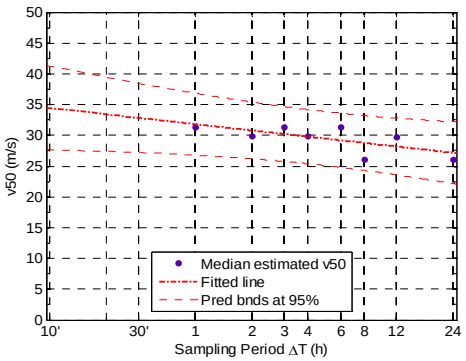
v50 (m/s)
Sampling Period ΔT (h)
Median estimated v50
Fitted line
Pred bnds at 95%

LIMR

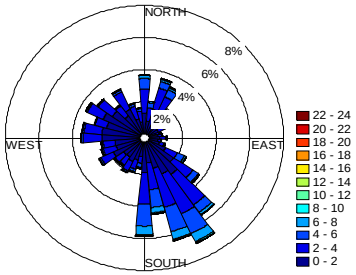
NORTH
8%
6%
4%
2%
WEST
EAST
SOUTH
22 - 24
20 - 22
18 - 20
16 - 18
14 - 16
12 - 14
10 - 12
8 - 10
6 - 8
4 - 6
2 - 4
0 - 2

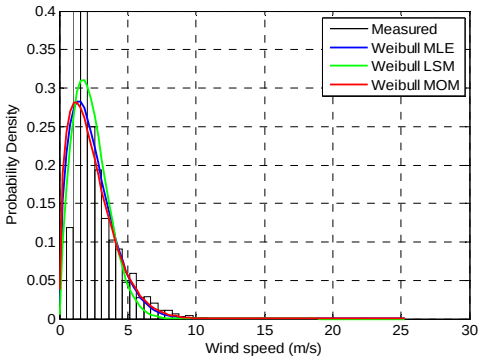
Measured
Weibull MLE
Weibull LSM
Weibull MOM
Probability Density
Wind speed (m/s)

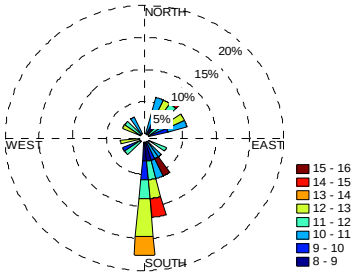
NORTH
20%
15%
10%
5%
WEST
EAST
SOUTH
15 - 16
14 - 15
13 - 14
12 - 13
11 - 12
10 - 11
9 - 10
8 - 9

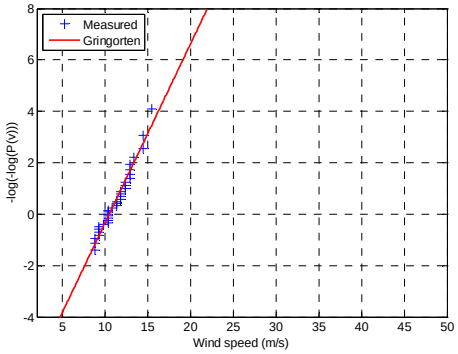
Measured
Gringorten
-log(-log(P(v)))
Wind speed (m/s)

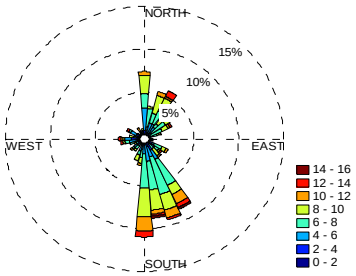
NORTH
15%
10%
5%
WEST
EAST
SOUTH
14 - 16
12 - 14
10 - 12
8 - 10
6 - 8
4 - 6
2 - 4
0 - 2

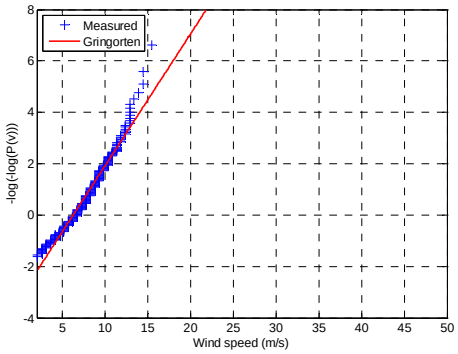
Measured
Gringorten
-log(-log(P(v)))
Wind speed (m/s)

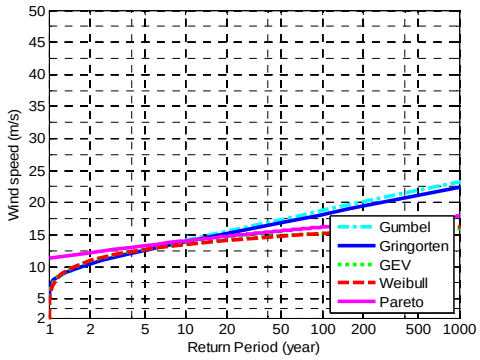
Wind speed (m/s)
Return Period (year)
Gumbel
Gringorten
GEV
Weibull
Pareto

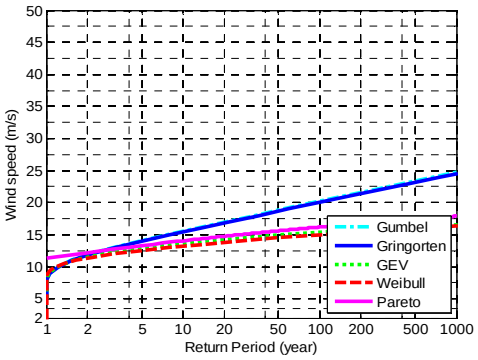
Wind speed (m/s)
Return Period (year)
Gumbel
Gringorten
GEV
Weibull
Pareto

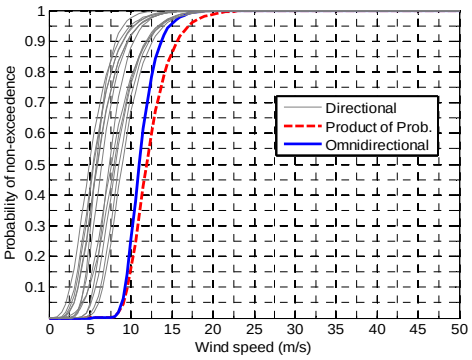
Probability of non-exceedence
Wind speed (m/s)
Directional
Product of Prob.
Omnidirectional

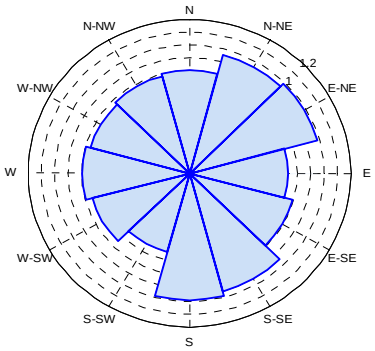
N
N-NE
E-NE
E
E-SE
S-SE
S
S-SW
W
W-NW
N-NW

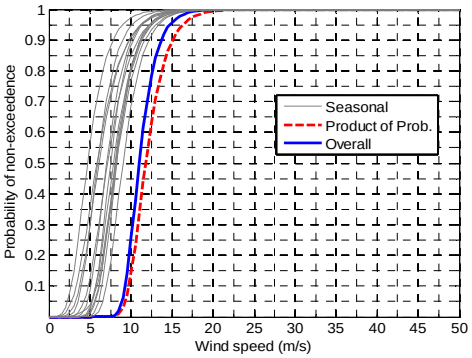
Probability of non-exceedence
Wind speed (m/s)
Seasonal
Product of Prob.
Overall

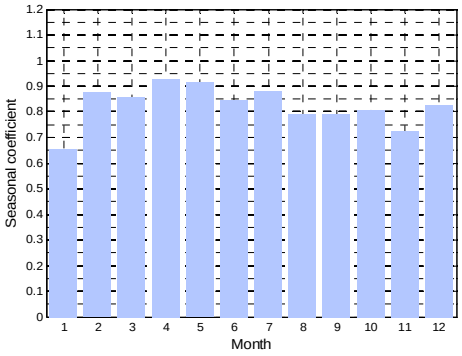
Seasonal coefficient
Month

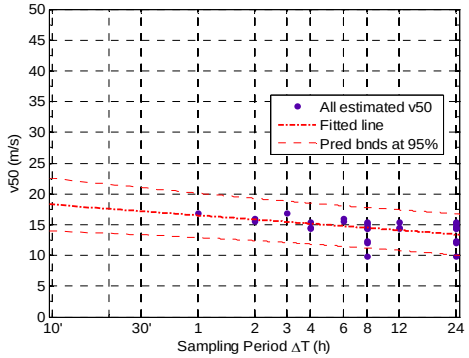
v50 (m/s)
Sampling Period ΔT (h)
All estimated v50
Fitted line
Pred bnds at 95%

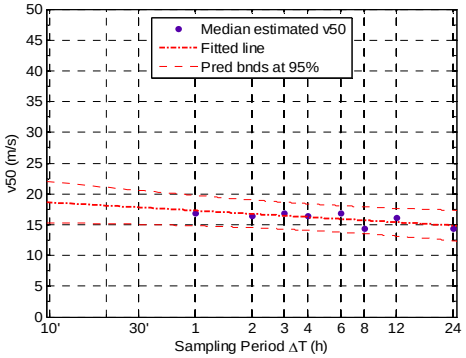
v50 (m/s)
Sampling Period ΔT (h)
Median estimated v50
Fitted line
Pred bnds at 95%

LIMS

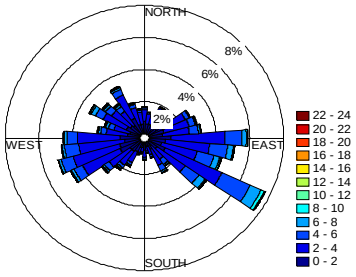
NORTH
8%
6%
4%
2%
WEST
EAST
SOUTH
22 - 24
20 - 22
18 - 20
16 - 18
14 - 16
12 - 14
10 - 12
8 - 10
6 - 8
4 - 6
2 - 4
0 - 2

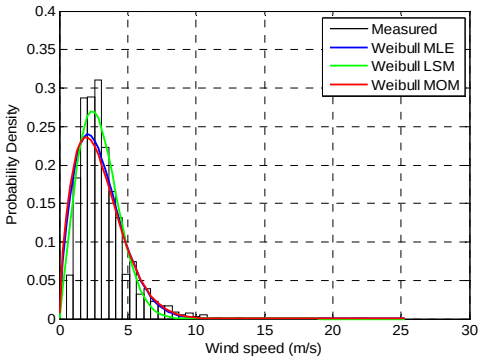
Measured
Weibull MLE
Weibull LSM
Weibull MOM
Probability Density
Wind speed (m/s)

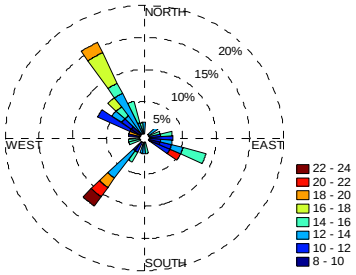
NORTH
20%
15%
10%
5%
WEST
EAST
SOUTH
22 - 24
20 - 22
18 - 20
16 - 18
14 - 16
12 - 14
10 - 12
8 - 10

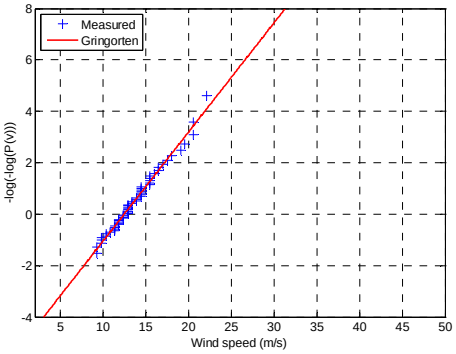
Measured
Gringorten
-log(-log(P(v)))
Wind speed (m/s)

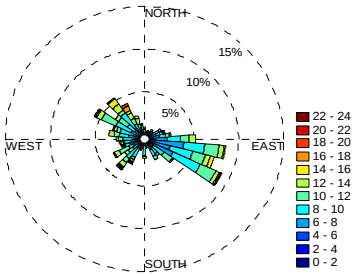
NORTH
15%
10%
5%
WEST
EAST
SOUTH
22 - 24
20 - 22
18 - 20
16 - 18
14 - 16
12 - 14
10 - 12
8 - 10
6 - 8
4 - 6
2 - 4
0 - 2

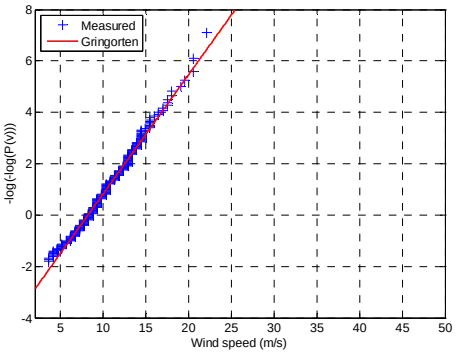
Measured
Gringorten
-log(-log(P(v)))
Wind speed (m/s)

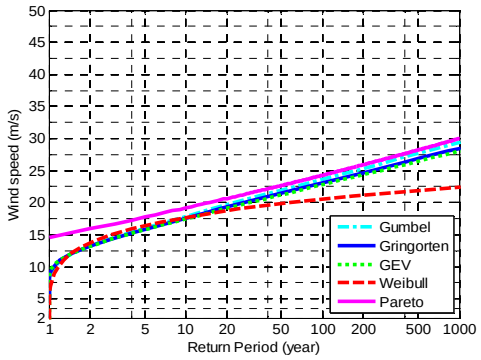
Wind speed (m/s)
Return Period (year)
Gumbel
Gringorten
GEV
Weibull
Pareto

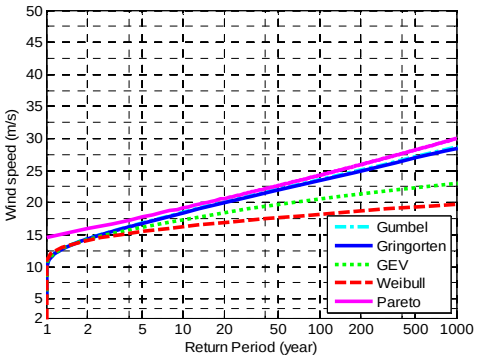
Wind speed (m/s)
Return Period (year)
Gumbel
Gringorten
GEV
Weibull
Pareto

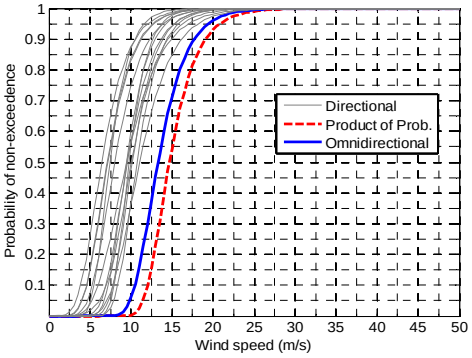
Probability of non-exceedence
Wind speed (m/s)
Directional
Product of Prob.
Omnidirectional

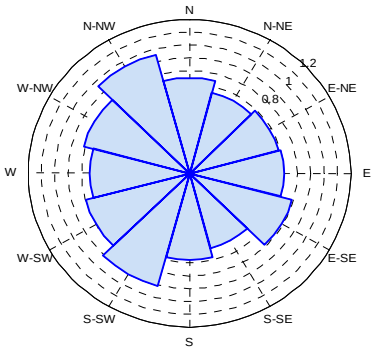
N
N-NE
E-NE
E
E-SE
S-SE
S
S-SW
W
W-NW
N-NW

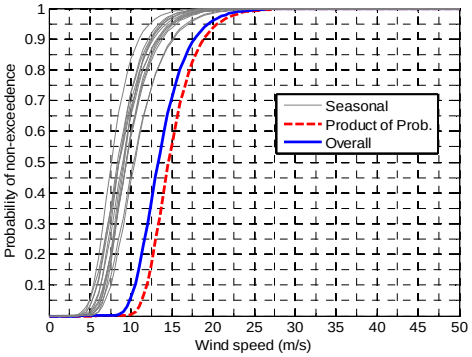
Probability of non-exceedence
Wind speed (m/s)
Seasonal
Product of Prob.
Overall

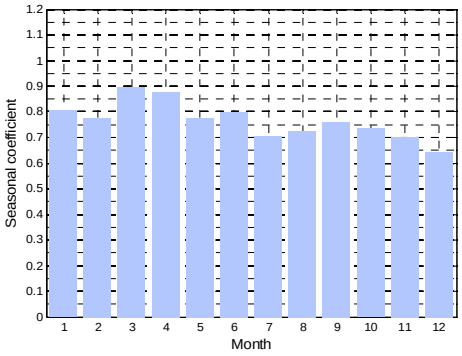
Seasonal coefficient
Month

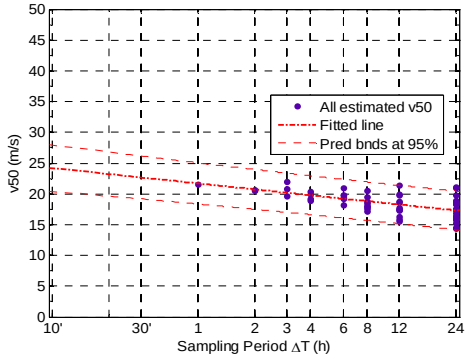
v50 (m/s)
Sampling Period ΔT (h)
All estimated v50
Fitted line
Pred bnds at 95%

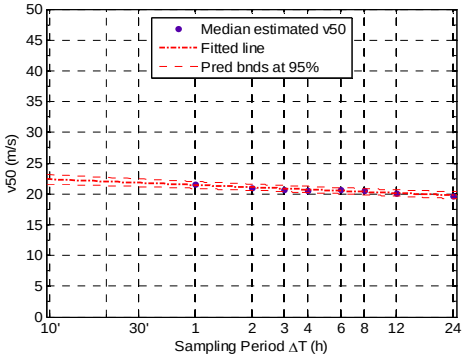
v50 (m/s)
Sampling Period ΔT (h)
Median estimated v50
Fitted line
Pred bnds at 95%

LIMT

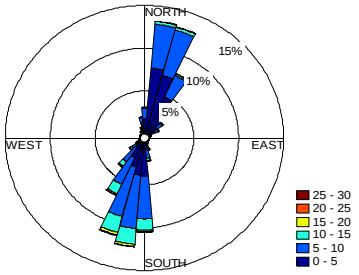
NORTH
15%
10%
5%
WEST
EAST
SOUTH
25 - 30
20 - 25
15 - 20
10 - 15
5 - 10
0 - 5

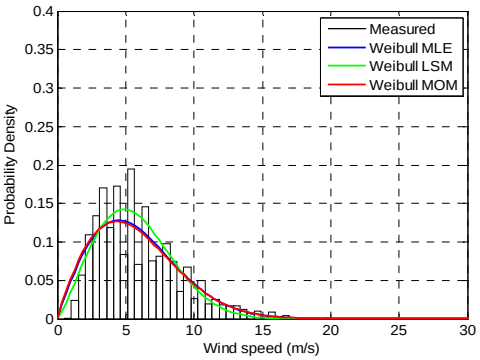
Measured
Weibull MLE
Weibull LSM
Weibull MOM
Probability Density
Wind speed (m/s)

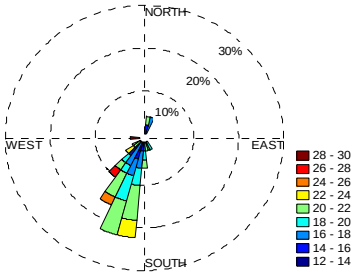
NORTH
30%
20%
10%
WEST
EAST
SOUTH
28 - 30
26 - 28
24 - 26
22 - 24
20 - 22
18 - 20
16 - 18
14 - 16
12 - 14

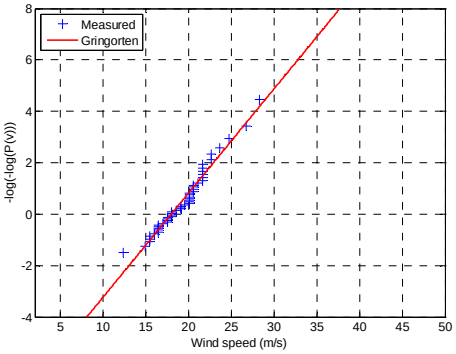
Measured
Gringorten
-log(-log(P(v)))
Wind speed (m/s)

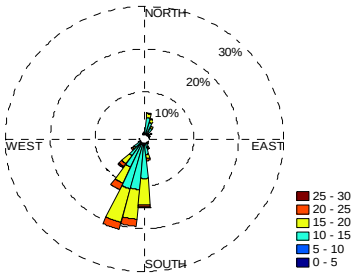
NORTH
30%
20%
10%
WEST
EAST
SOUTH
25 - 30
20 - 25
15 - 20
10 - 15
5 - 10
0 - 5

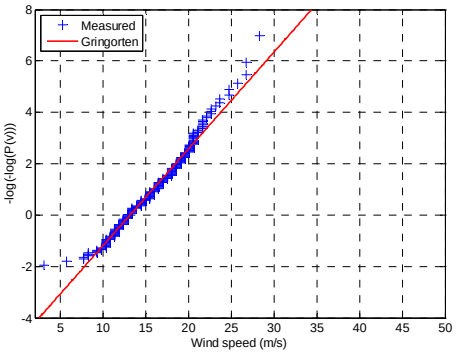
Measured
Gringorten
-log(-log(P(v)))
Wind speed (m/s)

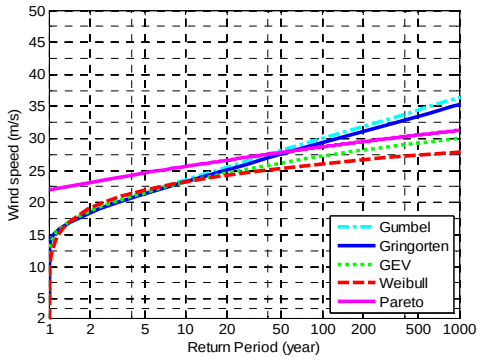
Wind speed (m/s)
Return Period (year)
Gumbel
Gringorten
GEV
Weibull
Pareto

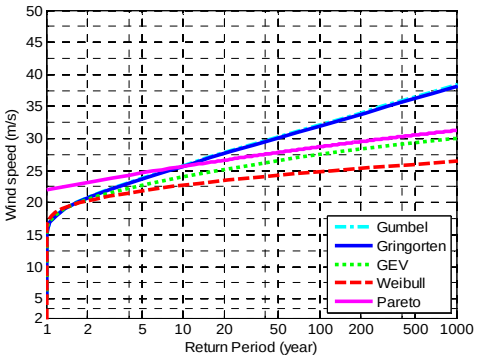
Wind speed (m/s)
Return Period (year)
Gumbel
Gringorten
GEV
Weibull
Pareto

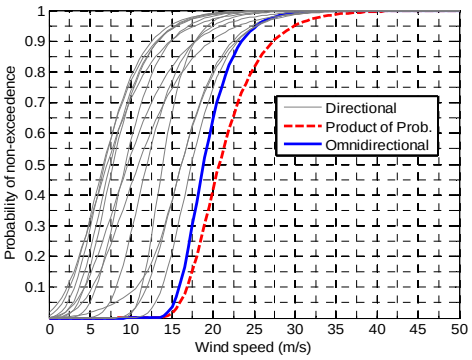
Probability of non-exceedence
Wind speed (m/s)
Directional
Product of Prob.
Omnidirectional

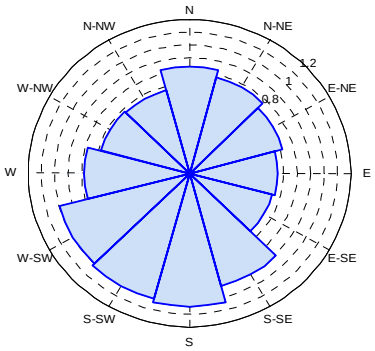
N
N-NE
E-NE
E
E-SE
S-SE
S
S-SW
W
W-NW
N-NW

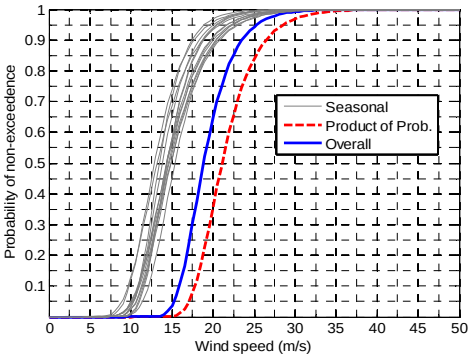
Probability of non-exceedence
Wind speed (m/s)
Seasonal
Product of Prob.
Overall

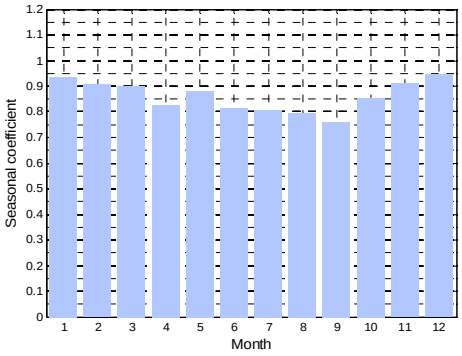
Seasonal coefficient
Month

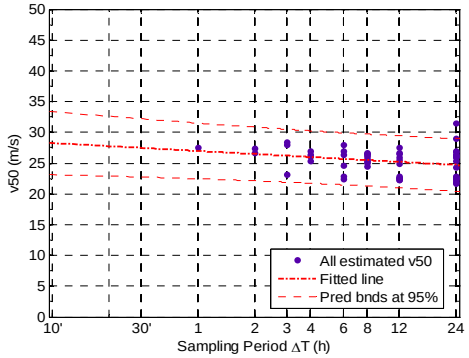
v50 (m/s)
Sampling Period ΔT (h)
All estimated v50
Fitted line
Pred bnds at 95%

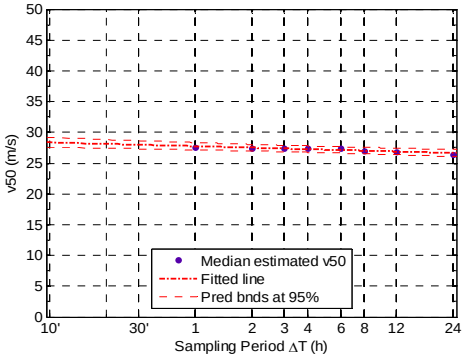
v50 (m/s)
Sampling Period ΔT (h)
Median estimated v50
Fitted line
Pred bnds at 95%

LIMU

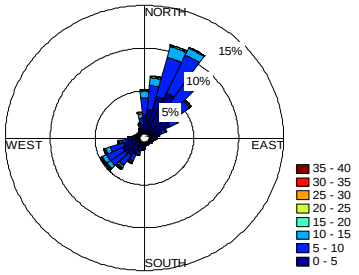
NORTH
15%
10%
5%
WEST
EAST
SOUTH
35 - 40
30 - 35
25 - 30
20 - 25
15 - 20
10 - 15
5 - 10
0 - 5

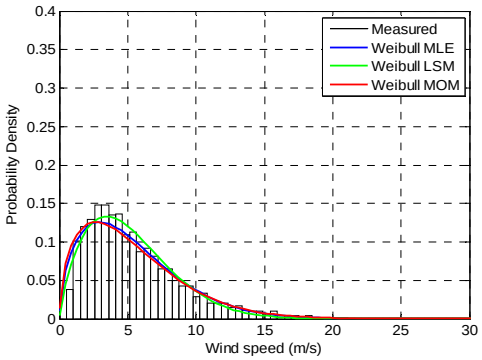
Measured
Weibull MLE
Weibull LSM
Weibull MOM
Probability Density
Wind speed (m/s)

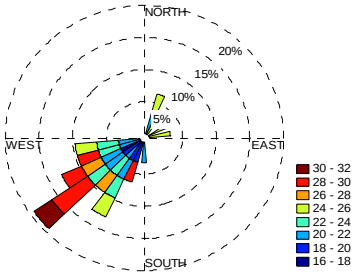
NORTH
20%
15%
10%
5%
WEST
EAST
SOUTH
30 - 32
28 - 30
26 - 28
24 - 26
22 - 24
20 - 22
18 - 20
16 - 18

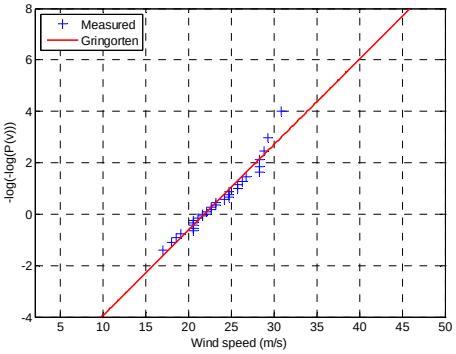
Measured
Gringorten
-log(-log(P(v)))
Wind speed (m/s)

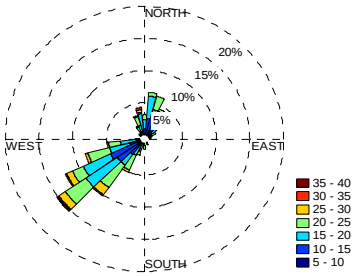
NORTH
20%
15%
10%
5%
WEST
EAST
SOUTH
35 - 40
30 - 35
25 - 30
20 - 25
15 - 20
10 - 15
5 - 10

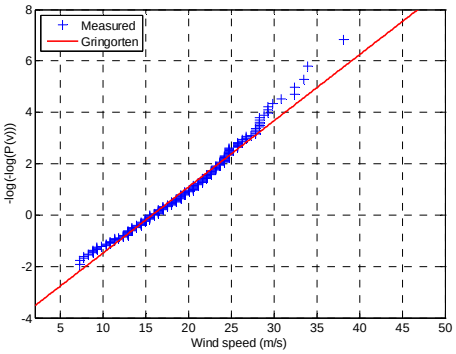
Measured
Gringorten
-log(-log(P(v)))
Wind speed (m/s)

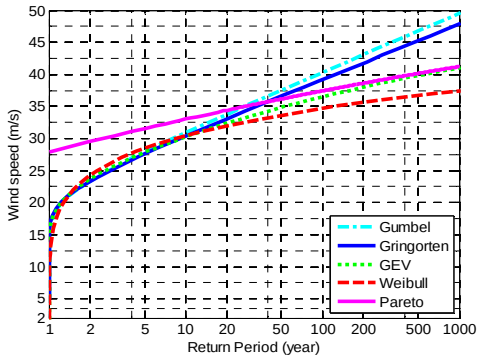
Wind speed (m/s)
Return Period (year)
Gumbel
Gringorten
GEV
Weibull
Pareto

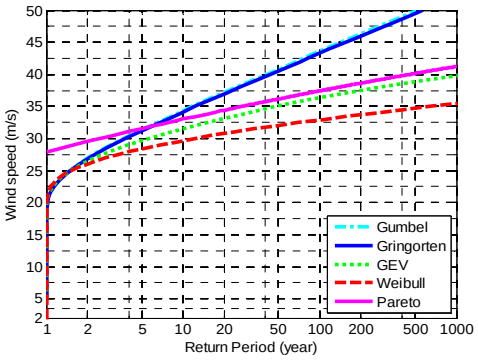
Wind speed (m/s)
Return Period (year)
Gumbel
Gringorten
GEV
Weibull
Pareto

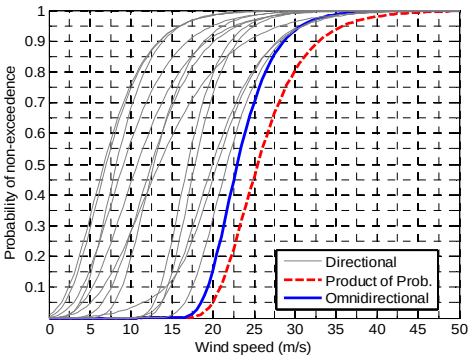
Probability of non-exceedence
Wind speed (m/s)
Directional
Product of Prob.
Omnidirectional

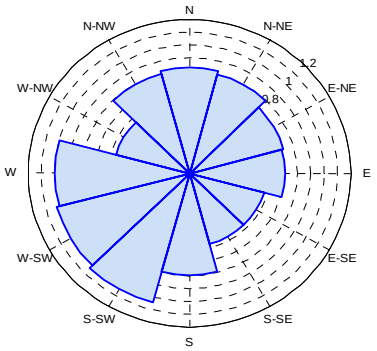
N
N-NE
E-NE
E
E-SE
S-SE
S
S-SW
W
W-NW
N-NW

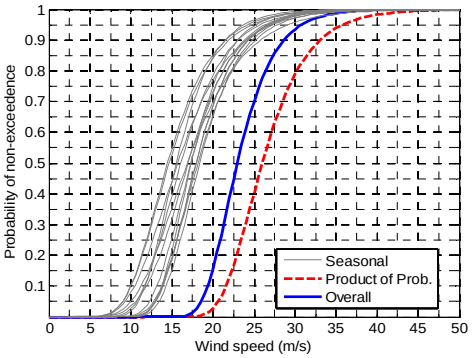
Probability of non-exceedence
Wind speed (m/s)
Seasonal
Product of Prob.
Overall

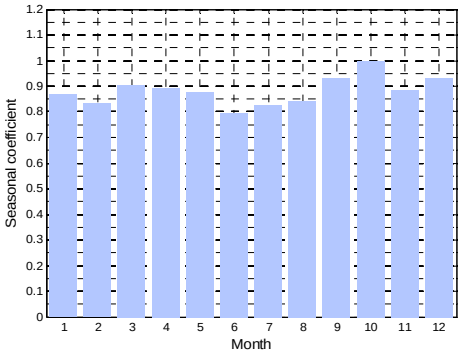
Seasonal coefficient
Month

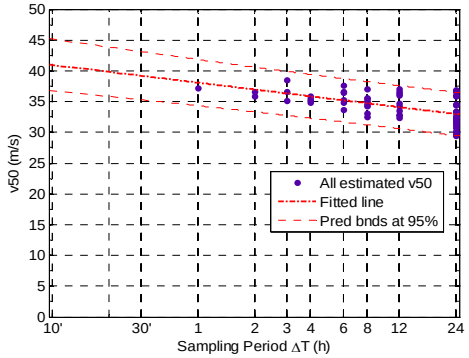
v50 (m/s)
Sampling Period ΔT (h)
All estimated v50
Fitted line
Pred bnds at 95%

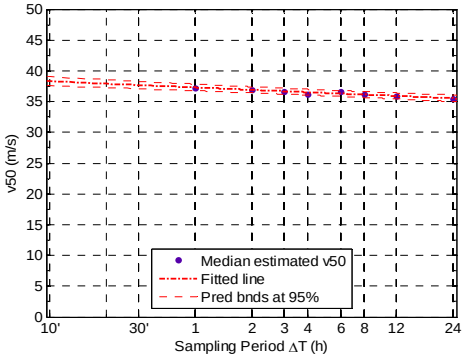
v50 (m/s)
Sampling Period ΔT (h)
Median estimated v50
Fitted line
Pred bnds at 95%

LIMV

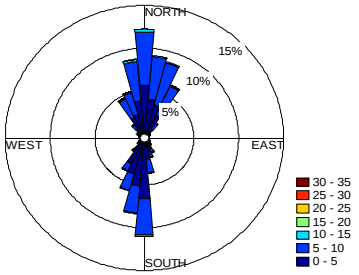
NORTH
15%
10%
5%
WEST
EAST
SOUTH
30 - 35
25 - 30
20 - 25
15 - 20
10 - 15
5 - 10
0 - 5

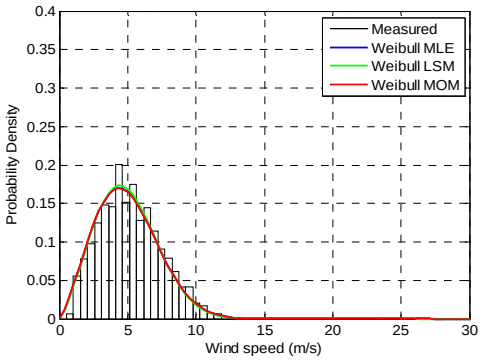
Measured
Weibull MLE
Weibull LSM
Weibull MOM
Probability Density
Wind speed (m/s)

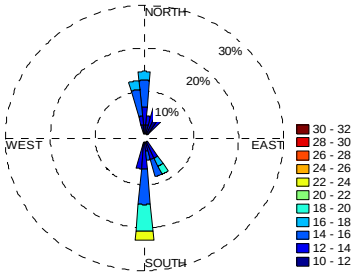
NORTH
30%
20%
10%
WEST
EAST
SOUTH
30 - 32
28 - 30
26 - 28
24 - 26
22 - 24
20 - 22
18 - 20
16 - 18
14 - 16
12 - 14
10 - 12

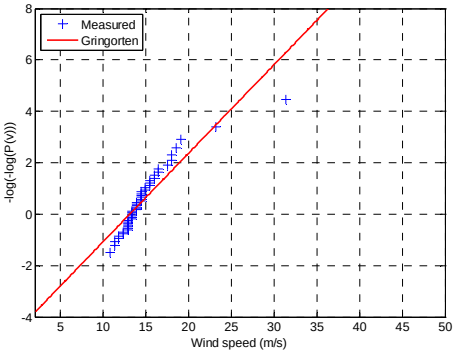
Measured
Gringorten
-log(-log(P(v)))
Wind speed (m/s)

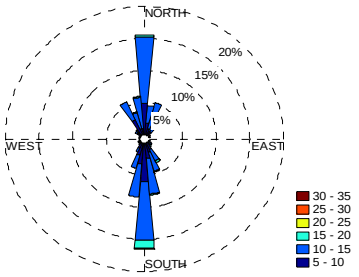
NORTH
20%
15%
10%
5%
WEST
EAST
SOUTH
30 - 35
25 - 30
20 - 25
15 - 20
10 - 15
5 - 10

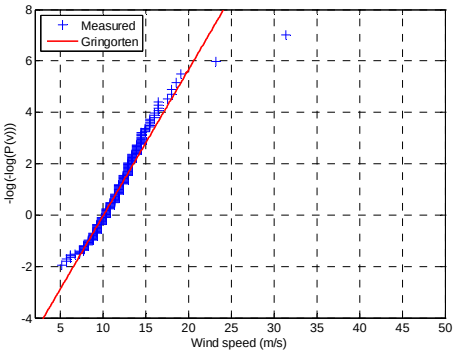
Measured
Gringorten
-log(-log(P(v)))
Wind speed (m/s)

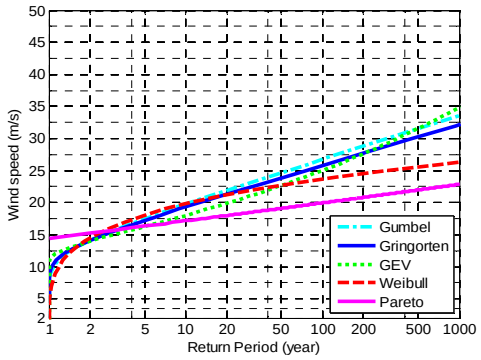
Wind speed (m/s)
Return Period (year)
Gumbel
Gringorten
GEV
Weibull
Pareto

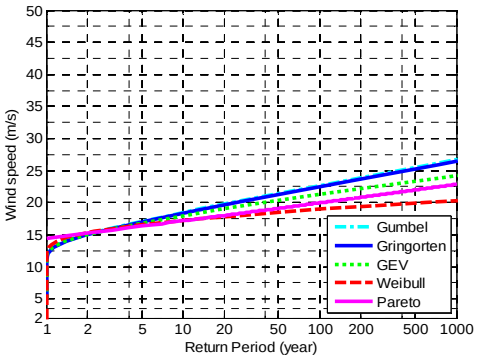
Wind speed (m/s)
Return Period (year)
Gumbel
Gringorten
GEV
Weibull
Pareto

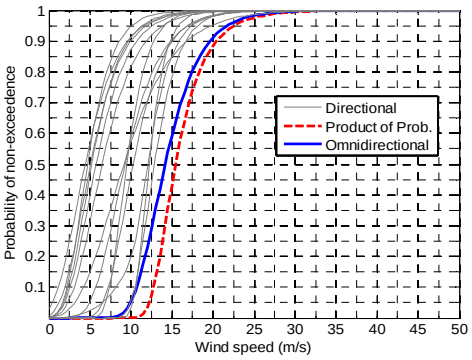
Probability of non-exceedence
Wind speed (m/s)
Directional
Product of Prob.
Omnidirectional

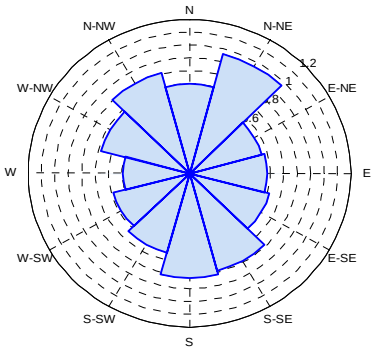
N
N-NE
E-NE
E
E-SE
S-SE
S
S-SW
W
W-NW
N-NW

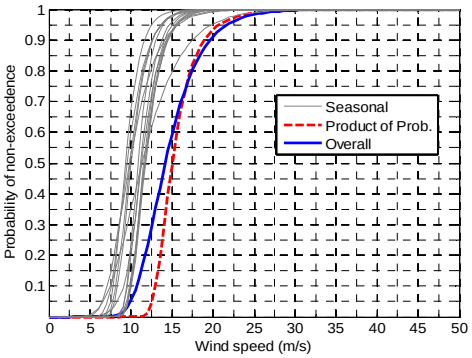
Probability of non-exceedence
Wind speed (m/s)
Seasonal
Product of Prob.
Overall

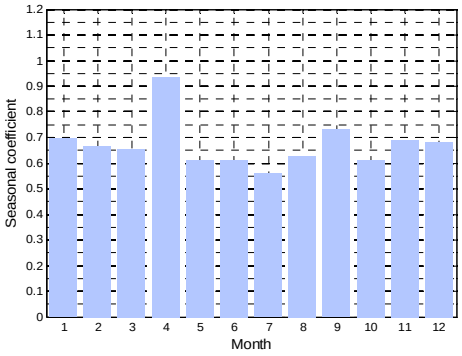
Seasonal coefficient
Month

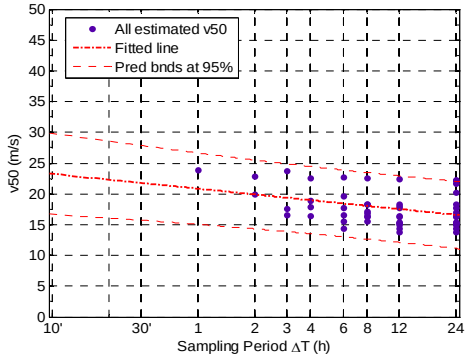
All estimated v50
Fitted line
Pred bnds at 95%
v50 (m/s)
Sampling Period ΔT (h)

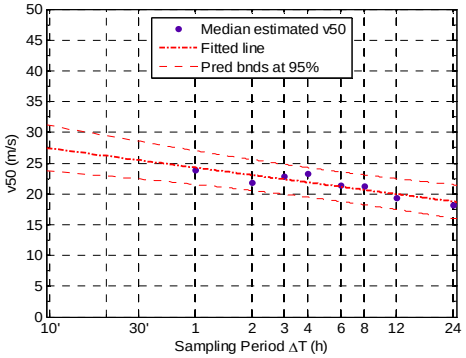
Median estimated v50
Fitted line
Pred bnds at 95%
v50 (m/s)
Sampling Period ΔT (h)

LIMY

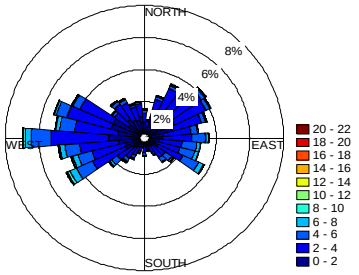
NORTH
8%
6%
4%
2%
WEST
EAST
SOUTH
20 - 22
18 - 20
16 - 18
14 - 16
12 - 14
10 - 12
8 - 10
6 - 8
4 - 6
2 - 4
0 - 2

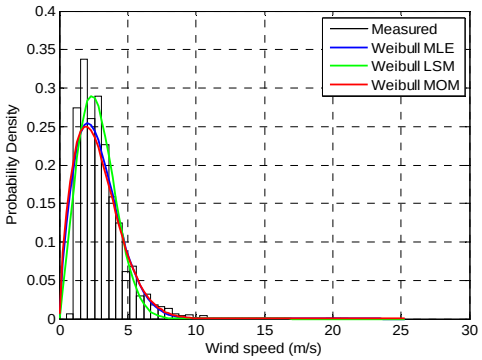
Measured
Weibull MLE
Weibull LSM
Weibull MOM
Probability Density
Wind speed (m/s)

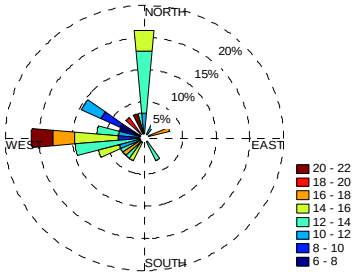
NORTH
20%
15%
10%
5%
WEST
EAST
SOUTH
20 - 22
18 - 20
16 - 18
14 - 16
12 - 14
10 - 12
8 - 10
6 - 8

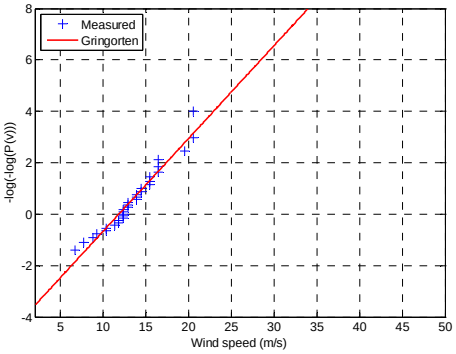
Measured
Gringorten
-log(-log(P(v)))
Wind speed (m/s)

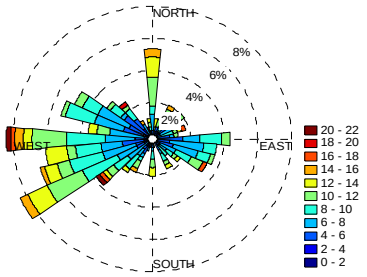
NORTH
8%
6%
4%
2%
WEST
EAST
SOUTH
20 - 22
18 - 20
16 - 18
14 - 16
12 - 14
10 - 12
8 - 10
6 - 8
4 - 6
2 - 4
0 - 2

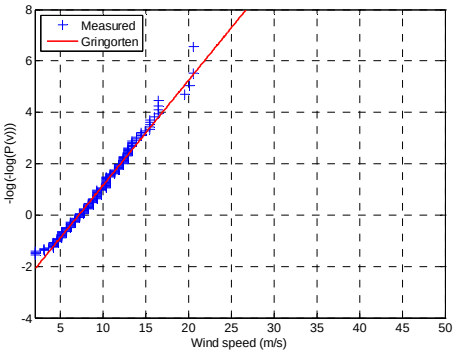
Measured
Gringorten
-log(-log(P(v)))
Wind speed (m/s)

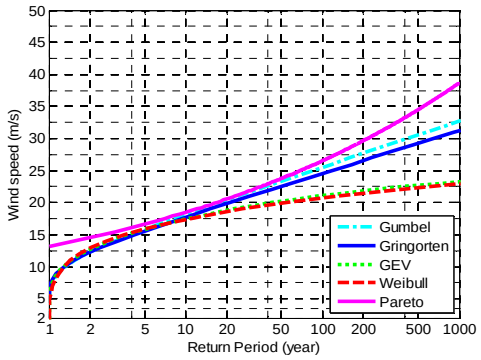
Wind speed (m/s)
Return Period (year)
Gumbel
Gringorten
GEV
Weibull
Pareto

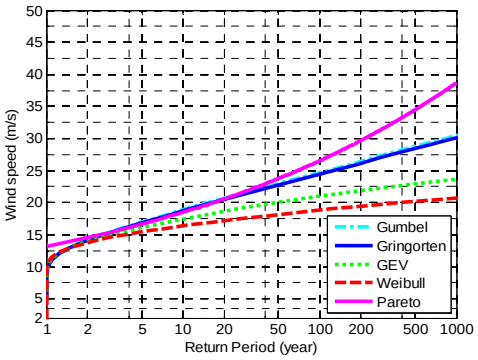
Wind speed (m/s)
Return Period (year)
Gumbel
Gringorten
GEV
Weibull
Pareto

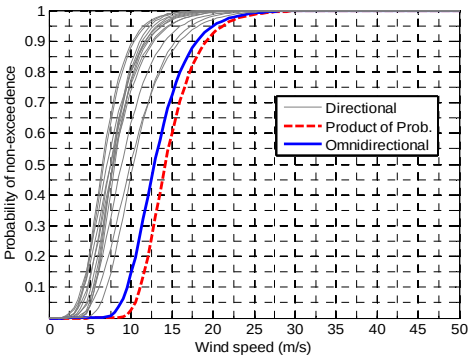
Probability of non-exceedence
Wind speed (m/s)
Directional
Product of Prob.
Omnidirectional

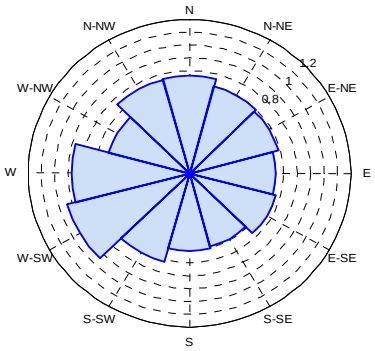
N
N-NE
E-NE
E
E-SE
S-SE
S
S-SW
W
W-NW
N-NW

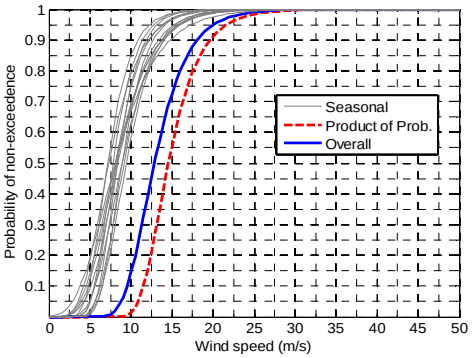
Probability of non-exceedence
Wind speed (m/s)
Seasonal
Product of Prob.
Overall

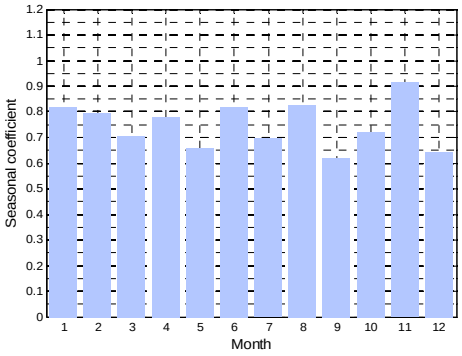
Seasonal coefficient
Month

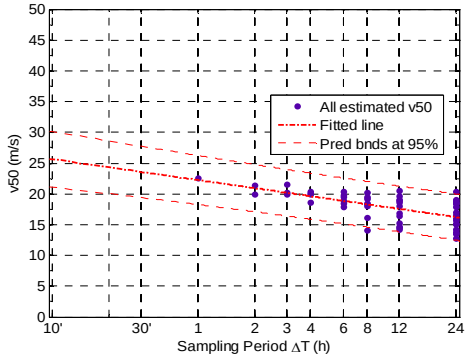
v50 (m/s)
Sampling Period ΔT (h)
All estimated v50
Fitted line
Pred bnds at 95%

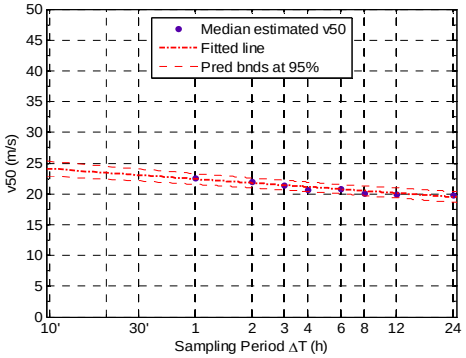
v50 (m/s)
Sampling Period ΔT (h)
Median estimated v50
Fitted line
Pred bnds at 95%

LIPA

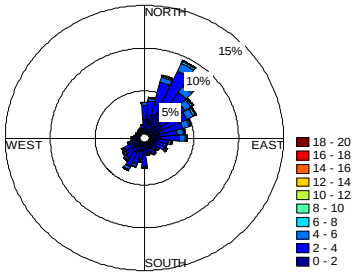
NORTH
15%
10%
5%
WEST
EAST
SOUTH
18 - 20
16 - 18
14 - 16
12 - 14
10 - 12
8 - 10
6 - 8
4 - 6
2 - 4
0 - 2

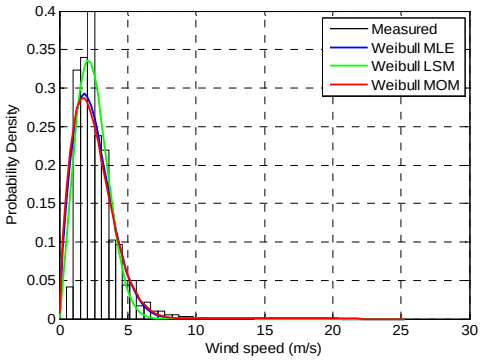
Measured
Weibull MLE
Weibull LSM
Weibull MOM
Probability Density
Wind speed (m/s)

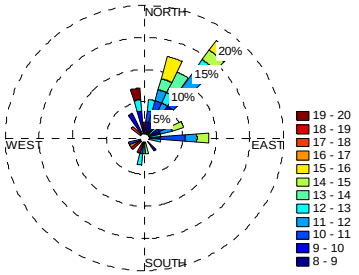
NORTH
20%
15%
10%
5%
WEST
EAST
SOUTH
19 - 20
18 - 19
17 - 18
16 - 17
15 - 16
14 - 15
13 - 14
12 - 13
11 - 12
10 - 11
9 - 10
8 - 9

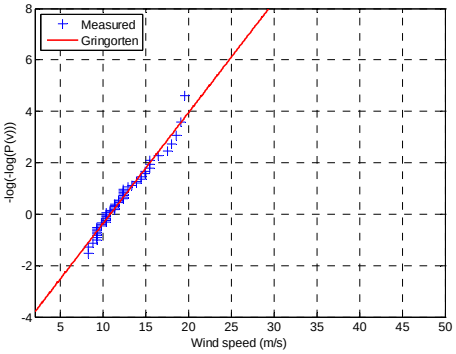
Measured
Gringorten
-log(-log(P(v)))
Wind speed (m/s)

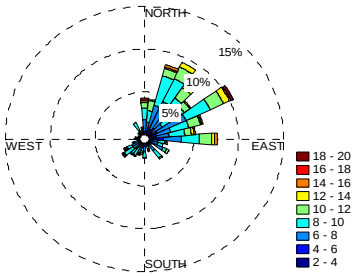
NORTH
15%
10%
5%
WEST
EAST
SOUTH
18 - 20
16 - 18
14 - 16
12 - 14
10 - 12
8 - 10
6 - 8
4 - 6
2 - 4

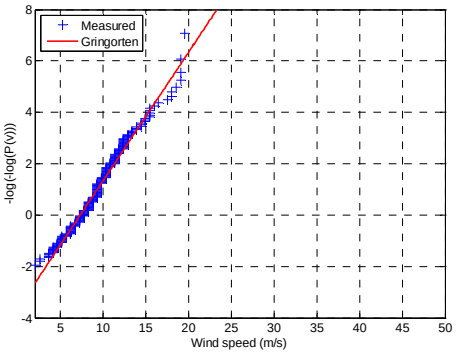
Measured
Gringorten
-log(-log(P(v)))
Wind speed (m/s)

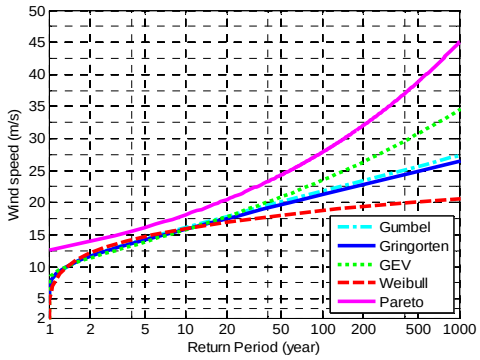
Wind speed (m/s)
Return Period (year)
Gumbel
Gringorten
GEV
Weibull
Pareto

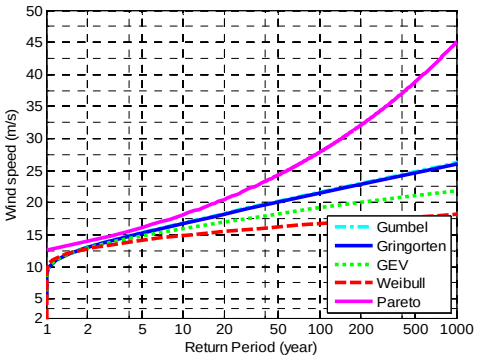
Wind speed (m/s)
Return Period (year)
Gumbel
Gringorten
GEV
Weibull
Pareto

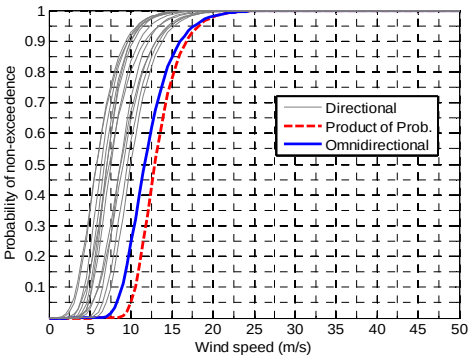
Probability of non-exceedence
Wind speed (m/s)
Directional
Product of Prob.
Omnidirectional

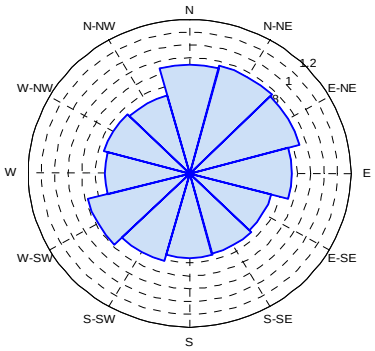
N
N-NE
E-NE
E
E-SE
S-SE
S
S-SW
W
W-NW
N-NW

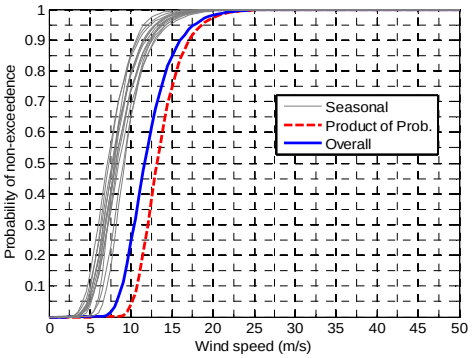
Probability of non-exceedence
Wind speed (m/s)
Seasonal
Product of Prob.
Overall

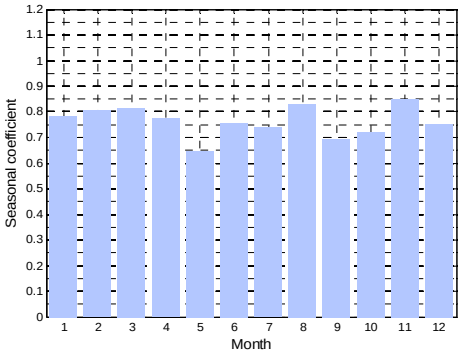
Seasonal coefficient
Month

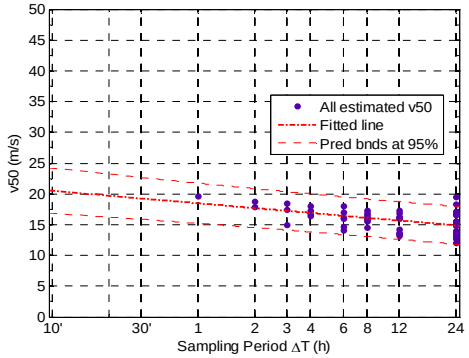
v50 (m/s)
Sampling Period ΔT (h)
All estimated v50
Fitted line
Pred bnds at 95%

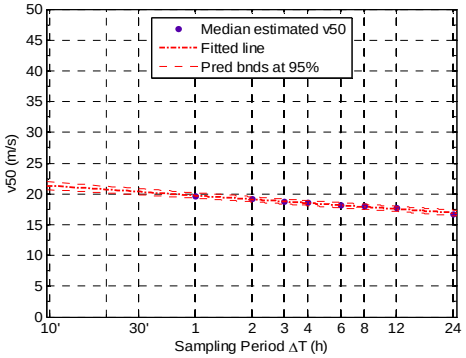
v50 (m/s)
Sampling Period ΔT (h)
Median estimated v50
Fitted line
Pred bnds at 95%

LIPB

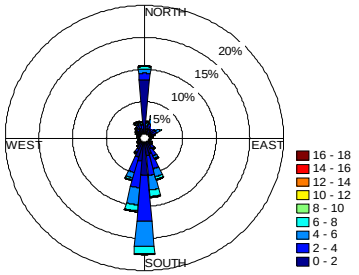
NORTH
20%
15%
10%
5%
WEST
EAST
SOUTH
16 - 18
14 - 16
12 - 14
10 - 12
8 - 10
6 - 8
4 - 6
2 - 4
0 - 2

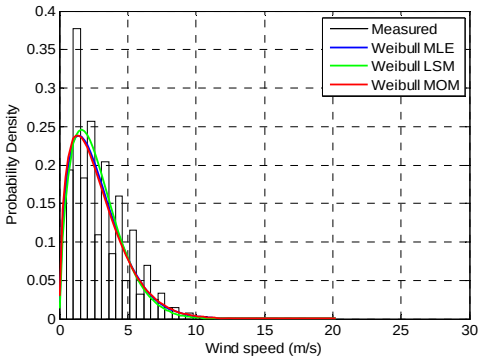
Measured
Weibull MLE
Weibull LSM
Weibull MOM
Probability Density
Wind speed (m/s)

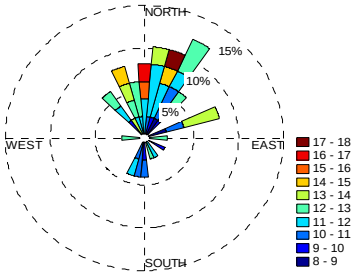
NORTH
15%
10%
5%
WEST
EAST
SOUTH
17 - 18
16 - 17
15 - 16
14 - 15
13 - 14
12 - 13
11 - 12
10 - 11
9 - 10
8 - 9

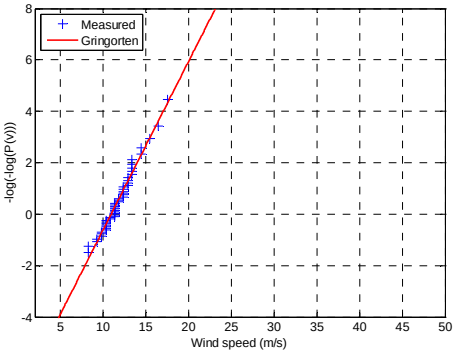
Measured
Gringorten
-log(-log(P(v)))
Wind speed (m/s)

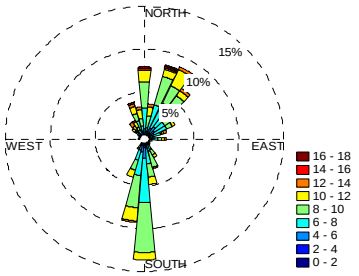
NORTH
15%
10%
5%
WEST
EAST
SOUTH
16 - 18
14 - 16
12 - 14
10 - 12
8 - 10
6 - 8
4 - 6
2 - 4
0 - 2

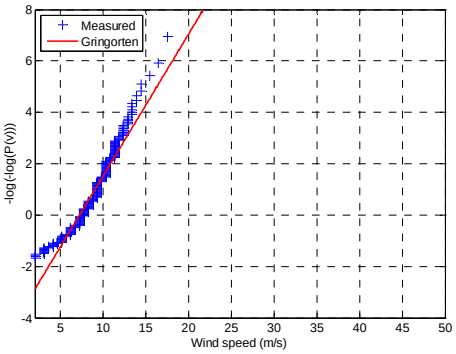
Measured
Gringorten
-log(-log(P(v)))
Wind speed (m/s)

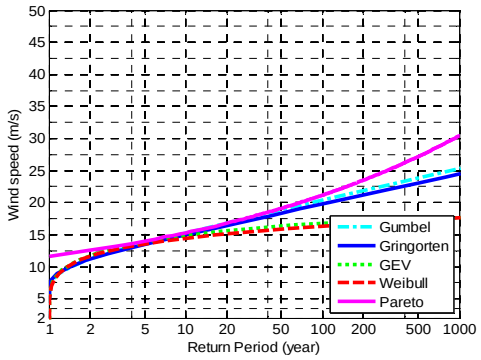
Wind speed (m/s)
Return Period (year)
Gumbel
Gringorten
GEV
Weibull
Pareto

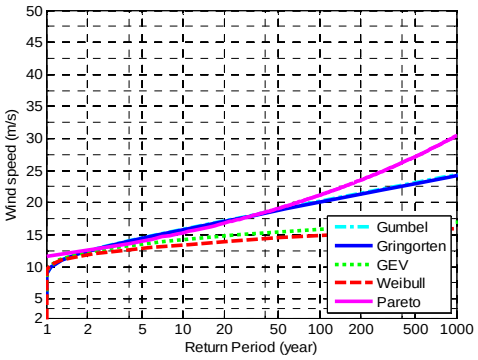
Wind speed (m/s)
Return Period (year)
Gumbel
Gringorten
GEV
Weibull
Pareto

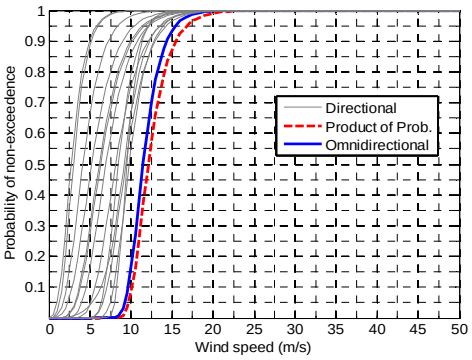
Probability of non-exceedence
Wind speed (m/s)
Directional
Product of Prob.
Omnidirectional

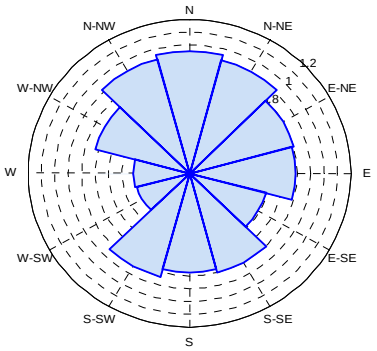
N
N-NE
E-NE
E
E-SE
S-SE
S
S-SW
W
W-NW
N-NW

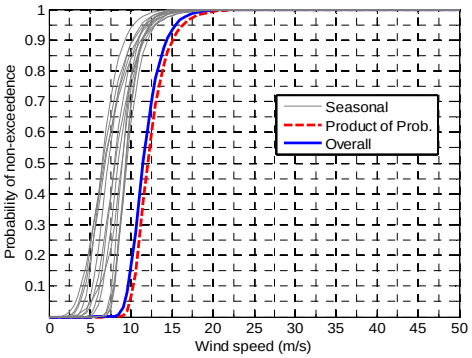
Probability of non-exceedence
Wind speed (m/s)
Seasonal
Product of Prob.
Overall

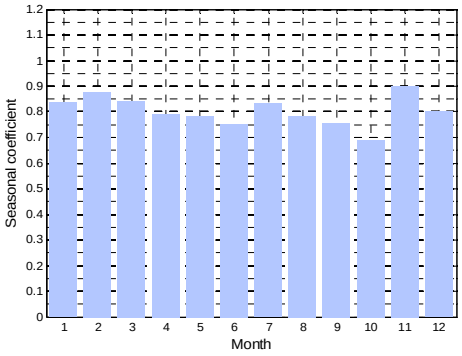
Seasonal coefficient
Month

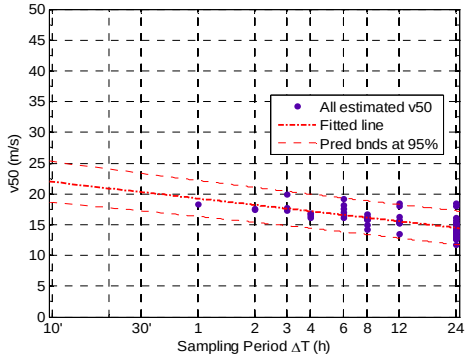
v50 (m/s)
Sampling Period ΔT (h)
All estimated v50
Fitted line
Pred bnds at 95%

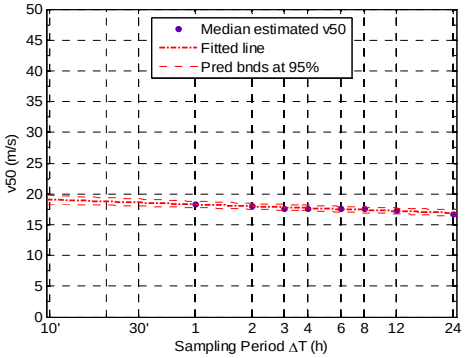
v50 (m/s)
Sampling Period ΔT (h)
Median estimated v50
Fitted line
Pred bnds at 95%

LIPC

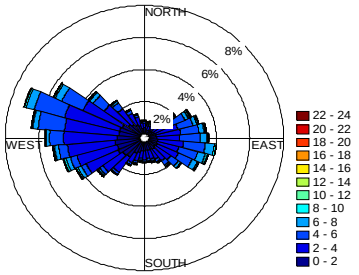
NORTH
8%
6%
4%
2%
WEST
EAST
SOUTH
22 - 24
20 - 22
18 - 20
16 - 18
14 - 16
12 - 14
10 - 12
8 - 10
6 - 8
4 - 6
2 - 4
0 - 2

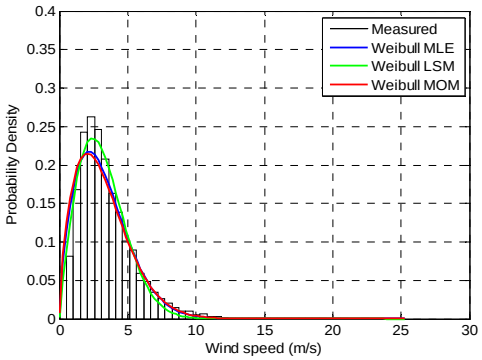
Measured
Weibull MLE
Weibull LSM
Weibull MOM
Probability Density
Wind speed (m/s)

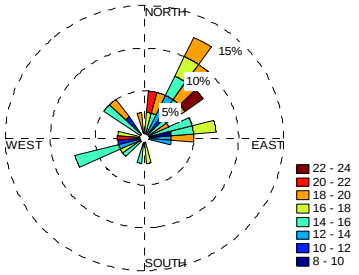
NORTH
15%
10%
5%
WEST
EAST
SOUTH
22 - 24
20 - 22
18 - 20
16 - 18
14 - 16
12 - 14
10 - 12
8 - 10

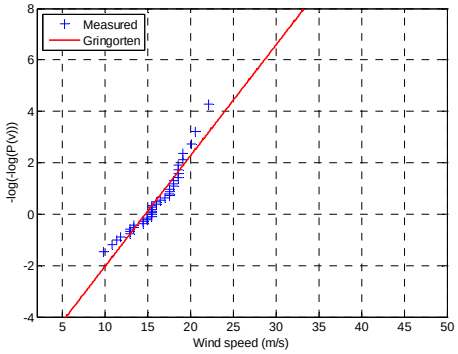
Measured
Gringorten
-log(-log(P(v)))
Wind speed (m/s)

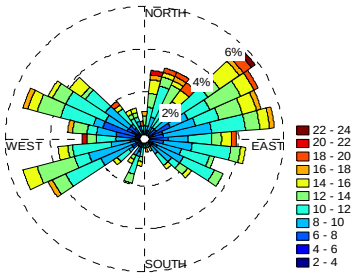
NORTH
6%
4%
2%
WEST
EAST
SOUTH
22 - 24
20 - 22
18 - 20
16 - 18
14 - 16
12 - 14
10 - 12
8 - 10
6 - 8
4 - 6
2 - 4

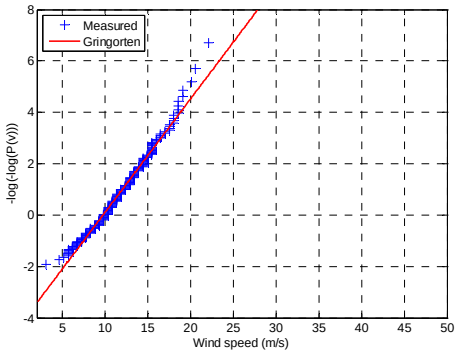
Measured
Gringorten
-log(-log(P(v)))
Wind speed (m/s)

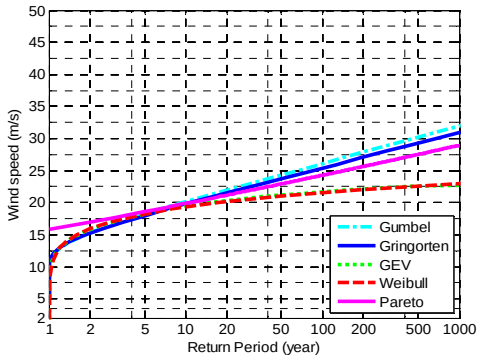
Wind speed (m/s)
Return Period (year)
Gumbel
Gringorten
GEV
Weibull
Pareto

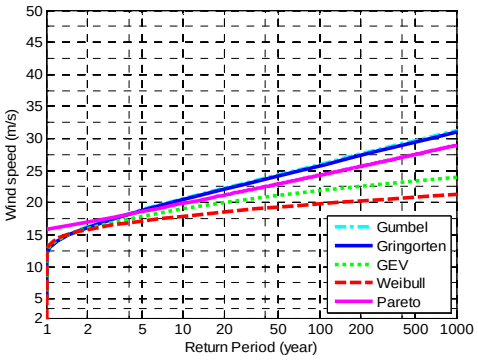
Wind speed (m/s)
Return Period (year)
Gumbel
Gringorten
GEV
Weibull
Pareto

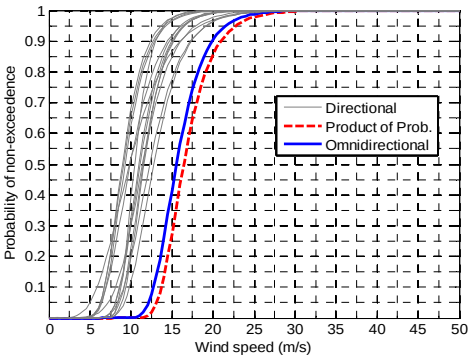
Probability of non-exceedence
Wind speed (m/s)
Directional
Product of Prob.
Omnidirectional

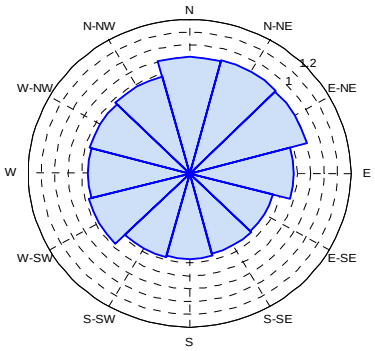
N
N-NE
E-NE
E
E-SE
S-SE
S
S-SW
W
W-NW
N-NW

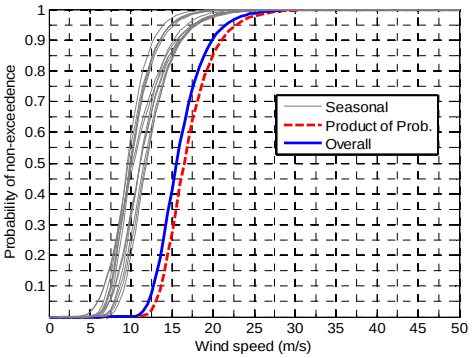
Probability of non-exceedence
Wind speed (m/s)
Seasonal
Product of Prob.
Overall

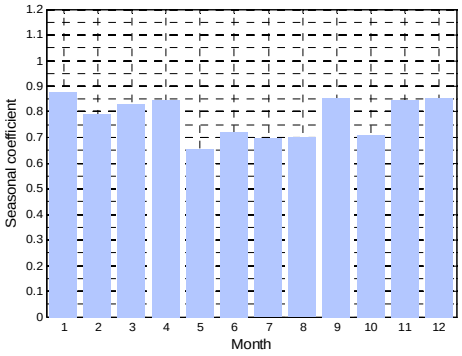
Seasonal coefficient
Month

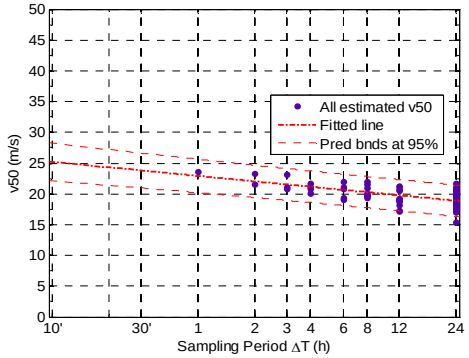
v50 (m/s)
Sampling Period ΔT (h)
All estimated v50
Fitted line
Pred bnds at 95%

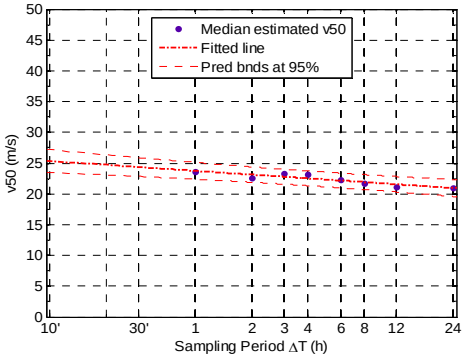
v50 (m/s)
Sampling Period ΔT (h)
Median estimated v50
Fitted line
Pred bnds at 95%

LIPD

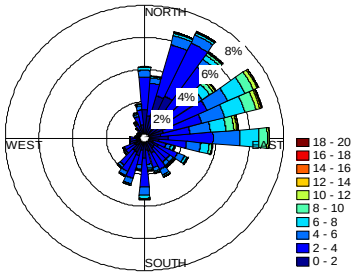
NORTH
8%
6%
4%
2%
WEST
EAST
SOUTH
18 - 20
16 - 18
14 - 16
12 - 14
10 - 12
8 - 10
6 - 8
4 - 6
2 - 4
0 - 2

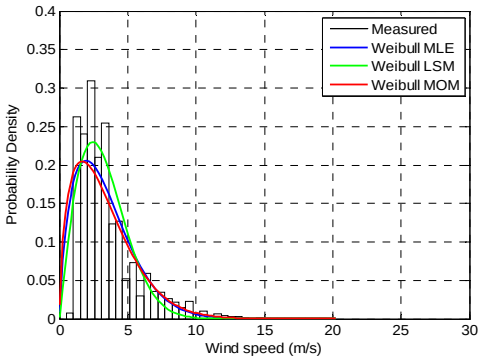
Measured
Weibull MLE
Weibull LSM
Weibull MOM
Probability Density
Wind speed (m/s)

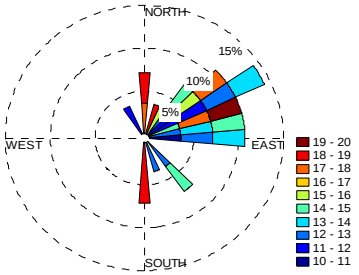
NORTH
15%
10%
5%
WEST
EAST
SOUTH
19 - 20
18 - 19
17 - 18
16 - 17
15 - 16
14 - 15
13 - 14
12 - 13
11 - 12
10 - 11

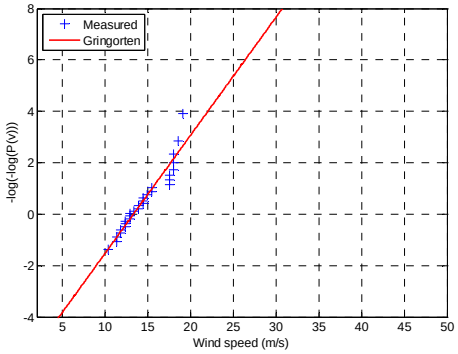
Measured
Gringorten
-log(-log(P(v)))
Wind speed (m/s)

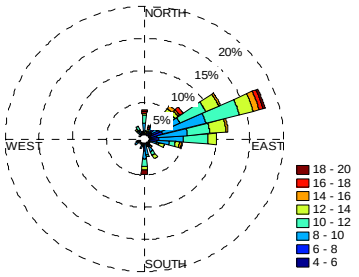
NORTH
20%
15%
10%
5%
WEST
EAST
SOUTH
18 - 20
16 - 18
14 - 16
12 - 14
10 - 12
8 - 10
6 - 8
4 - 6

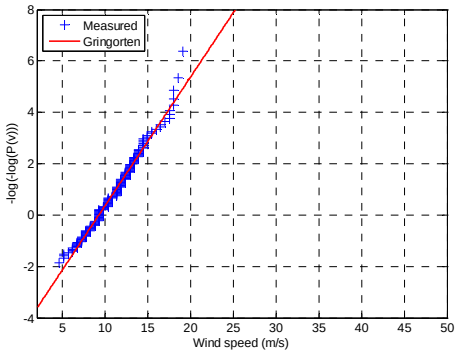
Measured
Gringorten
-log(-log(P(v)))
Wind speed (m/s)

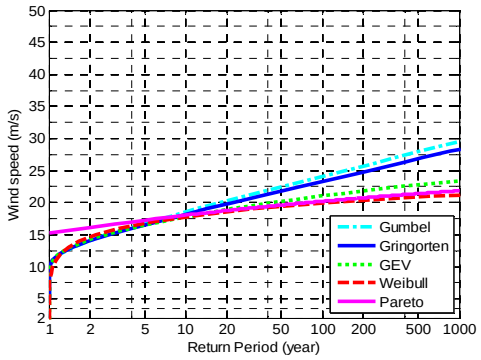
Wind speed (m/s)
Return Period (year)
Gumbel
Gringorten
GEV
Weibull
Pareto

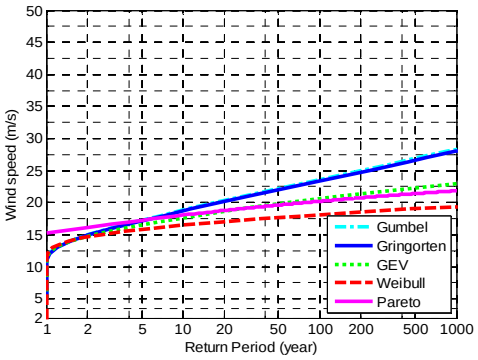
Wind speed (m/s)
Return Period (year)
Gumbel
Gringorten
GEV
Weibull
Pareto

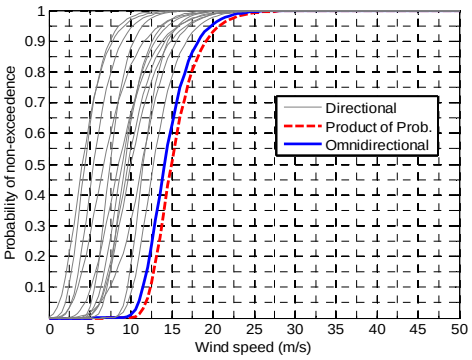
Probability of non-exceedence
Wind speed (m/s)
Directional
Product of Prob.
Omnidirectional

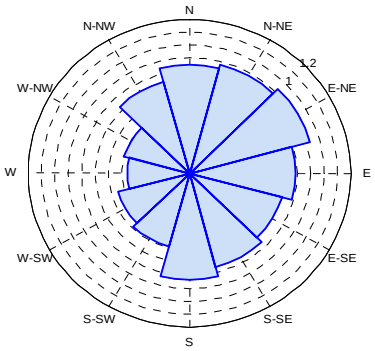
N
N-NE
E-NE
E
E-SE
S-SE
S
S-SW
W
W-NW
N-NW

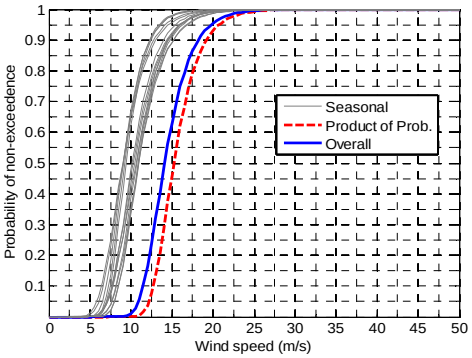
Probability of non-exceedence
Wind speed (m/s)
Seasonal
Product of Prob.
Overall

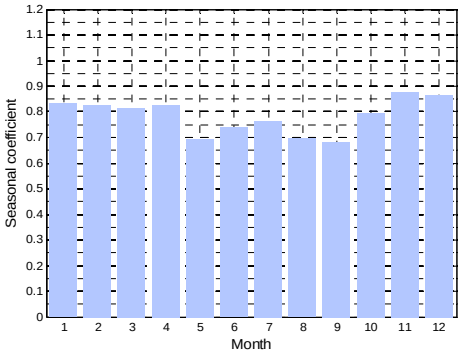
Seasonal coefficient
Month

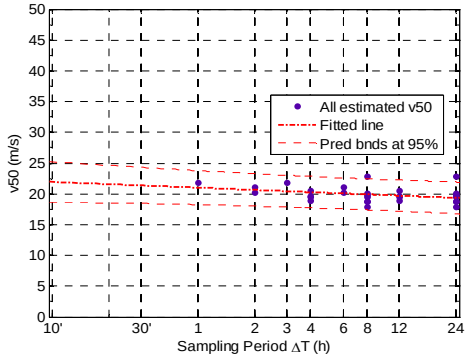
v50 (m/s)
Sampling Period ΔT (h)
All estimated v50
Fitted line
Pred bnds at 95%

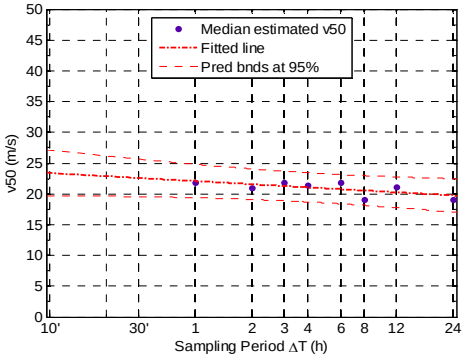
v50 (m/s)
Sampling Period ΔT (h)
Median estimated v50
Fitted line
Pred bnds at 95%

LIPE

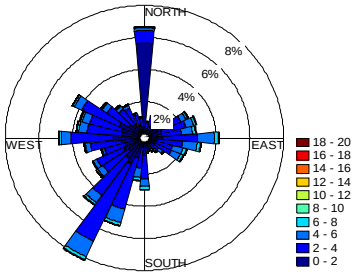
NORTH
8%
6%
4%
2%
WEST
EAST
SOUTH
18 - 20
16 - 18
14 - 16
12 - 14
10 - 12
8 - 10
6 - 8
4 - 6
2 - 4
0 - 2

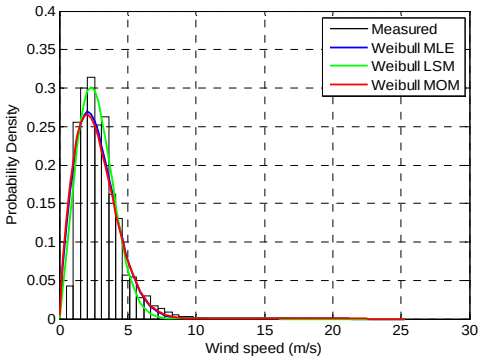
Measured
Weibull MLE
Weibull LSM
Weibull MOM
Probability Density
Wind speed (m/s)

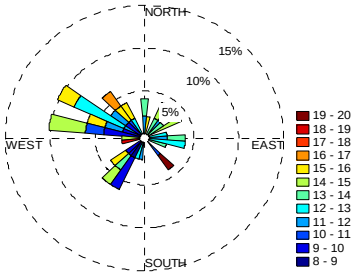
NORTH
15%
10%
5%
WEST
EAST
SOUTH
19 - 20
18 - 19
17 - 18
16 - 17
15 - 16
14 - 15
13 - 14
12 - 13
11 - 12
10 - 11
9 - 10
8 - 9

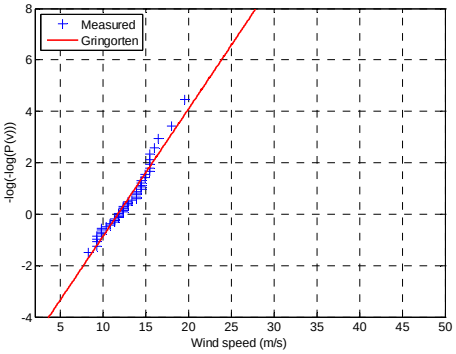
Measured
Gringorten
-log(-log(P(v)))
Wind speed (m/s)

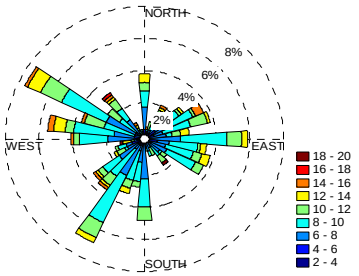
NORTH
8%
6%
4%
2%
WEST
EAST
SOUTH
18 - 20
16 - 18
14 - 16
12 - 14
10 - 12
8 - 10
6 - 8
4 - 6
2 - 4

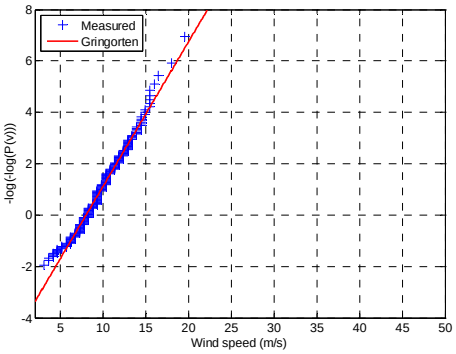
Measured
Gringorten
-log(-log(P(v)))
Wind speed (m/s)

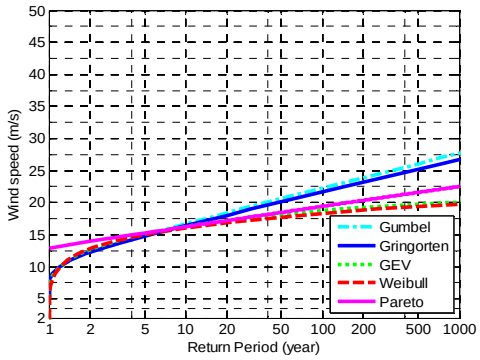
Wind speed (m/s)
Return Period (year)
Gumbel
Gringorten
GEV
Weibull
Pareto

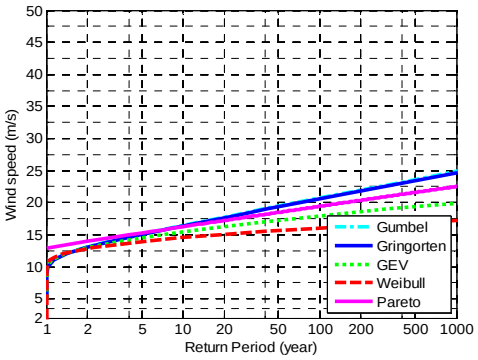
Wind speed (m/s)
Return Period (year)
Gumbel
Gringorten
GEV
Weibull
Pareto

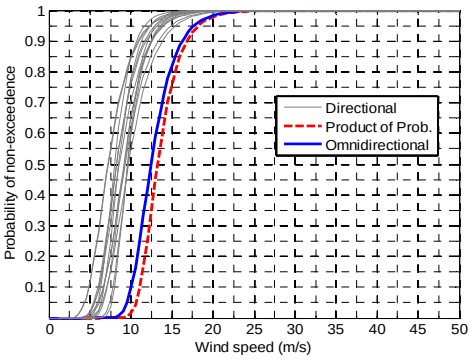
Probability of non-exceedence
Wind speed (m/s)
Directional
Product of Prob.
Omnidirectional

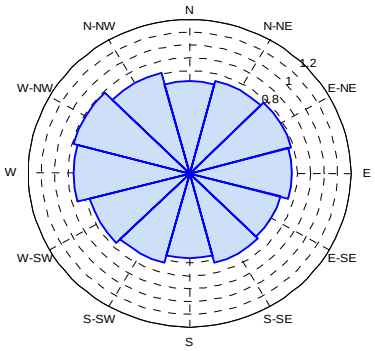
N
N-NE
E-NE
E
E-SE
S-SE
S
S-SW
W
W-NW
N-NW

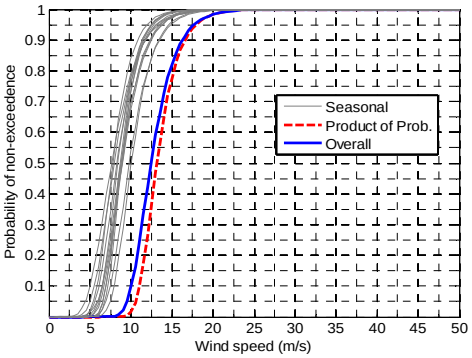
Probability of non-exceedence
Wind speed (m/s)
Seasonal
Product of Prob.
Overall

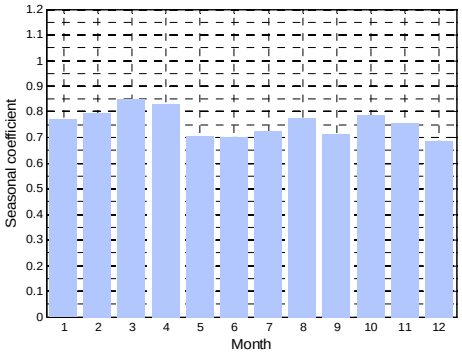
Seasonal coefficient
Month

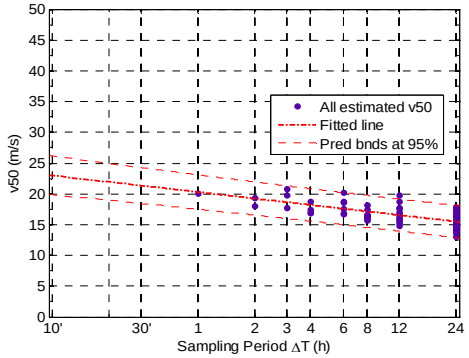
v50 (m/s)
Sampling Period ΔT (h)
All estimated v50
Fitted line
Pred bnds at 95%

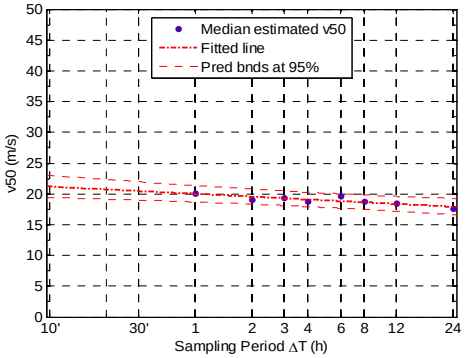
v50 (m/s)
Sampling Period ΔT (h)
Median estimated v50
Fitted line
Pred bnds at 95%

LIPF

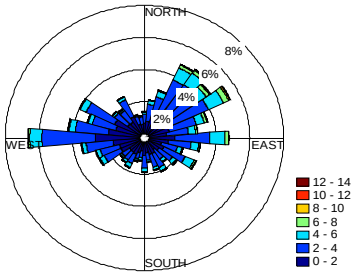
NORTH
8%
6%
4%
2%
WEST
EAST
SOUTH
12 - 14
10 - 12
8 - 10
6 - 8
4 - 6
2 - 4
0 - 2

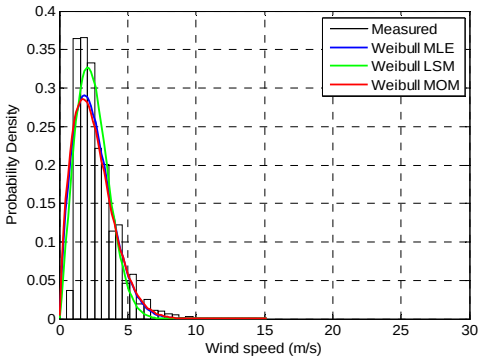
Measured
Weibull MLE
Weibull LSM
Weibull MOM
Probability Density
Wind speed (m/s)

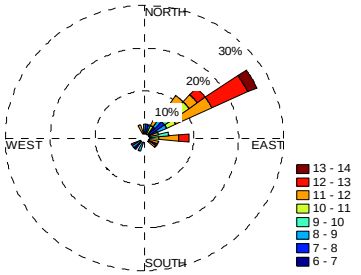
NORTH
30%
20%
10%
WEST
EAST
SOUTH
13 - 14
12 - 13
11 - 12
10 - 11
9 - 10
8 - 9
7 - 8
6 - 7

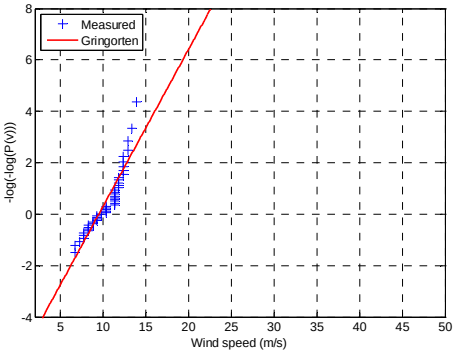
Measured
Gringorten
-log(-log(P(v)))
Wind speed (m/s)

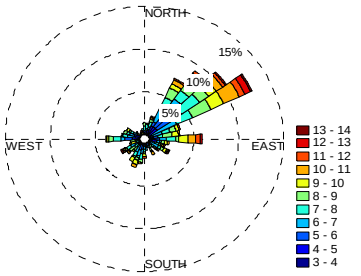
NORTH
15%
10%
5%
WEST
EAST
SOUTH
13 - 14
12 - 13
11 - 12
10 - 11
9 - 10
8 - 9
7 - 8
6 - 7
5 - 6
4 - 5
3 - 4

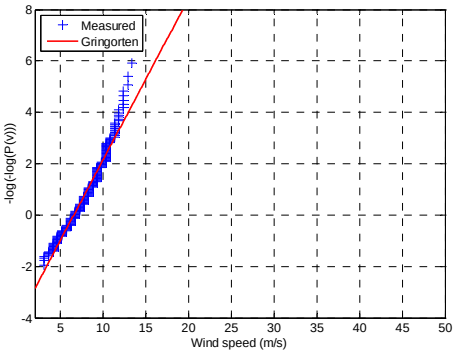
Measured
Gringorten
-log(-log(P(v)))
Wind speed (m/s)

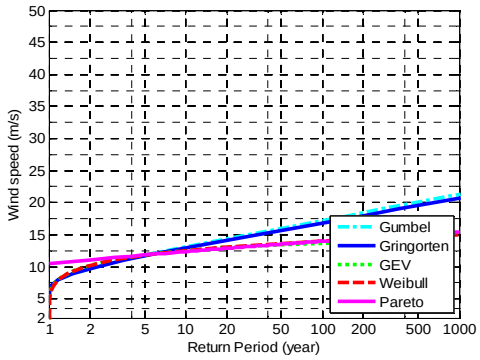
Wind speed (m/s)
Return Period (year)
Gumbel
Gringorten
GEV
Weibull
Pareto

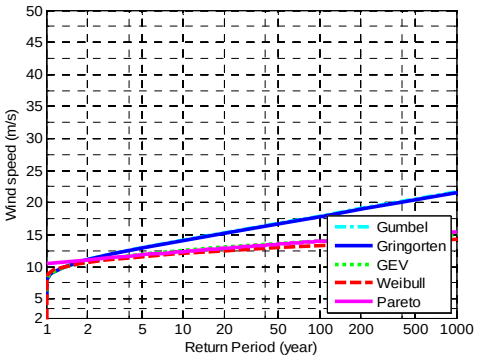
Wind speed (m/s)
Return Period (year)
Gumbel
Gringorten
GEV
Weibull
Pareto

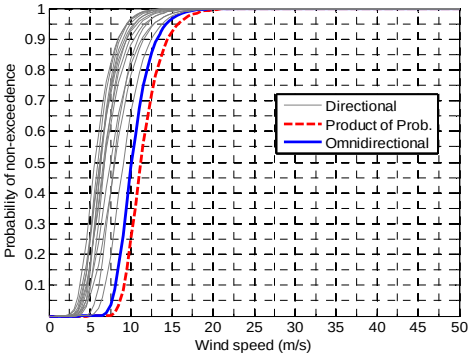
Probability of non-exceedence
Wind speed (m/s)
Directional
Product of Prob.
Omnidirectional

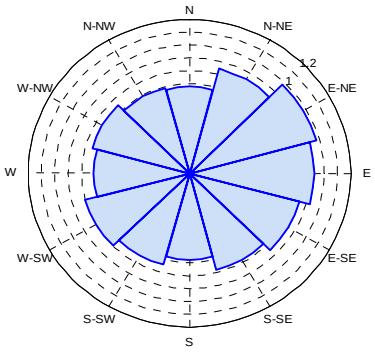
N
N-NE
E-NE
E
E-SE
S-SE
S
S-SW
W
W-NW
N-NW

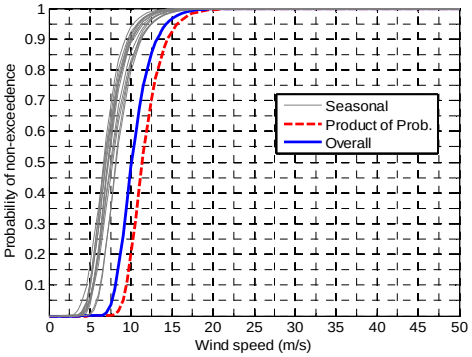
Probability of non-exceedence
Wind speed (m/s)
Seasonal
Product of Prob.
Overall

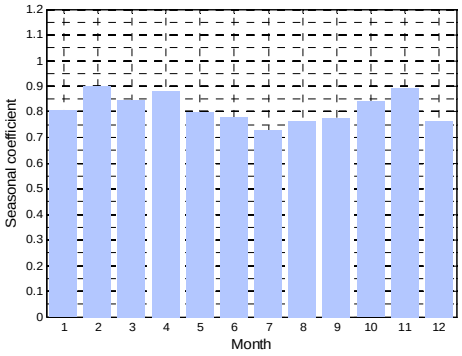
Seasonal coefficient
Month

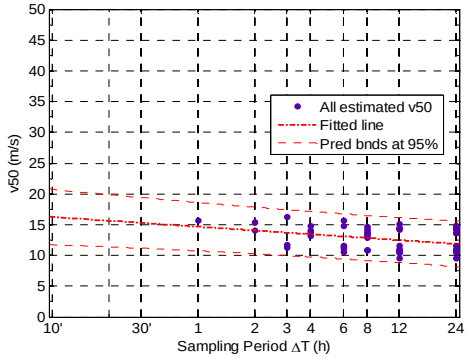
v50 (m/s)
Sampling Period ΔT (h)
All estimated v50
Fitted line
Pred bnds at 95%

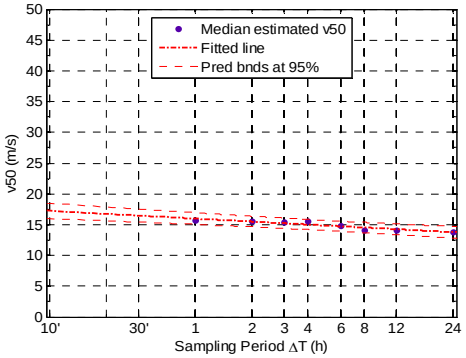
v50 (m/s)
Sampling Period ΔT (h)
Median estimated v50
Fitted line
Pred bnds at 95%

LIPH

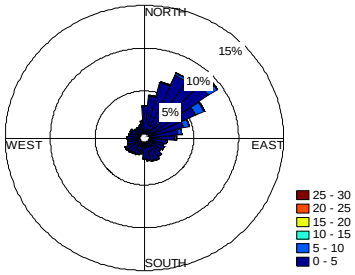
NORTH
15%
10%
5%
WEST
EAST
SOUTH
25 - 30
20 - 25
15 - 20
10 - 15
5 - 10
0 - 5

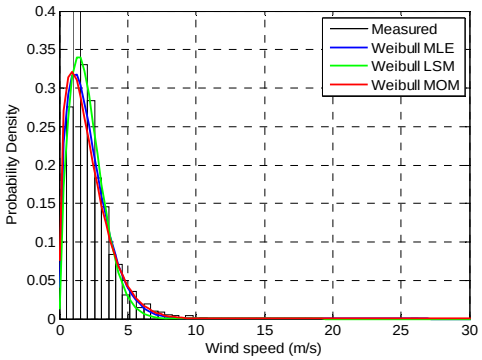
Measured
Weibull MLE
Weibull LSM
Weibull MOM
Probability Density
Wind speed (m/s)

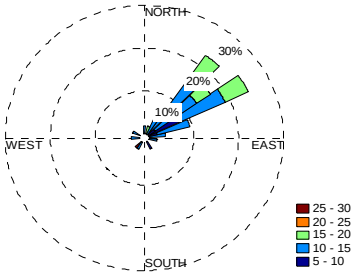
NORTH
30%
20%
10%
WEST
EAST
SOUTH
25 - 30
20 - 25
15 - 20
10 - 15
5 - 10

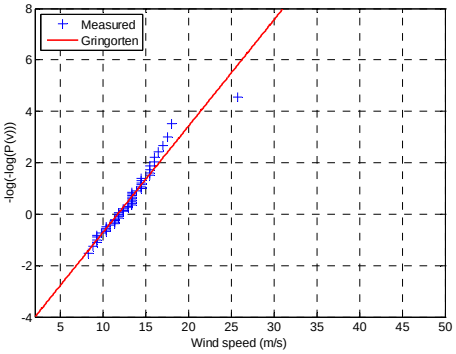
Measured
Gringorten
-log(-log(P(v)))
Wind speed (m/s)

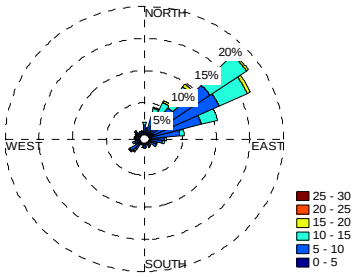
NORTH
20%
15%
10%
5%
WEST
EAST
SOUTH
25 - 30
20 - 25
15 - 20
10 - 15
5 - 10
0 - 5

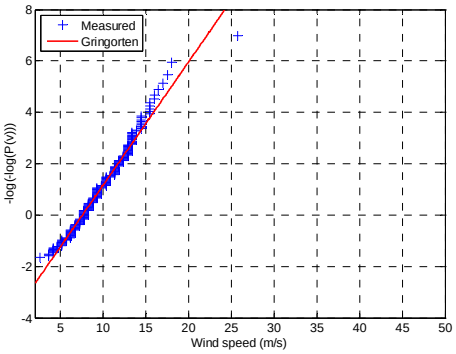
Measured
Gringorten
-log(-log(P(v)))
Wind speed (m/s)

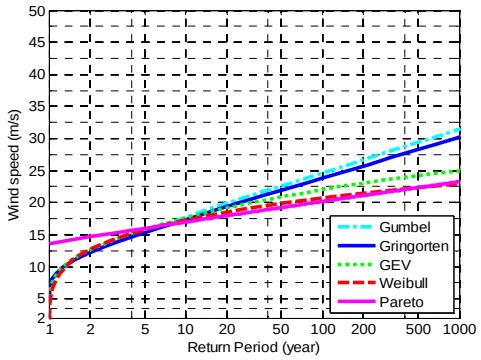
Wind speed (m/s)
Return Period (year)
Gumbel
Gringorten
GEV
Weibull
Pareto

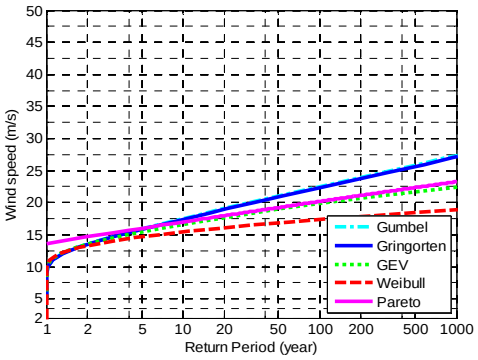
Wind speed (m/s)
Return Period (year)
Gumbel
Gringorten
GEV
Weibull
Pareto

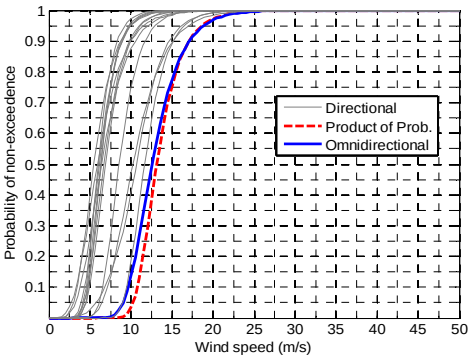
Probability of non-exceedence
Wind speed (m/s)
Directional
Product of Prob.
Omnidirectional

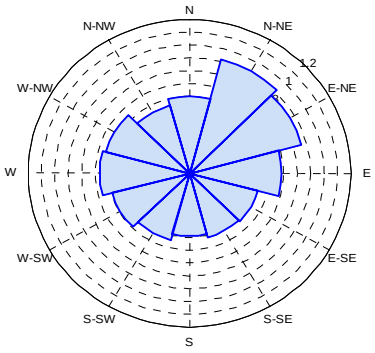
N
N-NE
E-NE
E
E-SE
S-SE
S
S-SW
W-SW
W
W-NW
N-NW

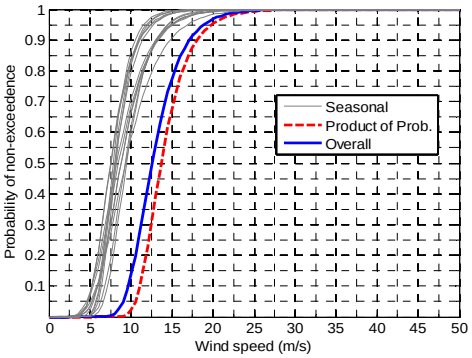
Probability of non-exceedence
Wind speed (m/s)
Seasonal
Product of Prob.
Overall

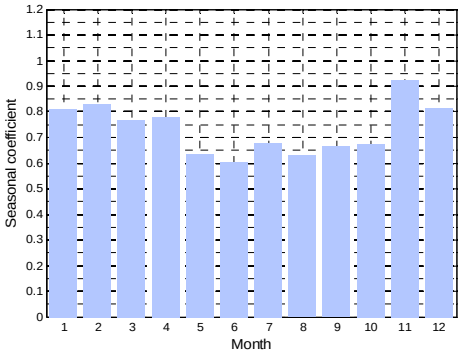
Seasonal coefficient
Month

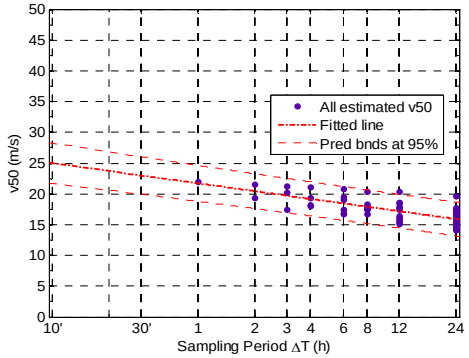
v50 (m/s)
Sampling Period ΔT (h)
All estimated v50
Fitted line
Pred bnds at 95%

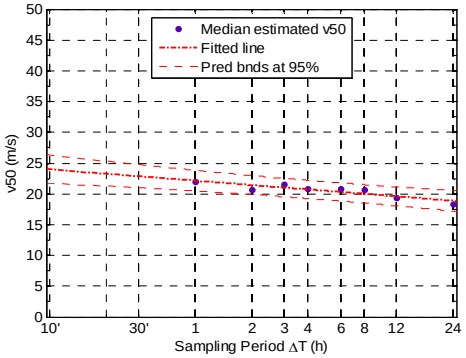
v50 (m/s)
Sampling Period ΔT (h)
Median estimated v50
Fitted line
Pred bnds at 95%

LIPI

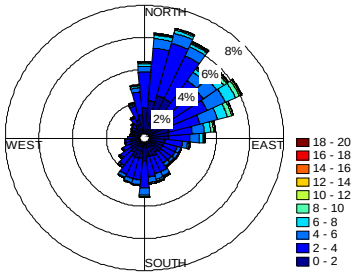
NORTH
EAST
SOUTH
WEST
8%
6%
4%
2%
18 - 20
16 - 18
14 - 16
12 - 14
10 - 12
8 - 10
6 - 8
4 - 6
2 - 4
0 - 2

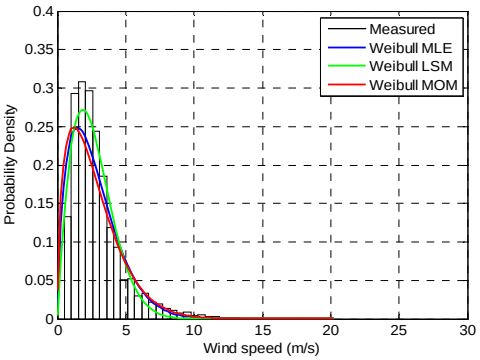
Measured
Weibull MLE
Weibull LSM
Weibull MOM
Probability Density
Wind speed (m/s)

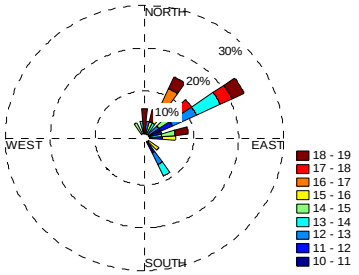
NORTH
EAST
SOUTH
WEST
30%
20%
10%
18 - 19
17 - 18
16 - 17
15 - 16
14 - 15
13 - 14
12 - 13
11 - 12
10 - 11

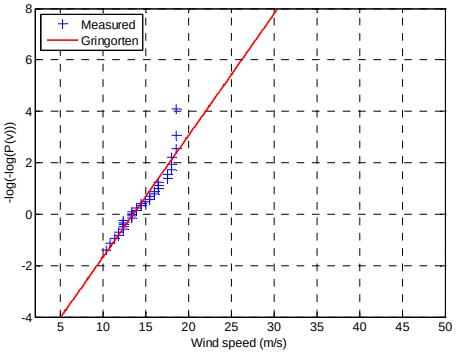
Measured
Gringorten
-log(-log(P(v)))
Wind speed (m/s)

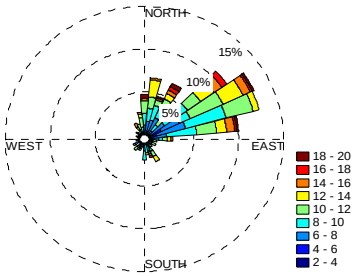
NORTH
EAST
SOUTH
WEST
15%
10%
5%
18 - 20
16 - 18
14 - 16
12 - 14
10 - 12
8 - 10
6 - 8
4 - 6
2 - 4

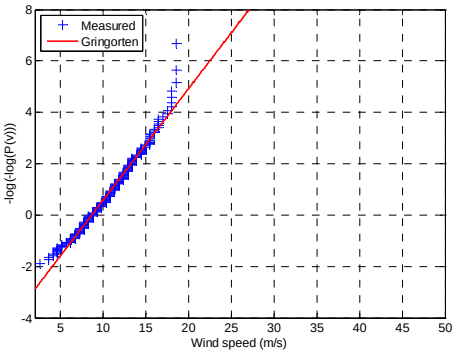
Measured
Gringorten
-log(-log(P(v)))
Wind speed (m/s)

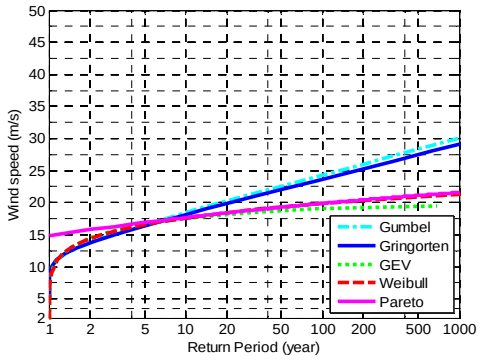
Wind speed (m/s)
Return Period (year)
Gumbel
Gringorten
GEV
Weibull
Pareto

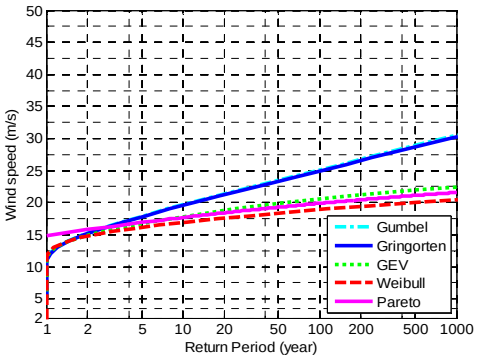
Wind speed (m/s)
Return Period (year)
Gumbel
Gringorten
GEV
Weibull
Pareto

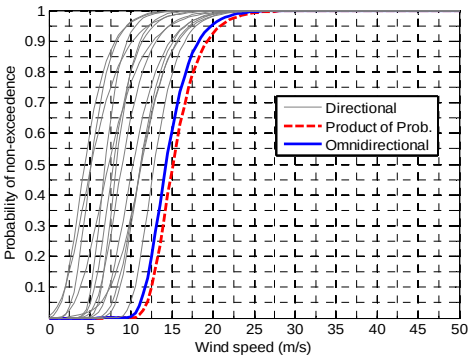
Probability of non-exceedence
Wind speed (m/s)
Directional
Product of Prob.
Omnidirectional

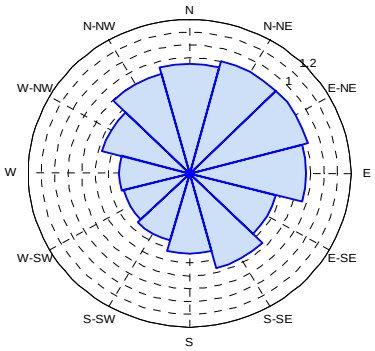
N
N-NE
E-NE
E
E-SE
S-SE
S
S-SW
W
W-NW
N-NW

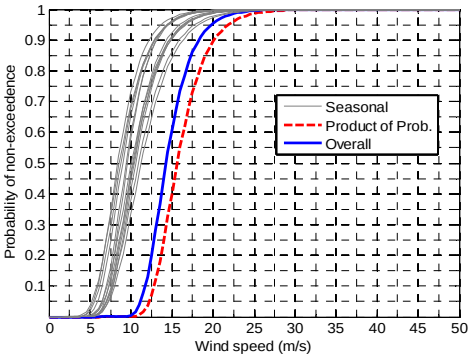
Probability of non-exceedence
Wind speed (m/s)
Seasonal
Product of Prob.
Overall

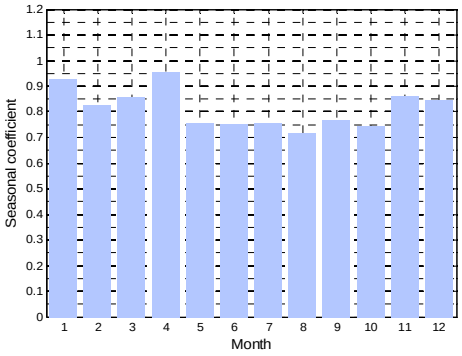
Seasonal coefficient
Month

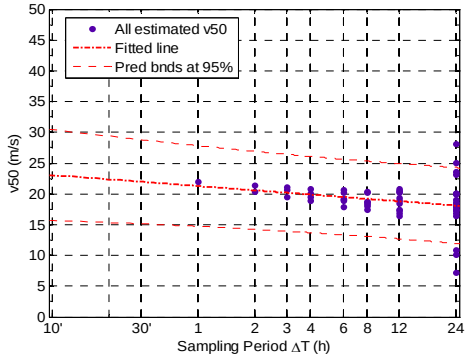
v50 (m/s)
Sampling Period ΔT (h)
All estimated v50
Fitted line
Pred bnds at 95%

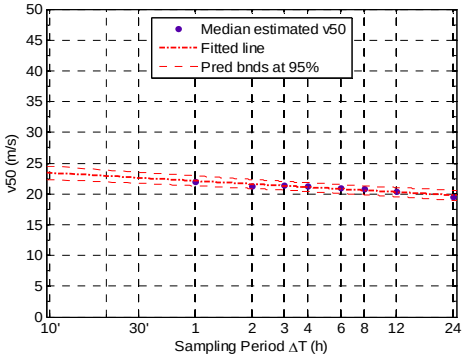
v50 (m/s)
Sampling Period ΔT (h)
Median estimated v50
Fitted line
Pred bnds at 95%

LIPK

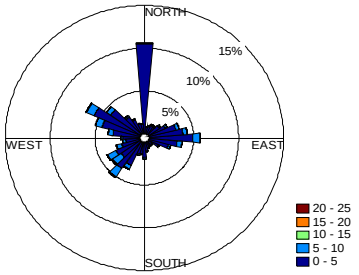
NORTH
15%
10%
5%
WEST
EAST
SOUTH
20 - 25
15 - 20
10 - 15
5 - 10
0 - 5

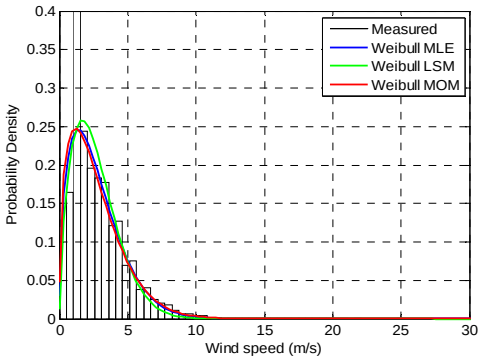
Measured
Weibull MLE
Weibull LSM
Weibull MOM
Probability Density
Wind speed (m/s)

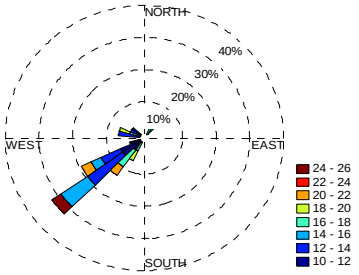
NORTH
40%
30%
20%
10%
WEST
EAST
SOUTH
24 - 26
22 - 24
20 - 22
18 - 20
16 - 18
14 - 16
12 - 14
10 - 12

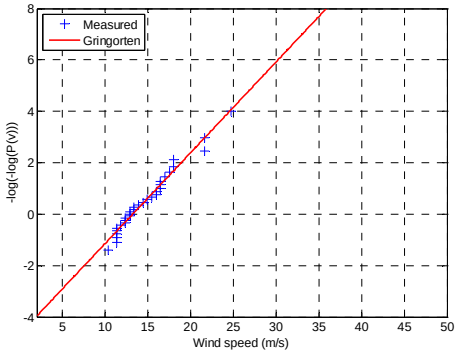
Measured
Gringorten
-log(-log(P(v)))
Wind speed (m/s)

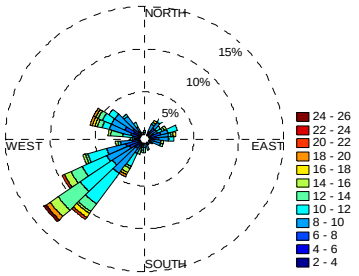
NORTH
15%
10%
5%
WEST
EAST
SOUTH
24 - 26
22 - 24
20 - 22
18 - 20
16 - 18
14 - 16
12 - 14
10 - 12
8 - 10
6 - 8
4 - 6
2 - 4

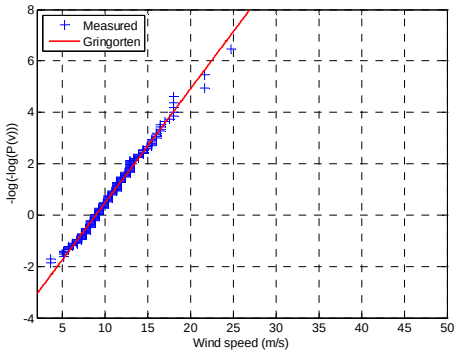
Measured
Gringorten
-log(-log(P(v)))
Wind speed (m/s)

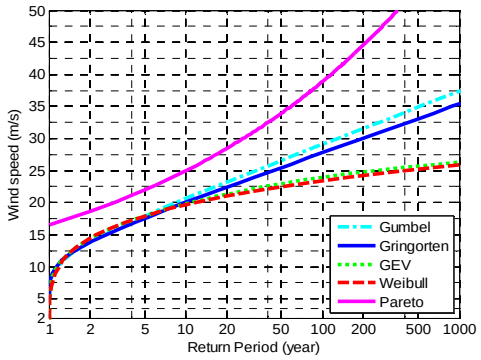
Wind speed (m/s)
Return Period (year)
Gumbel
Gringorten
GEV
Weibull
Pareto

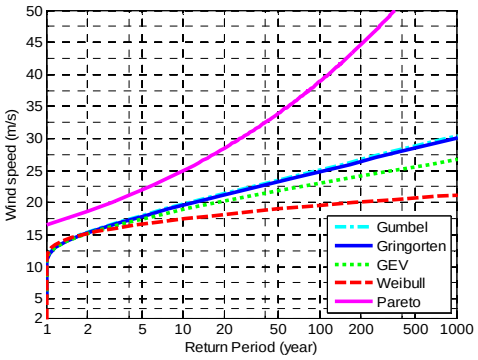
Wind speed (m/s)
Return Period (year)
Gumbel
Gringorten
GEV
Weibull
Pareto

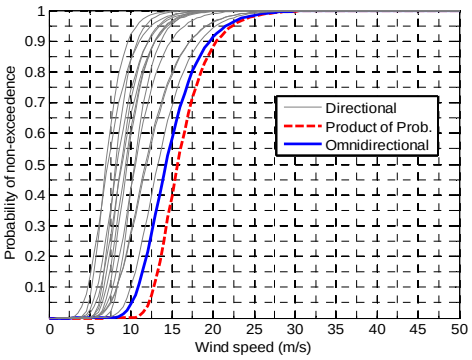
Probability of non-exceedence
Wind speed (m/s)
Directional
Product of Prob.
Omnidirectional

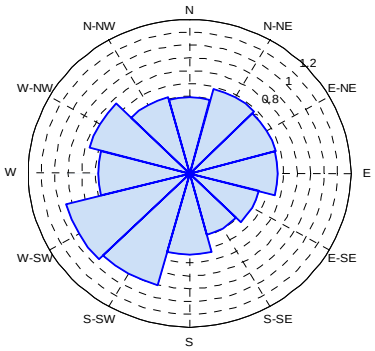
N
N-NE
E-NE
E
E-SE
S-SE
S
S-SW
W
W-NW
N-NW

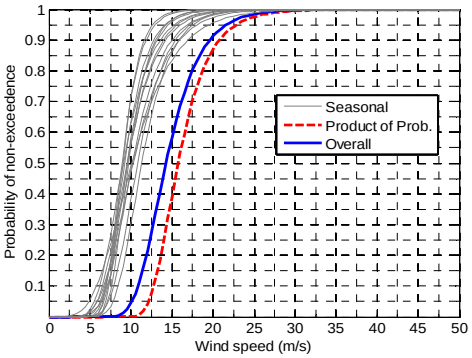
Probability of non-exceedence
Wind speed (m/s)
Seasonal
Product of Prob.
Overall

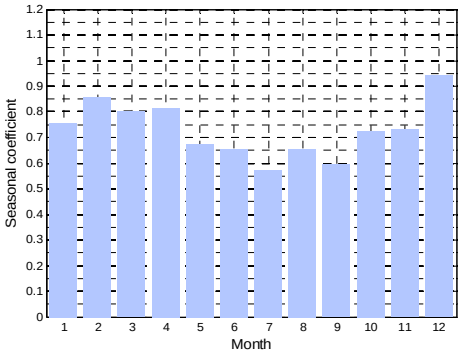
Seasonal coefficient
Month

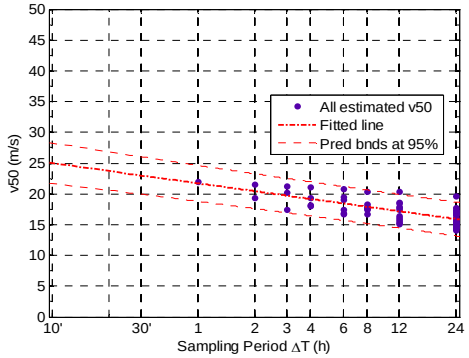
v50 (m/s)
Sampling Period ΔT (h)
All estimated v50
Fitted line
Pred bnds at 95%

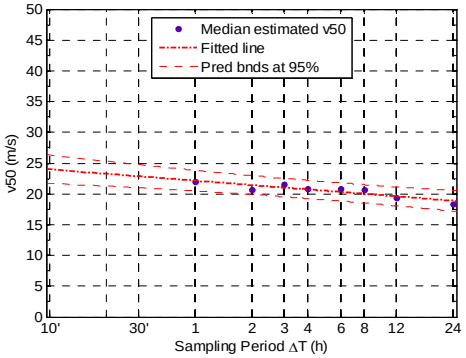
v50 (m/s)
Sampling Period ΔT (h)
Median estimated v50
Fitted line
Pred bnds at 95%

LIPL

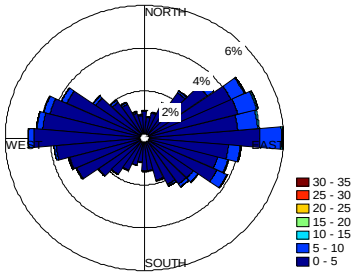
NORTH
6%
4%
2%
WEST
SOUTH
30 - 35
25 - 30
20 - 25
15 - 20
10 - 15
5 - 10
0 - 5

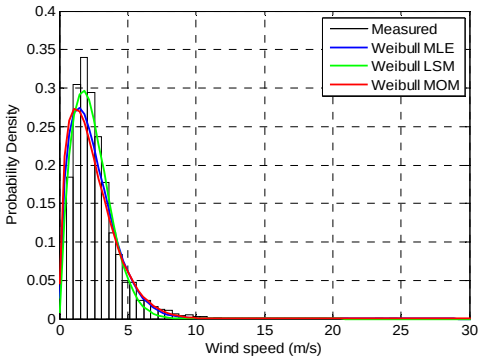
Measured
Weibull MLE
Weibull LSM
Weibull MOM
Probability Density
Wind speed (m/s)

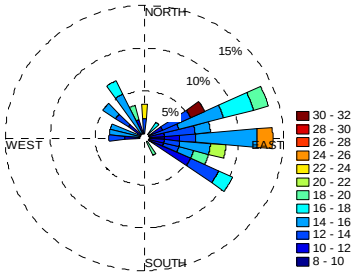
NORTH
15%
10%
5%
WEST
SOUTH
30 - 32
28 - 30
26 - 28
24 - 26
22 - 24
20 - 22
18 - 20
16 - 18
14 - 16
12 - 14
10 - 12
8 - 10

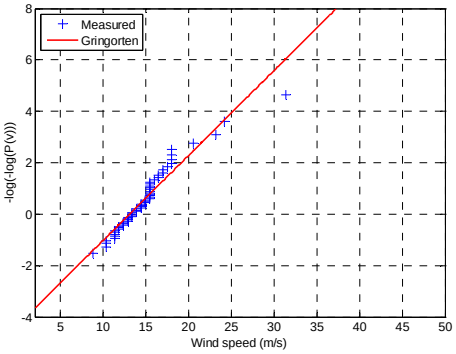
Measured
Gringorten
-log(-log(P(v)))
Wind speed (m/s)

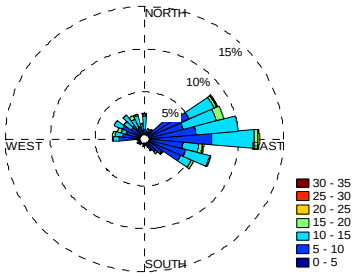
NORTH
15%
10%
5%
WEST
SOUTH
30 - 35
25 - 30
20 - 25
15 - 20
10 - 15
5 - 10
0 - 5

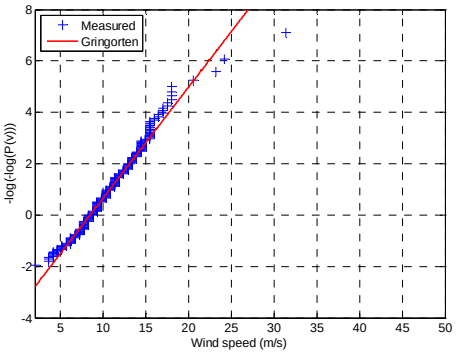
Measured
Gringorten
-log(-log(P(v)))
Wind speed (m/s)

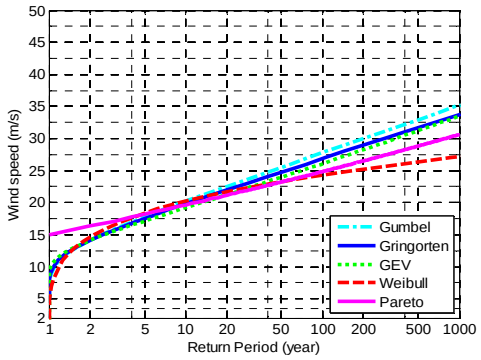
Wind speed (m/s)
Return Period (year)
Gumbel
Gringorten
GEV
Weibull
Pareto

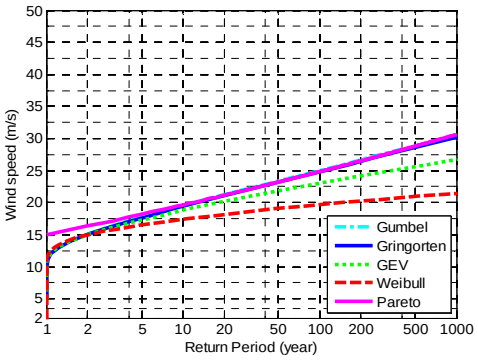
Wind speed (m/s)
Return Period (year)
Gumbel
Gringorten
GEV
Weibull
Pareto

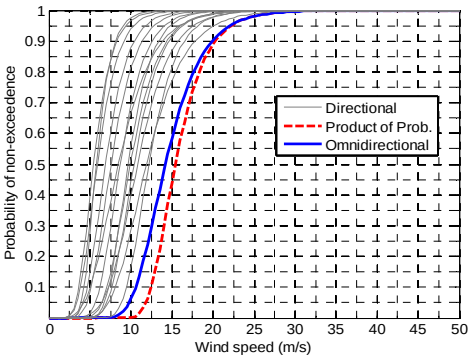
Probability of non-exceedence
Wind speed (m/s)
Directional
Product of Prob.
Omnidirectional

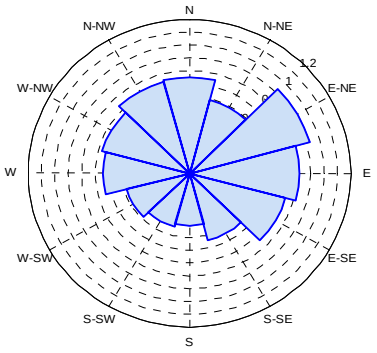
N
N-NE
E-NE
E
E-SE
S-SE
S
S-SW
W
W-NW
N-NW

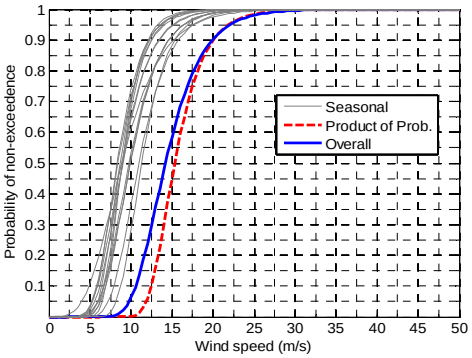
Probability of non-exceedence
Wind speed (m/s)
Seasonal
Product of Prob.
Overall

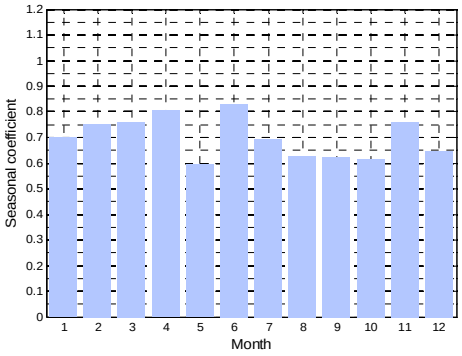
Seasonal coefficient
Month

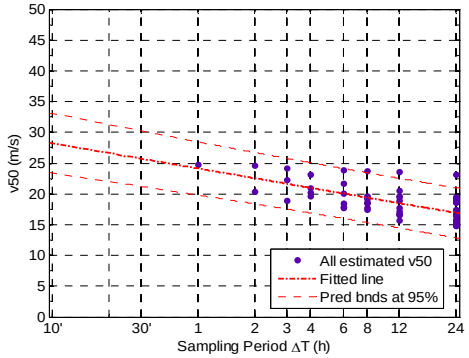
v50 (m/s)
Sampling Period ΔT (h)
All estimated v50
Fitted line
Pred bnds at 95%

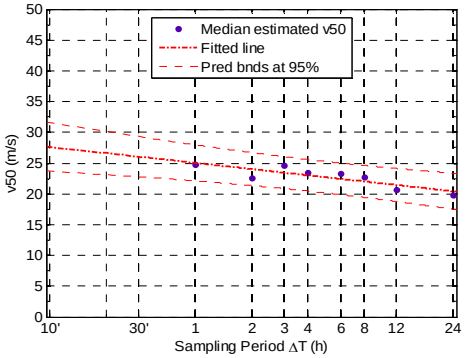
v50 (m/s)
Sampling Period ΔT (h)
Median estimated v50
Fitted line
Pred bnds at 95%

LIPQ

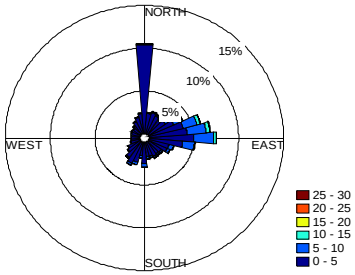
NORTH
15%
10%
5%
WEST
EAST
SOUTH
25 - 30
20 - 25
15 - 20
10 - 15
5 - 10
0 - 5

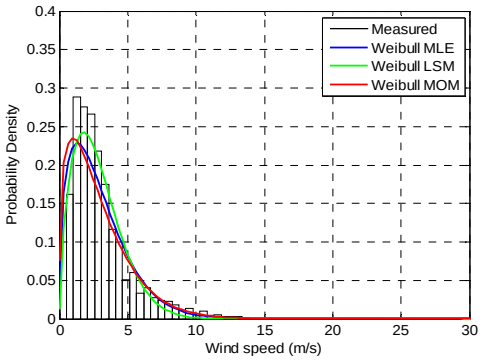
Measured
Weibull MLE
Weibull LSM
Weibull MOM
Probability Density
Wind speed (m/s)

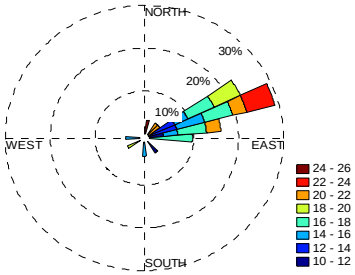
NORTH
30%
20%
10%
WEST
EAST
SOUTH
24 - 26
22 - 24
20 - 22
18 - 20
16 - 18
14 - 16
12 - 14
10 - 12

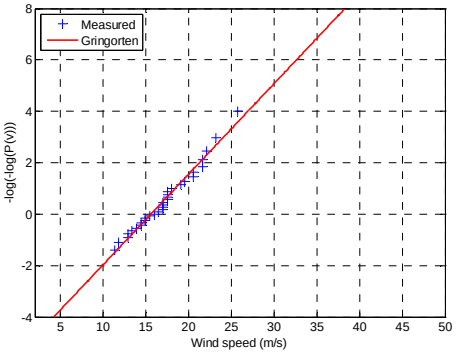
Measured
Gringorten
-log(-log(P(v)))
Wind speed (m/s)

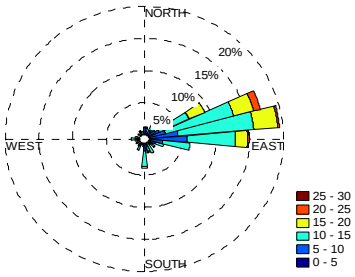
NORTH
20%
15%
10%
5%
WEST
EAST
SOUTH
25 - 30
20 - 25
15 - 20
10 - 15
5 - 10
0 - 5

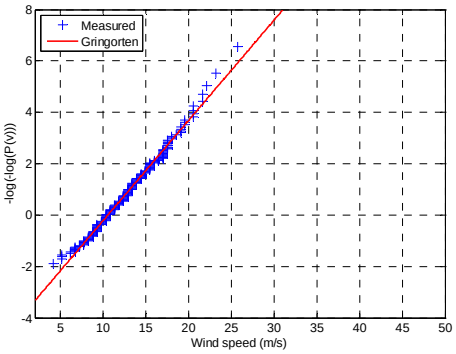
Measured
Gringorten
-log(-log(P(v)))
Wind speed (m/s)

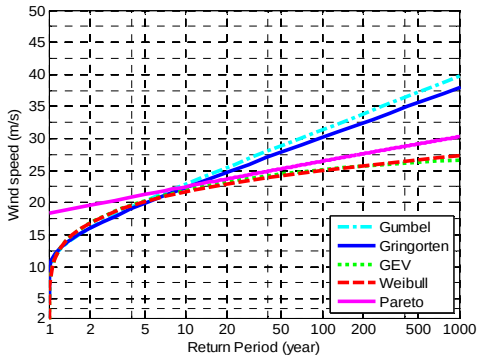
Wind speed (m/s)
Return Period (year)
Gumbel
Gringorten
GEV
Weibull
Pareto

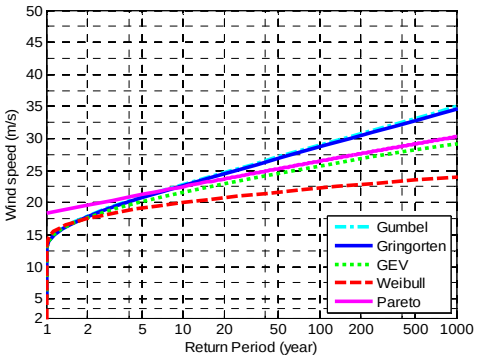
Wind speed (m/s)
Return Period (year)
Gumbel
Gringorten
GEV
Weibull
Pareto

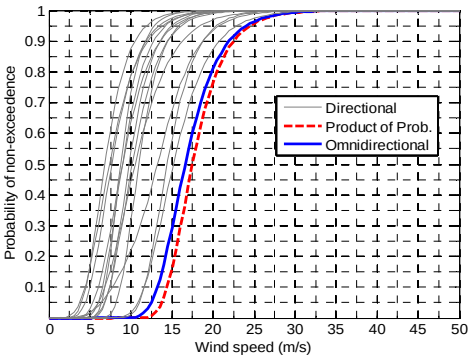
Probability of non-exceedence
Wind speed (m/s)
Directional
Product of Prob.
Omnidirectional

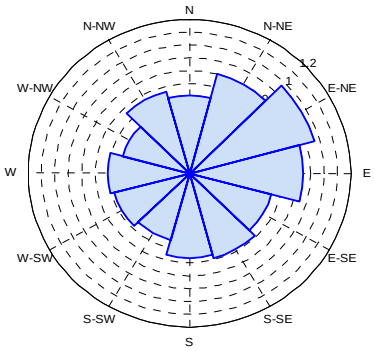
N
N-NE
E-NE
E
E-SE
S-SE
S
S-SW
W
W-NW
N-NW

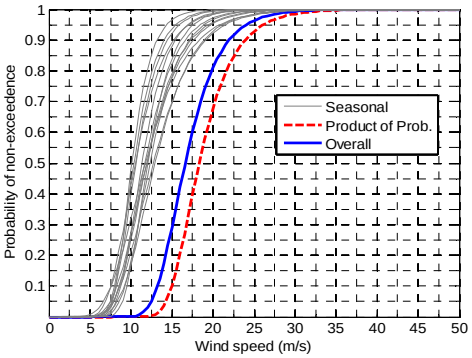
Probability of non-exceedence
Wind speed (m/s)
Seasonal
Product of Prob.
Overall

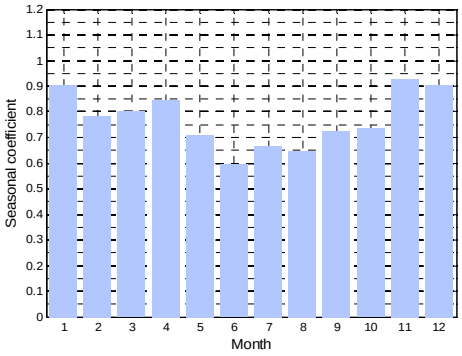
Seasonal coefficient
Month

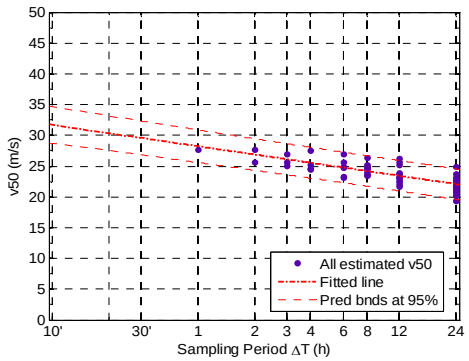
v50 (m/s)
Sampling Period ΔT (h)
All estimated v50
Fitted line
Pred bnds at 95%

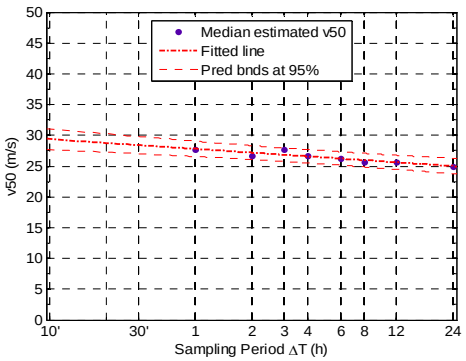
v50 (m/s)
Sampling Period ΔT (h)
Median estimated v50
Fitted line
Pred bnds at 95%

LIPR

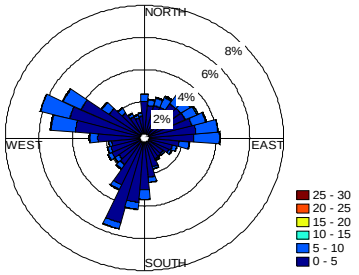
NORTH
8%
6%
4%
2%
WEST
EAST
SOUTH
25 - 30
20 - 25
15 - 20
10 - 15
5 - 10
0 - 5

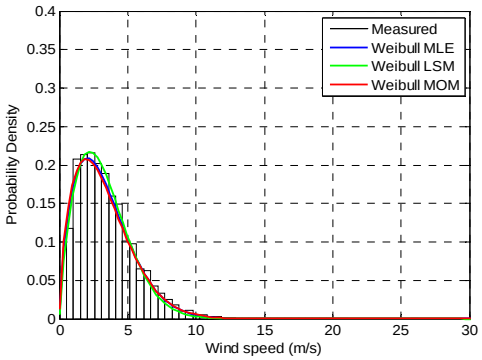
Measured
Weibull MLE
Weibull LSM
Weibull MOM
Probability Density
Wind speed (m/s)

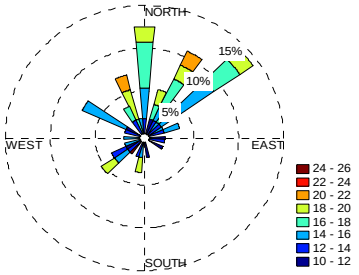
NORTH
15%
10%
5%
WEST
EAST
SOUTH
24 - 26
22 - 24
20 - 22
18 - 20
16 - 18
14 - 16
12 - 14
10 - 12

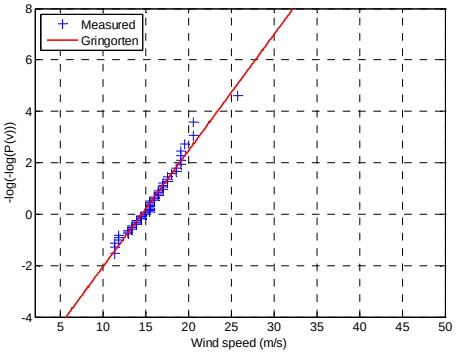
Measured
Gringorten
-log(-log(P(v)))
Wind speed (m/s)

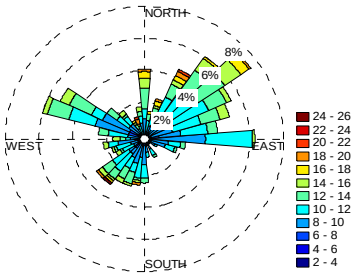
NORTH
8%
6%
4%
2%
WEST
EAST
SOUTH
24 - 26
22 - 24
20 - 22
18 - 20
16 - 18
14 - 16
12 - 14
10 - 12
8 - 10
6 - 8
4 - 6
2 - 4

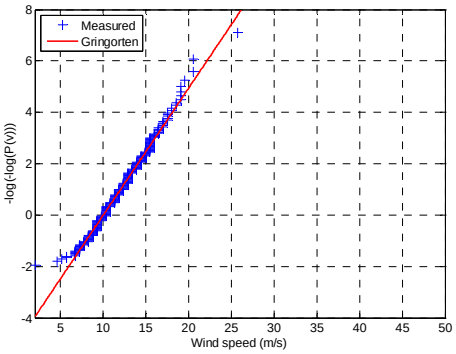
Measured
Gringorten
-log(-log(P(v)))
Wind speed (m/s)

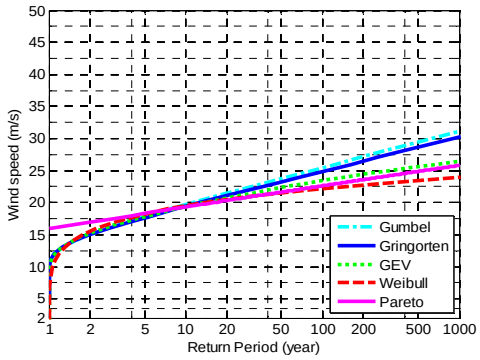
Wind speed (m/s)
Return Period (year)
Gumbel
Gringorten
GEV
Weibull
Pareto

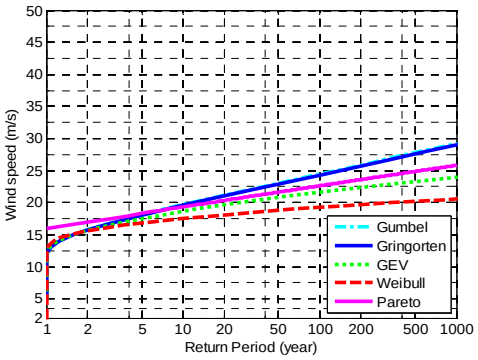
Wind speed (m/s)
Return Period (year)
Gumbel
Gringorten
GEV
Weibull
Pareto

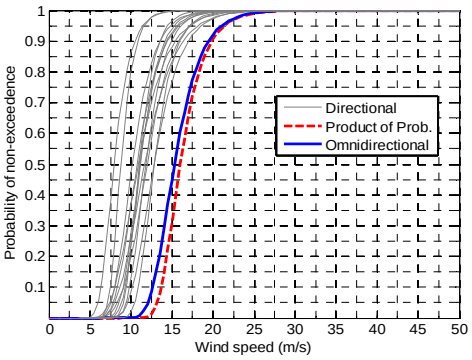
Probability of non-exceedence
Wind speed (m/s)
Directional
Product of Prob.
Omnidirectional

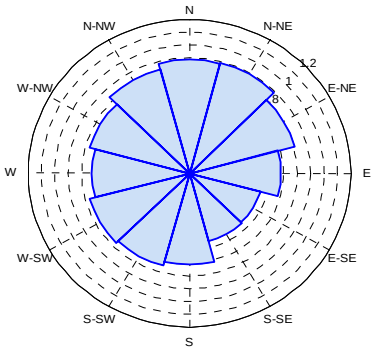
N
N-NE
E-NE
E
E-SE
S-SE
S
S-SW
W
W-NW
N-NW

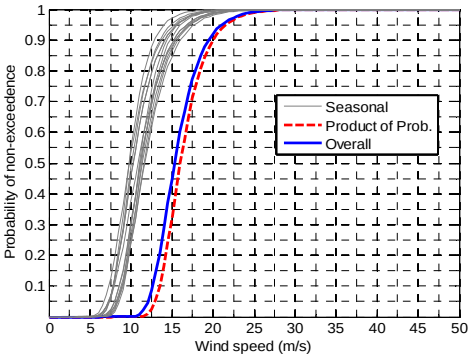
Probability of non-exceedence
Wind speed (m/s)
Seasonal
Product of Prob.
Overall

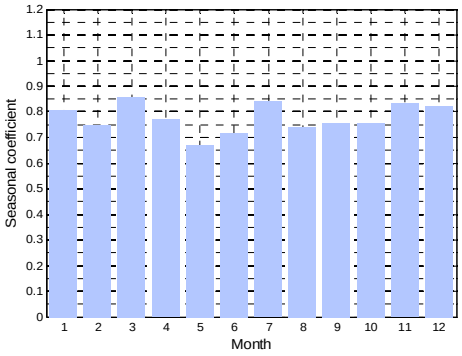
Seasonal coefficient
Month

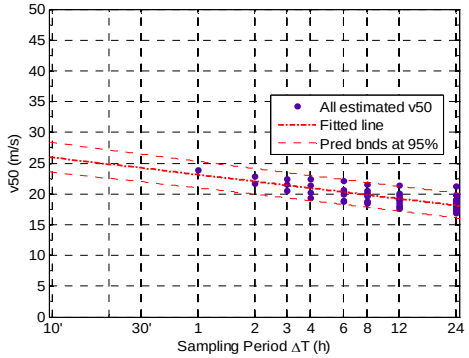
v50 (m/s)
Sampling Period ΔT (h)
All estimated v50
Fitted line
Pred bnds at 95%

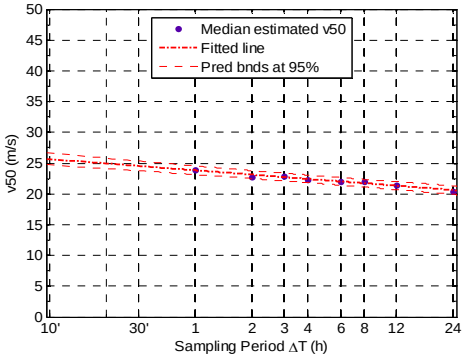
v50 (m/s)
Sampling Period ΔT (h)
Median estimated v50
Fitted line
Pred bnds at 95%

LIPS

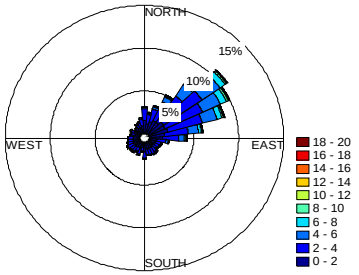
NORTH
15%
10%
5%
WEST
EAST
SOUTH
18 - 20
16 - 18
14 - 16
12 - 14
10 - 12
8 - 10
6 - 8
4 - 6
2 - 4
0 - 2

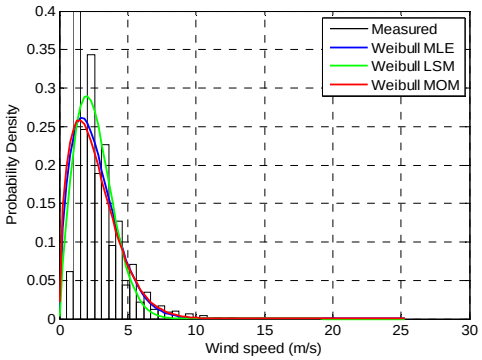
Measured
Weibull MLE
Weibull LSM
Weibull MOM
Probability Density
Wind speed (m/s)

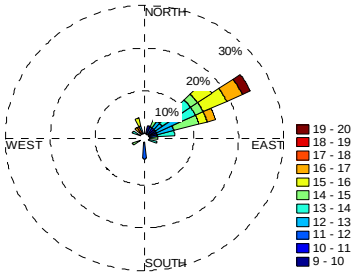
NORTH
30%
20%
10%
WEST
EAST
SOUTH
19 - 20
18 - 19
17 - 18
16 - 17
15 - 16
14 - 15
13 - 14
12 - 13
11 - 12
10 - 11
9 - 10

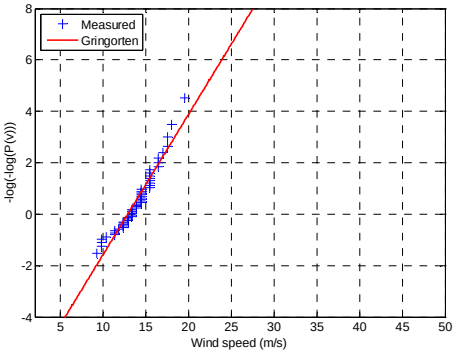
Measured
Gringorten
-log(-log(P(v)))
Wind speed (m/s)

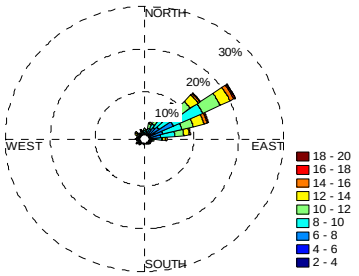
NORTH
30%
20%
10%
WEST
EAST
SOUTH
18 - 20
16 - 18
14 - 16
12 - 14
10 - 12
8 - 10
6 - 8
4 - 6
2 - 4

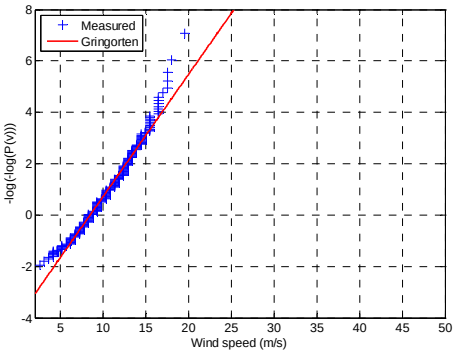
Measured
Gringorten
-log(-log(P(v)))
Wind speed (m/s)

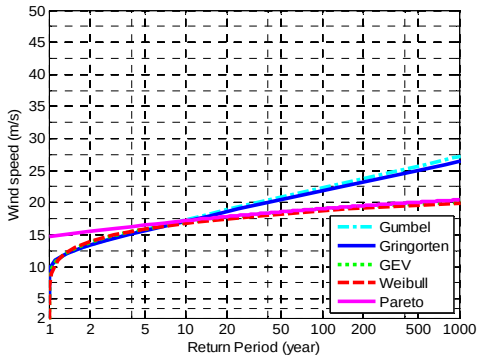
Wind speed (m/s)
Return Period (year)
Gumbel
Gringorten
GEV
Weibull
Pareto

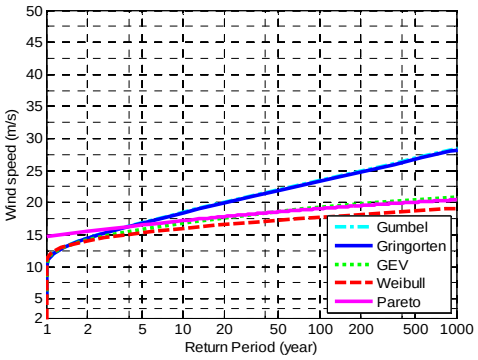
Wind speed (m/s)
Return Period (year)
Gumbel
Gringorten
GEV
Weibull
Pareto

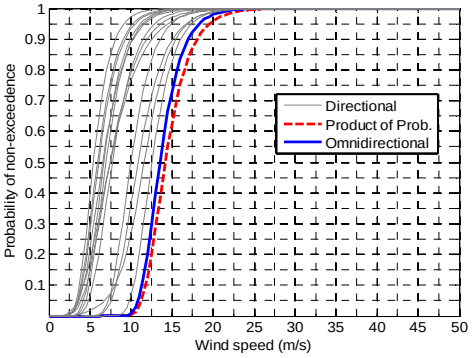
Probability of non-exceedence
Wind speed (m/s)
Directional
Product of Prob.
Omnidirectional

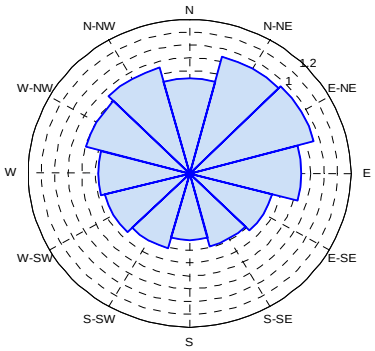
N
N-NE
E-NE
E
E-SE
S-SE
S
S-SW
W
W-NW
N-NW

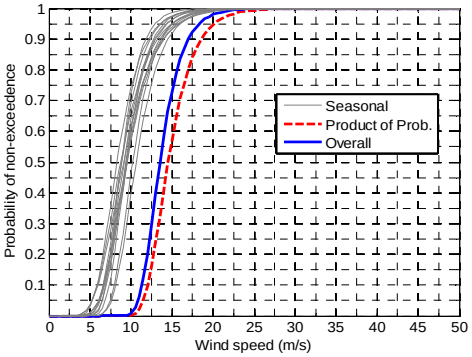
Probability of non-exceedence
Wind speed (m/s)
Seasonal
Product of Prob.
Overall

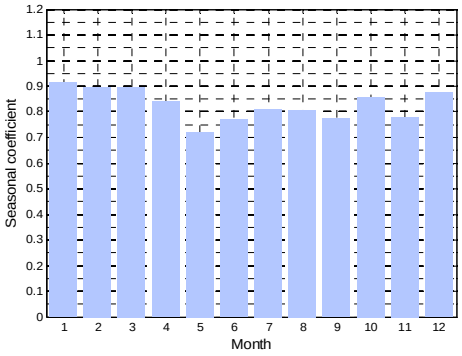
Seasonal coefficient
Month

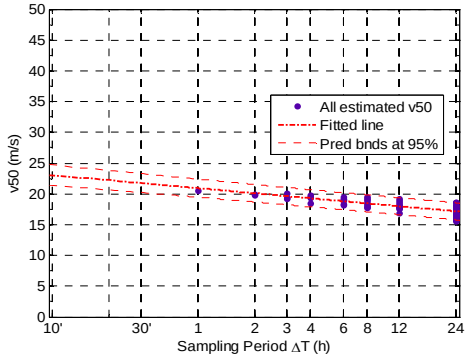
v50 (m/s)
Sampling Period ΔT (h)
All estimated v50
Fitted line
Pred bnds at 95%

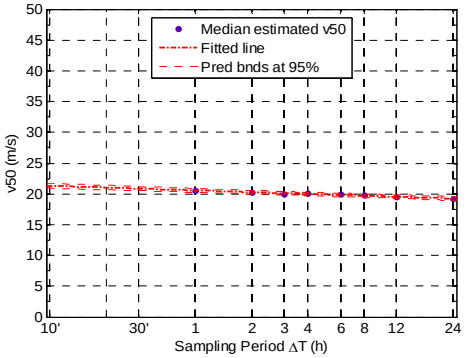
v50 (m/s)
Sampling Period ΔT (h)
Median estimated v50
Fitted line
Pred bnds at 95%

LIPT

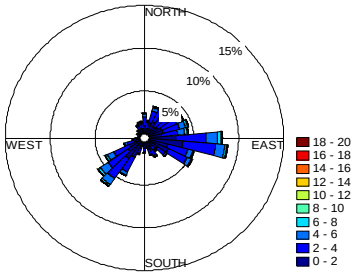
NORTH
15%
10%
5%
WEST
EAST
SOUTH
18 - 20
16 - 18
14 - 16
12 - 14
10 - 12
8 - 10
6 - 8
4 - 6
2 - 4
0 - 2

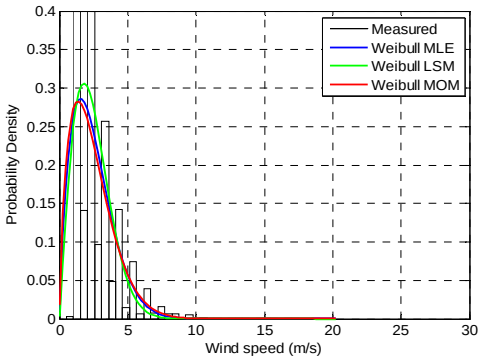
Measured
Weibull MLE
Weibull LSM
Weibull MOM
Probability Density
Wind speed (m/s)

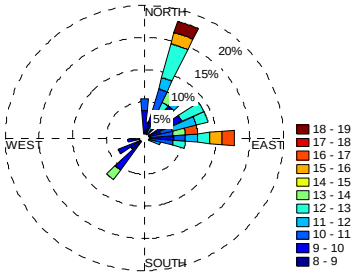
NORTH
20%
15%
10%
5%
WEST
EAST
SOUTH
18 - 19
17 - 18
16 - 17
15 - 16
14 - 15
13 - 14
12 - 13
11 - 12
10 - 11
9 - 10
8 - 9

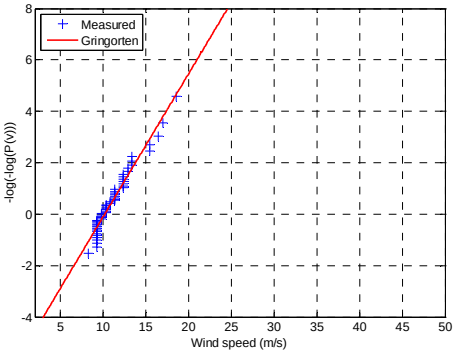
Measured
Gringorten
-log(-log(P(v)))
Wind speed (m/s)

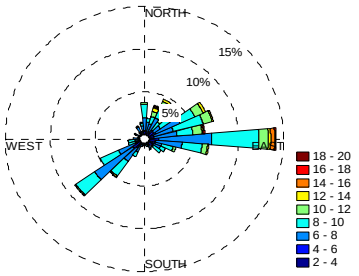
NORTH
15%
10%
5%
WEST
EAST
SOUTH
18 - 20
16 - 18
14 - 16
12 - 14
10 - 12
8 - 10
6 - 8
4 - 6
2 - 4

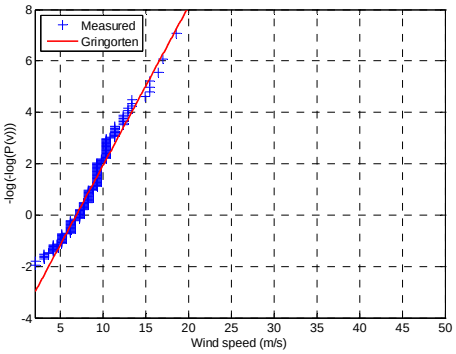
Measured
Gringorten
-log(-log(P(v)))
Wind speed (m/s)

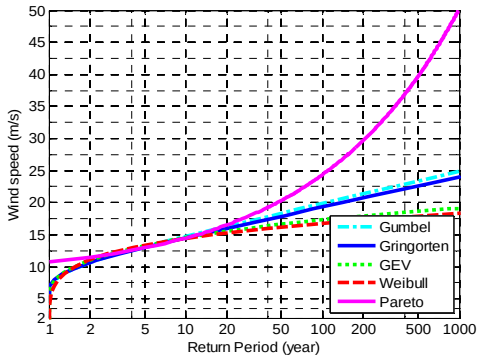
Wind speed (m/s)
Return Period (year)
Gumbel
Gringorten
GEV
Weibull
Pareto

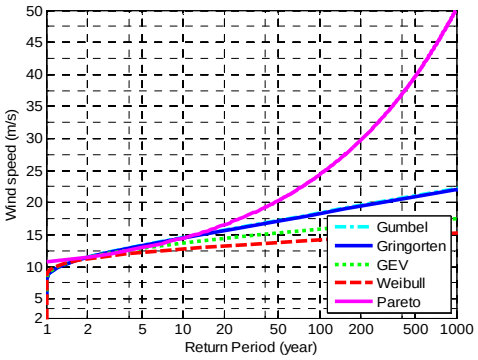
Wind speed (m/s)
Return Period (year)
Gumbel
Gringorten
GEV
Weibull
Pareto

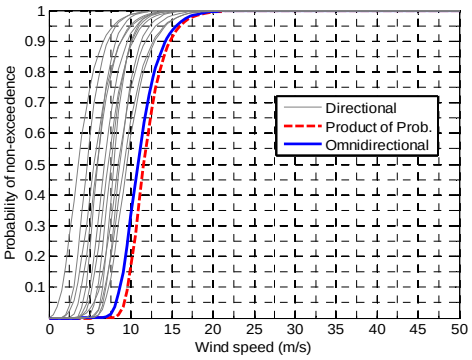
Probability of non-exceedence
Wind speed (m/s)
Directional
Product of Prob.
Omnidirectional

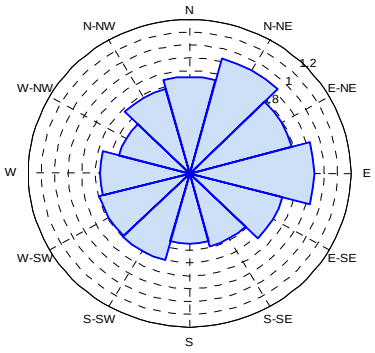
N
N-NE
E-NE
E
E-SE
S-SE
S
S-SW
W-SW
W
W-NW
N-NW

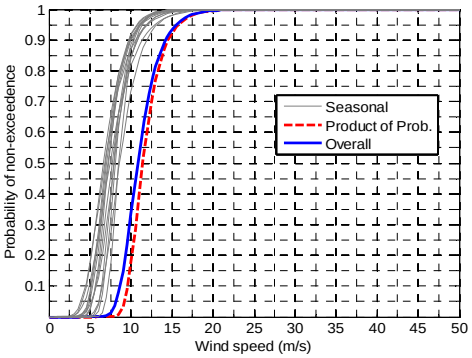
Probability of non-exceedence
Wind speed (m/s)
Seasonal
Product of Prob.
Overall

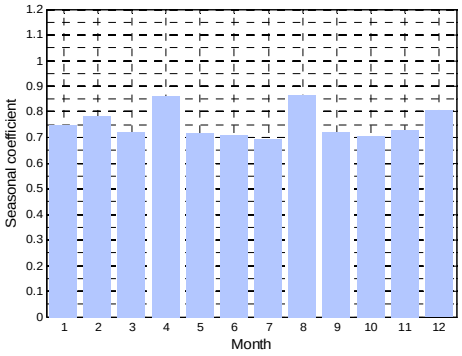
Seasonal coefficient
Month

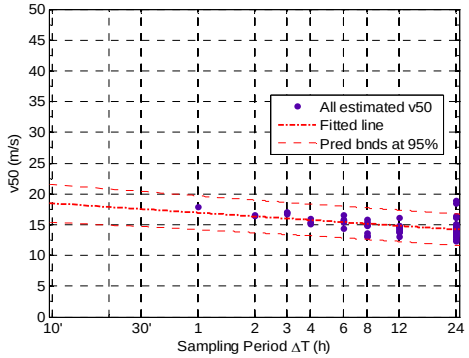
v50 (m/s)
Sampling Period ΔT (h)
All estimated v50
Fitted line
Pred bnds at 95%

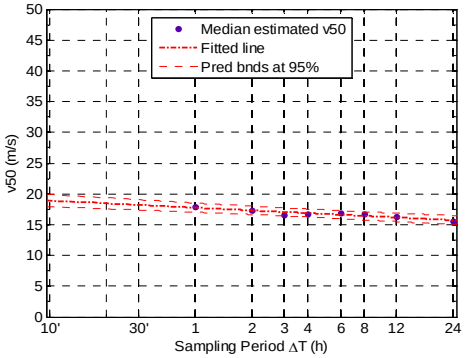
v50 (m/s)
Sampling Period ΔT (h)
Median estimated v50
Fitted line
Pred bnds at 95%

LIPX

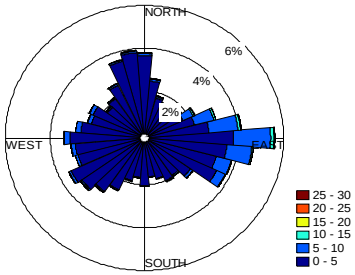
NORTH
6%
4%
2%
WEST
EAST
SOUTH
25 - 30
20 - 25
15 - 20
10 - 15
5 - 10
0 - 5

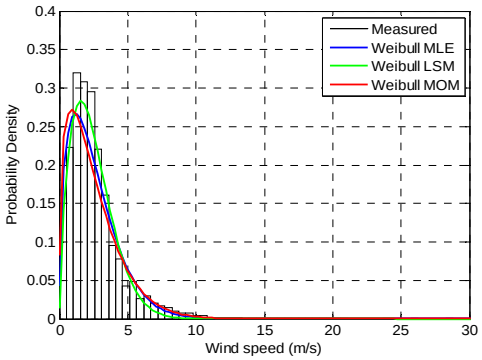
Measured
Weibull MLE
Weibull LSM
Weibull MOM
Probability Density
Wind speed (m/s)

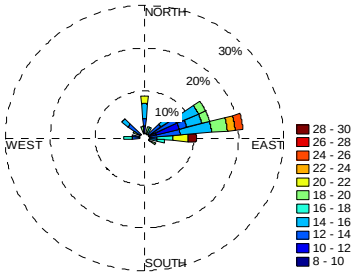
NORTH
30%
20%
10%
WEST
EAST
SOUTH
28 - 30
26 - 28
24 - 26
22 - 24
20 - 22
18 - 20
16 - 18
14 - 16
12 - 14
10 - 12
8 - 10

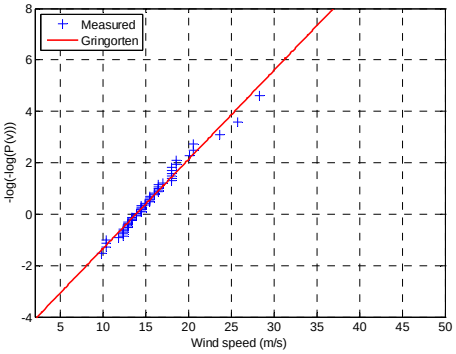
Measured
Gringorten
-log(-log(P(v)))
Wind speed (m/s)

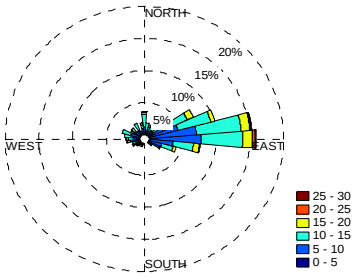
NORTH
20%
15%
10%
5%
WEST
EAST
SOUTH
25 - 30
20 - 25
15 - 20
10 - 15
5 - 10
0 - 5

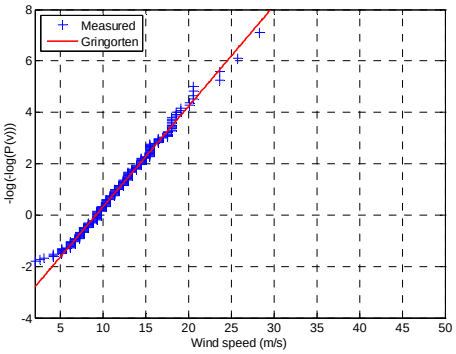
Measured
Gringorten
-log(-log(P(v)))
Wind speed (m/s)

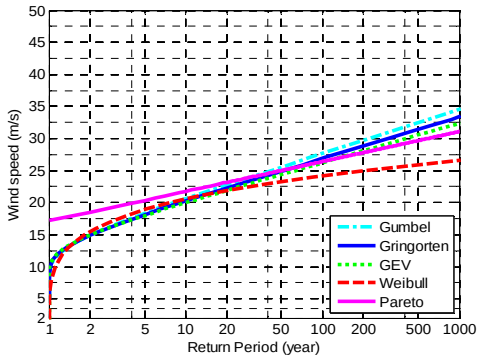
Wind speed (m/s)
Return Period (year)
Gumbel
Gringorten
GEV
Weibull
Pareto

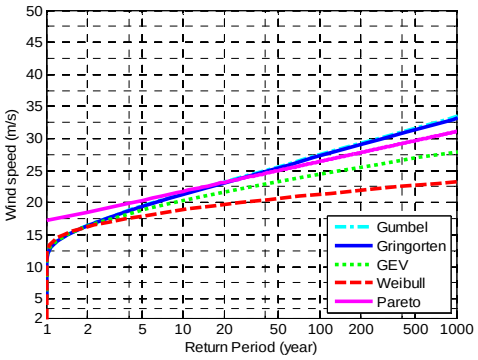
Wind speed (m/s)
Return Period (year)
Gumbel
Gringorten
GEV
Weibull
Pareto

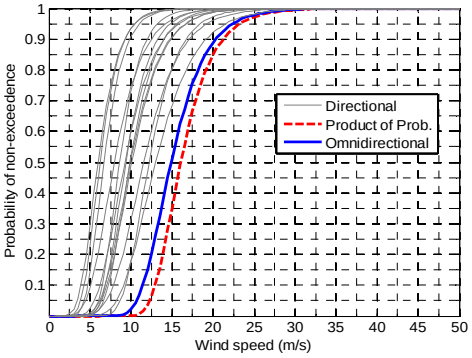
Probability of non-exceedence
Wind speed (m/s)
Directional
Product of Prob.
Omnidirectional

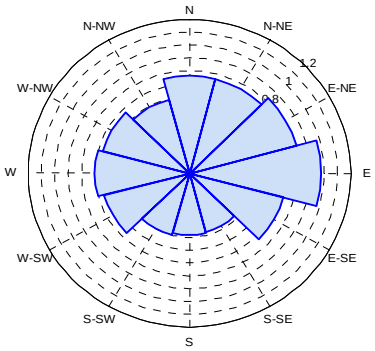
N
N-NE
E-NE
E
E-SE
S-SE
S
S-SW
W
W-NW
N-NW

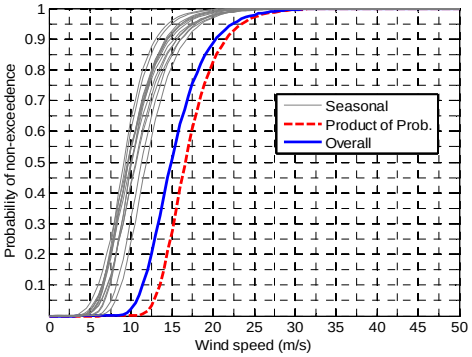
Probability of non-exceedence
Wind speed (m/s)
Seasonal
Product of Prob.
Overall

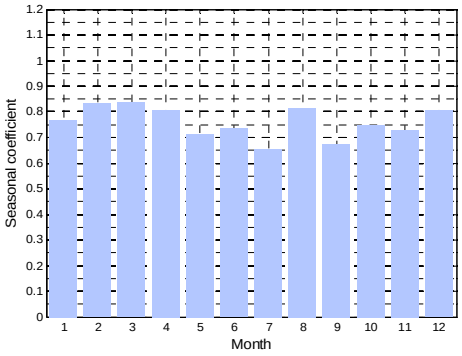
Seasonal coefficient
Month

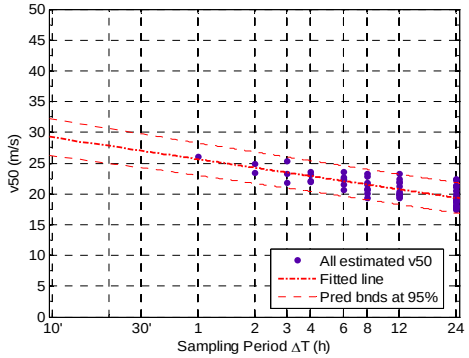
v50 (m/s)
Sampling Period ΔT (h)
All estimated v50
Fitted line
Pred bnds at 95%

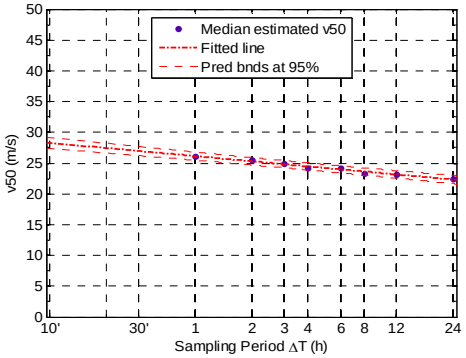
v50 (m/s)
Sampling Period ΔT (h)
Median estimated v50
Fitted line
Pred bnds at 95%

LIPY

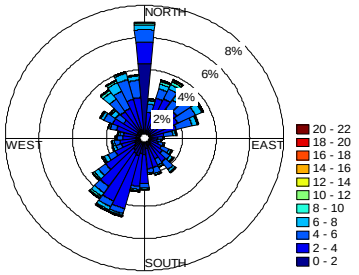
NORTH
8%
6%
4%
2%
WEST
EAST
SOUTH
20 - 22
18 - 20
16 - 18
14 - 16
12 - 14
10 - 12
8 - 10
6 - 8
4 - 6
2 - 4
0 - 2

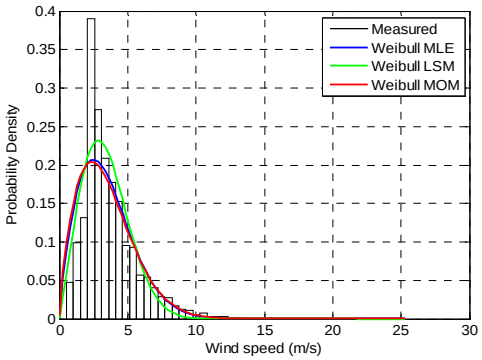
Measured
Weibull MLE
Weibull LSM
Weibull MOM
Probability Density
Wind speed (m/s)

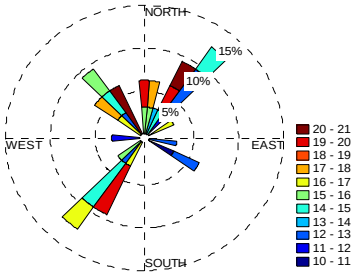
NORTH
15%
10%
5%
WEST
EAST
SOUTH
20 - 21
19 - 20
18 - 19
17 - 18
16 - 17
15 - 16
14 - 15
13 - 14
12 - 13
11 - 12
10 - 11

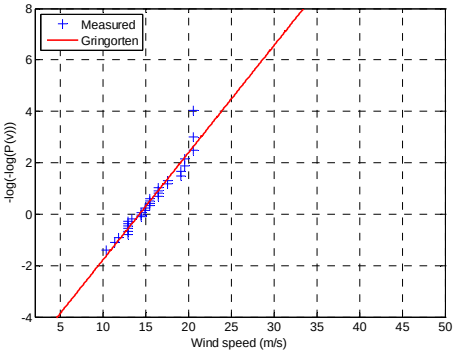
Measured
Gringorten
-log(-log(P(v)))
Wind speed (m/s)

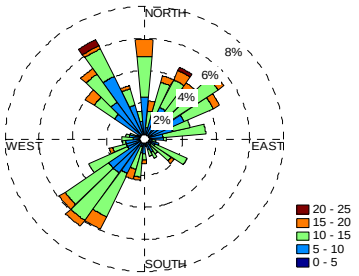
NORTH
8%
6%
4%
2%
WEST
EAST
SOUTH
20 - 25
15 - 20
10 - 15
5 - 10
0 - 5

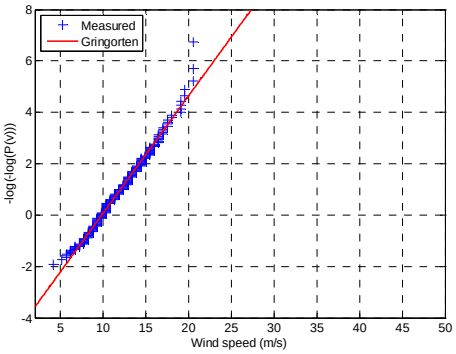
Measured
Gringorten
-log(-log(P(v)))
Wind speed (m/s)

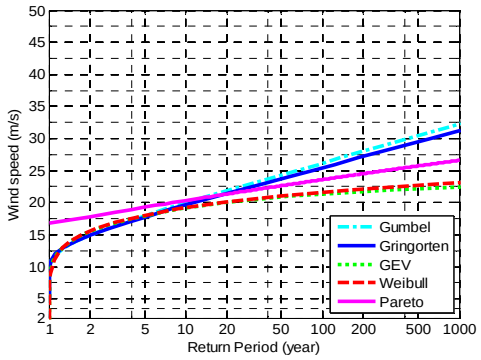
Wind speed (m/s)
Return Period (year)
Gumbel
Gringorten
GEV
Weibull
Pareto

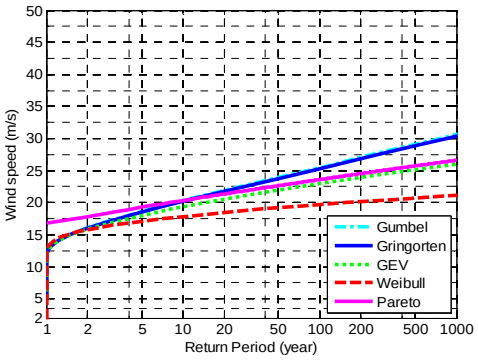
Wind speed (m/s)
Return Period (year)
Gumbel
Gringorten
GEV
Weibull
Pareto

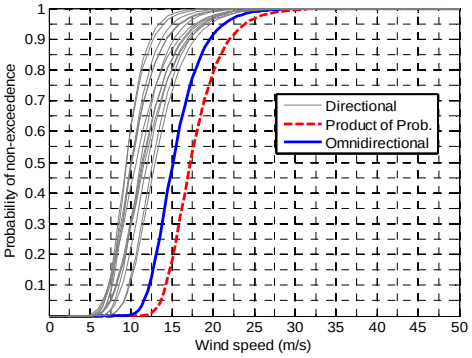
Probability of non-exceedence
Wind speed (m/s)
Directional
Product of Prob.
Omnidirectional

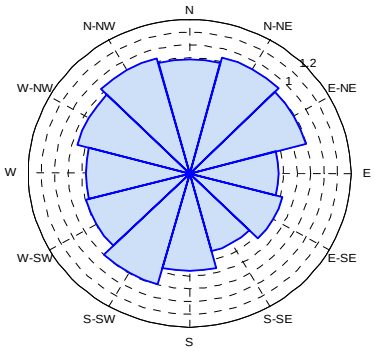
N
N-NE
E-NE
E
E-SE
S-SE
S
S-SW
W
W-NW
N-NW

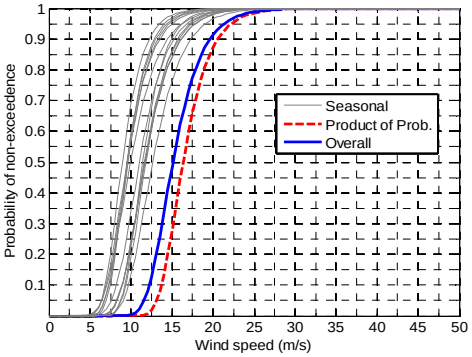
Probability of non-exceedence
Wind speed (m/s)
Seasonal
Product of Prob.
Overall

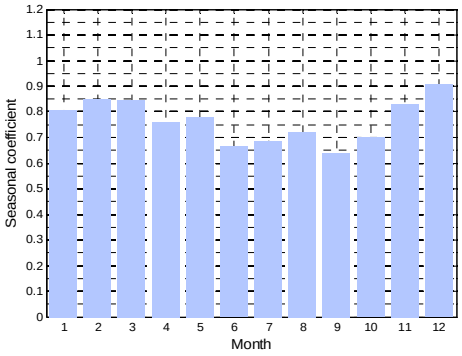
Seasonal coefficient
Month

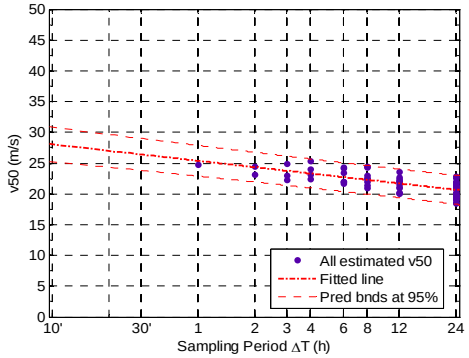
v50 (m/s)
Sampling Period ΔT (h)
All estimated v50
Fitted line
Pred bnds at 95%

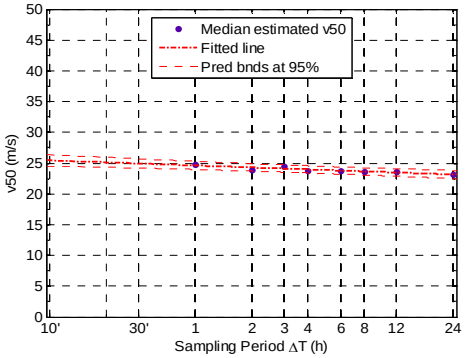
v50 (m/s)
Sampling Period ΔT (h)
Median estimated v50
Fitted line
Pred bnds at 95%

LIPZ

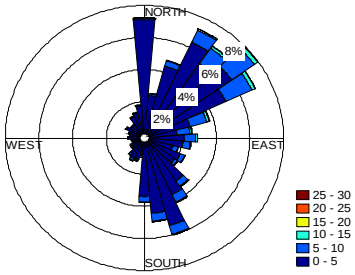
NORTH
EAST
SOUTH
WEST
2%
4%
6%
8%
25 - 30
20 - 25
15 - 20
10 - 15
5 - 10
0 - 5

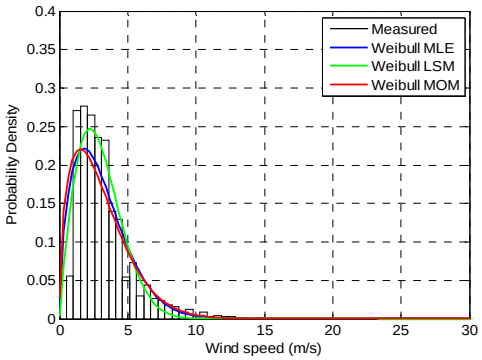
Measured
Weibull MLE
Weibull LSM
Weibull MOM
Probability Density
Wind speed (m/s)

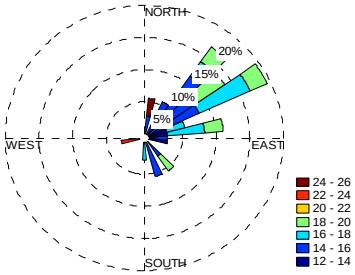
NORTH
EAST
SOUTH
WEST
5%
10%
15%
20%
24 - 26
22 - 24
20 - 22
18 - 20
16 - 18
14 - 16
12 - 14

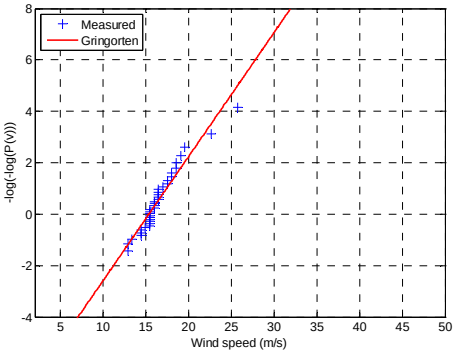
Measured
Gringorten
-log(-log(P(v)))
Wind speed (m/s)

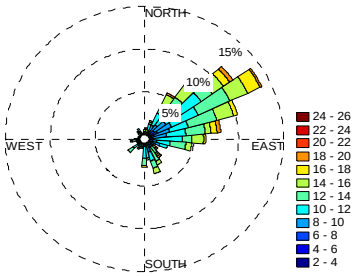
NORTH
EAST
SOUTH
WEST
5%
10%
15%
24 - 26
22 - 24
20 - 22
18 - 20
16 - 18
14 - 16
12 - 14
10 - 12
8 - 10
6 - 8
4 - 6
2 - 4

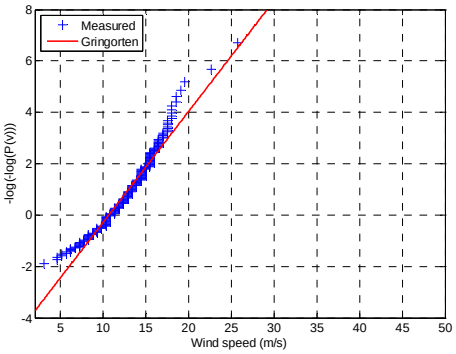
Measured
Gringorten
-log(-log(P(v)))
Wind speed (m/s)

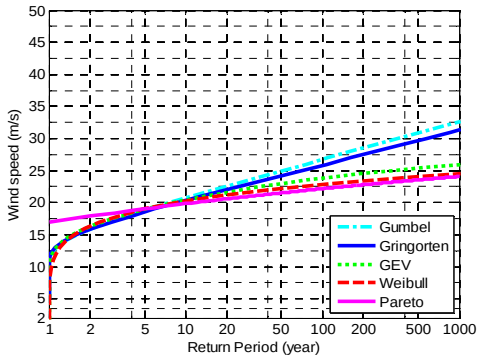
Wind speed (m/s)
Return Period (year)
Gumbel
Gringorten
GEV
Weibull
Pareto

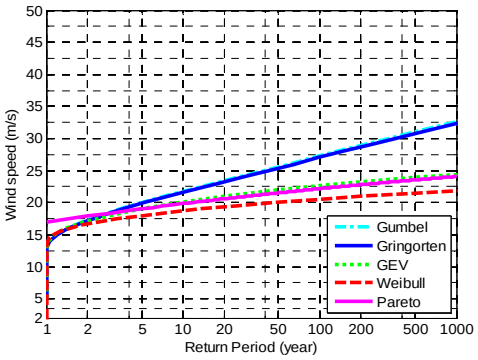
Wind speed (m/s)
Return Period (year)
Gumbel
Gringorten
GEV
Weibull
Pareto

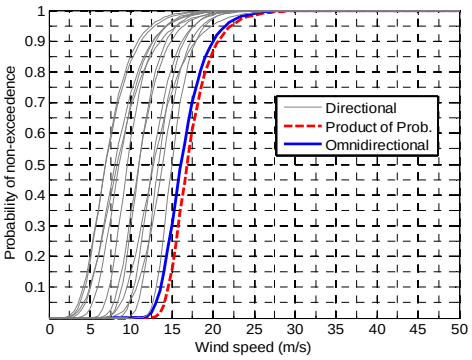
Probability of non-exceedence
Wind speed (m/s)
Directional
Product of Prob.
Omnidirectional

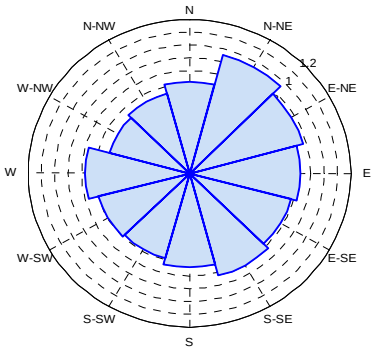
N
N-NE
E-NE
E
E-SE
S-SE
S
S-SW
W
W-NW
N-NW

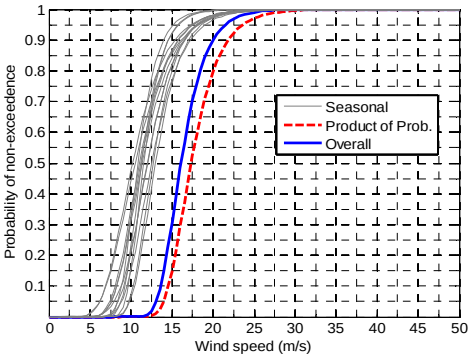
Probability of non-exceedence
Wind speed (m/s)
Seasonal
Product of Prob.
Overall

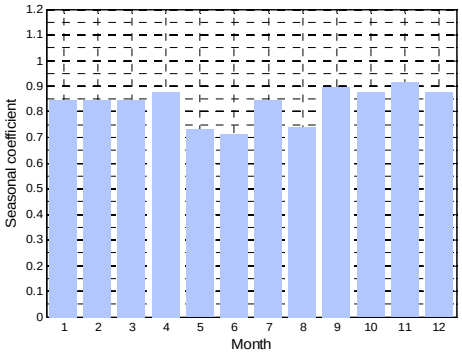
Seasonal coefficient
Month

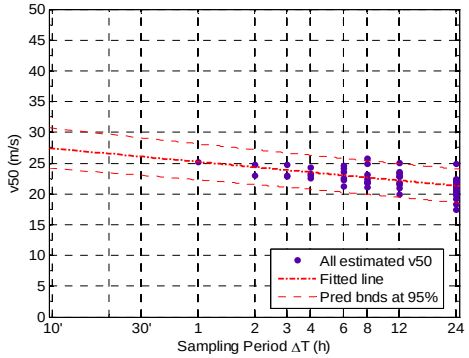
v50 (m/s)
Sampling Period ΔT (h)
All estimated v50
Fitted line
Pred bnds at 95%

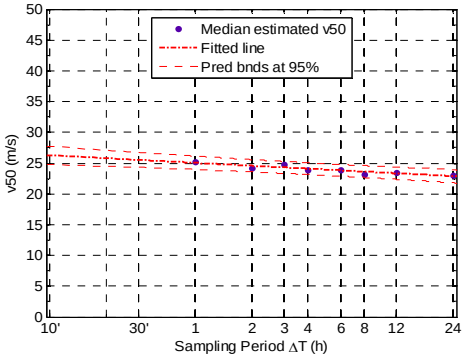
v50 (m/s)
Sampling Period ΔT (h)
Median estimated v50
Fitted line
Pred bnds at 95%

LIQB

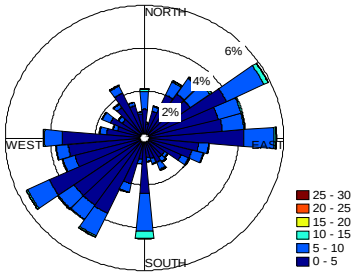
NORTH
6%
4%
2%
WEST
EAST
SOUTH
25 - 30
20 - 25
15 - 20
10 - 15
5 - 10
0 - 5

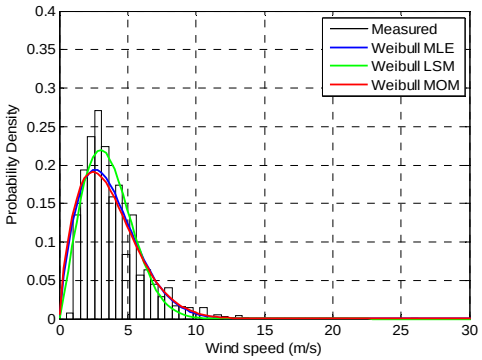
Measured
Weibull MLE
Weibull LSM
Weibull MOM
Probability Density
Wind speed (m/s)

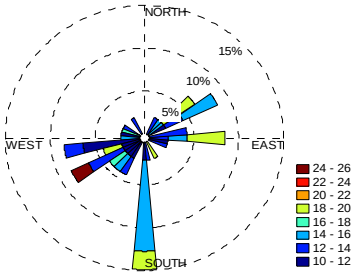
NORTH
15%
10%
5%
WEST
EAST
SOUTH
24 - 26
22 - 24
20 - 22
18 - 20
16 - 18
14 - 16
12 - 14
10 - 12

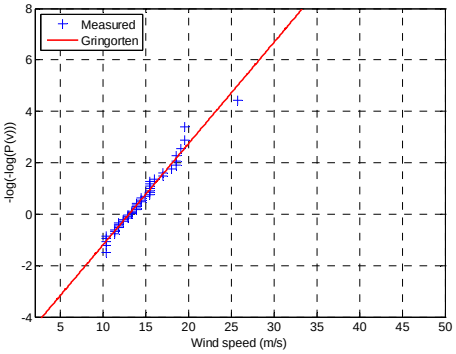
Measured
Gringorten
-log(-log(P(v)))
Wind speed (m/s)

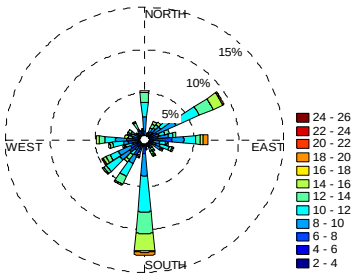
NORTH
15%
10%
5%
WEST
EAST
SOUTH
24 - 26
22 - 24
20 - 22
18 - 20
16 - 18
14 - 16
12 - 14
10 - 12
8 - 10
6 - 8
4 - 6
2 - 4

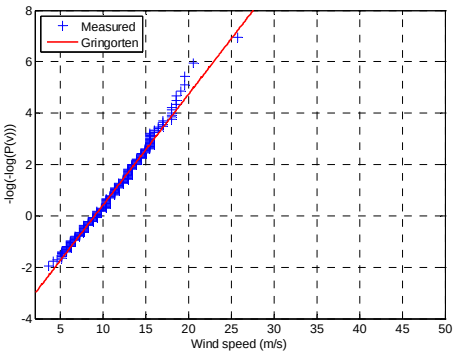
Measured
Gringorten
-log(-log(P(v)))
Wind speed (m/s)

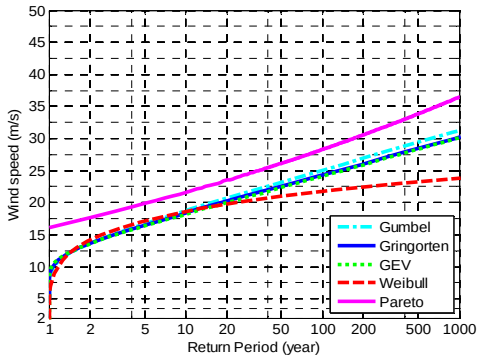
Wind speed (m/s)
Return Period (year)
Gumbel
Gringorten
GEV
Weibull
Pareto

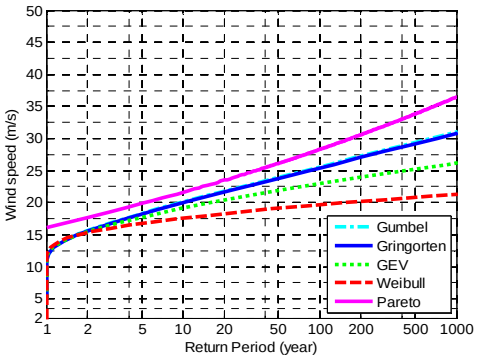
Wind speed (m/s)
Return Period (year)
Gumbel
Gringorten
GEV
Weibull
Pareto

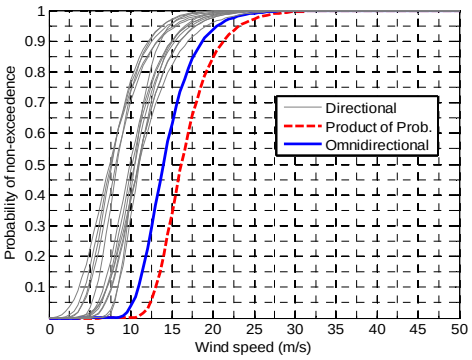
Probability of non-exceedence
Wind speed (m/s)
Directional
Product of Prob.
Omnidirectional

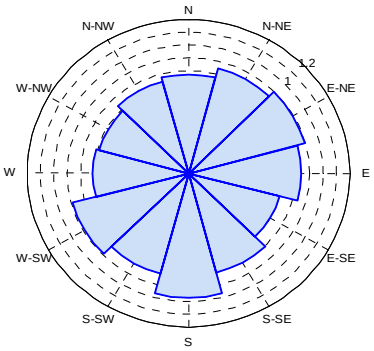
N
N-NE
E-NE
E
E-SE
S-SE
S
S-SW
W
W-NW
N-NW

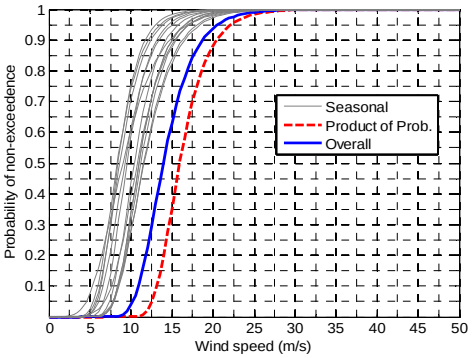
Probability of non-exceedence
Wind speed (m/s)
Seasonal
Product of Prob.
Overall

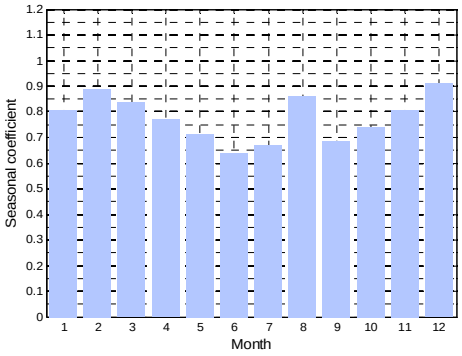
Seasonal coefficient
Month

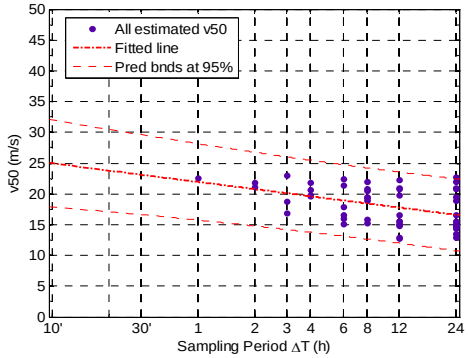
v50 (m/s)
Sampling Period ΔT (h)
All estimated v50
Fitted line
Pred bnds at 95%

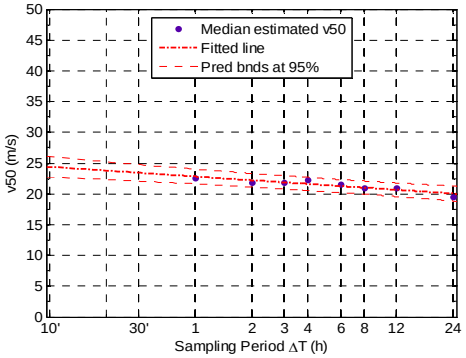
v50 (m/s)
Sampling Period ΔT (h)
Median estimated v50
Fitted line
Pred bnds at 95%

LIQC

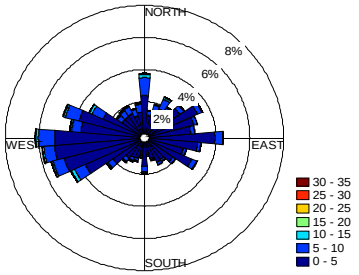
NORTH
8%
6%
4%
2%
WEST
EAST
SOUTH
30 - 35
25 - 30
20 - 25
15 - 20
10 - 15
5 - 10
0 - 5

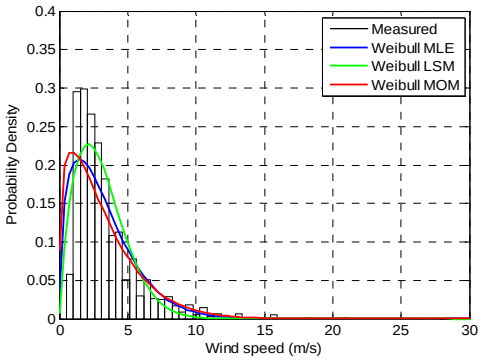
Measured
Weibull MLE
Weibull LSM
Weibull MOM
Probability Density
Wind speed (m/s)

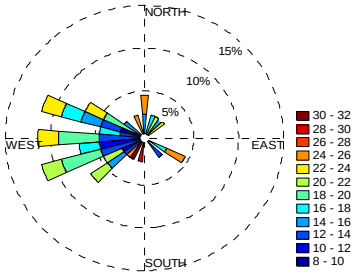
NORTH
15%
10%
5%
WEST
EAST
SOUTH
30 - 32
28 - 30
26 - 28
24 - 26
22 - 24
20 - 22
18 - 20
16 - 18
14 - 16
12 - 14
10 - 12
8 - 10

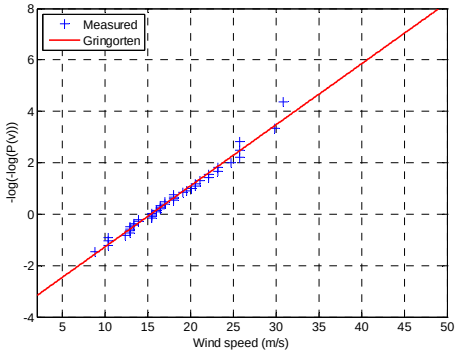
Measured
Gringorten
-log(-log(P(v)))
Wind speed (m/s)

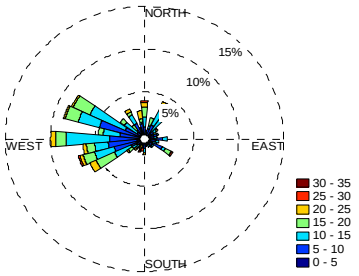
NORTH
15%
10%
5%
WEST
EAST
SOUTH
30 - 35
25 - 30
20 - 25
15 - 20
10 - 15
5 - 10
0 - 5

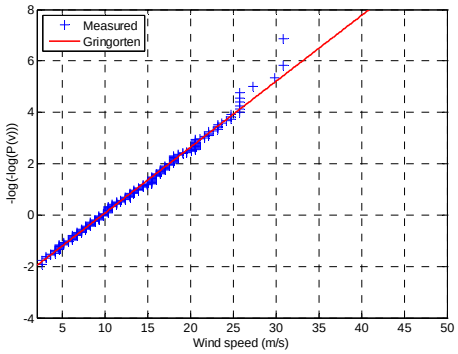
Measured
Gringorten
-log(-log(P(v)))
Wind speed (m/s)

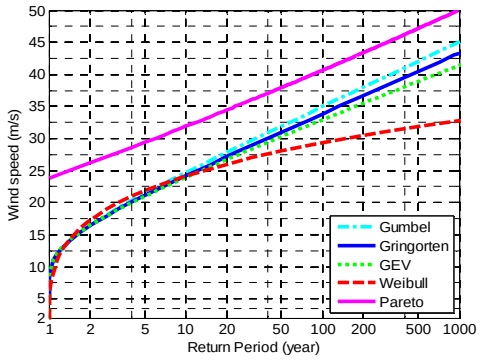
Wind speed (m/s)
Return Period (year)
Gumbel
Gringorten
GEV
Weibull
Pareto

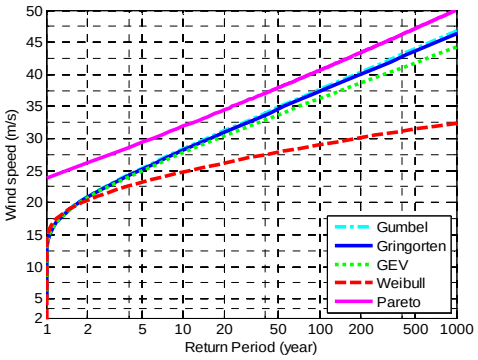
Wind speed (m/s)
Return Period (year)
Gumbel
Gringorten
GEV
Weibull
Pareto

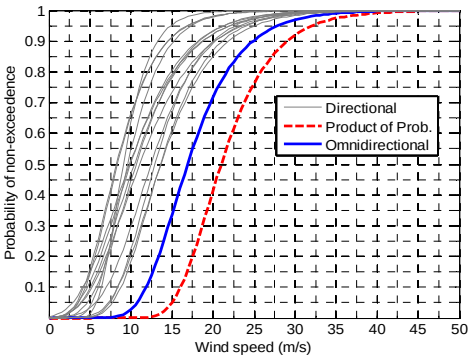
Probability of non-exceedence
Wind speed (m/s)
Directional
Product of Prob.
Omnidirectional

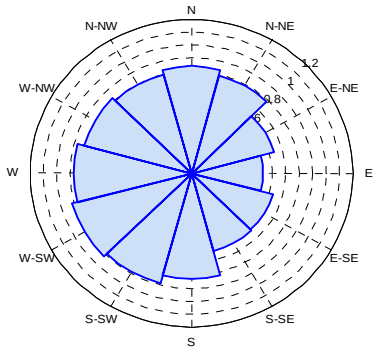
N
N-NE
E-NE
E
E-SE
S-SE
S
S-SW
W
W-NW
N-NW

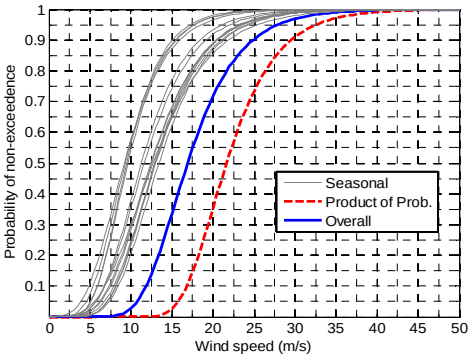
Probability of non-exceedence
Wind speed (m/s)
Seasonal
Product of Prob.
Overall

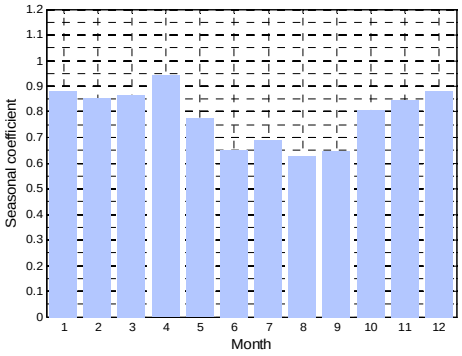
Seasonal coefficient
Month

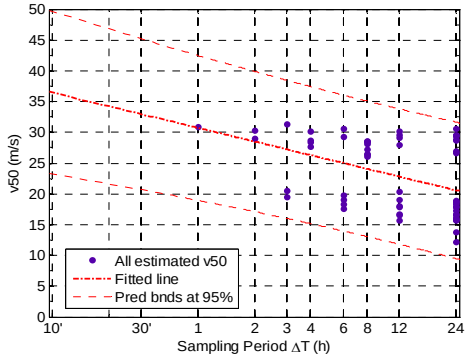
v50 (m/s)
Sampling Period ΔT (h)
All estimated v50
Fitted line
Pred bnds at 95%

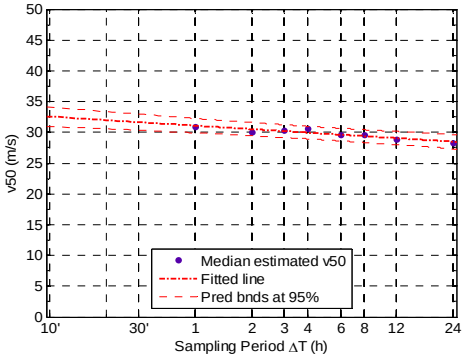
v50 (m/s)
Sampling Period ΔT (h)
Median estimated v50
Fitted line
Pred bnds at 95%

LIQD

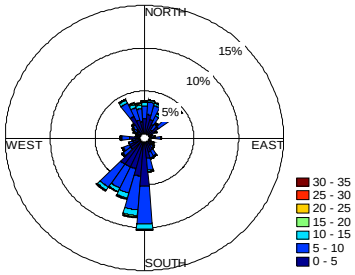
NORTH
15%
10%
5%
WEST
EAST
SOUTH
30 - 35
25 - 30
20 - 25
15 - 20
10 - 15
5 - 10
0 - 5

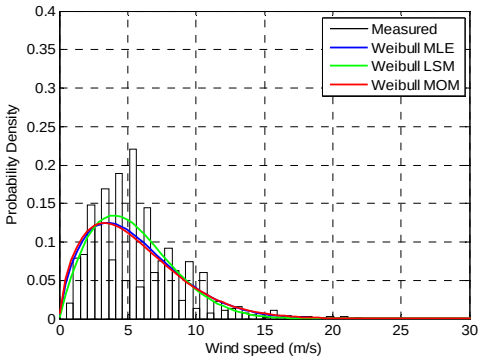
Measured
Weibull MLE
Weibull LSM
Weibull MOM
Probability Density
Wind speed (m/s)

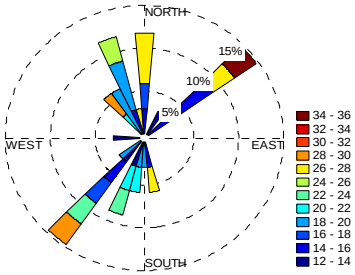
NORTH
15%
10%
5%
WEST
EAST
SOUTH
34 - 36
32 - 34
30 - 32
28 - 30
26 - 28
24 - 26
22 - 24
20 - 22
18 - 20
16 - 18
14 - 16
12 - 14

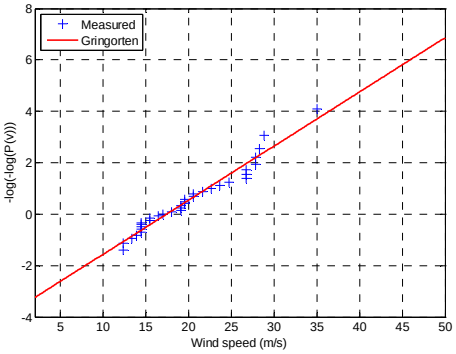
Measured
Gringorten
-log(-log(P(v)))
Wind speed (m/s)

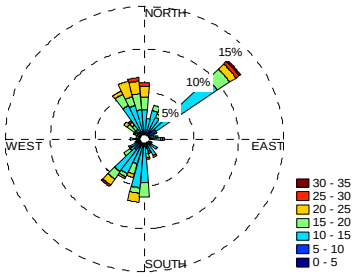
NORTH
15%
10%
5%
WEST
EAST
SOUTH
30 - 35
25 - 30
20 - 25
15 - 20
10 - 15
5 - 10
0 - 5

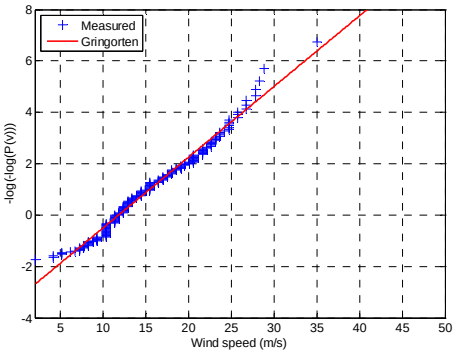
Measured
Gringorten
-log(-log(P(v)))
Wind speed (m/s)

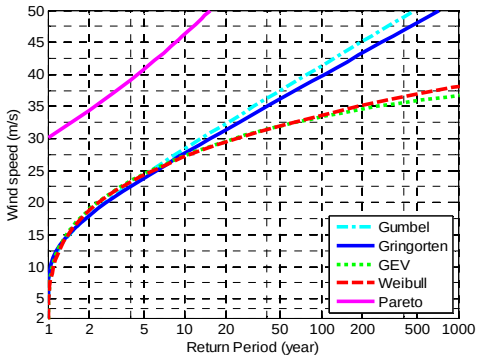
Wind speed (m/s)
Return Period (year)
Gumbel
Gringorten
GEV
Weibull
Pareto

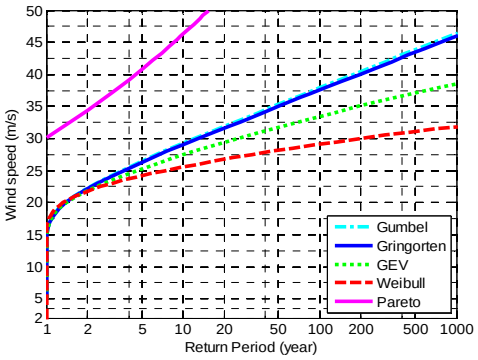
Wind speed (m/s)
Return Period (year)
Gumbel
Gringorten
GEV
Weibull
Pareto

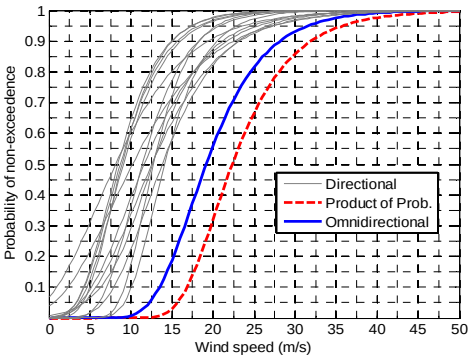
Probability of non-exceedence
Wind speed (m/s)
Directional
Product of Prob.
Omnidirectional

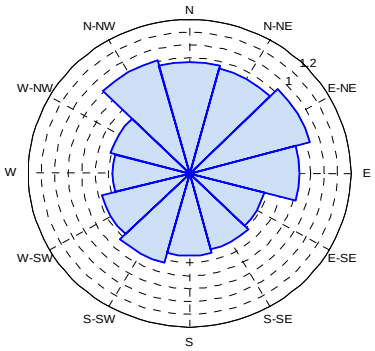
N
N-NE
E-NE
E
E-SE
S-SE
S
S-SW
W
W-NW
N-NW

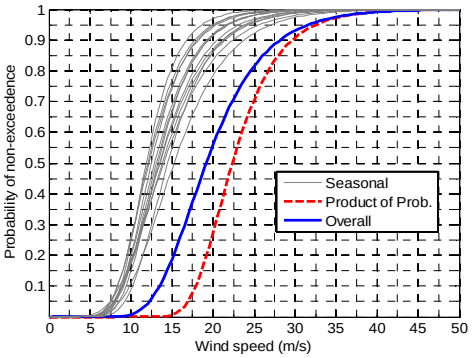
Probability of non-exceedence
Wind speed (m/s)
Seasonal
Product of Prob.
Overall

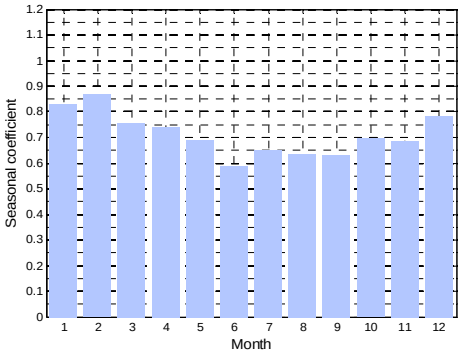
Seasonal coefficient
Month

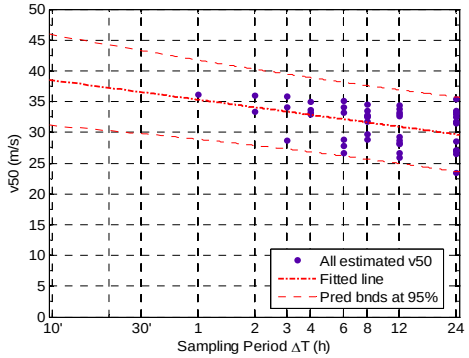
v50 (m/s)
Sampling Period ΔT (h)
All estimated v50
Fitted line
Pred bnds at 95%

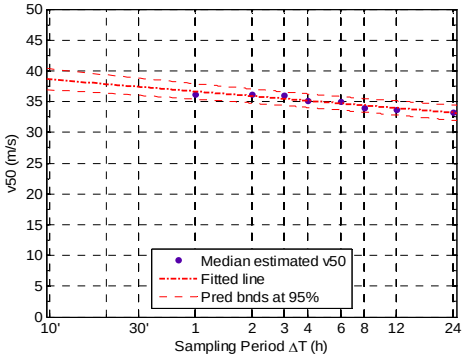
v50 (m/s)
Sampling Period ΔT (h)
Median estimated v50
Fitted line
Pred bnds at 95%

LIQI

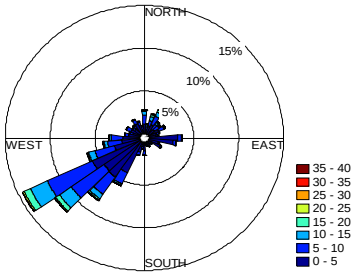
NORTH
15%
10%
5%
WEST
EAST
SOUTH
35 - 40
30 - 35
25 - 30
20 - 25
15 - 20
10 - 15
5 - 10
0 - 5

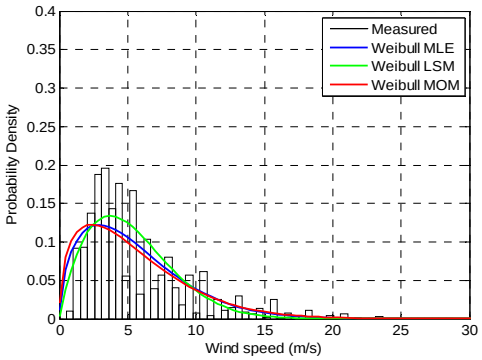
Measured
Weibull MLE
Weibull LSM
Weibull MOM
Probability Density
Wind speed (m/s)

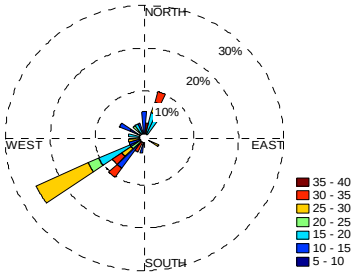
NORTH
30%
20%
10%
WEST
EAST
SOUTH
35 - 40
30 - 35
25 - 30
20 - 25
15 - 20
10 - 15
5 - 10

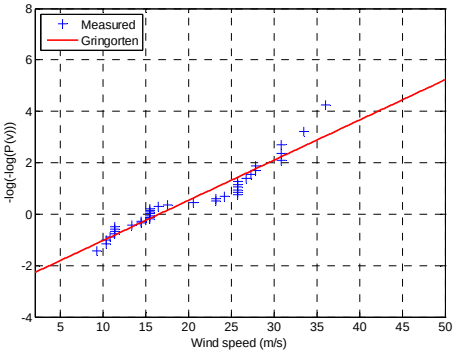
Measured
Gringorten
-log(-log(P(v)))
Wind speed (m/s)

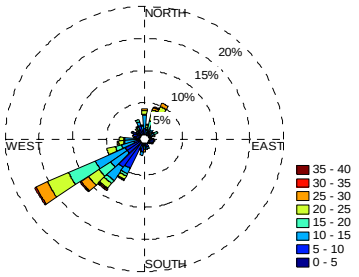
NORTH
20%
15%
10%
5%
WEST
EAST
SOUTH
35 - 40
30 - 35
25 - 30
20 - 25
15 - 20
10 - 15
5 - 10
0 - 5

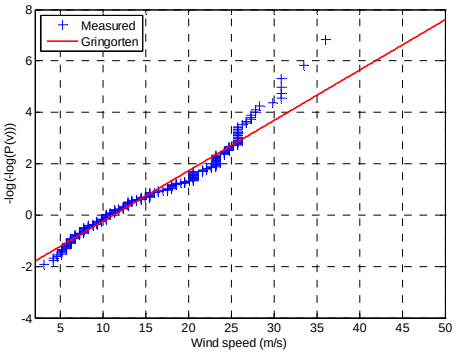
Measured
Gringorten
-log(-log(P(v)))
Wind speed (m/s)

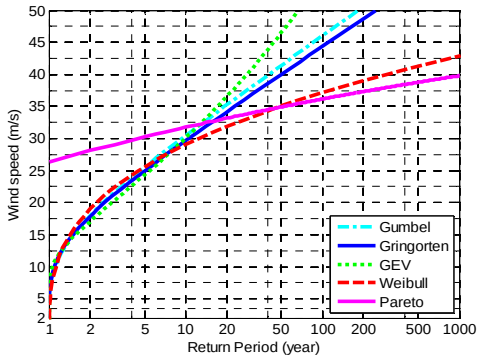
Wind speed (m/s)
Return Period (year)
Gumbel
Gringorten
GEV
Weibull
Pareto

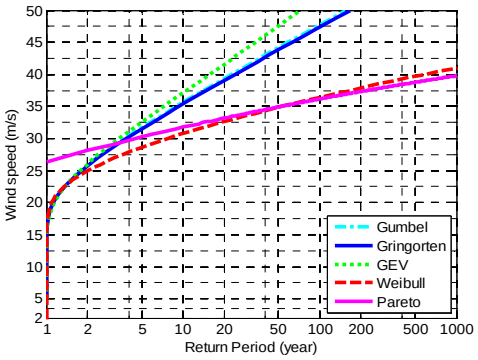
Wind speed (m/s)
Return Period (year)
Gumbel
Gringorten
GEV
Weibull
Pareto

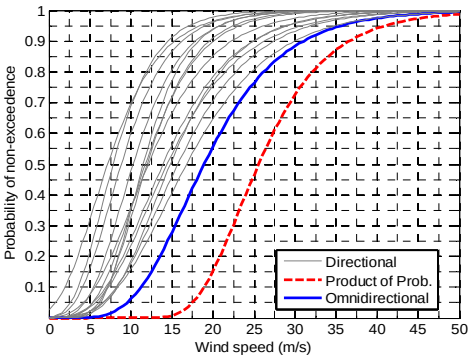
Probability of non-exceedence
Wind speed (m/s)
Directional
Product of Prob.
Omnidirectional

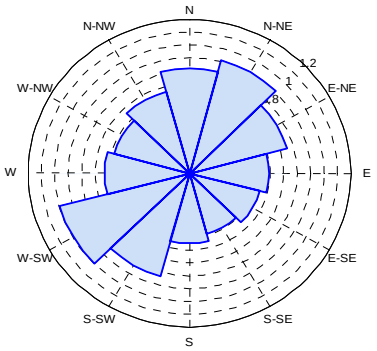
N
N-NE
E-NE
E
E-SE
S-SE
S
S-SW
W
W-NW
N-NW

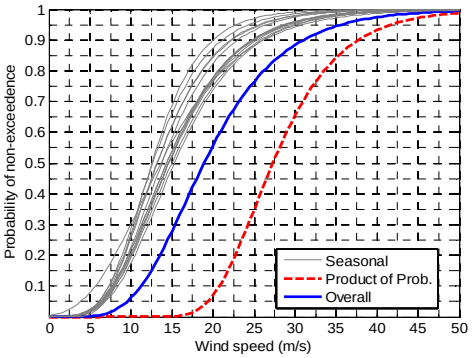
Probability of non-exceedence
Wind speed (m/s)
Seasonal
Product of Prob.
Overall

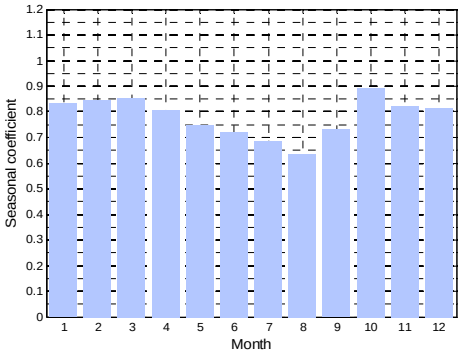
Seasonal coefficient
Month

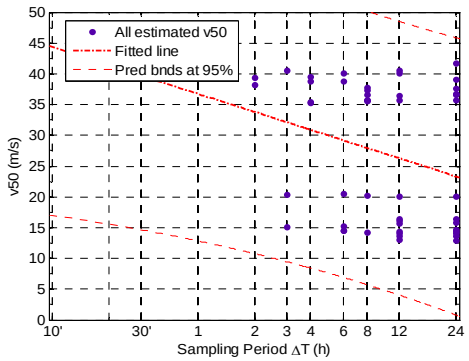
All estimated v50
Fitted line
Pred bnds at 95%
v50 (m/s)
Sampling Period ΔT (h)

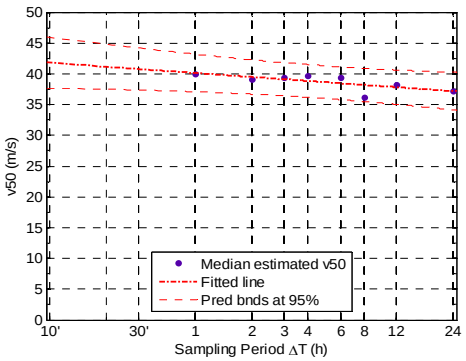
Median estimated v50
Fitted line
Pred bnds at 95%
v50 (m/s)
Sampling Period ΔT (h)

LIQJ

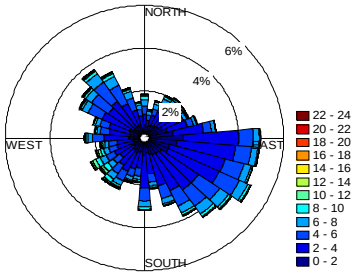
NORTH
6%
4%
2%
WEST
EAST
SOUTH
22 - 24
20 - 22
18 - 20
16 - 18
14 - 16
12 - 14
10 - 12
8 - 10
6 - 8
4 - 6
2 - 4
0 - 2

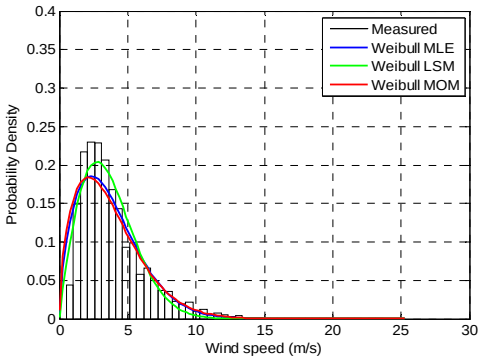
Measured
Weibull MLE
Weibull LSM
Weibull MOM
Probability Density
Wind speed (m/s)

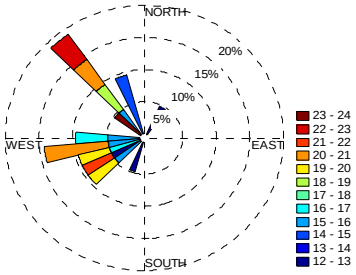
NORTH
20%
15%
10%
5%
WEST
EAST
SOUTH
23 - 24
22 - 23
21 - 22
20 - 21
19 - 20
18 - 19
17 - 18
16 - 17
15 - 16
14 - 15
13 - 14
12 - 13

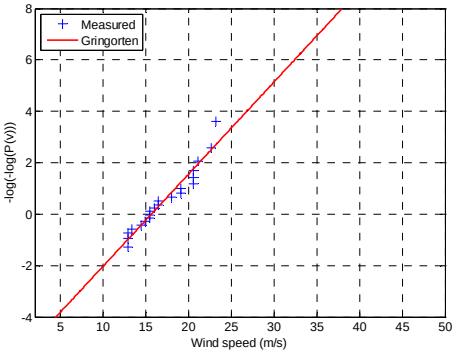
Measured
Gringorten
-log(-log(P(v)))
Wind speed (m/s)

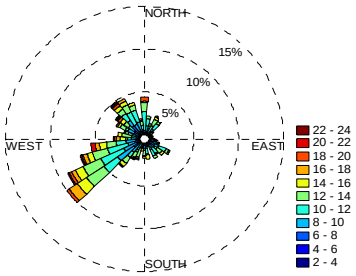
NORTH
15%
10%
5%
WEST
EAST
SOUTH
22 - 24
20 - 22
18 - 20
16 - 18
14 - 16
12 - 14
10 - 12
8 - 10
6 - 8
4 - 6
2 - 4

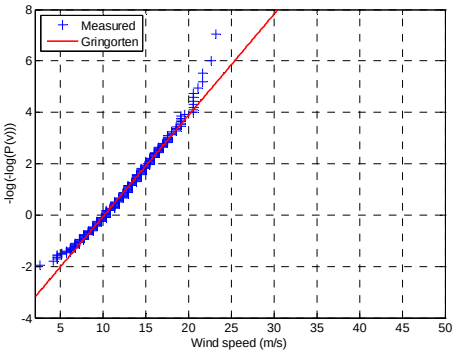
Measured
Gringorten
-log(-log(P(v)))
Wind speed (m/s)

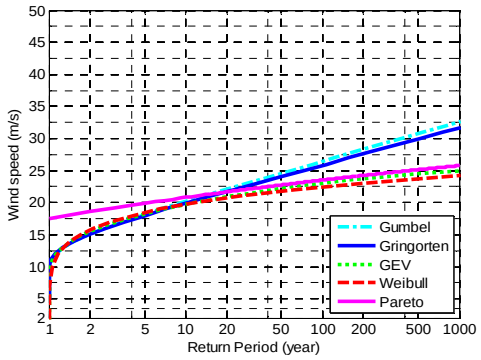
Wind speed (m/s)
Return Period (year)
Gumbel
Gringorten
GEV
Weibull
Pareto

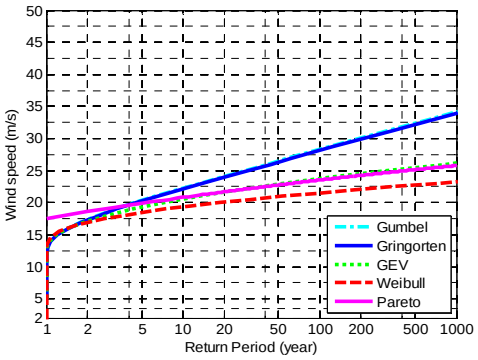
Wind speed (m/s)
Return Period (year)
Gumbel
Gringorten
GEV
Weibull
Pareto

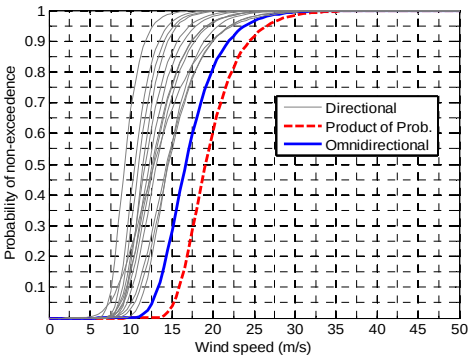
Probability of non-exceedence
Wind speed (m/s)
Directional
Product of Prob.
Omnidirectional

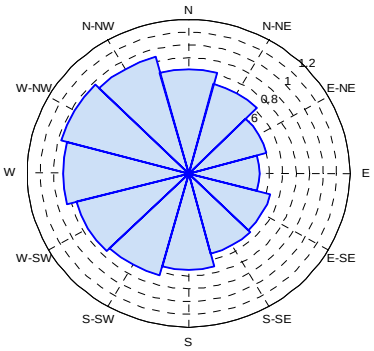
N
N-NE
E-NE
E
E-SE
S-SE
S
S-SW
W
W-NW
N-NW

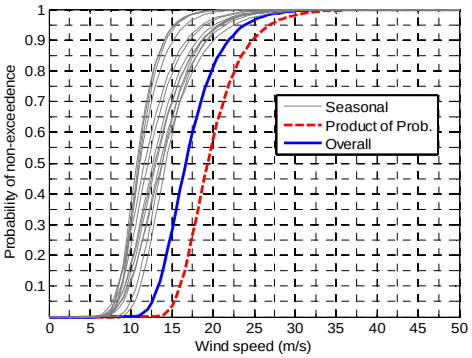
Probability of non-exceedence
Wind speed (m/s)
Seasonal
Product of Prob.
Overall

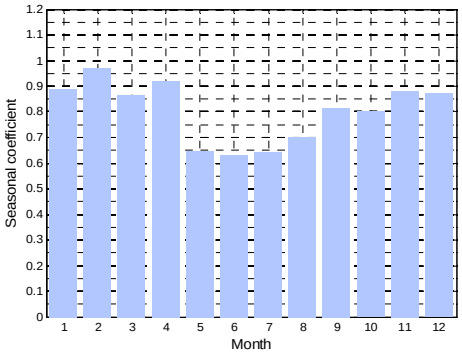
Seasonal coefficient
Month

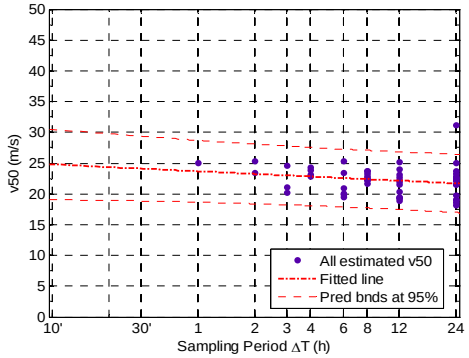
v50 (m/s)
Sampling Period ΔT (h)
All estimated v50
Fitted line
Pred bnds at 95%

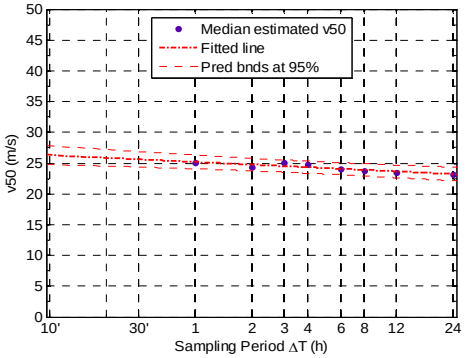
v50 (m/s)
Sampling Period ΔT (h)
Median estimated v50
Fitted line
Pred bnds at 95%

LIQK

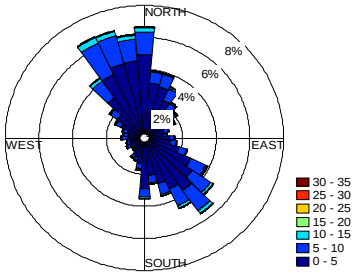
NORTH
EAST
SOUTH
WEST
2%
4%
6%
8%
30 - 35
25 - 30
20 - 25
15 - 20
10 - 15
5 - 10
0 - 5

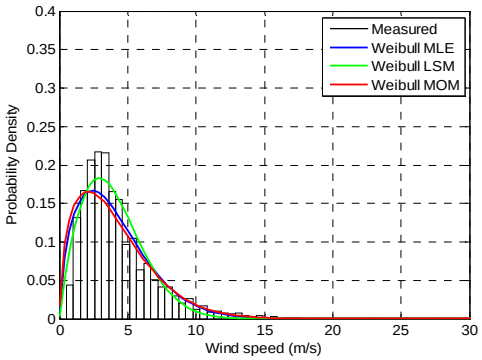
Measured
Weibull MLE
Weibull LSM
Weibull MOM
Probability Density
Wind speed (m/s)

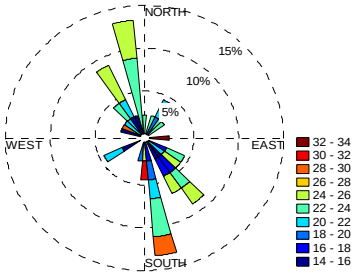
NORTH
EAST
SOUTH
WEST
5%
10%
15%
32 - 34
30 - 32
28 - 30
26 - 28
24 - 26
22 - 24
20 - 22
18 - 20
16 - 18
14 - 16

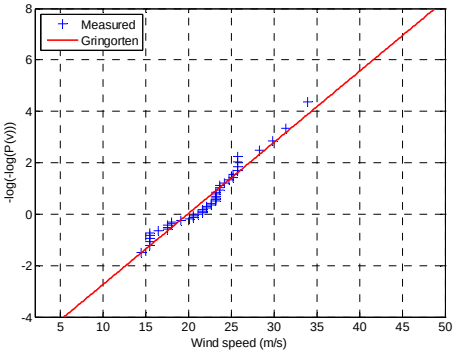
Measured
Gringorten
-log(-log(P(v)))
Wind speed (m/s)

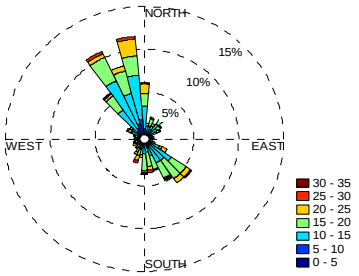
NORTH
EAST
SOUTH
WEST
5%
10%
15%
30 - 35
25 - 30
20 - 25
15 - 20
10 - 15
5 - 10
0 - 5

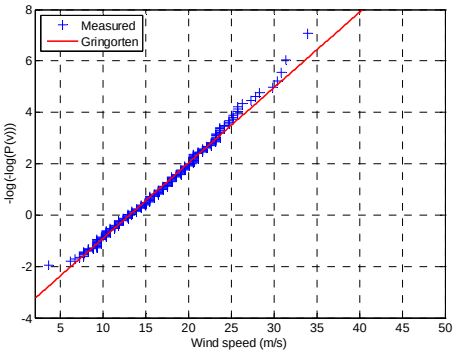
Measured
Gringorten
-log(-log(P(v)))
Wind speed (m/s)

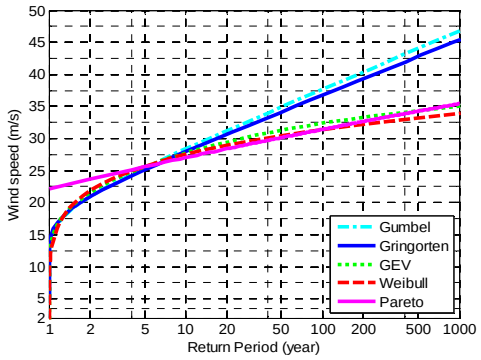
Wind speed (m/s)
Return Period (year)
Gumbel
Gringorten
GEV
Weibull
Pareto

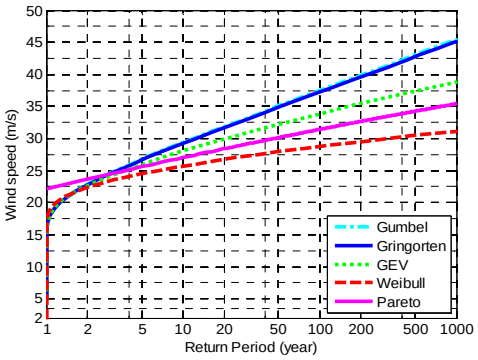
Wind speed (m/s)
Return Period (year)
Gumbel
Gringorten
GEV
Weibull
Pareto

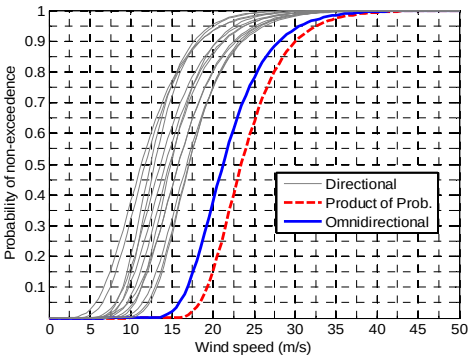
Probability of non-exceedence
Wind speed (m/s)
Directional
Product of Prob.
Omnidirectional

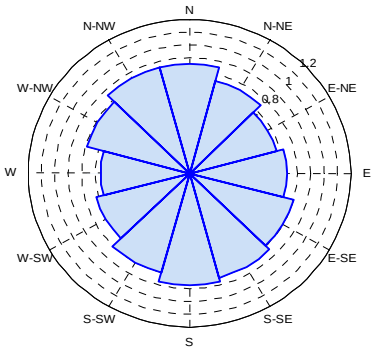
N
N-NE
E-NE
E
E-SE
S-SE
S
S-SW
W
W-NW
N-NW

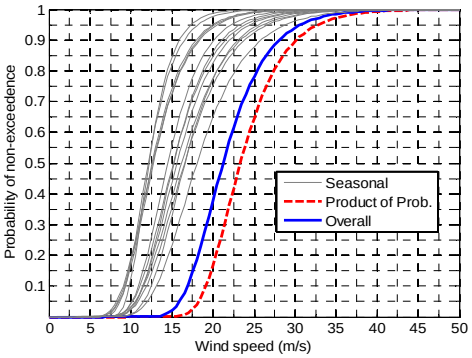
Probability of non-exceedence
Wind speed (m/s)
Seasonal
Product of Prob.
Overall

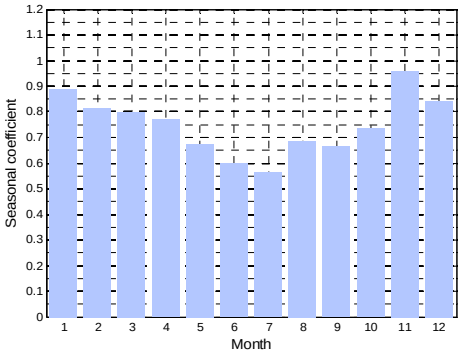
Seasonal coefficient
Month

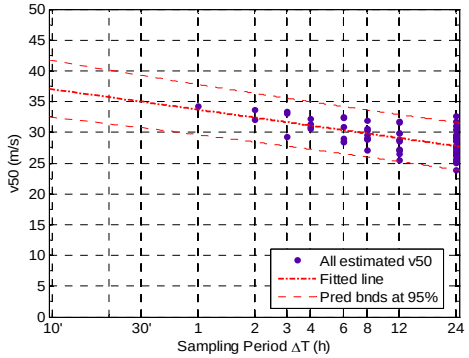
v50 (m/s)
Sampling Period ΔT (h)
All estimated v50
Fitted line
Pred bnds at 95%

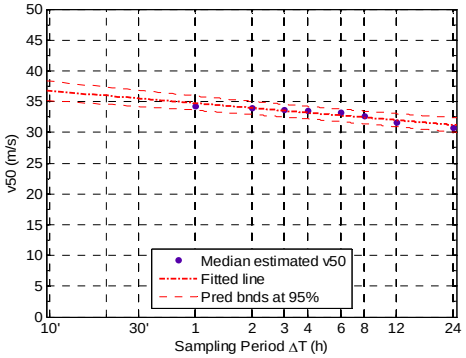
v50 (m/s)
Sampling Period ΔT (h)
Median estimated v50
Fitted line
Pred bnds at 95%

LIQM

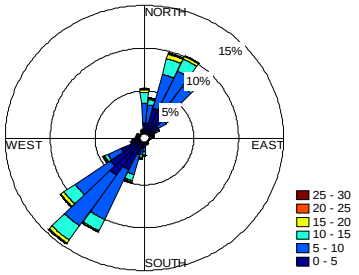
NORTH
15%
10%
5%
WEST
EAST
SOUTH
25 - 30
20 - 25
15 - 20
10 - 15
5 - 10
0 - 5

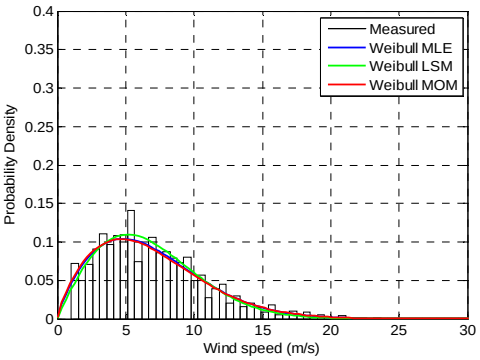
Measured
Weibull MLE
Weibull LSM
Weibull MOM
Probability Density
Wind speed (m/s)

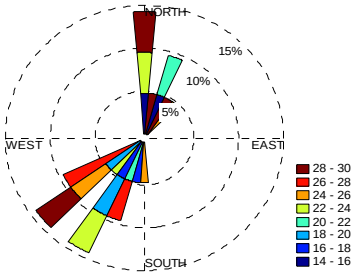
NORTH
15%
10%
5%
WEST
EAST
SOUTH
28 - 30
26 - 28
24 - 26
22 - 24
20 - 22
18 - 20
16 - 18
14 - 16

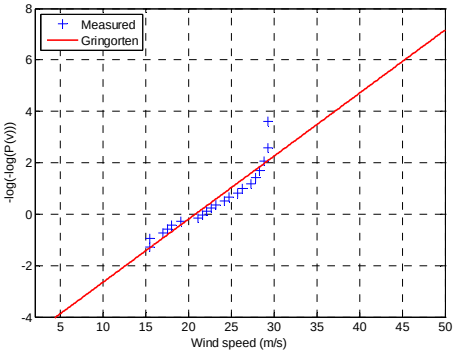
Measured
Gringorten
-log(-log(P(v)))
Wind speed (m/s)

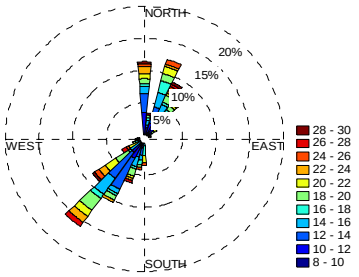
NORTH
20%
15%
10%
5%
WEST
EAST
SOUTH
28 - 30
26 - 28
24 - 26
22 - 24
20 - 22
18 - 20
16 - 18
14 - 16
12 - 14
10 - 12
8 - 10

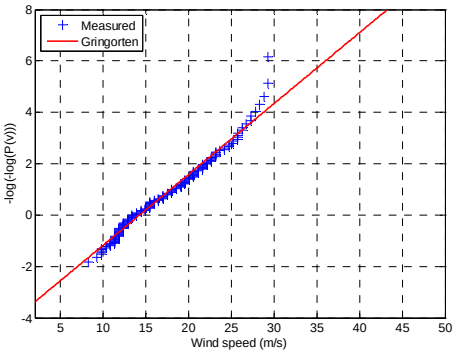
Measured
Gringorten
-log(-log(P(v)))
Wind speed (m/s)

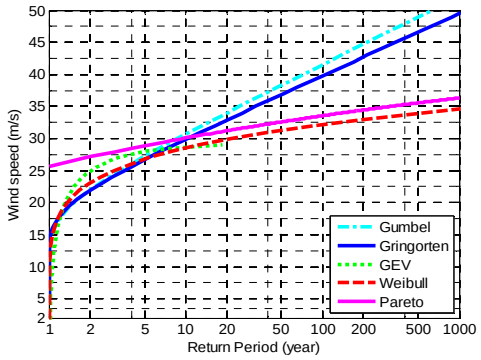
Wind speed (m/s)
Return Period (year)
Gumbel
Gringorten
GEV
Weibull
Pareto

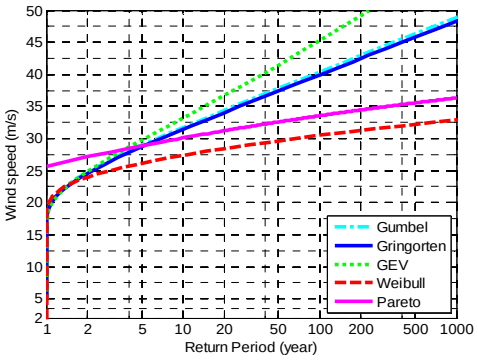
Wind speed (m/s)
Return Period (year)
Gumbel
Gringorten
GEV
Weibull
Pareto

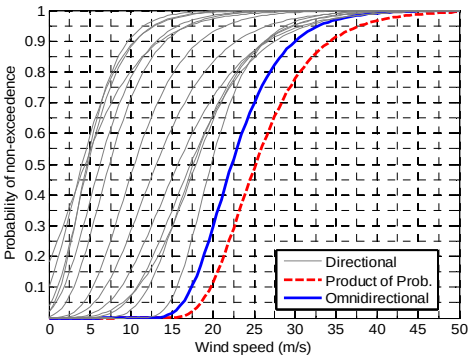
Probability of non-exceedence
Wind speed (m/s)
Directional
Product of Prob.
Omnidirectional

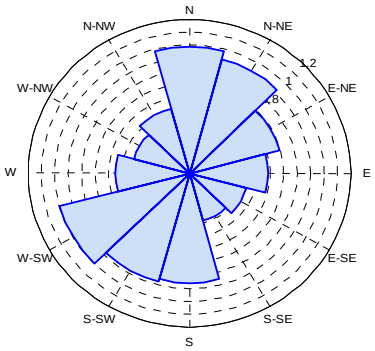
N
N-NE
E-NE
E
E-SE
S-SE
S
S-SW
W
W-NW
N-NW

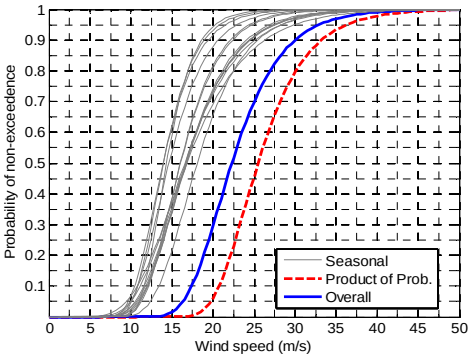
Probability of non-exceedence
Wind speed (m/s)
Seasonal
Product of Prob.
Overall

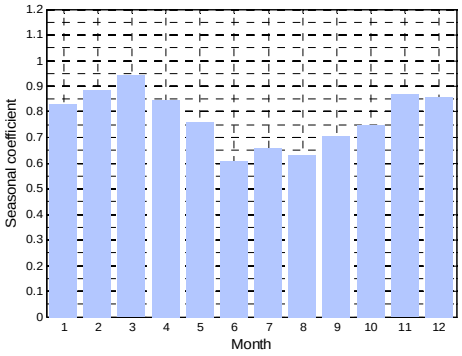
Seasonal coefficient
Month

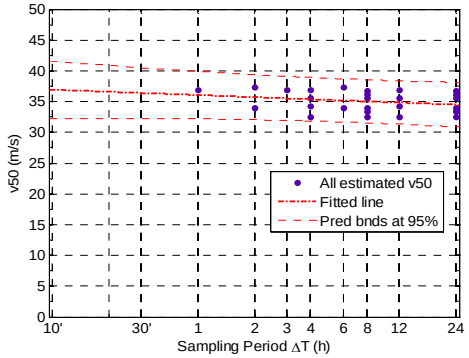
v50 (m/s)
Sampling Period ΔT (h)
All estimated v50
Fitted line
Pred bnds at 95%

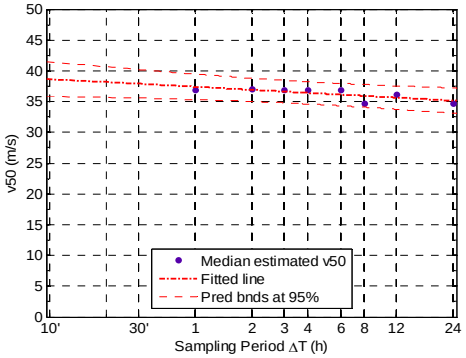
v50 (m/s)
Sampling Period ΔT (h)
Median estimated v50
Fitted line
Pred bnds at 95%

LIQN

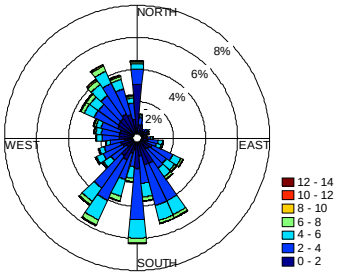
NORTH
8%
6%
4%
2%
WEST
EAST
SOUTH
12 - 14
10 - 12
8 - 10
6 - 8
4 - 6
2 - 4
0 - 2

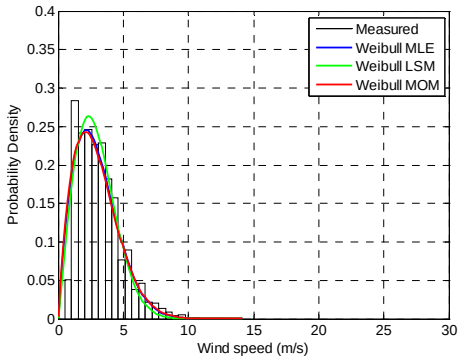
Measured
Weibull MLE
Weibull LSM
Weibull MOM
Probability Density
Wind speed (m/s)

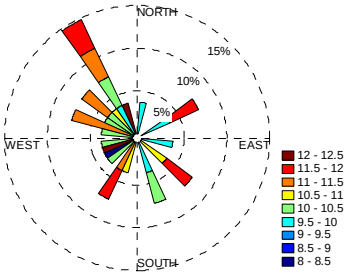
NORTH
15%
10%
5%
WEST
EAST
SOUTH
12 - 12.5
11.5 - 12
11 - 11.5
10.5 - 11
10 - 10.5
9.5 - 10
9 - 9.5
8.5 - 9
8 - 8.5

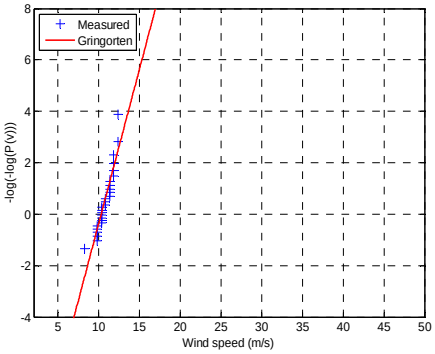
Measured
Gringorten
-log(-log(P(v)))
Wind speed (m/s)

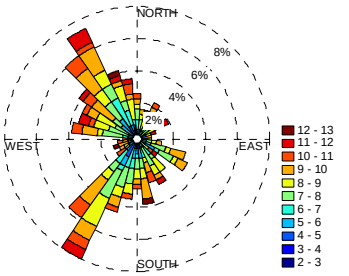
NORTH
8%
6%
4%
2%
WEST
EAST
SOUTH
12 - 13
11 - 12
10 - 11
9 - 10
8 - 9
7 - 8
6 - 7
5 - 6
4 - 5
3 - 4
2 - 3

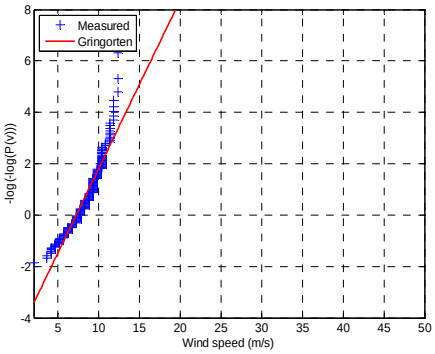
Measured
Gringorten
-log(-log(P(v)))
Wind speed (m/s)

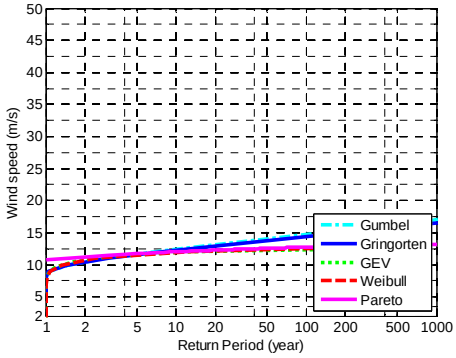
Wind speed (m/s)
Return Period (year)
Gumbel
Gringorten
GEV
Weibull
Pareto

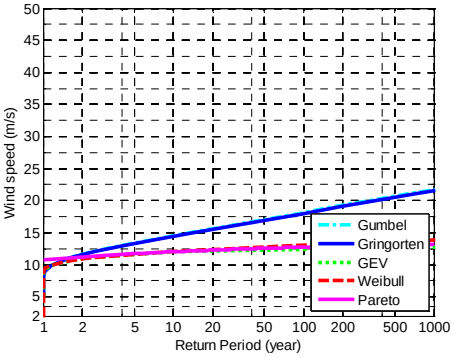
Wind speed (m/s)
Return Period (year)
Gumbel
Gringorten
GEV
Weibull
Pareto

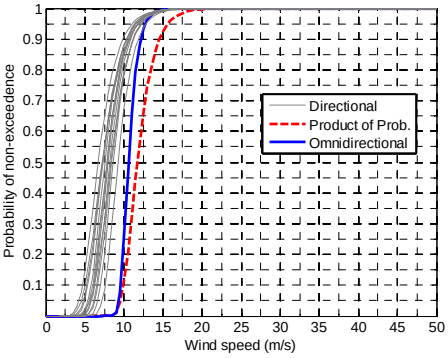
Probability of non-exceedence
Wind speed (m/s)
Directional
Product of Prob.
Omnidirectional

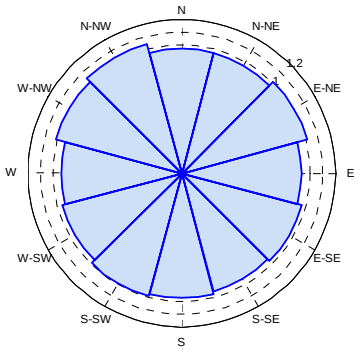
N
N-NE
E-NE
E
E-SE
S-SE
S
S-SW
W
W-NW
N-NW

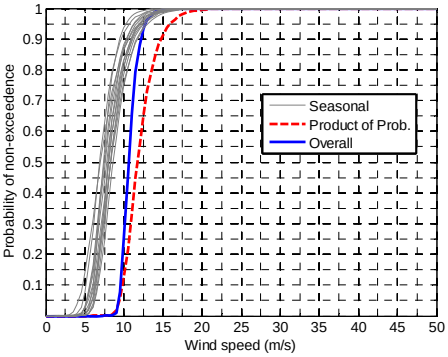
Probability of non-exceedence
Wind speed (m/s)
Seasonal
Product of Prob.
Overall

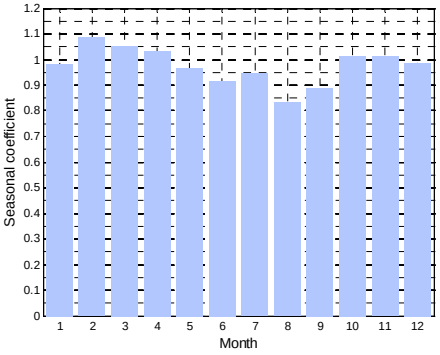
Seasonal coefficient
Month

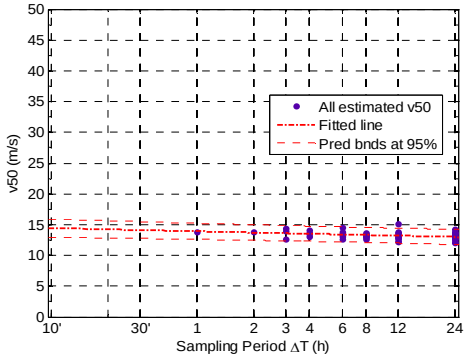
v50 (m/s)
Sampling Period ΔT (h)
All estimated v50
Fitted line
Pred bnds at 95%

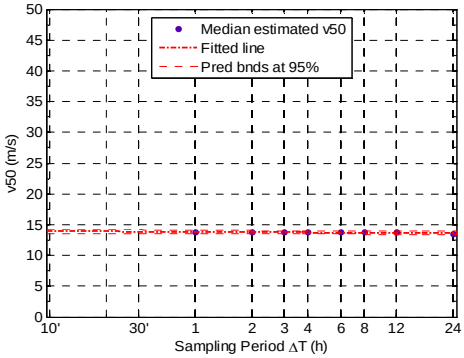
v50 (m/s)
Sampling Period ΔT (h)
Median estimated v50
Fitted line
Pred bnds at 95%

LIQO

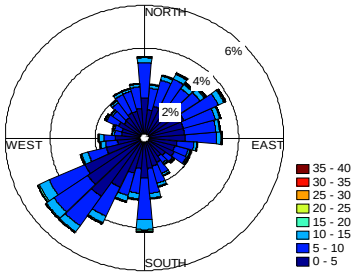
NORTH
6%
4%
2%
WEST
EAST
SOUTH
35 - 40
30 - 35
25 - 30
20 - 25
15 - 20
10 - 15
5 - 10
0 - 5

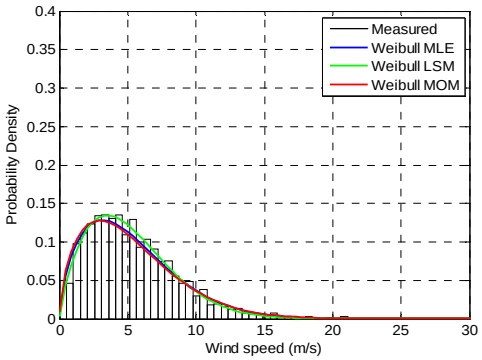
Measured
Weibull MLE
Weibull LSM
Weibull MOM
Probability Density
Wind speed (m/s)

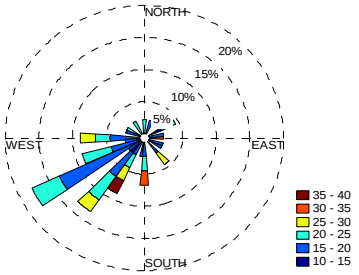
NORTH
20%
15%
10%
5%
WEST
EAST
SOUTH
35 - 40
30 - 35
25 - 30
20 - 25
15 - 20
10 - 15

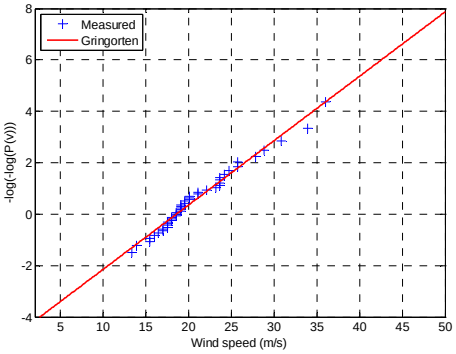
Measured
Gringorten
-log(-log(P(v)))
Wind speed (m/s)

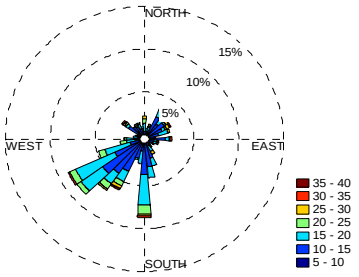
NORTH
15%
10%
5%
WEST
EAST
SOUTH
35 - 40
30 - 35
25 - 30
20 - 25
15 - 20
10 - 15
5 - 10

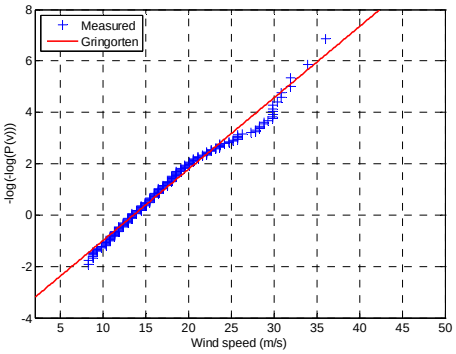
Measured
Gringorten
-log(-log(P(v)))
Wind speed (m/s)

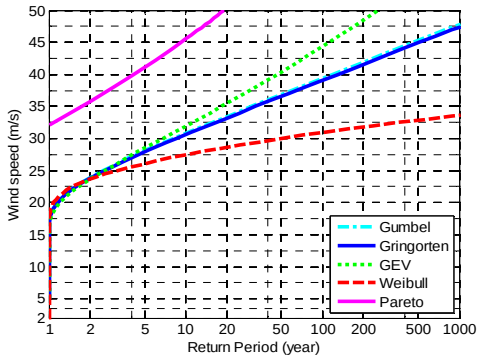
Wind speed (m/s)
Return Period (year)
Gumbel
Gringorten
GEV
Weibull
Pareto

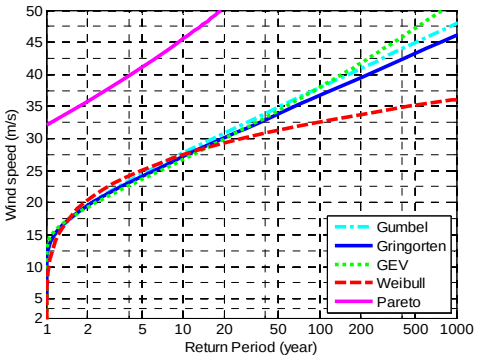
Wind speed (m/s)
Return Period (year)
Gumbel
Gringorten
GEV
Weibull
Pareto

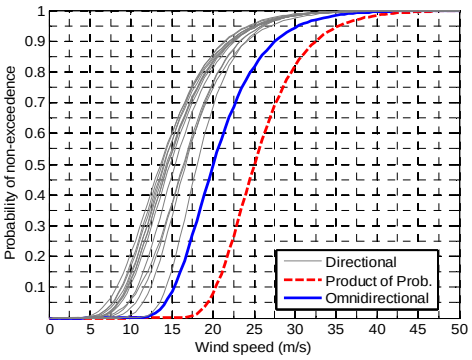
Probability of non-exceedence
Wind speed (m/s)
Directional
Product of Prob.
Omnidirectional

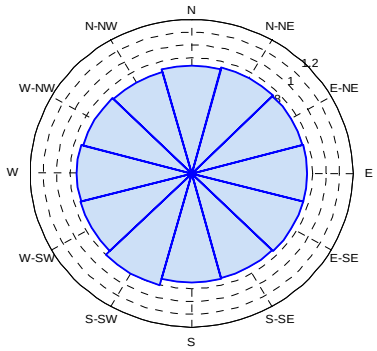
N
N-NE
E-NE
E
E-SE
S-SE
S
S-SW
W
W-NW
N-NW

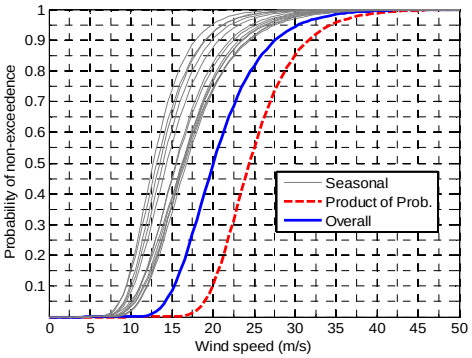
Probability of non-exceedence
Wind speed (m/s)
Seasonal
Product of Prob.
Overall

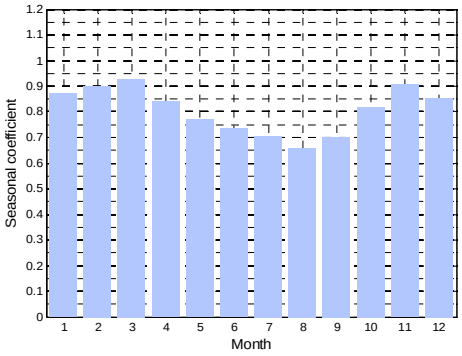
Seasonal coefficient
Month

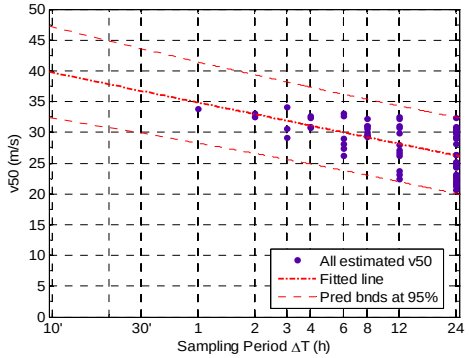
v50 (m/s)
Sampling Period ΔT (h)
All estimated v50
Fitted line
Pred bnds at 95%

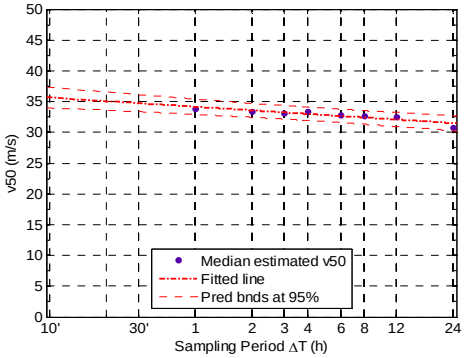
v50 (m/s)
Sampling Period ΔT (h)
Median estimated v50
Fitted line
Pred bnds at 95%

LIQR

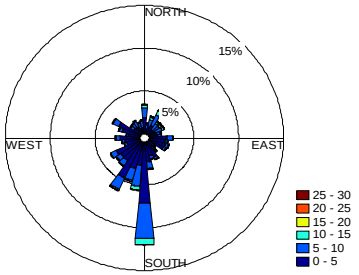
NORTH
15%
10%
5%
WEST
EAST
SOUTH
25 - 30
20 - 25
15 - 20
10 - 15
5 - 10
0 - 5

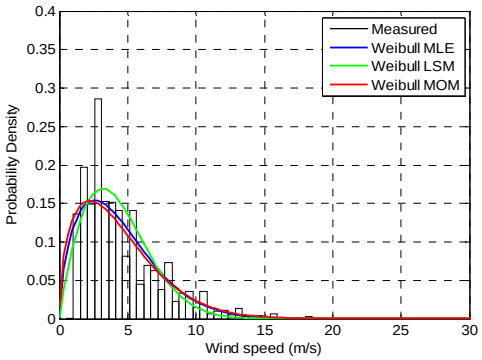
Measured
Weibull MLE
Weibull LSM
Weibull MOM
Probability Density
Wind speed (m/s)

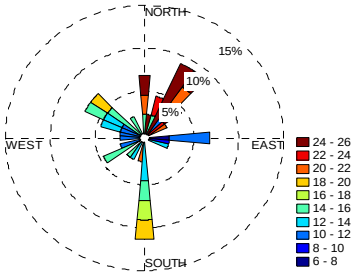
NORTH
15%
10%
5%
WEST
EAST
SOUTH
24 - 26
22 - 24
20 - 22
18 - 20
16 - 18
14 - 16
12 - 14
10 - 12
8 - 10
6 - 8

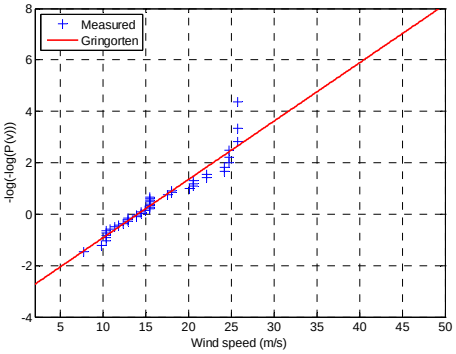
Measured
Gringorten
-log(-log(P(v)))
Wind speed (m/s)

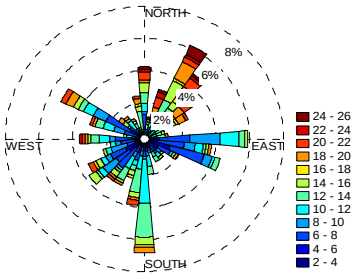
NORTH
8%
6%
4%
2%
WEST
EAST
SOUTH
24 - 26
22 - 24
20 - 22
18 - 20
16 - 18
14 - 16
12 - 14
10 - 12
8 - 10
6 - 8
4 - 6
2 - 4

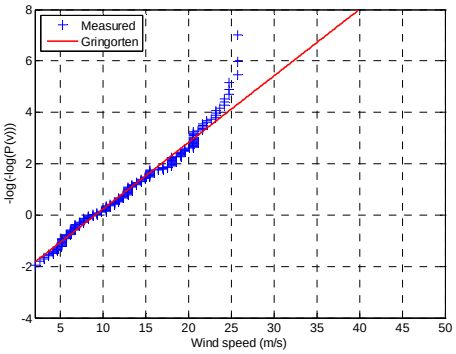
Measured
Gringorten
-log(-log(P(v)))
Wind speed (m/s)

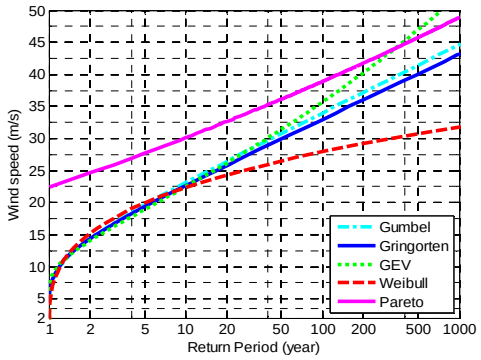
Wind speed (m/s)
Return Period (year)
Gumbel
Gringorten
GEV
Weibull
Pareto

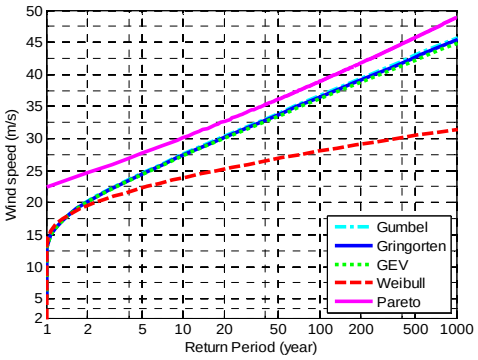
Wind speed (m/s)
Return Period (year)
Gumbel
Gringorten
GEV
Weibull
Pareto

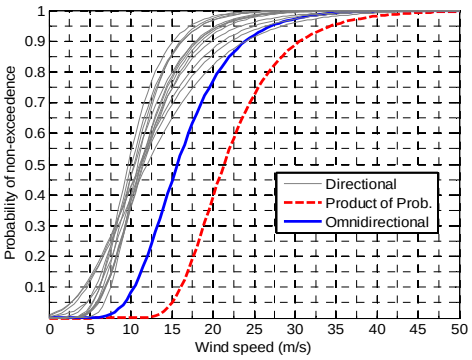
Probability of non-exceedence
Wind speed (m/s)
Directional
Product of Prob.
Omnidirectional

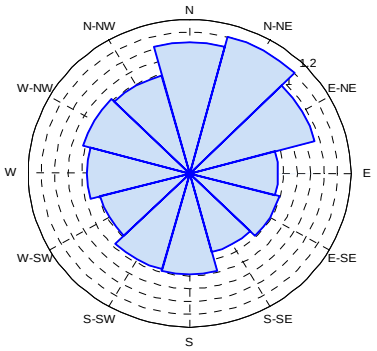
N
N-NE
E-NE
E
E-SE
S-SE
S
S-SW
W
W-NW
N-NW

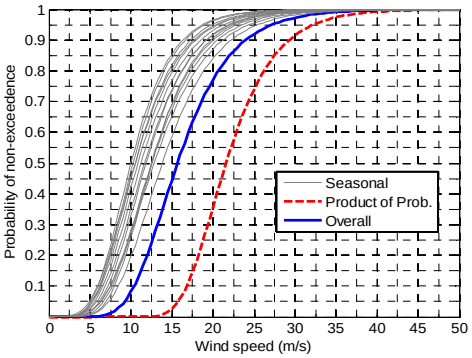
Probability of non-exceedence
Wind speed (m/s)
Seasonal
Product of Prob.
Overall

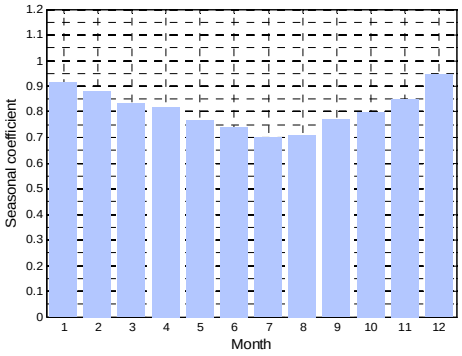
Seasonal coefficient
Month

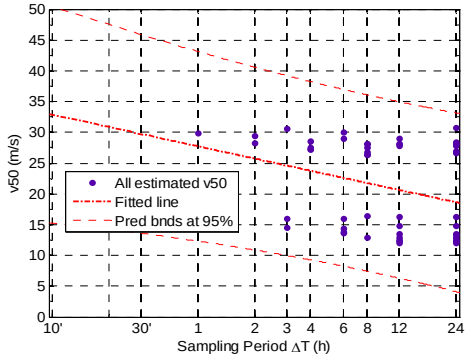
v50 (m/s)
Sampling Period ΔT (h)
All estimated v50
Fitted line
Pred bnds at 95%

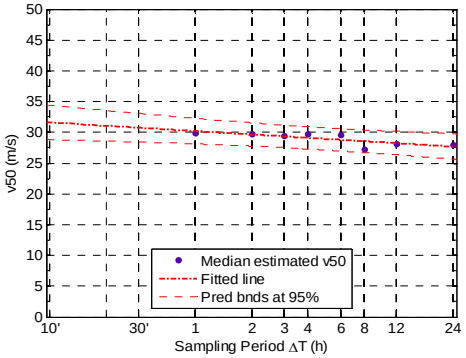
v50 (m/s)
Sampling Period ΔT (h)
Median estimated v50
Fitted line
Pred bnds at 95%

LIQV

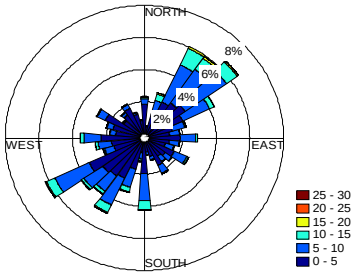
NORTH
EAST
SOUTH
WEST
8%
6%
4%
2%
25 - 30
20 - 25
15 - 20
10 - 15
5 - 10
0 - 5

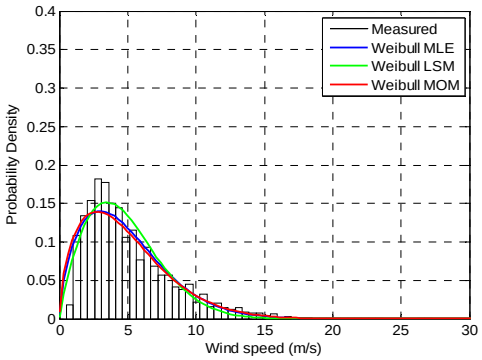
Measured
Weibull MLE
Weibull LSM
Weibull MOM
Probability Density
Wind speed (m/s)

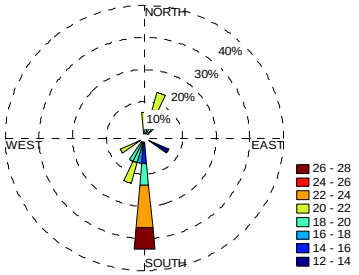
NORTH
EAST
SOUTH
WEST
40%
30%
20%
10%
26 - 28
24 - 26
22 - 24
20 - 22
18 - 20
16 - 18
14 - 16
12 - 14

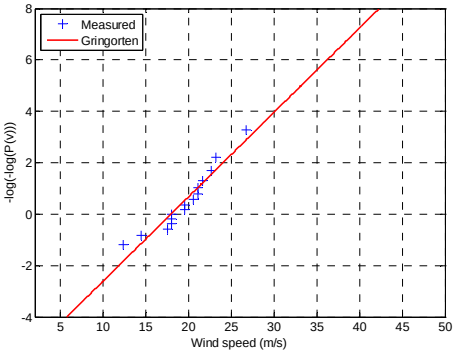
Measured
Gringorten
-log(-log(P(v)))
Wind speed (m/s)

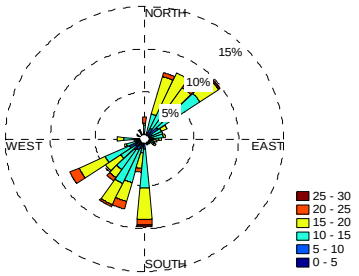
NORTH
EAST
SOUTH
WEST
15%
10%
5%
25 - 30
20 - 25
15 - 20
10 - 15
5 - 10
0 - 5

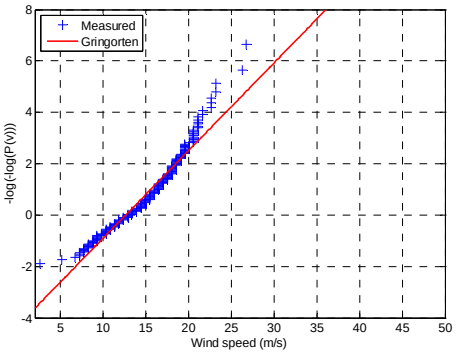
Measured
Gringorten
-log(-log(P(v)))
Wind speed (m/s)

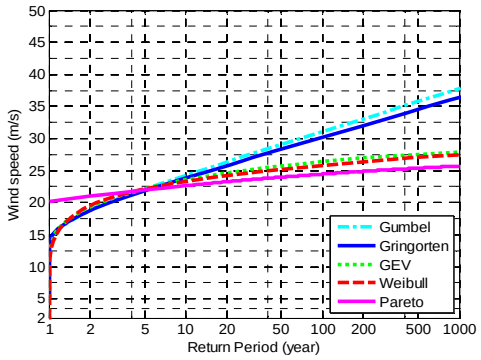
Wind speed (m/s)
Return Period (year)
Gumbel
Gringorten
GEV
Weibull
Pareto

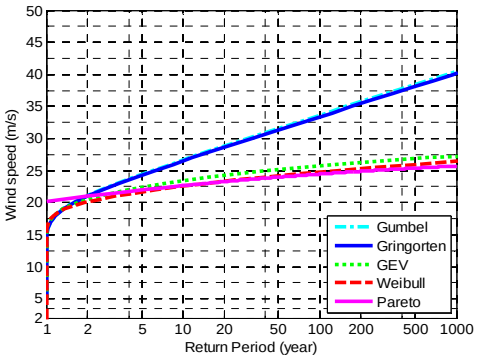
Wind speed (m/s)
Return Period (year)
Gumbel
Gringorten
GEV
Weibull
Pareto

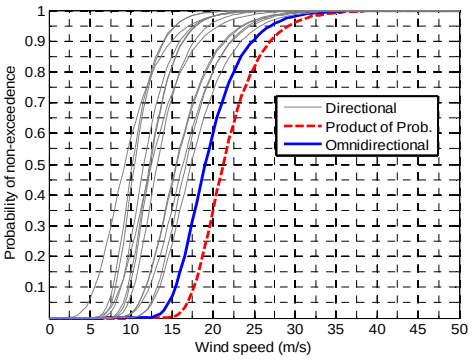
Probability of non-exceedence
Wind speed (m/s)
Directional
Product of Prob.
Omnidirectional

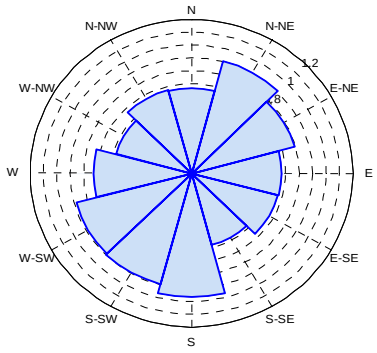
N
N-NE
E-NE
E
E-SE
S-SE
S
S-SW
W
W-NW
N-NW

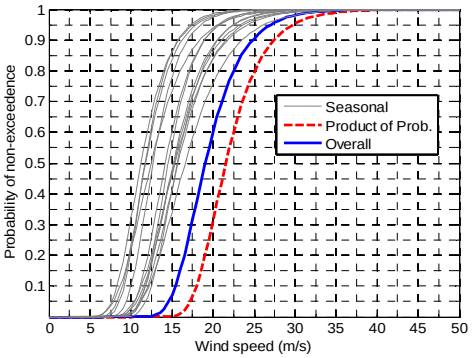
Probability of non-exceedence
Wind speed (m/s)
Seasonal
Product of Prob.
Overall

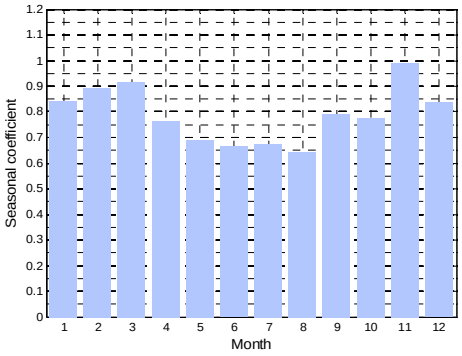
Seasonal coefficient
Month

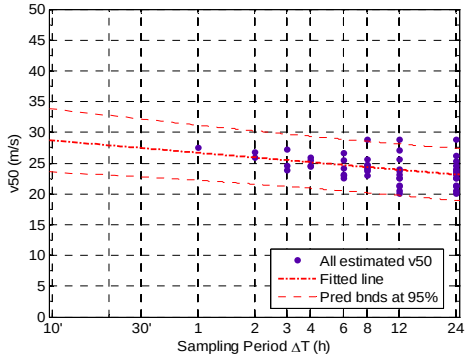
v50 (m/s)
Sampling Period ΔT (h)
All estimated v50
Fitted line
Pred bnds at 95%

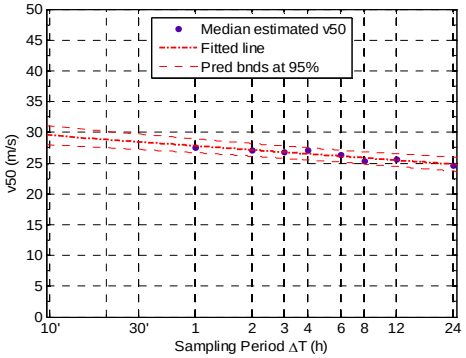
v50 (m/s)
Sampling Period ΔT (h)
Median estimated v50
Fitted line
Pred bnds at 95%

LIQW

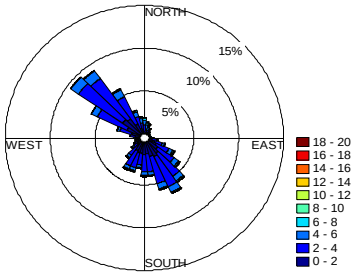
NORTH
15%
10%
5%
WEST
EAST
SOUTH
18 - 20
16 - 18
14 - 16
12 - 14
10 - 12
8 - 10
6 - 8
4 - 6
2 - 4
0 - 2

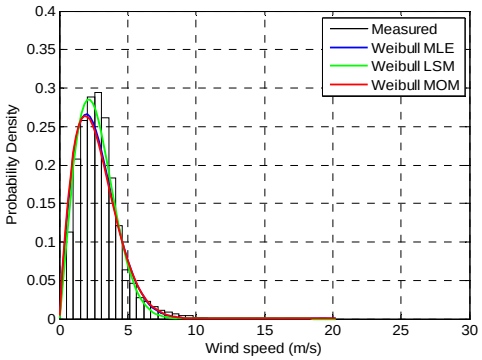
Measured
Weibull MLE
Weibull LSM
Weibull MOM
Probability Density
Wind speed (m/s)

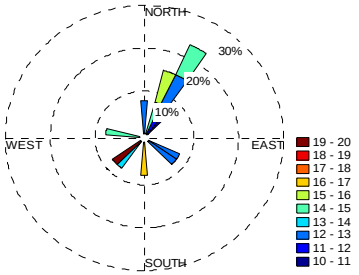
NORTH
30%
20%
10%
WEST
EAST
SOUTH
19 - 20
18 - 19
17 - 18
16 - 17
15 - 16
14 - 15
13 - 14
12 - 13
11 - 12
10 - 11

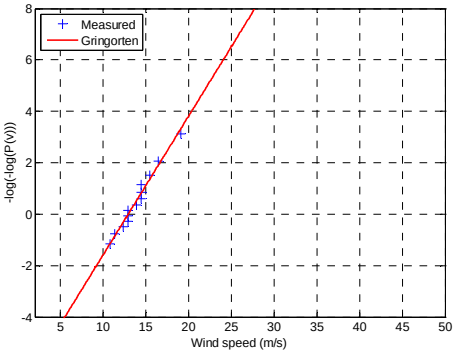
Measured
Gringorten
-log(-log(P(v)))
Wind speed (m/s)

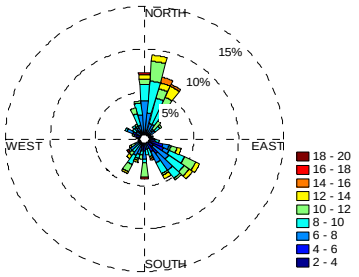
NORTH
15%
10%
5%
WEST
EAST
SOUTH
18 - 20
16 - 18
14 - 16
12 - 14
10 - 12
8 - 10
6 - 8
4 - 6
2 - 4

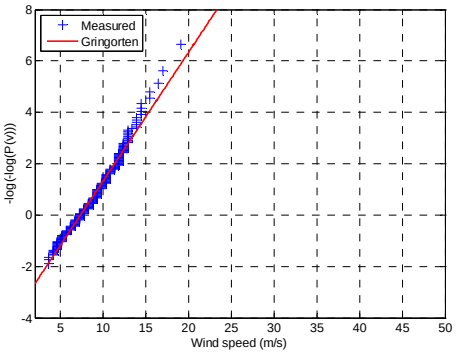
Measured
Gringorten
-log(-log(P(v)))
Wind speed (m/s)

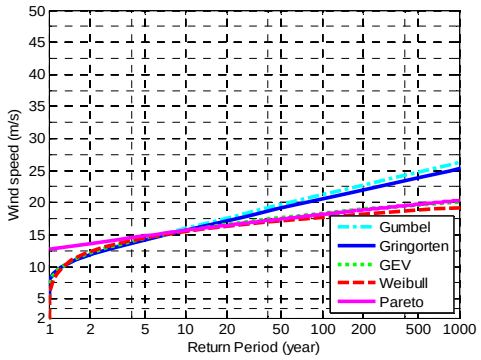
Wind speed (m/s)
Return Period (year)
Gumbel
Gringorten
GEV
Weibull
Pareto

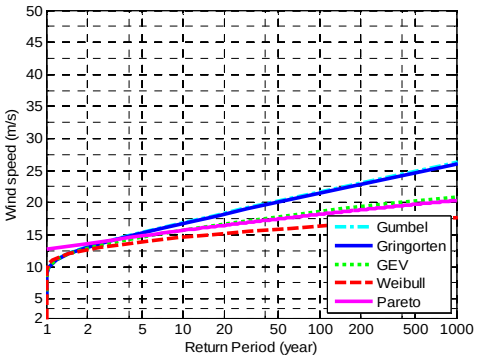
Wind speed (m/s)
Return Period (year)
Gumbel
Gringorten
GEV
Weibull
Pareto

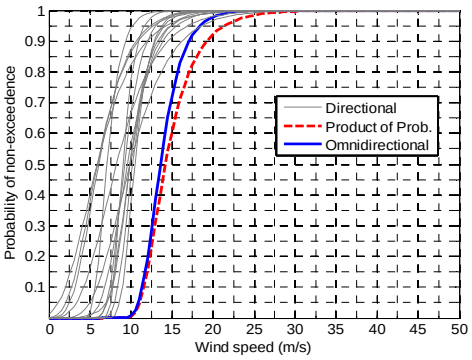
Probability of non-exceedence
Wind speed (m/s)
Directional
Product of Prob.
Omnidirectional

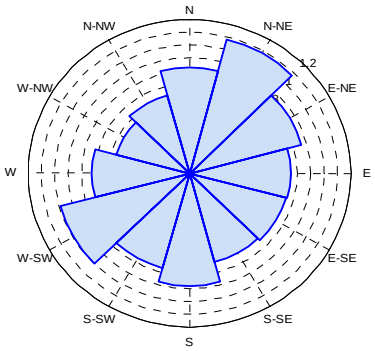
N
N-NE
E-NE
E
E-SE
S-SE
S
S-SW
W
W-NW
N-NW

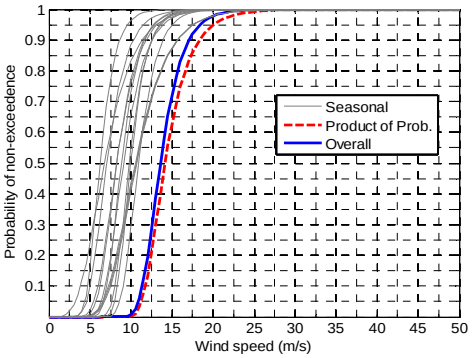
Probability of non-exceedence
Wind speed (m/s)
Seasonal
Product of Prob.
Overall

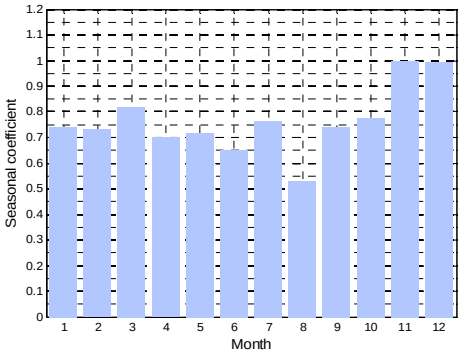
Seasonal coefficient
Month

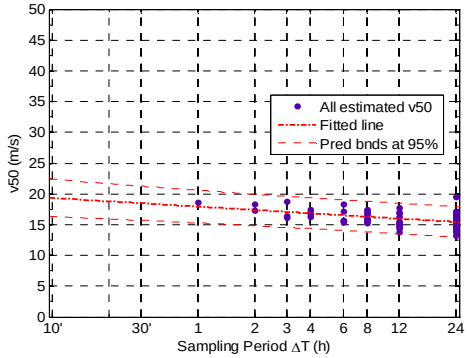
v50 (m/s)
Sampling Period ΔT (h)
All estimated v50
Fitted line
Pred bnds at 95%

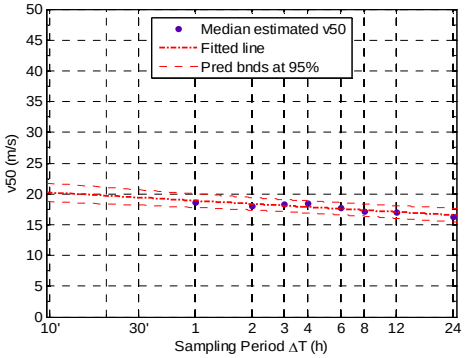
v50 (m/s)
Sampling Period ΔT (h)
Median estimated v50
Fitted line
Pred bnds at 95%

LIQZ

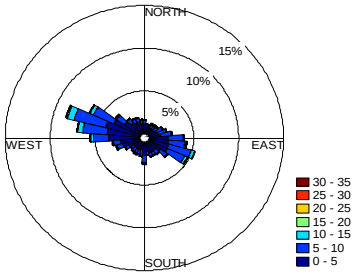
NORTH
15%
10%
5%
WEST
EAST
SOUTH
30 - 35
25 - 30
20 - 25
15 - 20
10 - 15
5 - 10
0 - 5

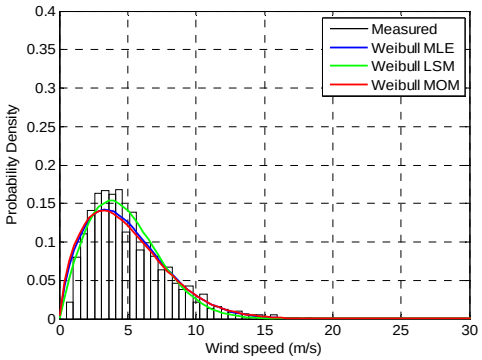
Measured
Weibull MLE
Weibull LSM
Weibull MOM
Probability Density
Wind speed (m/s)

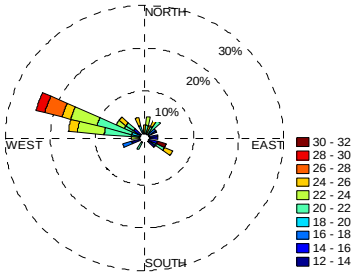
NORTH
30%
20%
10%
WEST
EAST
SOUTH
30 - 32
28 - 30
26 - 28
24 - 26
22 - 24
20 - 22
18 - 20
16 - 18
14 - 16
12 - 14

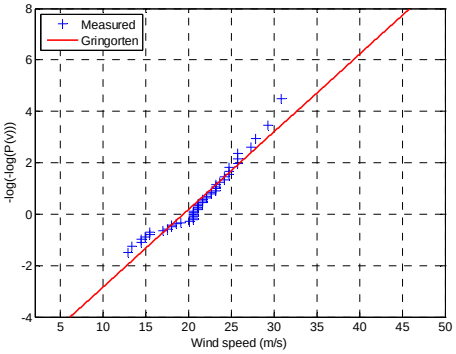
Measured
Gringorten
-log(-log(P(v)))
Wind speed (m/s)

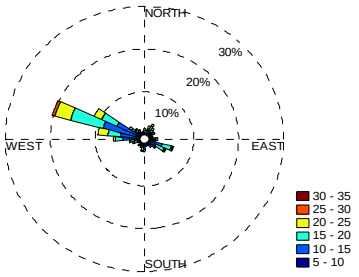
NORTH
30%
20%
10%
WEST
EAST
SOUTH
30 - 35
25 - 30
20 - 25
15 - 20
10 - 15
5 - 10

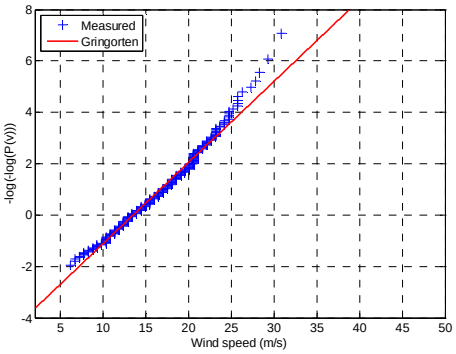
Measured
Gringorten
-log(-log(P(v)))
Wind speed (m/s)

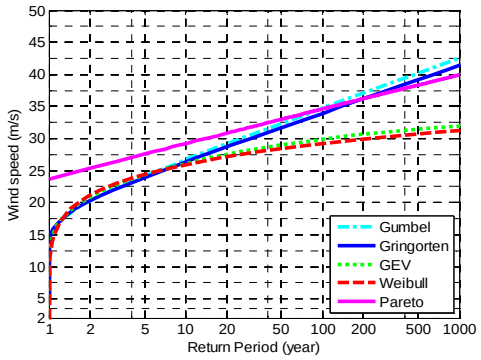
Wind speed (m/s)
Return Period (year)
Gumbel
Gringorten
GEV
Weibull
Pareto

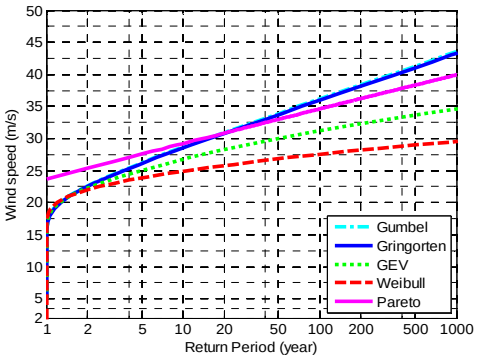
Wind speed (m/s)
Return Period (year)
Gumbel
Gringorten
GEV
Weibull
Pareto

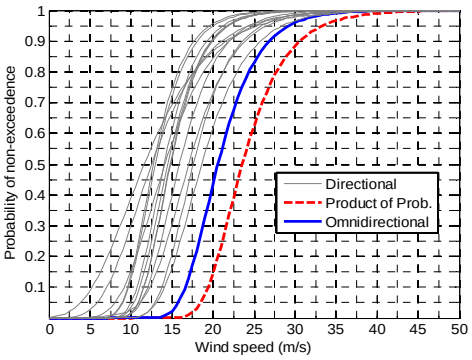
Probability of non-exceedence
Wind speed (m/s)
Directional
Product of Prob.
Omnidirectional

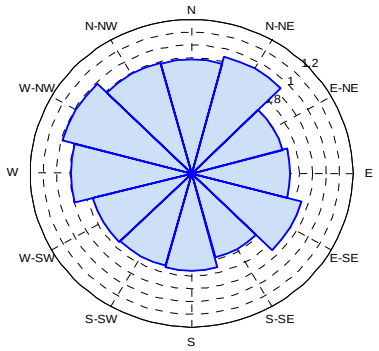
N
N-NE
E-NE
E
E-SE
S-SE
S
S-SW
W
W-NW
N-NW

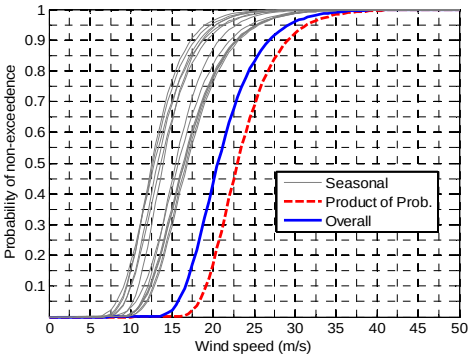
Probability of non-exceedence
Wind speed (m/s)
Seasonal
Product of Prob.
Overall

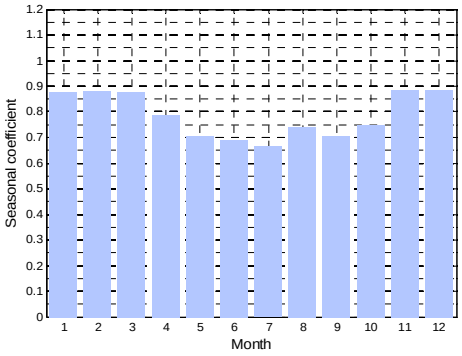
Seasonal coefficient
Month

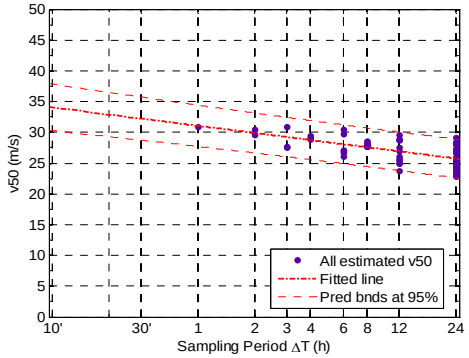
v50 (m/s)
Sampling Period ΔT (h)
All estimated v50
Fitted line
Pred bnds at 95%

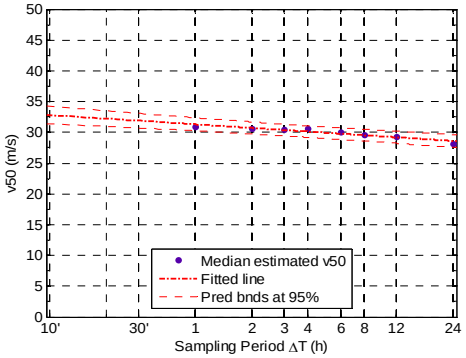
v50 (m/s)
Sampling Period ΔT (h)
Median estimated v50
Fitted line
Pred bnds at 95%

LIRA

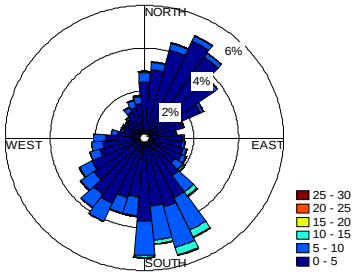
NORTH
EAST
SOUTH
WEST
6%
4%
2%
25 - 30
20 - 25
15 - 20
10 - 15
5 - 10
0 - 5

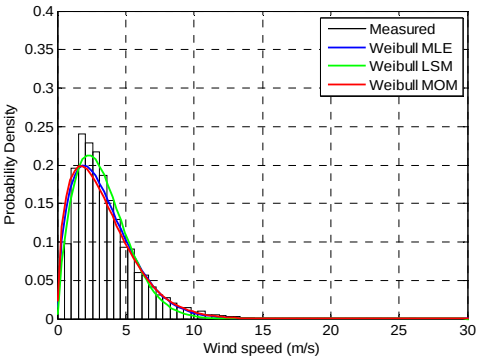
Measured
Weibull MLE
Weibull LSM
Weibull MOM
Probability Density
Wind speed (m/s)

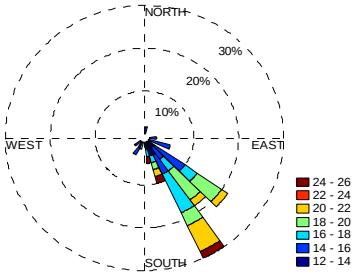
NORTH
EAST
SOUTH
WEST
30%
20%
10%
24 - 26
22 - 24
20 - 22
18 - 20
16 - 18
14 - 16
12 - 14

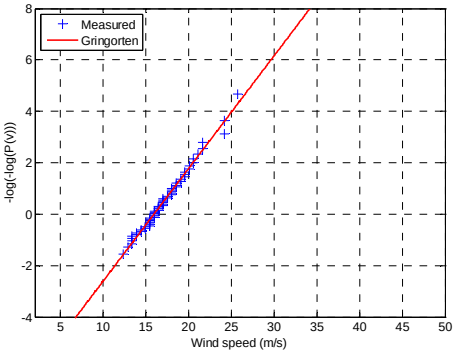
Measured
Gringorten
-log(-log(P(v)))
Wind speed (m/s)

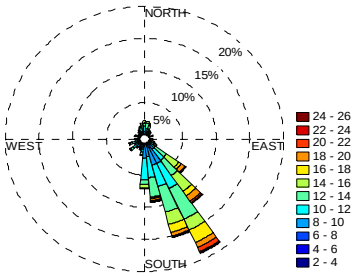
NORTH
EAST
SOUTH
WEST
20%
15%
10%
5%
24 - 26
22 - 24
20 - 22
18 - 20
16 - 18
14 - 16
12 - 14
10 - 12
8 - 10
6 - 8
4 - 6
2 - 4

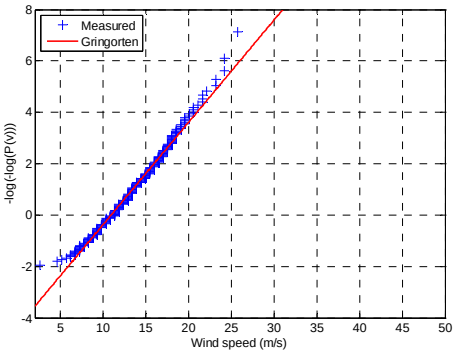
Measured
Gringorten
-log(-log(P(v)))
Wind speed (m/s)

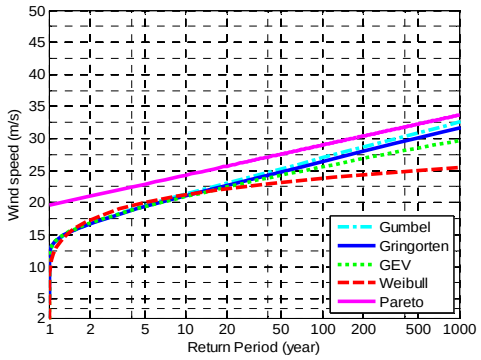
Wind speed (m/s)
Return Period (year)
Gumbel
Gringorten
GEV
Weibull
Pareto

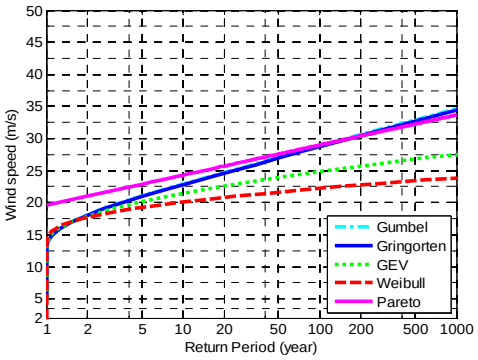
Wind speed (m/s)
Return Period (year)
Gumbel
Gringorten
GEV
Weibull
Pareto

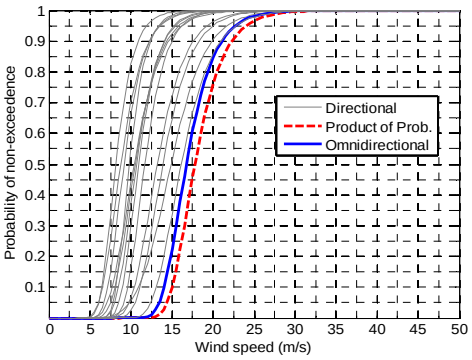
Probability of non-exceedence
Wind speed (m/s)
Directional
Product of Prob.
Omnidirectional

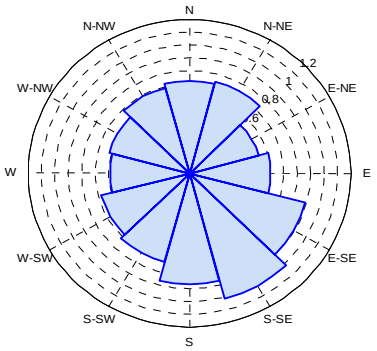
N
N-NE
E-NE
E
E-SE
S-SE
S
S-SW
W
W-NW
N-NW

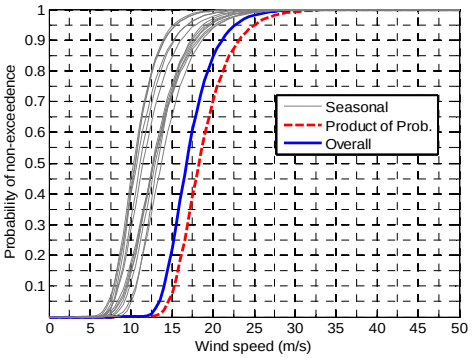
Probability of non-exceedence
Wind speed (m/s)
Seasonal
Product of Prob.
Overall

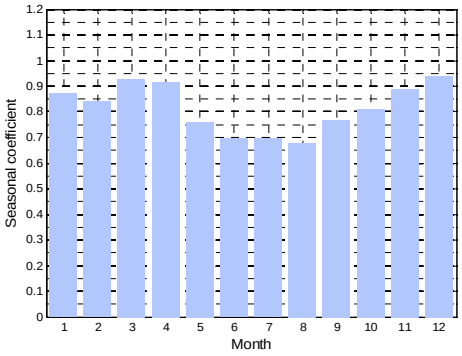
Seasonal coefficient
Month

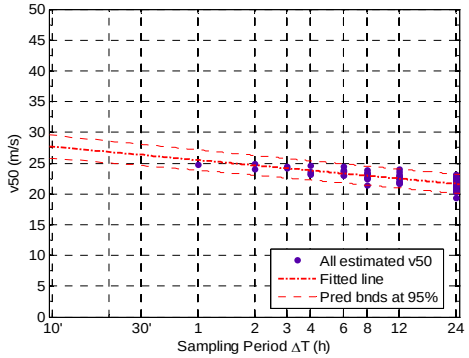
v50 (m/s)
Sampling Period ΔT (h)
All estimated v50
Fitted line
Pred bnds at 95%

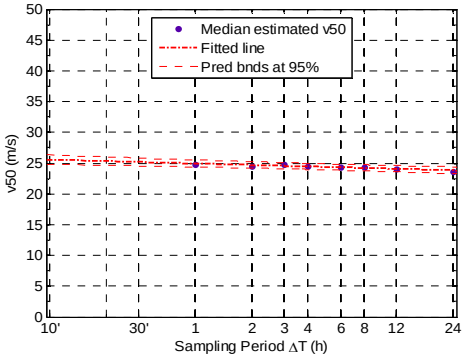
v50 (m/s)
Sampling Period ΔT (h)
Median estimated v50
Fitted line
Pred bnds at 95%

LIRB

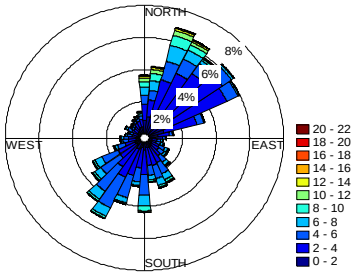
NORTH
EAST
SOUTH
WEST
8%
6%
4%
2%
20 - 22
18 - 20
16 - 18
14 - 16
12 - 14
10 - 12
8 - 10
6 - 8
4 - 6
2 - 4
0 - 2

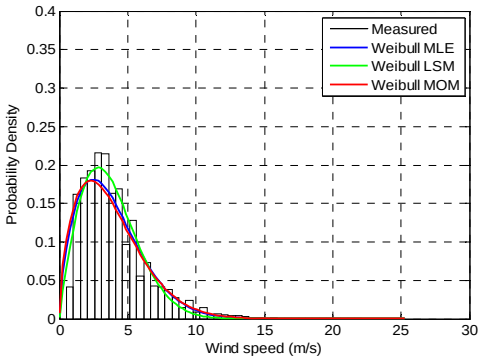
Measured
Weibull MLE
Weibull LSM
Weibull MOM
Probability Density
Wind speed (m/s)

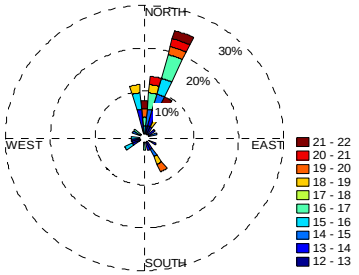
NORTH
EAST
SOUTH
WEST
30%
20%
10%
21 - 22
20 - 21
19 - 20
18 - 19
17 - 18
16 - 17
15 - 16
14 - 15
13 - 14
12 - 13

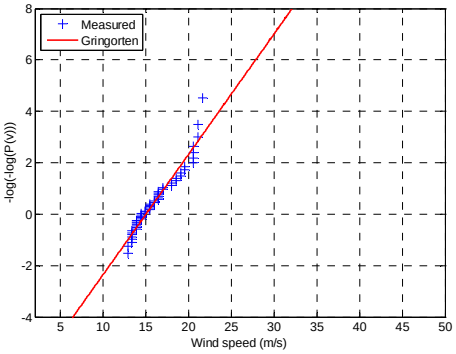
Measured
Gringorten
-log(-log(P(v)))
Wind speed (m/s)

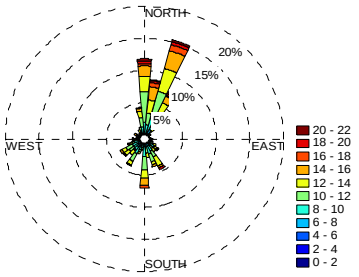
NORTH
EAST
SOUTH
WEST
20%
15%
10%
5%
20 - 22
18 - 20
16 - 18
14 - 16
12 - 14
10 - 12
8 - 10
6 - 8
4 - 6
2 - 4
0 - 2

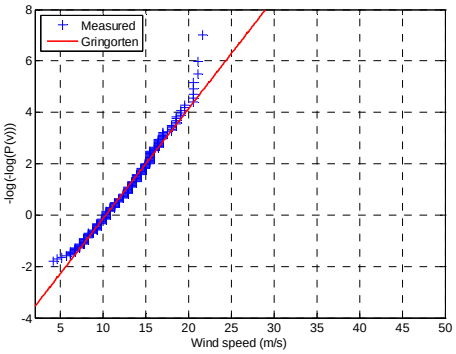
Measured
Gringorten
-log(-log(P(v)))
Wind speed (m/s)

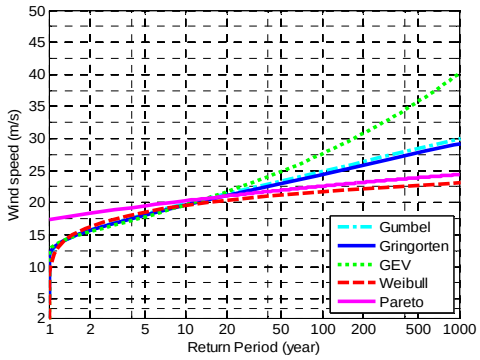
Wind speed (m/s)
Return Period (year)
Gumbel
Gringorten
GEV
Weibull
Pareto

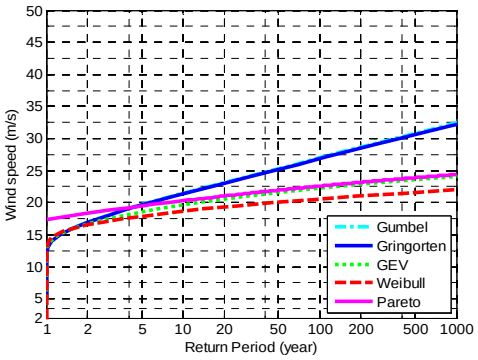
Wind speed (m/s)
Return Period (year)
Gumbel
Gringorten
GEV
Weibull
Pareto

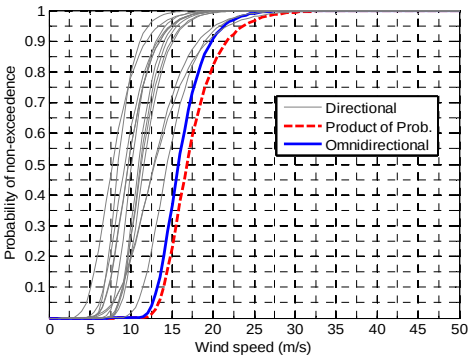
Probability of non-exceedence
Wind speed (m/s)
Directional
Product of Prob.
Omnidirectional

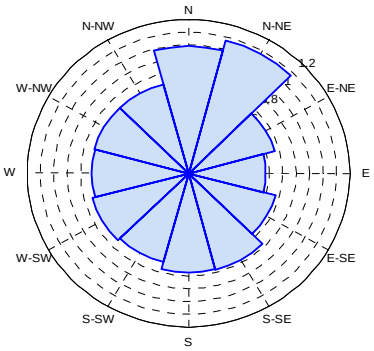
N
N-NE
E-NE
E
E-SE
S-SE
S
S-SW
W
W-NW
N-NW

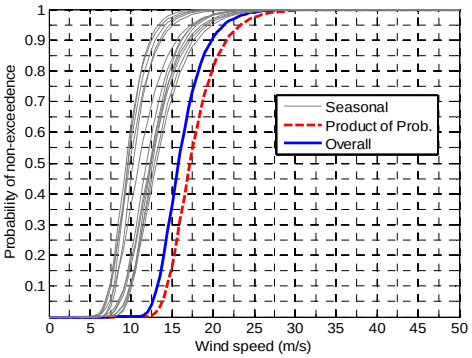
Probability of non-exceedence
Wind speed (m/s)
Seasonal
Product of Prob.
Overall

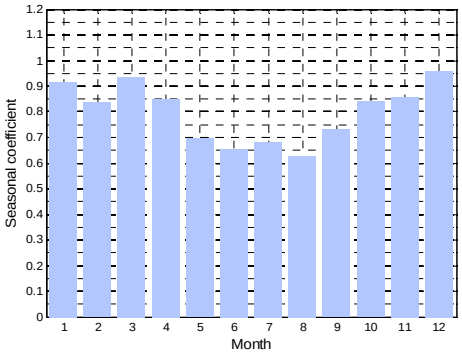
Seasonal coefficient
Month

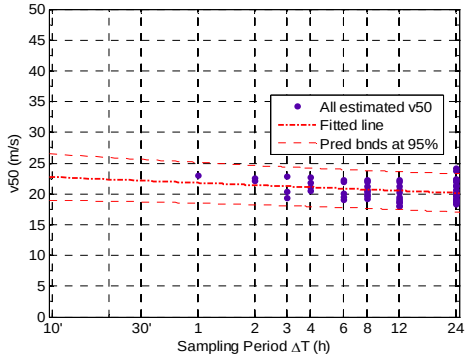
v50 (m/s)
Sampling Period ΔT (h)
All estimated v50
Fitted line
Pred bnds at 95%

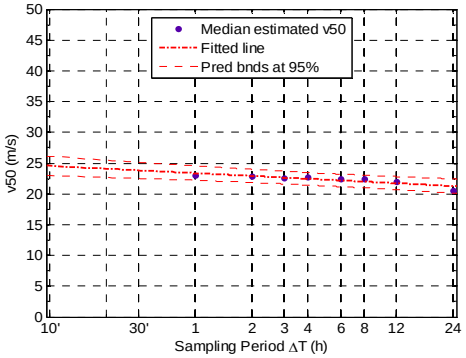
v50 (m/s)
Sampling Period ΔT (h)
Median estimated v50
Fitted line
Pred bnds at 95%

LIRE

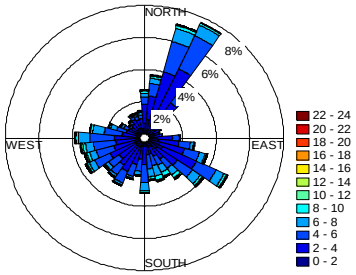
NORTH
EAST
SOUTH
WEST
2%
4%
6%
8%
22 - 24
20 - 22
18 - 20
16 - 18
14 - 16
12 - 14
10 - 12
8 - 10
6 - 8
4 - 6
2 - 4
0 - 2

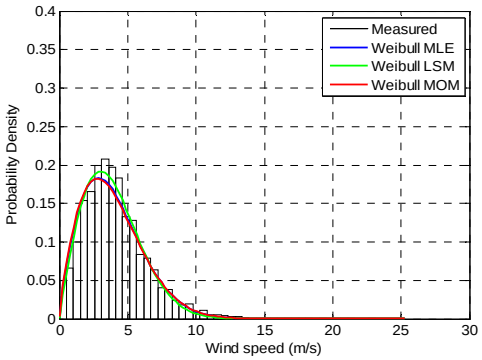
Measured
Weibull MLE
Weibull LSM
Weibull MOM
Probability Density
Wind speed (m/s)

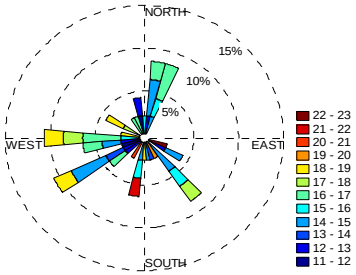
NORTH
EAST
SOUTH
WEST
5%
10%
15%
22 - 23
21 - 22
20 - 21
19 - 20
18 - 19
17 - 18
16 - 17
15 - 16
14 - 15
13 - 14
12 - 13
11 - 12

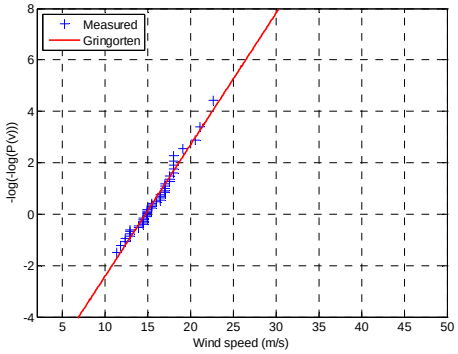
Measured
Gringorten
-log(-log(P(v)))
Wind speed (m/s)

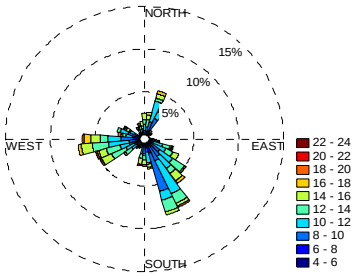
NORTH
EAST
SOUTH
WEST
5%
10%
15%
22 - 24
20 - 22
18 - 20
16 - 18
14 - 16
12 - 14
10 - 12
8 - 10
6 - 8
4 - 6

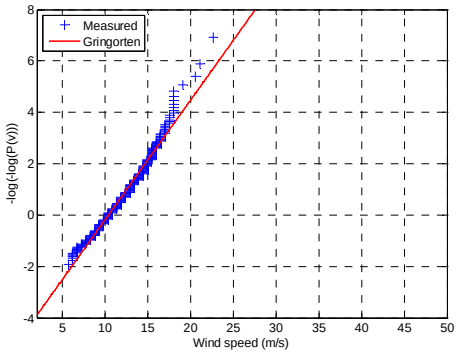
Measured
Gringorten
-log(-log(P(v)))
Wind speed (m/s)

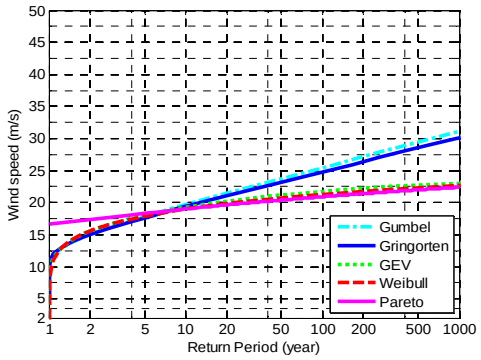
Wind speed (m/s)
Return Period (year)
Gumbel
Gringorten
GEV
Weibull
Pareto

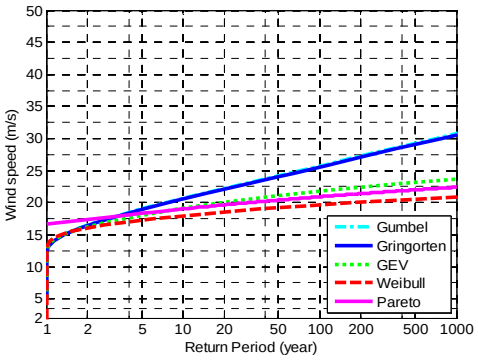
Wind speed (m/s)
Return Period (year)
Gumbel
Gringorten
GEV
Weibull
Pareto

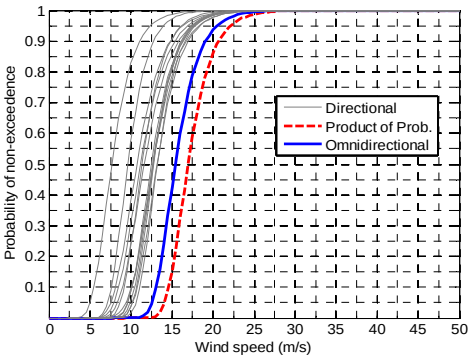
Probability of non-exceedence
Wind speed (m/s)
Directional
Product of Prob.
Omnidirectional

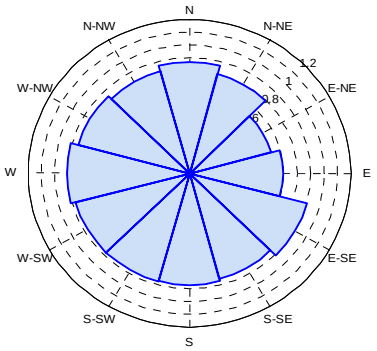
N
N-NE
E-NE
E
E-SE
S-SE
S
S-SW
W
W-NW
N-NW

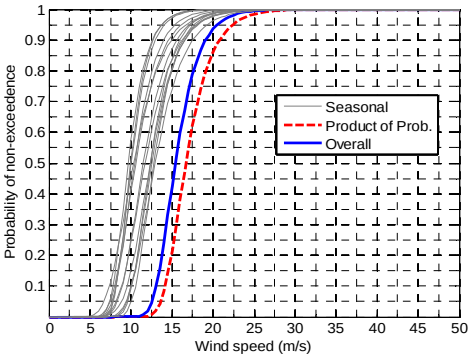
Probability of non-exceedence
Wind speed (m/s)
Seasonal
Product of Prob.
Overall

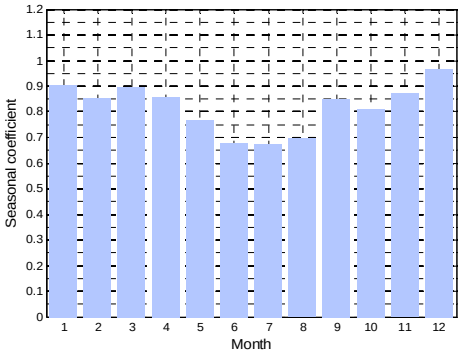
Seasonal coefficient
Month

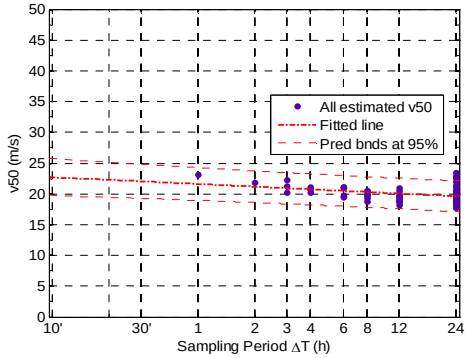
v50 (m/s)
Sampling Period ΔT (h)
All estimated v50
Fitted line
Pred bnds at 95%

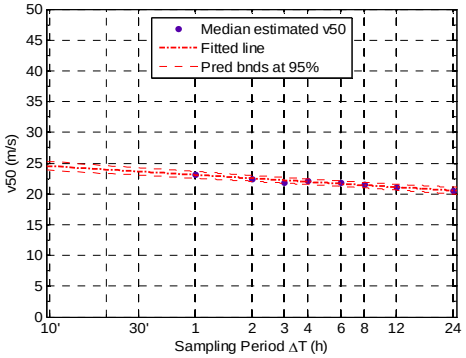
v50 (m/s)
Sampling Period ΔT (h)
Median estimated v50
Fitted line
Pred bnds at 95%

LIRF

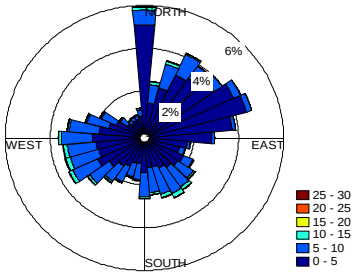
NORTH
6%
4%
2%
WEST
EAST
SOUTH
25 - 30
20 - 25
15 - 20
10 - 15
5 - 10
0 - 5

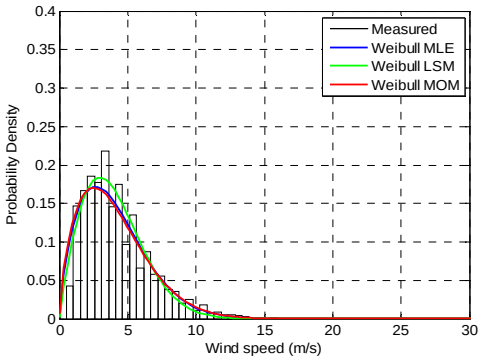
Measured
Weibull MLE
Weibull LSM
Weibull MOM
Probability Density
Wind speed (m/s)

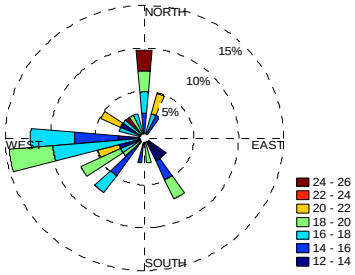
NORTH
15%
10%
5%
WEST
EAST
SOUTH
24 - 26
22 - 24
20 - 22
18 - 20
16 - 18
14 - 16
12 - 14

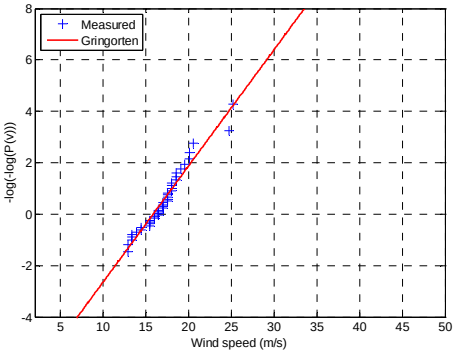
Measured
Gringorten
-log(-log(P(v)))
Wind speed (m/s)

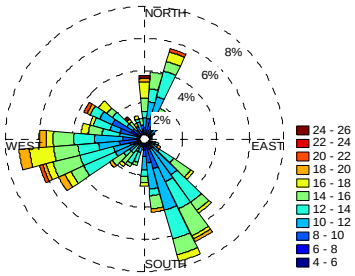
NORTH
8%
6%
4%
2%
WEST
EAST
SOUTH
24 - 26
22 - 24
20 - 22
18 - 20
16 - 18
14 - 16
12 - 14
10 - 12
8 - 10
6 - 8
4 - 6

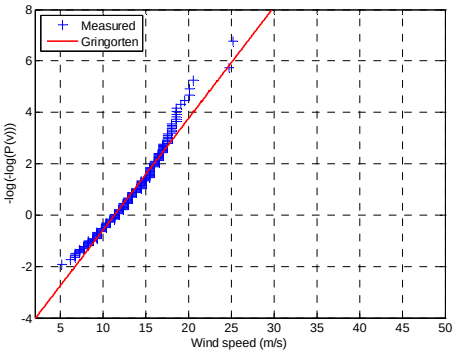
Measured
Gringorten
-log(-log(P(v)))
Wind speed (m/s)

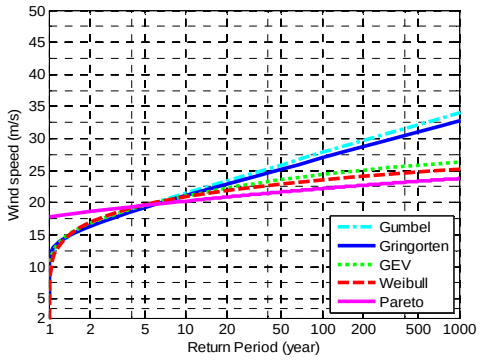
Wind speed (m/s)
Return Period (year)
Gumbel
Gringorten
GEV
Weibull
Pareto

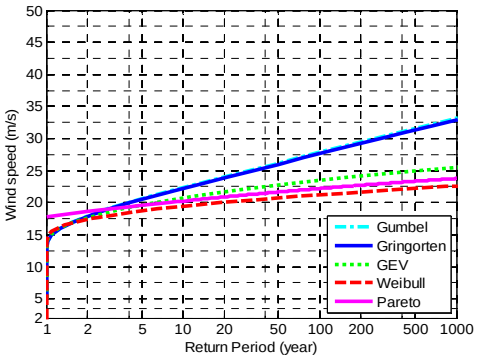
Wind speed (m/s)
Return Period (year)
Gumbel
Gringorten
GEV
Weibull
Pareto

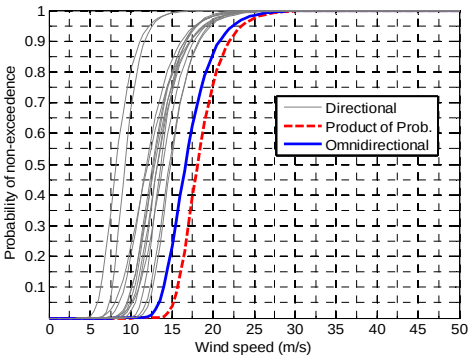
Probability of non-exceedence
Wind speed (m/s)
Directional
Product of Prob.
Omnidirectional

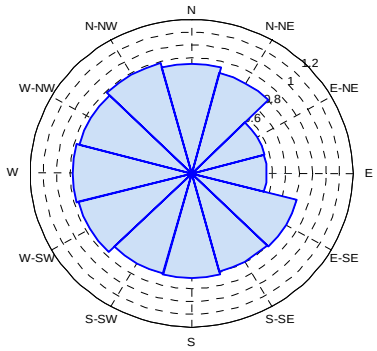
N
N-NE
E-NE
E
E-SE
S-SE
S
S-SW
W
W-NW
N-NW

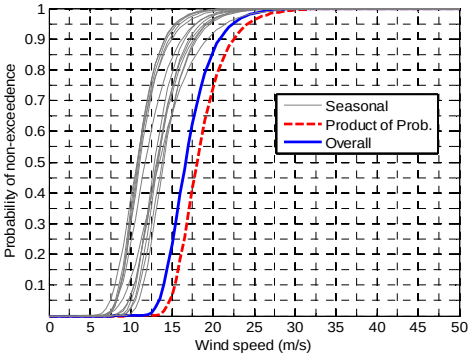
Probability of non-exceedence
Wind speed (m/s)
Seasonal
Product of Prob.
Overall

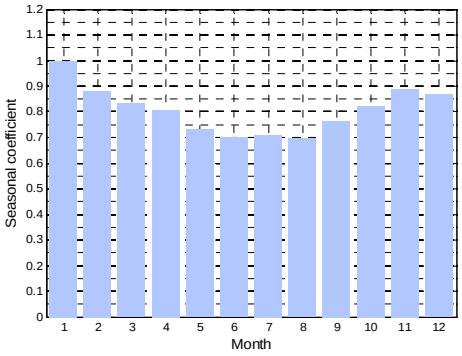
Seasonal coefficient
Month

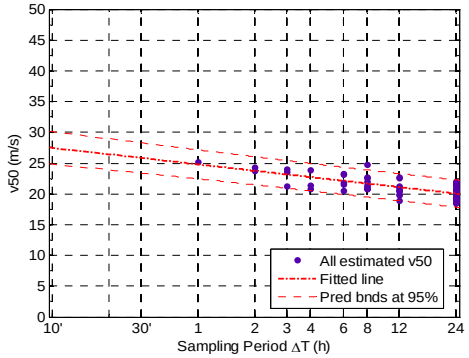
v50 (m/s)
Sampling Period ΔT (h)
All estimated v50
Fitted line
Pred bnds at 95%

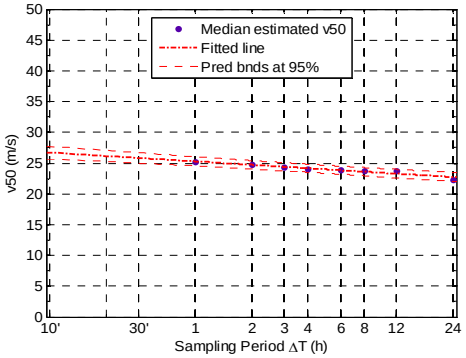
v50 (m/s)
Sampling Period ΔT (h)
Median estimated v50
Fitted line
Pred bnds at 95%

LIRG

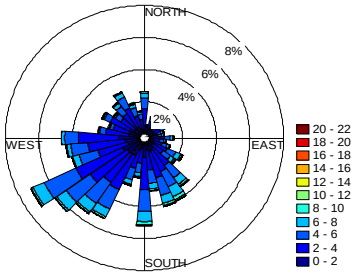
NORTH
8%
6%
4%
2%
WEST
EAST
SOUTH
20 - 22
18 - 20
16 - 18
14 - 16
12 - 14
10 - 12
8 - 10
6 - 8
4 - 6
2 - 4
0 - 2

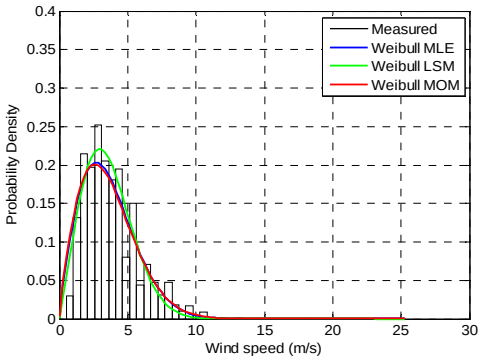
Measured
Weibull MLE
Weibull LSM
Weibull MOM
Probability Density
Wind speed (m/s)

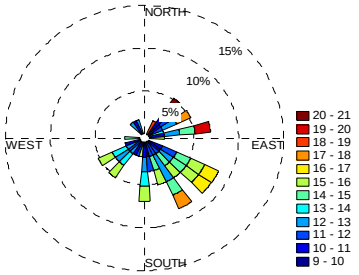
NORTH
15%
10%
5%
WEST
EAST
SOUTH
20 - 21
19 - 20
18 - 19
17 - 18
16 - 17
15 - 16
14 - 15
13 - 14
12 - 13
11 - 12
10 - 11
9 - 10

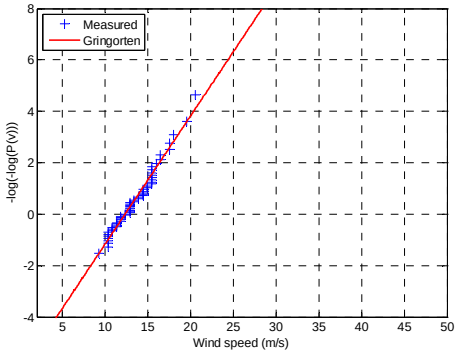
Measured
Gringorten
-log(-log(P(v)))
Wind speed (m/s)

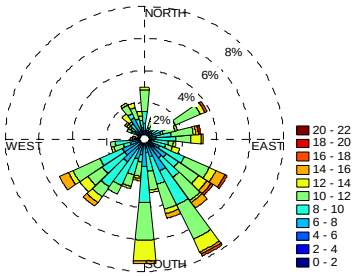
NORTH
8%
6%
4%
2%
WEST
EAST
SOUTH
20 - 22
18 - 20
16 - 18
14 - 16
12 - 14
10 - 12
8 - 10
6 - 8
4 - 6
2 - 4
0 - 2

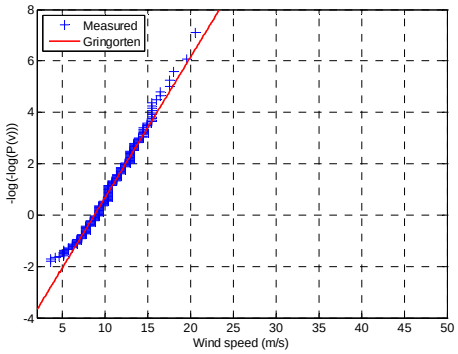
Measured
Gringorten
-log(-log(P(v)))
Wind speed (m/s)

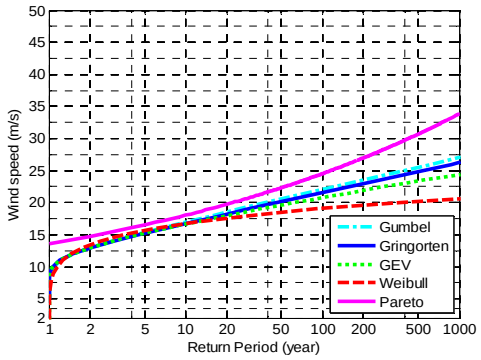
Wind speed (m/s)
Return Period (year)
Gumbel
Gringorten
GEV
Weibull
Pareto

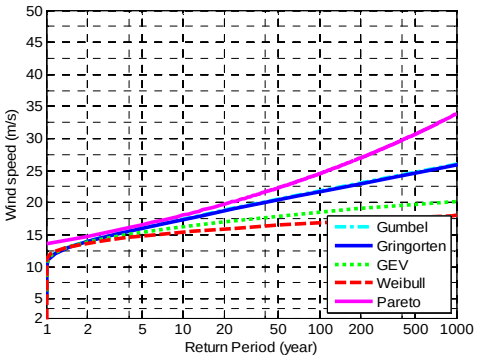
Wind speed (m/s)
Return Period (year)
Gumbel
Gringorten
GEV
Weibull
Pareto

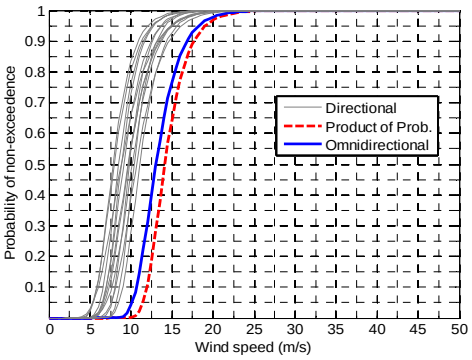
Probability of non-exceedence
Wind speed (m/s)
Directional
Product of Prob.
Omnidirectional

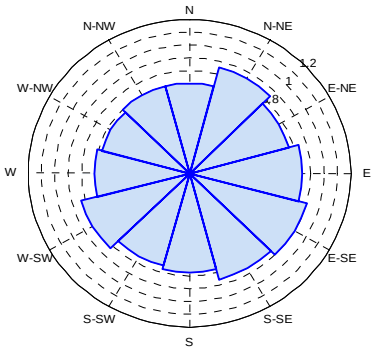
N
N-NE
E-NE
E
E-SE
S-SE
S
S-SW
W
W-NW
N-NW

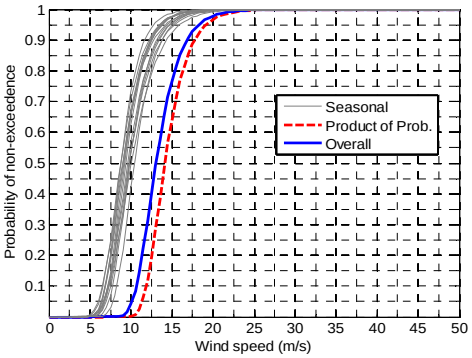
Probability of non-exceedence
Wind speed (m/s)
Seasonal
Product of Prob.
Overall

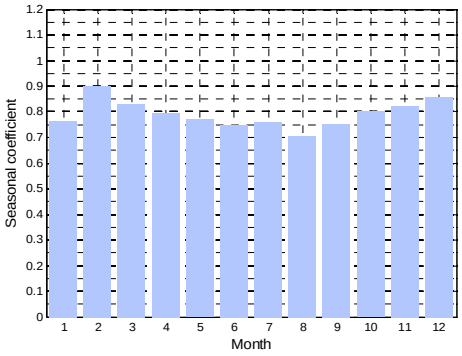
Seasonal coefficient
Month

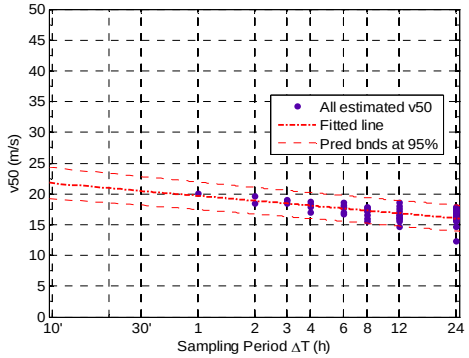
v50 (m/s)
Sampling Period ΔT (h)
All estimated v50
Fitted line
Pred bnds at 95%

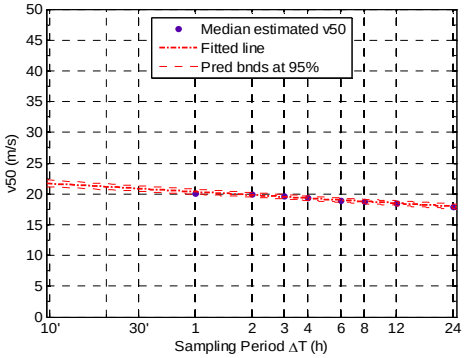
v50 (m/s)
Sampling Period ΔT (h)
Median estimated v50
Fitted line
Pred bnds at 95%

LIRH

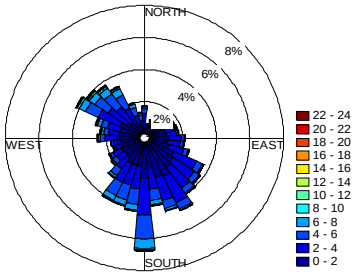
NORTH
8%
6%
4%
2%
WEST
EAST
SOUTH
22 - 24
20 - 22
18 - 20
16 - 18
14 - 16
12 - 14
10 - 12
8 - 10
6 - 8
4 - 6
2 - 4
0 - 2

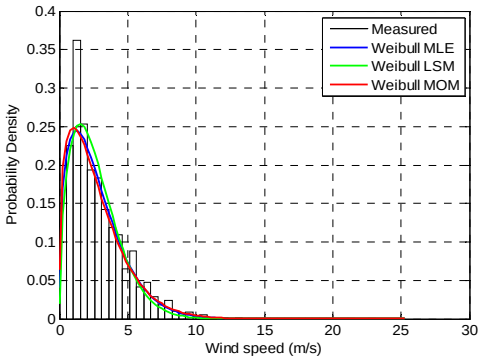
Measured
Weibull MLE
Weibull LSM
Weibull MOM
Probability Density
Wind speed (m/s)

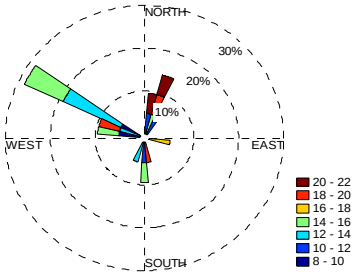
NORTH
30%
20%
10%
WEST
EAST
SOUTH
20 - 22
18 - 20
16 - 18
14 - 16
12 - 14
10 - 12
8 - 10

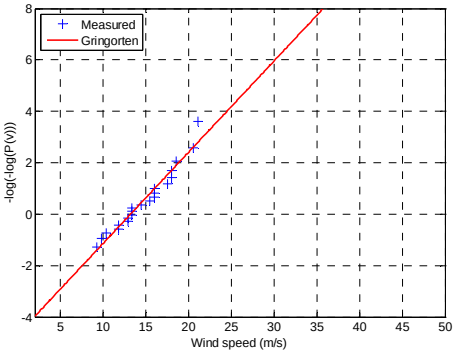
Measured
Gringorten
-log(-log(P(v)))
Wind speed (m/s)

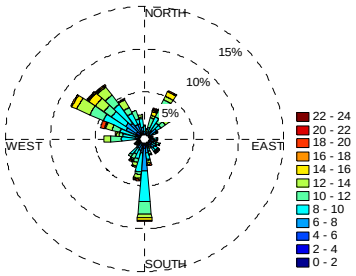
NORTH
15%
10%
5%
WEST
EAST
SOUTH
22 - 24
20 - 22
18 - 20
16 - 18
14 - 16
12 - 14
10 - 12
8 - 10
6 - 8
4 - 6
2 - 4
0 - 2

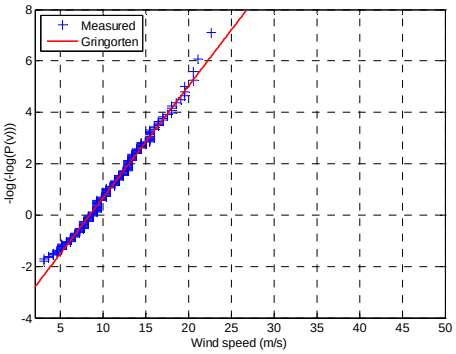
Measured
Gringorten
-log(-log(P(v)))
Wind speed (m/s)

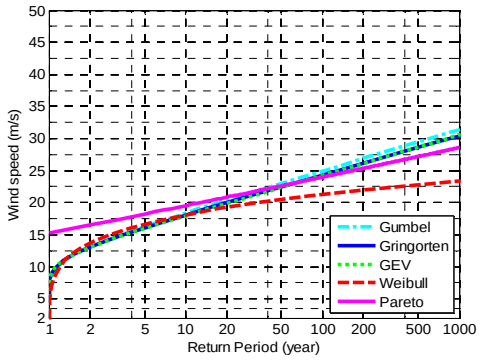
Wind speed (m/s)
Return Period (year)
Gumbel
Gringorten
GEV
Weibull
Pareto

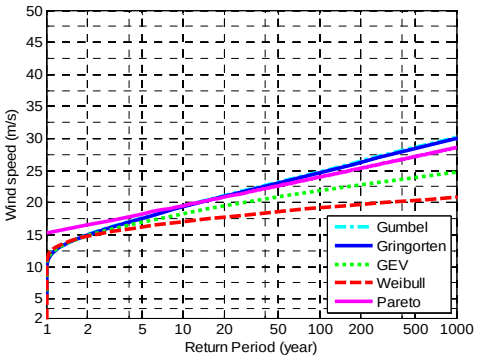
Wind speed (m/s)
Return Period (year)
Gumbel
Gringorten
GEV
Weibull
Pareto

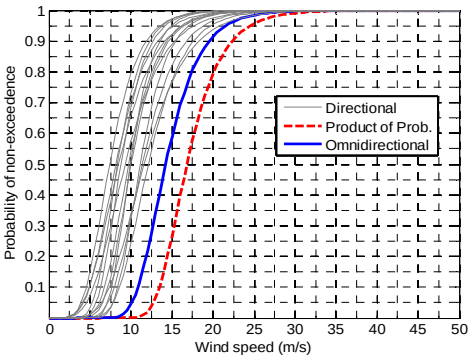
Probability of non-exceedence
Wind speed (m/s)
Directional
Product of Prob.
Omnidirectional

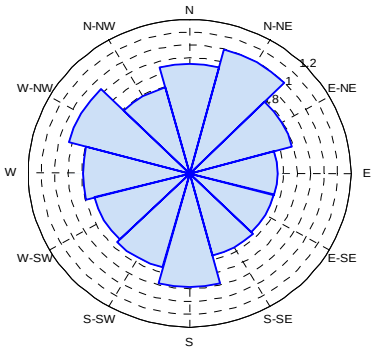
N
N-NE
E-NE
E
E-SE
S-SE
S
S-SW
W
W-NW
N-NW

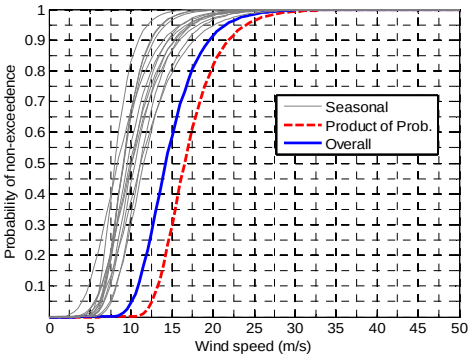
Probability of non-exceedence
Wind speed (m/s)
Seasonal
Product of Prob.
Overall

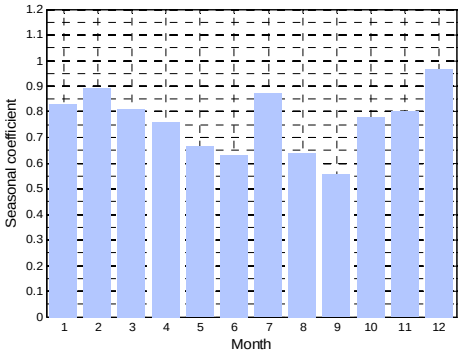
Seasonal coefficient
Month

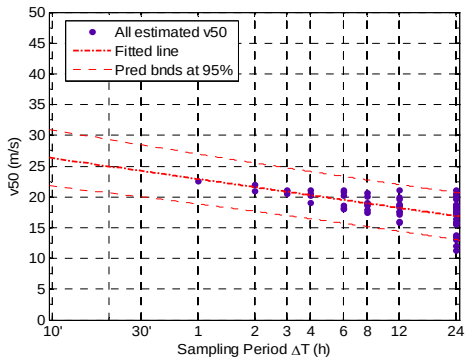
All estimated v50
Fitted line
Pred bnds at 95%
v50 (m/s)
Sampling Period ΔT (h)

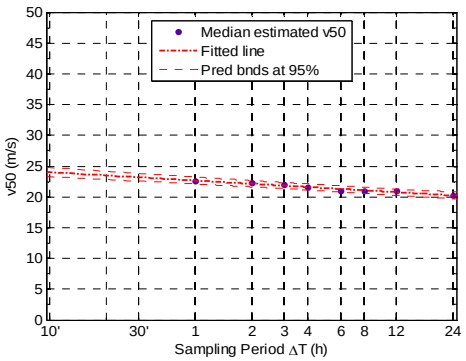
Median estimated v50
Fitted line
Pred bnds at 95%
v50 (m/s)
Sampling Period ΔT (h)

LIRK

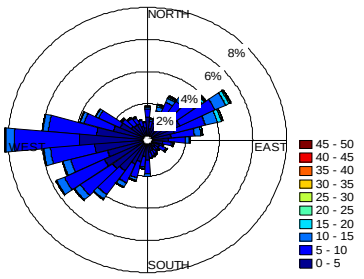
NORTH
8%
6%
4%
2%
WEST
EAST
SOUTH
45 - 50
40 - 45
35 - 40
30 - 35
25 - 30
20 - 25
15 - 20
10 - 15
5 - 10
0 - 5

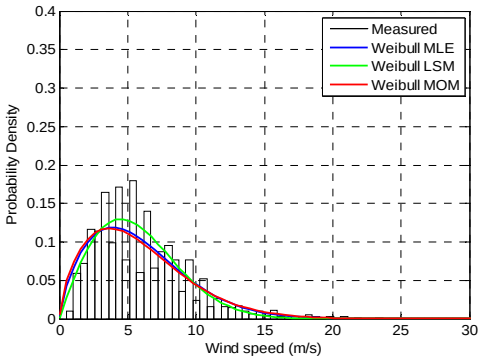
Measured
Weibull MLE
Weibull LSM
Weibull MOM
Probability Density
Wind speed (m/s)

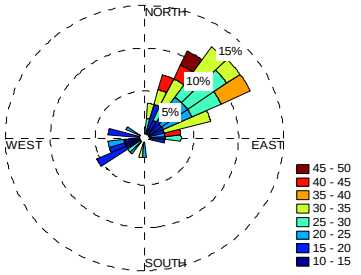
NORTH
15%
10%
5%
WEST
EAST
SOUTH
45 - 50
40 - 45
35 - 40
30 - 35
25 - 30
20 - 25
15 - 20
10 - 15

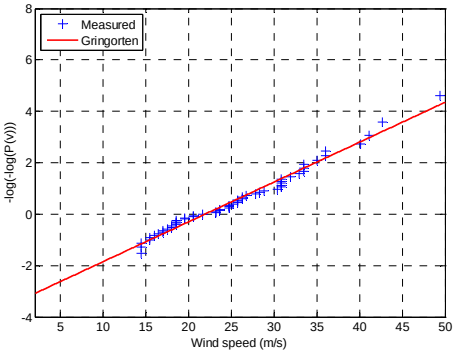
Measured
Gringorten
-log(-log(P(v)))
Wind speed (m/s)

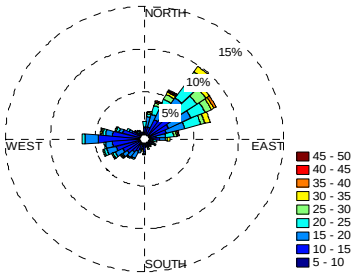
NORTH
15%
10%
5%
WEST
EAST
SOUTH
45 - 50
40 - 45
35 - 40
30 - 35
25 - 30
20 - 25
15 - 20
10 - 15
5 - 10

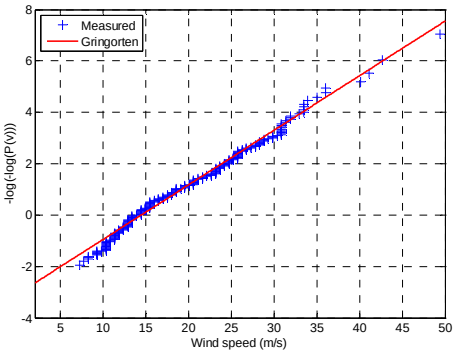
Measured
Gringorten
-log(-log(P(v)))
Wind speed (m/s)

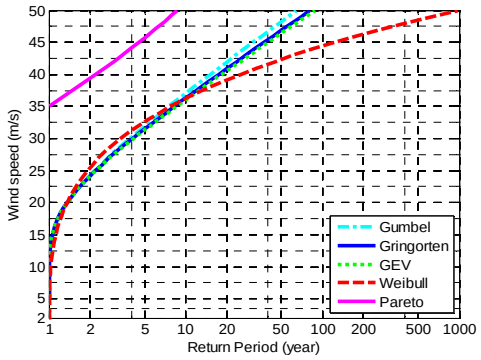
Wind speed (m/s)
Return Period (year)
Gumbel
Gringorten
GEV
Weibull
Pareto

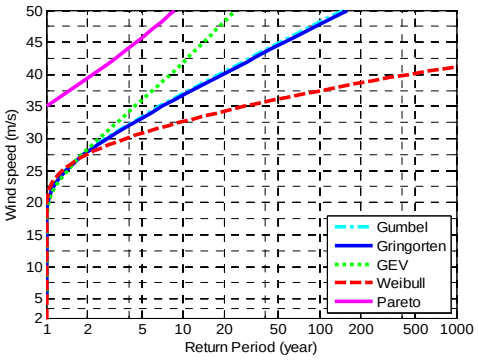
Wind speed (m/s)
Return Period (year)
Gumbel
Gringorten
GEV
Weibull
Pareto

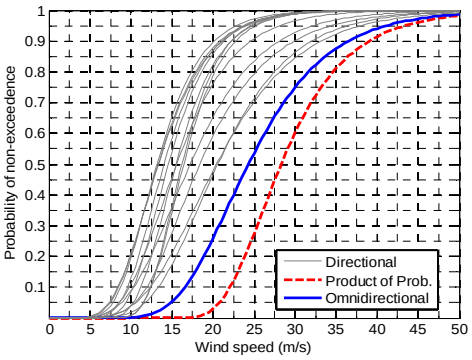
Probability of non-exceedence
Wind speed (m/s)
Directional
Product of Prob.
Omnidirectional

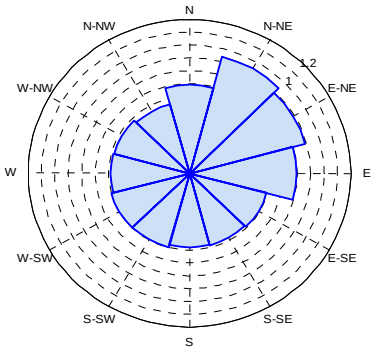
N
N-NE
E-NE
E
E-SE
S-SE
S
S-SW
W
W-NW
N-NW

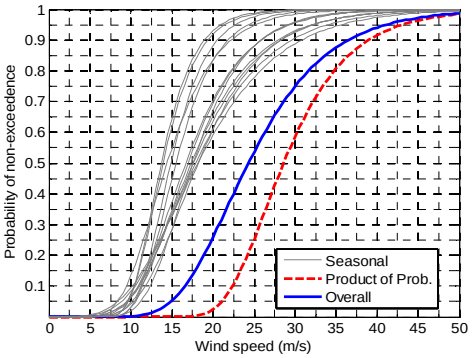
Probability of non-exceedence
Wind speed (m/s)
Seasonal
Product of Prob.
Overall

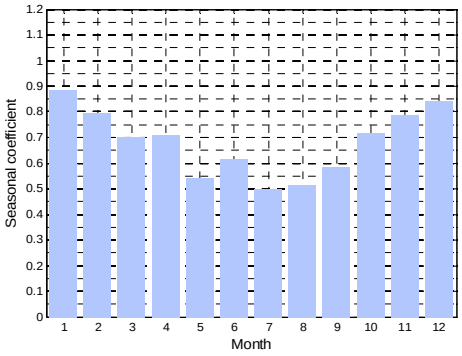
Seasonal coefficient
Month

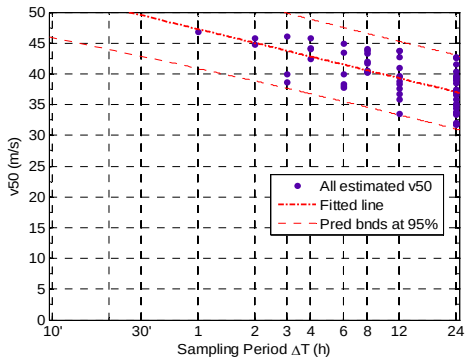
v50 (m/s)
Sampling Period ΔT (h)
All estimated v50
Fitted line
Pred bnds at 95%

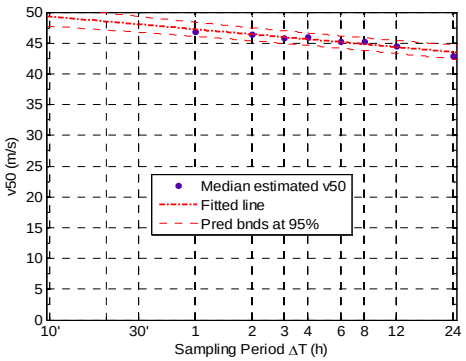
v50 (m/s)
Sampling Period ΔT (h)
Median estimated v50
Fitted line
Pred bnds at 95%

LIRL

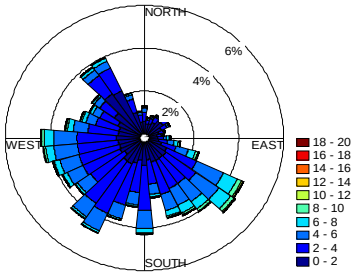
NORTH
6%
4%
2%
WEST
EAST
SOUTH
18 - 20
16 - 18
14 - 16
12 - 14
10 - 12
8 - 10
6 - 8
4 - 6
2 - 4
0 - 2

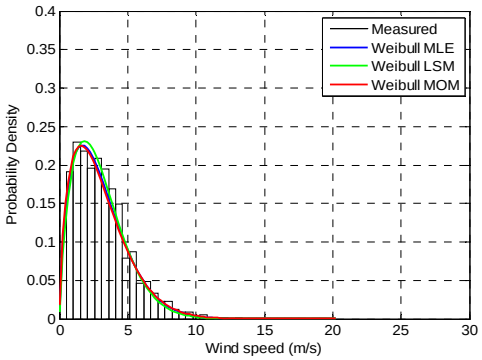
Measured
Weibull MLE
Weibull LSM
Weibull MOM
Probability Density
Wind speed (m/s)

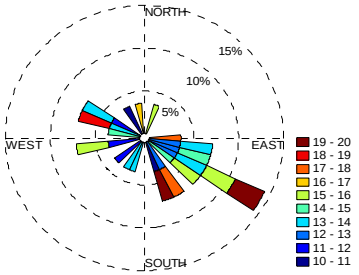
NORTH
15%
10%
5%
WEST
EAST
SOUTH
19 - 20
18 - 19
17 - 18
16 - 17
15 - 16
14 - 15
13 - 14
12 - 13
11 - 12
10 - 11

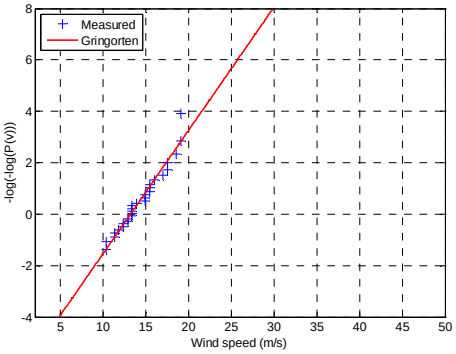
Measured
Gringorten
-log(-log(P(v)))
Wind speed (m/s)

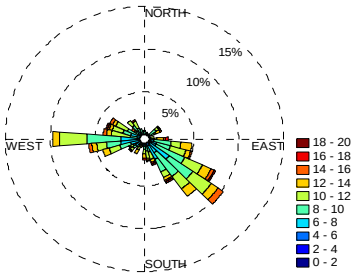
NORTH
15%
10%
5%
WEST
EAST
SOUTH
18 - 20
16 - 18
14 - 16
12 - 14
10 - 12
8 - 10
6 - 8
4 - 6
2 - 4
0 - 2

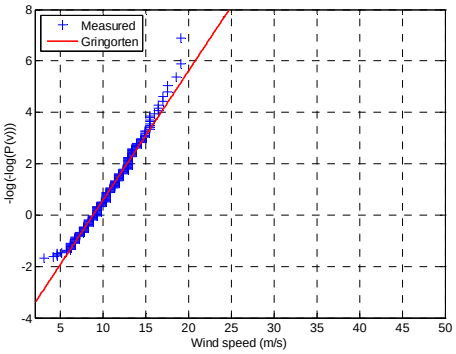
Measured
Gringorten
-log(-log(P(v)))
Wind speed (m/s)

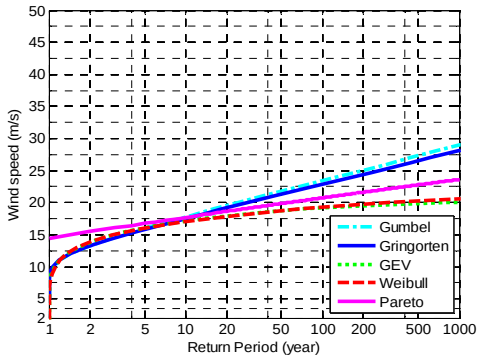
Wind speed (m/s)
Return Period (year)
Gumbel
Gringorten
GEV
Weibull
Pareto

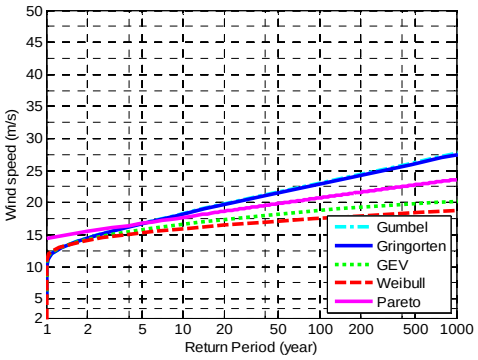
Wind speed (m/s)
Return Period (year)
Gumbel
Gringorten
GEV
Weibull
Pareto

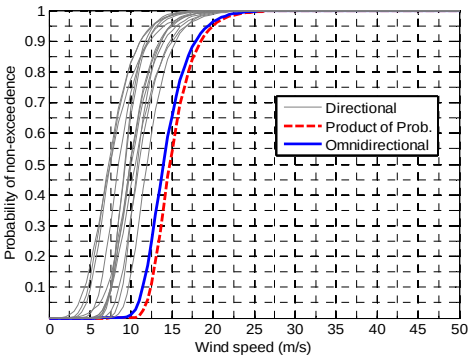
Probability of non-exceedence
Wind speed (m/s)
Directional
Product of Prob.
Omnidirectional

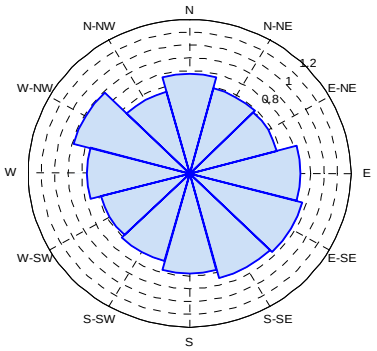
N
N-NE
E-NE
E
E-SE
S-SE
S
S-SW
W
W-NW
N-NW

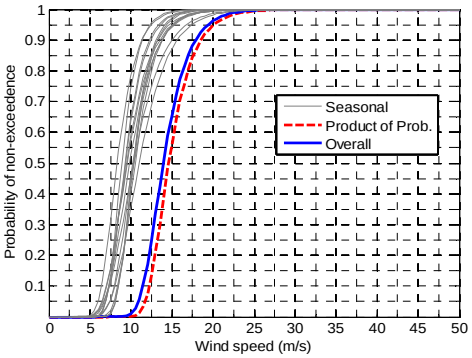
Probability of non-exceedence
Wind speed (m/s)
Seasonal
Product of Prob.
Overall

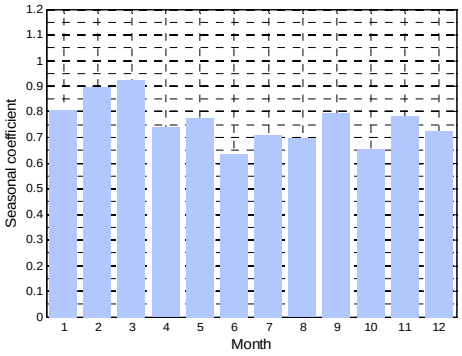
Seasonal coefficient
Month

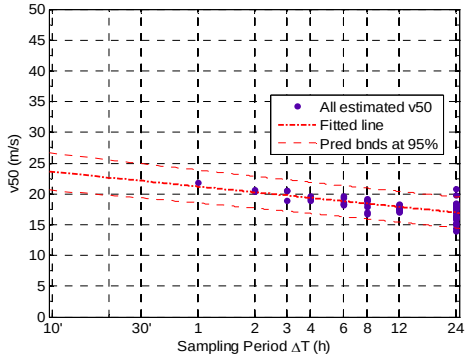
v50 (m/s)
Sampling Period ΔT (h)
All estimated v50
Fitted line
Pred bnds at 95%

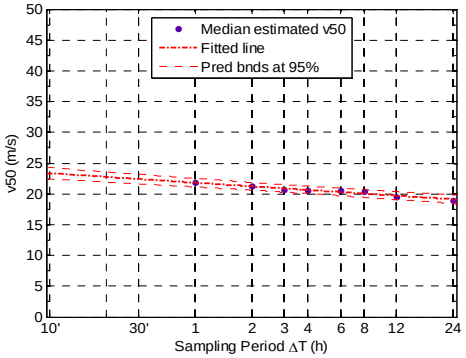
v50 (m/s)
Sampling Period ΔT (h)
Median estimated v50
Fitted line
Pred bnds at 95%

LIRM

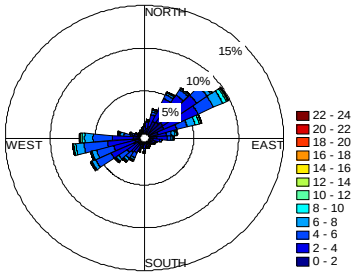
NORTH
15%
10%
5%
WEST
EAST
SOUTH
22 - 24
20 - 22
18 - 20
16 - 18
14 - 16
12 - 14
10 - 12
8 - 10
6 - 8
4 - 6
2 - 4
0 - 2

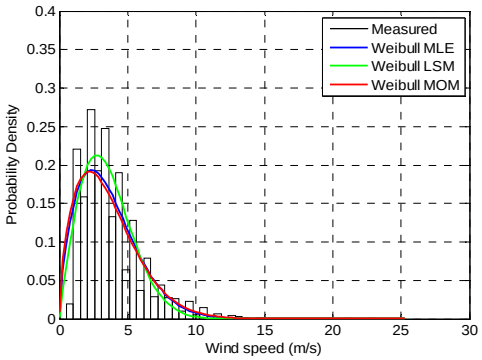
Measured
Weibull MLE
Weibull LSM
Weibull MOM
Probability Density
Wind speed (m/s)

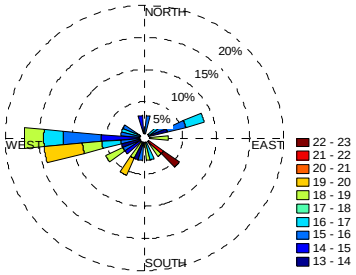
NORTH
20%
15%
10%
5%
WEST
EAST
SOUTH
22 - 23
21 - 22
20 - 21
19 - 20
18 - 19
17 - 18
16 - 17
15 - 16
14 - 15
13 - 14

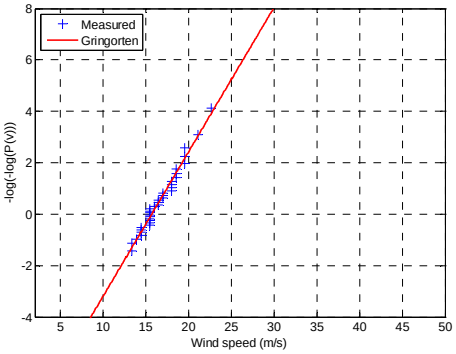
Measured
Gringorten
-log(-log(P(v)))
Wind speed (m/s)

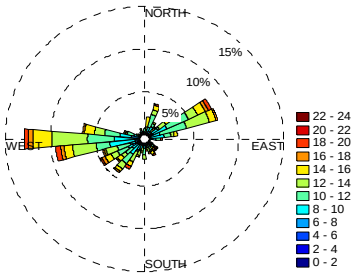
NORTH
15%
10%
5%
WEST
EAST
SOUTH
22 - 24
20 - 22
18 - 20
16 - 18
14 - 16
12 - 14
10 - 12
8 - 10
6 - 8
4 - 6
2 - 4
0 - 2

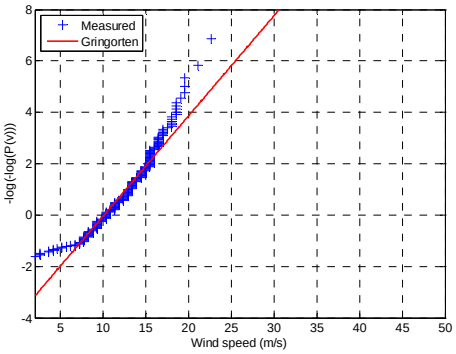
Measured
Gringorten
-log(-log(P(v)))
Wind speed (m/s)

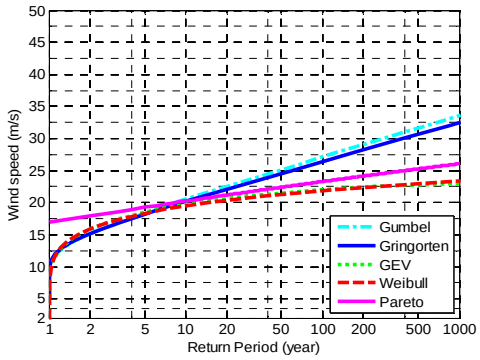
Wind speed (m/s)
Return Period (year)
Gumbel
Gringorten
GEV
Weibull
Pareto

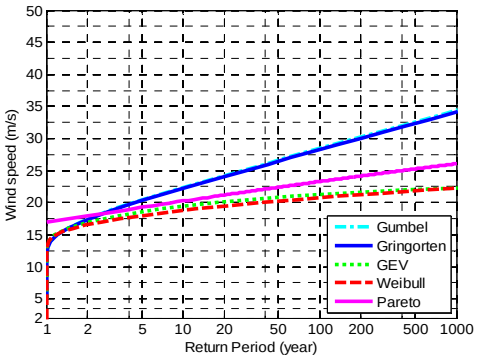
Wind speed (m/s)
Return Period (year)
Gumbel
Gringorten
GEV
Weibull
Pareto

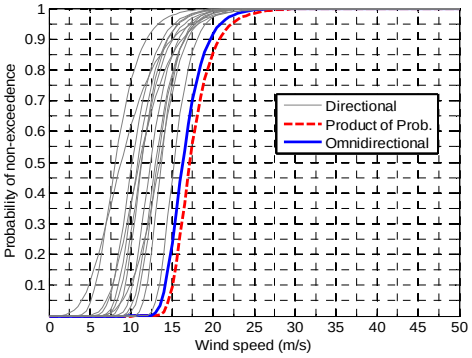
Probability of non-exceedence
Wind speed (m/s)
Directional
Product of Prob.
Omnidirectional

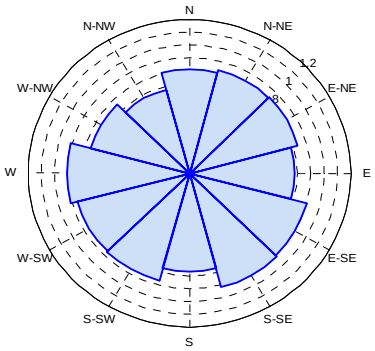
N
N-NE
E-NE
E
E-SE
S-SE
S
S-SW
W
W-NW
N-NW

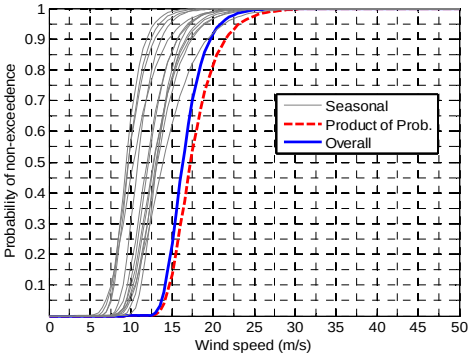
Probability of non-exceedence
Wind speed (m/s)
Seasonal
Product of Prob.
Overall

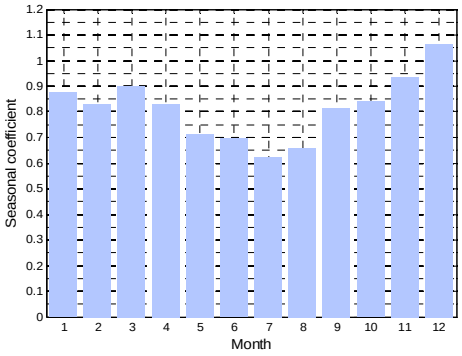
Seasonal coefficient
Month

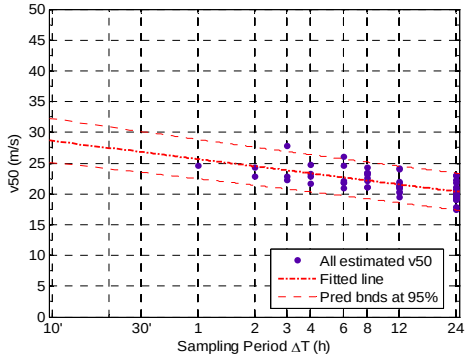
v50 (m/s)
Sampling Period ΔT (h)
All estimated v50
Fitted line
Pred bnds at 95%

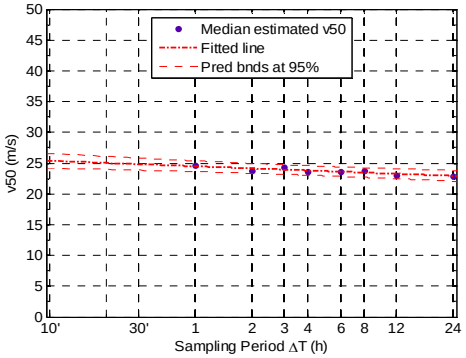
v50 (m/s)
Sampling Period ΔT (h)
Median estimated v50
Fitted line
Pred bnds at 95%

LIRN

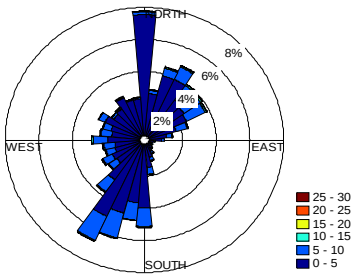
NORTH
8%
6%
4%
2%
WEST
EAST
SOUTH
25 - 30
20 - 25
15 - 20
10 - 15
5 - 10
0 - 5

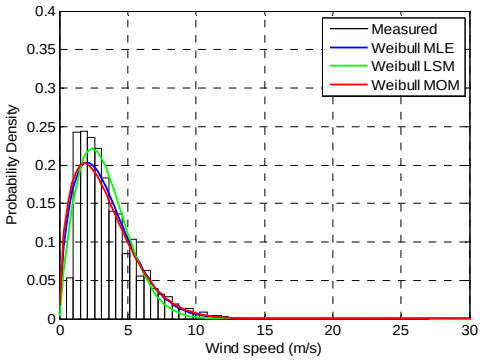
Measured
Weibull MLE
Weibull LSM
Weibull MOM
Probability Density
Wind speed (m/s)

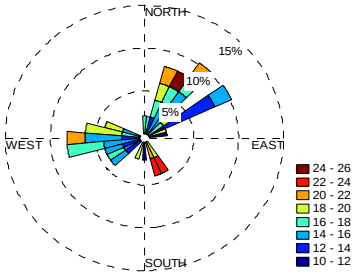
NORTH
15%
10%
5%
WEST
EAST
SOUTH
24 - 26
22 - 24
20 - 22
18 - 20
16 - 18
14 - 16
12 - 14
10 - 12

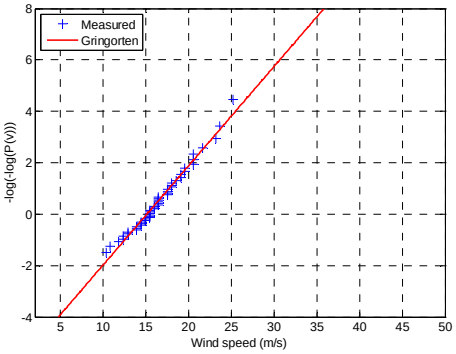
Measured
Gringorten
-log(-log(P(v)))
Wind speed (m/s)

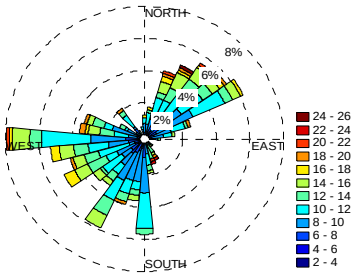
NORTH
8%
6%
4%
2%
WEST
EAST
SOUTH
24 - 26
22 - 24
20 - 22
18 - 20
16 - 18
14 - 16
12 - 14
10 - 12
8 - 10
6 - 8
4 - 6
2 - 4

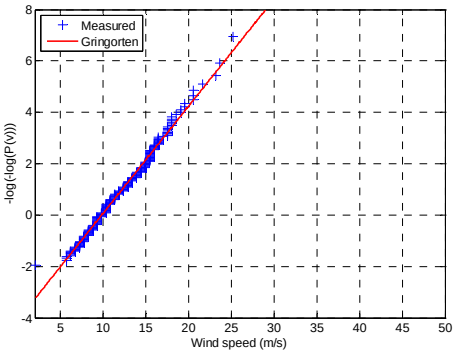
Measured
Gringorten
-log(-log(P(v)))
Wind speed (m/s)

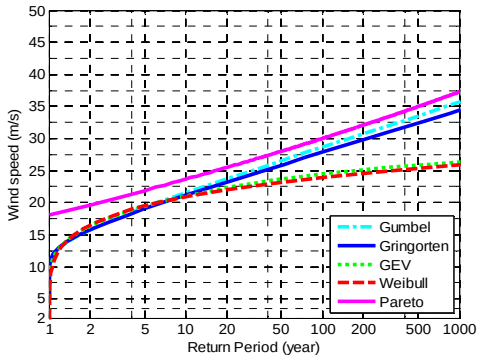
Wind speed (m/s)
Return Period (year)
Gumbel
Gringorten
GEV
Weibull
Pareto

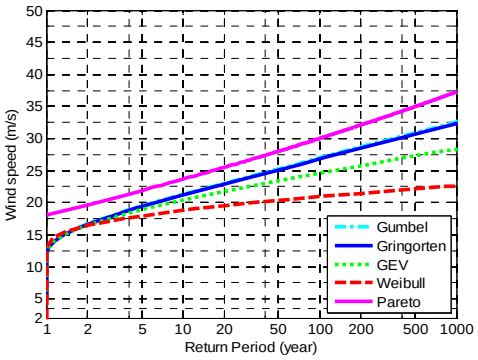
Wind speed (m/s)
Return Period (year)
Gumbel
Gringorten
GEV
Weibull
Pareto

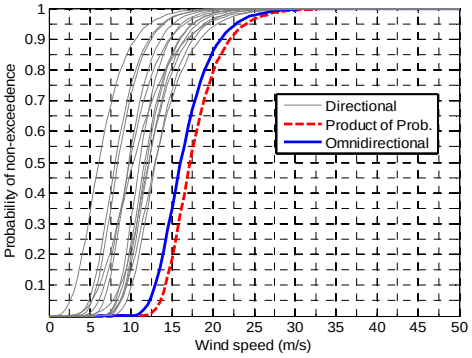
Probability of non-exceedence
Wind speed (m/s)
Directional
Product of Prob.
Omnidirectional

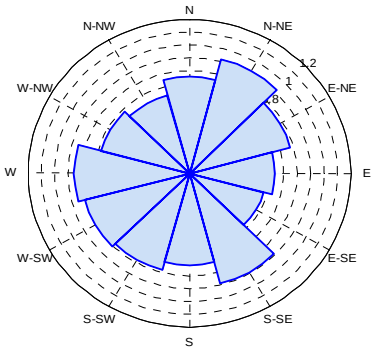
N
N-NE
E-NE
E
E-SE
S-SE
S
S-SW
W
W-NW
N-NW

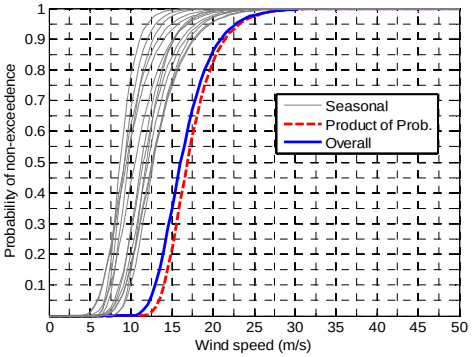
Probability of non-exceedence
Wind speed (m/s)
Seasonal
Product of Prob.
Overall

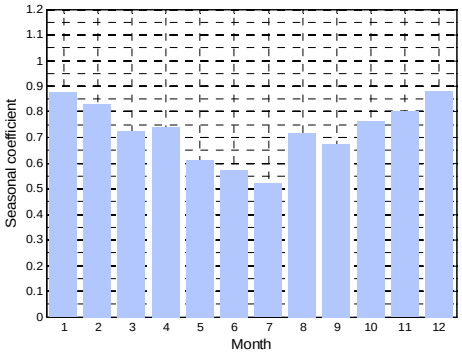
Seasonal coefficient
Month

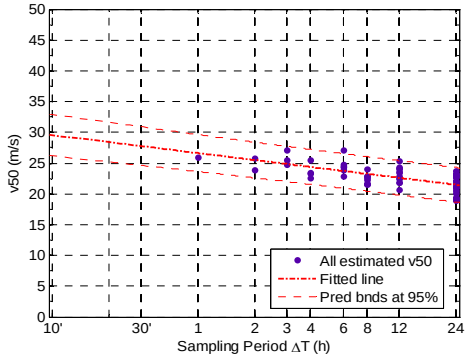
v50 (m/s)
Sampling Period ΔT (h)
All estimated v50
Fitted line
Pred bnds at 95%

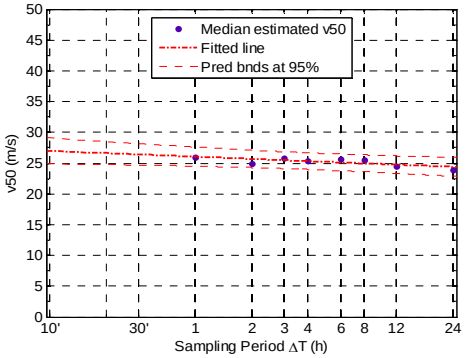
v50 (m/s)
Sampling Period ΔT (h)
Median estimated v50
Fitted line
Pred bnds at 95%

LIRP

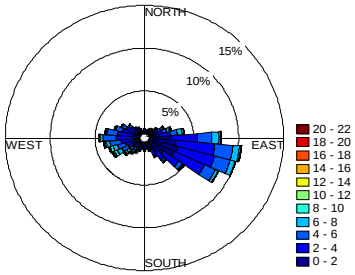
NORTH
15%
10%
5%
WEST
EAST
SOUTH
20 - 22
18 - 20
16 - 18
14 - 16
12 - 14
10 - 12
8 - 10
6 - 8
4 - 6
2 - 4
0 - 2

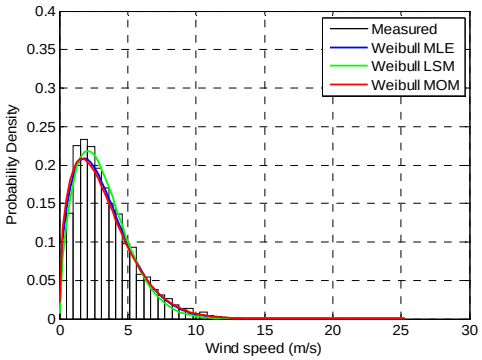
Measured
Weibull MLE
Weibull LSM
Weibull MOM
Probability Density
Wind speed (m/s)

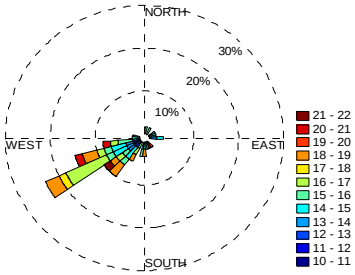
NORTH
30%
20%
10%
WEST
EAST
SOUTH
21 - 22
20 - 21
19 - 20
18 - 19
17 - 18
16 - 17
15 - 16
14 - 15
13 - 14
12 - 13
11 - 12
10 - 11

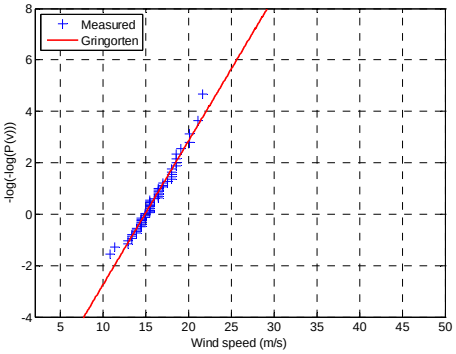
Measured
Gringorten
-log(-log(P(v)))
Wind speed (m/s)

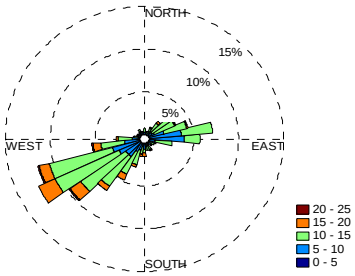
NORTH
15%
10%
5%
WEST
EAST
SOUTH
20 - 25
15 - 20
10 - 15
5 - 10
0 - 5

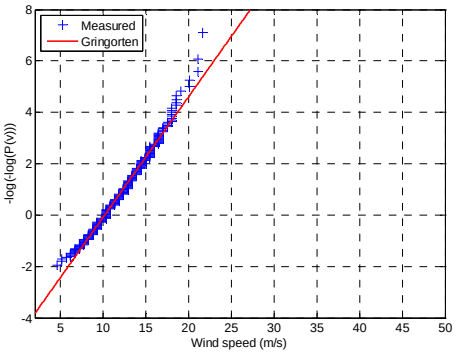
Measured
Gringorten
-log(-log(P(v)))
Wind speed (m/s)

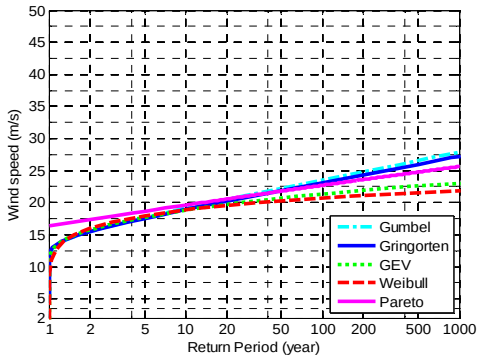
Wind speed (m/s)
Return Period (year)
Gumbel
Gringorten
GEV
Weibull
Pareto

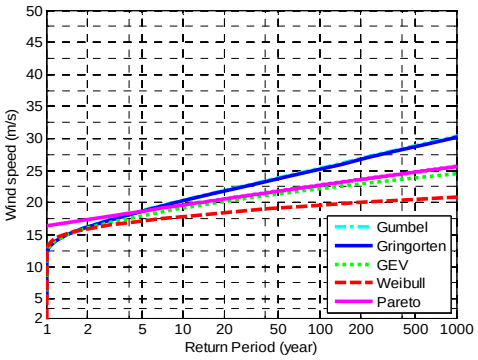
Wind speed (m/s)
Return Period (year)
Gumbel
Gringorten
GEV
Weibull
Pareto

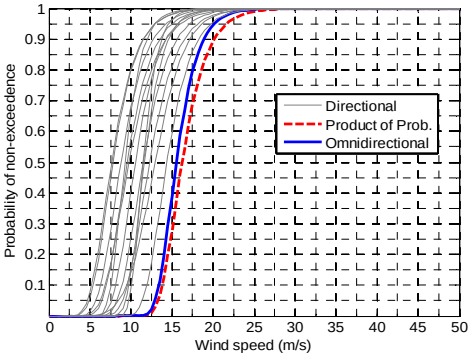
Probability of non-exceedence
Wind speed (m/s)
Directional
Product of Prob.
Omnidirectional

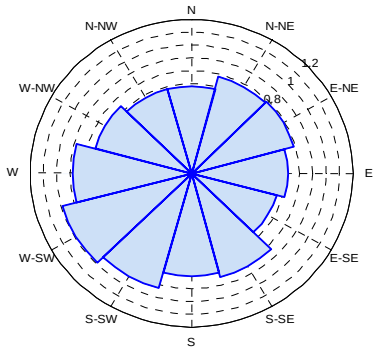
N
N-NE
E-NE
E
E-SE
S-SE
S
S-SW
W
W-NW
N-NW

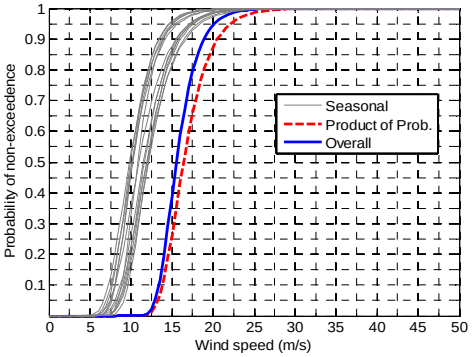
Probability of non-exceedence
Wind speed (m/s)
Seasonal
Product of Prob.
Overall

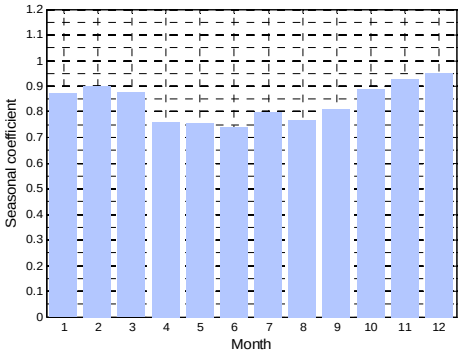
Seasonal coefficient
Month

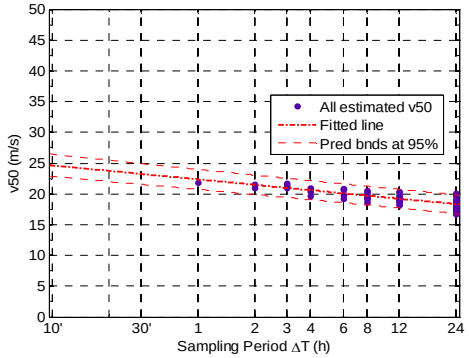
v50 (m/s)
Sampling Period ΔT (h)
All estimated v50
Fitted line
Pred bnds at 95%

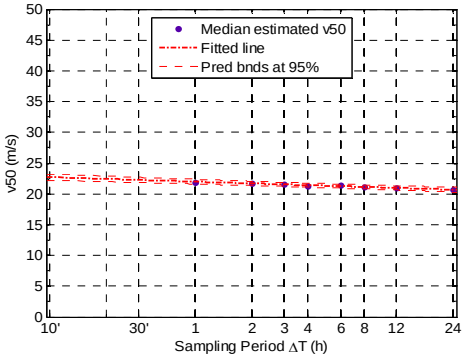
v50 (m/s)
Sampling Period ΔT (h)
Median estimated v50
Fitted line
Pred bnds at 95%

LIRQ

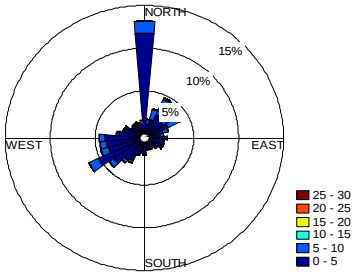
NORTH
15%
10%
5%
WEST
EAST
SOUTH
25 - 30
20 - 25
15 - 20
10 - 15
5 - 10
0 - 5

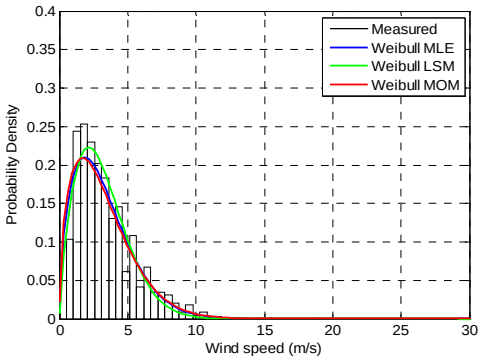
Measured
Weibull MLE
Weibull LSM
Weibull MOM
Probability Density
Wind speed (m/s)

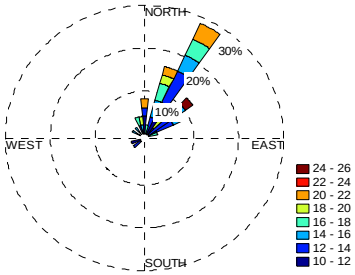
NORTH
30%
20%
10%
WEST
EAST
SOUTH
24 - 26
22 - 24
20 - 22
18 - 20
16 - 18
14 - 16
12 - 14
10 - 12

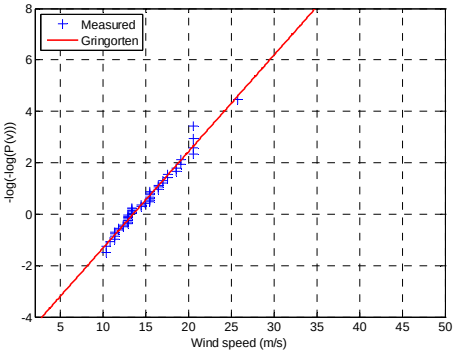
Measured
Gringorten
-log(-log(P(v)))
Wind speed (m/s)

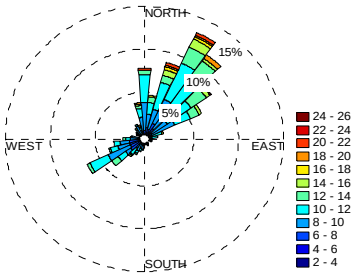
NORTH
15%
10%
5%
WEST
EAST
SOUTH
24 - 26
22 - 24
20 - 22
18 - 20
16 - 18
14 - 16
12 - 14
10 - 12
8 - 10
6 - 8
4 - 6
2 - 4

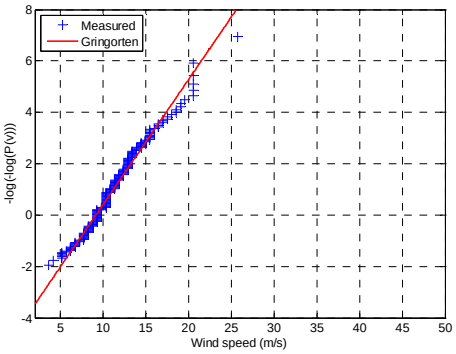
Measured
Gringorten
-log(-log(P(v)))
Wind speed (m/s)

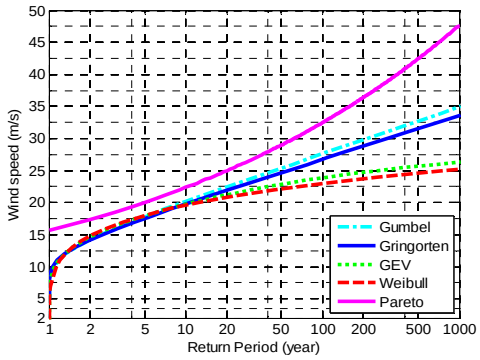
Wind speed (m/s)
Return Period (year)
Gumbel
Gringorten
GEV
Weibull
Pareto

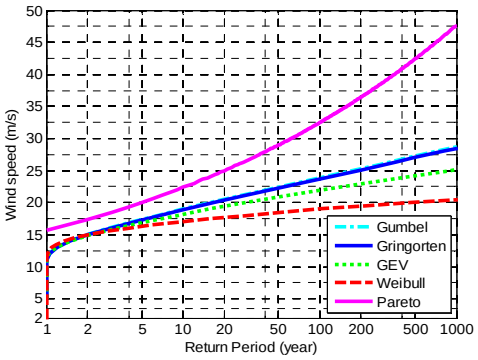
Wind speed (m/s)
Return Period (year)
Gumbel
Gringorten
GEV
Weibull
Pareto

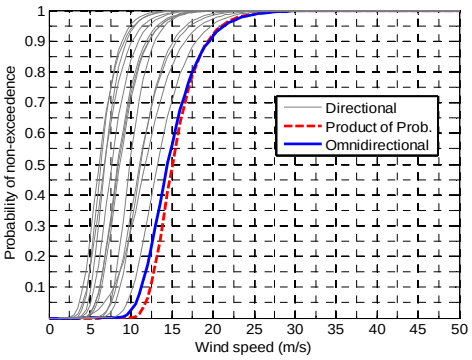
Probability of non-exceedence
Wind speed (m/s)
Directional
Product of Prob.
Omnidirectional

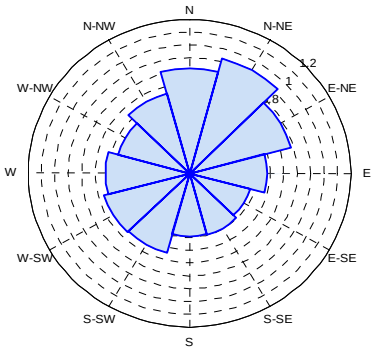
N
N-NE
E-NE
E
E-SE
S-SE
S
S-SW
W
W-NW
N-NW

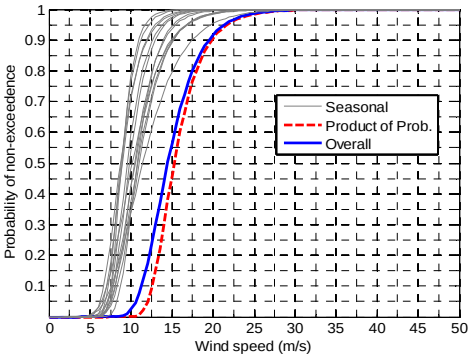
Probability of non-exceedence
Wind speed (m/s)
Seasonal
Product of Prob.
Overall

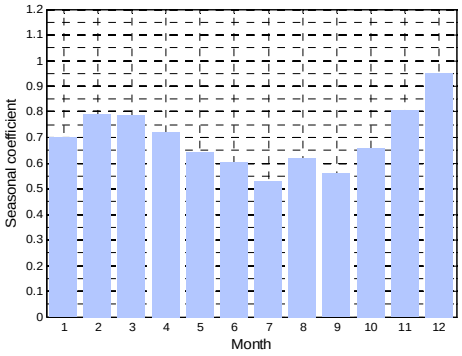
Seasonal coefficient
Month

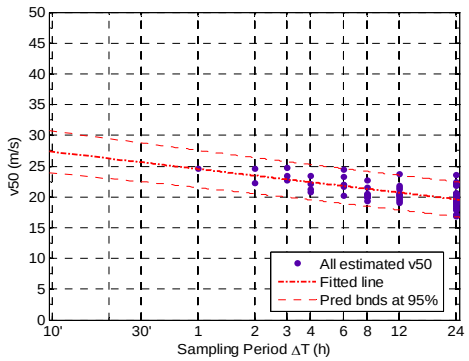
v50 (m/s)
Sampling Period ΔT (h)
All estimated v50
Fitted line
Pred bnds at 95%

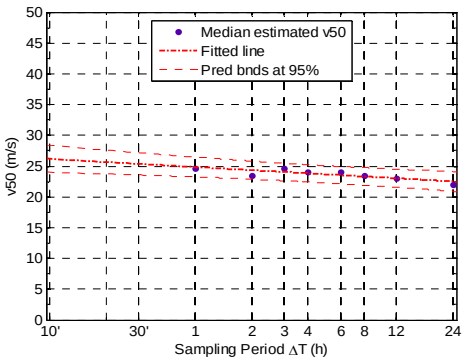
v50 (m/s)
Sampling Period ΔT (h)
Median estimated v50
Fitted line
Pred bnds at 95%

LIRS

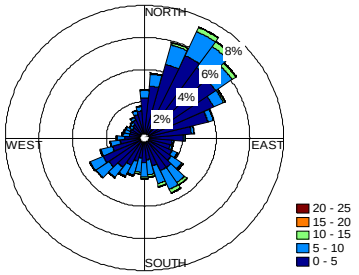
NORTH
EAST
SOUTH
WEST
8%
6%
4%
2%
20 - 25
15 - 20
10 - 15
5 - 10
0 - 5

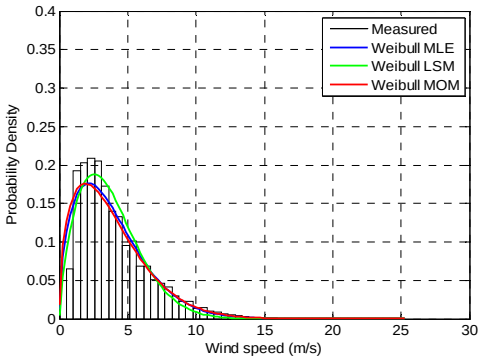
Measured
Weibull MLE
Weibull LSM
Weibull MOM
Probability Density
Wind speed (m/s)

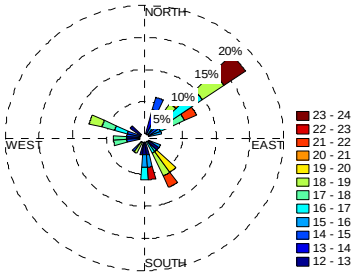
NORTH
EAST
SOUTH
WEST
20%
15%
10%
5%
23 - 24
22 - 23
21 - 22
20 - 21
19 - 20
18 - 19
17 - 18
16 - 17
15 - 16
14 - 15
13 - 14
12 - 13

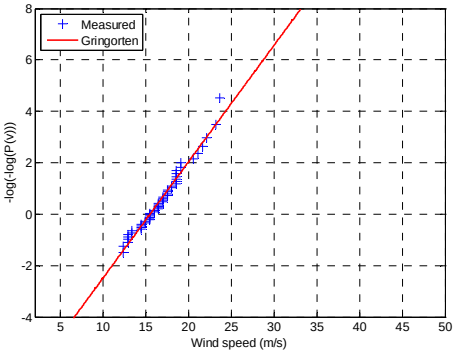
Measured
Gringorten
-log(-log(P(v)))
Wind speed (m/s)

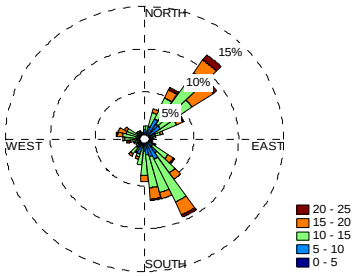
NORTH
EAST
SOUTH
WEST
15%
10%
5%
20 - 25
15 - 20
10 - 15
5 - 10
0 - 5

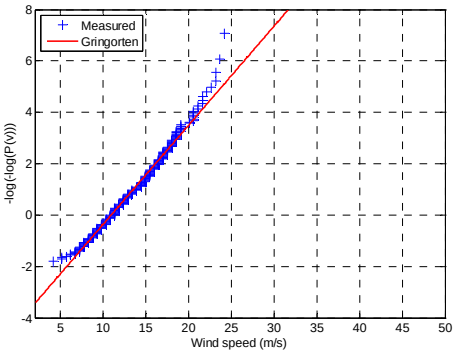
Measured
Gringorten
-log(-log(P(v)))
Wind speed (m/s)

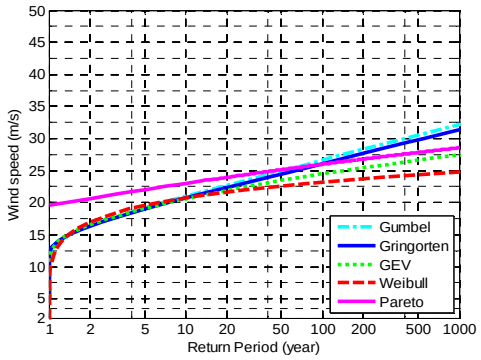
Wind speed (m/s)
Return Period (year)
Gumbel
Gringorten
GEV
Weibull
Pareto

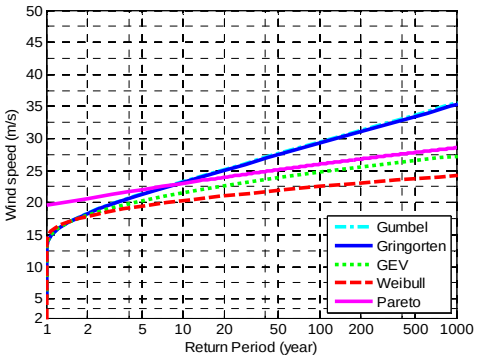
Wind speed (m/s)
Return Period (year)
Gumbel
Gringorten
GEV
Weibull
Pareto

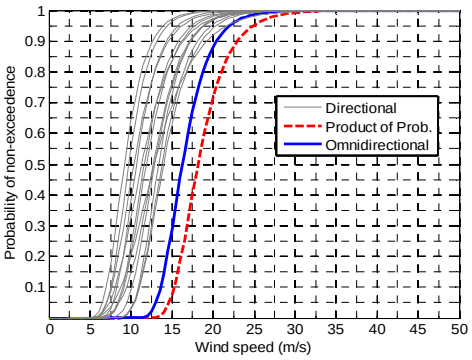
Probability of non-exceedence
Wind speed (m/s)
Directional
Product of Prob.
Omnidirectional

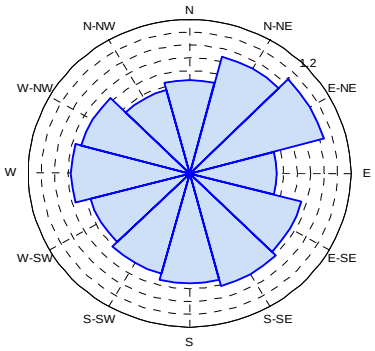
N
N-NE
E-NE
E
E-SE
S-SE
S
S-SW
W
W-NW
N-NW

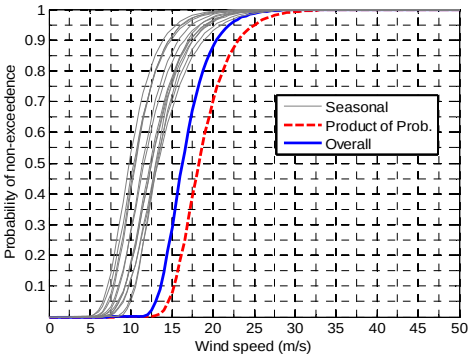
Probability of non-exceedence
Wind speed (m/s)
Seasonal
Product of Prob.
Overall

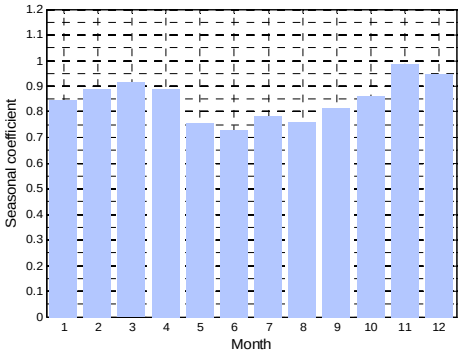
Seasonal coefficient
Month

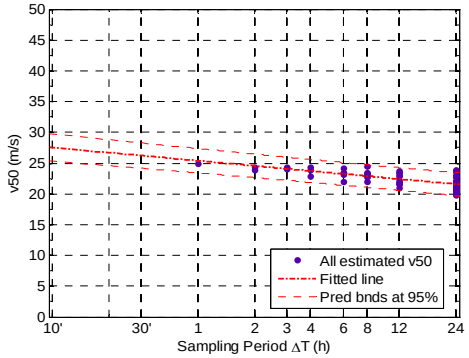
v50 (m/s)
Sampling Period ΔT (h)
All estimated v50
Fitted line
Pred bnds at 95%

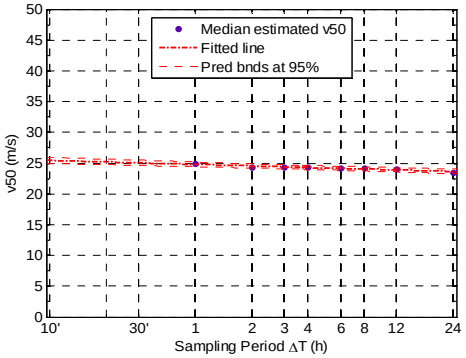
v50 (m/s)
Sampling Period ΔT (h)
Median estimated v50
Fitted line
Pred bnds at 95%

LIRT

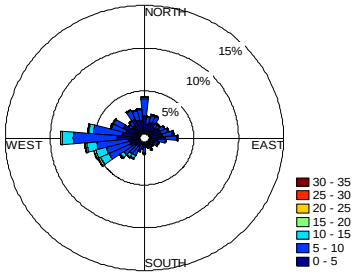
NORTH
15%
10%
5%
WEST
EAST
SOUTH
30 - 35
25 - 30
20 - 25
15 - 20
10 - 15
5 - 10
0 - 5

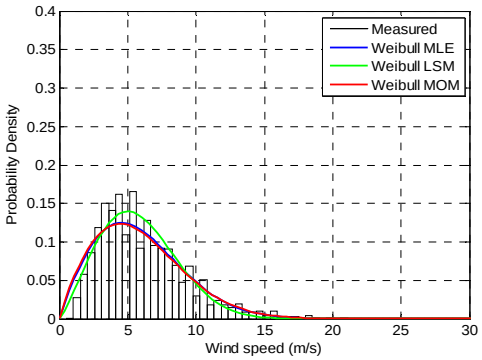
Measured
Weibull MLE
Weibull LSM
Weibull MOM
Probability Density
Wind speed (m/s)

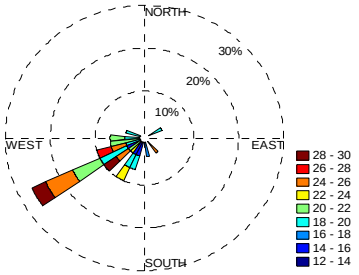
NORTH
30%
20%
10%
WEST
EAST
SOUTH
28 - 30
26 - 28
24 - 26
22 - 24
20 - 22
18 - 20
16 - 18
14 - 16
12 - 14

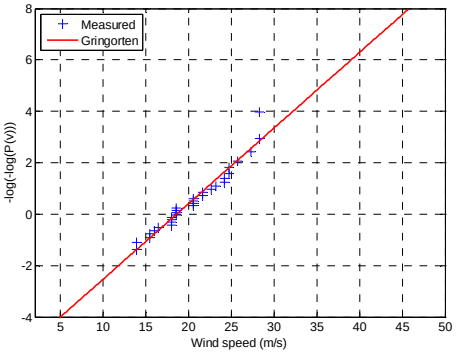
Measured
Gringorten
-log(-log(P(v)))
Wind speed (m/s)

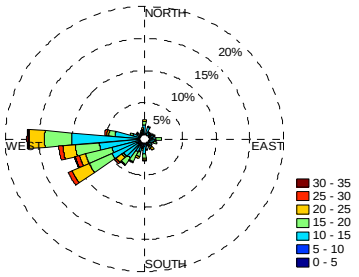
NORTH
20%
15%
10%
5%
WEST
EAST
SOUTH
30 - 35
25 - 30
20 - 25
15 - 20
10 - 15
5 - 10
0 - 5

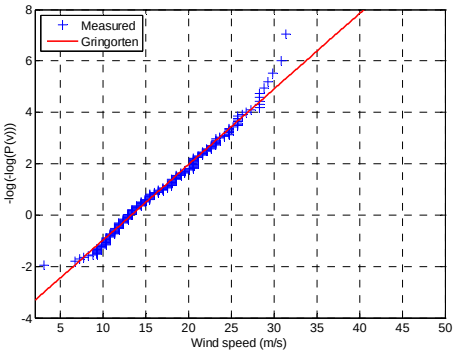
Measured
Gringorten
-log(-log(P(v)))
Wind speed (m/s)

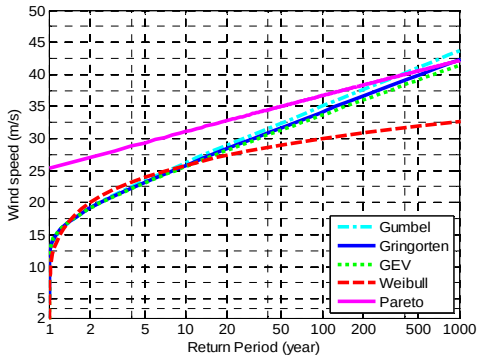
Wind speed (m/s)
Return Period (year)
Gumbel
Gringorten
GEV
Weibull
Pareto

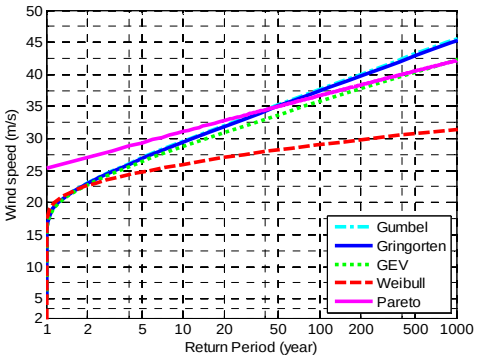
Wind speed (m/s)
Return Period (year)
Gumbel
Gringorten
GEV
Weibull
Pareto

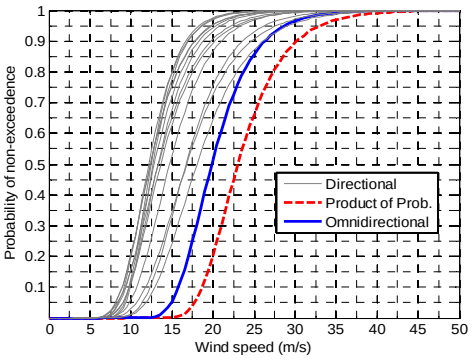
Probability of non-exceedence
Wind speed (m/s)
Directional
Product of Prob.
Omnidirectional

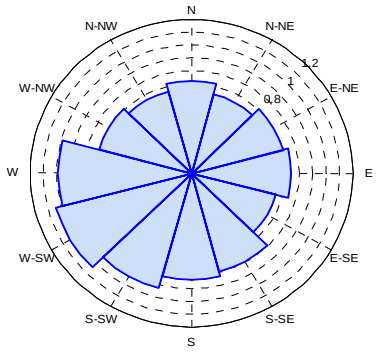
N
N-NE
E-NE
E
E-SE
S-SE
S
S-SW
W
W-NW
N-NW

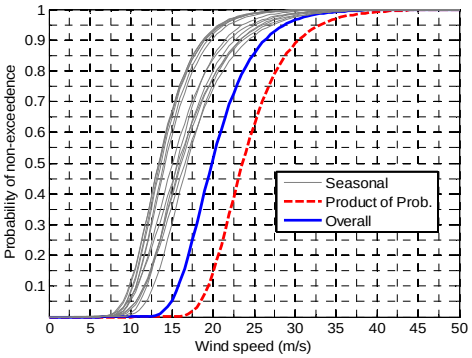
Probability of non-exceedence
Wind speed (m/s)
Seasonal
Product of Prob.
Overall

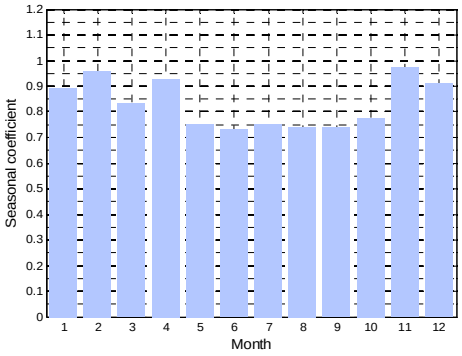
Seasonal coefficient
Month

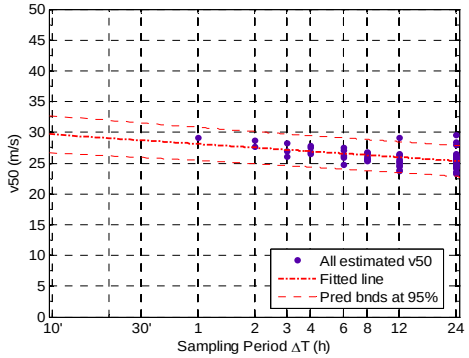
v50 (m/s)
Sampling Period ΔT (h)
All estimated v50
Fitted line
Pred bnds at 95%

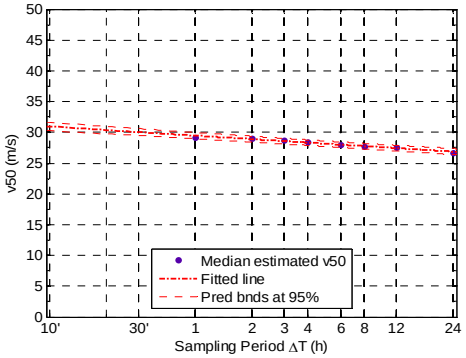
v50 (m/s)
Sampling Period ΔT (h)
Median estimated v50
Fitted line
Pred bnds at 95%

LIRU

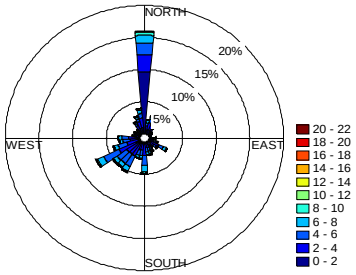
NORTH
20%
15%
10%
5%
WEST
EAST
SOUTH
20 - 22
18 - 20
16 - 18
14 - 16
12 - 14
10 - 12
8 - 10
6 - 8
4 - 6
2 - 4
0 - 2

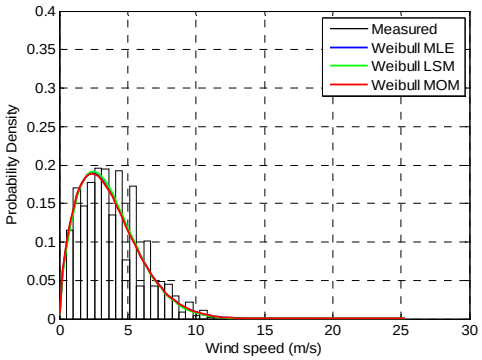
Measured
Weibull MLE
Weibull LSM
Weibull MOM
Probability Density
Wind speed (m/s)

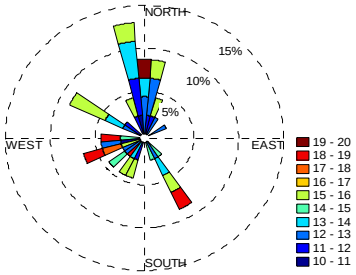
NORTH
15%
10%
5%
WEST
EAST
SOUTH
19 - 20
18 - 19
17 - 18
16 - 17
15 - 16
14 - 15
13 - 14
12 - 13
11 - 12
10 - 11

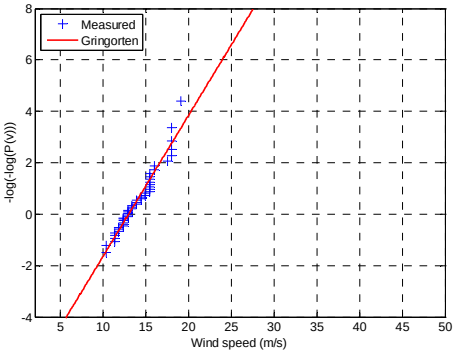
Measured
Gringorten
-log(-log(P(v)))
Wind speed (m/s)

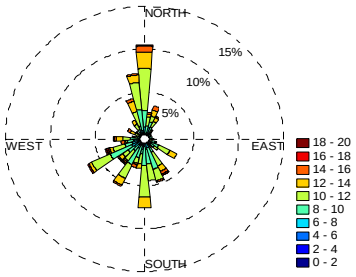
NORTH
15%
10%
5%
WEST
EAST
SOUTH
18 - 20
16 - 18
14 - 16
12 - 14
10 - 12
8 - 10
6 - 8
4 - 6
2 - 4
0 - 2

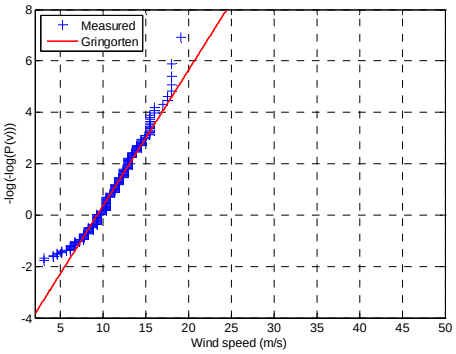
Measured
Gringorten
-log(-log(P(v)))
Wind speed (m/s)

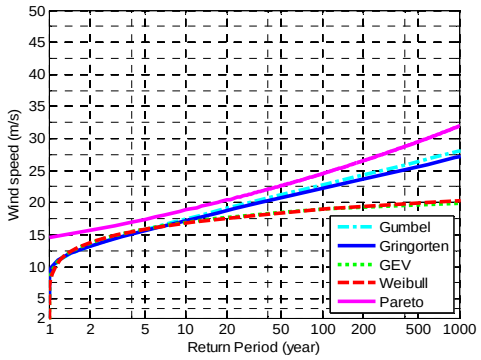
Wind speed (m/s)
Return Period (year)
Gumbel
Gringorten
GEV
Weibull
Pareto

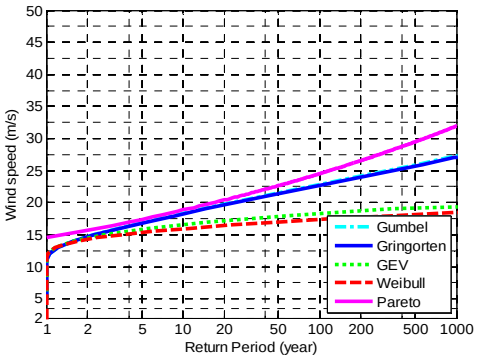
Wind speed (m/s)
Return Period (year)
Gumbel
Gringorten
GEV
Weibull
Pareto

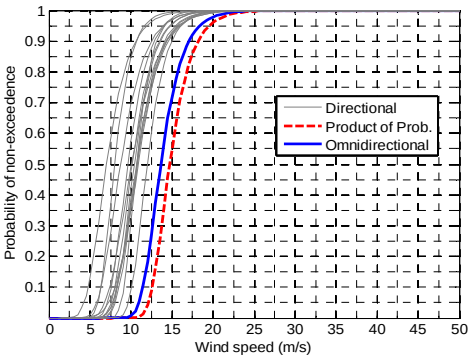
Probability of non-exceedence
Wind speed (m/s)
Directional
Product of Prob.
Omnidirectional

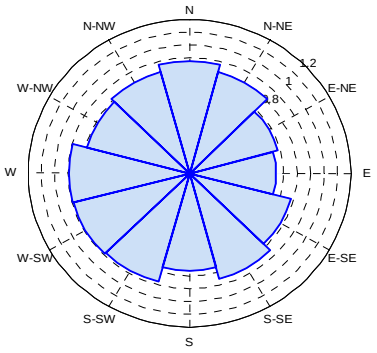
N
N-NE
E-NE
E
E-SE
S-SE
S
S-SW
W
W-NW
N-NW

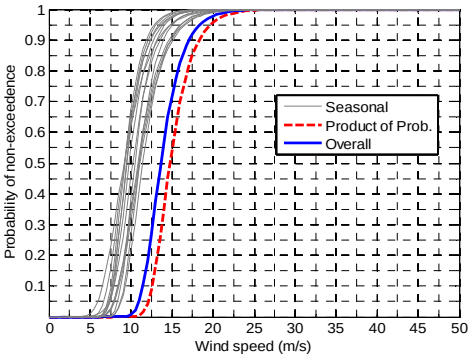
Probability of non-exceedence
Wind speed (m/s)
Seasonal
Product of Prob.
Overall

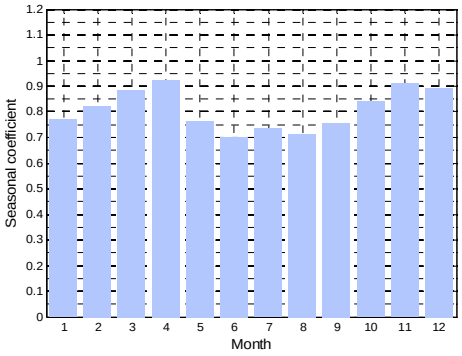
Seasonal coefficient
Month

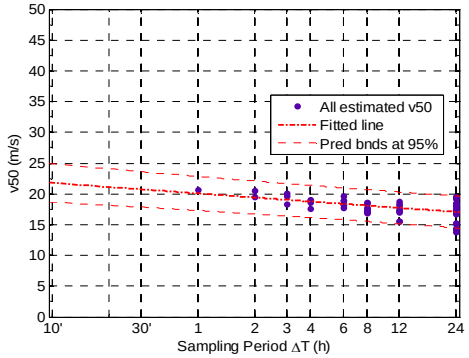
v50 (m/s)
Sampling Period ΔT (h)
All estimated v50
Fitted line
Pred bnds at 95%

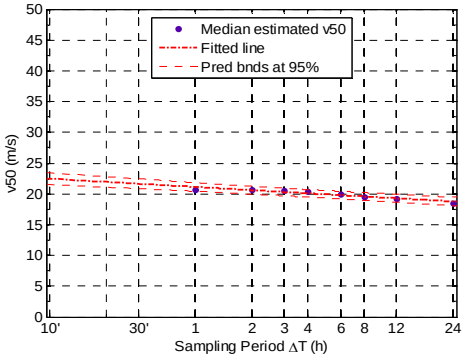
v50 (m/s)
Sampling Period ΔT (h)
Median estimated v50
Fitted line
Pred bnds at 95%

LIRV

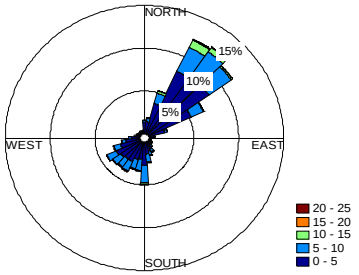
NORTH
EAST
SOUTH
WEST
15%
10%
5%
20 - 25
15 - 20
10 - 15
5 - 10
0 - 5

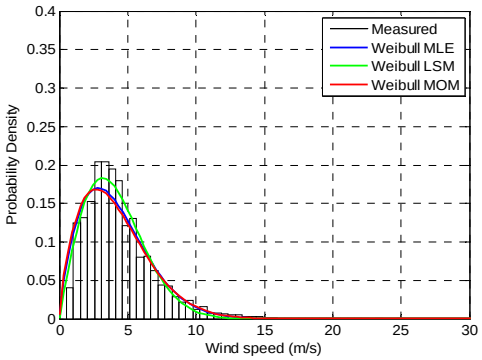
Measured
Weibull MLE
Weibull LSM
Weibull MOM
Probability Density
Wind speed (m/s)

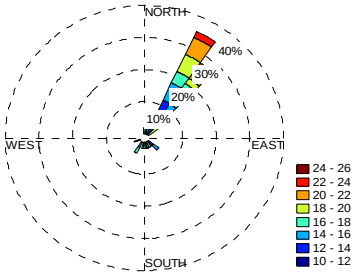
NORTH
EAST
SOUTH
WEST
40%
30%
20%
10%
24 - 26
22 - 24
20 - 22
18 - 20
16 - 18
14 - 16
12 - 14
10 - 12

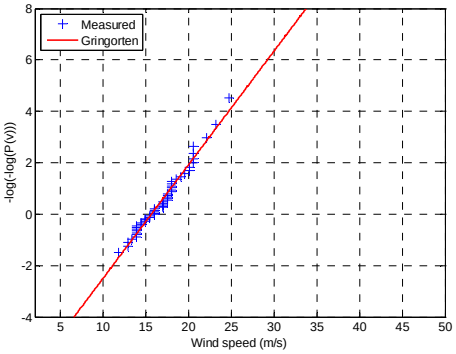
Measured
Gringorten
-log(-log(P(v)))
Wind speed (m/s)

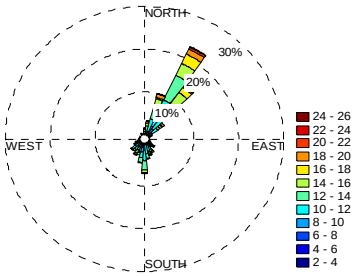
NORTH
EAST
SOUTH
WEST
30%
20%
10%
24 - 26
22 - 24
20 - 22
18 - 20
16 - 18
14 - 16
12 - 14
10 - 12
8 - 10
6 - 8
4 - 6
2 - 4

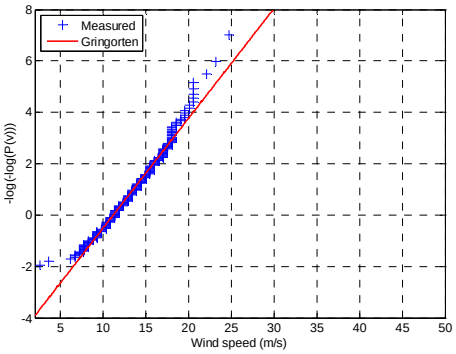
Measured
Gringorten
-log(-log(P(v)))
Wind speed (m/s)

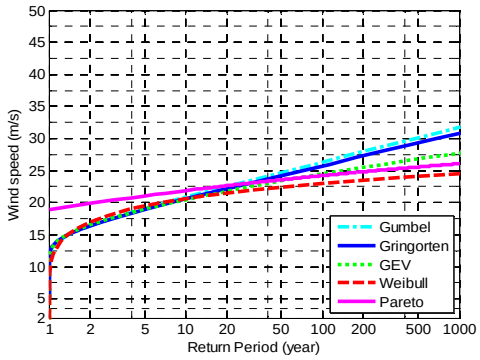
Wind speed (m/s)
Return Period (year)
Gumbel
Gringorten
GEV
Weibull
Pareto

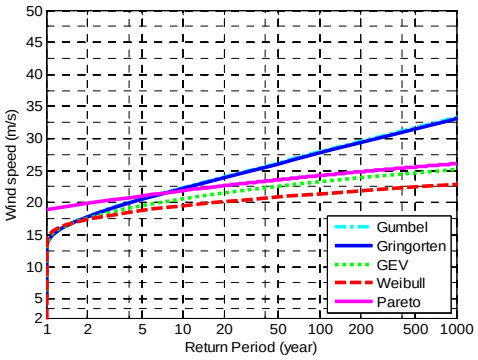
Wind speed (m/s)
Return Period (year)
Gumbel
Gringorten
GEV
Weibull
Pareto

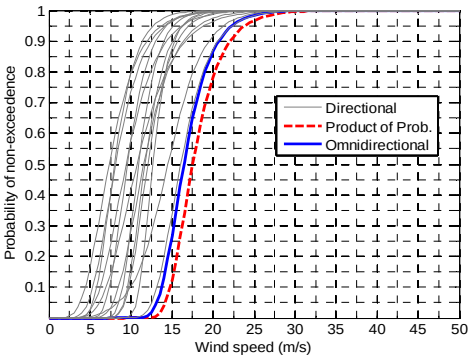
Probability of non-exceedence
Wind speed (m/s)
Directional
Product of Prob.
Omnidirectional

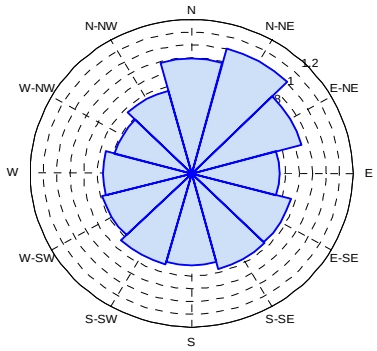
N
N-NE
E-NE
E
E-SE
S-SE
S
S-SW
W
W-NW
N-NW

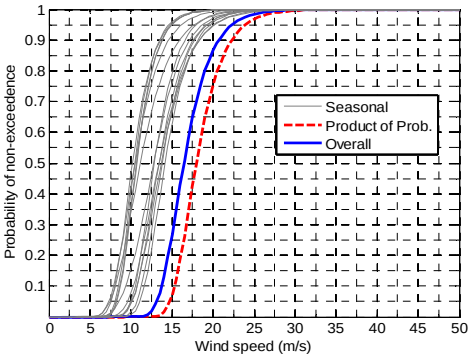
Probability of non-exceedence
Wind speed (m/s)
Seasonal
Product of Prob.
Overall

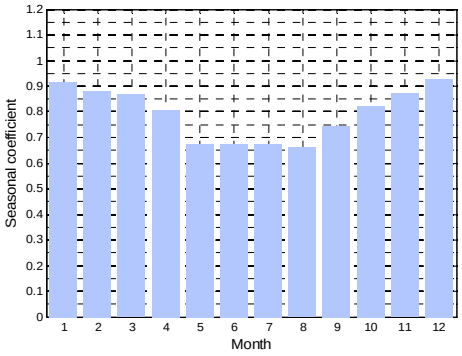
Seasonal coefficient
Month

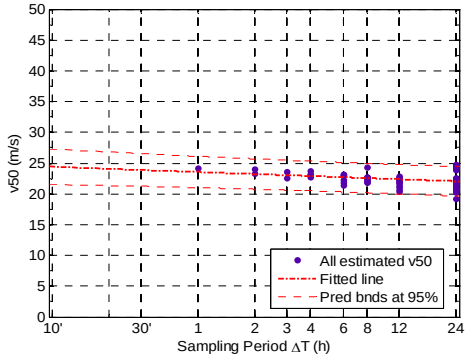
v50 (m/s)
Sampling Period ΔT (h)
All estimated v50
Fitted line
Pred bnds at 95%

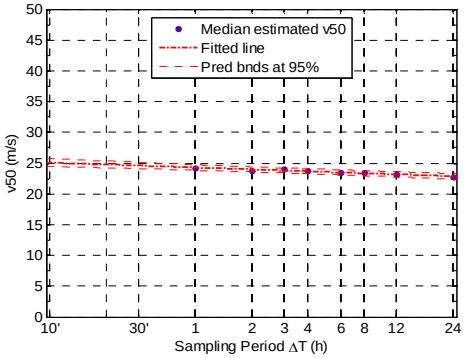
v50 (m/s)
Sampling Period ΔT (h)
Median estimated v50
Fitted line
Pred bnds at 95%

LIRX

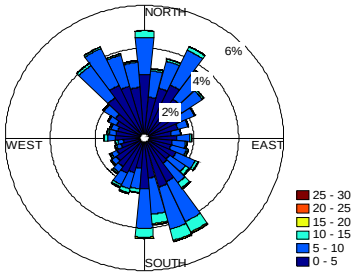
NORTH
6%
4%
2%
WEST
EAST
SOUTH
25 - 30
20 - 25
15 - 20
10 - 15
5 - 10
0 - 5

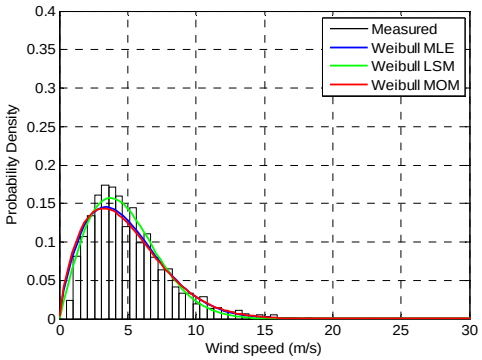
Measured
Weibull MLE
Weibull LSM
Weibull MOM
Probability Density
Wind speed (m/s)

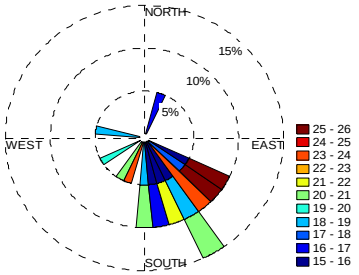
NORTH
15%
10%
5%
WEST
EAST
SOUTH
25 - 26
24 - 25
23 - 24
22 - 23
21 - 22
20 - 21
19 - 20
18 - 19
17 - 18
16 - 17
15 - 16

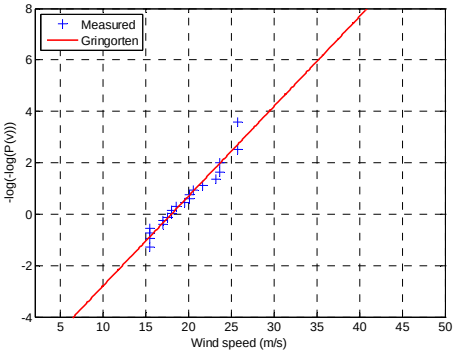
Measured
Gringorten
-log(-log(P(v)))
Wind speed (m/s)

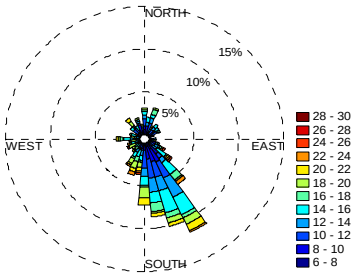
NORTH
15%
10%
5%
WEST
EAST
SOUTH
28 - 30
26 - 28
24 - 26
22 - 24
20 - 22
18 - 20
16 - 18
14 - 16
12 - 14
10 - 12
8 - 10
6 - 8

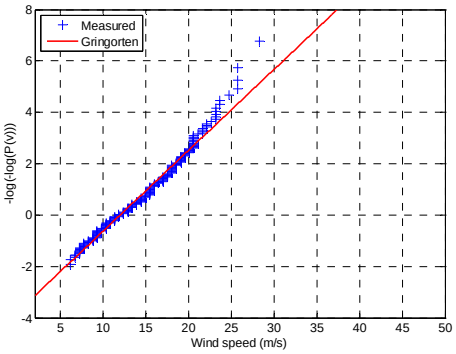
Measured
Gringorten
-log(-log(P(v)))
Wind speed (m/s)

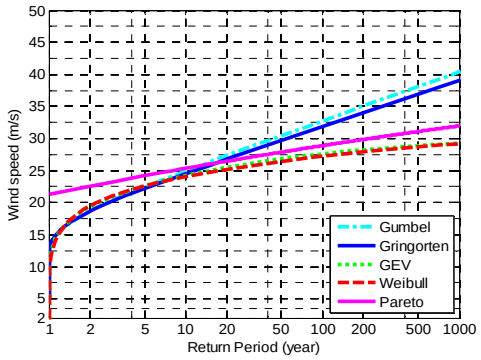
Wind speed (m/s)
Return Period (year)
Gumbel
Gringorten
GEV
Weibull
Pareto

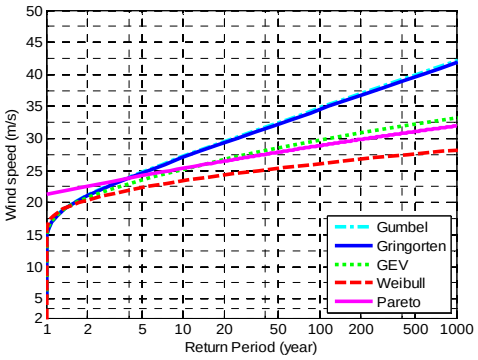
Wind speed (m/s)
Return Period (year)
Gumbel
Gringorten
GEV
Weibull
Pareto

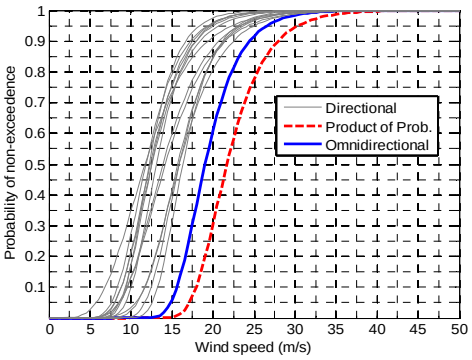
Probability of non-exceedence
Wind speed (m/s)
Directional
Product of Prob.
Omnidirectional

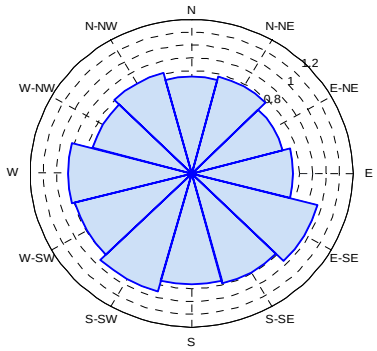
N
N-NE
E-NE
E
E-SE
S-SE
S
S-SW
W
W-NW
N-NW

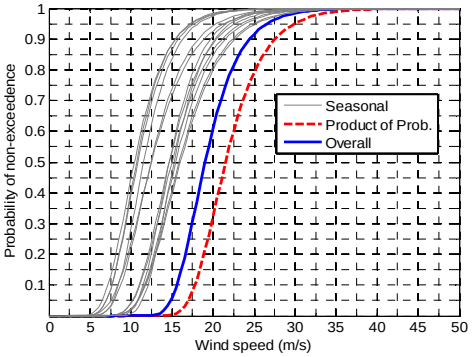
Probability of non-exceedence
Wind speed (m/s)
Seasonal
Product of Prob.
Overall

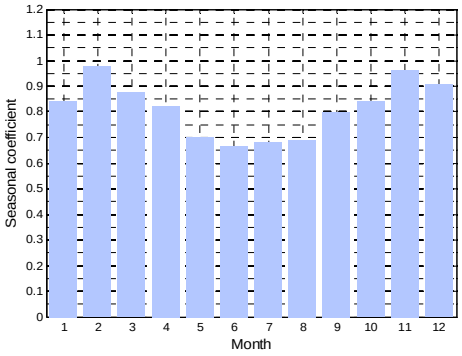
Seasonal coefficient
Month

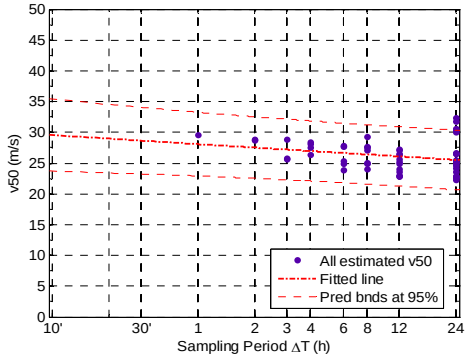
v50 (m/s)
Sampling Period ΔT (h)
All estimated v50
Fitted line
Pred bnds at 95%

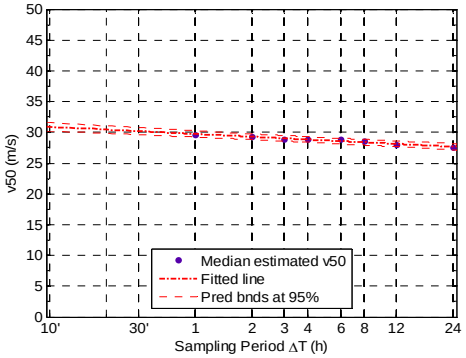
v50 (m/s)
Sampling Period ΔT (h)
Median estimated v50
Fitted line
Pred bnds at 95%

LIRZ

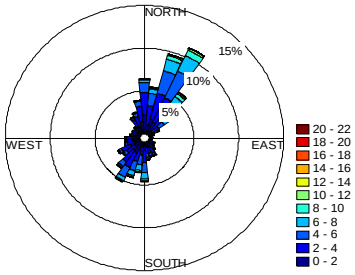
NORTH
EAST
SOUTH
WEST
15%
10%
5%
20 - 22
18 - 20
16 - 18
14 - 16
12 - 14
10 - 12
8 - 10
6 - 8
4 - 6
2 - 4
0 - 2

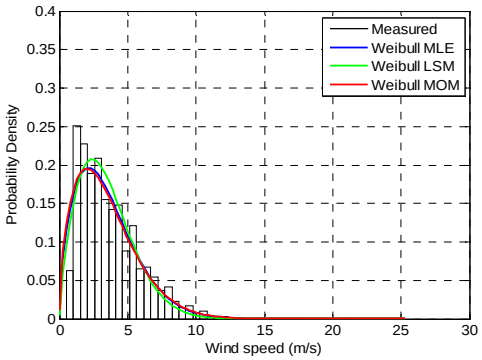
Measured
Weibull MLE
Weibull LSM
Weibull MOM
Probability Density
Wind speed (m/s)

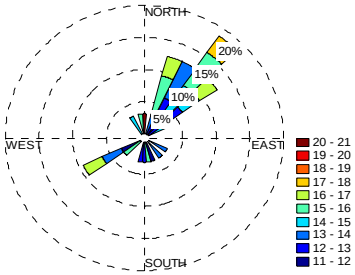
NORTH
EAST
SOUTH
WEST
20%
15%
10%
5%
20 - 21
19 - 20
18 - 19
17 - 18
16 - 17
15 - 16
14 - 15
13 - 14
12 - 13
11 - 12

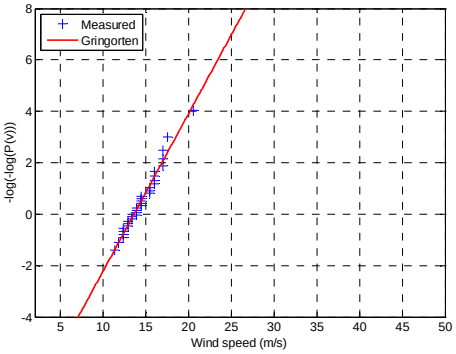
Measured
Gringorten
-log(-log(P(v)))
Wind speed (m/s)

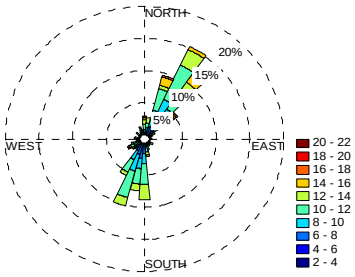
NORTH
EAST
SOUTH
WEST
20%
15%
10%
5%
20 - 22
18 - 20
16 - 18
14 - 16
12 - 14
10 - 12
8 - 10
6 - 8
4 - 6
2 - 4

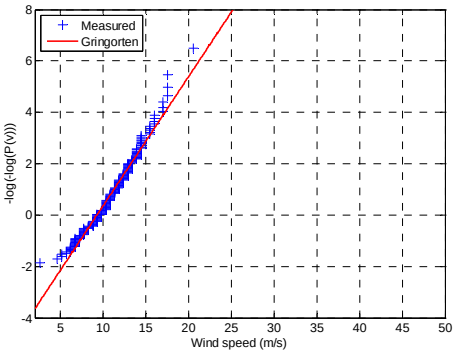
Measured
Gringorten
-log(-log(P(v)))
Wind speed (m/s)

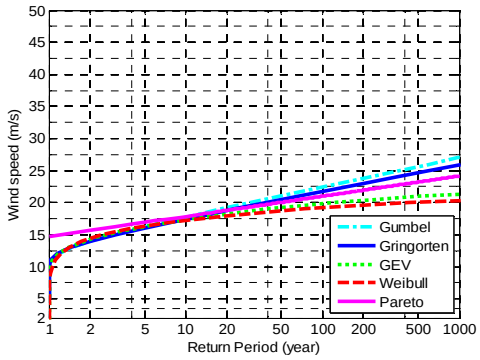
Wind speed (m/s)
Return Period (year)
Gumbel
Gringorten
GEV
Weibull
Pareto

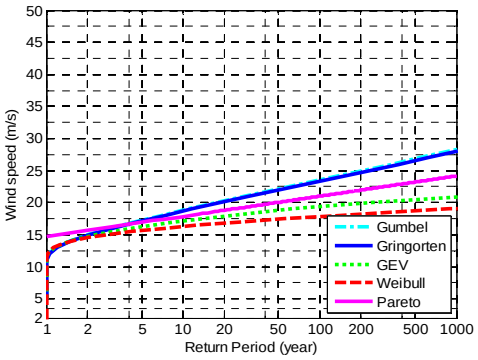
Wind speed (m/s)
Return Period (year)
Gumbel
Gringorten
GEV
Weibull
Pareto

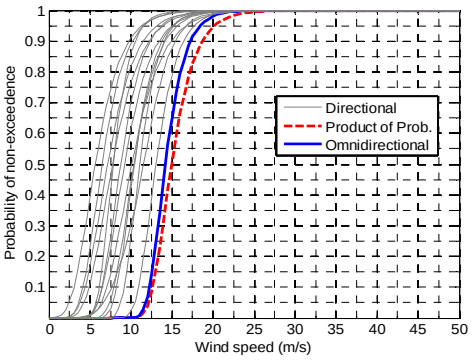
Probability of non-exceedence
Wind speed (m/s)
Directional
Product of Prob.
Omnidirectional

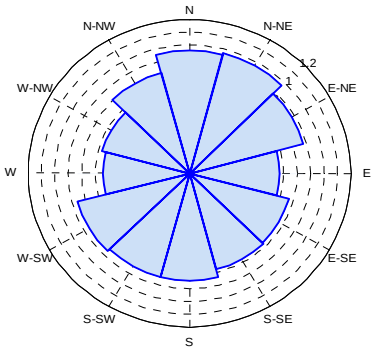
N
N-NE
E-NE
E
E-SE
S-SE
S
S-SW
W-SW
W
W-NW
N-NW

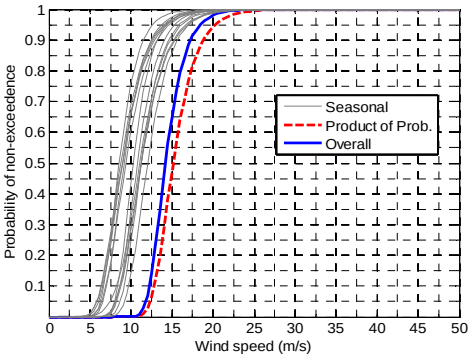
Probability of non-exceedence
Wind speed (m/s)
Seasonal
Product of Prob.
Overall

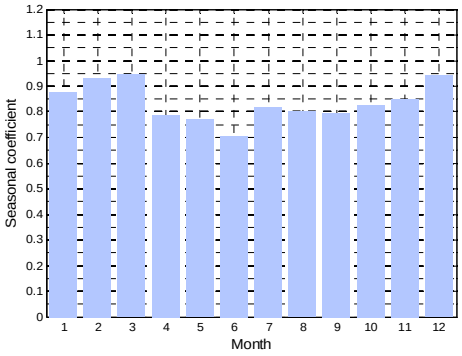
Seasonal coefficient
Month

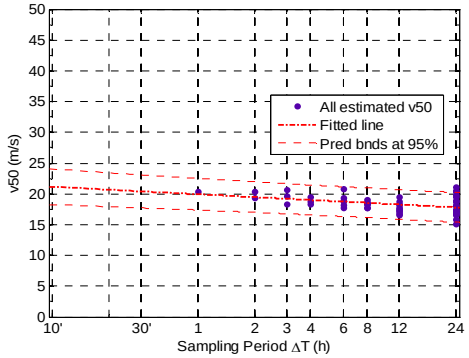
v50 (m/s)
Sampling Period ΔT (h)
All estimated v50
Fitted line
Pred bnds at 95%

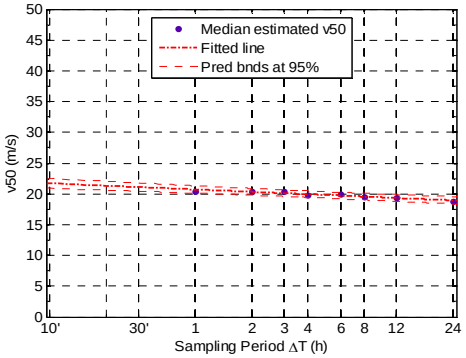
v50 (m/s)
Sampling Period ΔT (h)
Median estimated v50
Fitted line
Pred bnds at 95%

LIVC

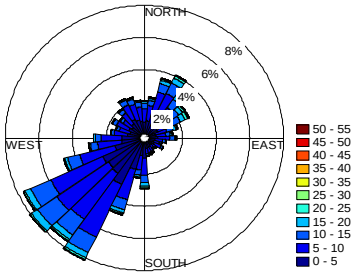
NORTH
8%
6%
4%
2%
WEST
EAST
SOUTH
50 - 55
45 - 50
40 - 45
35 - 40
30 - 35
25 - 30
20 - 25
15 - 20
10 - 15
5 - 10
0 - 5

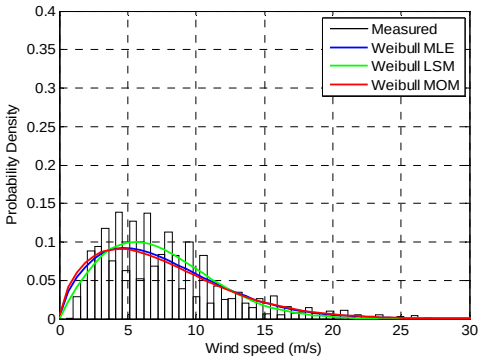
Measured
Weibull MLE
Weibull LSM
Weibull MOM
Probability Density
Wind speed (m/s)

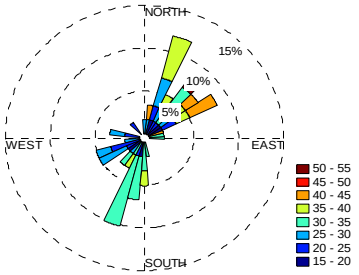
NORTH
15%
10%
5%
WEST
EAST
SOUTH
50 - 55
45 - 50
40 - 45
35 - 40
30 - 35
25 - 30
20 - 25
15 - 20

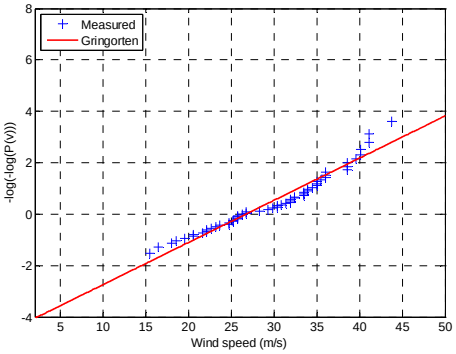
Measured
Gringorten
-log(-log(P(v)))
Wind speed (m/s)

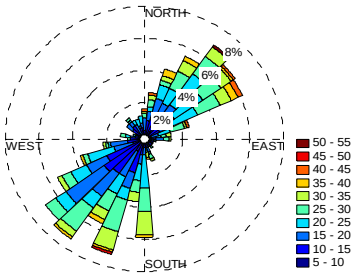
NORTH
8%
6%
4%
2%
WEST
EAST
SOUTH
50 - 55
45 - 50
40 - 45
35 - 40
30 - 35
25 - 30
20 - 25
15 - 20
10 - 15
5 - 10

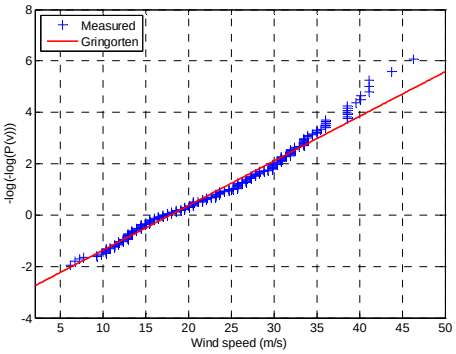
Measured
Gringorten
-log(-log(P(v)))
Wind speed (m/s)

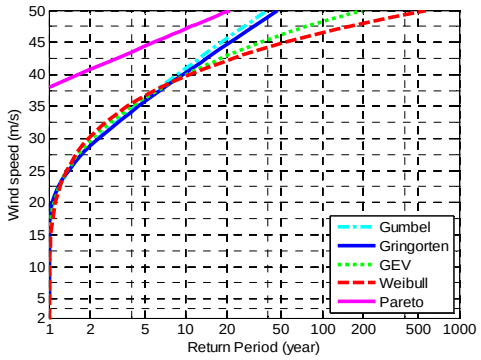
Wind speed (m/s)
Return Period (year)
Gumbel
Gringorten
GEV
Weibull
Pareto

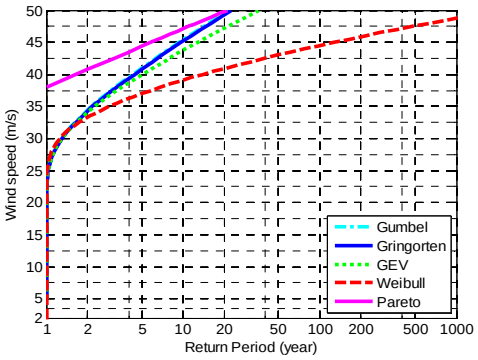
Wind speed (m/s)
Return Period (year)
Gumbel
Gringorten
GEV
Weibull
Pareto

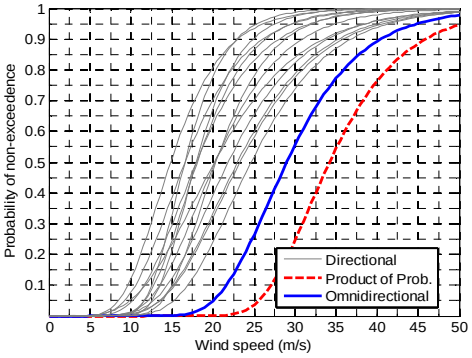
Probability of non-exceedence
Wind speed (m/s)
Directional
Product of Prob.
Omnidirectional

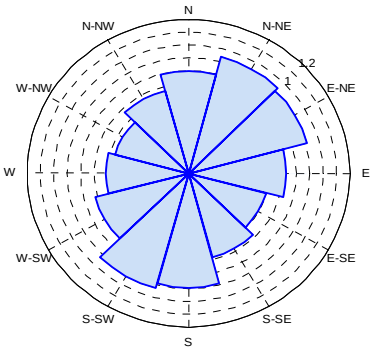
N
N-NE
E-NE
E
E-SE
S-SE
S
S-SW
W-SW
W
W-NW
N-NW

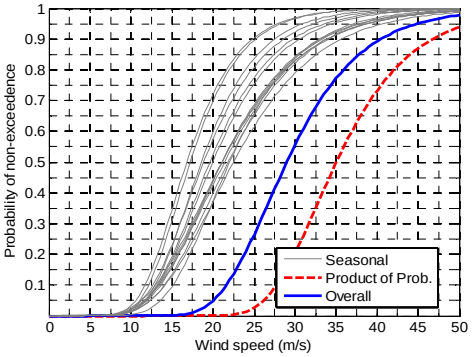
Probability of non-exceedence
Wind speed (m/s)
Seasonal
Product of Prob.
Overall

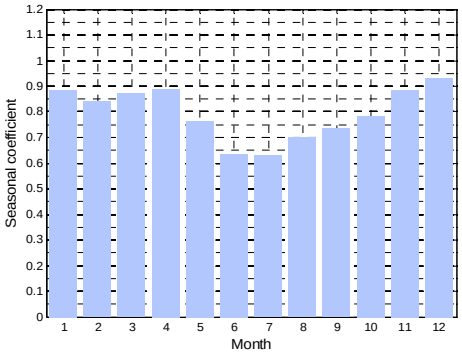
Seasonal coefficient
Month

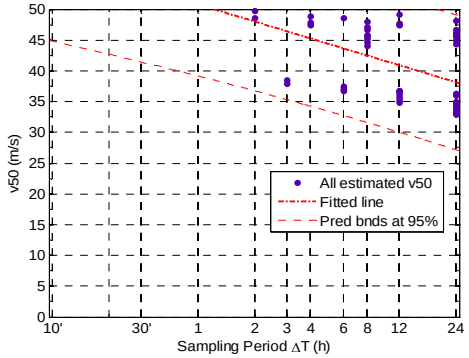
v50 (m/s)
Sampling Period ΔT (h)
All estimated v50
Fitted line
Pred bnds at 95%

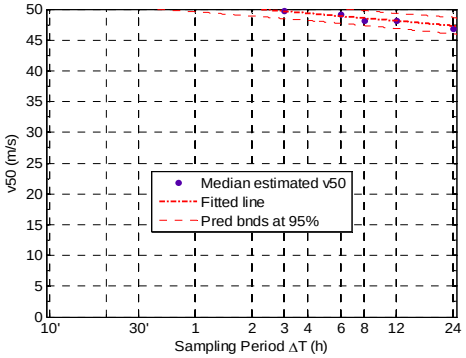
v50 (m/s)
Sampling Period ΔT (h)
Median estimated v50
Fitted line
Pred bnds at 95%

LIVD

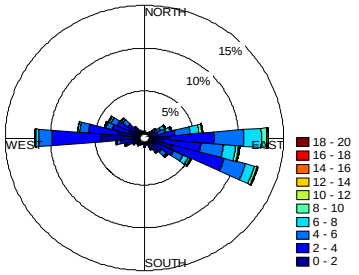
NORTH
15%
10%
5%
WEST
EAST
SOUTH
18 - 20
16 - 18
14 - 16
12 - 14
10 - 12
8 - 10
6 - 8
4 - 6
2 - 4
0 - 2

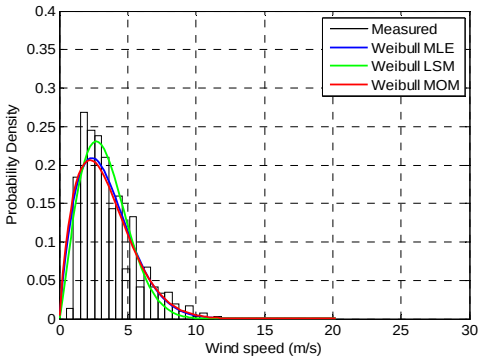
Measured
Weibull MLE
Weibull LSM
Weibull MOM
Probability Density
Wind speed (m/s)

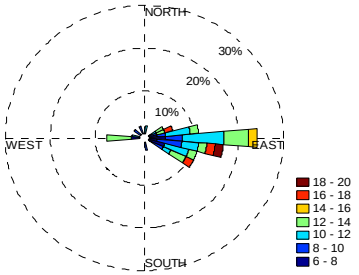
NORTH
30%
20%
10%
WEST
EAST
SOUTH
18 - 20
16 - 18
14 - 16
12 - 14
10 - 12
8 - 10
6 - 8

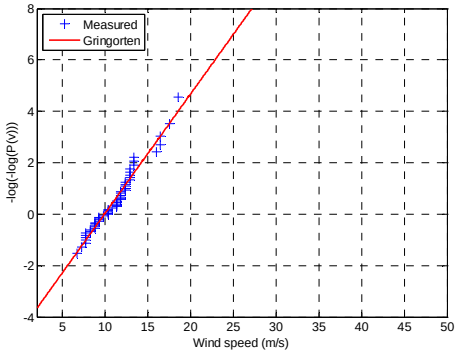
Measured
Gringorten
-log(-log(P(v)))
Wind speed (m/s)

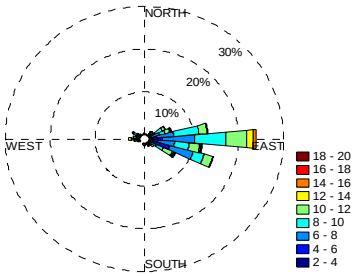
NORTH
30%
20%
10%
WEST
EAST
SOUTH
18 - 20
16 - 18
14 - 16
12 - 14
10 - 12
8 - 10
6 - 8
4 - 6
2 - 4

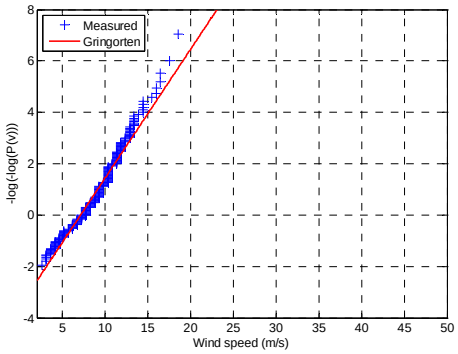
Measured
Gringorten
-log(-log(P(v)))
Wind speed (m/s)

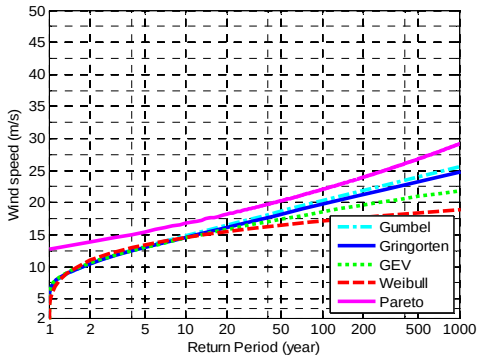
Wind speed (m/s)
Return Period (year)
Gumbel
Gringorten
GEV
Weibull
Pareto

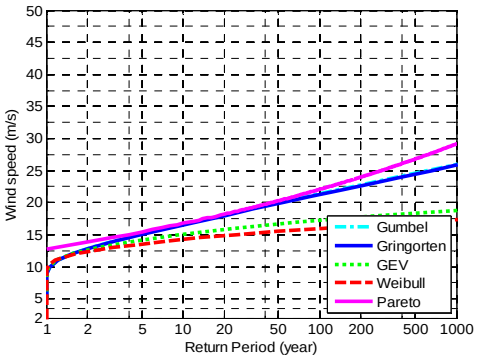
Wind speed (m/s)
Return Period (year)
Gumbel
Gringorten
GEV
Weibull
Pareto

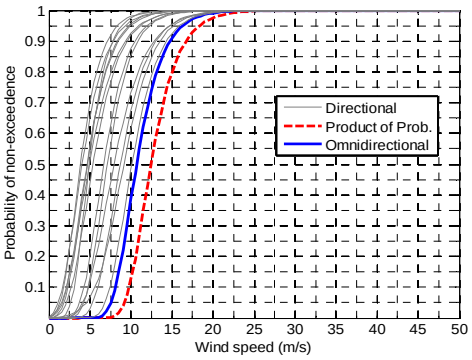
Probability of non-exceedence
Wind speed (m/s)
Directional
Product of Prob.
Omnidirectional

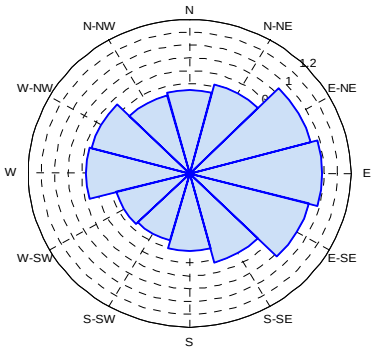
N
N-NE
E-NE
E
E-SE
S-SE
S
S-SW
W
W-NW
N-NW

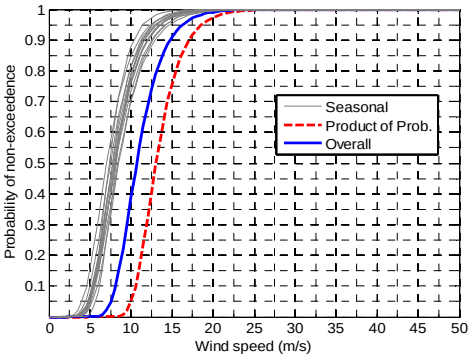
Probability of non-exceedence
Wind speed (m/s)
Seasonal
Product of Prob.
Overall

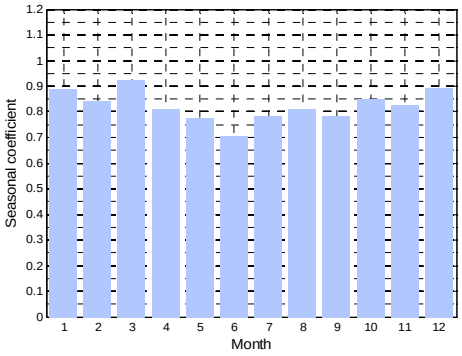
Seasonal coefficient
Month

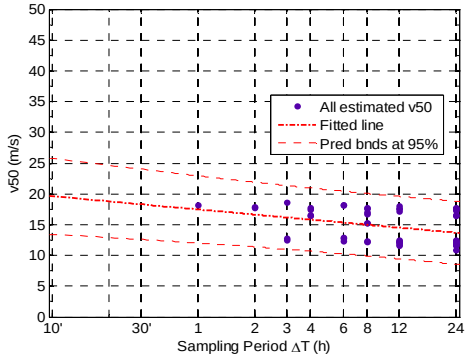
v50 (m/s)
Sampling Period ΔT (h)
All estimated v50
Fitted line
Pred bnds at 95%

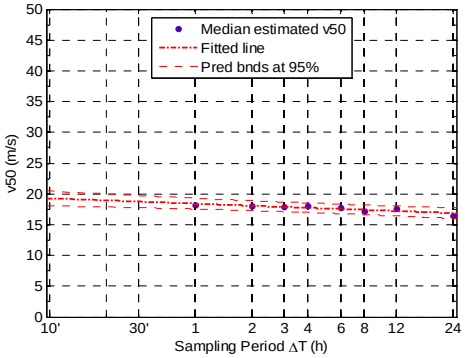
v50 (m/s)
Sampling Period ΔT (h)
Median estimated v50
Fitted line
Pred bnds at 95%

LIVE

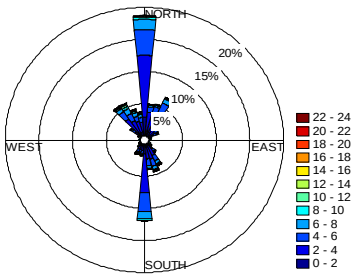
NORTH
20%
15%
10%
5%
WEST
EAST
SOUTH
22 - 24
20 - 22
18 - 20
16 - 18
14 - 16
12 - 14
10 - 12
8 - 10
6 - 8
4 - 6
2 - 4
0 - 2

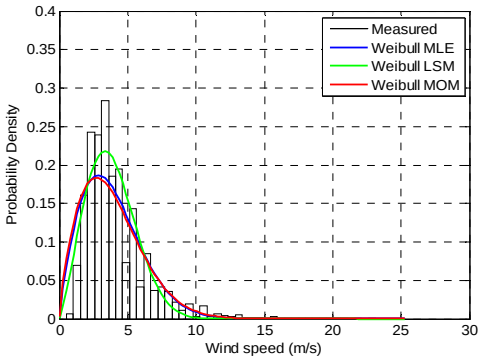
Measured
Weibull MLE
Weibull LSM
Weibull MOM
Probability Density
Wind speed (m/s)

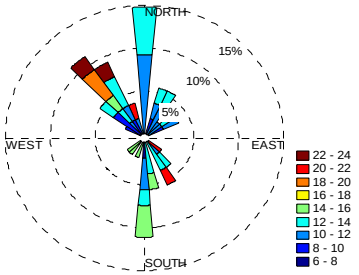
NORTH
15%
10%
5%
WEST
EAST
SOUTH
22 - 24
20 - 22
18 - 20
16 - 18
14 - 16
12 - 14
10 - 12
8 - 10
6 - 8

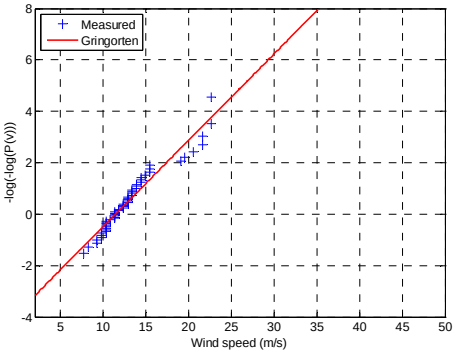
Measured
Gringorten
-log(-log(P(v)))
Wind speed (m/s)

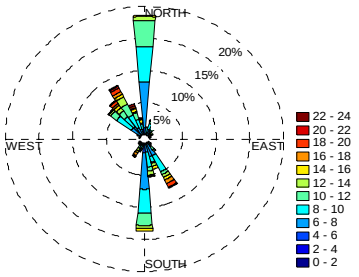
NORTH
20%
15%
10%
5%
WEST
EAST
SOUTH
22 - 24
20 - 22
18 - 20
16 - 18
14 - 16
12 - 14
10 - 12
8 - 10
6 - 8
4 - 6
2 - 4
0 - 2

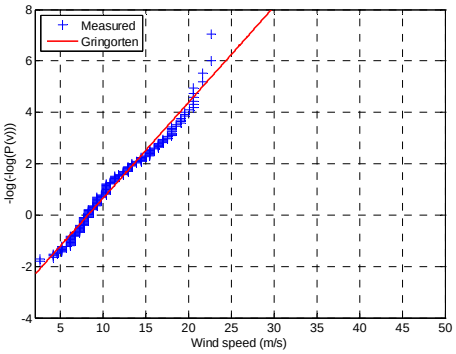
Measured
Gringorten
-log(-log(P(v)))
Wind speed (m/s)

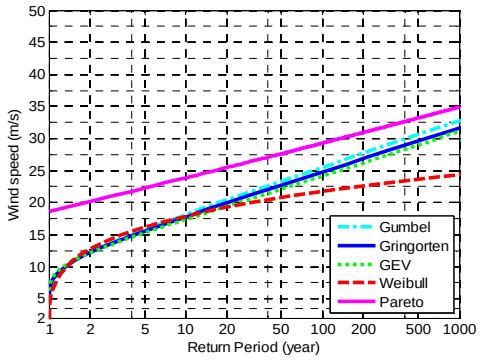
Wind speed (m/s)
Return Period (year)
Gumbel
Gringorten
GEV
Weibull
Pareto

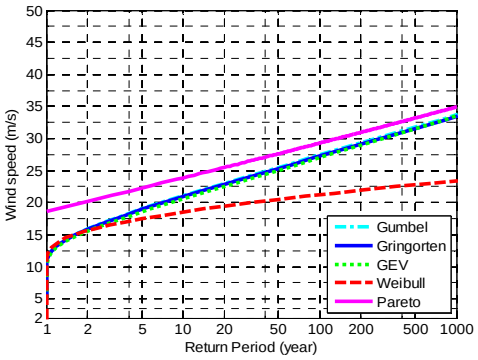
Wind speed (m/s)
Return Period (year)
Gumbel
Gringorten
GEV
Weibull
Pareto

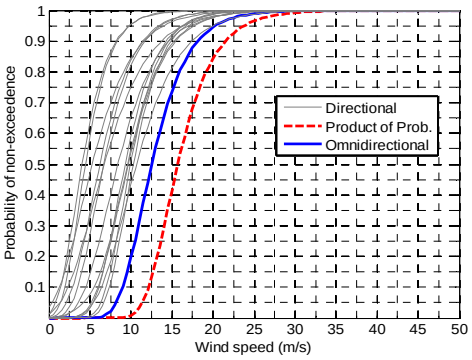
Probability of non-exceedence
Wind speed (m/s)
Directional
Product of Prob.
Omnidirectional

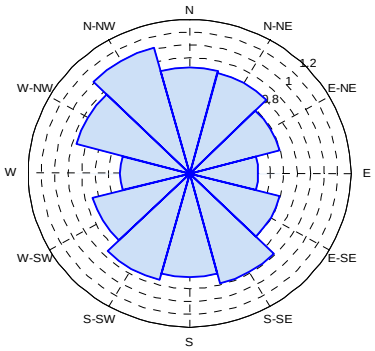
N
N-NE
E-NE
E
E-SE
S-SE
S
S-SW
W
W-NW
N-NW

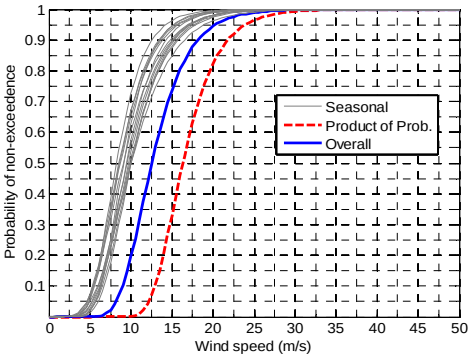
Probability of non-exceedence
Wind speed (m/s)
Seasonal
Product of Prob.
Overall

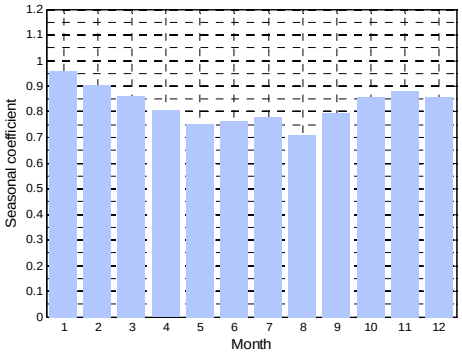
Seasonal coefficient
Month

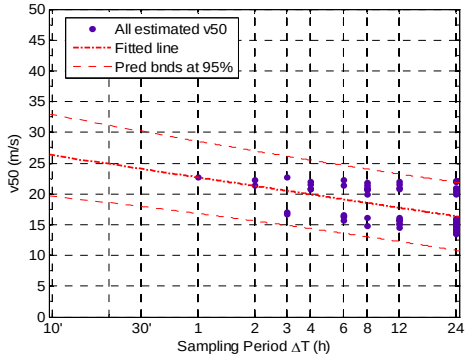
All estimated v50
Fitted line
Pred bnds at 95%
v50 (m/s)
Sampling Period ΔT (h)

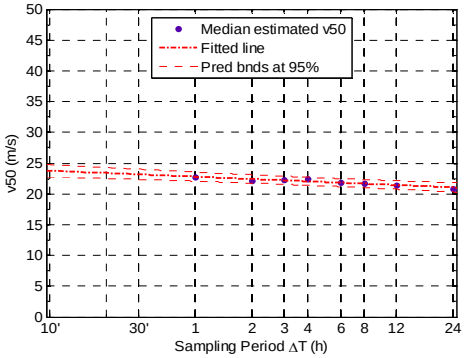
Median estimated v50
Fitted line
Pred bnds at 95%
v50 (m/s)
Sampling Period ΔT (h)

LIVF

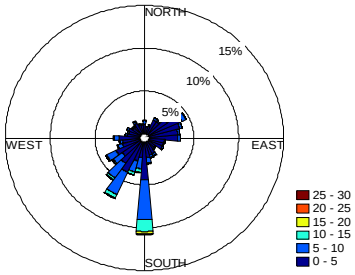
NORTH
15%
10%
5%
WEST
EAST
SOUTH
25 - 30
20 - 25
15 - 20
10 - 15
5 - 10
0 - 5

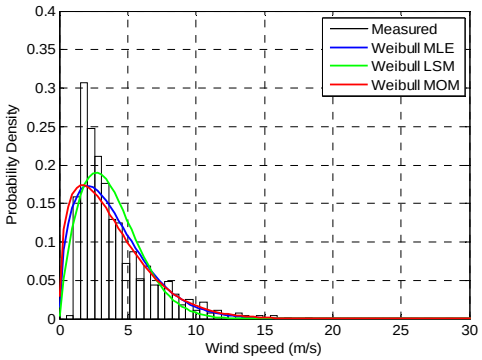
Measured
Weibull MLE
Weibull LSM
Weibull MOM
Probability Density
Wind speed (m/s)

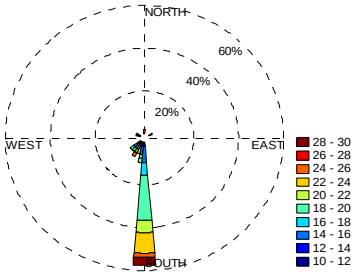
NORTH
60%
40%
20%
WEST
EAST
SOUTH
28 - 30
26 - 28
24 - 26
22 - 24
20 - 22
18 - 20
16 - 18
14 - 16
12 - 14
10 - 12

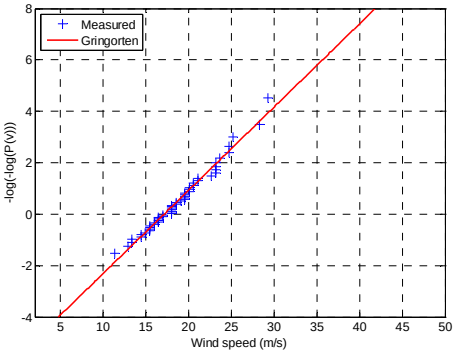
Measured
Gringorten
-log(-log(P(v)))
Wind speed (m/s)

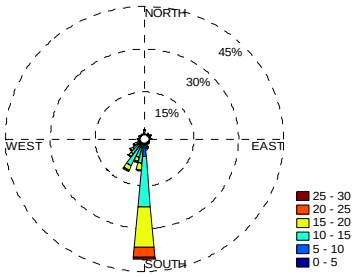
NORTH
45%
30%
15%
WEST
EAST
SOUTH
25 - 30
20 - 25
15 - 20
10 - 15
5 - 10
0 - 5

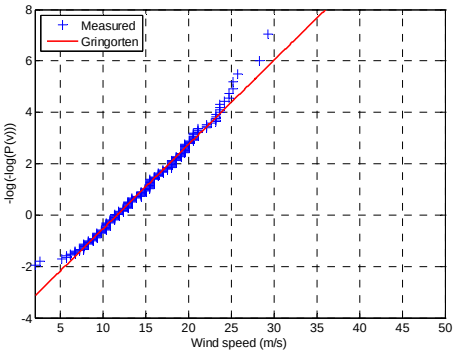
Measured
Gringorten
-log(-log(P(v)))
Wind speed (m/s)

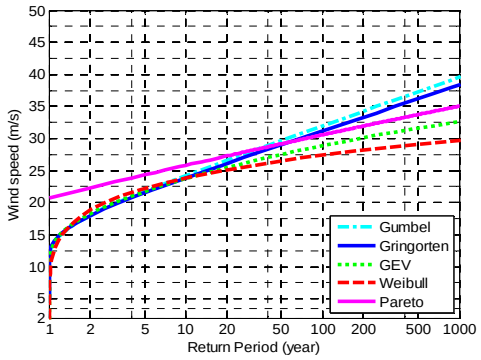
Wind speed (m/s)
Return Period (year)
Gumbel
Gringorten
GEV
Weibull
Pareto

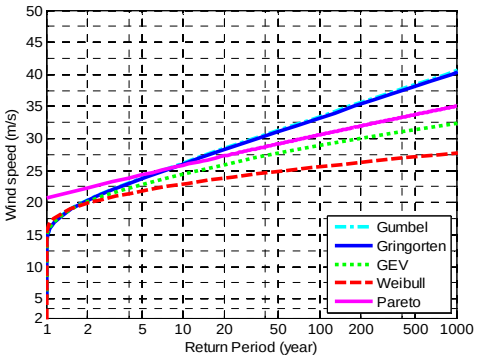
Wind speed (m/s)
Return Period (year)
Gumbel
Gringorten
GEV
Weibull
Pareto

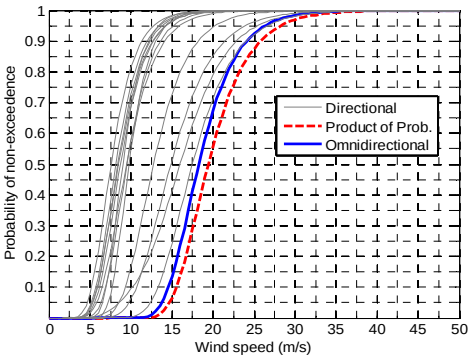
Probability of non-exceedence
Wind speed (m/s)
Directional
Product of Prob.
Omnidirectional

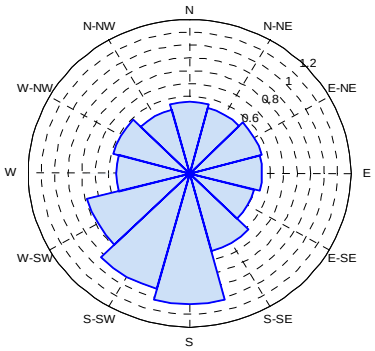
N
N-NE
E-NE
E
E-SE
S-SE
S
S-SW
W
W-NW
N-NW

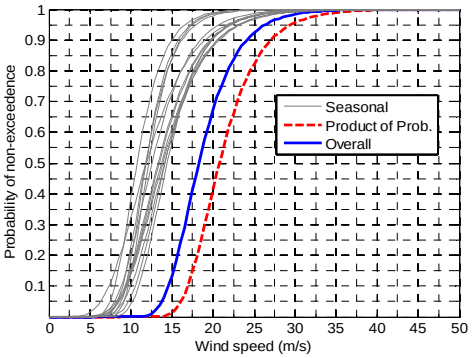
Probability of non-exceedence
Wind speed (m/s)
Seasonal
Product of Prob.
Overall

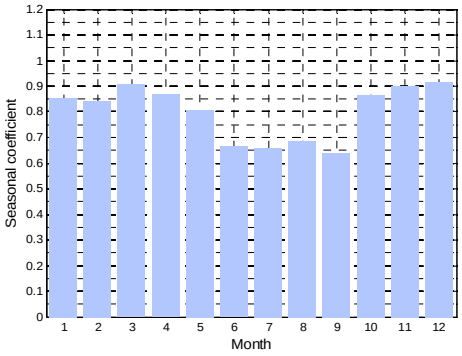
Seasonal coefficient
Month

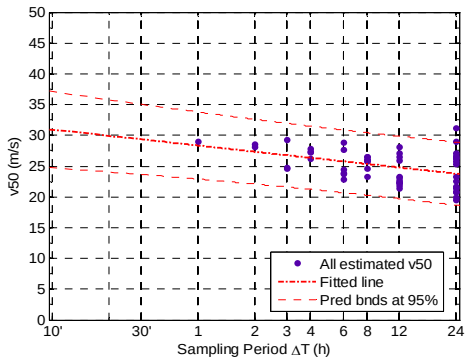
v50 (m/s)
Sampling Period ΔT (h)
All estimated v50
Fitted line
Pred bnds at 95%

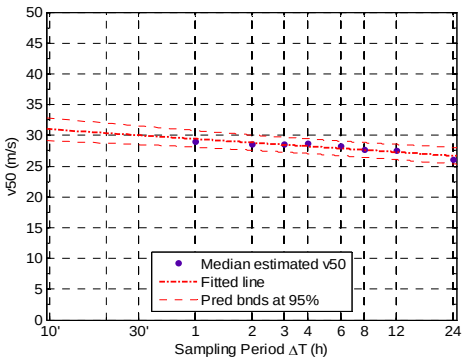
v50 (m/s)
Sampling Period ΔT (h)
Median estimated v50
Fitted line
Pred bnds at 95%

LIVM

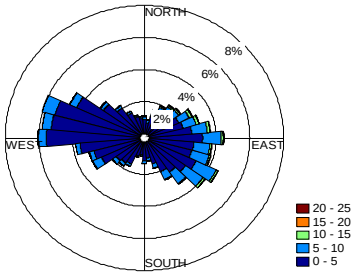
NORTH
8%
6%
4%
2%
WEST
EAST
SOUTH
20 - 25
15 - 20
10 - 15
5 - 10
0 - 5

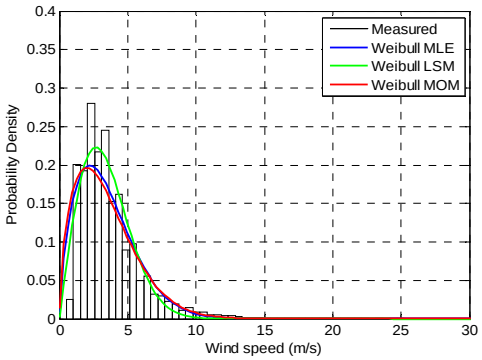
Measured
Weibull MLE
Weibull LSM
Weibull MOM
Probability Density
Wind speed (m/s)

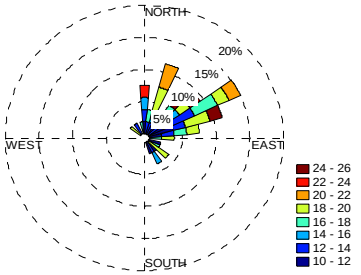
NORTH
20%
15%
10%
5%
WEST
EAST
SOUTH
24 - 26
22 - 24
20 - 22
18 - 20
16 - 18
14 - 16
12 - 14
10 - 12

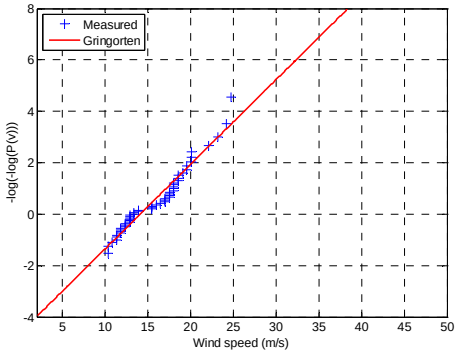
Measured
Gringorten
-log(-log(P(v)))
Wind speed (m/s)

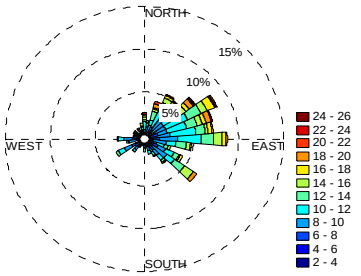
NORTH
15%
10%
5%
WEST
EAST
SOUTH
24 - 26
22 - 24
20 - 22
18 - 20
16 - 18
14 - 16
12 - 14
10 - 12
8 - 10
6 - 8
4 - 6
2 - 4

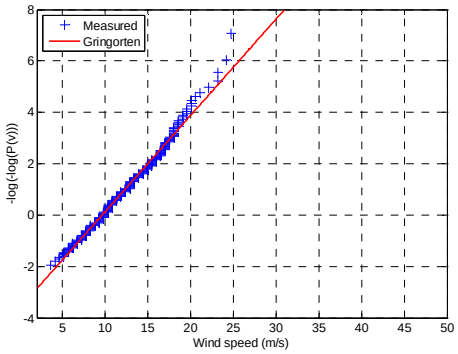
Measured
Gringorten
-log(-log(P(v)))
Wind speed (m/s)

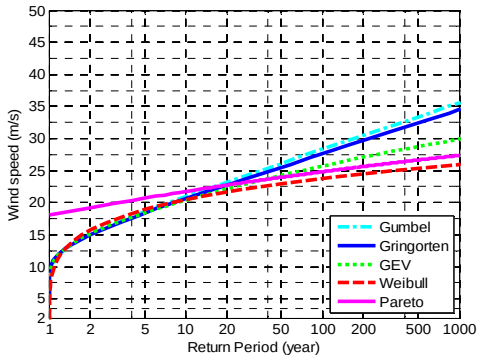
Wind speed (m/s)
Return Period (year)
Gumbel
Gringorten
GEV
Weibull
Pareto

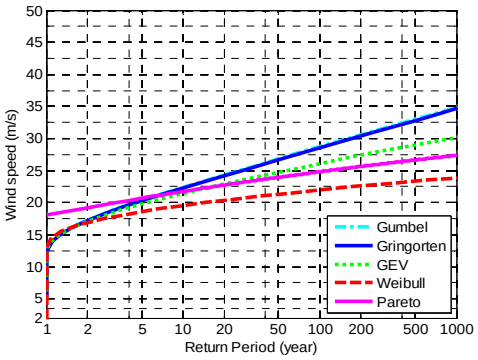
Wind speed (m/s)
Return Period (year)
Gumbel
Gringorten
GEV
Weibull
Pareto

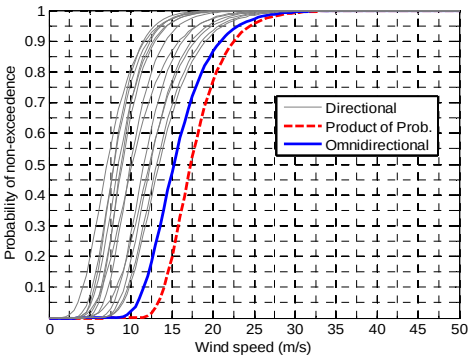
Probability of non-exceedence
Wind speed (m/s)
Directional
Product of Prob.
Omnidirectional

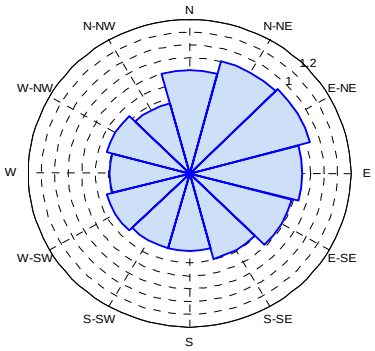
N
N-NE
E-NE
E
E-SE
S-SE
S
S-SW
W
W-NW
N-NW

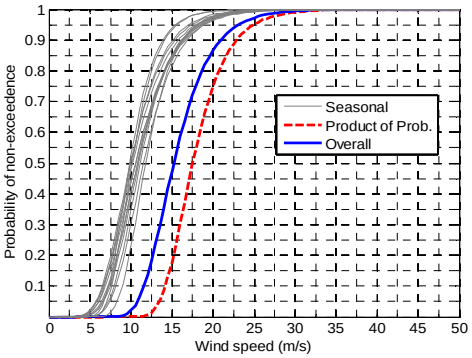
Probability of non-exceedence
Wind speed (m/s)
Seasonal
Product of Prob.
Overall

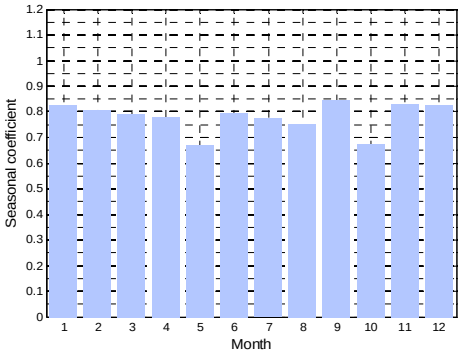
Seasonal coefficient
Month

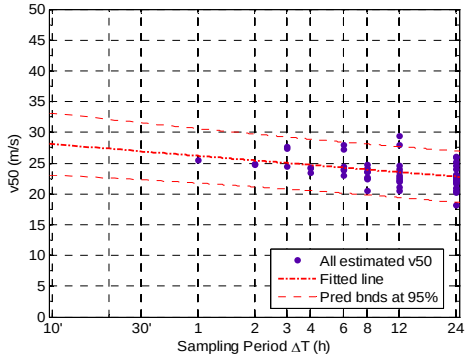
v50 (m/s)
Sampling Period ΔT (h)
All estimated v50
Fitted line
Pred bnds at 95%

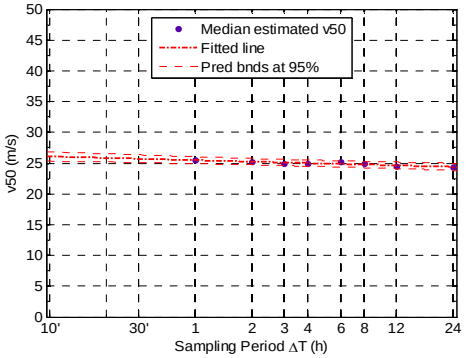
v50 (m/s)
Sampling Period ΔT (h)
Median estimated v50
Fitted line
Pred bnds at 95%

LIVO

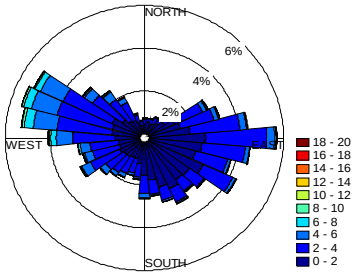
NORTH
6%
4%
2%
WEST
EAST
SOUTH
18 - 20
16 - 18
14 - 16
12 - 14
10 - 12
8 - 10
6 - 8
4 - 6
2 - 4
0 - 2

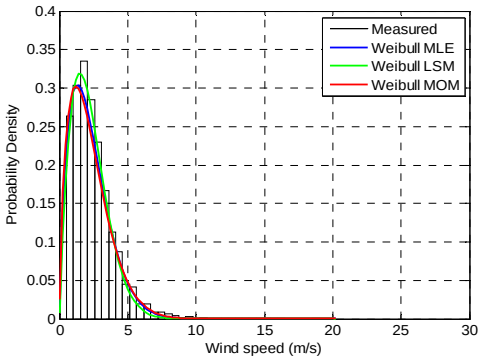
Measured
Weibull MLE
Weibull LSM
Weibull MOM
Probability Density
Wind speed (m/s)

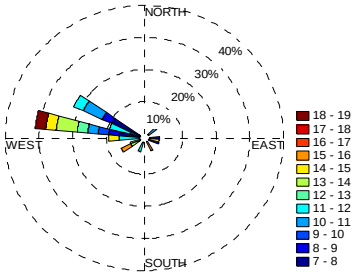
NORTH
40%
30%
20%
10%
WEST
EAST
SOUTH
18 - 19
17 - 18
16 - 17
15 - 16
14 - 15
13 - 14
12 - 13
11 - 12
10 - 11
9 - 10
8 - 9
7 - 8

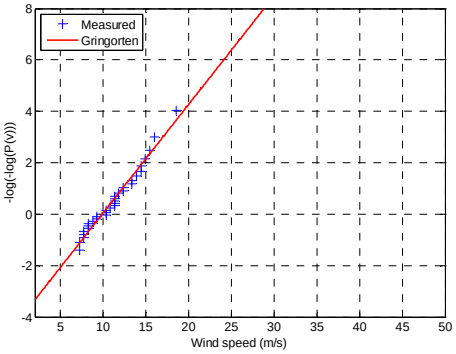
Measured
Gringorten
-log(-log(P(v)))
Wind speed (m/s)

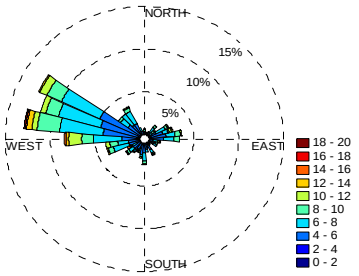
NORTH
15%
10%
5%
WEST
EAST
SOUTH
18 - 20
16 - 18
14 - 16
12 - 14
10 - 12
8 - 10
6 - 8
4 - 6
2 - 4
0 - 2

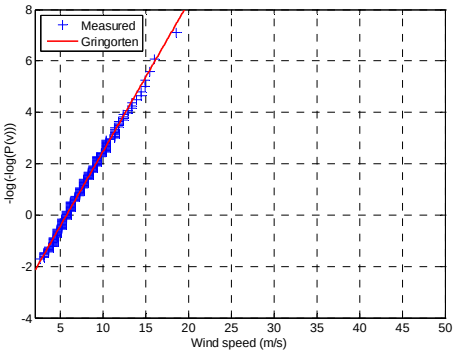
Measured
Gringorten
-log(-log(P(v)))
Wind speed (m/s)

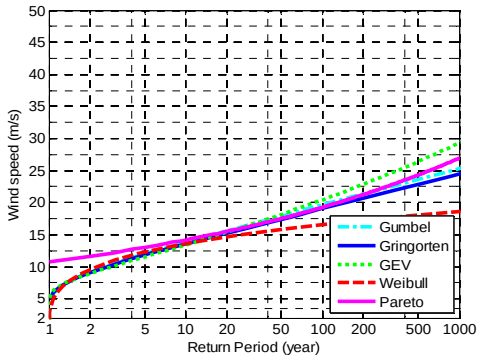
Wind speed (m/s)
Return Period (year)
Gumbel
Gringorten
GEV
Weibull
Pareto

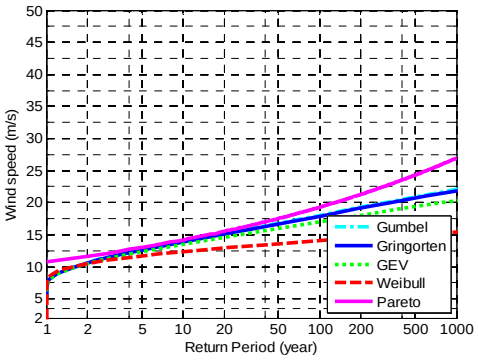
Wind speed (m/s)
Return Period (year)
Gumbel
Gringorten
GEV
Weibull
Pareto

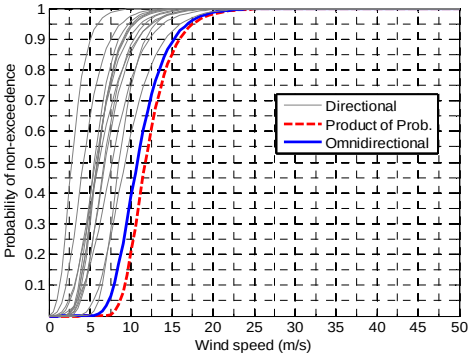
Probability of non-exceedence
Wind speed (m/s)
Directional
Product of Prob.
Omnidirectional

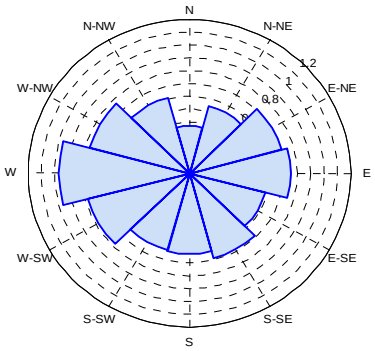
N
N-NE
E-NE
E
E-SE
S-SE
S
S-SW
W-SW
W
W-NW
N-NW

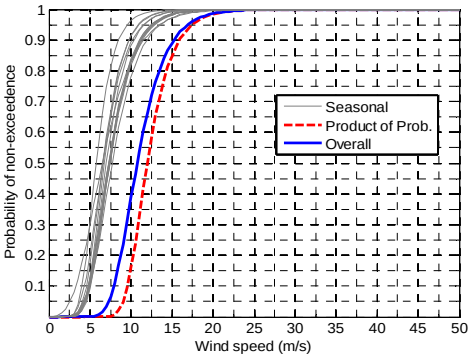
Probability of non-exceedence
Wind speed (m/s)
Seasonal
Product of Prob.
Overall

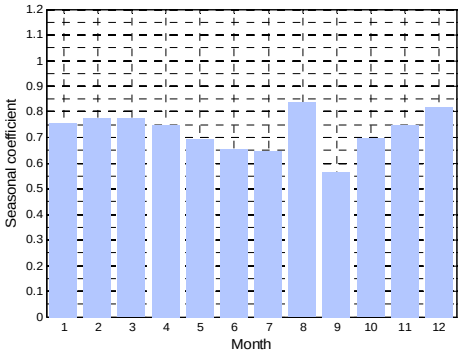
Seasonal coefficient
Month

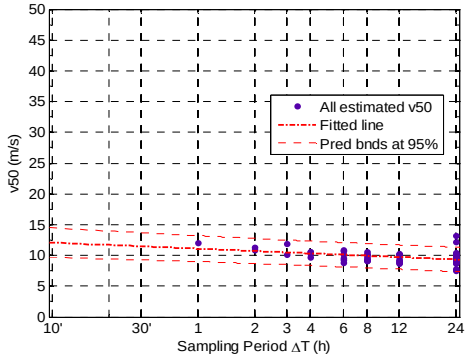
v50 (m/s)
Sampling Period ΔT (h)
All estimated v50
Fitted line
Pred bnds at 95%

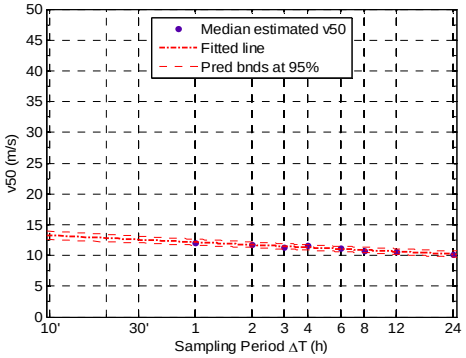
v50 (m/s)
Sampling Period ΔT (h)
Median estimated v50
Fitted line
Pred bnds at 95%

LIVP

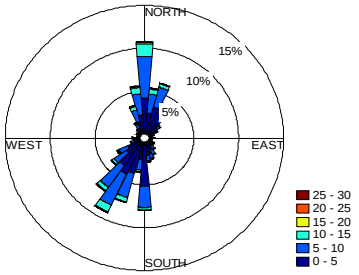
NORTH
15%
10%
5%
WEST
EAST
SOUTH
25 - 30
20 - 25
15 - 20
10 - 15
5 - 10
0 - 5

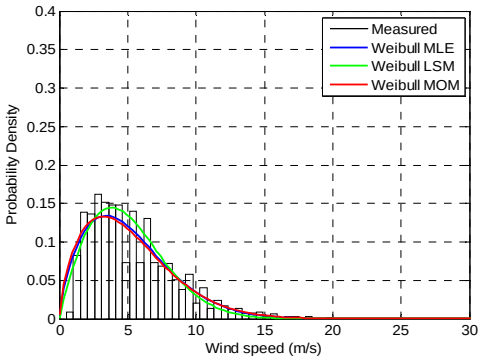
Measured
Weibull MLE
Weibull LSM
Weibull MOM
Probability Density
Wind speed (m/s)

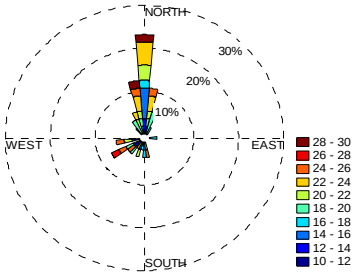
NORTH
30%
20%
10%
WEST
EAST
SOUTH
28 - 30
26 - 28
24 - 26
22 - 24
20 - 22
18 - 20
16 - 18
14 - 16
12 - 14
10 - 12

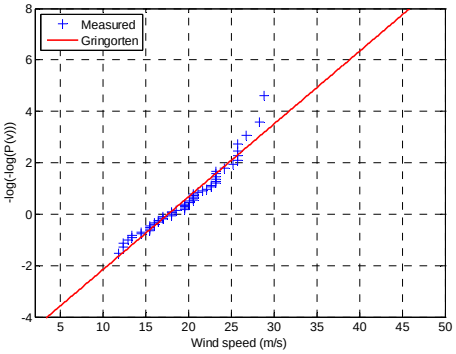
Measured
Gringorten
-log(-log(P(v)))
Wind speed (m/s)

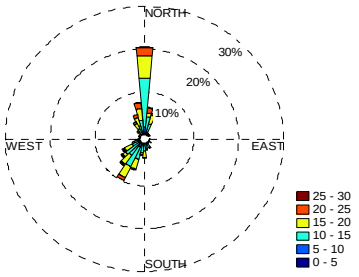
NORTH
30%
20%
10%
WEST
EAST
SOUTH
25 - 30
20 - 25
15 - 20
10 - 15
5 - 10
0 - 5

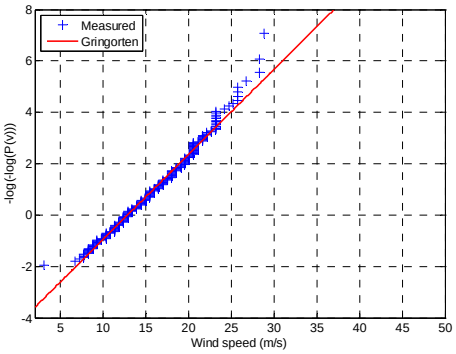
Measured
Gringorten
-log(-log(P(v)))
Wind speed (m/s)

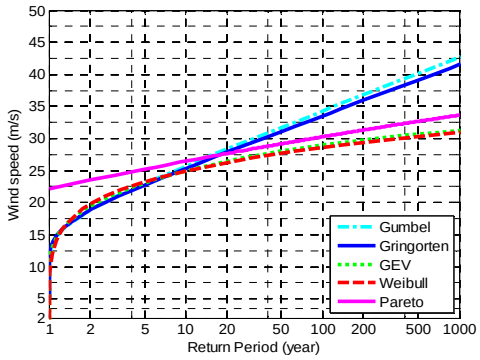
Wind speed (m/s)
Return Period (year)
Gumbel
Gringorten
GEV
Weibull
Pareto

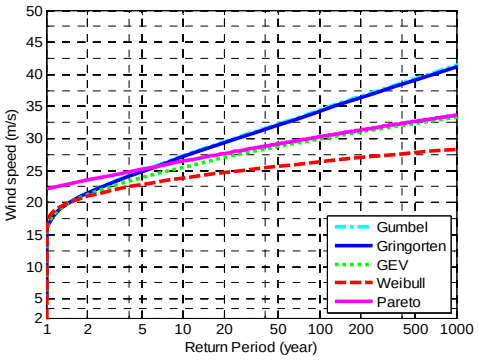
Wind speed (m/s)
Return Period (year)
Gumbel
Gringorten
GEV
Weibull
Pareto

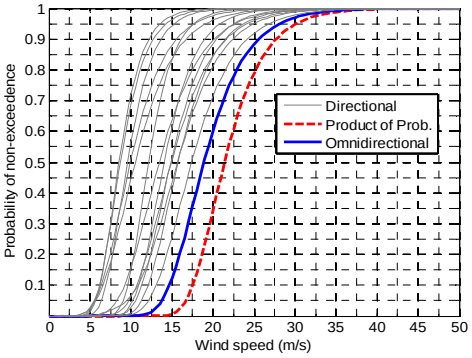
Probability of non-exceedence
Wind speed (m/s)
Directional
Product of Prob.
Omnidirectional

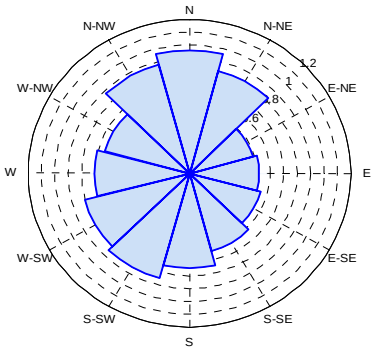
N
N-NE
E-NE
E
E-SE
S-SE
S
S-SW
W
W-NW
N-NW

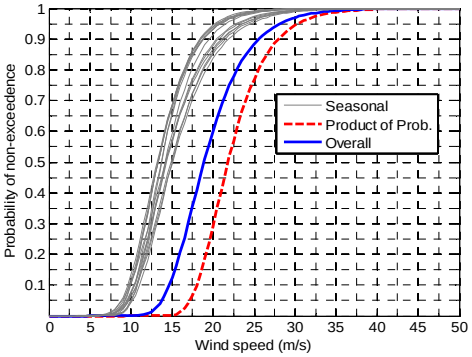
Probability of non-exceedence
Wind speed (m/s)
Seasonal
Product of Prob.
Overall

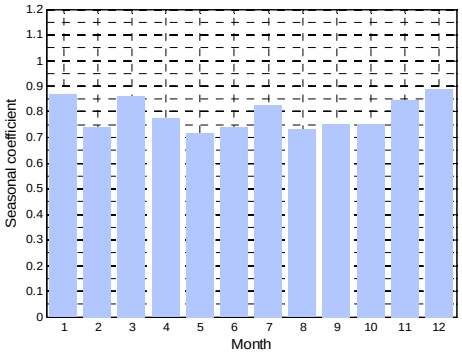
Seasonal coefficient
Month

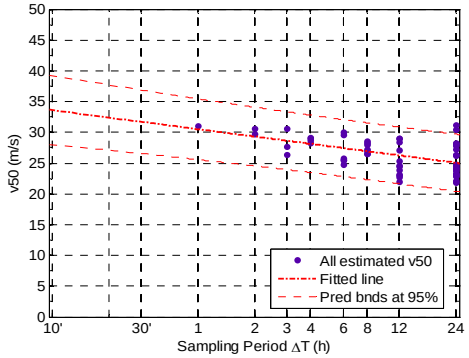
v50 (m/s)
Sampling Period ΔT (h)
All estimated v50
Fitted line
Pred bnds at 95%

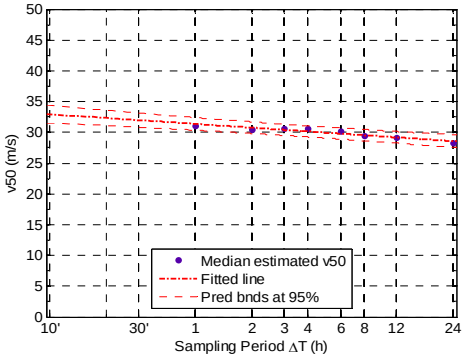
v50 (m/s)
Sampling Period ΔT (h)
Median estimated v50
Fitted line
Pred bnds at 95%

LIVR

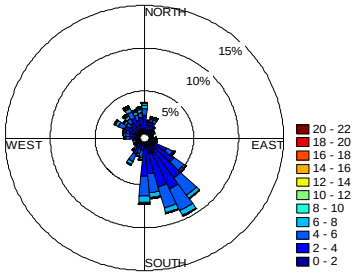
NORTH
15%
10%
5%
WEST
EAST
SOUTH
20 - 22
18 - 20
16 - 18
14 - 16
12 - 14
10 - 12
8 - 10
6 - 8
4 - 6
2 - 4
0 - 2

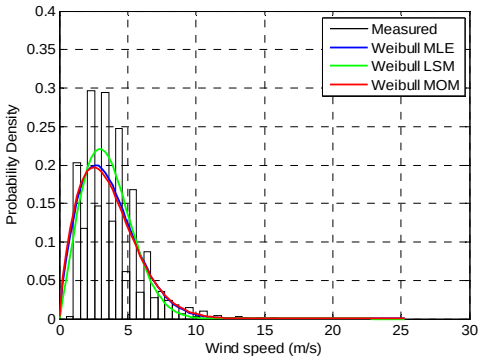
Measured
Weibull MLE
Weibull LSM
Weibull MOM
Probability Density
Wind speed (m/s)

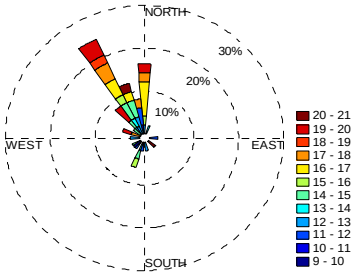
NORTH
30%
20%
10%
WEST
EAST
SOUTH
20 - 21
19 - 20
18 - 19
17 - 18
16 - 17
15 - 16
14 - 15
13 - 14
12 - 13
11 - 12
10 - 11
9 - 10

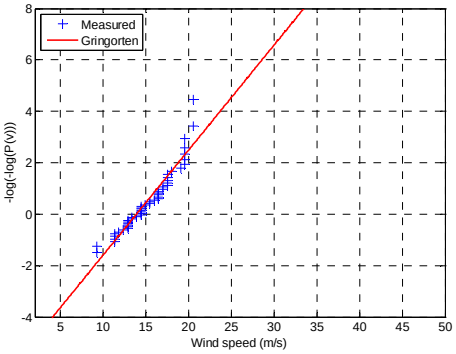
Measured
Gringorten
-log(-log(P(v)))
Wind speed (m/s)

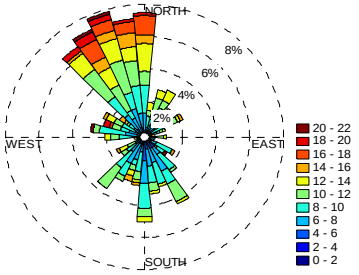
NORTH
8%
6%
4%
2%
WEST
EAST
SOUTH
20 - 22
18 - 20
16 - 18
14 - 16
12 - 14
10 - 12
8 - 10
6 - 8
4 - 6
2 - 4
0 - 2

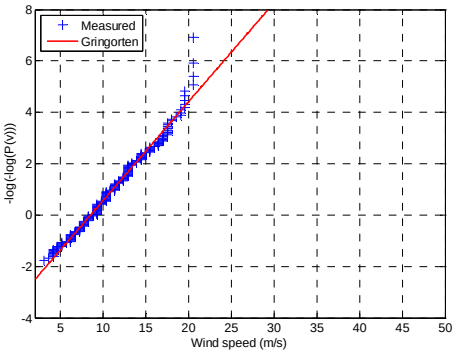
Measured
Gringorten
-log(-log(P(v)))
Wind speed (m/s)

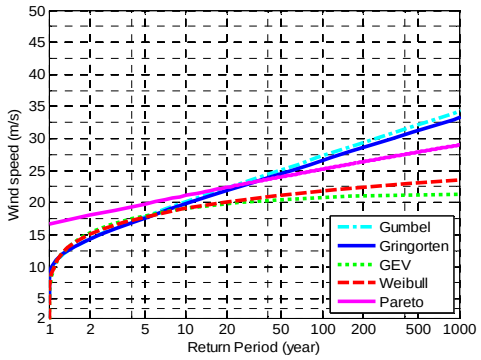
Wind speed (m/s)
Return Period (year)
Gumbel
Gringorten
GEV
Weibull
Pareto

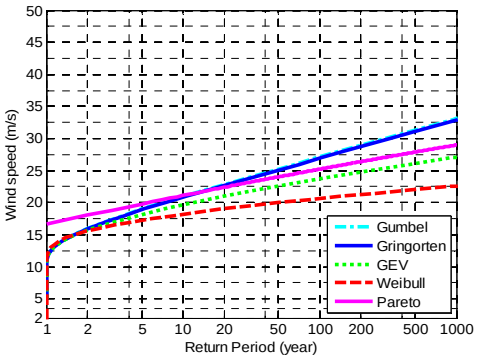
Wind speed (m/s)
Return Period (year)
Gumbel
Gringorten
GEV
Weibull
Pareto

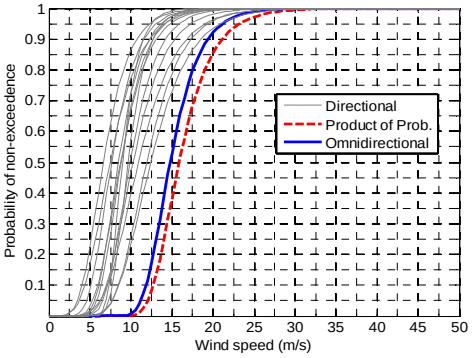
Probability of non-exceedence
Wind speed (m/s)
Directional
Product of Prob.
Omnidirectional

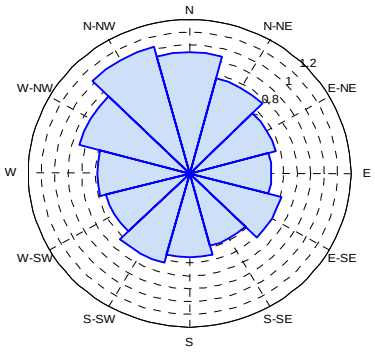
N
N-NE
E-NE
E
E-SE
S-SE
S
S-SW
W
W-NW
N-NW

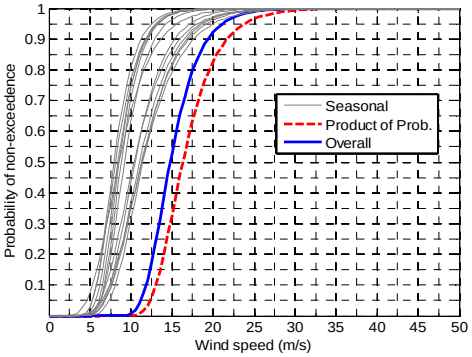
Probability of non-exceedence
Wind speed (m/s)
Seasonal
Product of Prob.
Overall

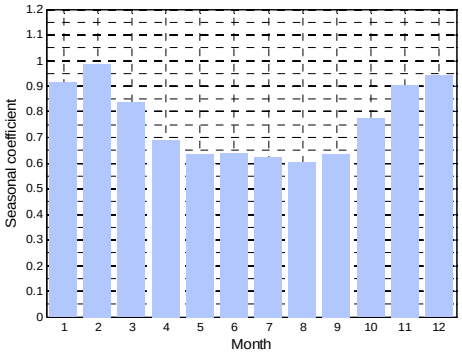
Seasonal coefficient
Month

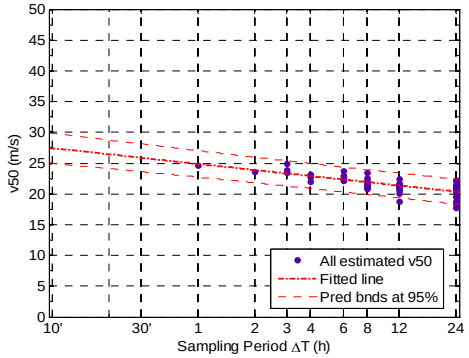
v50 (m/s)
Sampling Period ΔT (h)
All estimated v50
Fitted line
Pred bnds at 95%

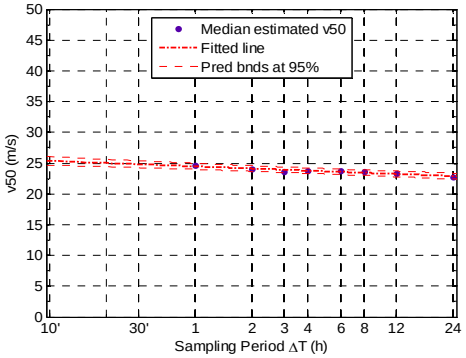
v50 (m/s)
Sampling Period ΔT (h)
Median estimated v50
Fitted line
Pred bnds at 95%

LIVT

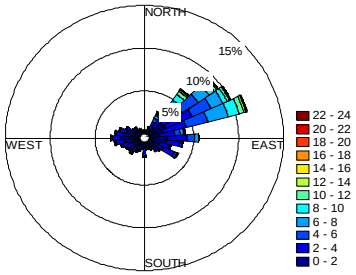
NORTH
15%
10%
5%
WEST
EAST
SOUTH
22 - 24
20 - 22
18 - 20
16 - 18
14 - 16
12 - 14
10 - 12
8 - 10
6 - 8
4 - 6
2 - 4
0 - 2

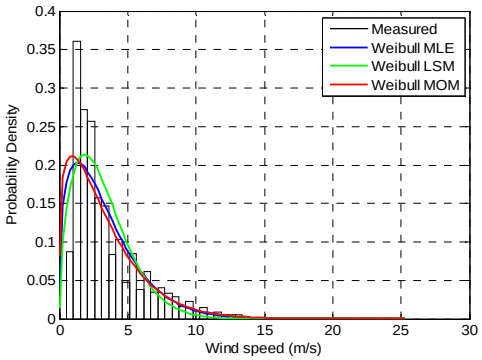
Measured
Weibull MLE
Weibull LSM
Weibull MOM
Probability Density
Wind speed (m/s)

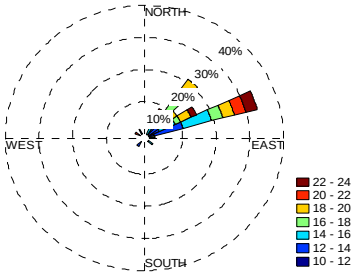
NORTH
40%
30%
20%
10%
WEST
EAST
SOUTH
22 - 24
20 - 22
18 - 20
16 - 18
14 - 16
12 - 14
10 - 12

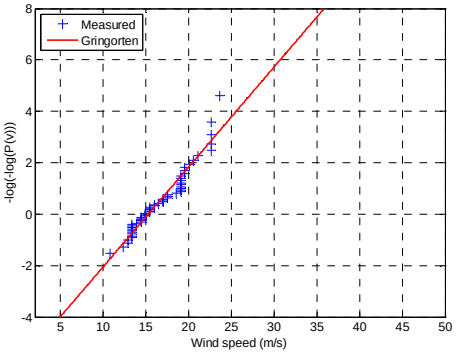
Measured
Gringorten
-log(-log(P(v)))
Wind speed (m/s)

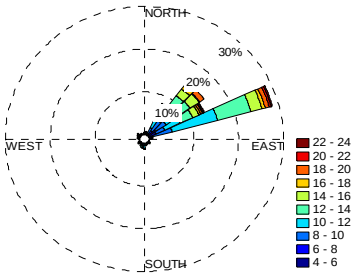
NORTH
30%
20%
10%
WEST
EAST
SOUTH
22 - 24
20 - 22
18 - 20
16 - 18
14 - 16
12 - 14
10 - 12
8 - 10
6 - 8
4 - 6

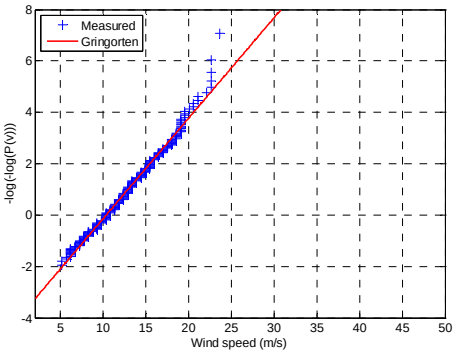
Measured
Gringorten
-log(-log(P(v)))
Wind speed (m/s)

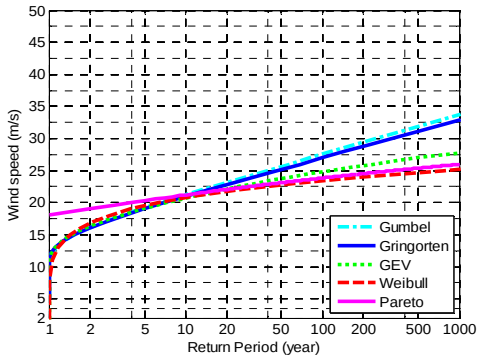
Wind speed (m/s)
Return Period (year)
Gumbel
Gringorten
GEV
Weibull
Pareto

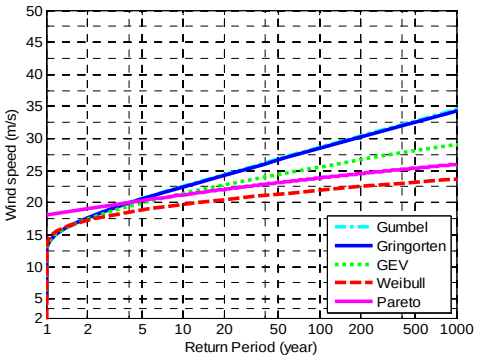
Wind speed (m/s)
Return Period (year)
Gumbel
Gringorten
GEV
Weibull
Pareto

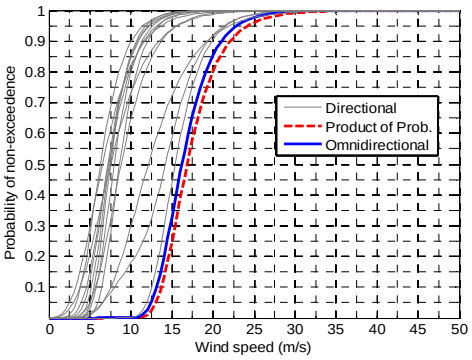
Probability of non-exceedence
Wind speed (m/s)
Directional
Product of Prob.
Omnidirectional

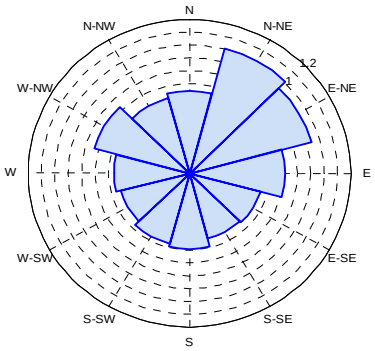
N
N-NE
E-NE
E
E-SE
S-SE
S
S-SW
W
W-NW
N-NW

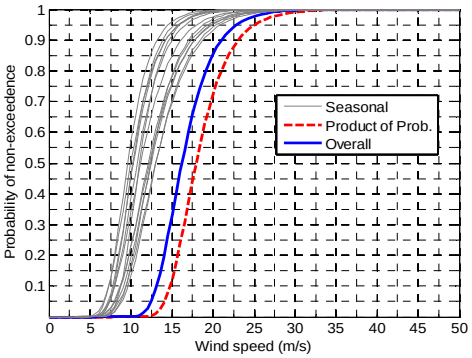
Probability of non-exceedence
Wind speed (m/s)
Seasonal
Product of Prob.
Overall

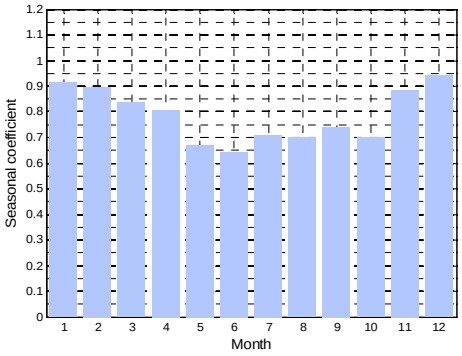
Seasonal coefficient
Month

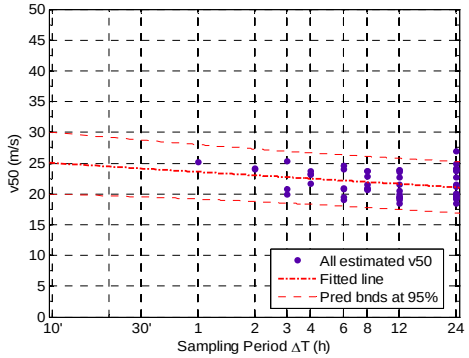
v50 (m/s)
Sampling Period ΔT (h)
All estimated v50
Fitted line
Pred bnds at 95%

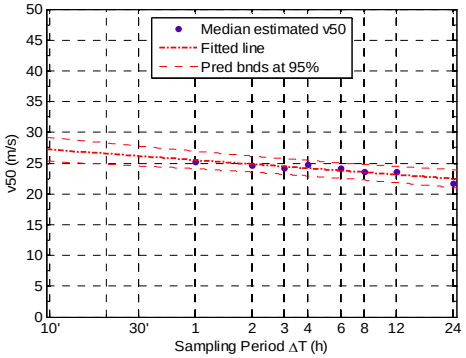
v50 (m/s)
Sampling Period ΔT (h)
Median estimated v50
Fitted line
Pred bnds at 95%

APPENDIX 3 – DETAILED RESULTS OF DOWNSAMPLING OF DATA

The detailed results of downsampling are presented. In the first column the ICAO Code of the meteorological station is reported with the aim at identify the station. Columns 2 and 3 represent the beginning and the end of the interval of data available. The meaning of the symbols on the columns 4, 5, 10-14 is exhaustively explained in the section 2.8. The column 6 contains the R-square value associated to the logarithm equation fitted to median values calculated for each sampling period whereas the column 7 contains the mean of the coefficients of variation calculated for each sampling period. Finally, columns 8 and 9 contain the slopes of the logarithm equations fitted to the median values minus and plus one standard deviation, respectively.

Table 6 Detailed results of downsampling of data

Station	Interval		$v_{50}(\Delta T=1)$ (m/s)	a (m/s/h)	ρ^2	Iv	a (μ−σ) (m/s/h)	a (μ+σ) (m/s/h)	$v_{50}(\Delta T=10')$ (m/s)	ρ_1	ρ_2	ρ_3	ρ_4
LIBA	1959	2010	25,37	-0,72	96,1%	3,1%	-1,05	-0,39	26,67	1,03	1,05	1,09	1,16
LIBC	1951	2005	25,34	-0,64	82,6%	2,7%	-1,04	-0,23	26,49	1,03	1,05	1,07	1,14
LIBD	1951	2005	24,18	-0,50	66,8%	4,2%	-0,83	-0,18	25,09	1,02	1,04	1,06	1,11
LIBE	1951	2009	41,12	-1,02	87,1%	3,4%	-1,69	-0,36	42,95	1,03	1,04	1,07	1,13
LIBG	1960	2005	23,14	-0,45	90,0%	2,3%	-0,82	-0,09	23,95	1,02	1,04	1,06	1,10
LIBH	1968	2010	26,58	-0,56	84,6%	3,8%	-1,11	-0,02	27,59	1,02	1,04	1,06	1,11
LIBN	1951	2010	24,69	-0,82	79,8%	4,3%	-1,07	-0,57	26,16	1,04	1,06	1,10	1,18
LIBP	1951	2005	26,49	-0,71	98,5%	2,5%	-0,99	-0,42	27,75	1,03	1,05	1,08	1,14
LIBQ	1952	2010	31,71	-0,66	91,0%	2,5%	-1,05	-0,27	32,89	1,02	1,04	1,06	1,11
LIBR	1951	2010	28,20	-0,93	94,0%	4,2%	-1,34	-0,52	29,86	1,04	1,06	1,10	1,18
LIBS	1958	2009	34,08	-0,89	86,2%	2,8%	-1,42	-0,35	35,67	1,03	1,05	1,08	1,14
LIBT	1951	2009	34,23	-0,70	83,6%	3,4%	-1,43	0,02	35,49	1,02	1,04	1,06	1,11
LIBU	1951	2010	38,04	-1,22	95,3%	6,4%	-2,57	0,13	40,23	1,03	1,06	1,10	1,18
LIBV	1959	2010	27,70	-0,35	89,9%	1,9%	-0,58	-0,13	28,33	1,01	1,02	1,04	1,07
LIBW	1960	2010	34,33	-0,16	62,7%	1,4%	-0,58	0,26	34,61	1,01	1,01	1,01	1,02
LIBY	1951	2010	25,37	-0,73	85,6%	3,4%	-1,23	-0,22	26,67	1,03	1,05	1,09	1,16
LIBZ	1951	2007	27,01	-0,70	87,5%	3,5%	-1,21	-0,20	28,27	1,03	1,05	1,08	1,14
LICA	1978	1999	24,31	-0,75	80,1%	5,6%	-1,31	-0,19	25,66	1,03	1,06	1,09	1,17
LICC	1951	2005	24,96	-0,87	82,0%	4,5%	-1,12	-0,62	26,51	1,04	1,06	1,10	1,19
LICD	1959	2005	27,11	-0,69	85,2%	4,2%	-1,44	0,06	28,34	1,03	1,05	1,08	1,14
LICE	1951	2010	27,29	-0,23	54,1%	4,0%	-1,01	0,55	27,69	1,01	1,01	1,02	1,04
LICF	1951	2010	20,57	-0,79	80,5%	5,2%	-1,07	-0,51	21,99	1,04	1,07	1,12	1,22
LICG	1951	2010	34,49	-0,92	99,3%	2,6%	-1,31	-0,52	36,14	1,03	1,05	1,08	1,14
LICJ	1960	2005	26,24	-0,41	94,5%	2,3%	-0,70	-0,12	26,98	1,02	1,03	1,05	1,08
LICL	1965	2010	28,15	-0,93	91,7%	4,4%	-1,52	-0,35	29,82	1,04	1,06	1,10	1,18

Station	Interval		$v_{50}(\Delta T=1)$ (m/s)	a (m/s/h)	ρ^2	Iv	a (μ−σ) (m/s/h)	a (μ+σ) (m/s/h)	$v_{50}(\Delta T=10')$ (m/s)	ρ_1	ρ_2	ρ_3	ρ_4
LICO	1951	2010	28,27	-0,84	81,4%	6,6%	-1,88	0,20	29,77	1,03	1,05	1,09	1,16
LICP	1951	2008	25,69	-0,65	70,5%	4,6%	-1,17	-0,13	26,86	1,03	1,05	1,08	1,14
LICR	1951	2005	25,34	-0,47	97,3%	2,2%	-0,77	-0,18	26,18	1,02	1,03	1,05	1,10
LICT	1962	2010	30,72	-0,72	78,7%	3,9%	-1,47	0,03	32,01	1,03	1,04	1,07	1,13
LICU	1951	2010	41,36	-1,05	84,2%	6,5%	-2,90	0,79	43,25	1,03	1,05	1,08	1,14
LICX	1951	2010	25,36	-0,64	92,1%	3,2%	-1,06	-0,23	26,51	1,03	1,05	1,08	1,14
LICZ	1961	2010	22,87	-0,35	91,7%	2,2%	-0,49	-0,21	23,50	1,02	1,03	1,05	1,08
LIEA	1951	2005	23,64	-0,49	87,0%	2,9%	-0,81	-0,18	24,52	1,02	1,04	1,06	1,11
LIEB	1951	2010	35,73	-1,25	89,2%	3,7%	-1,92	-0,59	37,98	1,04	1,06	1,11	1,20
LIEC	1951	2010	44,77	-1,06	90,5%	2,7%	-1,56	-0,55	46,66	1,03	1,04	1,07	1,13
LIED	1962	2010	23,34	-0,91	85,8%	4,6%	-1,37	-0,45	24,97	1,04	1,07	1,12	1,22
LIEE	1951	2010	25,03	-0,42	95,0%	2,0%	-0,65	-0,18	25,78	1,02	1,03	1,05	1,09
LIEF	1962	2010	29,96	-0,64	91,7%	2,5%	-1,04	-0,24	31,10	1,02	1,04	1,06	1,11
LIEG	1951	1999	39,99	-0,85	83,3%	2,8%	-1,41	-0,28	41,50	1,02	1,04	1,06	1,11
LIEH	1975	2010	34,75	-1,22	75,9%	6,1%	-2,21	-0,24	36,94	1,04	1,06	1,11	1,20
LIEL	1953	2006	20,71	-0,24	45,0%	2,9%	-0,55	0,06	21,15	1,01	1,02	1,03	1,06
LIEN	1951	2006	25,50	-0,96	85,3%	9,8%	-2,08	0,17	27,22	1,04	1,07	1,11	1,21
LIEO	1969	2005	25,62	-0,36	85,8%	2,0%	-0,62	-0,10	26,26	1,02	1,02	1,04	1,07
LIEP	1961	2007	25,99	-0,01	0,2%	1,5%	-0,46	0,44	26,01	1,00	1,00	1,00	1,00
LIEZ	1951	1996	37,38	-1,38	52,6%	5,8%	-3,10	0,34	39,86	1,04	1,07	1,11	1,21
LIMC	1951	1999	25,23	-0,73	95,5%	4,0%	-1,11	-0,35	26,54	1,03	1,05	1,09	1,16
LIME	1951	2005	22,01	-0,82	93,1%	4,3%	-1,22	-0,43	23,48	1,04	1,07	1,11	1,21
LIMF	1951	2005	22,74	-0,64	77,4%	4,9%	-0,99	-0,29	23,89	1,03	1,05	1,08	1,15
LIMG	1951	2005	25,23	-0,29	51,1%	2,2%	-0,66	0,07	25,75	1,01	1,02	1,03	1,06
LIMH	1951	2010	44,78	-1,52	88,1%	5,0%	-2,19	-0,86	47,51	1,04	1,06	1,10	1,19
LIMJ	1962	2005	25,25	-0,87	88,5%	3,9%	-1,28	-0,47	26,82	1,04	1,06	1,10	1,19
LIMK	1952	2010	23,49	-0,96	87,9%	5,3%	-1,28	-0,63	25,20	1,04	1,07	1,12	1,23
LIML	1951	1999	22,60	-0,44	91,2%	2,5%	-0,63	-0,24	23,38	1,02	1,03	1,06	1,10

Station	Interval		$v_{50}(\Delta T=1)$ (m/s)	a (m/s/h)	ρ^2	Iv	a (μ−σ) (m/s/h)	a (μ+σ) (m/s/h)	$v_{50}(\Delta T=10')$ (m/s)	ρ_1	ρ_2	ρ_3	ρ_4
LIMN	1957	2010	21,41	-0,64	89,9%	3,0%	-0,99	-0,30	22,56	1,03	1,05	1,09	1,17
LIMO	1952	1998	26,24	-0,98	88,8%	6,6%	-1,57	-0,39	27,99	1,04	1,07	1,11	1,21
LIMQ	1951	1985	31,82	-1,46	47,3%	5,4%	-2,36	-0,56	34,44	1,05	1,08	1,14	1,27
LIMR	1951	1998	17,28	-0,76	50,1%	5,2%	-1,38	-0,14	18,64	1,05	1,08	1,13	1,25
LIMS	1951	2010	21,44	-0,52	90,2%	3,8%	-0,88	-0,17	22,38	1,03	1,04	1,07	1,13
LIMT	1951	2009	27,75	-0,35	78,7%	3,8%	-1,06	0,37	28,37	1,01	1,02	1,04	1,06
LIMU	1963	2010	37,29	-0,55	91,9%	2,4%	-0,99	-0,12	38,29	1,02	1,03	1,04	1,08
LIMV	1951	2010	24,28	-1,73	80,9%	11,4%	-2,55	-0,91	27,38	1,07	1,13	1,22	1,46
LIMY	1951	2010	22,43	-0,92	92,2%	4,5%	-1,16	-0,68	24,08	1,04	1,07	1,12	1,23
LIPA	1951	2010	19,73	-0,88	97,5%	5,4%	-1,33	-0,43	21,31	1,05	1,08	1,14	1,26
LIPB	1951	2005	18,29	-0,43	88,3%	4,2%	-0,83	-0,03	19,07	1,03	1,04	1,07	1,13
LIPC	1968	2010	23,75	-0,88	81,5%	4,7%	-1,12	-0,64	25,33	1,04	1,07	1,11	1,21
LIPD	1951	1978	22,08	-0,73	43,5%	3,8%	-1,18	-0,29	23,40	1,04	1,06	1,10	1,18
LIPE	1951	2005	20,01	-0,66	72,2%	6,1%	-1,00	-0,32	21,19	1,04	1,06	1,10	1,18
LIPF	1951	2009	15,99	-0,70	85,3%	8,3%	-1,42	0,02	17,24	1,05	1,08	1,13	1,25
LIPH	1955	2009	22,15	-1,03	79,8%	6,7%	-1,40	-0,65	23,99	1,05	1,08	1,14	1,27
LIPI	1969	2010	22,12	-0,73	89,9%	4,0%	-0,98	-0,48	23,43	1,04	1,06	1,10	1,18
LIPK	1969	2005	25,43	-0,57	91,3%	3,2%	-0,86	-0,29	26,45	1,02	1,04	1,07	1,12
LIPL	1951	2010	25,04	-1,45	72,1%	9,6%	-1,87	-1,02	27,63	1,06	1,10	1,18	1,35
LIPQ	1967	2005	27,80	-0,88	84,1%	4,2%	-1,14	-0,61	29,38	1,03	1,06	1,09	1,17
LIPR	1951	2010	23,84	-1,01	95,6%	5,3%	-1,29	-0,73	25,65	1,05	1,08	1,13	1,24
LIPS	1951	2009	20,56	-0,42	95,2%	2,2%	-0,59	-0,25	21,31	1,02	1,04	1,06	1,11
LIPT	1951	2008	17,76	-0,64	88,7%	4,2%	-0,90	-0,38	18,91	1,04	1,06	1,11	1,20
LIPX	1951	2010	26,13	-1,19	97,2%	5,4%	-1,66	-0,73	28,27	1,05	1,08	1,14	1,27
LIPY	1960	2005	24,62	-0,46	83,6%	3,8%	-0,75	-0,17	25,45	1,02	1,03	1,06	1,10
LIPZ	1961	2005	25,04	-0,68	80,6%	4,4%	-0,86	-0,50	26,26	1,03	1,05	1,08	1,15
LIQB	1957	2010	22,82	-0,87	84,6%	7,2%	-1,73	-0,01	24,38	1,04	1,07	1,11	1,22
LIQC	1951	2009	31,09	-0,81	83,7%	9,8%	-2,61	0,98	32,55	1,03	1,05	1,08	1,14

Station	Interval		$v_{50}(\Delta T=1)$ (m/s)	a (m/s/h)	ρ^2	Iv	a (μ−σ) (m/s/h)	a (μ+σ) (m/s/h)	$v_{50}(\Delta T=10')$ (m/s)	ρ_1	ρ_2	ρ_3	ρ_4
LIQD	1951	2002	36,66	-1,09	88,9%	4,9%	-2,11	-0,06	38,61	1,03	1,05	1,09	1,16
LIQI	1954	1999	40,13	-0,93	49,6%	3,2%	-1,56	-0,29	41,79	1,03	1,04	1,07	1,12
LIQJ	1951	2010	25,19	-0,62	76,3%	5,6%	-1,22	-0,01	26,29	1,03	1,04	1,07	1,13
LIQK	1951	2009	34,75	-1,11	90,6%	3,7%	-1,77	-0,45	36,74	1,03	1,06	1,10	1,18
LIQM	1961	1982	37,40	-0,71	55,3%	2,3%	-1,26	-0,15	38,66	1,02	1,03	1,06	1,10
LIQN	1973	2005	13,83	-0,06	34,6%	2,6%	-0,29	0,16	13,94	1,00	1,01	1,01	1,02
LIQO	1961	2009	34,16	-0,83	82,8%	3,8%	-1,60	-0,07	35,65	1,03	1,04	1,07	1,13
LIQR	1951	2010	30,20	-0,79	60,5%	2,5%	-1,12	-0,46	31,61	1,03	1,05	1,08	1,14
LIQV	1961	1998	27,81	-0,94	88,1%	3,6%	-1,40	-0,48	29,49	1,04	1,06	1,10	1,19
LIQW	1970	2010	18,90	-0,74	82,2%	4,8%	-1,02	-0,45	20,22	1,04	1,07	1,12	1,22
LIQZ	1951	2010	31,30	-0,85	87,1%	3,0%	-1,34	-0,35	32,82	1,03	1,05	1,08	1,15
LIRA	1951	2010	24,94	-0,35	79,8%	1,9%	-0,53	-0,16	25,56	1,02	1,02	1,04	1,07
LIRB	1951	2009	23,37	-0,66	77,2%	3,8%	-1,19	-0,13	24,55	1,03	1,05	1,08	1,15
LIRE	1960	2009	23,09	-0,80	96,0%	3,7%	-1,05	-0,55	24,53	1,04	1,06	1,10	1,19
LIRF	1958	1999	25,28	-0,80	92,4%	4,2%	-1,28	-0,32	26,72	1,03	1,06	1,09	1,18
LIRG	1951	2010	20,35	-0,75	97,4%	3,7%	-1,06	-0,44	21,69	1,04	1,07	1,11	1,21
LIRH	1951	2010	22,66	-0,76	95,2%	3,5%	-1,14	-0,37	24,02	1,04	1,06	1,10	1,19
LIRK	1951	2007	47,24	-1,16	91,4%	4,2%	-2,27	-0,05	49,31	1,03	1,04	1,07	1,13
LIRL	1961	2010	21,82	-0,85	94,2%	3,9%	-1,15	-0,54	23,34	1,04	1,07	1,12	1,22
LIRM	1962	2009	24,49	-0,49	76,9%	5,5%	-1,00	0,02	25,37	1,02	1,04	1,06	1,11
LIRN	1951	2005	26,05	-0,52	54,5%	4,5%	-0,87	-0,17	26,98	1,02	1,04	1,06	1,11
LIRP	1951	2010	21,98	-0,41	92,4%	2,1%	-0,65	-0,16	22,71	1,02	1,03	1,05	1,10
LIRQ	1951	2005	24,85	-0,74	69,0%	5,2%	-1,07	-0,40	26,17	1,03	1,05	1,09	1,16
LIRS	1951	2009	24,80	-0,36	90,5%	1,9%	-0,51	-0,21	25,44	1,02	1,03	1,04	1,08
LIRT	1952	2009	29,47	-0,82	96,6%	2,9%	-1,20	-0,44	30,94	1,03	1,05	1,08	1,15
LIRU	1951	2005	21,13	-0,74	92,1%	3,5%	-1,12	-0,36	22,45	1,04	1,06	1,11	1,20
LIRV	1955	2010	24,29	-0,45	90,8%	2,2%	-0,61	-0,28	25,09	1,02	1,03	1,05	1,10
LIRX	1961	2009	29,74	-0,65	94,4%	3,6%	-1,29	-0,01	30,90	1,02	1,04	1,06	1,12

Station	Interval		$v_{50}(\Delta T=1)$ (m/s)	a (m/s/h)	ρ^2	Iv	a (μ−σ) (m/s/h)	a (μ+σ) (m/s/h)	$v_{50}(\Delta T=10')$ (m/s)	ρ_1	ρ_2	ρ_3	ρ_4
LIRZ	1967	2005	20,72	-0,55	90,0%	3,2%	-0,85	-0,26	21,71	1,03	1,05	1,08	1,14
LIVC	1951	2010	50,93	-1,13	88,2%	6,0%	-3,21	0,95	52,96	1,02	1,04	1,07	1,12
LIVD	1953	2010	18,41	-0,48	75,7%	8,0%	-1,52	0,57	19,27	1,03	1,05	1,08	1,14
LIVE	1951	2010	22,80	-0,54	85,0%	7,2%	-1,49	0,40	23,77	1,03	1,04	1,07	1,13
LIVF	1954	2010	29,42	-0,86	81,2%	4,3%	-1,61	-0,11	30,96	1,03	1,05	1,09	1,16
LIVM	1951	2010	25,47	-0,34	79,0%	3,6%	-0,90	0,23	26,08	1,01	1,02	1,04	1,07
LIVO	1951	2010	12,15	-0,61	94,2%	5,8%	-0,88	-0,34	13,25	1,05	1,09	1,15	1,30
LIVP	1951	2010	31,37	-0,88	88,5%	4,0%	-1,49	-0,27	32,95	1,03	1,05	1,08	1,15
LIVR	1951	2009	24,47	-0,50	91,3%	2,7%	-0,77	-0,22	25,36	1,02	1,04	1,06	1,11
LIVT	1951	2010	25,50	-0,95	82,5%	5,5%	-1,68	-0,23	27,21	1,04	1,07	1,11	1,21

APPENDIX 4 – DIRECTIONAL COEFFICIENTS

Station	ICAO Code	v50 (m/s)	Directional coefficients											
			345°-15°	15°-45°	45°-75°	75°-105°	105°-135°	135°-165°	165°-195°	195°-225°	225°-255°	255°-285°	285°-315°	315°-345°
Albenga (SV)	LIMG	23.7	0.96	0.77	0.65	0.51	0.43	0.57	0.62	0.61	0.61	0.64	0.98	0.99
Alghero (SS)	LIEA	23.4	0.81	0.77	0.79	0.68	0.67	0.67	0.85	0.75	0.75	0.90	1.03	0.92
Ancona Falconara	LIPY	23.6	0.89	0.94	0.89	0.66	0.72	0.63	0.76	0.90	0.80	0.77	0.87	0.93
Arezzo	LIQB	22.9	0.77	0.84	0.90	0.84	0.70	0.81	0.97	0.81	0.89	0.71	0.69	0.74
Aviano (PN)	LIPA	19.9	0.85	0.87	0.85	0.76	0.63	0.65	0.66	0.71	0.78	0.63	0.65	0.63
Bari Palese	LIBD	23.2	0.76	0.80	0.79	0.65	0.65	0.87	0.95	0.81	0.71	0.75	0.83	0.81
Bergamo Orio al Serio	LIME	20.8	0.82	0.72	0.75	0.71	0.71	0.60	0.55	0.62	0.72	0.86	0.85	0.90
Bologna Borgo Panigale	LIPE	19.6	0.72	0.75	0.78	0.76	0.70	0.72	0.66	0.73	0.77	0.86	0.89	0.81
Bolzano	LIPB	16.9	0.95	0.91	0.80	0.79	0.59	0.80	0.77	0.84	0.41	0.42	0.73	0.92
Brescia Ghedi	LIPL	24.9	0.75	0.59	0.93	0.81	0.74	0.54	0.41	0.43	0.48	0.64	0.67	0.74
Brindisi	LIBR	28.2	0.85	0.75	0.67	0.67	0.73	0.80	0.76	0.69	0.64	0.74	0.94	0.89
Cagliari Decimomannu	LIED	23.1	0.73	0.62	0.59	0.76	0.77	0.72	0.64	0.48	0.68	0.89	0.91	0.92
Cagliari Elmas	LIEE	25.0	0.71	0.57	0.60	0.82	0.85	0.61	0.67	0.70	0.68	0.78	0.96	0.96
Cameri (NO)	LIMN	22.4	1.00	0.90	0.75	0.62	0.67	0.50	0.59	0.46	0.44	0.52	0.62	0.81
Campobasso	LIBS	31.7	0.95	0.89	0.65	0.61	0.59	0.73	0.86	0.87	1.03	1.00	0.79	0.87
Capo Bellavista (OG)	LIEB	34.6	0.89	0.98	0.78	0.74	0.69	0.69	0.68	0.58	0.61	0.77	0.85	0.83
Capo Bonifati (CS)	LIBW	34.7	0.73	0.88	1.03	0.86	0.69	0.72	0.72	0.77	0.76	0.71	0.75	0.77
Capo Caccia (SS)	LIEH	31.4	1.00	0.85	0.82	0.75	0.81	0.91	0.89	1.02	0.81	0.79	0.88	0.94
Capo Carbonara (CA)	LIEC	45.3	0.62	0.70	0.65	0.57	0.57	0.57	0.54	0.58	0.80	0.98	0.90	0.60
Capo Frasca (CA)	LIEF	29.0	0.87	0.66	0.63	0.92	0.94	0.90	0.67	0.77	0.71	0.86	0.95	1.01

Station	ICAO Code	v50 (m/s)	Directional coefficients											
			345°-15°	15°-45°	45°-75°	75°-105°	105°-135°	135°-165°	165°-195°	195°-225°	225°-255°	255°-285°	285°-315°	315°-345°
Capo Mele (SV)	LIMU	33.6	0.82	0.80	0.73	0.71	0.58	0.57	0.80	1.04	1.02	1.00	0.56	0.80
Capo Palinuro (SA)	LIQK	34.0	0.85	0.75	0.67	0.73	0.80	0.84	0.87	0.80	0.72	0.66	0.79	0.86
Capo S. Lorenzo (CA)	LIEL	21.3	0.70	0.88	0.71	0.74	0.66	0.63	0.71	0.65	0.76	0.88	0.99	0.86
Capri (NA)	LIQC	31.8	0.84	0.79	0.63	0.53	0.63	0.63	0.82	0.89	0.92	0.87	0.82	0.80
Carloforte (CI)	LIEZ	31.7	0.93	0.72	0.68	0.68	0.67	0.58	0.71	0.48	0.66	0.74	0.70	0.90
Catania Fontanarossa	LICC	23.5	0.66	0.85	0.82	0.71	0.65	0.65	0.57	0.84	0.87	0.90	0.88	0.79
Catania Sigonella	LICZ	23.0	0.63	0.78	0.92	0.87	0.73	0.62	0.64	0.76	0.87	0.95	0.97	0.81
Cervia (RA)	LIPC	23.7	0.91	0.91	0.90	0.77	0.64	0.65	0.67	0.68	0.78	0.75	0.76	0.78
Civitavecchia (RM)	LIQJ	26.5	0.81	0.72	0.60	0.53	0.63	0.65	0.76	0.82	0.86	0.93	0.98	0.94
Cozzo Spadaro (SR)	LICO	27.9	0.78	0.98	0.92	0.75	0.72	0.67	0.69	0.76	0.82	0.92	0.88	0.69
Crotone	LIBC	24.9	0.91	0.77	0.61	0.66	0.82	0.77	0.80	0.86	0.93	0.83	0.78	0.91
Dobbiaco (BZ)	LIVD	18.3	0.65	0.72	0.94	0.98	0.92	0.72	0.61	0.55	0.56	0.77	0.76	0.63
Elba Monte Calamita (LI)	LIRX	29.2	0.75	0.78	0.71	0.76	0.97	0.89	0.87	0.96	0.89	0.92	0.76	0.81
Enna	LICE	26.7	0.81	0.80	0.82	0.87	0.89	0.74	0.80	0.85	0.86	0.89	0.91	0.79
Ferrara	LIPF	15.9	0.68	0.84	0.98	0.93	0.85	0.78	0.68	0.74	0.80	0.71	0.75	0.69
Firenze Peretola	LIRQ	23.9	0.82	0.93	0.78	0.58	0.47	0.50	0.49	0.64	0.65	0.63	0.55	0.64
Foggia Amendola	LIBA	24.9	0.84	0.70	0.64	0.71	0.68	0.70	0.62	0.80	0.83	0.90	1.00	0.93
Fonni (NU)	LIEN	26.7	0.52	0.50	0.57	0.74	0.75	0.67	0.56	0.64	0.70	0.97	0.94	0.63
Forli	LIPK	24.3	0.59	0.68	0.66	0.65	0.54	0.49	0.64	0.90	0.95	0.68	0.77	0.62
Frontone (PU)	LIVF	29.2	0.56	0.53	0.56	0.54	0.50	0.63	1.02	0.93	0.79	0.54	0.59	0.51
Frosinone	LIRH	24.2	0.86	1.00	0.79	0.65	0.65	0.67	0.89	0.76	0.73	0.79	0.93	0.69
Gela (CL)	LICL	27.9	0.74	0.55	0.69	0.59	0.64	0.78	0.72	0.80	0.94	0.97	0.87	0.72
Genova	LIMJ	23.8	0.94	0.88	0.76	0.63	0.93	0.84	0.79	0.78	0.76	0.64	0.64	0.91
Gioia del Colle (BA)	LIBV	27.7	0.76	0.68	0.51	0.64	1.01	0.98	0.85	0.72	0.76	0.71	0.85	0.87
Govone (CN)	LIMQ	31.2	0.75	0.84	0.57	0.55	0.46	0.57	0.56	0.57	0.62	0.66	0.82	0.90
Grazzanise (CE)	LIRM	22.6	0.81	0.83	0.84	0.78	0.90	0.92	0.77	0.87	0.86	0.91	0.76	0.67

Station	ICAO Code	v50 (m/s)	Directional coefficients											
			345°-15°	15°-45°	45°-75°	75°-105°	105°-135°	135°-165°	165°-195°	195°-225°	225°-255°	255°-285°	285°-315°	315°-345°
Grosseto	LIRS	24.1	0.73	0.94	1.03	0.65	0.86	0.91	0.86	0.81	0.76	0.88	0.83	0.67
Grottaglie (TA)	LIBG	22.8	0.87	0.67	0.56	0.68	0.94	0.92	0.81	0.79	0.70	0.67	0.79	0.94
Guardiavecchia (SS)	LIEG	39.7	0.75	0.73	0.75	0.71	0.60	0.55	0.47	0.69	0.84	0.94	0.97	0.75
Guidonia (RM)	LIRG	20.1	0.70	0.85	0.76	0.84	0.90	0.86	0.77	0.75	0.83	0.71	0.67	0.70
Lamezia Terme (CZ)	LICA	23.7	0.68	0.79	0.82	0.85	0.79	0.76	0.67	0.86	0.90	1.05	0.95	0.79
Lampedusa (AG)	LICD	26.6	0.87	0.64	0.67	0.82	0.78	0.66	0.61	0.73	0.77	0.79	0.87	0.99
L'Aquila Preturo	LIQI	41.5	0.82	0.91	0.75	0.59	0.54	0.49	0.55	0.83	1.00	0.63	0.58	0.66
Latina	LIRL	21.3	0.78	0.69	0.68	0.82	0.87	0.85	0.78	0.71	0.68	0.76	0.89	0.66
Latronico (PZ)	LIBU	36.9	0.86	0.88	0.79	0.66	0.64	0.56	0.90	0.94	0.90	0.68	0.68	0.83
Lecce Galatina	LIBN	24.4	0.78	0.80	0.54	0.73	0.87	0.93	0.89	0.79	0.71	0.76	0.80	0.81
Marina di Ginosa (TA)	LIBH	26.5	0.67	0.64	0.80	0.86	1.07	0.95	0.78	0.64	0.65	0.66	0.65	0.69
Messina	LICF	20.5	0.68	0.72	0.62	0.55	0.56	0.89	0.97	0.93	0.79	0.78	0.82	0.73
Milano Linate	LIML	22.4	0.91	0.71	0.63	0.65	0.70	0.50	0.53	0.58	0.56	0.63	0.86	0.92
Milano Malpensa	LIMC	25.3	0.95	0.93	0.60	0.61	0.66	0.49	0.49	0.44	0.45	0.39	0.60	0.91
Mondovi (CN)	LIMY	22.6	0.76	0.70	0.68	0.64	0.67	0.59	0.61	0.72	0.94	0.88	0.62	0.76
Monte Argentario (GR)	LIQO	34.2	0.84	0.86	0.85	0.86	0.86	0.85	0.86	0.90	0.85	0.85	0.83	0.82
Monte Bisbino (CO)	LIMO	23.2	0.83	0.94	0.97	0.77	0.81	0.86	0.93	0.67	0.53	0.62	0.65	0.87
Monte Cimone (MO)	LIVC	50.5	0.80	0.94	0.91	0.73	0.60	0.68	0.89	0.93	0.72	0.61	0.56	0.67
Monte S. Angelo (FG)	LIBE	40.7	0.95	0.68	0.49	0.56	0.53	0.62	0.65	0.71	0.68	0.65	0.80	0.93
Monte Scuro (CS)	LIBQ	31.4	0.61	0.69	0.84	0.88	0.87	0.84	0.77	0.75	0.90	0.94	0.80	0.63
Monte Terminillo (RI)	LIRK	47.1	0.69	0.94	0.89	0.80	0.59	0.58	0.58	0.60	0.60	0.59	0.58	0.56
Napoli Capodichino	LIRN	25.2	0.75	0.92	0.78	0.63	0.57	0.89	0.72	0.78	0.81	0.86	0.68	0.63
Novi Ligure (AL)	LIMR	16.1	0.81	0.96	0.98	0.73	0.80	0.95	0.99	0.64	0.75	0.80	0.76	0.78
Olbia (OT)	LIEO	23.1	0.66	0.87	0.67	0.85	0.82	0.71	0.57	0.65	0.90	1.10	1.06	0.80
Paganella (TN)	LIVP	31.4	0.96	0.83	0.49	0.52	0.55	0.63	0.74	0.85	0.81	0.71	0.65	0.88
Palermo Boccadifalco	LICP	25.8	0.68	0.56	0.56	0.59	0.78	0.79	0.91	0.87	0.90	0.90	0.86	0.75

Station	ICAO Code	v50 (m/s)	Directional coefficients											
			345°-15°	15°-45°	45°-75°	75°-105°	105°-135°	135°-165°	165°-195°	195°-225°	225°-255°	255°-285°	285°-315°	315°-345°
Palermo Punta Raisi	LICJ	25.7	0.89	0.86	0.80	0.89	0.91	1.03	1.00	0.83	0.90	0.97	0.89	0.89
Pantelleria (TP)	LICG	34.7	0.73	0.59	0.69	0.89	0.99	0.90	0.75	0.68	0.65	0.66	0.73	0.76
Passo dei Giovi (GE)	LIMV	24.4	0.70	0.96	0.56	0.58	0.62	0.79	0.82	0.64	0.59	0.49	0.68	0.81
Passo della Cisa (MS)	LIMT	27.6	0.83	0.77	0.72	0.66	0.64	0.91	1.04	1.02	1.00	0.78	0.68	0.67
Passo Porretta (PT)	LIQD	36.0	0.87	0.85	0.93	0.82	0.58	0.62	0.64	0.73	0.67	0.57	0.60	0.91
Passo Rolle (TN)	LIVR	23.4	0.94	0.77	0.66	0.61	0.71	0.59	0.66	0.73	0.64	0.69	0.85	1.02
Perdasdefogu (OG)	LIEP	27.4	0.54	0.77	0.83	0.77	0.64	0.55	0.46	0.68	0.87	1.00	1.04	0.86
Perugia S. Egidio	LIRZ	20.0	0.96	0.97	0.88	0.67	0.77	0.78	0.84	0.84	0.86	0.64	0.67	0.81
Pescara	LIBP	25.7	0.69	0.64	0.56	0.52	0.58	0.56	0.80	0.97	0.87	0.85	0.81	0.80
Piacenza	LIMS	21.6	0.74	0.65	0.69	0.70	0.79	0.61	0.68	0.91	0.80	0.74	0.81	0.96
Pisa S.Giusto	LIRP	21.9	0.68	0.78	0.79	0.72	0.66	0.84	0.80	0.93	0.99	0.88	0.74	0.68
Plateau Rosa (AO)	LIMH	42.1	0.89	1.01	0.88	0.71	0.69	0.63	0.74	0.65	0.60	0.66	0.73	0.85
Ponza (LT)	LIQZ	32.3	0.89	0.94	0.70	0.74	0.85	0.68	0.76	0.75	0.76	0.89	0.99	0.89
Potenza	LIBZ	25.9	0.87	0.76	0.64	0.58	0.63	0.61	0.71	0.78	0.94	1.04	0.75	0.74
Prizzi (PA)	LICX	25.3	0.80	0.83	0.55	0.80	0.84	0.90	0.84	0.76	0.80	0.89	0.92	0.96
Punta Marina (RA)	LIVM	26.0	0.81	0.91	0.93	0.84	0.79	0.69	0.61	0.61	0.63	0.59	0.63	0.57
Radicofani (SI)	LIQR	31.3	1.02	1.10	0.97	0.66	0.69	0.64	0.79	0.78	0.69	0.76	0.82	0.79
Reggio Calabria	LICR	24.9	0.84	0.69	0.61	0.71	0.97	0.96	0.78	0.78	0.80	0.72	0.91	0.93
Rieti	LIQN	13.5	0.97	0.97	1.01	0.93	0.97	0.95	0.97	0.99	0.96	0.94	1.01	1.04
Rifredo Mugello (FI)	LIQM	36.7	0.99	0.92	0.69	0.59	0.44	0.38	0.86	0.88	1.00	0.55	0.43	0.52
Rimini	LIPR	23.1	0.89	0.89	0.81	0.68	0.55	0.55	0.71	0.75	0.77	0.72	0.76	0.84
Roma Ciampino	LIRA	24.8	0.72	0.74	0.53	0.60	0.89	1.01	0.87	0.72	0.68	0.59	0.62	0.69
Roma Fiumicino	LIRF	24.5	0.85	0.81	0.56	0.56	0.81	0.80	0.82	0.81	0.87	0.88	0.86	0.89
Roma Pratica di Mare	LIRE	22.3	0.87	0.80	0.63	0.70	0.91	0.85	0.87	0.87	0.88	0.91	0.85	0.82
Roma Urbe	LIRU	20.1	0.88	0.81	0.68	0.65	0.78	0.85	0.76	0.88	0.89	0.89	0.79	0.82
Ronchi dei Legionari (GO)	LIPQ	26.7	0.60	0.80	0.96	0.85	0.63	0.69	0.66	0.54	0.58	0.61	0.51	0.66

Station	ICAO Code	v50 (m/s)	Directional coefficients											
			345°-15°	15°-45°	45°-75°	75°-105°	105°-135°	135°-165°	165°-195°	195°-225°	225°-255°	255°-285°	285°-315°	315°-345°
S. Maria di Leuca (LE)	LIBY	25.2	0.89	0.86	0.81	0.86	0.90	0.90	0.83	0.87	0.84	0.79	0.77	0.79
S.Valentino alla Muta (BZ)	LIVE	23.1	0.82	0.81	0.70	0.51	0.70	0.89	0.81	0.86	0.74	0.51	0.87	1.01
Sarzana Luni (SP)	LIQW	20.1	0.83	1.08	0.86	0.75	0.74	0.72	0.88	0.77	0.99	0.73	0.56	0.63
Tarvisio (UD)	LIVO	19.1	0.37	0.55	0.71	0.75	0.59	0.69	0.63	0.62	0.78	0.97	0.77	0.61
Termoli (CB)	LIBT	33.1	0.98	0.93	0.60	0.56	0.57	0.57	0.55	0.55	0.59	0.68	0.87	0.98
Torino Bric Della Croce	LIMK	23.5	0.74	0.71	0.67	0.59	0.57	0.52	0.54	0.54	0.67	0.88	0.94	0.89
Torino Caselle	LIMF	22.0	0.71	0.66	0.59	0.55	0.42	0.38	0.50	0.61	0.71	0.89	0.94	0.82
Trapani Birgi	LICT	30.2	0.79	0.68	0.48	0.63	1.03	0.86	0.71	0.68	0.75	0.88	0.86	0.85
Trevico (AV)	LIRT	31.9	0.72	0.64	0.71	0.74	0.65	0.80	0.83	0.93	1.04	0.99	0.71	0.66
Treviso Istrana	LIPS	20.0	0.74	0.94	0.96	0.83	0.64	0.59	0.52	0.61	0.65	0.68	0.80	0.85
Treviso S. Angelo	LIPH	21.1	0.60	0.92	0.86	0.69	0.53	0.52	0.49	0.54	0.59	0.67	0.64	0.55
Trieste	LIVT	25.3	0.64	1.01	0.94	0.71	0.55	0.53	0.59	0.57	0.53	0.56	0.73	0.60
Udine Campoformido	LIPD	21.8	0.85	0.88	0.93	0.79	0.71	0.76	0.83	0.59	0.55	0.46	0.50	0.73
Udine Rivolto	LIPI	21.8	0.86	0.91	0.91	0.87	0.67	0.77	0.63	0.54	0.51	0.52	0.67	0.80
Ustica (PA)	LICU	40.9	0.92	0.86	0.64	0.65	0.71	0.68	0.75	0.77	0.72	0.77	0.94	1.00
Venezia Tessera	LIPZ	23.4	0.71	0.96	0.88	0.82	0.78	0.83	0.74	0.68	0.70	0.78	0.61	0.64
Verona Villafranca	LIPX	25.1	0.76	0.76	0.83	0.98	0.73	0.48	0.48	0.50	0.66	0.70	0.67	0.59
Vicenza	LIPT	17.2	0.75	0.92	0.79	0.93	0.72	0.59	0.55	0.70	0.69	0.66	0.54	0.68
Vigna di Valle (RM)	LIRB	23.3	0.99	1.07	0.66	0.58	0.67	0.78	0.77	0.72	0.74	0.72	0.72	0.72
Viterbo	LIRV	24.5	0.89	1.01	0.85	0.65	0.76	0.77	0.72	0.74	0.68	0.66	0.59	0.67
Volterra (PI)	LIQV	29.8	0.66	0.91	0.79	0.67	0.67	0.58	0.97	0.89	0.89	0.73	0.58	0.67

APPENDIX 5 – SEASONAL COEFFICIENTS

Station	ICAO Code	v50 (m/s)	Seasonal coefficients											
			1 Jan.	2 Feb.	3 Mar.	4 Apr.	5 May	6 Jun.	7 Jul.	8 Aug.	9 Sep.	10 Oct.	11 Nov.	12 Dec.
Albenga (SV)	LIMG	23.71	0.92	0.91	0.81	0.78	0.78	0.65	0.54	0.57	0.75	0.88	0.90	0.93
Alghero (SS)	LIEA	23.37	0.93	0.87	0.84	0.86	0.68	0.68	0.66	0.67	0.62	0.84	0.84	0.95
Ancona Falconara	LIPY	23.59	0.81	0.85	0.85	0.76	0.78	0.67	0.69	0.72	0.64	0.70	0.83	0.91
Arezzo	LIQB	22.92	0.81	0.89	0.84	0.77	0.71	0.64	0.67	0.86	0.69	0.74	0.81	0.91
Aviano (PN)	LIPA	19.86	0.78	0.81	0.82	0.77	0.65	0.76	0.74	0.83	0.69	0.72	0.85	0.75
Bari Palese	LIBD	23.18	0.79	0.82	0.82	0.81	0.81	0.63	0.62	0.68	0.63	0.83	0.78	0.85
Bergamo Orio al Serio	LIME	20.82	0.80	0.79	0.83	0.74	0.61	0.76	0.91	0.84	0.75	0.68	0.74	0.73
Bologna Borgo Panigale	LIPE	19.58	0.77	0.79	0.85	0.83	0.71	0.70	0.72	0.78	0.71	0.79	0.76	0.69
Bolzano	LIPB	16.87	0.84	0.88	0.85	0.79	0.78	0.75	0.83	0.78	0.76	0.69	0.90	0.80
Brescia Ghedi	LIPL	24.90	0.70	0.75	0.76	0.80	0.59	0.83	0.69	0.63	0.62	0.62	0.76	0.65
Brindisi	LIBR	28.18	0.86	0.73	0.92	0.71	0.66	0.71	0.64	0.65	0.69	0.73	0.76	0.80
Cagliari Decimomannu	LIED	23.08	0.93	0.93	0.82	0.80	0.74	0.69	0.67	0.71	0.73	0.74	0.78	0.91
Cagliari Elmas	LIEE	24.98	0.98	0.86	0.86	0.81	0.75	0.67	0.68	0.71	0.78	0.79	0.86	0.92
Cameri (NO)	LIMN	22.36	0.78	0.82	0.81	0.84	0.67	0.63	0.64	0.62	0.65	0.60	0.95	0.71
Campobasso	LIBS	31.70	0.99	0.92	0.91	0.92	0.83	0.80	0.75	0.74	0.75	0.92	0.87	1.01

Station	ICAO Code	v50 (m/s)	Seasonal coefficients											
			1 Jan.	2 Feb.	3 Mar.	4 Apr.	5 May	6 Jun.	7 Jul.	8 Aug.	9 Sep.	10 Oct.	11 Nov.	12 Dec.
Capo Bellavista (OG)	LIEB	34.63	0.92	0.89	0.81	0.80	0.77	0.61	0.61	0.62	0.68	0.82	0.79	0.91
Capo Bonifati (CS)	LIBW	34.72	0.85	0.82	0.99	0.82	0.79	0.63	0.49	0.60	0.69	0.86	0.85	0.86
Capo Caccia (SS)	LIEH	31.37	0.98	0.95	0.78	0.92	0.70	0.73	0.68	0.73	0.71	0.93	0.91	0.95
Capo Carbonara (CA)	LIEC	45.33	0.83	0.89	0.79	0.79	0.68	0.75	0.76	0.62	0.72	0.72	0.79	0.81
Capo Frasca (CA)	LIEF	28.99	1.04	0.87	0.97	0.98	0.86	0.74	0.70	0.68	0.69	0.84	0.87	0.96
Capo Mele (SV)	LIMU	33.59	0.87	0.83	0.90	0.89	0.88	0.80	0.83	0.84	0.93	1.00	0.89	0.93
Capo Palinuro (SA)	LIQK	34.02	0.89	0.82	0.80	0.77	0.67	0.60	0.56	0.69	0.67	0.74	0.96	0.85
Capo S. Lorenzo (CA)	LIEL	21.26	0.83	0.88	0.82	0.79	0.79	0.75	0.82	0.68	0.65	0.79	0.64	0.98
Capri (NA)	LIQC	31.80	0.88	0.86	0.87	0.94	0.78	0.65	0.69	0.63	0.65	0.81	0.85	0.88
Carloforte (CI)	LIEZ	31.75	0.73	0.89	0.69	0.69	0.65	0.53	0.57	0.52	0.87	0.66	0.73	0.71
Catania Fontanarossa	LICC	23.47	0.82	0.94	0.88	0.87	0.72	0.65	0.71	0.65	0.65	0.73	0.77	0.85
Catania Sigonella	LICZ	23.04	0.92	0.92	0.97	0.93	0.85	0.73	0.78	0.80	0.77	0.81	0.93	1.01
Cervia (RA)	LIPC	23.75	0.88	0.79	0.83	0.85	0.65	0.72	0.70	0.70	0.85	0.71	0.85	0.85
Civitavecchia (RM)	LIQJ	26.53	0.89	0.97	0.86	0.92	0.65	0.64	0.64	0.71	0.82	0.80	0.88	0.87
Cozzo Spadaro (SR)	LICO	27.89	0.90	0.95	0.88	0.83	0.79	0.75	0.74	0.70	0.74	0.85	0.80	0.93
Crotone	LIBC	24.88	0.93	0.90	0.84	0.72	0.68	0.72	0.66	0.70	0.69	0.82	0.78	0.94
Dobbiaco (BZ)	LIVD	18.31	0.89	0.85	0.93	0.81	0.78	0.71	0.78	0.81	0.78	0.85	0.83	0.89
Elba Monte Calamita (LI)	LIRX	29.16	0.84	0.98	0.88	0.82	0.70	0.67	0.68	0.69	0.80	0.84	0.96	0.91
Enna	LICE	26.72	0.84	0.84	0.89	0.86	0.77	0.68	0.61	0.65	0.75	0.74	0.86	0.92
Ferrara	LIPF	15.87	0.81	0.90	0.85	0.88	0.80	0.78	0.73	0.76	0.78	0.84	0.89	0.76
Firenze Peretola	LIRQ	23.89	0.70	0.79	0.79	0.72	0.64	0.60	0.53	0.62	0.56	0.66	0.81	0.95
Foggia Amendola	LIBA	24.92	0.91	0.84	0.94	0.76	0.73	0.74	0.78	0.76	0.70	0.80	0.81	0.92

Station	ICAO Code	v50 (m/s)	Seasonal coefficients											
			1 Jan.	2 Feb.	3 Mar.	4 Apr.	5 May	6 Jun.	7 Jul.	8 Aug.	9 Sep.	10 Oct.	11 Nov.	12 Dec.
Fonni (NU)	LIEN	26.67	0.85	0.84	0.78	0.72	0.62	0.69	0.59	0.61	0.57	0.70	0.74	0.93
Forli	LIPK	24.28	0.76	0.86	0.80	0.82	0.68	0.66	0.57	0.66	0.59	0.72	0.73	0.94
Frontone (PU)	LIVF	29.20	0.85	0.84	0.91	0.87	0.81	0.67	0.66	0.69	0.64	0.87	0.90	0.92
Frosinone	LIRH	24.20	0.83	0.89	0.81	0.76	0.67	0.63	0.87	0.64	0.56	0.78	0.80	0.97
Gela (CL)	LICL	27.91	0.90	0.82	0.86	0.88	0.75	0.80	0.71	0.75	0.74	0.80	0.93	0.91
Genova	LIMJ	23.80	0.83	0.96	0.90	0.84	0.69	0.71	0.74	0.76	0.80	0.91	0.85	0.85
Gioia del Colle (BA)	LIBV	27.75	0.89	0.86	0.94	0.91	0.80	0.73	0.64	0.74	0.69	0.82	0.84	0.95
Govone (CN)	LIMQ	31.15	0.69	0.74	0.75	0.73	0.53	0.47	0.73	0.61	0.52	0.71	0.67	0.77
Grazzanise (CE)	LIRM	22.61	0.88	0.83	0.90	0.83	0.72	0.70	0.62	0.66	0.81	0.84	0.94	1.06
Grosseto	LIRS	24.09	0.85	0.89	0.92	0.89	0.76	0.73	0.78	0.76	0.82	0.86	0.99	0.95
Grottaglie (TA)	LIBG	22.85	0.77	0.89	0.86	0.79	0.66	0.67	0.61	0.61	0.79	0.85	0.87	0.88
Guardiavecchia (SS)	LIEG	39.68	0.82	0.96	0.85	0.83	0.69	0.72	0.69	0.74	0.70	0.82	0.86	0.89
Guidonia (RM)	LIRG	20.14	0.76	0.90	0.83	0.80	0.77	0.75	0.76	0.71	0.75	0.80	0.82	0.86
Lamezia Terme (CZ)	LICA	23.67	0.98	0.89	0.89	0.79	0.75	0.65	0.63	0.66	0.78	0.73	0.97	1.07
Lampedusa (AG)	LICD	26.60	0.92	0.87	0.80	0.88	0.74	0.67	0.69	0.62	0.73	0.66	0.79	0.86
L'Aquila Preturo	LIQI	41.55	0.83	0.85	0.86	0.81	0.75	0.72	0.69	0.64	0.73	0.89	0.82	0.81
Latina	LIRL	21.31	0.81	0.90	0.93	0.74	0.78	0.64	0.71	0.70	0.80	0.66	0.79	0.73
Latronico (PZ)	LIBU	36.93	0.89	0.90	0.83	0.79	0.70	0.62	0.58	0.60	0.71	0.83	0.91	0.96
Lecce Galatina	LIBN	24.37	0.83	0.82	0.90	0.86	0.74	0.71	0.71	0.79	0.83	0.84	0.89	0.87
Marina di Ginosa (TA)	LIBH	26.47	0.99	0.91	0.89	0.85	0.77	0.63	0.64	0.61	0.77	0.92	0.97	1.02
Messina	LICF	20.45	0.88	0.88	0.85	0.88	0.79	0.70	0.65	0.64	0.67	0.85	0.81	0.86
Milano Linate	LIML	22.39	0.82	0.86	0.89	0.76	0.62	0.71	0.62	0.67	0.65	0.74	0.75	0.89

Station	ICAO Code	v50 (m/s)	Seasonal coefficients											
			1 Jan.	2 Feb.	3 Mar.	4 Apr.	5 May	6 Jun.	7 Jul.	8 Aug.	9 Sep.	10 Oct.	11 Nov.	12 Dec.
Milano Malpensa	LIMC	25.34	0.91	0.81	0.85	0.86	0.69	0.64	0.61	0.59	0.62	0.67	0.83	0.90
Mondovi (CN)	LIMY	22.64	0.82	0.80	0.71	0.78	0.66	0.82	0.70	0.83	0.62	0.72	0.91	0.64
Monte Argentario (GR)	LIQO	34.18	0.87	0.90	0.93	0.84	0.77	0.74	0.71	0.66	0.70	0.82	0.91	0.85
Monte Bisbino (CO)	LIMO	23.19	0.87	0.88	0.86	0.79	0.79	0.83	0.75	0.85	0.88	0.87	0.88	0.80
Monte Cimone (MO)	LIVC	50.52	0.89	0.84	0.87	0.89	0.76	0.64	0.63	0.70	0.74	0.79	0.89	0.93
Monte S. Angelo (FG)	LIBE	40.73	0.92	0.80	0.88	0.76	0.70	0.70	0.64	0.72	0.73	0.69	0.79	0.87
Monte Scuro (CS)	LIBQ	31.44	0.90	0.86	0.84	0.76	0.73	0.70	0.63	0.66	0.75	0.84	0.88	0.89
Monte Terminillo (RI)	LIRK	47.13	0.89	0.79	0.70	0.71	0.54	0.62	0.50	0.51	0.58	0.72	0.79	0.84
Napoli Capodichino	LIRN	25.21	0.87	0.83	0.72	0.74	0.61	0.57	0.52	0.72	0.68	0.76	0.80	0.88
Novi Ligure (AL)	LIMR	16.06	0.66	0.88	0.86	0.93	0.92	0.85	0.88	0.79	0.79	0.81	0.73	0.83
Olbia (OT)	LIEO	23.13	1.03	0.96	0.94	0.82	0.78	0.79	0.80	0.79	0.82	0.87	0.84	0.95
Paganella (TN)	LIVP	31.40	0.87	0.74	0.86	0.77	0.72	0.74	0.83	0.73	0.75	0.75	0.85	0.89
Palermo Boccadifalco	LICP	25.83	0.88	0.94	0.92	0.77	0.79	0.60	0.63	0.66	0.74	0.84	0.84	0.87
Palermo Punta Raisi	LICJ	25.73	0.97	0.96	0.92	0.87	0.85	0.66	0.72	0.77	0.88	0.88	0.93	0.97
Pantelleria (TP)	LICG	34.75	0.79	0.79	0.86	0.98	0.80	0.70	0.58	0.60	0.65	0.72	0.74	0.75
Passo dei Giovi (GE)	LIMV	24.44	0.70	0.67	0.65	0.94	0.61	0.61	0.56	0.63	0.73	0.61	0.69	0.68
Passo della Cisa (MS)	LIMT	27.58	0.94	0.91	0.90	0.83	0.88	0.82	0.81	0.80	0.76	0.86	0.91	0.94
Passo Porretta (PT)	LIQD	35.97	0.83	0.87	0.76	0.74	0.69	0.59	0.65	0.64	0.63	0.70	0.69	0.78
Passo Rolle (TN)	LIVR	23.43	0.91	0.99	0.84	0.69	0.64	0.64	0.62	0.61	0.64	0.77	0.90	0.94
Perdasdefogu (OG)	LIEP	27.37	1.01	0.92	0.88	0.81	0.73	0.71	0.79	0.80	0.79	0.78	0.91	0.99
Perugia S. Egidio	LIRZ	19.97	0.88	0.93	0.95	0.79	0.77	0.71	0.82	0.80	0.80	0.83	0.85	0.94
Pescara	LIBP	25.68	0.84	0.87	0.80	0.73	0.80	0.66	0.74	0.66	0.68	0.75	0.84	0.99

Station	ICAO Code	v50 (m/s)	Seasonal coefficients											
			1 Jan.	2 Feb.	3 Mar.	4 Apr.	5 May	6 Jun.	7 Jul.	8 Aug.	9 Sep.	10 Oct.	11 Nov.	12 Dec.
Piacenza	LIMS	21.63	0.81	0.78	0.90	0.88	0.78	0.80	0.71	0.72	0.76	0.74	0.70	0.65
Pisa S.Giusto	LIRP	21.86	0.87	0.90	0.88	0.76	0.76	0.74	0.80	0.77	0.81	0.89	0.93	0.95
Plateau Rosa (AO)	LIMH	42.07	0.92	0.85	0.88	0.82	0.68	0.67	0.76	0.74	0.73	0.78	0.90	0.94
Ponza (LT)	LIQZ	32.33	0.88	0.88	0.88	0.79	0.71	0.69	0.67	0.74	0.71	0.75	0.89	0.89
Potenza	LIBZ	25.85	0.87	0.83	0.90	0.78	0.74	0.70	0.75	0.70	0.77	0.78	0.91	0.97
Prizzi (PA)	LICX	25.25	0.91	0.92	0.90	0.85	0.80	0.61	0.54	0.63	0.64	0.70	0.85	0.90
Punta Marina (RA)	LIVM	25.96	0.83	0.81	0.79	0.78	0.67	0.80	0.77	0.75	0.85	0.68	0.83	0.83
Radicofani (SI)	LIQR	31.26	0.91	0.88	0.83	0.82	0.77	0.74	0.70	0.71	0.77	0.80	0.85	0.95
Reggio Calabria	LICR	24.94	0.93	0.86	0.88	0.83	0.77	0.71	0.69	0.68	0.69	0.80	0.83	0.86
Rieti	LIQN	13.53	0.99	1.09	1.05	1.03	0.97	0.92	0.95	0.83	0.89	1.02	1.01	0.99
Rifredo Mugello (FI)	LIQM	36.72	0.83	0.89	0.94	0.85	0.76	0.61	0.66	0.63	0.71	0.75	0.87	0.86
Rimini	LIPR	23.13	0.81	0.75	0.86	0.77	0.67	0.72	0.84	0.74	0.76	0.76	0.83	0.82
Roma Ciampino	LIRA	24.83	0.87	0.84	0.93	0.92	0.76	0.70	0.70	0.68	0.77	0.81	0.89	0.94
Roma Fiumicino	LIRF	24.46	1.00	0.88	0.83	0.81	0.73	0.70	0.71	0.70	0.76	0.82	0.89	0.87
Roma Pratica di Mare	LIRE	22.33	0.91	0.85	0.90	0.86	0.77	0.68	0.68	0.70	0.85	0.81	0.87	0.97
Roma Urbe	LIRU	20.09	0.77	0.82	0.89	0.92	0.77	0.71	0.74	0.71	0.76	0.84	0.91	0.89
Ronchi dei Legionari (GO)	LIPQ	26.66	0.90	0.78	0.80	0.85	0.71	0.60	0.67	0.65	0.73	0.73	0.93	0.90
S. Maria di Leuca (LE)	LIBY	25.19	0.94	0.88	0.88	0.82	0.73	0.68	0.69	0.73	0.75	0.80	0.94	0.92
S.Valentino alla Muta (BZ)	LIVE	23.06	0.96	0.90	0.86	0.80	0.75	0.76	0.78	0.71	0.80	0.86	0.88	0.86
Sarzana Luni (SP)	LIQW	20.15	0.74	0.73	0.82	0.70	0.72	0.65	0.76	0.53	0.74	0.78	1.00	1.00
Tarvisio (UD)	LIVO	19.11	0.76	0.78	0.77	0.75	0.69	0.66	0.65	0.84	0.57	0.70	0.75	0.82
Termoli (CB)	LIBT	33.13	0.89	0.89	0.85	0.75	0.69	0.73	0.71	0.71	0.75	0.75	0.84	0.94

Station	ICAO Code	v50 (m/s)	Seasonal coefficients											
			1 Jan.	2 Feb.	3 Mar.	4 Apr.	5 May	6 Jun.	7 Jul.	8 Aug.	9 Sep.	10 Oct.	11 Nov.	12 Dec.
Torino Bric Della Croce	LIMK	23.46	0.85	0.77	0.87	0.80	0.68	0.66	0.74	0.61	0.72	0.80	0.86	0.82
Torino Caselle	LIMF	22.04	0.86	0.94	0.85	0.67	0.64	0.65	0.65	0.80	0.65	0.67	0.74	0.78
Trapani Birgi	LICT	30.21	0.89	0.92	0.96	0.99	0.87	0.78	0.61	0.64	0.71	0.79	0.86	0.87
Trevico (AV)	LIRT	31.88	0.89	0.96	0.83	0.93	0.75	0.73	0.75	0.74	0.74	0.78	0.98	0.91
Treviso Istrana	LIPS	20.01	0.91	0.90	0.90	0.84	0.72	0.77	0.81	0.81	0.77	0.86	0.78	0.88
Treviso S. Angelo	LIPH	21.12	0.81	0.83	0.77	0.78	0.64	0.61	0.68	0.63	0.67	0.67	0.93	0.82
Trieste	LIVT	25.30	0.91	0.90	0.84	0.81	0.67	0.65	0.71	0.70	0.74	0.70	0.89	0.94
Udine Campoformido	LIPD	21.79	0.83	0.83	0.82	0.83	0.69	0.74	0.76	0.70	0.68	0.80	0.88	0.86
Udine Rivolto	LIPI	21.76	0.93	0.83	0.86	0.96	0.76	0.75	0.76	0.72	0.77	0.75	0.86	0.85
Ustica (PA)	LICU	40.90	0.89	0.87	0.87	0.76	0.63	0.55	0.62	0.61	0.69	0.73	0.86	0.94
Venezia Tessera	LIPZ	23.42	0.85	0.85	0.85	0.88	0.73	0.71	0.85	0.74	0.90	0.88	0.91	0.87
Verona Villafranca	LIPX	25.11	0.77	0.83	0.84	0.81	0.71	0.74	0.66	0.82	0.68	0.75	0.73	0.80
Vicenza	LIPT	17.18	0.75	0.78	0.72	0.86	0.72	0.71	0.69	0.87	0.72	0.71	0.73	0.81
Vigna di Valle (RM)	LIRB	23.34	0.92	0.84	0.93	0.85	0.70	0.66	0.68	0.63	0.73	0.84	0.86	0.96
Viterbo	LIRV	24.45	0.92	0.88	0.87	0.81	0.68	0.68	0.68	0.66	0.75	0.82	0.87	0.93
Volterra (PI)	LIQV	29.83	0.84	0.89	0.92	0.77	0.69	0.67	0.68	0.65	0.79	0.78	0.99	0.84